Characterization and Evolution of Primary and Secondary Aerosols During $PM_{2.5}$ and PM_{10} Episodes in the South Coast Air Basin

Final Report
September 26, 2000

Jonathan O. Allen, Lara S. Hughes, Lynn G. Salmon,
Paul R. Mayo, Robert J. Johnson, and Glen R. Cass

Environmental Engineering and Science Department
California Institute of Technology
Pasadena, California 91125

This project was supported by the Coordinating Research Council, Inc., and the U.S. DOE Office of Heavy Vehicle Technologies through the National Renewable Energy Laboratory under CRC Project No. A-22.

Executive Summary

Annually averaged airborne fine particle mass concentrations in Southern California have declined in recent years as a result of specific emission control programs including sulfur oxides emission controls, diesel engine improvements, and light-duty vehicle emission controls. Despite these improvements, aerosol concentrations in the South Coast Air Basin (SoCAB) continue to exceed air quality standards. The 24-h average national ambient air quality standard for PM_{10}, which is set at 150 $\mu g\ m^{-3}$, was exceeded on between 1% and 8% of the sampling days in the mid-1990s. During the period 1994–1996, the SoCAB registered the highest 24-hour-average fine particle ($PM_{2.5}$) concentration (115 $\mu g\ m^{-3}$) observed in California. This level exceeds the proposed National Ambient Air Quality Standard for fine particles, set at a 24-h average of 65 $\mu g\ m^{-3}$, by nearly a factor of two.

The major contributors to aerosol mass in the SoCAB on days with high fine particle concentrations are NH_4^+, NO_3^-, and organic carbon. Aerosol NH_4^+ originates from NH_3 gas that can be emitted from both vehicle exhaust and agricultural operations. Aerosol NO_3^- originates from atmospheric reactions that begin with NO gas emitted from vehicles and other combustion sources. Aerosol organic carbon is directly emitted from numerous source types including motor vehicles, woodsmoke, and food cooking. Gas-phase organic compounds also can react in the atmosphere to produce low vapor pressure products that condense to form secondary organic aerosol. If aerosol concentrations in the SoCAB are to be reduced to meet air quality standards in a cost-effective manner, we must understand the contributions of various sources to aerosol and aerosol precursor concentrations, as well as the aerosol transport and transformation processes in the atmosphere. Detailed measurements are needed to aid our understanding of the sources and transformation of aerosols in the SoCAB.

In the summer and fall of 1997, the Aerosol Project of the 1997 Southern California Ozone Study—North American Research Strategy for Tropospheric Ozone (SCOS97) experiments took place in California's South Coast Air Basin. A program of airborne particle research took place as part of those experiments. This report documents the results of three portions of the particle research effort: the Vehicle-Oriented Trajectory Study, the Nitrate-Oriented Trajectory Study, and the Caldecott Tunnel Study. The trajectory studies were designed to observe aerosol evolution in an urban atmosphere that is influenced by source emissions and physical and chemical transformation processes. The specific objective of the Vehicle-Oriented Trajectory Study was to observe the influence of vehicle emissions

on aerosol evolution. In the Nitrate-Oriented Trajectory Study, the objective was to observe the formation of nitrogen-containing aerosols, including ammonium nitrate, at sites located upwind, inside, and downwind of the Chino dairy area, a large source of ammonia. The third study was the Caldecott Tunnel Study in which traffic-generated aerosol samples were collected from two bores of a highway tunnel located in the San Francisco Bay area. The objective of that study was to determine aerosol emission rates for the California in-use vehicle fleet.

In each study, aerosol samples were collected using filter samplers, cascade impactors, and electronic particle size distribution monitors. Two sets of filter samples were collected, one for particles smaller than 1.9 μm aerodynamic diameter ($PM_{1.9}$) and another for particles smaller than 10 μm aerodynamic diameter (PM_{10}). The filter and impactor samples were analyzed for aerosol mass and for the major aerosol chemical components including organic carbon, elemental carbon, sulfate, nitrate, ammonium, and 36 trace elements.

Vehicle-Oriented Trajectory Study

The Vehicle-Oriented Trajectory Study was conducted in August of 1997 at three sites in Southern California. The monitoring sites were located in Central Los Angeles, near the highest density of vehicle traffic in the Los Angeles area, in Azusa, which is often downwind of Central Los Angeles, and in Riverside. The objective of the experiment was to use trajectory-oriented sampling to observe single air parcels that are heavily influenced by primary particle emissions from motor vehicles at several locations along an air parcel trajectory and by comparison to document the effects of emissions, chemical reactions, deposition, and other processes on the particle population.

Fine particle ($PM_{1.9}$) mass, ammonium ion, organic carbon, and elemental carbon concentrations at Central Los Angeles generally exhibited very strong diurnal cycles with concentration peaks during or soon after the period of the morning traffic peak and concentration minima overnight. Fine particle mass and elemental carbon concentrations at Azusa exhibited a similar diurnal pattern. $PM_{1.9}$ and PM_{10} mass balances were generally dominated by organic compounds and elemental carbon at both Central Los Angeles and Azusa.

During these experiments, two air parcels were identified that passed near both the Central Los Angeles and Azusa monitoring sites in succession. The compositions of aerosols in these single air parcels at the upwind and downwind sites were compared in order to assess the extent of aerosol transformation in the presence of continuing emissions, atmospheric reactions and deposition. Both of the air parcels passed near Central Los Angeles in the afternoon and progressed to the Azusa area

where they stagnated overnight. Along these trajectories, the particle chemical composition and concentration changed very little between Central Los Angeles and Azusa. Less than 1.5% of the nitrogen in the air parcels stagnating in Azusa was in the form of HNO_3, however, and there was little particulate ammonium nitrate formation, which together indicate that nitric acid production was effectively balanced by dry deposition within the air parcels studied. With the onset of the morning traffic peak in Azusa, however, fine particle elemental and organic carbon concentrations within these air parcels increased by factors of 1.6–3.6 and 1.2–2.5 respectively, and NO and NO_2 concentrations increased by factors of 2.3–3.6 and 1.4–1.8, respectively.

Nitrate-Oriented Trajectory Study

In September and October of 1997, the Nitrate-Oriented Trajectory Study was conducted at three Southern California sites. These air monitoring stations were located in Diamond Bar, Mira Loma, and Riverside, sites which were upwind of, within, and downwind of the Chino dairy area, a large source of gas-phase ammonia. This was the first time that air monitoring stations have been placed to observe the effects of a major source of ammonia emissions at close range.

Ammonium nitrate was the largest component of fine particle ($PM_{1.9}$) mass at all three sites. Nitrogen species balances show that NO and NO_2 concentrations were generally very high in comparison to the other nitrogen species. Together they almost always contained at least half, and sometimes as much as 87%, of the total nitrogen present. Conversely, very little of the nitrogen, generally less than 5%, was present in the form of HNO_3. Nitric acid was produced by NO_2 oxidation, but because gas-phase ammonia was available in large concentrations nitric acid was quickly converted to particulate ammonium nitrate.

Air parcel trajectories were identified that passed successively over two air monitoring sites while sampling was taking place. The composition of aerosols within these air parcels at the upwind and downwind sites were compared in order to monitor aerosol transformation due to continuing emissions, atmospheric reactions and deposition. One of these air parcel trajectories passed the Diamond Bar air monitoring site in the morning, and stagnated near Mira Loma in the evening of the same day. Between Diamond Bar and Mira Loma, NO was oxidized to NO_2, and the ammonia concentration increased by a factor of 5. A second air parcel trajectory which stagnated near the Mira Loma site during the early morning hours and passed near the Riverside site approximately 24 hours later showed a decrease in ammonia concentration over time that is consistent with dilution as the air mass moves downwind from the virtual point source of ammonia in the dairy area. The particulate ammonium

nitrate concentration in that air parcel remained approximately constant over time, consistent with a continued excess of NH_3 relative to HNO_3 and a widespread mass of air containing inorganic nitrate upwind of the dairy area.

Caldecott Tunnel Study

In November 1997, the Caldecott Tunnel Study was conducted to measure direct aerosol emissions from the in-use vehicle fleet traveling through the Caldecott Tunnel that connects Berkeley, CA, and Orinda, CA. Approximately 37500 vehicles traveled through the tunnel during four experiments, each of 3-hours duration. Aerosol concentrations were measured in two tunnel bores and at a background site. Particle mass concentrations measured inside the tunnel were significantly elevated relative to background concentrations in all the samples. These measurements provide a complete set of size-segregated data on the chemical composition of fine particles emitted by in-use vehicles. Most of the fine particle ($PM_{1.9}$) mass was contained in particles with aerodynamic diameters smaller than 0.5 μm with the highest concentration of aerosol mass in the 0.1–0.18 μm particle size fraction.

The Caldecott Tunnel is divided into separate bores, one which carries light-duty vehicle traffic and one which carries a mixture of light- and heavy-duty vehicles. Aerosol emissions in each bore were computed per unit of fuel consumed in the tunnel based on the increased carbon concentration in the tunnel air. From experiments conducted in both bores, estimates are made of emissions rates and particle chemical composition extrapolated to 100% light-duty and 100% heavy-duty vehicle fleets. Heavy-duty and light-duty vehicles emitted 809 and 46 mg of $PM_{1.9}$ mass per liter of gasoline-equivalent fuel burned, respectively. This corresponds to fine particle ($PM_{1.9}$) emissions of approximately 430 and 5 mg km^{-1} driven by the heavy-duty and light-duty fleets, respectively. The bulk of the aerosol emissions consisted of elemental carbon and organic compounds. Gas phase ammonia emissions were also observed to be 267 and 194 mg per liter of fuel burned by vehicles passing through Bore 1 (mixed heavy- and light-duty vehicle traffic) and Bore 2 (light-duty vehicle traffic) of the tunnel, respectively.

Conclusions

During experiments in the western SoCAB during periods of moderate fine particulate ($PM_{1.9}$) concentrations (15–55 μg m^{-3}) and low photochemical activity, we measured the composition of ambient aerosol composed mainly of primary emissions. The largest contributors to fine particulate mass at Azusa were, in order of importance:

Organic Matter mainly emitted by vehicles and food cooking

Sulfate Ion mainly due to marine background sulfate, but also due to SO_x emitted by ships and diesel-powered vehicles

Elemental Carbon mainly emitted by diesel-powered vehicles

Ammonium Ion originally emitted as ammonia by a wide variety of sources including biological decay and vehicle catalysts

Nitrate Ion originally emitted as NO_x by vehicles and stationary source fuel combustors

During experiments in the eastern SoCAB during periods of high fine particulate ($PM_{1.9}$) concentrations (50–170 μg m^{-3}), we measured the composition of aerosols in air parcels which had spent several days over the most concentrated ammonia emission sources of the SoCAB. The largest contributors to fine particulate mass at Riverside during this experiment were, in order of importance:

Nitrate Ion originally emitted as NO_x by vehicles and stationary source fuel combustion

Ammonium Ion originally emitted as ammonia from dairy operations but also by vehicle catalysts and other agricultural operations

Organic Matter mainly emitted by vehicles and food cooking

Elemental Carbon mainly emitted by diesel-powered vehicles

Sulfate Ion mainly due to marine background sulfate but also due to SO_x emitted by ships and diesel-powered vehicles

Nitrate and ammonium ions are the largest contributors to the high 24-hour averaged fine particulate matter concentrations observed in this study, but are expected to be relatively smaller contributors to the annual-averaged concentrations. This suggests that different strategies may be required to control annual and 24-hour averaged fine particulate matter concentrations.

Aerosol emissions for the light-duty vehicle fleet measured in the Caldecott Tunnel were comparable to recent dynamometer-based laboratory measurements of particulate matter emitted from light duty catalyst-equipped automobiles. These results indicate that if there are gasoline-powered vehicles which have high emission rates, these vehicles are from the gasoline-powered truck fleet, a vehicle subpopulation whose emissions are not well characterized.

Ammonia is emitted in substantial quantities from the in-use motor vehicle fleet passing through the Caldecott Tunnel, consistent with the behavior of 3-way catalyst equipped cars that are running

with a rich air/fuel mixture. Ammonia concentration increases measured during the morning traffic peak in Central Los Angeles were at levels consistent with measurements of ammonia emissions from motor vehicles in the Caldecott tunnel.

These results will be useful in designing cost-effective attainment strategies to control $PM_{2.5}$ concentrations. For example, these results can be used as air quality model evaluation data sets, and can also be used for consistency checks on emissions inventories for the eastern and western SoCAB.

Acknowledgements

A study as large and ambitious as the one described here can only succeed with the help of many colleagues, collaborators, and administrators. We offer our heartfelt thanks to everyone who has helped with this study! We are especially grateful to those listed below who made notable contributions to this project.

Prof. Kimberly Prather and her research group at the University of California, Riverside — Rich Carlin, Keith Coffee, Tas Dienes, Markus Gälli, Eric Gard, Deborah Gross, Sergio Guazzotti, Don Liu, Chris Noble, Phil Silva, Dave Suess, Jeff Whiteaker, and Sylvia Pastor — collaborated in the design and execution of the study. They collected collocated data with their Aerosol Time-of-Flight Mass Spectrometry instruments, and generously assisted in setting up and running the sampling sites. Deborah Gross helped choose and manage the sampling sites. The close collaboration between our research groups has been very rewarding.

Susanne Hering of Aerosol Dynamics generously loaned us an optical particle counter and an electrical aerosol analyzer for use in this study.

Michael Ames at the MIT nuclear reactor laboratory conducted instrumental neutron activation analyses of the samples for trace metals.

Thanks are due to Rudy Eden and his staff at the South Coast Air Quality Management District for help in securing several of the air monitoring sites used in these experiments. Ozone, NO, and NO_2 concentrations also were measured by the South Coast Air Quality Management District. Thanks go to Kevin Durkee of the California Air Resources Board for help in obtaining the data. Meteorological data were provided by Leon Dosilager of the California Air Resources Board.

Bart Croes, Tony van Curen, and Nehzat Motallebi of the California Air Resources Board coordinated the study. They managed interaction among the research groups, and organized access to the Mira

Loma and Caldecott Tunnel sampling sites.

Ray Mailot, Louis Herce and others at the CalTrans Caldecott Tunnel made extraordinary efforts to provide electrical power and site access for the tunnel sampling experiments.

Prof. Robert Harley, Brett Singer, and Tom Kirchstetter of the University of California, Berkeley, shared their expertise in sampling at the Caldecott Tunnel.

Michael Kleeman of the California Institute of Technology measured mass loadings on some impactor samples. Russ Green, also at Caltech, manufactured crucial parts for the samplers on short notice.

This project was supported by the Coordinating Research Council, Inc., and the U.S. DOE Office of Heavy Vehicle Technologies through the National Renewable Energy Laboratory under CRC Project No. A-22. Brent Bailey and Tim Belian of CRC oversaw the project. The CRC's Atmospheric Impacts Committee, especially Kent Hoekman and Steve Japar, oversaw the technical content of the project.

Contents

List of Figures

List of Tables

Chapter 1

Introduction

1.1 Southern California Aerosol

Annually averaged airborne fine particle mass concentrations in Southern California have declined over the period 1982–1993 [1]. In certain cases, reduction in the concentration of major aerosol chemical species can be seen to result from specific emission control programs. Fine particle sulfate concentrations have declined as a strict sulfur oxides emission control program was implemented. Fine particle elemental (black) carbon particle concentrations have declined as newer diesel engines and improved diesel fuels were introduced. Fine organic carbon particle emissions from motor vehicles have also declined with the introduction of catalyst-equipped cars having lower particle mass emission rates.

Despite these improvements, aerosol concentrations in the South Coast Air Basin (SoCAB) continue to exceed air quality standards. Between 59% and 74% of the days on which aerosol mass concentrations were measured in the years 1990–1996 violated the California ambient air quality standard for particulate matter smaller than 10 μm in diameter (PM_{10}), which specifies that the 24-h average PM_{10} concentration is not to exceed 50 μg m^{-3} [2]. Between 1% and 8% of these days also exceeded the 24-h average national ambient air quality standard for PM_{10}, which is set at 150 μg m^{-3}. During the period 1994–1996, the SoCAB registered the highest 24-hour-average fine particle ($PM_{2.5}$) concentration (115 μg m^{-3}) observed in California. This level exceeds the proposed National Ambient Air Quality Standard for fine particles, set at a 24-h average of 65 μg m^{-3}, by nearly a factor of two.

The major contributors to aerosol mass in the SoCAB on days with high fine particle concentrations

are NH_4^+, NO_3^-, and organic carbon [1, 3]. Organic carbon particles and the gas-phase precursors of secondary particulate matter are emitted from multiple source types. Aerosol NH_4^+ originates from NH_3 gas that can be emitted from both vehicle exhaust [4] and agricultural operations [5]. Aerosol NO_3^- originates from atmospheric reactions that begin with NO gas emitted from vehicles and other combustion sources. Aerosol organic carbon is directly emitted from numerous source types including motor vehicles, woodsmoke, and food cooking. Gas-phase organic compounds also can react in the atmosphere to produce low vapor pressure products that condense to form secondary organic aerosol.

If aerosol concentrations in the SoCAB are to be reduced to meet air quality standards in a cost-effective manner, we must understand the contributions of various sources to aerosol and aerosol precursor concentrations, as well as the aerosol transport and transformation processes in the atmosphere. Our current understanding of aerosol sources and transformation processes is expressed in aerosol air quality models. The latest generation of such models can track aerosols on a single-particle level while maintaining an account of the emission source type from which the primary core of each particle was originally emitted [5, 6]. Detailed measurements of aerosol concentrations and composition during air parcel evolution in the atmosphere are required to develop and test these models. Through testing, confidence in the model predictions can be gained before they are used to evaluate the likely outcomes of proposed emission control policies.

1.2 SCOS97-NARSTO Aerosol Program

The 1997 Southern California Ozone Study-North American Research Strategy for Tropospheric Ozone (SCOS97-NARSTO) experiment was a large multi-investigator monitoring study conducted from June 16 through October 15, 1997 [7, 8, 9]. Study participants measured ozone, ozone precursors, and meteorological parameters aloft and at ground-based stations. The study was designed to provide aerometric and emission data to support detailed photochemical modeling and analysis for a better understanding of the processes involved in the formation of high ozone concentrations in the SoCAB and across Southern California.

Nested within the larger study that focused on ozone air quality, a second set of experiments was designed to explore particulate air quality in Southern California [2]. These studies, coordinated with each other and the main SCOS97-NARSTO ozone experiments, made up the SCOS97-NARSTO Aerosol Program and Radiation Study, referred to simply as *SCOS97* in this report. The goals of the SCOS97

study were to develop a three-dimensional picture of the generation and evolution of aerosols in the SoCAB, and to provide observations to support modeling of the emissions, transport, dispersion, deposition, and photochemical reactions that affect ozone, $PM_{2.5}$, and PM_{10} concentrations.

SCOS97 consisted of these seven interconnected studies:

1. Vehicle-Oriented Trajectory Study
2. Nitrate-Oriented Trajectory Study
3. Caldecott Tunnel Study
4. Fine Particle Measurement Study
5. $PM_{2.5}$ Federal Reference Method Nitrate Loss Study
6. Radiation Study
7. Aerosol Aircraft Study

Fourteen research groups (see Table 1.1) collected measurements between August and November, 1997. The purpose of the present report is to document data collected by the Caltech participants in the first three of these studies: the Vehicle- and Nitrate-Oriented Trajectory Studies as well as the Caldecott Tunnel Study. These data will provide the basis for subsequent work to develop, evaluate, and improve photochemical models that simulate the chemical and physical transformations that occur as particles age while they are transported in the atmosphere.

1.2.1 Vehicle-Oriented Trajectory Study

The Vehicle-Oriented Trajectory Study was conducted from August 16 through 31, 1997, at the Central Los Angeles, Azusa, and Riverside sampling sites (see Figure 1.1). Central Los Angeles was chosen because it is surrounded by the highest density of motor vehicle traffic in Southern California. Azusa was chosen because it is generally downwind of Central LA. These sites were selected in the hope that individual air parcels could be observed as they were transported from Central LA to Azusa in the presence of continuing emissions and atmospheric transformations. The Riverside site was chosen in order to collect samples colocated with Prof. Prather's laboratory-based aerosol time of flight mass spectrometry (ATOFMS) instrument in Riverside, which is not transportable.

Table 1.1: SCOS97-NARSTO Aerosol Program and Radiation Study Research Participants (Adapted from [2])

Organization	Investigators
Aerosol Dynamics, Inc. (ADI)	Susanne Hering
Brigham Young University (BYU)	Delbert Eatough, Norman Eatough
California Air Resources Board (CARB)	Curtis Schreiber, Thelma Yoosephiance
California Institute of Technology (Caltech)	Glen Cass, Jonathan Allen, Lara Hughes, Robert Johnson, Paul Mayo, Lynn Salmon
Center for Interdisciplinary Remotely Piloted Aircraft Studies (CIRPAS)	John Seinfeld, Richard Flagan, Haflichi Johnson, Mark Frolli, Paul Finn, Kenneth Liao, Lynn Russell
Colorado State University — National Renewable Energy Laboratory (CSU-NREL)	James Gibson, George Janson, William Durham
Desert Research Institute (DRI)	Barbara Zielinska, Larry Sheetz
Harvard University School of Public Health (Harvard)	Petros Koutrakis, George Allen, Mark Davey
South Coast Air Quality Management District (SCAQMD)	Rudy Eden, Steve Barbosa, Solomon Teffera, Mel Zeldin
University of California, Davis (UCD)	Debbie Niemeier, Britt Holmen, Judi Charles
University of California, Riverside, Department of Chemistry (UCR)	Kimberly Prather, Deborah Gross, Markus Gälli, Eric Gard, Sylvia Pastor, and the rest of the Prather Group
University of California, Riverside, College of Engineering-Center for Environmental Research and Technology (CE-CERT)	William Carter, Dennis Fitz, Michael McClanahan
University of California, Riverside, Statewide Air Pollution Research Center (SAPRC)	Ernesto Tuazon, Janet Arey, Roger Atkinson
University of Georgia	John Rives, Wanfeng Mou

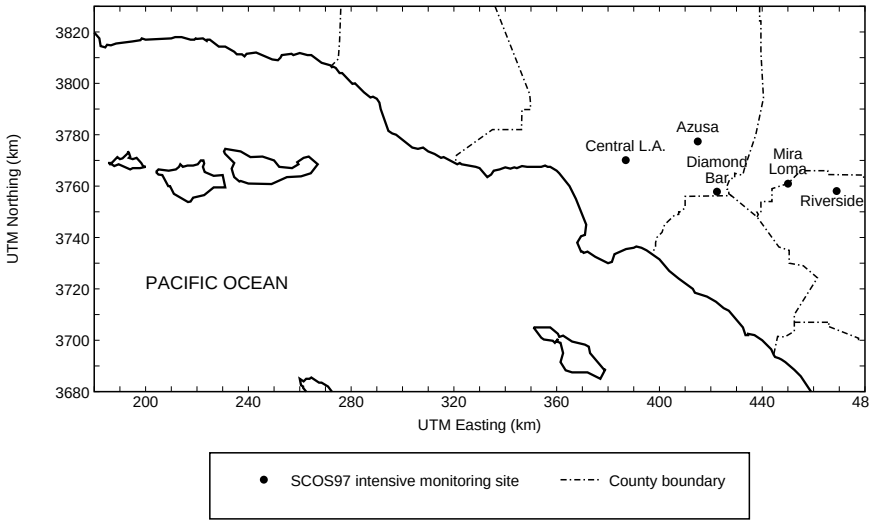

Figure 1.1: Map of sampling sites for the Vehicle-Oriented and Nitrate-Oriented Trajectory Studies.

The Caltech group deployed filter samplers for collection of particles with aerodynamic diameters, D_a, less than 1.9 μm ($PM_{1.9}$) and $D_a < 10$ μm (PM_{10}). This group also deployed denuder difference samplers for nitric acid, stacked filter samplers for NH_3, impactors, and continuous electronic particle size monitors at the sampling sites. These instruments were colocated with ATOFMS instruments operated by Prof. Prather's research group at all the sampling sites. In addition, Federal Reference Method samplers for fine particulate matter and a continuous aerosol nitrate instrument were operated by other investigators at the Riverside Agricultural Operations site which was approximately 2 miles away from the Caltech sampling site in Riverside, at Pierce Hall, on the campus of the University of California, Riverside [10]. These data have been reported separately by the research groups that made those measurements.

Two 2-day intensive operating periods (IOPs) were selected based on meteorological and air quality forecasts (see Table 1.2). During the IOPs, $PM_{1.9}$ and PM_{10} filter samples were collected on the same 5-sample per day schedule as that used during the 1987 Southern California Air Quality Study (SCAQS). These filter samples were analyzed for aerosol mass, ionic species, trace elements, organic carbon and

Table 1.2: SCOS97 Aerosol Study Intensive Operating Periods.

Description	Time	Locations
First Vehicle-Oriented Trajectory Study	21 Aug 97 01:20 PDT to 23 Aug 97 01:00 PDT	Central LA Azusa Riverside
Second Vehicle-Oriented Trajectory Study	27 Aug 97 01:20 PDT to 29 Aug 97 01:00 PDT	Central LA Azusa Riverside
Nitrate-Oriented Calibration Study	27 Sep 97 01:20 PDT to 30 Sep 97 01:00 PDT	Mira Loma
Nitrate-Oriented Trajectory Study	31 Oct 97 01:20 PST to 02 Nov 97 01:00 PST	Diamond Bar Mira Loma Riverside
Tunnel Study Day 1	17 Nov 97 12:00–15:00 PST	Caldecott Tunnel Bore 1 Outside Tunnel
Tunnel Study Day 2	18 Nov 97 12:00–15:00 PST	Caldecott Tunnel Bore 1 Outside Tunnel
Tunnel Study Day 3	19 Nov 97 15:30–18:30 PST	Caldecott Tunnel Bore 2 Outside Tunnel
Tunnel Study Day 4	20 Nov 97 15:30–18:30 PST	Caldecott Tunnel Bore 2 Outside Tunnel

elemental carbon. These data were used to create a material balance on the bulk chemical composition of the aerosol in sizes smaller than 10 and 1.9 μm diameter. Additional filter samplers were run at all three sites to collect enough fine particulate matter for quantification of the trace organic species by gas chromatography/mass spectrometry (GC/MS). These samples were composited over the entire episode at each site and will later be analyzed for individual organic compounds. One or two sets of impactor samples were collected for four hours each day at each site. Impactor samples were also analyzed for aerosol mass, ionic species, trace elements, organic carbon and elemental carbon. These data were used to create material balances on the bulk chemical composition of the aerosol in six size ranges from 0.056 to 1.8 μm particle aerodynamic diameter. These data were compared with data from analyses of simultaneously collected fine particle filter samples. Optical particle counters and electronic aerosol analyzers continuously collected data on aerosol size distributions.

1.2.2 Nitrate-Oriented Trajectory Study

During the Nitrate-Oriented Trajectory Study aerosols were sampled along trajectories crossing the Chino dairy area to examine the formation of ammonium nitrate aerosol. Aerosol nitrate is the most important contributor to peak-day fine particle concentration events in the SoCAB [1]. The NO_x involved in its formation is emitted in part from vehicle traffic and thus the study of aerosol nitrate formation and transport is relevant to vehicle exhaust effects on particle concentrations. This study was conducted from September 2 through November 2, 1997 at three sampling sites. The Diamond Bar station was located to the west of the Chino dairy area. High ammonia emissions originate near Chino from agricultural and livestock husbandry operations. The Mira Loma station was located within the dairy area, and the Riverside station was generally downwind of the Chino area (see Figure 1.1). Aerosol nitrate formation was studied as single air parcels were observed to pass over the Diamond Bar and Mira Loma sites consecutively, and over the Mira Loma and Riverside sites consecutively, while nitric acid and ammonia concentrations were changed by activities in the dairy area. This was the first study of aerosol nitrate formation in which samples were collected within the dairy area itself.

The Caltech group deployed filter samplers ($PM_{1.9}$ and PM_{10}), denuder difference samplers for nitric acid and aerosol nitrate, filter pack samplers for NH_3, impactors, and continuous electronic particle size monitors at the sampling sites. These instruments were colocated with ATOFMS instruments operated by Prof. Prather's research group at the Riverside and Mira Loma (September event only) sampling sites. In addition, Federal Reference Method samplers for fine particulate matter and a continuous aerosol nitrate instrument were operated by other investigators at the Mira Loma site [10]. These data have been reported separately by the research groups that made those measurements.

Three intensive operating periods (IOPs) were selected based on meteorological and air quality forecasts. The first IOP was conducted from September 4-6, 1997, the second and third IOPs are listed in Table 1.2. The study plan called for one Nitrate-Oriented Trajectory Study IOP to be analyzed; because of the high ambient fine particle concentrations present during the October 31-November 2 IOP, samples from this IOP were chosen for analysis.

During the Nitrate-Oriented Trajectory Study, $PM_{1.9}$ and PM_{10} filter samples were collected at three sampling sites on the same 5-sample per day schedule as that used during SCAQS. These filter samples were analyzed for aerosol mass, ionic species, trace elements, organic carbon and elemental carbon. These data were used to create a material balance on the bulk chemical composition of the aerosol in sizes smaller than about 10 and 1.9 μm diameter. Additional filter samplers were run at all three

sites to collect enough fine particulate matter for quantification of the trace organic species by gas chromatography/mass spectrometry (GC/MS). These samples were composited over the entire episode at each site and will be analyzed for individual organic compounds. One or two sets of impactor samples were collected for four hours each day at each site. Impactor samples were also analyzed for aerosol mass, ionic species, trace elements, organic carbon and elemental carbon. These data were used to create material balances on the bulk chemical composition of the aerosol in six size ranges from 0.056 to 1.8 μm diameter. These data were compared with data from analyses of simultaneously collected fine particle filter samples.

An additional IOP experiment was conducted in late September, 1997, at only the Mira Loma site. The primary goal of this study, the Nitrate-Oriented Calibration Study, was to provide calibration data for comparison with Susanne Hering's real-time aerosol nitrate analyzer and the ATOFMS instrument. $PM_{1.9}$ filter and impactor samples were collected and analyzed in the same manner as for the Nitrate-Oriented Trajectory Study. This study was done in addition to those called for in the original study plan.

1.2.3 Caldecott Tunnel Study

Analysis and modeling of the air quality data collected during the Vehicle-Oriented Trajectory Study depends on the acquisition of detailed emission source profiles for gasoline- and diesel-fueled motor vehicles. The Caldecott Tunnel east of Oakland, CA, is operated with the center bore open only to light-duty vehicles and the side bores open to both light- and heavy-duty vehicles. The particulate matter concentrations in the center bore are dominated by light-duty vehicles, while the aerosol burden in the side bores is primarily due to emissions from heavy-duty diesel-powered and gasoline-powered trucks. Between November 17 and 21, 1997, four experiments were conducted to characterize the aerosol emissions from vehicles within the tunnels. Two experiments were conducted in a side bore (Bore 1), and two experiments were conducted in the center bore (Bore 2). Samples were collected from Bore 1 from noon through 3:00 p.m., the period of highest heavy-duty vehicle traffic. Samples were collected from Bore 2 from 3:30 through 6:30 p.m., the period of highest light-duty vehicle traffic. During each experiment, samples of the background air outside the tunnel were characterized and pollutants contributed from the ambient background were subtracted from measurements made in the tunnel. Note that the study plan called for only one sampling experiment in each bore; the additional data collected allow the calculation of confidence intervals on the sampling results.

The Caltech group deployed filter samplers ($PM_{1.9}$ and PM_{10}), denuder difference samplers for nitric acid, stacked filter samplers for NH_3, and cascade impactors at the tunnel and background sampling sites. Prof. Prather's research group operated an ATOFMS instrument during the tunnel experiments. Other research groups made related measurements which will be reported separately: gas-phase compounds including CO, CO_2, CH_4, and non-methane hydrocarbons were measured so that the carbon balance in the tunnel could be calculated. An aerosol LIDAR was operated outside the tunnel, and vehicle counts were made to help in interpreting the emissions results.

Filter samples were analyzed for aerosol mass, ionic species, trace elements, organic carbon and elemental carbon. These data were used to create a material balance on the bulk chemical composition of the aerosol in sizes smaller than 10 and 1.9 μm aerodynamic diameter. Additional filter samplers were run at the tunnel sampling site to collect enough fine particulate matter for future quantification of the trace organic species by gas chromatography/mass spectrometry (GC/MS). These samples were composited for each tunnel bore and will be analyzed for individual organic compounds. Impactor samples were collected inside the tunnel and at the background sampling site. Impactor samples were also analyzed for aerosol mass, ionic species, trace elements, organic carbon and elemental carbon. These data were used to create material balances on the bulk chemical composition of the aerosol in six size ranges from 0.056 to 1.8 μm aerodynamic diameter. These data were compared with data from analyses of simultaneously collected fine particle filter samples.

Data from the Tunnel Study were reduced to produce separate detailed source emissions profiles that describe light- and heavy-duty vehicle exhaust aerosols. These motor vehicle emission profiles were then compared to the ambient outdoor aerosol composition seen during the Vehicle-Oriented Trajectory Study.

1.3 Air Quality during the SCOS97 Measurement Period

In order to place the SCOS97 particulate matter intensive study periods into a broader context, it is useful to visualize how air quality during those short periods of observation related to overall air quality during the late summer and early fall of 1997 at Riverside. Figure 1.2 shows the time series of daily

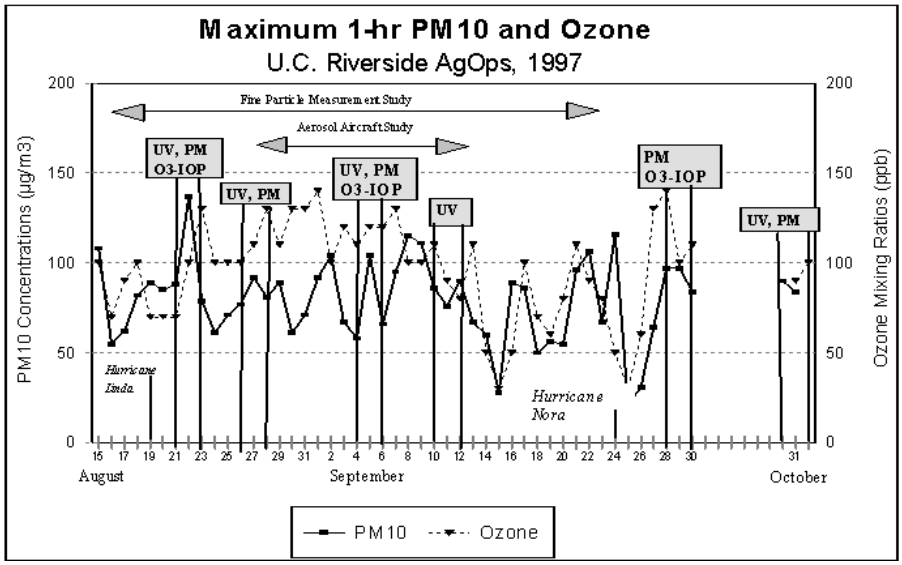

Figure 1.2: Maximum PM_{10} and ozone concentrations measured during SCOS97 at Riverside, CA. Adapted from [2].

maximum 1-h average ozone and PM_{10} concentrations[1] during the SCOS97 study period. Superimposed on those time series data are narrow time slices that show the ozone (O3-IOP), particulate matter (PM) and ultra-violet radiation (UV) intensive operating periods. Many of the lowest pollutant concentrations occurred during periods in mid-August and mid-September as hurricanes off the coast of Mexico brought large amounts of moisture and disturbed atmospheric conditions to the SoCAB. Air sampling was avoided during those periods. The first Vehicle-Oriented Trajectory experiment occurred during a period of higher than usual particle concentrations in the Riverside area. The remaining SCOS97 aerosol experiments occurred on days with closer to average PM_{10} concentrations for this year and season. Ozone concentrations and photochemical activity were unusually low by comparison to past years in the SoCAB throughout the entire study period. An increased frequency of positive vorticity advection and mid-atmospheric troughing just west of the Pacific Coast (associated with El Niño activity) is thought to have contributed to a deeper marine layer and better mixing than usual over the SoCAB during the summer and early fall of 1997.

[1] PM_{10} data shown in Figure 1.2 were measured by the SCAQMD with a tapered element oscillating microbalance (TEOM) that is heated to between 30 and 50°C; actual PM_{10} concentrations may be much higher than shown because heating can evaporate semi-volatile aerosol material such as ammonium nitrate and some organic compounds.

Chapter 2

Vehicle-Oriented Trajectory Study

2.1 Introduction

Motor vehicle exhaust emissions and their physical and chemical behavior in the atmosphere need to be clearly understood in order to judge the effectiveness of potential vehicle-related air quality control programs. Among the more complex issues that must be addressed is the effect of motor vehicle exhaust on airborne fine particle concentrations. Motor vehicles contribute both primary particles that are emitted in the particle phase directly from automobile and truck tailpipes, as well as reactive gases such as NO, SO_2, ammonia, and hydrocarbon vapors that can react chemically in the atmosphere to form secondary aerosol mass.

In late August of 1997, a field experiment was conducted in conjunction with the 1997 Southern California Ozone Study [7, 8, 9] in which a network of three airborne particle observatories was established, employing advanced instrumentation for determination of the size and chemical composition distribution of atmospheric particles. At each air monitoring site, measurements were made of the particle size distribution, bulk fine particle ($PM_{1.9}$) and PM_{10} chemical composition, chemical composition segregated into narrow particle size intervals, and single-particle chemical composition. Two of these air monitoring station locations were chosen along a seasonally typical wind trajectory passing over downtown Los Angeles and extending downwind to Azusa, CA, with the intent of first observing air parcels in an area dominated by high motor vehicle traffic density, and subsequently observing the same air parcels after they had been transported downwind. This sampling scheme was designed to provide data on the evolution over time of the size and chemical composition of ambient aerosols at the bulk,

size-segregated, and single-particle levels as those particles are potentially altered by gas-to-particle conversion processes and affected by continuing emissions, dilution, and dry deposition.

Several studies of particle evolution using multiple observation points along a single air parcel trajectory have been conducted previously in the Los Angeles area. In a 1982 field study, gas- and particle-phase nitrogen species were sampled from a single air parcel which passed over or near three monitoring sites in succession: Long Beach, Anaheim, and Rubidoux, CA, providing insight into the process of aerosol nitrate formation and the interrelationship between gas phase HNO_3 and NH_3 versus particulate NH_4NO_3 [11]. Measurements made at that time showed that the aerosol nitrate behaved as would be expected from analyses based on thermodynamic equilibrium between the gas and particle phases [12], and verified the presence of a large ammonia source located in the agricultural and dairy area between Anaheim and Rubidoux leading to large aerosol nitrate concentrations in the Riverside (Rubidoux) area. In 1996, a similarly designed field study was conducted using more advanced instrumentation. A battery of aerosol sampling instruments similar to those employed in the present study, including samplers for fine and total suspended particulate matter chemical composition, size-segregated particulate matter chemical composition, and single-particle size and composition measurements, were used to obtain information about the evolution of the particle population in the presence of significant aerosol nitrate formation and continuing emissions [3, 13]. Two air parcel trajectories were identified which passed over or near three or four air monitoring stations along the Santa Catalina Island—Long Beach—Fullerton—Riverside pollutant transport corridor [13]. It was shown that the relatively fresh aerosol at Long Beach consisted largely of sea salt particles, primary carbon particles and background sulfate particles. Over a one and a half day transport period from Long Beach to Riverside, sea salt particles were transformed to sodium nitrate while the population of carbon-containing particles which consisted mostly of organic and elemental carbon at Long Beach was transformed into a population of very complex particles containing aerosol carbon as well as ammonium and nitrate ion at the single-particle level. The purpose of the present study is to apply the method of trajectory-oriented field experiments to the problem of observing air parcels that are heavily influenced by primary particle emissions from motor vehicles.

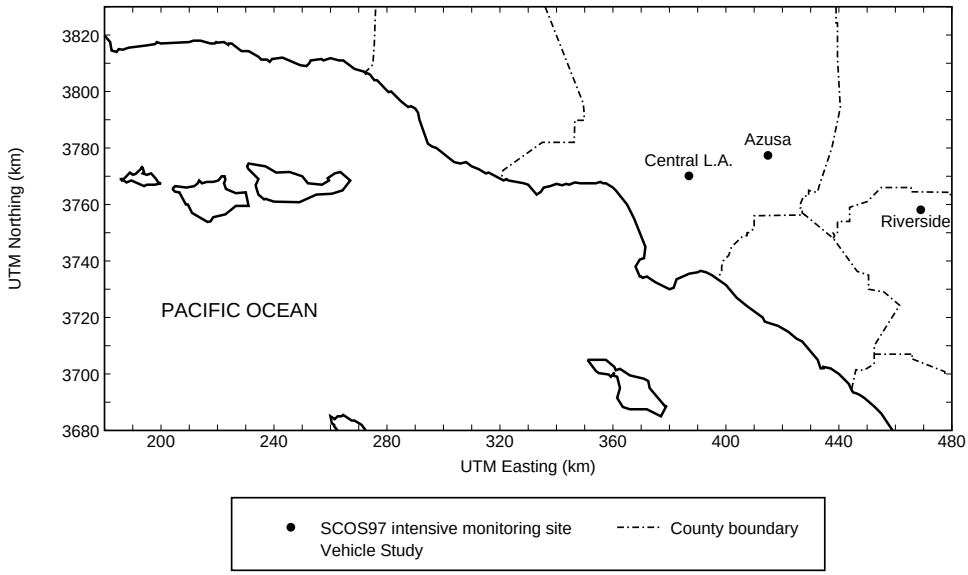

Figure 2.1: South Coast Air Basin and Vehicle-Oriented Trajectory Study sampling site locations.

2.2 Experimental Methods

2.2.1 Sample Collection

Three urban air monitoring stations were established in the Los Angeles metropolitan area to observe ambient particulate matter concentrations in the presence of atmospheric transport and transformation. These sites were located in Central Los Angeles, Azusa, and Riverside (see Figure 2.1). Two of the sampling sites were chosen to focus on the transport of motor vehicle-derived aerosol: Central Los Angles because of its proximity to the highest traffic densities in the South Coast Air Basin (SoCAB), and Azusa because it is often located directly downwind of Central Los Angeles. The Riverside site was chosen primarily because one of the three existing aerosol time-of-flight mass spectrometer (ATOFMS) instruments used to measure single particle size and chemical composition is permanently located there.

Sampling was conducted over two 48-hour periods on August 21-23, 1997, and August 27-29, 1997. Fine particle ($PM_{1.9}$) and PM_{10} samples for mass and chemical composition determination were collected sequentially on a 5-sample per day schedule, and a pair of micro-orifice impactors (MOIs) was operated at each site for one or two of these time periods each day. Times of operation for the filter samplers and impactors are shown in Figure 2.2 for both 48-h events.

An electrical aerosol analyzer (EAA, TSI Inc., model 3030) was used at each site to continuously

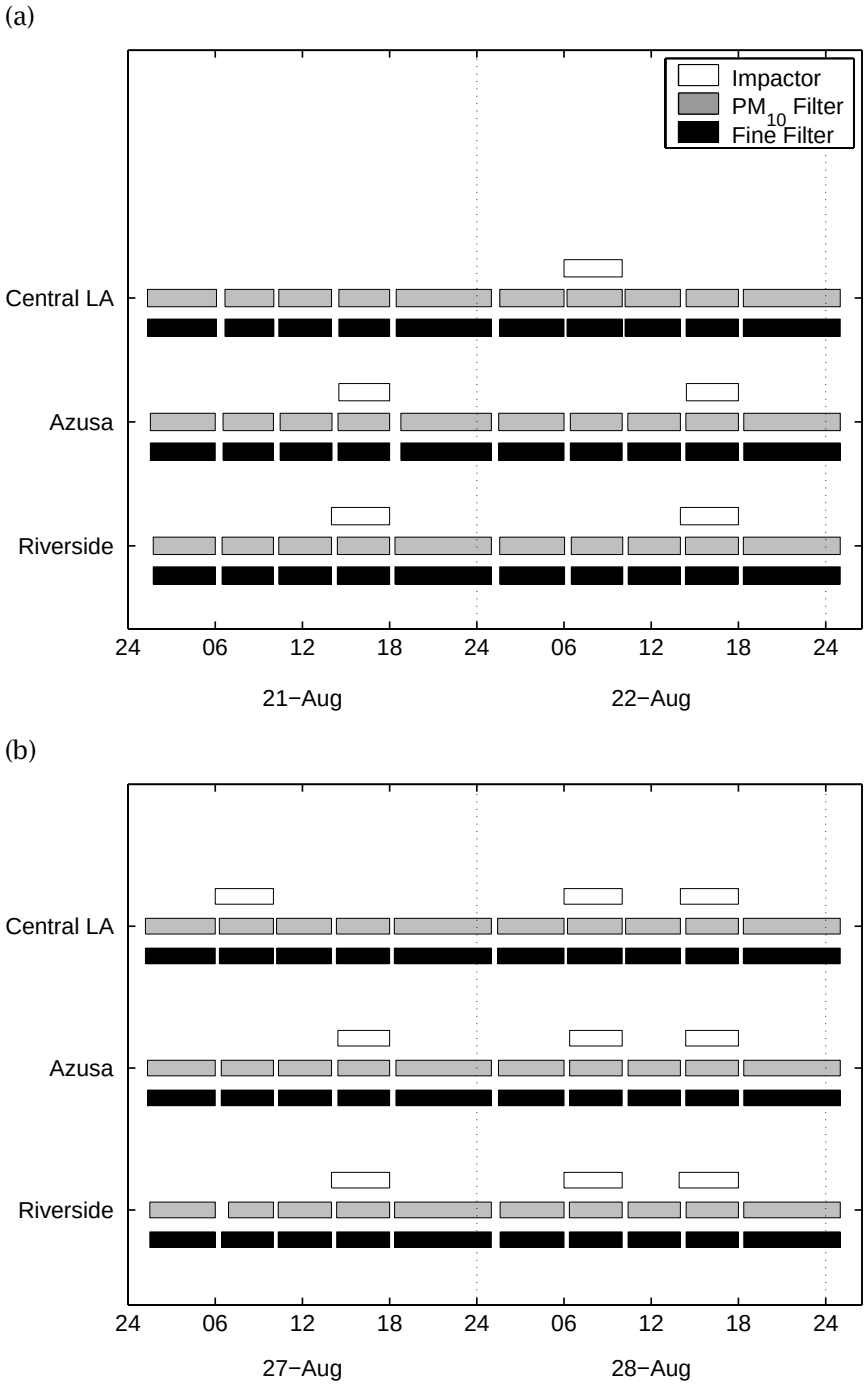

Figure 2.2: Times of operation (in PDT) of impactors and filter samplers at each site during the 48-h periods of (a) August 21-23, 1997, and (b) August 27-29, 1997.

measure particle number concentrations in the particle physical diameter, D_p, range $0.03 < D_p < 0.23$ μm. The particle number distribution over the EAA's size range was acquired once every 4-7 minutes.

Laser optical particle counters (OPC; Particle Measuring Systems, model ASASP-X at the Central Los Angeles and Azusa sites; Particle Measuring Systems, model LAS-X, at Riverside) were used to extend size distribution measurements to larger particle sizes. The OPCs at the Central Los Angeles and Azusa sites recorded particle number distributions over the size range $0.23 < D_p < 2.55$ μm in 22 channels every 5 seconds. The OPC at the Riverside site recorded particle number distributions over the size range $0.23 < D_p < 3.5$ μm in 12 channels every 21 seconds. Size distributions from the OPCs were corrected as suggested by Hering [14] to take into account the difference in the refractive index between the polystyrene latex (PSL) spheres used to calibrate the instruments and typical Los Angeles area atmospheric aerosols.

Three aerosol time-of-flight mass spectrometry (ATOFMS) instruments were used; the Central LA and Azusa sites each had a transportable ATOFMS instrument [15], and a laboratory-bound ATOFMS instrument [16] was operated in Riverside. The ATOFMS instruments operated continuously, collecting number distribution data in the particle aerodynamic diameter, D_a, range $0.2 < D_a < 5$ μm, and obtaining mass spectra for a subset of the sampled particles. The ATOFMS data were taken by Professor Kimberly Prather's research group at the University of California, Riverside (UCR), and will be reported separately by them.

Four filter-based sampling systems were operated at each air monitoring station: one to collect PM_{10} samples ($D_a < 10$ μm) and three to collect fine particle ($PM_{1.9}$, $D_a < 1.9$ μm) samples. The PM_{10} sampler and two of the three fine particle samplers were used to collect consecutive short time average samples for bulk ionic and carbonaceous species and elemental analysis. Five complete sets of filter samples were collected each day according to the following time schedule: 0120-0600, 0620-1000, 1020-1400, 1420-1800, 1820-0100 hours PDT (see Figure 2.2). All times during this study are given in Pacific Daylight Time (PDT). This filter sampling schedule provides relatively fine temporal resolution data for comparison with the continuous ATOFMS data and future air quality modeling results. One fine particle sampler at each site operated over 24-h sampling intervals in order to collect enough material for later analysis for individual particulate organic compounds by GC/MS.

The PM_{10} samplers assembled for this study were similar to those deployed by Solomon et al. to collect the PM_{10} database that was used for regulatory purposes in Los Angeles from 1987 to 1995 [17]. The PM_{10} sampler drew air through an EPA-approved low volume PM_{10} inlet [17] and distributed

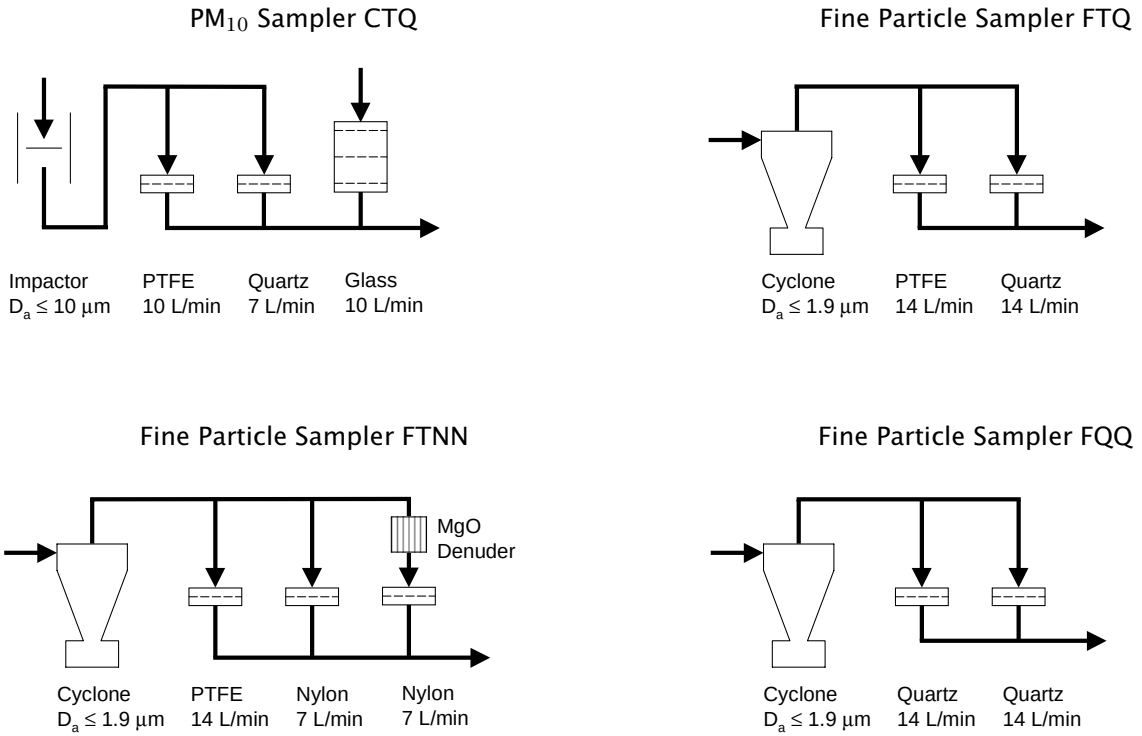

Figure 2.3: Schematic diagram of the particulate matter sampling systems used in this study

the air between two filter holders (see Figure 2.3), one containing a polytetrafluoroethylene (PTFE) filter (Gelman Sciences, Teflo, 47mm, 1.0 μm pore size) and one containing a quartz fiber filter (Pallflex, 2500 QAO, 47mm). The air flow through each filter was controlled by a critical orifice downstream of the filter. The PTFE filter collected aerosol particles for gravimetric and inorganic species analyses, while the quartz fiber filter collected particles for aerosol carbon and organic species analyses. This sampler also housed an open face filter stack in which gas-phase ammonia was collected on two oxalic acid impregnated glass fiber filters located downstream of a PTFE pre-filter used to remove airborne particles.

In fine particle sampling systems FTQ and FTNN shown in Figure 2.3, ambient air was drawn under a stainless steel rain cap and then through an acid-washed Pyrex glass inlet line at a nominal air flow rate of 28 lpm. The air was then passed through a Teflon-coated AIHL-design cyclone separator [18] which, when operated at flow rate of 28 lpm, removed coarse particles with aerodynamic diameters larger than 1.9 μm (see Figure 2.3). Following the cyclone, the airstream containing only fine particles and gases entered a Teflon-coated sampling manifold where it was split and ducted via Teflon tubing to several low-volume filter holder assemblies arranged in parallel. Fine particles were collected in

parallel on two PTFE filters, one quartz fiber filter, one nylon filter, and another nylon filter located downstream of a MgO denuder. Samplers FTQ and FTNN were operated on the 5-sampling period per day schedule described above (see Figure 2.2). Gravimetric mass, ionic species, and trace metals were determined from the PTFE filter samples. Organic and elemental carbon were determined from the quartz fiber filters. Aerosol nitrate and HNO_3 were determined by the denuder difference method from the nylon filter samples. Fine particle sampler FQQ shown in Figure 2.3 collected larger samples for organic aerosol determination over 24-hr sampling intervals.

A pair of 10-stage micro-orifice impactors (MOI, MSP Corp., model 110) [19] was operated at each air monitoring site. The impactors collocated at a site were operated simultaneously to measure fine particulate mass and chemical composition as a function of particle size. A cyclone separator [18] was placed upstream of each impactor in order to capture coarse particles ($D_a > 1.8$ μm) that might otherwise enter the impactor and distort the mass distribution measurements by bouncing from their appropriate collection stages. Particles reported here were collected on stages 5-10 of the impactors over the size range $0.056 < D_a < 1.8$ μm. One member of each pair of impactors was loaded with aluminum foil impaction substrates (MSP Corp.), while the other was loaded with PTFE impaction substrates (Gelman Sciences, Teflo, 47mm). No grease or oil was used on the substrates to avoid adding a source of organic contamination.

After sample collection, the PTFE, nylon, and oxalic acid-impregnated filters, and impactor substrates were stored in petri dishes which were then sealed with Teflon tape; quartz fiber filters were stored in petri dishes lined with prebaked aluminum foil and sealed with Teflon tape. All samples were refrigerated until returned from the field, a period not longer than 48 hours, and then frozen at -20°C until sample analysis.

2.2.2 Sample Analysis

Mass measurements were made gravimetrically before and after sampling on all PTFE filters and all PTFE and aluminum foil impaction substrates, providing the basis for atmospheric fine particle ($PM_{1.9}$), PM_{10}, and size-distributed mass concentration determinations. Each filter or substrate was weighed at least twice before and twice after sample collection on a Mettler Model M-55-A mechanical microbalance maintained in a temperature- and humidity-controlled environment (22.9±0.3°C and 48±3% RH). Unexposed PTFE filters and substrates were equilibrated in the same controlled conditions for at least 24 hours prior to weighing. PTFE filters and substrates with collected aerosol samples were equilibrated in

the controlled environment for about 4 hours prior to weighing; a shorter equilibration time was used for collected samples to reduce the time that a sample spent at above-freezing temperatures, and so reduce the opportunity for species volatilization. A set of control filters was weighed during each daily weighing session to verify the consistency of the balance calibration between pre- and post-sample collection weighings.

Elemental carbon (EC) and organic carbon (OC) concentrations were determined by thermal-optical analysis [20, 21] of samples collected on quartz fiber filters and aluminum foil impaction substrates. Organic matter concentrations were estimated from measured organic carbon concentrations by multiplying by a factor of 1.4 to account for the additional mass of associated H, O, N, and S present in typical atmospheric organic aerosols [22]. Prior to sample collection, all quartz fiber filters were baked at 550°C in air for 8 hours to lower their carbon blank levels. Aluminum foil substrates were similarly baked at 550°C in air for 48 hours prior to initial weighing and sample collection.

Impactor and PM_{10} samples collected on PTFE substrates or filters were cut in half prior to analysis to allow the use of several chemical analysis methods. Cutting was unnecessary for the fine particle samples due to the existence of redundant samples collected on pairs of PTFE filters. Half of each set of PTFE filters and impaction substrates were extracted, and the extract analyzed using a Dionex Model 2020i ion chromatograph for determination of the atmospheric concentrations of the major ionic species: NO_3^-, $SO_4^=$, and Cl^- [23]. These extracts were analyzed for ammonium ion (NH_4^+) by an indophenol colorimetric procedure [24] using an Alpkem rapid flow analyzer (Model RFA-300). Gas phase ammonia collected on oxalic acid-impregnated glass fiber filters was measured as ammonium ion using the same procedure. Aerosol nitrate and nitric acid samples collected on nylon filters were analyzed using the ion chromatographic process prescribed by Solomon et al. [25].

The remaining half of each set of PTFE samples underwent instrumental neutron activation analysis, from which the bulk concentrations of 39 major and minor trace elements were determined [26]. The elements measured were Al, As, Au, Ba, Br, Ce, Cs, Cd, Cl, Co, Cr, Eu, Fe, Ga, Hg, In, K, La, Lu, Mg, Mo, Mn, Na, Nd, Rb, Sb, Sc, Se, Sm, Sr, Ta, Tb, Th, Ti, U, V, Yb, Zn, and Zr. The elements Ta, Tb, and Zr were not found in any of the atmospheric aerosol samples.

2.2.3 Meteorology

Wind fields over the South Coast Air Basin for each hour of the episodes studied were reconstructed with a 5 km $\times$ 5 km grid resolution using the method of Goodin et al. [27] based on hourly averaged wind

speed and direction measurements at 29 meteorological stations maintained by the South Coast Air Quality Management District (SCAQMD). From the wind fields, back trajectories from the sampling sites were calculated, establishing the time and location history of the air parcels arriving at the sampling sites.

Wind patterns were relatively consistent across the two 48-h episodes studied. Air parcels arriving at Central Los Angeles generally approached from the southwest, having crossed the coastline near Hawthorne. Air parcels reaching Azusa generally approached from the southwest as well, setting up the possibility that the same air parcel would pass over both Central Los Angeles and Azusa as planned. Air stagnation at Central Los Angeles occurred daily beginning between 1800 and 2200 PDT in the evening and ending between 1100 and 1200 PDT the following morning. Temperatures at Central Los Angeles ranged between 18.3 and 32.2°C, with relative humidities measured between 31 and 60%. By mid-day at Los Angeles, the sky was generally hazy, though most evenings were clear. On August 22 there was significant cloud cover, but all other sampling days had few clouds. Fog was seen around the Central Los Angeles site in the early morning of August 21. Air stagnation occurred at Azusa beginning between 2000 and 2100 PDT in the evening and ending between 1000 and 1200 PDT the following morning. Temperatures at Azusa were between 18.3 and 35.6°C, and relative humidities were 24 to 86%. Mornings were generally clear, with haziness during some afternoons. Air parcels arriving at Riverside were advected from the ocean along routes passing near Long Beach and Fullerton, CA, south of both Central Los Angeles and Azusa. This is a similar path to those taken by air parcels arriving at Riverside during September, 1996 [3]. Air stagnation occurred at Riverside beginning between 2000 and 2100 PDT and ending between 1200 and 1400 PDT the following morning. Temperatures at Riverside were between 17.8 and 35.7°C, and relative humidities were measured between 20 and 91%.

2.3 Results and Discussion

2.3.1 August 21-23, 1997, Sampling Event

Figure 2.4 shows the time series of fine particle ($PM_{1.9}$) mass and major aerosol chemical species concentrations at Central Los Angeles over the August 21-23 time period. The fine particle mass concentration shows a strong diurnal cycle, generally peaking during the morning 0600-1000 PDT peak traffic period. The fine particle mass concentration remains at a high level during the late morning and early afternoon of the second day. Elemental and organic carbon particle concentrations generally follow this

strong diurnal cycle, with elemental carbon concentrations highest during the 0600-1000 PDT traffic peak and organic compounds highest during the late morning/early afternoon period from 1000-1400 PDT.

Gas phase ammonia at Central LA shows a nearly constant baseline concentration of about 8 to 9.5 μg m^{-3} (11.4-13.6 ppb) with a near doubling of ammonia concentrations during those hours when the elemental carbon concentrations are highest, possibly reflecting a traffic-derived source of NH_3 emissions as reported earlier by Fraser and Cass [4] based on experiments in the Van Nuys Tunnel. On the basis of ΔNH_3, ΔNH_4^+, and ΔEC defined as the increases in NH_3 nitrogen, fine particulate NH_4^+ nitrogen, and fine particulate EC concentrations from a previous sampling period to the time period of interest, the $(\Delta NH_3 + \Delta NH_4^+)/\Delta EC$ ratios for periods 0600-1000 PDT on August 21 and August 22 were 1.51±0.68 and 1.39±1.22, respectively. These ratios are approximately the same as the background-subtracted $(NH_3 + NH_4^+)$ nitrogen to black carbon mass ratio measured in the mixed light- and heavy-duty vehicle bore of the Caldecott Tunnel on November 17, 1997, (see Chapter 4), which was 1.38±0.10. For purposes of comparison, the $(NH_3 + NH_4^+)$ nitrogen to black carbon mass ratio seen in the Van Nuys Tunnel experiments was 2.80 [4, 28], which is within ±2 standard errors of the incremental increases in the $(NH_3 + NH_4^+)$ nitrogen to EC ratio just discussed during the time periods that contain the morning traffic peak in Figure 2.4. Nitric acid concentrations show a strong diurnal profile, with the peak concentrations during daylight hours of about 5 to 11 μg m^{-3} (2.1-4.2 ppb) and nearly zero concentrations at night. Fine particle nitrate levels at Central LA are generally low throughout this experiment; the highest aerosol nitrate levels occurred overnight and during the 0600-1000 PDT period on August 21, a period with overnight fog turning to haze later in the morning. Aerosol sulfate concentrations are only marginally higher, and at times lower, than marine fine particle sulfate background levels recently reported for Santa Catalina Island (4.51 μg m^{-3}).

Fine aerosol behavior at Azusa over the August 21-22 episode, shown in Figure 2.5, is qualitatively similar to that at Central Los Angeles, except that the organic aerosol diurnal peak is broader and extends later into the day than at Central LA, possibly reflecting both early morning local traffic plus transport of organic aerosol to Azusa from upwind later in the same day. Fine particle sulfate concentrations are generally lower than at Central LA, indicating that the effects of dilution and surface removal are exceeding new sulfate formation between Central LA and Azusa. Nitric acid vapor concentrations at Azusa still show the strong diurnal cycle expected for a photochemcially generated pollutant. Gaseous ammonia concentrations at Azusa do not show a diurnal variation that peaks during the early morning traffic peak, suggesting less influence from NH_3 emissions from autos with 3-way

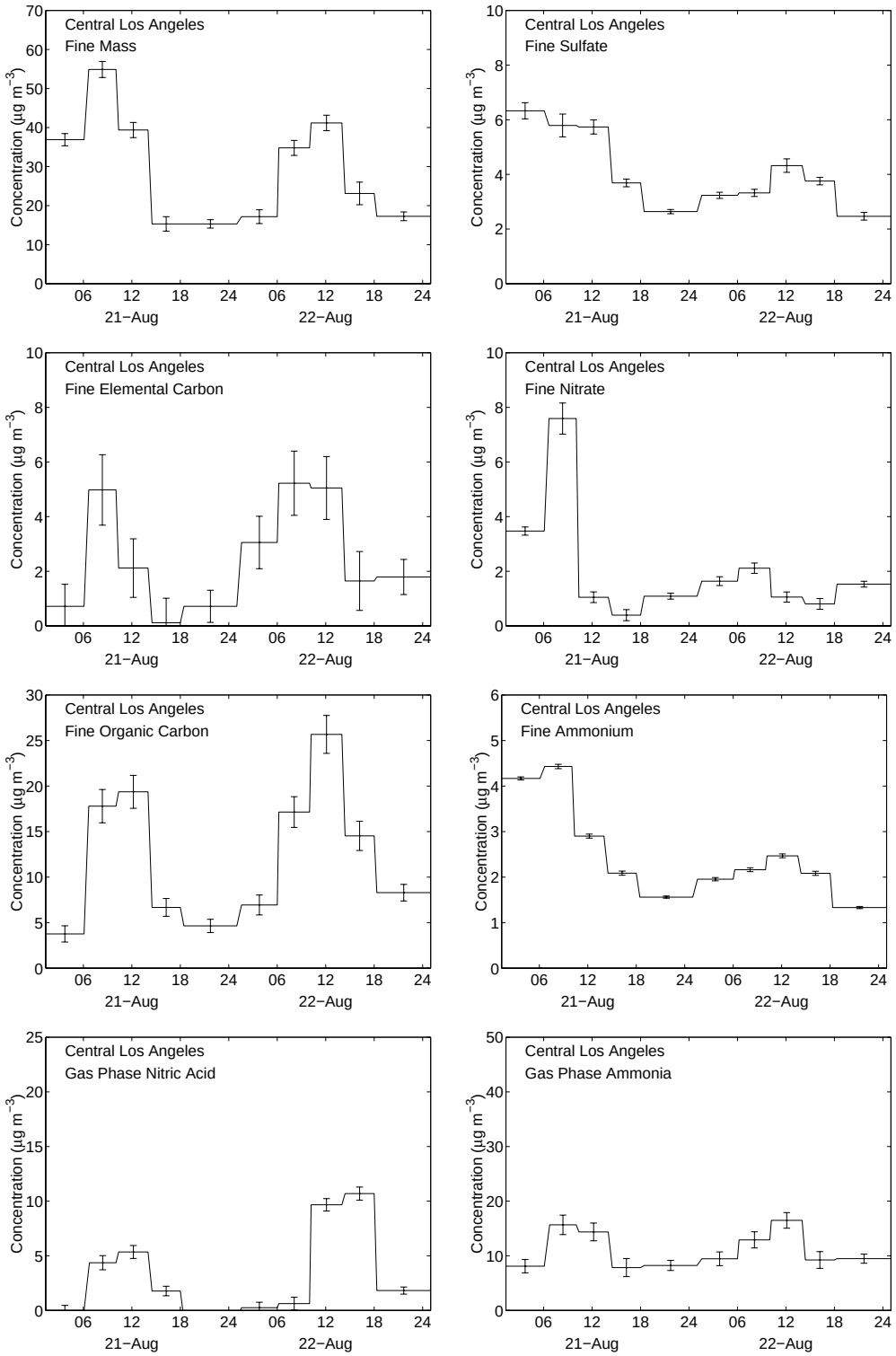

Figure 2.4: Fine particle ($PM_{1.9}$) and gas-phase concentrations for individual species measured during the August 21-23, 1997, sampling event at Central Los Angeles.

catalytic converters. Elemental carbon shows strong early morning concentration peaks, suggesting that considerable diesel truck traffic occurs near the Azusa monitoring site.

Figure 2.6 shows the time series of fine particle mass and major aerosol chemical species concentrations at Riverside over the August 21-23 time period. Fine aerosol mass concentrations at Riverside show a diurnal variation that differs from that seen at Central LA and Azusa, which is not surprising since Riverside does not lie on the same air parcel trajectory pathway as Central LA and Azusa. Relative peaks that correspond in time to peaks in individual aerosol chemical species can be seen clearly in the overall Riverside fine particle mass concentration time series. The fine elemental carbon particle concentrations increase sharply during the morning traffic peak. The organic aerosol concentration peaks are detached from the timing of the EC peak, with OC concentrations increasing later in the day as aerosol is transported to this inland location from the city upwind. Ammonia concentrations at Riverside are quite high, as expected given Riverside's location downwind of the agricultural ammonia sources in the Chino dairy area [29, 30, 31]. Nitric acid concentrations however are generally lower than at Central LA and Azusa, and on these days there is little aerosol nitrate, suggesting that HNO_3 formation from NO_2 was not running much faster than dry deposition of HNO_3 during the August 21-23 period.

2.3.2 August 27-29, 1997, Sampling Event

During the August 27-29 experiments, fine aerosol mass concentrations at Central Los Angeles and Azusa ranged between 12.8 and 30.1 μg m^{-3} with a diurnal variation having comparable minimum values but smaller peak values than were seen during the August 21-23 episode. Elemental and organic carbon concentrations at Central LA were similar between the two experiments, while sulfate aerosol levels at that site were generally lower than in the earlier episode. Nitric acid showed peak concentrations of about 10 μg m^{-3} (3.9 ppb) during the middle of the day at Central LA and 20.5-22.5 μg m^{-3} (8.2-8.9 ppb) at Azusa with the usual daytime concentration peak and near-zero values at night. Aerosol nitrate concentrations were low, generally between 1-2.5 μg m^{-3} at both Central LA and Azusa.

Fine particle concentration and composition trends at Riverside likewise were fairly similar between the August 21-23 and August 27-29 episodes, and thus will not be described further. Plots showing the time series of pollutant concentrations during the August 27-29 episode at all 3 monitoring sites are given in Appendix C to this report in a format similar to Figures 2.4- 2.6.

Figure 2.7 shows a material balance on fine particle chemical composition at Central Los Angeles

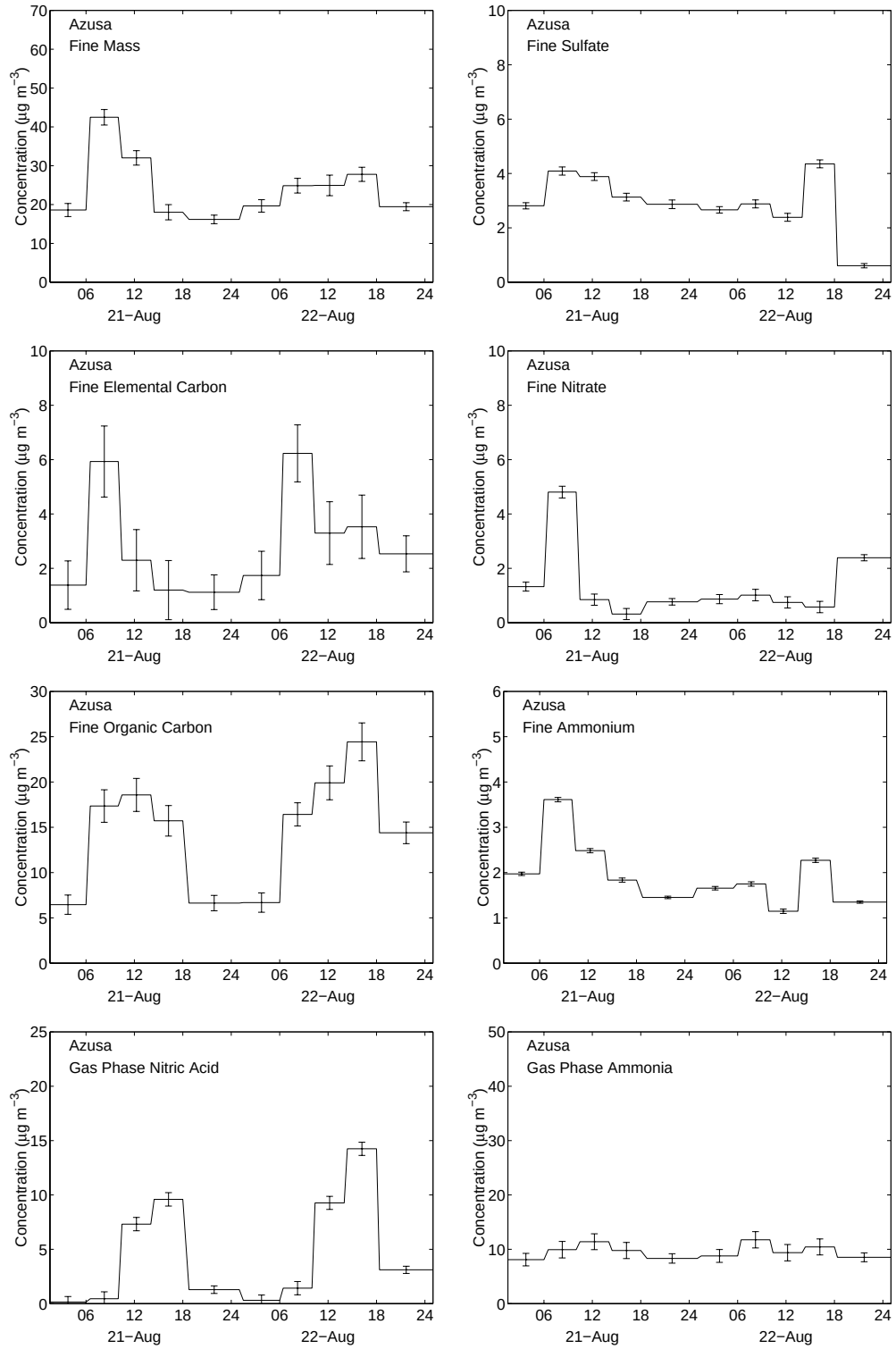

Figure 2.5: Fine particle ($PM_{1.9}$) and gas-phase concentrations for individual species measured during the August 21-23, 1997, sampling event at Azusa.

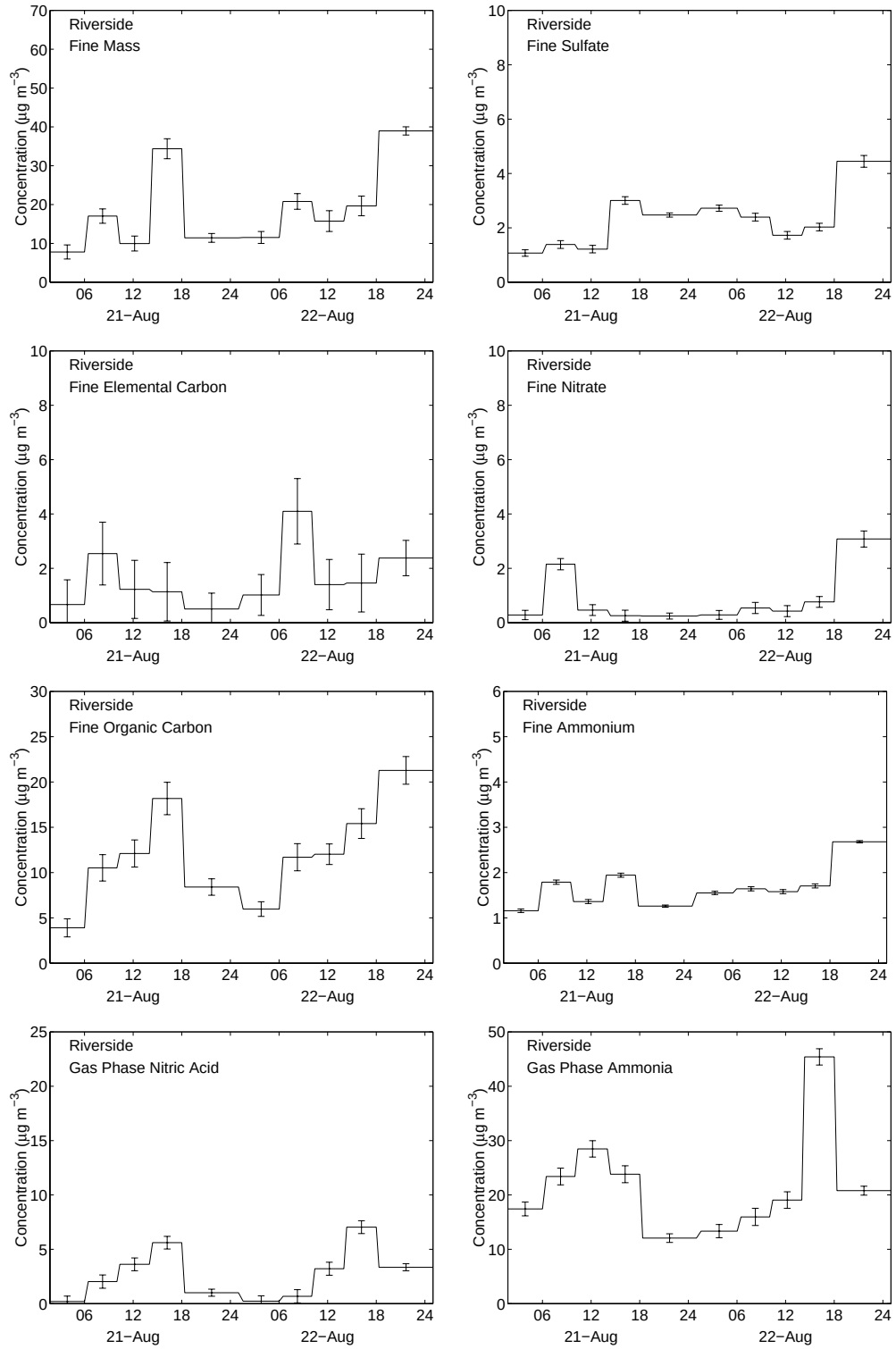

Figure 2.6: Fine particle ($PM_{1.9}$) and gas-phase concentrations for individual species measured during the August 21-23, 1997, sampling event at Riverside.

during the August 27-29 episode from the filter-based data during all sampling periods, as well as the size-segregated mass distribution and chemical composition of the fine particulate matter (D_a < 1.8 μm) collected by the micro-orifice impactors during two sampling time periods: 0600-1000 PDT and 1400-1800 PDT on August 28, 1997. In these plots, as well as in mass balance presentations in Figures 2.8, 2.9, and 2.10, the designation "Unidentified" applies to the difference between mass concentration determined gravimetrically and the sum of species concentrations identified by chemical analysis methods. Silicon- and calcium-containing mineral matter are among the materials not detected by the methods used in the present study, and these make up some portion of the unidentified matter. In addition, because samples were equilibrated and weighed in an environment with controlled low relative humidity, water may have been retained by some ionic species. "Metals and Metal Oxides" refers to the sum of trace elements measured by neutron activation analysis, with elemental concentrations converted to equivalent concentrations of their most common oxides, where appropriate.

The decreases in fine EC, OC, and aerosol nitrate apparent between the 0600-1000 PDT versus 1400-1800 PDT in Figure 2.7a also can be seen by a comparison of the two sets of impactor data. The EC concentration reduction between the morning traffic rush hour period versus the later period is accompanied by a size shift from an EC concentration peak in the 0.1-0.18 μm particle size range during the morning traffic peak to a relatively even distribution of EC between 0.1 and 0.56 μm diameter particles later in the day. The OC concentration reduction over this same pair of time periods is likewise accompanied by a shift of the peak in the OC size distribution to a larger size, moving from the 0.18-0.32 μm size range in the 0600-1000 PDT time period to the 0.32-0.56 μm size range in the 1400-1800 time period. The EC and OC concentration peaks during the morning in the 0.18-0.32 μm particle size range occur in the same size range as the predominant fine particle emissions from gasoline- and diesel-powered engines [32]. The appearance of EC and OC in larger particle sizes late in the day could result from advection into Central Los Angeles of aged aerosol having accumulated coatings of gas-to-particle conversion products over time. Alternatively, additional sources may contribute to the afternoon aerosol. NO_3^-, Cl^-, and Na are found in significant quantities only in the largest size range measured by the impactor (1.0 < D_a < 1.8 μm); these substances are associated with sea salt or transformed sea salt, which is generally found in particle sizes larger than 1 μm in diameter. If all of the Na and Cl^- began as NaCl in sea salt particles, then the Cl^- measured between 0600 and 1000 PDT suggests that about 82% of the sea salt has undergone a chloride substitution reaction during atmospheric transport prior to that time. The lack of Cl^- seen between 1400 and 1800 PDT implies that all of the chlorine originally associated with sea-salt aerosol has been driven from the aerosol by

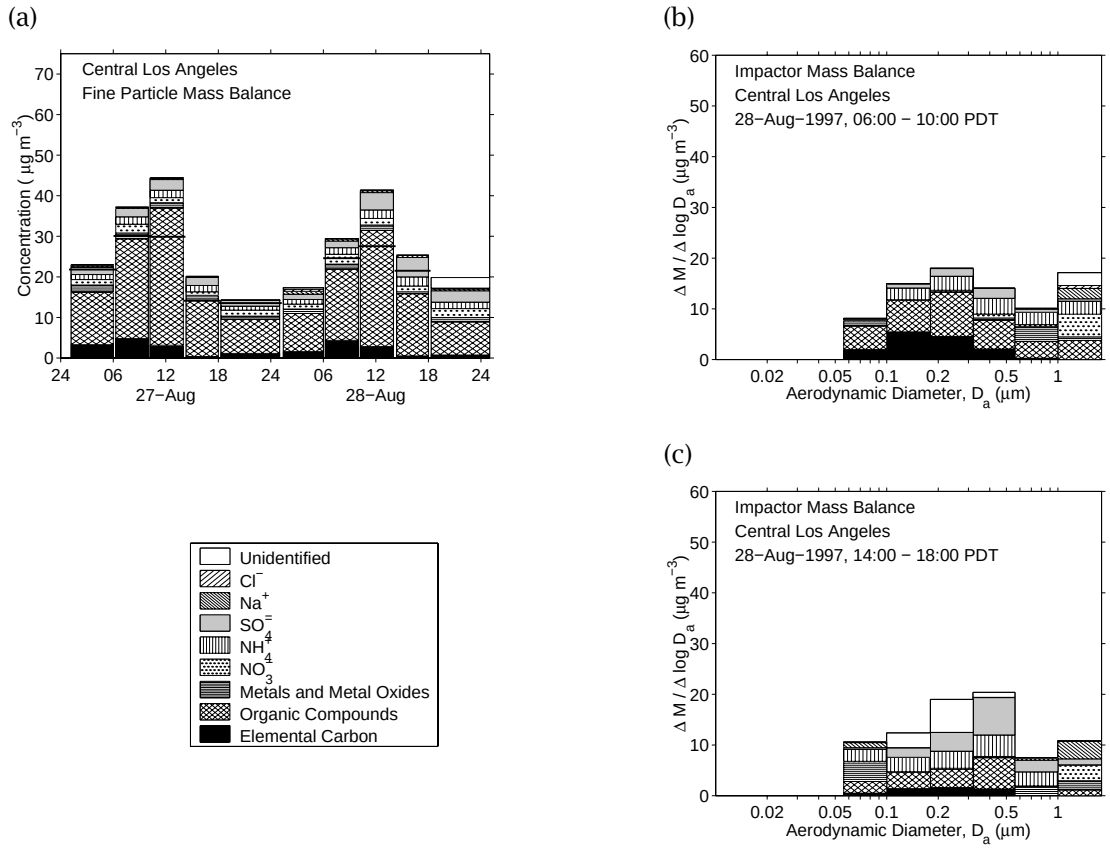

Figure 2.7: Fine particle results for a typical sampling event at Central Los Angeles. (a) Bulk fine particle ($PM_{1.9}$) concentrations and chemical compositions measured during the August 27-29, 1997, sampling event. (b) Size-resolved fine particle mass distribution and chemical composition measured on August 28, 1997, during the 0600-1000 PDT sampling period. (c) Size-resolved fine particle mass distribution and chemical composition measured on August 28, 1997, during the 1400-1800 PDT sampling period.

late in the afternoon on the day studied. The reaction of nitric acid vapor with NaCl to produce $NaNO_3$ aerosol and hydrochloric acid vapor is well-documented [15, 33, 34, 35, 36, 37, 38]. The nitric acid concentration peaks in the daylight hours between 1000 and 1800 PDT. The air parcels which were sampled on the morning of August 28, 1997, at Central Los Angeles were over the ocean during the previous day's nitric acid peak, and crossed the coast at about 1800 PDT on August 27, 1997, arriving at Central LA before the time of the HNO_3 peak on August 28. In contrast, air parcels sampled at Central Los Angeles on the afternoon of August 28, 1997, stagnated over or near the ocean the night before, but were exposed to peak nitric acid concentrations during transport over land at mid-day on August 28, driving the chloride substitution reaction to completion.

Figure 2.8a shows the time series of fine particle concentrations and chemical compositions measured on August 27-29, 1997, during a typical sampling event at Azusa. As in Los Angeles, the highest concentrations of EC occurred during the 0600-1000 PDT time period when vehicle traffic was heavy, and OC concentrations were much larger during daylight hours than at night.

Figures 2.8b and c show the size-segregated mass distribution and chemical composition of the fine particulate matter ($D_a < 1.8$ μm) at Azusa during the two sampling time periods: 0600-1000 PDT and 1400-1800 PDT on August 28, 1997. The air parcels sampled in the morning of August 28 at Azusa stagnated over the ocean on the evening of August 26-27, crossed the coastline at approximately 1400 PDT August 27, and proceeded to Azusa, where stagnation occurred overnight between August 27-28. The air parcels sampled in the afternoon at Azusa on August 28 stagnated overnight over land, having come inland across the coast the afternoon before. Elemental and organic carbon particle concentrations and size distributions measured in the morning of August 28 at Azusa are similar to those measured at Azusa that afternoon. As in the Los Angeles morning and afternoon impactor samples (Figure 2.7), sulfate is present in greater quantities in the afternoon, particularly in the 0.32-0.56 μm size range. On this day, NO_3^- and Na are found only in particles larger than 1 μm, and the sea salt had been exposed to enough nitric acid vapor for complete Cl^- substitution to have occurred. The afternoon impactor samples show a larger NH_4^+ concentration in the 0.1-0.56 μm particle diameter size range than was the case in the morning, corresponding to the increased $SO_4^=$ concentration.

2.3.3 Evolution Along Air Parcel Trajectories

Several air parcel trajectories during the study were determined to have passed over or near the Central Los Angeles and Azusa air monitoring sites in succession, thereby permitting a comparison of aerosol

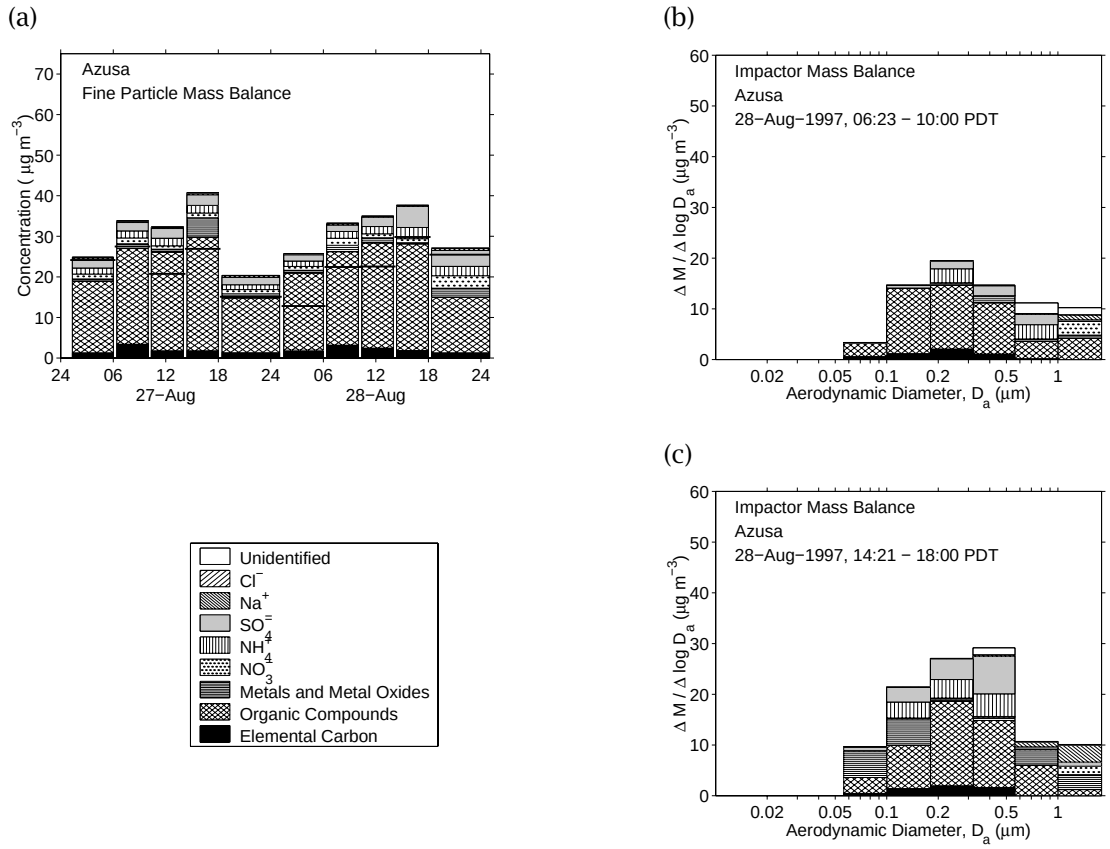

Figure 2.8: Fine particle results for a typical sampling event at Azusa. (a) Bulk fine particle ($PM_{1.9}$) concentrations and chemical compositions measured during the August 27-29, 1997, sampling event. (b) Size-resolved fine particle mass distribution and chemical composition measured on August 28, 1997, during the 0600-1000 PDT sampling period. (c) Size-resolved fine particle mass distribution and chemical composition measured on August 28, 1997, during the 1400-1800 PDT sampling period.

evolution over time; two such air parcel trajectories are examined closely here. These two air parcel trajectories are of similar character; in each case the air mass which stagnated overnight within 5 km of Azusa passed within 5 km of the Central Los Angeles monitoring site during the afternoon of the previous day. Trajectory analysis indicates that the air mass stagnating overnight within 5 km of Azusa on the night of August 21-22, 1997, passed within 5 km of Central LA at around 1400-1600 PDT on the afternoon of August 21. Figure 2.9a shows that air parcel path; each open circle indicates the air parcel location at successive hours during transport. Similarly, during the second 48-h experiment, the air mass stagnating overnight within 5 km of Azusa on the night of August 27-28 passed within 5 km of Central LA at around 1500-1630 PDT on the afternoon of August 27. This air parcel path is shown in Figure 2.10a. Examination of data obtained from these sites and time periods permits study of particle evolution within the same air mass.

Figures 2.9b and 2.10b show the composition of the nitrogen-containing air pollutant concentrations present within the August 21-22 and the August 27-28 air parcels studied, respectively. Most notable in both cases are the sharp increases in NO, by factors of 2.3-3.6, and NO_2, by factors of 1.4-1.8, that occur at Azusa between the 0100-0600 PDT and 0600-1000 PDT time periods. These increases are presumably due to the increase in motor vehicle exhaust emissions during the morning traffic peak. While ammonia is present at noticeable concentrations in the range 4.0-13.6 μg N m^{-3} (equivalent to 7.0-24.5 ppb NH_3), there is little HNO_3 and little aerosol nitrate. This indicates that there is little NH_4NO_3 formation from HNO_3, and that HNO_3 formation from NO_2 is not faster than HNO_3 dry deposition along these trajectories. This is consistent with the comparatively low level of photochemical oxidant formation during the episodes studied here when compared to historical conditions in Southern California. Daily peak concentrations of hourly-averaged ozone ranged between 50 and 70 ppb at Central Los Angeles and 70 and 100 ppb at Azusa over the August 21-23 and August 27-29 sampling events. California air quality standards specify that the hourly average ozone concentration should not exceed 90 ppb. This standard was exceeded during two hours of the sampling events in this study at Azusa; the standard was not exceeded at the other two sites. In general, the smog season of 1997 was mild in comparison with previous years; there was only one Stage One ozone episode during the entire year (hourly average O_3 concentration > 200 ppb), in contrast to 41, 24, 23, 14, and 7 such episodes over the 5 consecutive years 1992-1996, respectively [9].

Figures 2.9c and 2.10c show material balances on fine particle ($PM_{1.9}$) chemical composition along the August 21-22 trajectory and the August 27-28 trajectory, respectively. "Unidentified" material indicates the difference between gravimetrically determined mass concentrations and the sum of the

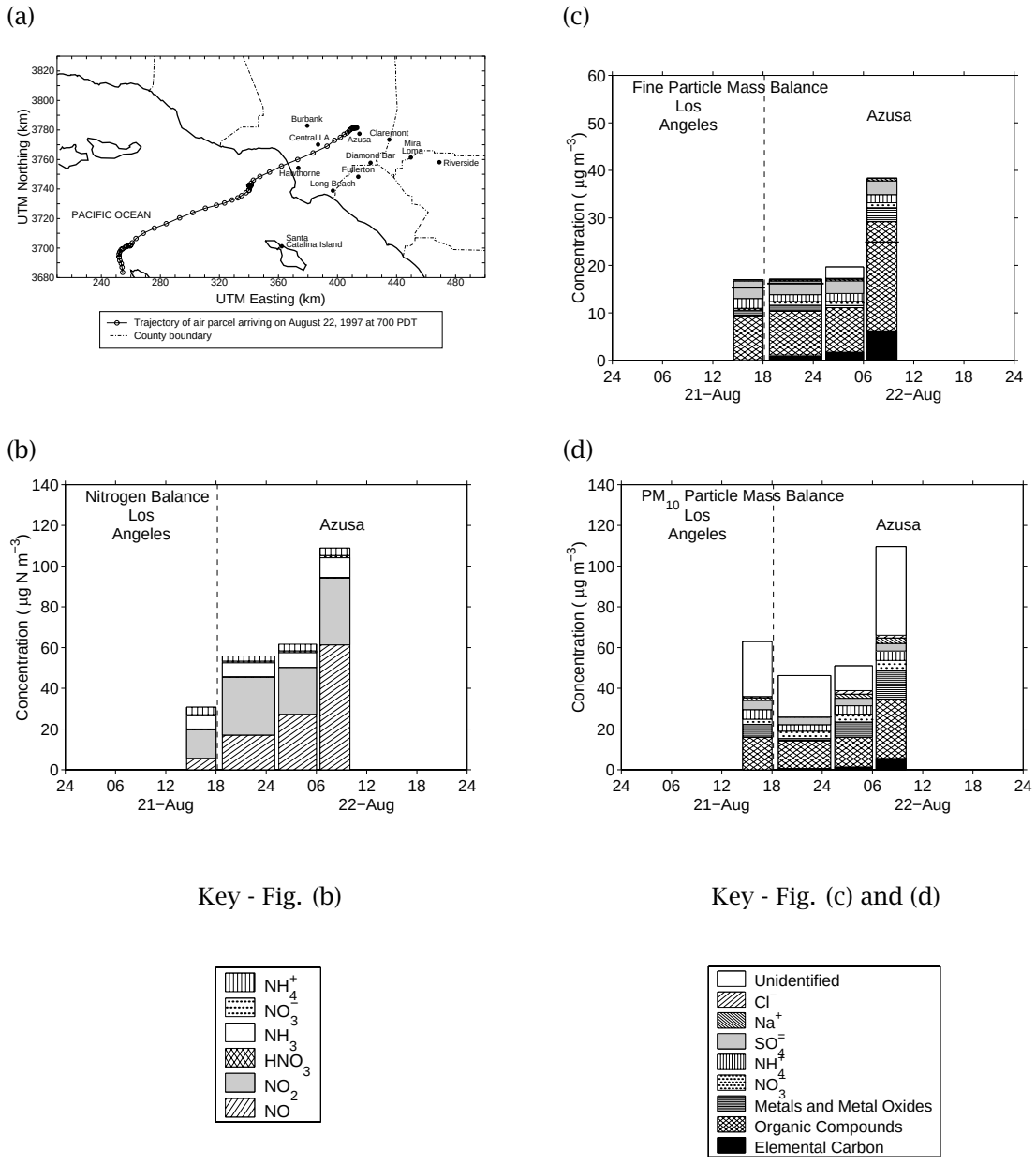

Figure 2.9: Aerosol evolution along the trajectory between Central Los Angeles and Azusa, August 21-22, 1997. (a) Representative air parcel trajectory reaching Azusa, CA at 0700 PDT August 22, 1997. The air parcel passed within 5 km of the Central Los Angeles sampling site between 1400 and 1800 PDT on August 21 before stagnating at Azusa over the night and morning of August 21-22. Circles represent air parcel location at consecutive hours. (b) Nitrogen balance, (c) Fine particle ($PM_{1.9}$) mass balance, and (d) PM_{10} mass balance.

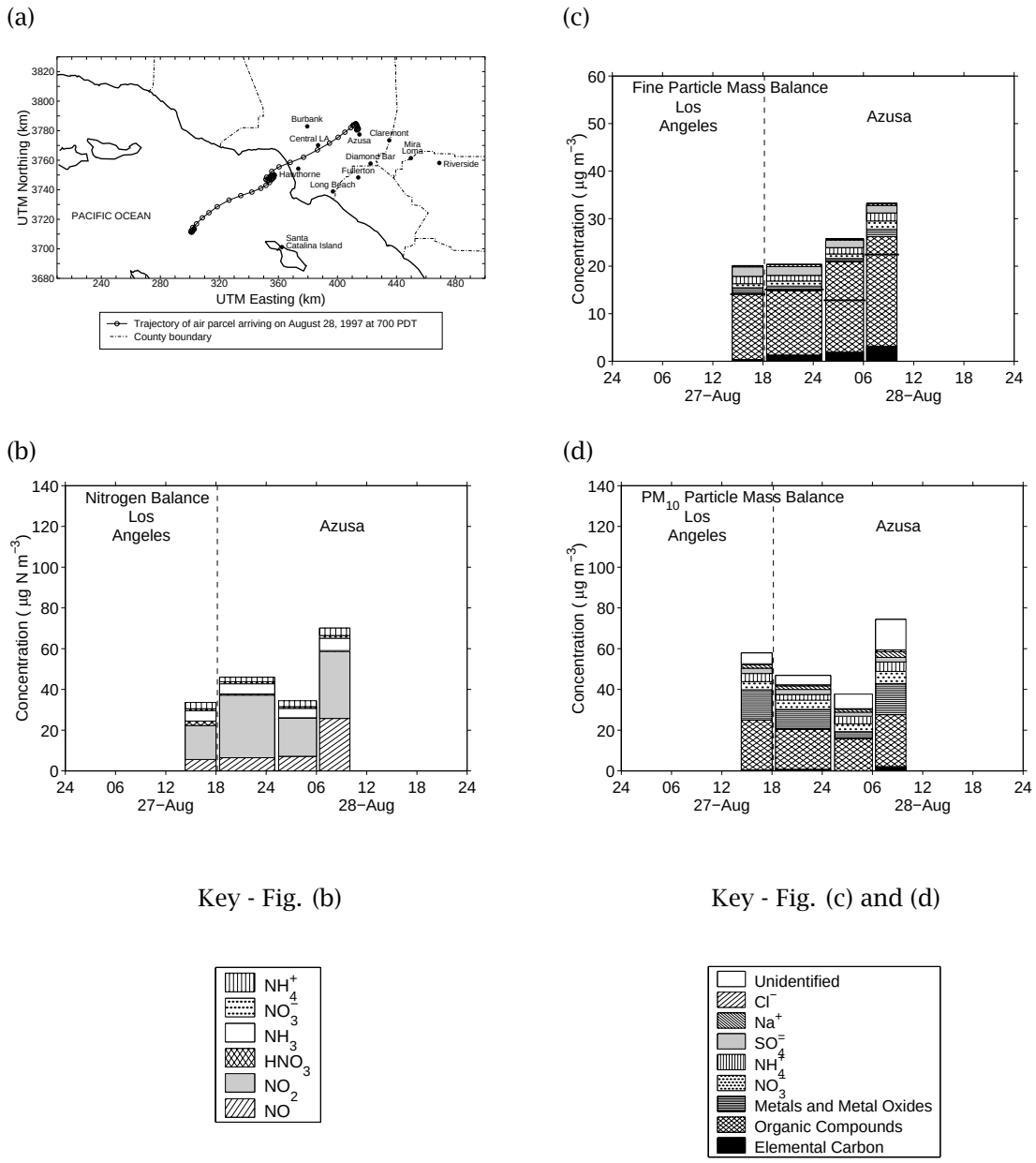

Figure 2.10: Aerosol evolution along the trajectory between Central Los Angeles and Azusa, August 27-28, 1997. (a) Representative air parcel trajectory reaching Azusa, CA at 0700 PDT August 28, 1997. The air parcel passed within 5 km of the Central Los Angeles sampling site between 1400 and 1800 PDT on August 27 before stagnating at Azusa over the night and morning of August 27-28. Circles represent air parcel location at consecutive hours. (b) Nitrogen balance, (c) Fine particle ($PM_{1.9}$) mass balance, and (d) PM_{10} mass balance.

identified analyte concentrations. A thick horizontal line indicates the gravimetrically determined mass concentration on the one occasion when this is less than the sum of the identified analyte concentrations. During transport along both trajectories, the relative composition of the aerosol did not change appreciably between 1400 PDT at Central Los Angeles and 0600 PDT the next morning at Azusa. The exception to this observation is that elemental carbon concentrations increased steadily over time in both air parcels, as did organic aerosol during the early morning hours on August 28 at Azusa. There was not significant NO_3^- or $SO_4^=$ formation during the overnight stagnation periods up until 0600 PDT. In both cases, on the second morning of each experiment the particle population changed noticeably during the morning traffic peak period through increases in aerosol elemental carbon (65-258% increase), organic matter (21-146% increase), metals and metal oxides (138-538% increase), nitrate (17-84% increase), ammonium (6-25% increase), and fine aerosol mass (27-75% increase) during periods when the air mass motion was relatively stagnant.

Figures 2.9d and 2.10d show PM_{10} material balances on aerosol chemical composition along the August 21-22 and the August 27-28 air parcel trajectories studied, respectively. At least a portion of the large unidentified mass concentrations includes silicate minerals and calcium-containing mineral matter which were not measured by neutron activation analysis in this experiment. These minerals are found primarily in dust and crustal material, which are largely present in the coarse particle size range; therefore unidentified matter is generally greater for PM_{10} particulate matter than for fine particle matter. As with fine aerosol, on the second morning of each experiment the PM_{10} particle population changed significantly during the morning peak traffic period through increases in aerosol organic matter (60-100% increase), metals and metal oxides (88-353% increase), nitrate (27-58% increase), ammonium (13-24% increase), and fine aerosol mass (97-115% increase).

Chapter 3

Nitrate-Oriented Trajectory Study

3.1 Introduction

In autumn of 1997 a field experiment was conducted in conjunction with the 1997 Southern California Ozone Study [7, 8, 9] in which a network of three air monitoring stations was established, with the purpose of determining the size and chemical composition of the airborne particle population in an area having high secondary aerosol ammonium nitrate formation. Measurements were made of the particle size distribution, bulk fine particle ($PM_{1.9}$) and PM_{10} chemical composition, chemical composition segregated into narrow particle size intervals, and single-particle chemical composition. Air monitoring station locations were chosen along a seasonally typical wind trajectory that crosses an agricultural area located to the east of Los Angeles, CA, that has significant ammonia emissions due to livestock husbandry operations and fertilizer use. The intent was to first observe air parcels at the leading edge of the ammonia source area, and to subsequently observe the same air parcels after they have been carried downwind through the source area. This sampling scheme was designed to provide data on the evolution over time of the size and chemical composition of ambient aerosols at the bulk, size-segregated, and single-particle levels as those particles are potentially altered by gas-to-particle conversion processes and affected by continuing emissions, dilution, and dry deposition.

Several studies of nitrate-containing particle evolution using multiple observation points along a single air parcel trajectory have been conducted previously in the Los Angeles area. In a 1982 field study, gas- and particle-phase nitrogen species were sampled from a single air parcel which passed over or near three monitoring sites in succession: Long Beach, Anaheim, and Rubidoux, CA, providing insight

into the process of aerosol nitrate formation and the interrelationship between gas-phase HNO_3 and NH_3 versus particulate NH_4NO_3 [11, 12, 29]. Measurements made at that time showed that the aerosol nitrate behaved as would be expected from analyses based on thermodynamic equilibrium between the gas and particle phases and verified the presence of a large ammonia source located in the agricultural and dairy area between Anaheim and Rubidoux leading to large aerosol nitrate concentrations in the Riverside (Rubidoux) area.

In 1996, a similarly designed field study was conducted using more advanced instrumentation. A battery of aerosol sampling instruments similar to those employed in the present study, including samplers for fine and total suspended particulate matter chemical composition, size-segregated particulate matter chemical composition, and single-particle size and composition measurements, were used to obtain information about the evolution of the particle population as particles aged in the presence of significant aerosol nitrate formation as well as continuing emissions [3, 13]. Two air parcel trajectories were identified which passed over or near three or four air monitoring stations along the Santa Catalina Island—Long Beach—Fullerton—Riverside pollutant transport corridor [13]. Notable in the results of this study was the observation of large increases in particulate ammonium and nitrate concentrations between Fullerton and Riverside in air parcels which stagnated overnight in the area of large livestock and agricultural ammonia sources just west of Riverside. The present study differs from previous work in that, for the first time, air monitoring stations are placed just upwind of and directly within the Chino dairy area in order to observe the effect of a major source of ammonia emissions at close range.

3.2 Experimental Methods

3.2.1 Sample Collection and Analysis

Three urban air monitoring stations were established in the Los Angeles metropolitan area to measure the effect of nitrogen species emissions on ambient particulate matter concentrations. These sites were located in Diamond Bar, Mira Loma, and Riverside, as labeled on the map in Figure 3.1. The three sites were chosen because they are located along a seasonally typical wind path inland across the South Coast Air Basin. This allows the possibility of successive sampling of the same air parcels at multiple locations as they are transported downwind. In addition, the area traversed by an air parcel advected between two or more of these sites is exposed to substantial agricultural and livestock ammonia sources

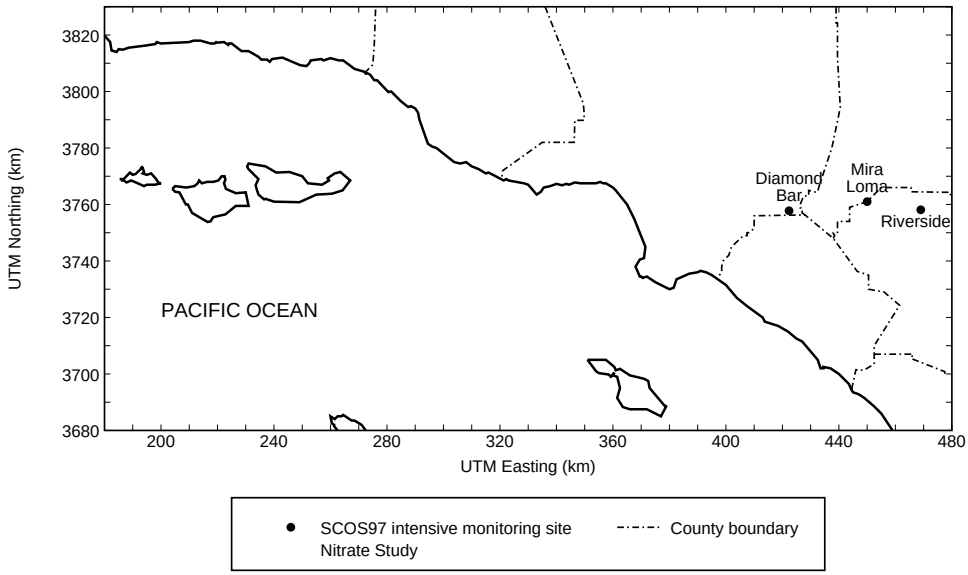

Figure 3.1: South Coast Air Basin and Nitrate-Oriented Trajectory Study sampling site locations.

(see Figure 2 of [30]).

Sampling was conducted at all three sites during one 48-hour period on October 31-November 2, 1997. In addition, continuous sampling at the Mira Loma monitoring station alone was conducted during one 59-hour period, September 27-29, 1997. Fine particle ($PM_{1.9}$) and PM_{10} samples for mass and chemical composition determination were collected sequentially on a 5-sample per day schedule, and a pair of micro-orifice impactors (MOIs) were operated at each site for one or two of these time periods each day. Times of operation for the filter samplers and impactors are shown in Figure 3.2 for both sampling events.

During the September 27-29, 1997, sampling at Mira Loma, a transportable aerosol time-of-flight mass spectrometry (ATOFMS) instrument [15] was in operation at that site. During the October 31-November 2, 1997, sampling period, a laboratory-bound ATOFMS instrument [16] was operated in Riverside. Where used, the ATOFMS instruments operated continuously, collecting number distribution data in the particle aerodynamic diameter, D_a, range $0.2 < D_a < 5$ μm, and obtaining mass spectra for a subset of the input particle population. The ATOFMS instrument data will be reported separately by Professor Kimberly Prather's research group at the University of California, Riverside.

Four filter sampling systems were used to collect particles at each air monitoring station: one to collect PM_{10} samples ($D_a < 10$ μm) and three to collect fine particle ($PM_{1.9}$) samples. The PM_{10} sampler and two of the three fine particle samplers were used to collect consecutive short time average samples

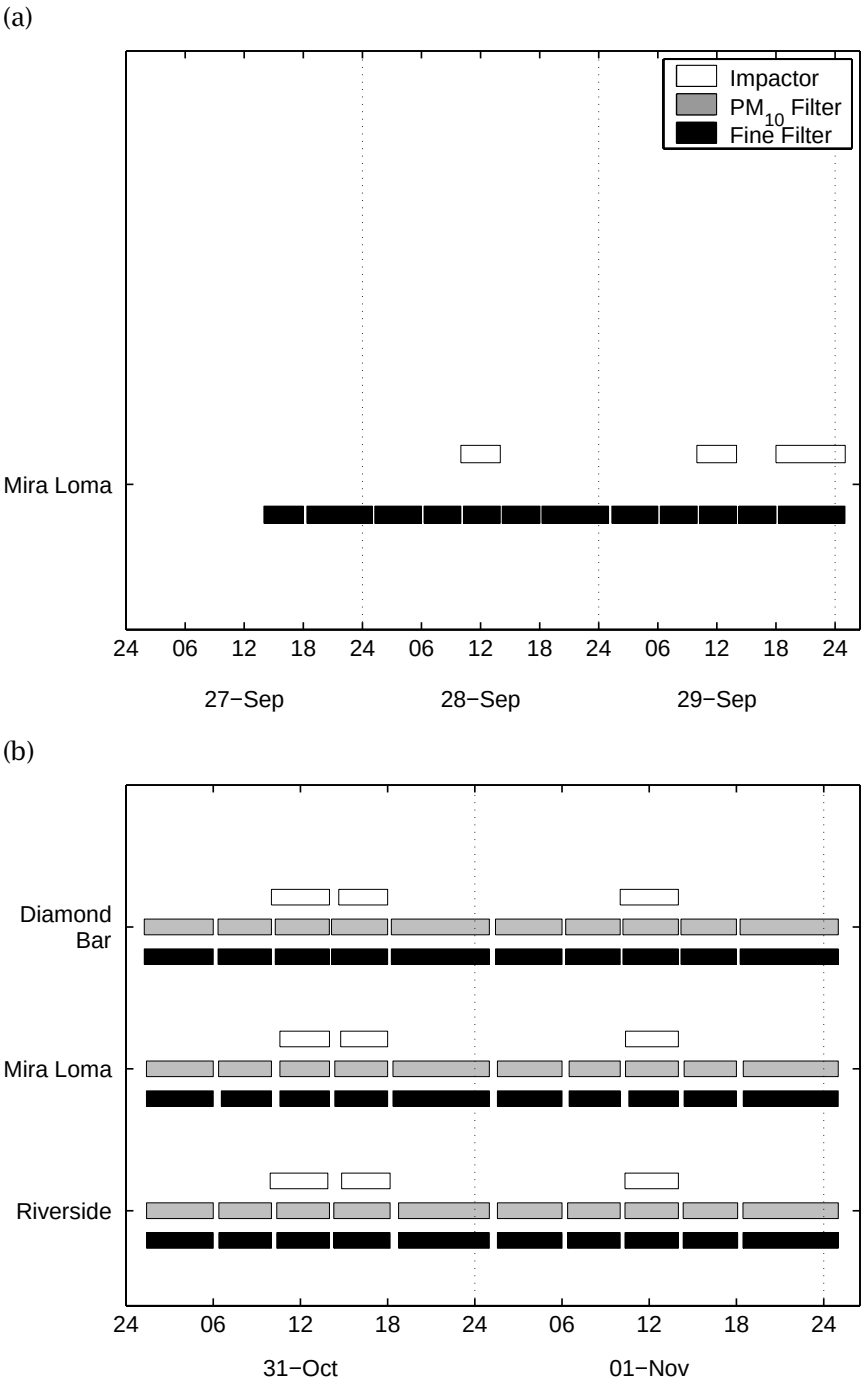

Figure 3.2: Times of operation of impactors and filter samplers at each site during the two sampling events, stated in terms of local time during the experiments. (a) Extended sampling at Mira Loma, September 27-20, 1997 (local time was PDT). (b) Three-site experiment, October 31-November 2, 1997 (local time was PST).

for bulk and elemental analysis. Five complete sets of filter samples were collected each day according to the following time schedule: 0120-0600 hours, 0620-1000 hours, 1020-1400 hours, 1420-1800 hours, 1820-0100 hours (the following day). All times in this study were in the local time system, therefore times before October 26, 1997, are in Pacific Daylight Time (PDT), and times after October 26, 1997, are in Pacific Standard Time (PST). This filter sampling schedule provides relatively fine temporal resolution data for comparison with the continuous ATOFMS data and future air quality modeling results. One fine particle sampler at each site collected 24-h average samples to facilitate collection of enough material for later analysis of individual particulate organic compounds by GC/MS.

The impactors, filter samplers, and sample analysis methods are identical to samplers used in the Vehicle-Oriented Trajectory Study, and are described in detail in Chapter 2. Impactor substrates and filter samples were analyzed for mass gravimetrically, for Cl^-, NO_3^-, and $SO_4^=$ by ion chromatography, for NH_4^+ by indophenol colorimetry, for elemental black carbon and organic carbon by thermal evolution and combustion analysis, and by neutron activation analysis for 39 trace elements. HNO_3 was measured using the denuder difference method. Gas-phase NH_3 was detected as NH_4^+ collected on oxalic acid-impregnated glass fiber filters used downstream of a PTFE pre-filter. Measurement methods are discussed in more detail in Chapter 2. A factor of 1.4 was applied to measured organic carbon concentrations to convert these measurements to an estimate of organic compound concentrations. This scale factor accounts for the additional mass of associated H, O, N, and S present in the organic matter of typical atmospheric organic aerosols [22].

3.2.2 Meteorology

Wind fields over the South Coast Air Basin were reconstructed over a 5 km $\times$ 5 km grid system superimposed over the airshed for each hour during the study using the method of Goodin et al. [27], based on hourly averaged wind speed and direction measurements at 27-28 meteorological stations maintained by the South Coast Air Quality Management District (SCAQMD). From the wind fields, back trajectories from the sampling sites were calculated, establishing the time and location history of the air parcels arriving at the sampling sites.

At Mira Loma during the September 27-30 sampling event, temperatures were between 17.2 and 39.2°C, relative humidities were 15 to 94%, and optical conditions were hazy. Air stagnation occurred beginning between 2000 and 2300 PDT in the evening until between 0900 and 1100 PDT the following morning.

Temperatures at Diamond Bar during the October 31-November 2 sampling episode ranged between 11.5 and 34.8°C, with relative humidities measured between 12 and 78%. Air stagnation occurred at Diamond Bar beginning at about 1700 PST in the evening each day until about 1300 PST the afternoon of the following day. Mornings were hazy, and the haze cleared in the afternoon of November 1. During the October 31-November 2 sampling event at Mira Loma, the temperature range was 8.5 to 34.8°C and the relative humidity range was 10 to 85%. Air stagnation occurred at Mira Loma on the evening of October 31 at about 1700 PST, lasting until about 0600 PST the following morning; no air stagnation occurred the evening of November 1. Mornings were hazy and misty; the afternoon of October 31 was hazy, but conditions cleared beginning early in the morning of November 1. Temperatures at Riverside during the October 31-November 2 sampling event ranged between 12.4 and 33.3°C, and the relative humidity range was 26 to 62%. Air stagnation occurred at Riverside on the evening of October 31 at about 1700 PST, and lasting until about 0700 PST the following morning; no air stagnation occurred at Riverside the evening of November 1. October 31 was hazy, but November 1 was clear from the early morning on. None of the three sites had significant cloud cover at any time during sampling, and air quality cleared significantly at all three sites beginning on the morning or early afternoon of November 1 and lasting through the rest of that day. Wind pattern shifts likely explain this phenomenon; air parcels reaching Mira Loma and Riverside for the latter half of November 1 were transported from the north, rather than across the heavily populated area to the west of those locations.

3.3 Results and Discussion

3.3.1 September 27-30, 1997, Sampling Event

Figure 3.3 shows the time series of fine particle mass and major aerosol chemical species concentrations at Mira Loma over the sampling period of September 27-30. Fine particle mass concentrations are high, averaging 81.9 μg m^{-3}, 63.9 μg m^{-3} and 58.2 μg m^{-3} on September 27 (after 1400 PDT), September 28, and September 29, respectively. By comparison, the recently proposed Federal $PM_{2.5}$ air quality standard limits 24-h average fine particle concentrations to not more than 65 μg m^{-3} and annual average $PM_{2.5}$ concentrations to not more than 15 μg m^{-3}. The fine particle mass concentration at Mira Loma on these days is dominated by ammonium nitrate aerosol, with significant quantities of organic aerosol also present.

September 27, 28, and 29 fell on Saturday, Sunday, and Monday, respectively, and it is interesting to

note the differences between species concentration patterns on a weekend and a weekday. For example, Monday, September 29 exhibits a strong peak in the elemental carbon concentration during the 0600-1000 PDT time period. This pattern was also noted on weekdays in Central LA and Azusa, areas in which vehicle traffic emissions are a major source (see Figures 2.4 and 2.5). However, this pattern does not appear on Sunday, September 28.

In addition to the weekend/weekday distinctions, some of the concentration time series behaviors can be explained by the source of the air mass sampled. Concentrations of fine particulate nitrate, ammonium, and mass are all relatively high and constant from the evening of September 27 through the morning of September 28. Fine particulate sulfate concentrations were relatively high, but steadily decreasing. Average concentrations during this time period were 8.5 μg m^{-3} fine $SO_4^=$, 43.9 μg m^{-3} fine NO_3^-, 12.7 μg m^{-3} fine NH_4^+, and 111 μg m^{-3} fine particulate mass. The consistency of these concentrations over time was due to the fact that this air mass was stagnant at Mira Loma overnight. After 1000 PDT, air mass stagnation ended, and the air parcels transported into the Mira Loma area came from north of Mira Loma, an area absent the ammonia source-driven ammonium nitrate production associated with the dairy area near Mira Loma. This difference in air mass origin is reflected in the precipitous drop in measured concentrations of gas-phase ammonia and fine particle mass, EC, organic compounds, sulfate, nitrate, and ammonium. (Two independent gravimetric measurements of this minimum in the fine particle mass concentration agreed within 6%.) The fine mass concentration minimum during this time period was 7.5 $\pm$ 1.9 μg m^{-3}, compared to maximum and average fine particle mass concentrations of 114.9 $\pm$ 1.1 μg m^{-3} and 64.5 $\pm$ 0.50 μg m^{-3}, respectively, over the entire sampling event. Later in the afternoon of September 28, particulate species concentrations increased again; the air arriving at Mira Loma in these time periods stagnated the night before in the corridor between Claremont, Diamond Bar, and Fullerton, and most back-calculated trajectories indicate several hours of travel across the ammonia sources between Diamond Bar and Mira Loma before these air parcels reached Mira Loma.

Figure 3.4a shows a material balance on the fine particle chemical composition at Mira Loma during the September 27-30 episode. Ammonium nitrate is the most abundant species present, followed by organic compounds. In this plot, as well as in mass balance presentations in Figures 3.6, 3.8, 3.10, 3.11 and 3.12, the designation “Unidentified” applies to the difference between mass concentration determined gravimetrically and the sum of species concentrations identified by chemical analysis methods. Silicates and calcium-containing mineral matter are among the materials not detected by the methods used in the present study, and these may be included in the unidentified matter. While samples were

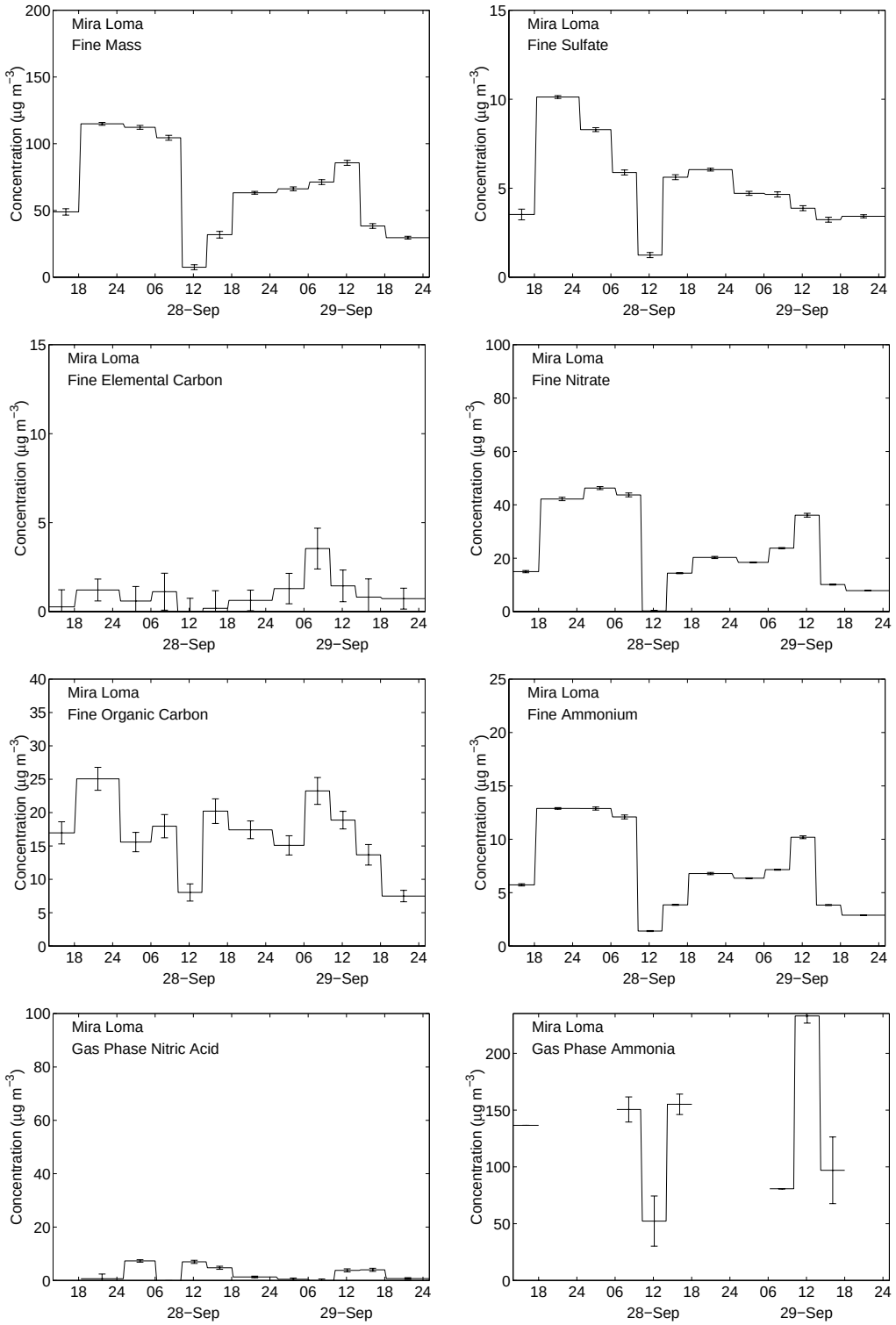

Figure 3.3: Fine particle ($PM_{1.9}$) and gas-phase results for individual species measured during the September 27-30, 1997, sampling event at Mira Loma.

equilibrated and weighed in an environment with low relative humidity, some water may have been retained in the samples despite dessication. "Metals and Metal Oxides" refers to the sum of trace elements measured by neutron activation analysis, with elemental concentrations converted to the equivalent concentrations of their most common oxides, where appropriate (see Table A.3 for a list of these oxides and the conversion factors used).

Figure 3.4b shows a material balance on nitrogen-containing air pollutant concentrations present at Mira Loma during the September 27-30 episode. Data are presented in terms of μg of nitrogen m^{-3}. Gas-phase NH_3 data for this sampling period were taken by Dr. Dennis Fitz's group at CE-CERT, UC-Riverside. Ammonia was measured only during daylight hours, 0600-1800. Dashed lines connect the intervals where ammonia data are missing to indicate the likely ammonia concentrations present. The most important point demonstrated in Figure 3.4 is that ammonia concentrations are extraordinarily high at the Mira Loma site; so high that virtually all of the HNO_3 produced in the plume downwind of the Los Angeles/Long Beach/Orange County urban complex will be converted to ammonium nitrate aerosol to the extent that that plume passes over Mira Loma. The nitrogen species concentrations echo the mid-day minimum concentrations seen on September 28 and mid-day maximum concentrations seen on September 29 in the fine particle species data of Figures 3.3 and 3.4a. NO and NO_2 concentration patterns are similar between the two days. During both days, there is a general increase in NO + NO_2 nitrogen concentrations after 1800, peaking in the 0600-1000 PDT time period, after which NO + NO_2 concentrations decrease, followed by HNO_3 concentration peaks between the hours of 1000 and 1800 PDT.

3.3.2 October 31-November 2, 1997, Sampling Event

During the October 31-November 2, 1997, sampling period, all three of the air monitoring stations were in operation. All three sites had periods of relatively high pollutant concentrations on Friday, October 31, and all three sites experienced drastic reductions in particle concentrations beginning in the morning of November 1 and lasting for the rest of that day. Changing wind patterns account for the sudden change in conditions. During the period of clean air at the end of the day on November 1, incoming air parcels at Mira Loma and Riverside approached from the mountains to the north and northeast instead of from urban and agricultural areas to the west.

Figure 3.5 shows the time series of fine particle mass and major fine aerosol chemical species concentrations at Diamond Bar over the October 31-November 2, 1997, sampling period. October 31 and

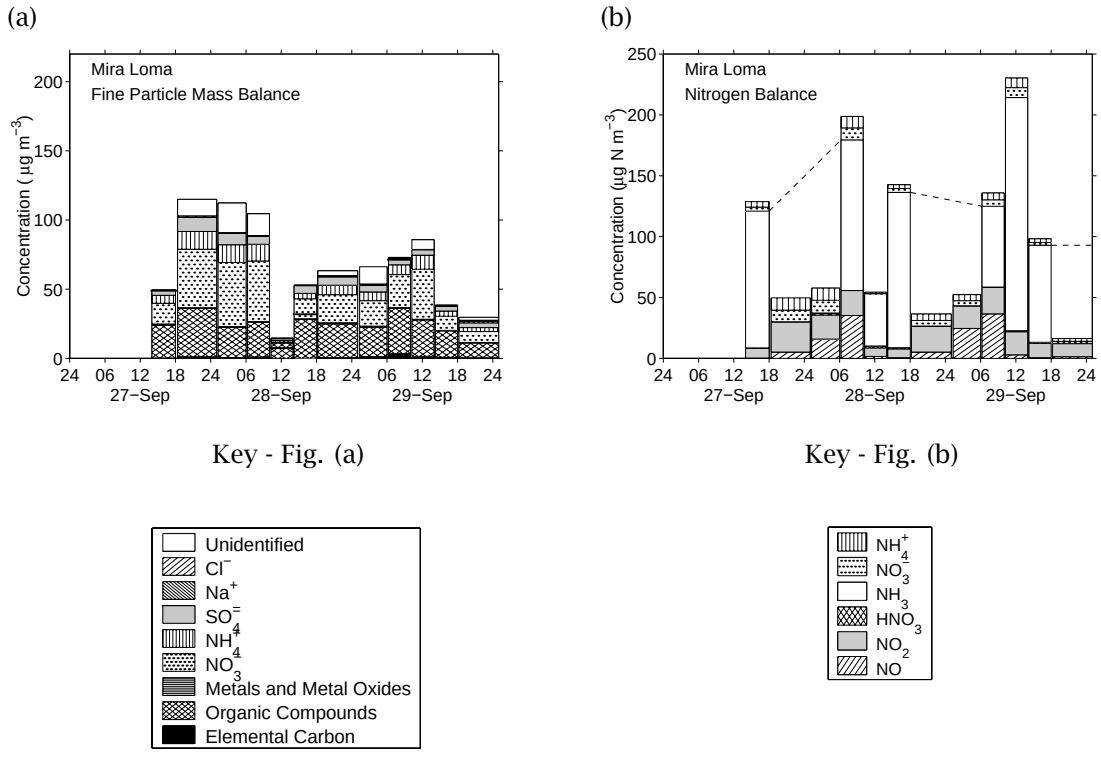

Figure 3.4: (a) Fine particle ($PM_{1.9}$) mass balance and (b) nitrogen species mass balance during sampling at Mira Loma, September 27-30, 1997. NH_3(g) measurements were not taken by the Fitz group at UC-Riverside between the hours of 1800 and 0600 each day; dashed lines roughly indicate the likely ammonia concentrations present overnight.

November 1 were on Friday and Saturday, respectively. Fine particulate mass, NO_3^-, and NH_4^+ concentrations are essentially constant for the first half of the day on October 31. These concentrations are relatively high, with an average fine particle mass concentration of 98.6 ± 1.7 μg m^{-3}, containing 40.8 ± 0.7 μg m^{-3} fine particle NO_3^- and 10.5 ± 0.2 μg m^{-3} fine particle NH_4^+. The air parcels reaching Diamond Bar during this night and morning period of low-to-stagnant wind speeds approached Diamond Bar from the northeast during a condition of mild off-shore wind flow after having crossed the Pacific Coast along the Santa Monica Bay two to three days earlier. The air mass stagnating overnight at Diamond Bar in this case already contains high particulate ammonium nitrate concentrations. In contrast, air parcels arriving during the 1400-1800 time period were transported by on-shore winds after stagnating only once overnight near Fullerton; these air parcels have been over the urban area for a much shorter time, and there are minimums in the particulate NO_3^-, NH_4^+, and fine mass concentrations as a result. The fine particulate elemental carbon concentration increased by more than a factor of 2.5 during the 0600-1000 PST morning traffic peak period on October 31 when compared to the previous time period. This 0600-1000 PST peak in EC concentrations did not occur on Saturday, November 1, reflecting the differences between weekday and weekend traffic patterns.

Figure 3.6a shows the time series of fine particle concentrations and chemical compositions measured at Diamond Bar during the October 31-November 1, 1997, sampling event. Figures 3.6b and c show the size-segregated mass mass distribution and chemical composition of the fine particulate matter ($D_a < 1.8$ μm) at Diamond Bar during the two sampling time periods 1000-1400 PST and 1400-1800 PST on October 31, 1997. The particle size distribution data show that aerosol nitrate accumulation is occurring mainly on particles larger than 0.3 μm aerodynamic diameter. The air sampled during the 1000-1400 PST time period stagnated overnight in and to the northeast of the Diamond Bar area; the air sampled in the subsequent time period was transported from west of Diamond Bar. The decreases in fine particulate NO_3^-, NH_4^+, and mass, the slight decrease in fine aerosol carbon, and the slight increase in fine particle $SO_4^=$ between the two time periods apparent in Figure 3.6a can also be seen in the size-segregated chemical composition data.

Figure 3.7 shows the time series of fine particle mass and major aerosol chemical species concentrations at Mira Loma over the October 31-November 2, 1997, sampling period. Gas phase NH_3 concentrations between 1000 PST and 0100 PST October 31-November 1 were among the highest concentrations measured during the study, peaking at 123.9 ± 2.3 μg m^{-3} (equivalent to 180 ± 3.4 ppb). Fine elemental carbon and organic compound concentrations peaked during the 0600-1000 PST peak traffic period on Friday, October 31. Other fine particulate species remained relatively constant from

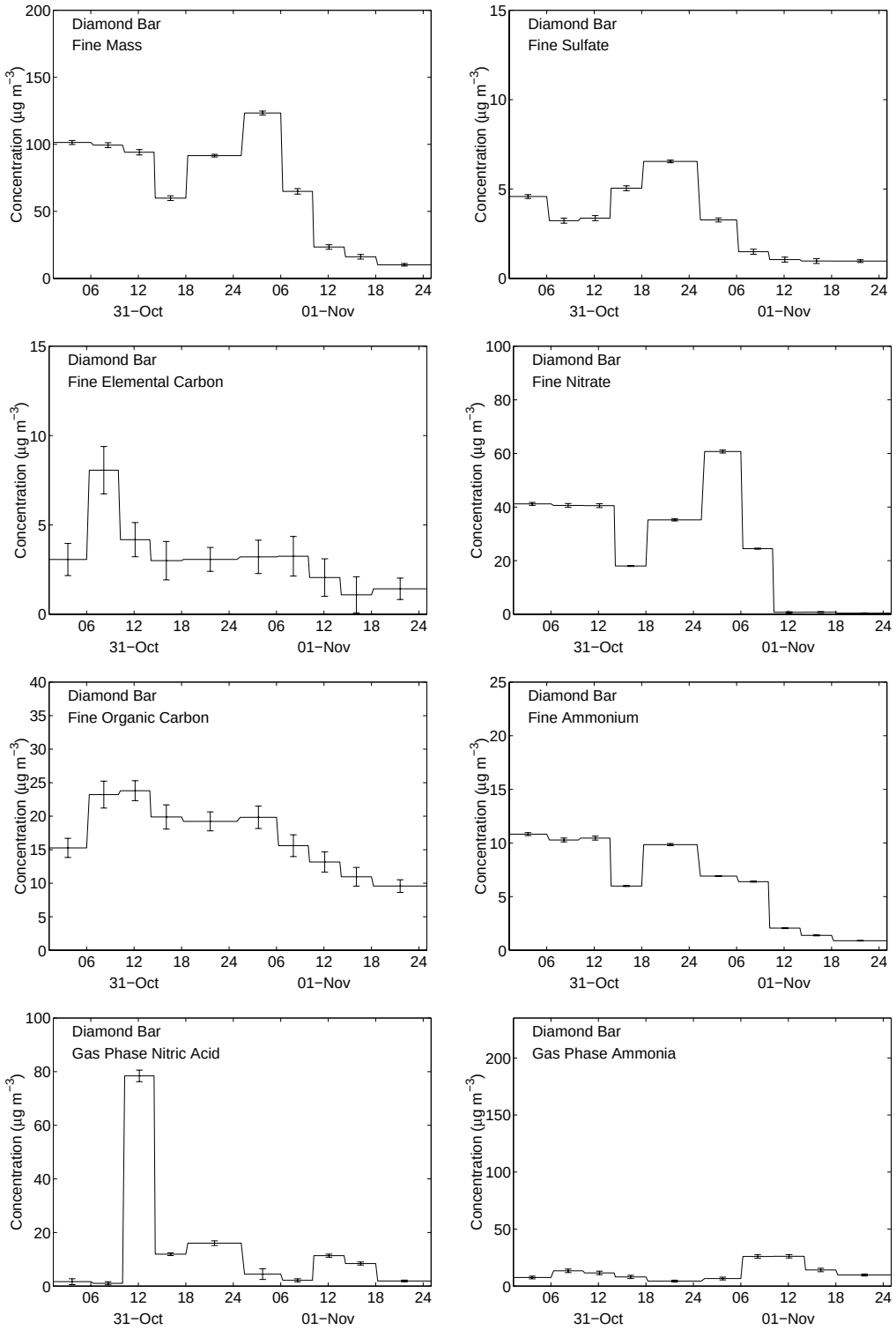

Figure 3.5: Fine particle ($PM_{1.9}$) and gas-phase results for individual species measured during the October 31-November 2, 1997, sampling event at Diamond Bar.

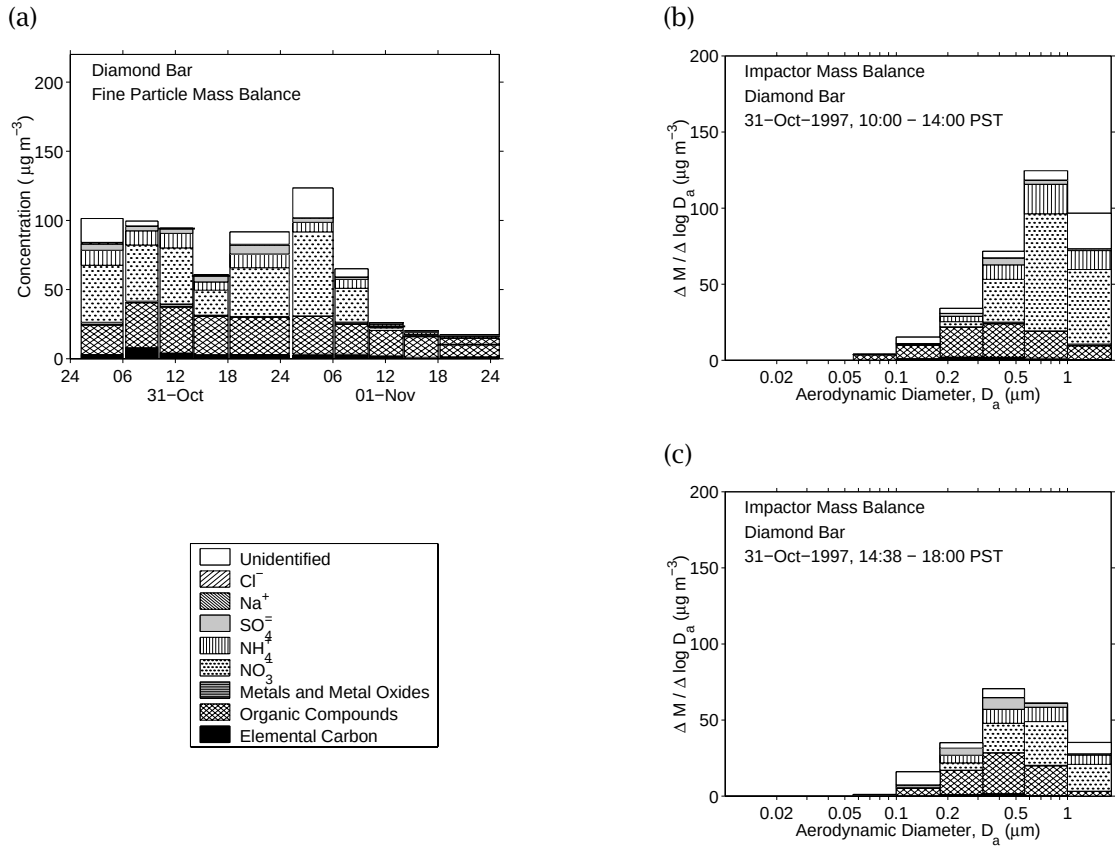

Figure 3.6: Fine particle concentration and chemical composition at Diamond Bar. (a) Bulk fine particle ($PM_{1.9}$) concentrations and chemical compositions measured during the October 31-November 2, 1997, sampling event. (b) Size-resolved fine particle mass distribution and chemical composition measured on October 31, 1997, during the 1000-1400 PST sampling period. (c) Size-resolved fine particle mass distribution and chemical composition measured on October 31, 1997, during the 1400-1800 PST sampling period.

0100 through 1000 hours PST on October 31. Air parcel trajectories arriving at Mira Loma changed around 1100 hours PST from a pattern which approached Mira Loma from the north to one which approached Mira Loma from the west. Air parcels arriving after 1100 hours PST contained higher concentrations of fine particulate NO_3^- and NH_4^-, and gas-phase NH_3, and lower concentrations of EC. The center of the Chino dairy area is located to the west of Mira Loma, and thus it is not surprising that the highest ammonia concentrations recorded occur at this time. Overnight between October 31 and November 1 as air parcels stagnated at Mira Loma, the concentrations of all species remained relatively high. As mentioned previously, the wind direction shifted to produce flow from the north after 0700 PST on November 1, resulting in very low fine particle concentrations for the rest of that day.

Figure 3.8a shows a chemical material balance on the time series of fine particle concentrations and chemical compositions measured at Mira Loma during the October 31-November 2, 1997, sampling event. Figures 3.6b and c show the size-segregated mass distribution and chemical composition of the fine particulate matter ($D_a < 1.8$ μm) at Mira Loma as measured by the cascade impactors during the two sampling time periods 1000-1400 PST and 1400-1800 PST on October 31, 1997. Increases in fine particle mass, EC, organic compounds, NO_3^-, $SO_4^=$, and NH_4^+ between the mid-day and afternoon time periods seen in Figure 3.8a also can be seen in the size-segregated fine particle composition data as well. Again, the greatest accumulation of nitrate is occurring on particles larger than 0.3 μm aerodynamic diameter.

Figure 3.9 shows the time series of fine particle mass and major aerosol chemical species concentrations at Riverside over the October 31-November 2, 1997, sampling event. Elemental carbon concentrations were relatively constant through October 31 and the following morning. Fine particulate mass, organic compounds, NH_4^+, and NO_3^- peaked during the 1400-1800 PST time period on October 31; wind speeds increased at this time after the overnight stagnation period ended, thereby transporting more polluted air parcels into Riverside from the west. $SO_4^=$ concentrations peaked at 3.0 ± 0.1 μg m^{-3} in the 1800-0100 PST period.

Figure 3.10a shows a material balance on the time series of fine particle concentrations and chemical compositions measured at Riverside during the October 31-November 1, 1997, sampling event. Figures 3.10b and c show the size-segregated mass distribution and chemical composition of the fine particulate matter ($D_a < 1.8$ μm) at Riverside as measured from the cascade impactor samples during the two sampling time periods 1000-1400 PST and 1400-1800 PST on October 31, 1997. Again, the ammonium nitrate concentration increase between these two time periods occurs in the form of

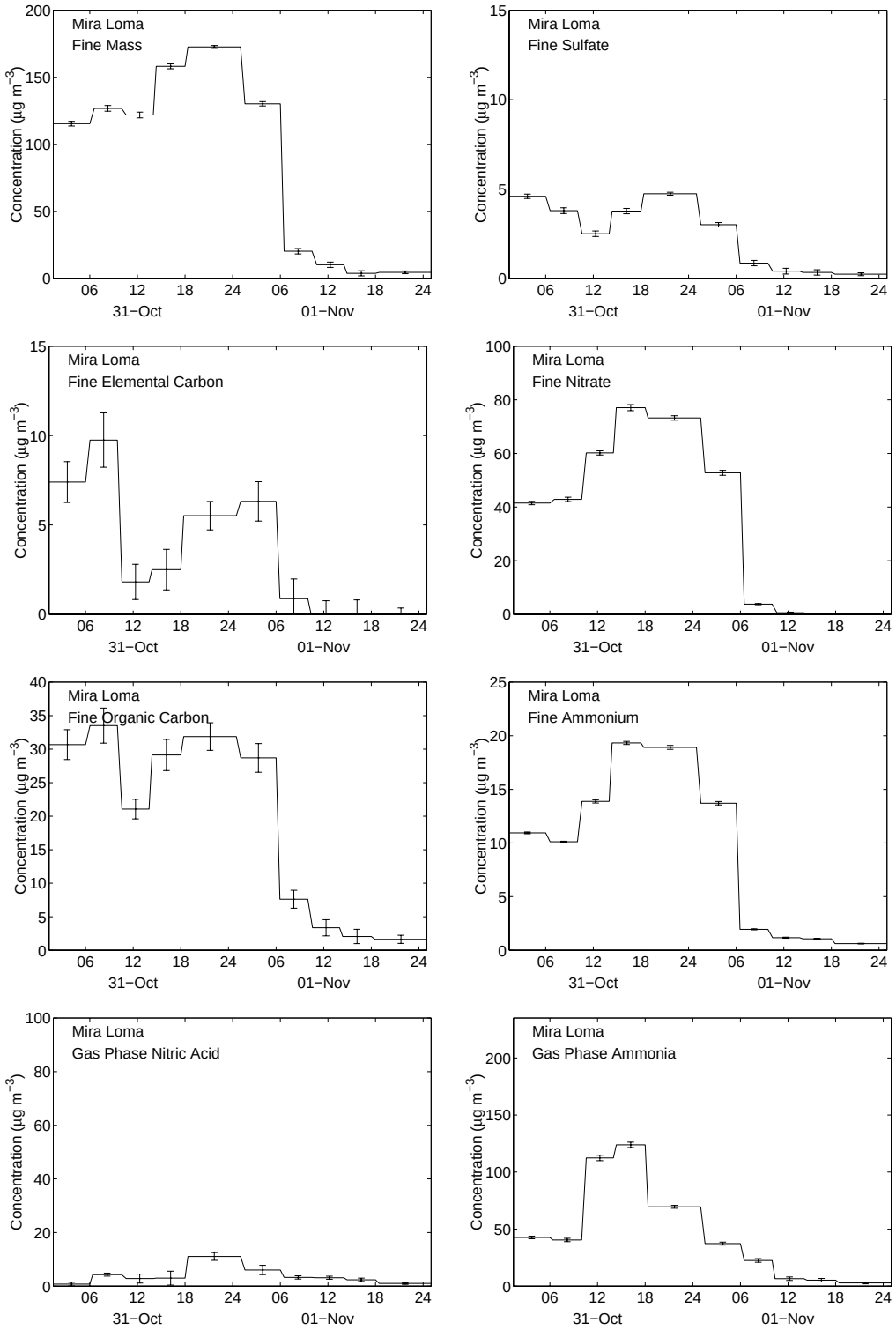

Figure 3.7: Fine particle ($PM_{1.9}$) and gas-phase results for individual species measured during the October 31-November 2, 1997, sampling event at Mira Loma.

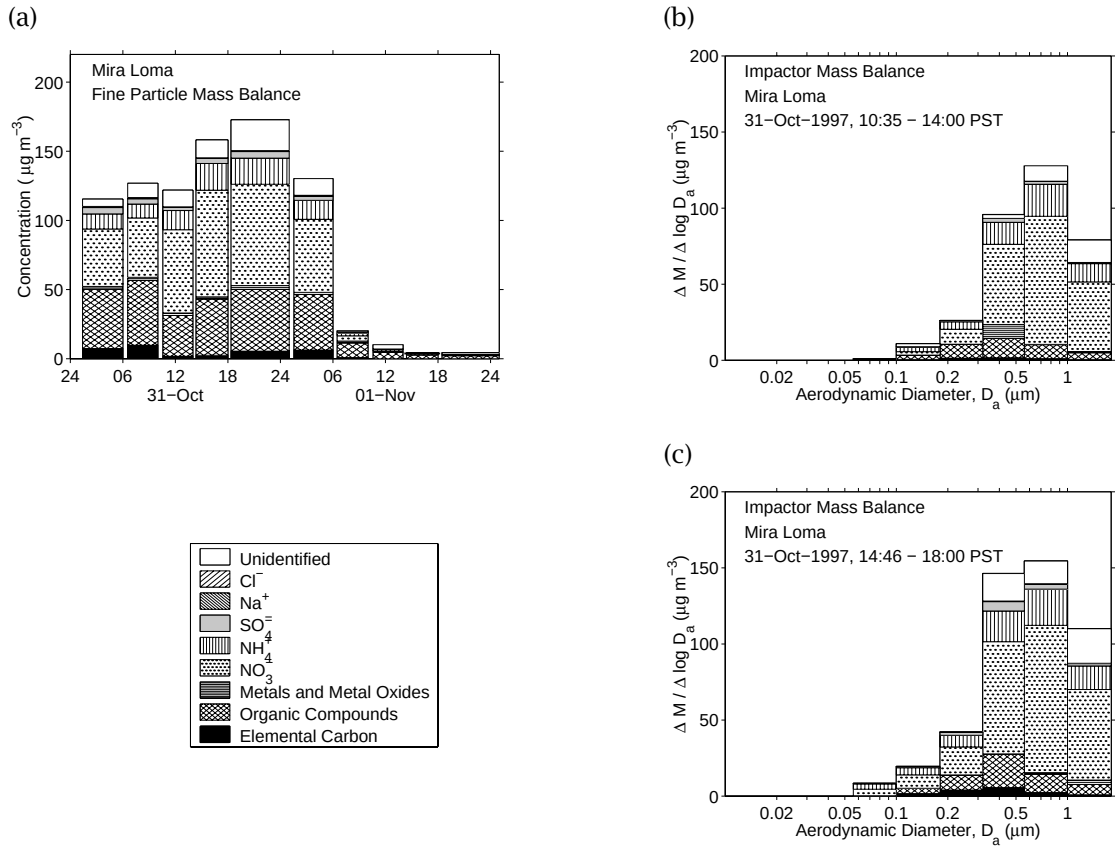

Figure 3.8: Fine particle concentration and chemical composition at Mira Loma. (a) Bulk fine particle ($PM_{1.9}$) concentrations and chemical compositions measured during the October 31-November 2, 1997, sampling event. (b) Size-resolved fine particle mass distribution and chemical composition measured on October 31, 1997, during the 1000-1400 PST sampling period. (c) Size-resolved fine particle mass distribution and chemical composition measured on October 31, 1997, during the 1400-1800 PST sampling period.

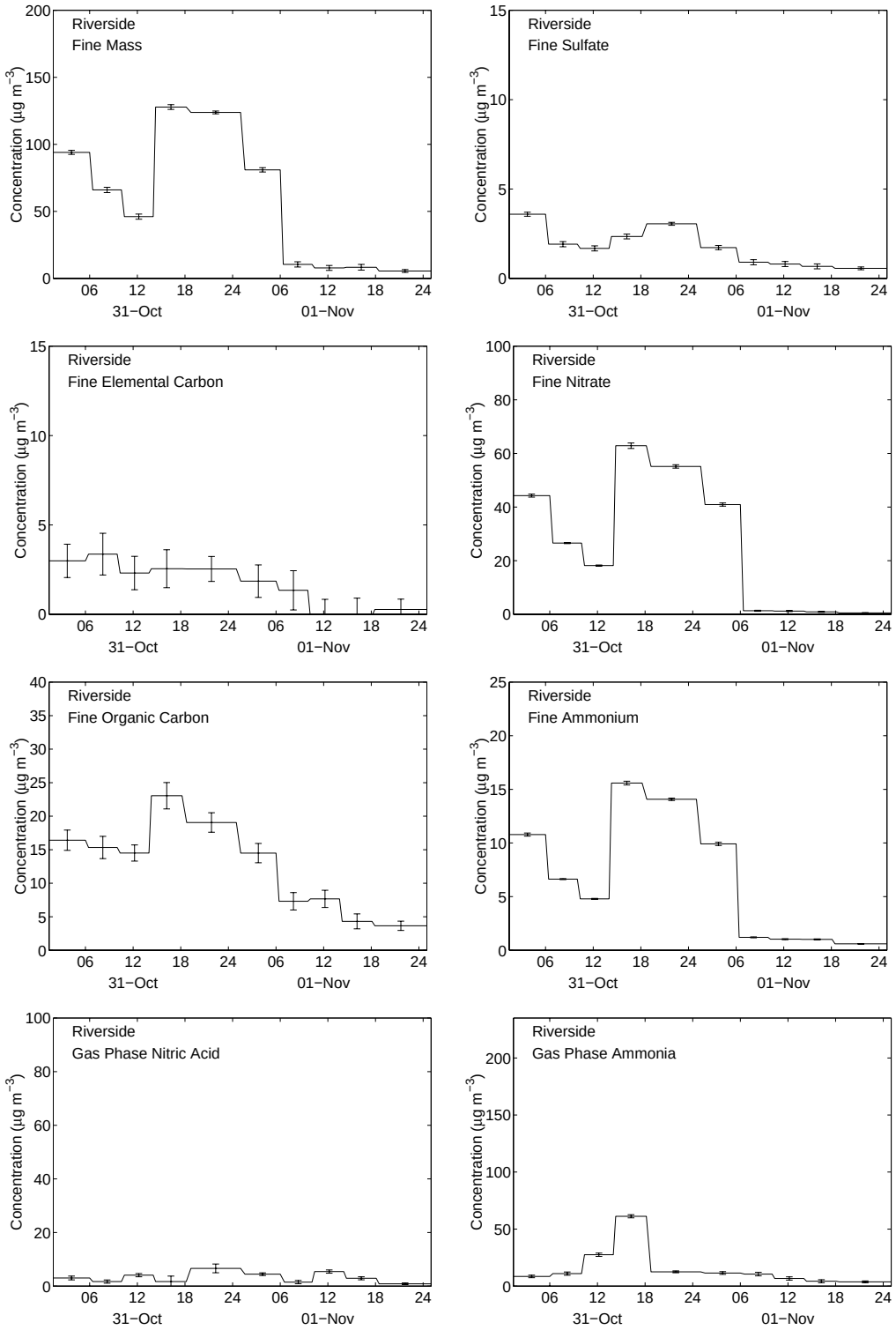

Figure 3.9: Fine particle ($PM_{1.9}$) and gas-phase results for individual species measured during the October 31-November 2, 1997, sampling event at Riverside.

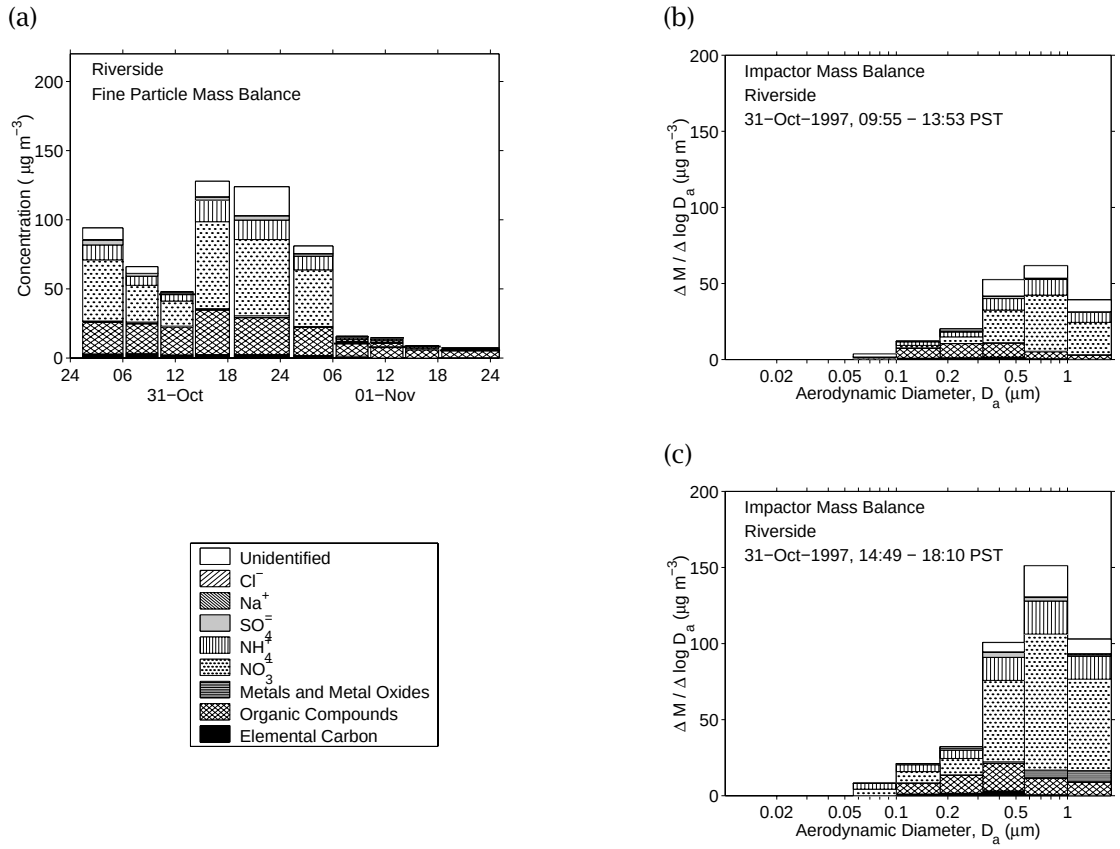

Figure 3.10: Fine particle concentration and chemical composition at Riverside. (a) Bulk fine particle ($PM_{1.9}$) concentrations and chemical compositions measured during the October 31-November 2, 1997, sampling event. (b) Size-resolved fine mass distribution and chemical composition measured on October 31, 1997, during the 1000-1400 PST sampling period. (c) Size-resolved fine mass distribution and chemical composition measured on October 31, 1997, during the 1400-1800 PST sampling period.

additional ammonium nitrate accumulation on particles larger than 0.3 μm aerodynamic diameter.

3.3.3 Evolution Along Air Parcel Trajectories

Several air parcel trajectories during the October 31-November 2 sampling event passed over or near two of the three air monitoring stations in succession, allowing a comparison of the pollutant concentrations and aerosol populations within single air parcels as pollutants age in the presence of continuing emissions and dry deposition.

The first of these air parcel trajectories to be discussed is shown in Figure 3.11a; each open circle indicates the air parcel location at successive hours during transport across the air basin. Trajectory analysis shows that an air parcel passing within 5 km of Diamond Bar between 0830-0930 hours PST on October 31 later was advected across the ammonia sources in the Chino dairy area and arrived within 5 km of the Mira Loma site between 1800-2200 PST later that day. Study of particle evolution within this air parcel provides direct insight into the effect of transport across the largest ammonia source area in Southern California. A material balance on the nitrogen-containing pollutants within this air parcel is shown in Figure 3.11b. The air parcel begins its travels that morning at Diamond Bar with more than 100 μg N m^{-3} present as NO and lesser quantities of NO_2; nitric acid concentrations initially are close to zero while excess NH_3 is still present in the gas phase, indicating that NH_4NO_3 present at Diamond Bar is limited by the amount of inorganic nitrate (e.g. HNO_3) available to form aerosol. During transport from Diamond Bar to Mira Loma, Figure 3.11b shows that NO is converted to NO_2; that same reaction system will lead eventually to NO_2 oxidation to form additional nitric acid. Ammonia concentrations increase by more than a factor of 5 between Diamond Bar and Mira Loma as the air parcel passes over the local ammonia sources. The additional ammonia drives the additional HNO_3 formed into the particle phase and aerosol nitrate concentrations increase, as shown in Figure 3.11c.

Trajectory analysis also shows that the air parcels stagnating near the Riverside air monitoring station in the early morning hours (0100-0800 PST) of November 1 previously passed slowly near the monitoring station at Mira Loma approximately 24 hours earlier, on October 31 from about 0100-0700 hours PST. This air parcel path is shown in Figure 3.12a; again, each open circle indicates the air parcel location at successive hours. This air parcel was over land for approximately 3 days before arriving at Mira Loma, and was over land for 4 days before arriving at Riverside.

Figures 3.12b, c, and d show a material balance on the nitrogen-containing pollutant, fine particulate matter ($PM_{1.9}$), and PM_{10} concentrations present over time within that air parcel. NH_3 concentrations

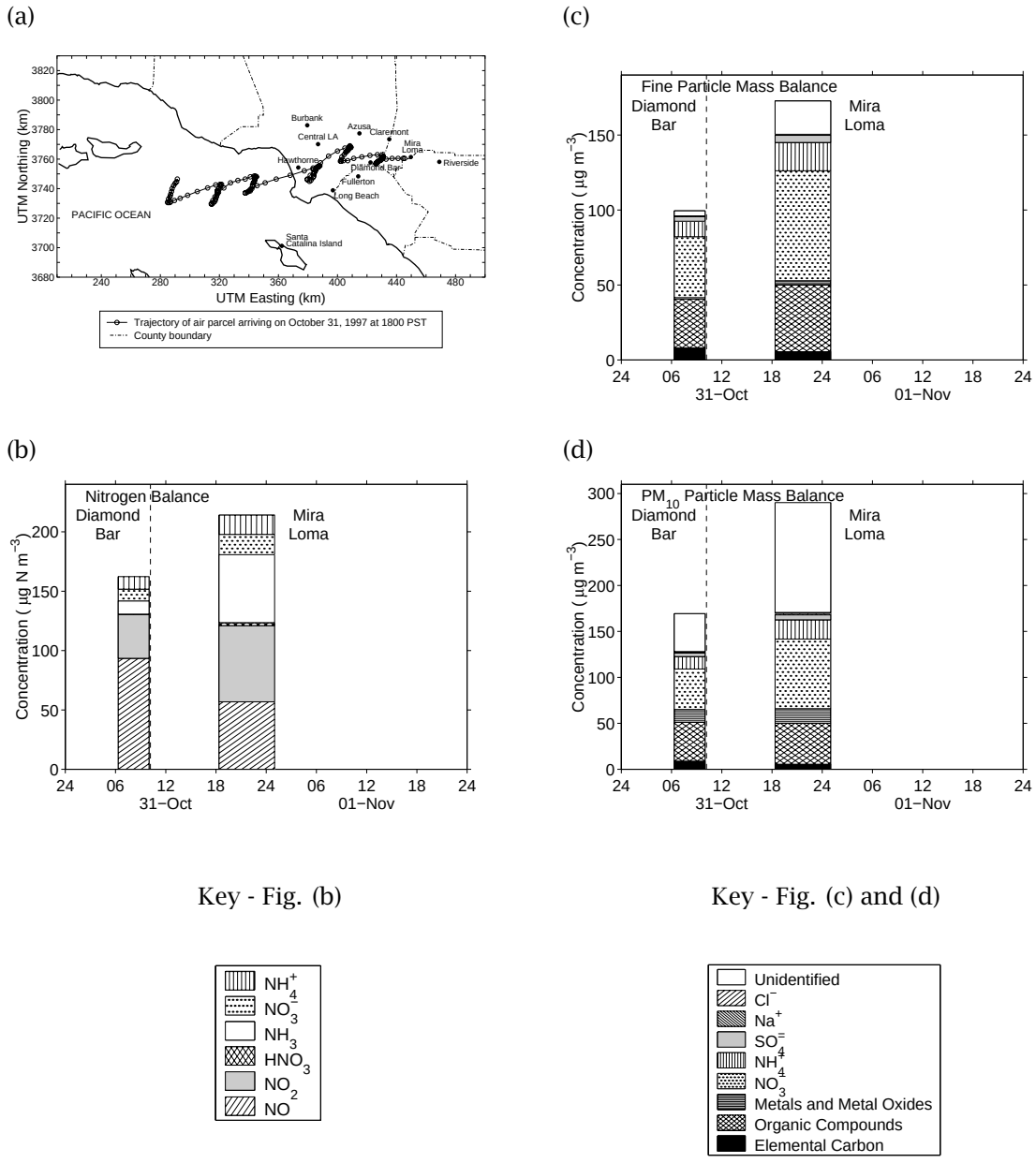

Figure 3.11: Aerosol evolution along the trajectory between Diamond Bar and Mira Loma, October 31-November 1, 1997. a) Representative air parcel trajectory reaching Mira Loma at 1800 PST November 1, 1997. The air parcel passed within 5 km of Diamond Bar at 0830-0930 PST on October 31 before being transported to near Mira Loma during 1800-2200 PST later that day. Each circle represents an elapsed hour. b) Nitrogen balance, c) Fine particle ($PM_{1.9}$) mass balance, and d) PM_{10} mass balance.

at Riverside decreased to about 25% of the concentration present at Mira Loma, within the NH_3 source area. This NH_3 concentration decrease is consistent with the dilution expected as one moves away from the virtual point source of ammonia in the Chino dairy area (see Russell et al. [30]). NO_3^- and NH_4^+ concentrations are approximately the same at both Mira Loma and Riverside, reflecting a balance between NH_4NO_3 aerosol formation versus pollutant dispersion and dry deposition. PM_{10} mass decreased proportionally more than fine particle mass; the 24-h transit time facilitated depositional losses of PM_{10}.

A final perspective on the aerosol nitrate formation problem in the South Coast Air Basin can be gained from Figure 3.13. That figure shows a nitrogen balance on the air masses over consecutive time periods at all three air monitoring sites over the October 31-November 2 sampling period. Generally, NO and NO_2 concentrations are much higher than either HNO_3 concentrations or aerosol nitrate concentrations. Thus the precursor gases needed for more HNO_3 production are available in abundance. Excess ammonia is present at most times, thus any HNO_3 formed usually will be driven quickly into the aerosol phase. Although the aerosol nitrate concentrations are small relative to the total nitrogen burden in the atmosphere, the resulting NH_4NO_3 aerosol is large in comparison to both other aerosol species as well as the fine particle air quality standards recently proposed by the US EPA.

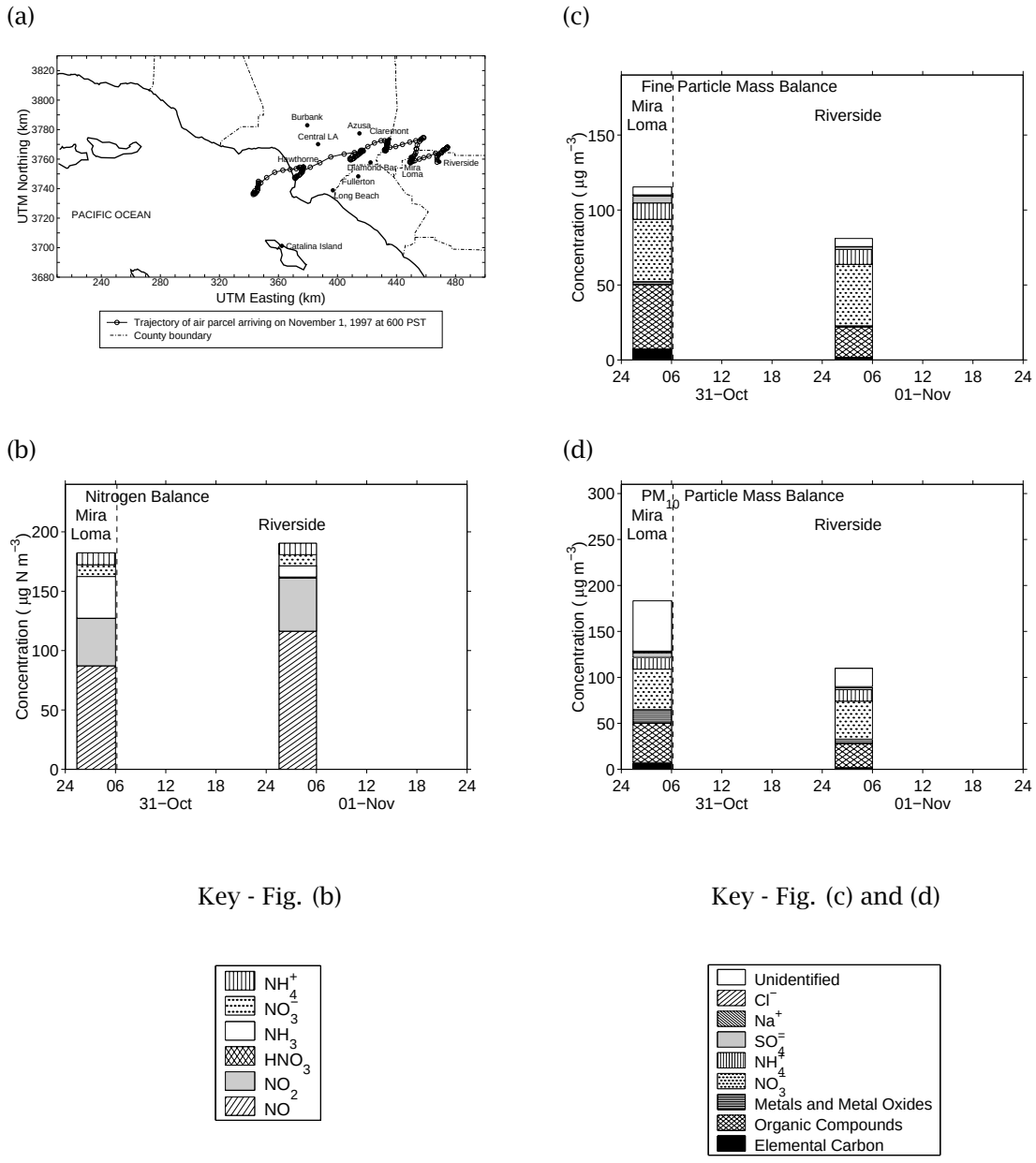

Figure 3.12: Aerosol evolution along the trajectory between Mira Loma and Riverside, October 31-November 1, 1997. a) Representative air parcel trajectory reaching Riverside at 0600 PST November 1, 1997. Air parcel passed within 5 km of Mira Loma during 0100-0700 PST on October 31 before passing within 5 km of Riverside during 0100-0800 PST on November 1. Each circle represents an elapsed hour. b) Nitrogen balance, c) Fine particle ($PM_{1.9}$) mass balance, and d) PM_{10} mass balance.

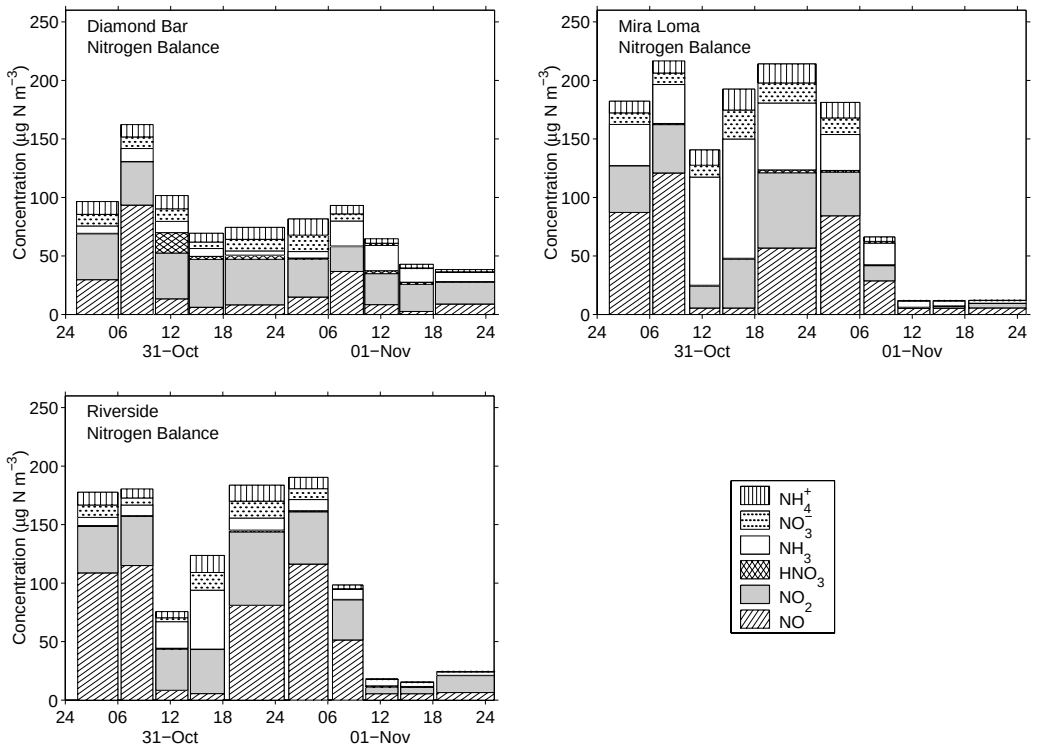

Figure 3.13: Nitrogen balances at the three sites monitored during the October 31-November 2, 1997, sampling event.

Chapter 4

Caldecott Tunnel Study

4.1 Introduction

Vehicle emissions make substantial contributions, both directly and indirectly, to atmospheric particle concentrations. Direct contributions include particulate emissions from tailpipes, brake lining wear, and tire wear. Indirect contributions include the emission of reactive gases, both organic and inorganic, which form secondary particulate matter via atmospheric transformations. In a recent estimate for the Los Angeles basin in September 1996, primary particles emitted from motor vehicles contributed 9–11% of the fine particle mass concentrations [5]. Some compounds emitted by motor vehicles in the gas phase can contribute to aerosol mass when transformed by atmospheric chemical reactions. These gas-to-particle conversion products include nitrate, sulfate, and ammonium ions as well as organic compounds. Gas-to-particle conversion products due to the emissions from all mobile plus stationary sources in the Los Angeles area contributed 37–65% of the fine particle mass during the 1996 case study reference above; these products include transformed species originally emitted from motor vehicles as organic vapors, NO_x, SO_2 and NH_3. In addition, paved road dust reentrained into the atmosphere by vehicle traffic accounted for 5–10% of the atmospheric fine particle mass concentration during the 1996 study period.

Air quality models that simulate atmospheric pollutant transport and chemical reaction are used to calculate these and similar estimates of source contributions to atmospheric particulate matter. Motor vehicle emission inventories normally used in these models are derived from tailpipe emissions measurements conducted on motor vehicles operated over simulated driving cycles on a chassis

dynamometer. Source tests to determine the particulate matter size distribution and chemical composition are difficult and expensive to conduct; thus the number of vehicles tested to date is relatively small. Further, conventional chassis dynamometer tests do not measure non-tailpipe emissions including those from tire and brake wear.

An alternative to single vehicle emissions measurements is to measure the emissions from a large population of on-road vehicles as they are driven through a highway tunnel. Particulate matter emissions measurements made in highway tunnels are of particular interest to the present study [39, 40, 28, 41]. Over the years 1970–1979, Pierson and colleagues measured gas and particulate pollutant emissions in the Allegheny and Tuscarora Mountain Tunnels of the Pennsylvania Turnpike [39]. They measured 35 analytes collected on filter samples and attributed emissions to either light-duty or heavy-duty vehicles. The particulate mass emission rate calculated for the heavy-duty vehicles observed during 10 studies in the period 1970–79 was 870 mg km^{-1} compared to 25 mg km^{-1} for light-duty vehicles. The most important contributor to aerosol mass in these studies was carbonaceous particles from the heavy-duty trucks. In 1993 Weingartner et al. measured fine particle emissions in the Gubrist Tunnel near Zurich, Switzerland [40]. They measured fine particle mass emission rates of 383.5 mg km^{-1} for heavy-duty vehicles, and 8.53 mg km^{-1} for light-duty vehicles. In 1993, Fraser, Cass and Simoneit measured emissions in the Los Angeles area Van Nuys Tunnel [28]. Fine particle mass emission rates for a mixed vehicle fleet composed of 4% heavy-duty and 96% light-duty vehicles were 491 mg l^{-1} of fuel burned in the tunnel. This emission rate can be converted to 78 mg km^{-1} using the authors' estimated fleet-averaged fuel economy [4]. The main components of fine particle mass in the Van Nuys Tunnel were carbonaceous species and NH_4NO_3; the NH_4NO_3 was likely formed in the tunnel from the reaction of background HNO_3 with NH_3 emitted by the vehicles. In the summer of 1997 Kirchstetter et al. measured fine particle emissions in the Caldecott Tunnel, four months before the present study [41]. These authors calculated fine particle mass emission factors of 2.5 g kg^{-1} of fuel burned in the tunnel for heavy-duty diesel trucks and 0.11 g kg^{-1} of fuel burned for light-duty vehicles. Using the fuel and fleet fuel economy data recommended by these authors, these emission factors are equivalent to 990 and 9.8 mg km^{-1} for heavy-duty diesel trucks and light-duty vehicles, respectively. Comparison between the 1997 Caldecott Tunnel and the 1970–79 Pennsylvania Turnpike tunnel experiments does not show the significant reduction in the emissions from heavy-duty diesel trucks that in fact has been achieved over the past two decades. This is due in part to the fact that the Caldecott Tunnel has a 4.2% upward sloping grade which is expected to increase emissions over those measured in earlier years in tunnels where the road bed is more nearly level.

In the present work we report ammonia and primary particle emissions measurements made during November 1997 from the vehicle fleet traveling through the Caldecott Tunnel that connects Berkeley, CA, and Orinda, CA. The emissions from approximately 37500 vehicles were sampled during four experiments, each of 3-hours duration. Measurements were made of fine particle ($D_a < 1.9\ \mu m$) and PM_{10} mass, carbonaceous particulate matter, inorganic ion, and trace element concentrations in the tunnel and at a background site. From these concentration data, emission rates were calculated per liter of fuel consumed and per kilometer driven. Further, size-segregated fine aerosol samples were collected using cascade impactors from which the size distributions of major chemical species emitted in the tunnel were determined. In addition, ammonia emission rates were determined per liter of fuel consumed and per kilometer driven. These measurements provide a complete set of size-segregated data on the chemical composition of fine particle emissions measured in a traffic tunnel. We can then compare these results with selected measurements made in other tunnel studies. During the same experiments, Professor Kimberly Prather's research group from the University of California, Riverside (UCR) measured the composition of single particles in the tunnel using aerosol time-of-flight mass spectrometry [42]. These single particle data will be reported by UCR.

The Caldecott Tunnel is divided into separate bores, one which carries light-duty vehicle traffic and one which carries a mixture of light- and heavy-duty vehicles. From experiments conducted in both bores, estimates are made of emissions rates and particle chemical composition extrapolated to the 100% light-duty and 100% heavy-duty vehicle fleets.

4.2 Experimental Methods

4.2.1 Sample Collection

The Caldecott Tunnel consists of three two-lane bores, running east—west between Berkeley, CA and Orinda, CA, on a major commuting corridor into San Francisco. The tunnel is approximately 1.1 km long and slopes upward from west to east with a grade of approximately 4.2% [43]. Ventilation shafts run the length of the tunnel bores. The tunnel bores are equipped with fans for forced ventilation; the fans were not operated during these experiments. Bore 1 carries mixed light-duty vehicle (LDV) and heavy-duty vehicle (HDV) traffic from west to east, and Bore 3 carries mixed vehicle traffic from east to west. Only LDVs are legally permitted to travel through Bore 2 in the direction of the prevailing flow of traffic; i.e., westward in the morning, and eastward in the afternoon and evening. Thus, the eastbound

Table 4.1: Caldecott Tunnel Sampling Events

Date	Time (PST)	Location	Vehicle Counts[a]	
			Light Duty	Heavy Duty
17 Nov 97	1200–1500	Bore 1	5657	342
18 Nov 97	1200–1500	Bore 1[b]	5978	436
19 Nov 97	1530–1830	Bore 2	12681	30
20 Nov 97	1530–1830	Bore 2[c]	12406	31

[a]Vehicle counts provided by Prof. Deborah Niemeir at the University of California, Davis.
[b]Only fine particle filters operated at background site.
[c]Only fine particle and PM_{10}filters operated at background site.

traffic in the afternoon is driven uphill under load and is segregated by vehicle type in Bores 1 and 2, such that Bore 1 contains a mix of LDVs and HDVs, whereas Bore 2 contains almost exclusively LDVs plus a few stray HDVs that defy the rules (see Table 4.1). Since approximately 7% of the HDV traffic during the study actually uses the light-duty vehicle bore of the tunnel, we place "LDV Only" in quotes when referring to Bore 2 of the tunnel. The emissions from HDVs are much greater than those from LDVs, thus the stray HDVs in Bore 2 have an important influence on the results and interpretations of this study which is taken into account in analysis of these data.

Pollutant concentrations in the tunnel bores were measured with a suite of sampling equipment positioned inside the ventilation shaft located directly above the roadway at a site approximately 50 m from the eastern exit of Bores 1 and 2. The equipment consisted of one filter sampler to collect PM_{10} samples, three fine particle filter samplers, and two cascade impactors (see Figure 2.3). An identical suite of sampling equipment was operated concurrently at an outdoor background site in order to measure the outdoor pollutant concentrations. This site was located south of the East Fan house, approximately 400 m from the eastern exit of the tunnel.

Particles were sampled from Bore 1 (containing both LDVs and HDVs) during the period of highest expected HDV traffic, from 1200 to 1500 hours PST, on November 17 and 18, 1997 (see Table 4.1). Particles were sampled from Bore 2 of the tunnel ("LDV Only") during the period of highest expected LDV traffic, from 1530 to 1830 PST, on November 19 and 20, 1997. Background air samplers were operated concurrently.

The sampling equipment was identical to that used in the ambient aerosol sampling program of the 1997 Southern California Ozone Study and is fully described in Section 2.2.1 and Appendix B; an abbreviated description of the equipment is presented here.

In the PM_{10} samplers, air was drawn at a rate of 16.7 l min^{-1} through an EPA-approved low volume

PM_{10} inlet (Andersen Instruments, Smyrna, GA) and distributed between two parallel filter holders. A polytetrafluoroethylene (PTFE) filter was used to collect particulate matter for gravimetric and inorganic species analyses. A quartz fiber filter was used to collect particles for aerosol carbon and organic species analyses. In each of three fine particle samplers, ambient air was drawn at a nominal flow rate of 28 l min^{-1} through acid-washed Pyrex glass inlet lines. The air then passed through a PTFE-coated AIHL-design cyclone separator which removed particles with aerodynamic diameters larger than 1.9 μm [18]. Following the cyclone, the airstream of one sampler was split in half and ducted to one PTFE filters and one quartz fiber filter arranged in parallel. In the second fine particle sampler, the airstream was split in half and ducted to two quartz fiber filters in parallel. A denuder difference system was used to measure gas-phase reactive chlorine and "nitric acid" concentrations in the third fine particle sampler; samples were collected on one PTFE filter at 14 l min^{-1} and two parallel nylon filters at 7 l min^{-1} each, one of which was downstream of a MgO coated tubular denuder [44]. We caution the reader that there may be interferences (e.g. from HONO) that affect the HNO_3 measurements within a highway tunnel that would not be encountered when measurements are made in outdoor air. An open-faced filter stack also was operated at 10 l min^{-1} to collect gas-phase ammonia. This consisted of a PTFE filter to remove aerosol particles followed by two glass fiber filters in series which had been impregnated with oxalic acid [44]. The air flow rate across each filter was controlled by a critical orifice downstream of the filter. Actual flow rates were measured with a calibrated rotameter at the beginning and end of each sampling period.

Two cascade impactors were operated at each sampling site. These were 10 stage micro-orifice impactors (MOI) manufactured by MSP Corporation (Minneapolis, MN) [19]. Each MOI was preceded by an AIHL-design cyclone separator which removed particles larger than 1.8 μm. Ambient air was drawn through the impactor sampling systems at a nominal flow rate of 30 L min^{-1}. Pressures at impactor stages 5 and 10 were monitored and the flow rate controlled to maintain the pressure on these stages within the instrument design values. The actual flow rate through the impactors was subsequently determined from pressure drop measurements made across a calibrated orifice (MSP Corporation). In order to avoid sample contamination, no coatings were applied to the impaction substrates. Coarse particles were removed by the cyclone separators because these larger particles may be more likely to bounce off their intended impaction stage and contaminate the fine particle samples. Samples collected on impactor stages 5 though 10 and the afterfilter were analyzed; these stages have designed lower aerodynamic diameter, D_a, cut-offs of 1.0, 0.56, 0.32, 0.18, 0.1, and 0.056 μm. One MOI was equipped with polytetrafluoroethylene (PTFE) impaction substrates (47 mm diameter, Gelman Teflo, 1.0 μm pore

size) for gravimetric, ionic species, and elemental analysis. The other MOI was equipped with 47 mm diameter aluminum foil substrates supplied by MSP Corporation and baked at 550°C for at least 8 hours. The aluminum foil substrates were used to collect samples for determination of mass, organic carbon, and elemental carbon.

4.2.2 Sample Analyses

Methods for chemical analysis of samples were identical to those used in the aerosol sampling program of the 1997 Southern California Ozone Study. That work is fully described elsewhere Section 2.2.2; abbreviated descriptions of the analytical methods are presented here.

PTFE filters and impaction substrates were weighed before and after sampling using a mechanical microgram balance with a 1 μg sensitivity (Mettler Instruments, Model M-5S-A) to determine aerosol mass concentrations gravimetrically. The filters and impaction substrates were equilibrated at a temperature of 22.9±0.3°C and a relative humidity of 48±3% for 4 or 24 hours prior to weighing.

PTFE and oxalic acid coated glass-fiber filters were extracted into deionized water. The nylon filters were extracted in a buffer solution. Concentrations of the major ionic species, $SO_4^=$, NO_3^-, and Cl^-, in the extracts were determined using a Dionex Model 2020i ion chromatograph. Filter extracts were also analyzed for ammonium ion (NH_4^+) by an indophenol colorimetric procedure employing a rapid flow analyzer (Alpkem Corp., RFA-300 TM). Gas phase nitric acid concentrations were determined by the denuder difference method [44]. Ammonia concentrations were determined from the oxalic acid-impregnated filters by the colorimetric procedure described previously for aerosol NH_4^+.

Elemental carbon (EC) and organic carbon (OC) concentrations in the aerosol samples were measured by a thermal-optical technique [20, 21]. Prior to sample collection, these filters were heat treated at 550°C in air for at least 8 hours to lower their carbon blank levels. EC and OC analyses of aluminum impaction substrates were performed in a similar manner according to the procedures described by Kleeman et al. [45]. These media also were heat treated prior to use at 550°C in air for 48 hours. Organic matter concentrations were estimated from measured organic carbon concentrations by multiplying by a factor of 1.2 to account for the additional mass of associated H, O, N, and S present in typical atmospheric organic aerosols.

The concentrations of 39 major and minor trace elements were measured by instrumental neutron activation analysis [26]. These elements were Al, As, Au, Ba, Br, Ce, Cs, Cd, Cl, Co, Cr, Eu, Fe, Ga, Hg, In,

K, La, Lu, Mg, Mo, Mn, Na, Nd, Rb, Sb, Sc, Se, Sm, Sr, Ta, Tb, Th, Ti, U, V, Yb, Zn, and Zr. The elements Ta, Tb, and Zr were not found in any of the tunnel samples.

All concentration values reported here have been blank corrected by subtracting the appropriate field blank concentrations, and the variances were estimated by adding the field blank and sample concentration variances.

4.3 Results and Discussion

4.3.1 Particle Concentrations

Particulate matter samples were collected from the Caldecott Tunnel with three types of samplers; filter samplers with a 10 μm D_a cutoff (PM_{10}), filter samplers with a 1.9 μm D_a cutoff ($PM_{1.9}$), and microorifice impactors (MOI). Using the impactors, size-segregated fine particulate matter was collected in 6 size ranges below 1.8 μm aerodynamic diameter with lower D_a cutoffs at 1.0, 0.56, 0.32, 0.18, 0.1, and 0.056 μm plus an afterfilter. Particle mass concentrations measured inside the tunnel were significantly elevated relative to background concentrations in all the samples. For example, the average $PM_{1.9}$ mass concentration in Bore 1 was 102 μg m^{-3}, and 32 μg m^{-3} in Bore 2, while the average background $PM_{1.9}$ mass concentration was 7.1 μg m^{-3}.

Aerosol concentration data for the remainder of this section are reported as background-subtracted concentrations with analytical uncertainties calculated from the sum of the tunnel and background sample variances. $PM_{1.9}$ background samples were collected on every day of the study. PM_{10} samples were collected at the background site on 3 days of the 4 days studied (see Table 4.1). Day to day variations in PM_{10} background concentrations were found to be significantly greater than analytical uncertainties, therefore PM_{10} data from days when background samples were not collected are not included in the background-subtracted concentrations. Impactor samples were collected at the background site on 2 of the 4 study days. Fine particle background concentrations were found to be similar from day to day within analytical uncertainties, therefore average background concentrations were subtracted from impactor data on days that background impactor samples were not collected. The original data can be found in Appendix D.

The background-subtracted mass concentrations measured for the aerosol samples in each experiment are shown in Tables 4.2, 4.3, and 4.4. Aerosol mass measurements in the same tunnel bore on

different days agree within experimental error. The sum of aerosol mass measured on the impactor stages is significantly lower than that collected on the fine particle filter. One cause for this difference is that the impactor afterfilters which collect particles smaller than 0.056 μm were quartz filters which cannot be analyzed gravimetrically.

Concentrations of elemental carbon and organic material in the tunnel also were measured. Duplicate measurements in the tunnel bores agree within the experimental error. For elemental carbon the sum of impactor sample concentrations agrees with the fine filter sample within experimental error. The organic matter concentrations measured in impactor samples are systematically lower than those measured on filters; this is discussed at length in Appendix A. The PM_{10} and $PM_{1.9}$ concentrations of organic matter are identical within experimental error, indicating that the particulate organics emissions are dominated by fine particles. The impactor sample measurements can be used to show the relative distribution of organic matter with particle size. The 0.1–0.18 μm particle size fraction has the highest concentration of both elemental carbon and organic matter. This is in agreement with laboratory measurements of gasoline and diesel vehicle emissions [32].

Aerosol concentrations of the inorganic ions NH_4^+, NO_3^-, and $SO_4^=$ were measured (see Tables 4.2 and 4.3). The concentrations of certain of these species are below detection limits in some of the filter samples as well as in many of the impactor samples. In those cases where there are sufficient data to compare duplicate measurements, these data generally agree within experimental error. As discussed below, substantial gas phase NH_3 emissions were observed in the Caldecott Tunnel. The apparent emissions of aerosol NH_4^+ and NO_3^- are likely influenced by the formation of secondary particulate matter within the tunnel from the reaction of gas phase NH_3 with HNO_3. The molar charge concentrations measured in the fine aerosol on November 17, 1997, were 0.042, 0.022, and 0.042 μmol m^{-3} for NH_4^+, NO_3^-, and $SO_4^=$, respectively. The excess of negative ions may be due to an acidic aerosol or the kinetics of gas-particle conversion reactions. The presence of aerosol $SO_4^=$ in higher concentrations in Bore 1 suggests that HDVs emit primary sulfates.

Aerosol concentrations of the trace elements Al, As, Au, Ba, Br, Cd, Ce, Cl, Co, Cr, Cs, Eu, Fe, Ga, Hg, In, K, La, Lu, Mg, Mn, Mo, Na, Nd, Rb, Sb, Sc, Se, Sm, Sr, Th, Ti, U, V, Tb, and Zn were measured. Elements which were detected at concentrations significantly greater than zero in at least one sample are listed in Tables 4.2 and 4.3.

Mass balances constructed for the aerosol samples show that the majority of the PM_{10} mass in the tunnel is carbonaceous (see Figure 4.1). Elemental carbon is the largest contributor to PM_{10} in Bore 1

Table 4.2: PM_{10} Concentrations in the Caldecott Tunnel ($\mu g\ m^{-3}$)

	Bore 1 (LDV and HDV)						Bore 2 ("LDV only")					
	17 Nov 97			18 Nov 97			19 Nov 97			20 Nov 97		
Mass	**128.54**	±	**6.99**	-			**30.32**	±	**6.58**	**42.62**	±	**6.63**
Organic Compounds	**45.15**	±	**10.26**	-			**21.38**	±	**9.21**	**22.65**	±	**9.18**
Elemental Carbon	**72.92**	±	**6.64**	-			**21.80**	±	**6.06**	**20.49**	±	**5.93**
NH_4^+	**5.46**	±	**0.28**	-			**4.64**	±	**0.27**	**4.78**	±	**0.27**
NO_3^-	0.72	±	1.18	-			0.40	±	1.17	0.62	±	1.16
$SO_4^=$	**3.15**	±	**0.86**	-			1.10	±	0.85	0.68	±	0.84
Al	0.7477	±	1.0418	-			0.2039	±	0.9897	0.3419	±	0.9835
Ba		-		-				-		**0.2708**	±	**0.0646**
Cr	**0.0804**	±	**0.0145**	-			-0.0086	±	0.0108	**0.0236**	±	**0.0115**
Fe		-		-			**2.2902**	±	**0.8491**		-	
Hg	0.000046	±	0.000200	-				-		**0.000438**	±	**0.000154**
La	0.001062	±	0.001113	-			0.000551	±	0.001097	0.000656	±	0.001088
Mg	0.3855	±	0.3086	-			0.2353	±	0.2398	0.2665	±	0.2984
Mn	0.04253	±	0.02179	-			0.01652	±	0.02149	0.02925	±	0.02130
Na	0.1045	±	0.1398	-			**0.3703**	±	**0.1482**	**0.3292**	±	**0.0476**
Sb	**0.025722**	±	**0.003890**	-			**0.017563**	±	**0.003552**	**0.031971**	±	**0.003989**
Sc	0.000083	±	0.000180	-			0.000057	±	0.000165	0.000083	±	0.000167
V	0.001562	±	0.003540	-			0.001618	±	0.003145	0.001982	±	0.003121
Zn	**1.9351**	±	**0.5404**	-			-0.2115	±	0.4773	0.4104	±	0.4718

Table 4.3: Fine Particle Concentrations in the Caldecott Tunnel ($\mu g\ m^{-3}$)

	Bore 1 (LDV and HDV)				Bore 2 ("LDV only")			
	17 Nov 97	18 Nov 97	19 Nov 97	20 Nov 97				
Mass	**89.79** ± **4.71**	**87.10** ± **4.70**	**34.45** ± **3.33**	**29.29** ± **3.31**				
Organic Compounds	**37.01** ± **5.00**	**34.71** ± **4.83**	**16.82** ± **3.03**	**15.73** ± **3.29**				
Elemental Carbon	**59.51** ± **4.14**	**39.50** ± **3.22**	**8.22** ± **1.93**	**6.65** ± **2.00**				
NH_4^+	**0.76** ± **0.08**	**0.88** ± **0.08**	**1.36** ± **0.08**	0.13 ± 0.08				
NO_3^-	**1.39** ± **0.36**	**2.07** ± **0.35**	0.20 ± 0.35	0.19 ± 0.36				
$SO_4^=$	**2.03** ± **0.25**	**1.89** ± **0.24**	**0.50** ± **0.25**	0.41 ± 0.26				
Al	**0.6027** ± **0.0673**	-0.0284 ± 0.0530	-0.0361 ± 0.0512	-0.1247 ± 0.0543				
Ba	**0.1109** ± **0.0143**	-	-	-0.0253 ± 0.0127				
Cr	-0.0256 ± 0.0078	-0.0372 ± 0.0044	-0.0035 ± 0.0022	-0.0056 ± 0.0027				
Fe	0.1976 ± 0.3965	-0.2059 ± 0.2664	-	**0.8855** ± **0.1220**				
Hg	**0.000634** ± **0.000121**	0.000075 ± 0.000073	0.000041 ± 0.000056	0.000044 ± 0.000070				
La	**0.000326** ± **0.000137**	**0.000207** ± **0.000059**	-	0.000076 ± 0.000056				
Mg	**0.3732** ± **0.1466**	-	0.0646 ± 0.0490	-0.0523 ± 0.0518				
Mn	**0.01897** ± **0.00057**	-0.00450 ± 0.00030	-	-0.00342 ± 0.00037				
Na	**0.2198** ± **0.0564**	-0.0395 ± 0.0199	**0.1566** ± **0.0404**	0.0240 ± 0.0195				
Sb	**0.005780** ± **0.001434**	-0.000178 ± 0.000173	**0.009258** ± **0.000747**	**0.004582** ± **0.001229**				
Sc	**0.000140** ± **0.000041**	0.000029 ± 0.000043	-0.000000 ± 0.000017	-0.000015 ± 0.000021				
V	**0.001833** ± **0.000449**	-0.000403 ± 0.000186	0.000018 ± 0.000255	-0.000604 ± 0.000162				
Zn	**0.1581** ± **0.0690**	0.0080 ± 0.0438	0.0282 ± 0.0281	-0.0834 ± 0.0368				

Table 4.4: Size-Segregated Aerosol Concentrations in the Caldecott Tunnel (μg m^{-3})

	Bore 1 (LDV and HDV)		Bore 2 ("LDV only")	
	17 Nov 97	18 Nov 97	19 Nov 97	20 Nov 97
$D_a = 1.8 - 1.0\mu$m				
Mass	**5.96 ± 1.77**	2.71 ± 1.46	0.28 ± 1.66	-1.10 ± 1.47
Organic Compounds	2.32 ± 1.22	**1.83 ± 0.81**	0.34 ± 1.13	0.09 ± 0.74
Elemental Carbon	**3.11 ± 0.49**	**2.56 ± 0.30**	0.17 ± 0.38	0.15 ± 0.24
$D_a = 1.0 - 0.56\mu$m				
Mass	2.52 ± 1.71	1.57 ± 1.60	-0.32 ± 1.83	-1.17 ± 1.52
Organic Compounds	**4.68 ± 1.26**	**2.24 ± 0.80**	0.98 ± 1.14	0.60 ± 0.73
Elemental Carbon	**2.72 ± 0.48**	**2.96 ± 0.31**	0.41 ± 0.38	0.46 ± 0.24
$D_a = 0.56 - 0.32\mu$m				
Mass	**9.11 ± 1.76**	**8.04 ± 1.59**	2.66 ± 1.72	0.76 ± 1.50
Organic Compounds	**4.44 ± 1.30**	**3.24 ± 0.84**	1.70 ± 1.14	1.26 ± 0.75
Elemental Carbon	**8.08 ± 0.71**	**7.80 ± 0.42**	**1.11 ± 0.39**	**1.50 ± 0.25**
$D_a = 0.32 - 0.18\mu$m				
Mass	**12.61 ± 1.71**	**11.27 ± 1.50**	**3.54 ± 1.75**	1.57 ± 1.53
Organic Compounds	**3.89 ± 1.23**	**2.95 ± 0.82**	1.17 ± 1.14	**1.78 ± 0.76**
Elemental Carbon	**9.09 ± 0.76**	**9.32 ± 0.47**	**1.76 ± 0.44**	**2.06 ± 0.27**
$D_a = 0.18 - 0.1\mu$m				
Mass	**21.07 ± 1.74**	**20.78 ± 1.51**	**7.11 ± 1.68**	**8.14 ± 1.49**
Organic Compounds	**5.39 ± 1.32**	**5.07 ± 0.91**	**4.23 ± 1.25**	**2.92 ± 0.79**
Elemental Carbon	**15.54 ± 1.07**	**14.94 ± 0.62**	**3.64 ± 0.51**	**3.76 ± 0.30**
$D_a = 0.1 - 0.056\mu$m				
Mass	**14.61 ± 1.80**	**13.80 ± 1.54**	3.36 ± 1.72	**3.20 ± 1.49**
Organic Compounds	**3.94 ± 1.24**	**4.14 ± 0.89**	**3.27 ± 1.27**	1.51 ± 0.77
Elemental Carbon	**9.79 ± 0.79**	**10.32 ± 0.49**	**1.97 ± 0.43**	**1.56 ± 0.26**
$D_a < 0.056\mu$m				
Mass	-	-	-	-
Organic Compounds	**6.96 ± 1.36**	**6.52 ± 1.01**	**3.18 ± 1.08**	**3.62 ± 0.79**
Elemental Carbon	**5.43 ± 0.65**	**4.33 ± 0.38**	0.32 ± 0.44	**0.59 ± 0.28**

(HDV and LDV) and organic carbon is the largest contributor to PM_{10} in Bore 2 ("LDV Only"). Other important contributors to PM_{10} are NH_4^+, $SO_4^=$, Fe, and Zn. The majority of $PM_{1.9}$ also is carbonaceous (see Figure 4.2); as was the case for PM_{10}, elemental carbon is the largest contributor to $PM_{1.9}$ in Bore 1 (HDV and LDV) and organic carbon is the largest contributor in Bore 2 ("LDV Only"). Other important contributors to $PM_{1.9}$ are NH_4^+ and $SO_4^=$.

The unidentified mass shown in Figure 4.2 represents the difference between the gravimetrically determined mass concentration and the sum of the identified species. One source of this "unidentified mass" may be analytic uncertainty which is generally larger for the gravimetric mass measurements than for the chemical analyses. Other contributors to the unidentified mass are species which are not determined, most important among these are Ca and Si which are commonly present as their respective carbonates in the case of Ca and oxides in the case of Si in soil and road dust samples. Water retained in the samples at the weighing conditions ($\approx$ 48% RH) would also contribute to the unidentified mass. The horizontal bar drawn across the results in Figures 4.1 and 4.2 shows the gravimetrically determined mass concentration which in that case is lower than the sum of the identified species; again most probably due to the uncertainties in the gravimetric analysis.

The impactor samples also were analyzed to determine the size-resolved aerosol chemical composition (see Figure 4.3). Aerosol mass concentrations in both Bore 1 (HDV and LDV) and Bore 2 ("LDV Only") have peaks at 0.1–0.18 μm particle aerodynamic diameter. These peaks occur at a size similar to that recorded in recent dynamometer-based measurements of motor vehicle exhaust by Kleeman et al. [32]. In Bore 1, the peak is comparatively broader (0.056–0.56 μm) and composed mainly of elemental carbon with lesser amounts of organic material; ammonium and sulfate ions are present in most of the size fractions. In Bore 2, the peak is narrower and contains more organic material than elemental carbon. Data shown in Figure 4.3 for the afterfilter sample ($D_a < 0.056$ μm) should be viewed with caution since the quartz fiber filter is subject to a positive artifact due to the adsorption of organic vapors.

4.3.2 Aerosol Emissions

Aerosol concentration measurements can be used to calculate emission rates from the vehicle fleet in the tunnel. The emission rate of individual species i, $E_{C,i}$ per mass of carbon burned in the tunnel is a precise and directly-measured emission rate. This is similar to emission rates stated as pollutant mass emitted per volume fuel burned as recommended by Singer and Harley [46]. $E_{C,i}$ can be calculated from

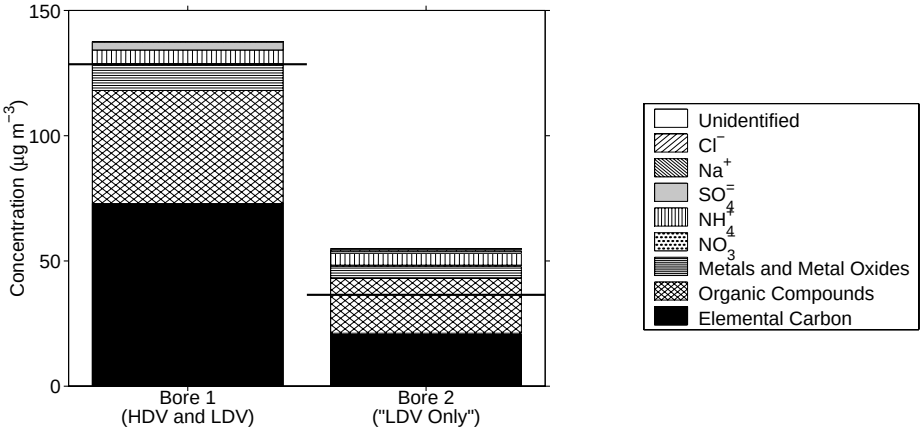

Figure 4.1: Mass balance on average PM_{10} concentrations in Bores 1 and 2 of the Caldecott Tunnel

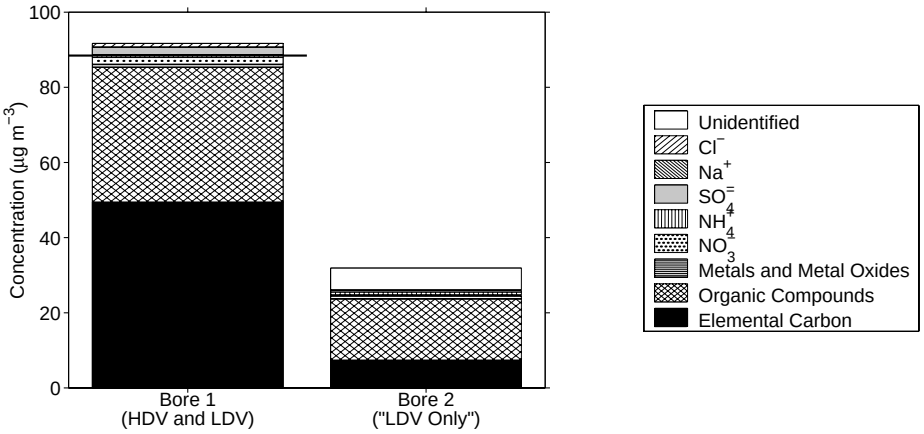

Figure 4.2: Mass balance on average fine particle concentrations in Bores 1 and 2 of the Caldecott Tunnel

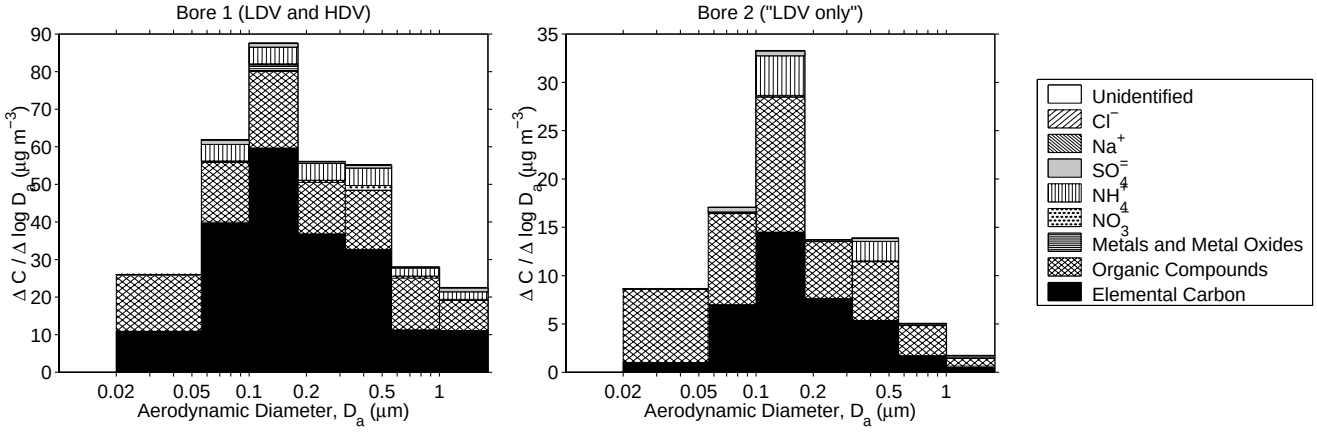

Figure 4.3: Size-segregated aerosol concentrations in the Caldecott Tunnel

a material balance on the carbon in the fuel burned as

$$E_{C,i} = \frac{\Delta C_i}{\sum_j \Delta C_{C,j}} \tag{4.1}$$

where ΔC_i is the increase in concentration of species i between the tunnel interior and outdoor background, $\Delta C_{C,j}$ is the increase in carbon concentration between the tunnel and background air due to species j. The increase in carbon concentration in the tunnel due to all species combined is a direct measure of fuel consumption and is calculated as

$$\sum_j \Delta C_{C,j} = \Delta[CO_2] + \Delta[CO] + \Delta[CH_4] + \Delta[\text{NMHC}] \tag{4.2}$$

where concentrations are expressed as carbon mass per unit air volume, and NMHC is the sum of gas-phase nonmethane hydrocarbons. Dr. Barbara Zielinska of the Desert Research Institute measured the concentrations of CO_2, CO, CH_4, and NMHC in the tunnel and background air as part of this study. Carbonaceous aerosol species are not included in this summation because they make a negligible contribution to $\sum_j \Delta C_{C,j}$.

The emission rates of most species are greater in the heavy-duty vehicle-influenced Bore 1 than in the "light-duty only" Bore 2. Possible reasons for this are differences between the bores in 1) the proportion of HDVs, 2) the composition of the LDV fleet, and 3) driving conditions. Bore 1 was sampled in the early afternoon (1200 to 1500 hours PST) while Bore 2 was sampled in the late afternoon (1530 to 1830 hours PST) during the homeward-bound commuter rush. The LDV fleet driven in the early afternoon may include a higher proportion of older or poorly maintained cars than the commuter vehicle fleet going home from work in the late afternoon. Driving conditions also differed between the early and late afternoon when there was a higher traffic density. Kirchstetter et al. measured vehicle speeds in the Caldecott Tunnel to be approximately 20 km h^{-1} faster in the early afternoon (1300 to 1500 hours PDT) than during rush hour (1600 to 1800 hours PDT) [47]. In the same study, LDV CO emissions per unit fuel burned declined from 1300 to 1800 hours PDT. We believe that the higher emission rates in Bore 1 are mostly due to the higher fraction of HDVs, although the different LDV fleet and higher average speeds in Bore 2 at different times of day may also have affected emissions.

Using the assumption that the differences in emission rates between Bores 1 and 2 are due entirely to the differences in the number of HDVs, one can estimate emission rates of species i for the LDV fleet, $E_{C,i}$(LDV), and the HDV fleet, $E_{C,i}$(HDV). These estimates are derived from a linear regression

analysis of the emission rates measured in the four experiments, j, as

$$E_{C,ij} = \phi_j E_{C,i}(\text{HDV}) + (1 - \phi_j) E_{C,i}(\text{LDV}) + \epsilon_{ij} \tag{4.3}$$

where $E_{C,ij}$ is the emission rate of species i per mass of carbon burned from the entire vehicle fleet measured in experiment j, ϕ_j is the fraction of carbon emitted by HDVs in the tunnel during experiment j, and ϵ_{ij} is the residual difference between predicted and observed values. $E_{C,i}(\text{LDV})$ and $E_{C,i}(\text{HDV})$ were estimated using the linear regression function implemented in the Matlab Statistics Package (The Mathworks, Natick, MA).

The fraction of carbon emitted by the HDV fleet was estimated from vehicle counts and fleet-averaged fuel consumption estimates as

$$\phi = \frac{\sum_{\text{HDV}} n_k U_k \rho_k w_k}{\sum_{\text{AllVehicles}} n_k U_k \rho_k w_k} \tag{4.4}$$

where n_k is the number of vehicles of type k, U_k is the fuel consumption (l km^{-1}), ρ_k is the fuel density (kg l^{-1}), and w_k is the weight fraction carbon in the fuel.

For vehicle fleet calculations, the fleet was divided into 4 types: diesel-powered trucks with 3 or more axles, diesel-powered trucks with 2 axles and 6 tires, gasoline-powered trucks with 2 axles and 6 tires, and vehicles with 2 axles and 4 tires. Vehicles with 3 or more axles and those with 2 axles and 6 tires were considered HDVs here. This separation follows that of Kirchstetter et al. [41], who recorded vehicle types and determined the type of fuel used from license plate surveys. They report that 39% of the HDVs in Bore 1 had 3 or more axles while only 4% of the HDVs in Bore 2 had 3 or more axles. Kirchstetter et al. also surveyed vehicle license plates and estimated that >99% of vehicles with 3 or more axles were diesel powered and that 50% of vehicles with 2 axles and 6 tires were diesel powered. We use the distributions of vehicle type and fuel use reported by Kirchstetter et al. to estimate the diesel-powered vehicle population in the fleet sampled here. The number of vehicles in each type were calculated by scaling the relative distribution of vehicle types measured by Kirchstetter et al. to match the vehicle counts made for this study. Note that, based on California Air Resource Board motor vehicle emission inventory program (MVEI7G) [48], the LDV fleet in Contra Costa County, CA, includes 1% diesel-powered vehicles and 28% light duty trucks.

Fuel consumption rates used were those measured in the uphill section of the Fort McHenry tunnel for which Pierson et al. report fuel economies of 4.8 and 23 mi gal^{-1} for the HDV and LDV fleets, respectively [49]. The uphill part of the Fort McHenry Tunnel has a 3.8% grade, similar to that for the

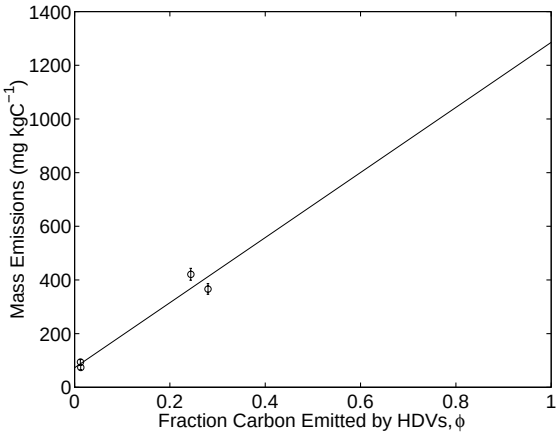

Figure 4.4: Linear regression to determine fine particulate mass emissions for the HDV and LDV fleets

Caldecott. Kirchstetter et al. sampled gasolines sold in the vicinity of the Caldecott Tunnel in 1997 [47]. They report w to be 0.85 and ρ to be 0.74 g cm^{-3} for these California Phase II reformulated gasoline samples. For diesel fuel we use 0.87 for w and 0.84 g cm^{-3} for ρ [41].

The measured and extrapolated emission rates for aerosol mass show the expected strong influence of HDVs on emissions (see Figure 4.4); emission data for other analytes show similar scatter. The uncertainties shown for the calculated values represent 69% confidence intervals; this interval was chosen to be comparable with the one standard deviation confidence interval shown for the laboratory analytical results. However, the linear regression analysis does not include analytical uncertainties. The LDV extrapolated fleet emission rates are generally not greater than zero with 95% confidence. However, the Bore 2 emission rates generally agree with the 100% LDV fleet emission rate estimates and are more accurate; these values can be used to place an upper limit on the LDV fleet emissions in place of the extrapolated values.

The majority of PM_{10} and $PM_{1.9}$ mass emitted by the HDV fleet is carbonaceous (see Figures 4.5 and 4.6). Elemental carbon is the largest component, and organic matter is the second largest component of these emissions. Other significant contributors to PM_{10} and $PM_{1.9}$ emissions by the HDV fleet are NH_4^+, NO_3^-, $SO_4^=$, Al, Cr, Mg, and Zn. Size-resolved aerosol emissions extrapolated to the condition of a 100% HDV fleet show a relatively broad peak (0.056–0.56 μm) which is composed mainly of elemental carbon with lesser amounts of organic material; ammonium and sulfate ions are present in most of the size fractions (see Figure 4.7). The PM_{10} and $PM_{1.9}$ mass emitted by the LDV fleet is much smaller than that emitted by the HDV fleet; the bar graphs for the LDV fleet in Figures 4.5 and 4.6 are scaled

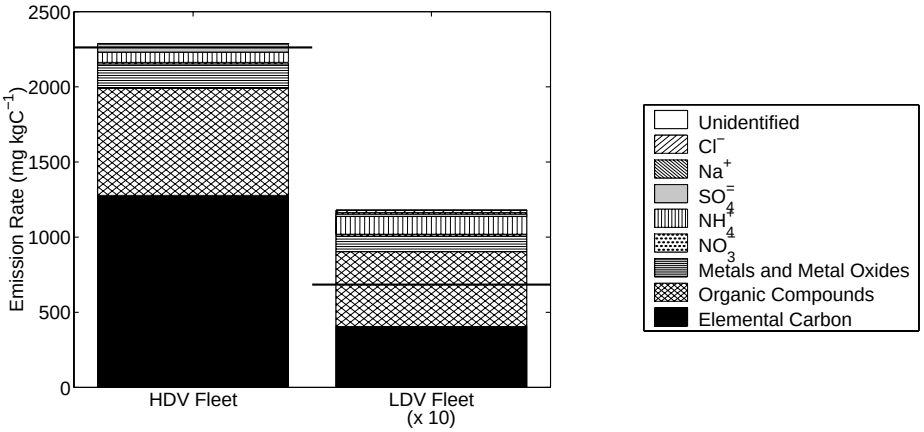

Figure 4.5: Mass balance on PM_{10} emissions for the HDV and LDV fleets

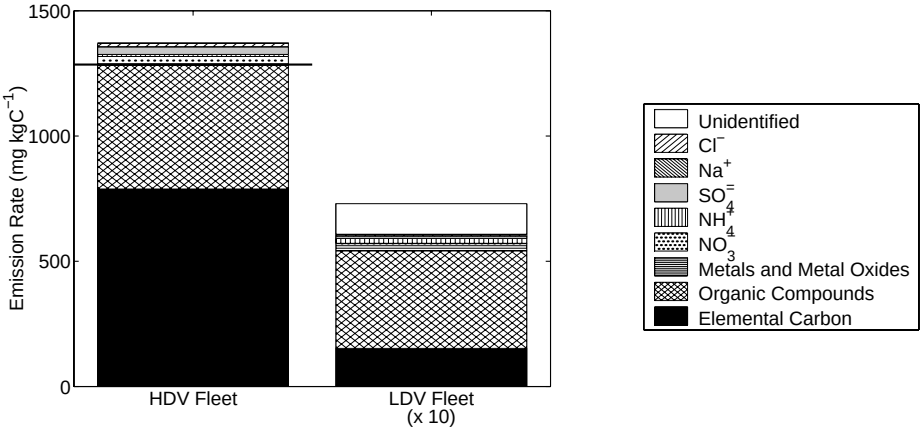

Figure 4.6: Mass balance on fine particle emissions for the HDV and LDV fleets

upward by a factor of 10 in order to display the chemical composition data. PM_{10} emissions per kg carbon burned from the LDV fleet are approximately 30 times lower than the HDV fleet; LDV $PM_{1.9}$ emissions are not significantly different from zero. The largest component of LDV fleet emissions is organic compounds. Fine particle elemental carbon emissions by the LDV fleet are not significantly different from zero in a statistical sense. The size-resolved aerosol emissions from the LDV fleet are not graphed because none of these were significantly different from zero outside of organic material in the sub-0.18 μm aerodynamic diameter particle size range.

It is convenient to convert emission rates stated on the basis of carbon burned, $E_{C,i}$, to emission rates stated on the basis of a fuel volume consumed or distance driven. Emissions of species i on a gasoline-equivalent fuel-volume basis, $E_{V,i}$ were calculated as

$$E_{V,i} = \rho w E_{C,i} \tag{4.5}$$

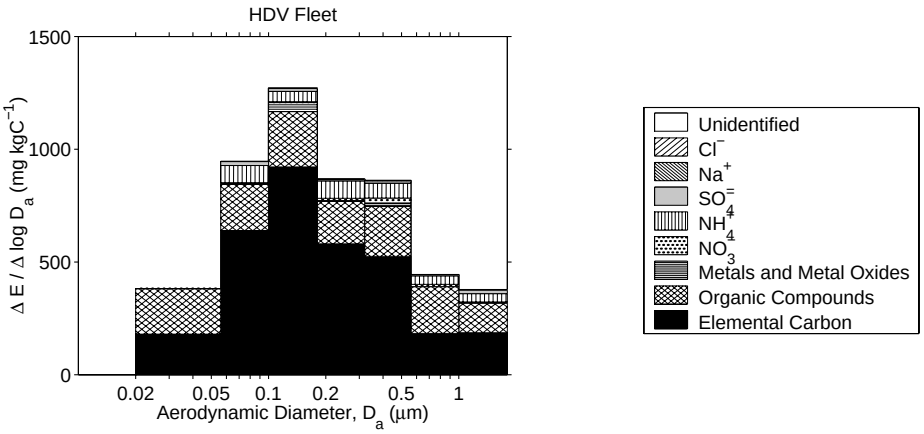

Figure 4.7: Mass balance on size-segregated aerosol emissions estimated for the heavy-duty vehicle fleet in the Caldecott Tunnel

where ρ and w are values for gasoline. Emission rates per volume of gasoline-equivalent fuel burned in Bores 1 and 2 and extrapolated to 100% HDV and LDV fleets are reported in Tables 4.5, 4.6, and 4.7. Emissions of species i on a distance-driven basis, $E_{D,i}$ were calculated as

$$E_{D,i} = \overline{U\rho w} E_{C,i} \tag{4.6}$$

where $\overline{U\rho w}$ is the product of fuel consumption, density, and carbon content averaged across vehicle types weighted by distance traveled by vehicles of each type calculated as

$$\overline{U\rho w} = \frac{\sum_{\text{AllVehicles}} n_k U_k \rho_k w_k}{\sum_{\text{AllVehicles}} n_k} \tag{4.7}$$

Emission rates per distance driven are reported in Tables 4.8, 4.9, and 4.10 based on the fuel economy estimates stated previously. Note that the emissions in mg km^{-1} represent the particular driving conditions in the Caldecott Tunnel; specifically, the emissions from warm vehicles driving at steady highway speeds up a fairly steep grade.

Emission rates also can be extrapolated to a fleet of 100% heavy-duty diesel powered versus all other vehicles. The fraction of carbon emitted by diesel-powered vehicles was calculated from an equation analogous to 4.4 and the emissions data regressed using Equation 4.3. Emission rates on a fuel volume consumed basis were calculated using Equation 4.5 (see Tables 4.11–4.13). Emission rates on a distance traveled basis were calculated using Equations 4.6 and 4.7 using the previously stated fuel economy values (see Tables 4.14–4.16).

As for the HDV fleet overall, the majority of PM_{10} and $PM_{1.9}$ mass emitted by the heavy-duty diesel

Table 4.5: PM_{10} Emissions on a Gasoline-Equivalent Fuel Basis in the Caldecott Tunnel (mg l^{-1})

	Measured						Calculated					
	Bore 1 (LDV and HDV)			Bore 2 ("LDV Only")			100% HDV			100% LDV		
Mass	**379.31**	±	**20.62**	**60.29**	±	**7.77**	**1423.01**	±	**98.41**	**43.06**	±	**15.14**
Organic Compounds	**133.22**	±	**30.29**	**36.57**	±	**10.82**	**449.36**	±	**5.18**	**31.36**	±	**0.80**
Elemental Carbon	**215.18**	±	**19.60**	**35.21**	±	**7.06**	**803.87**	±	**33.99**	**25.50**	±	**5.23**
NH_4^+	**16.11**	±	**0.82**	**7.83**	±	**0.32**	**43.20**	±	**2.36**	**7.38**	±	**0.36**
NO_3^-	2.12	±	3.49	0.85	±	1.37	**6.27**	±	**1.95**	**0.78**	±	**0.30**
$SO_4^=$	**9.31**	±	**2.54**	1.49	±	0.99	**34.89**	±	**5.37**	1.06	±	0.83
Al	2.2065	±	3.0742	0.4498	±	1.1613	**7.9547**	±	**1.2447**	0.3548	±	0.1915
Ba		-		**0.4342**	±	**0.1036**		-			-	
Cr	**0.2372**	±	**0.0428**	0.0115	±	0.0131	**0.9756**	±	**0.3374**	-0.0007	±	0.0519
Fe		-		**3.9458**	±	**1.4629**		-			-	
Hg	0.000136	±	0.000589	**0.000702**	±	**0.000247**		-			-	
La	0.003135	±	0.003283	0.001001	±	0.001286	**0.010117**	±	**0.000624**	**0.000886**	±	**0.000096**
Mg	1.1376	±	0.9107	0.4164	±	0.3161	**3.4968**	±	**0.1278**	**0.3774**	±	**0.0197**
Mn	0.12551	±	0.06431	0.03768	±	0.02519	**0.41295**	±	**0.11796**	0.03293	±	0.01815
Na	0.3083	±	0.4125	**0.5829**	±	**0.1332**	-0.5911	±	0.7099	**0.5978**	±	**0.1092**
Sb	**0.075903**	±	**0.011479**	**0.040763**	±	**0.004426**	0.191032	±	0.135593	0.038849	±	0.020859
Sc	0.000244	±	0.000532	0.000115	±	0.000195	**0.000667**	±	**0.000222**	**0.000108**	±	**0.000034**
V	0.004609	±	0.010447	0.002983	±	0.003688	**0.009931**	±	**0.002509**	**0.002895**	±	**0.000386**
Zn	**5.7104**	±	**1.5946**	0.1469	±	0.5587	**23.9183**	±	**6.5274**	-0.1542	±	1.0041

Table 4.6: Fine Particle Emissions on a Gasoline-Equivalent Fuel Basis in the Caldecott Tunnel (mg l^{-1})

	Measured				Calculated			
	Bore 1 (LDV and HDV)		Bore 2 ("LDV Only")		100% HDV		100% LDV	
Mass	**247.82**	± **9.33**	**53.16**	± **3.91**	**808.56**	± **149.11**	45.91	± 31.77
Organic Compounds	**100.56**	± **9.76**	**27.10**	± **3.71**	**311.11**	± **65.85**	24.53	± 14.03
Elemental Carbon	**140.10**	± **7.44**	**12.42**	± **2.31**	**495.87**	± **209.08**	9.57	± 44.54
NH_4^+	**2.29**	± **0.16**	**1.28**	± **0.10**	5.27	± 5.05	1.23	± 1.08
NO_3^-	**4.79**	± **0.70**	0.33	± 0.42	**18.19**	± **1.66**	0.08	± 0.35
$SO_4^=$	**5.51**	± **0.49**	**0.76**	± **0.30**	**19.13**	± **3.96**	0.59	± 0.84
Al	**0.8518**	± **0.1216**	-0.1311	± 0.0620	3.2647	± 4.6690	-0.1012	± 0.9948
Ba	**0.3272**	± **0.0421**	-0.0406	± 0.0203	-	-	-	
Cr	-0.0871	± 0.0129	-0.0075	± 0.0029	-0.3255	± 0.0275	-0.0031	± 0.0059
Fe	0.0190	± 0.6832	**1.4199**	± **0.1957**	-4.4622	± 4.9605	1.5633	± 1.2818
Hg	**0.001034**	± **0.000203**	0.000071	± 0.000074	0.003437	± 0.004226	0.000094	± 0.000900
La	**0.000756**	± **0.000217**	0.000123	± 0.000089	0.002453	± 0.002716	0.000129	± 0.000702
Mg	**1.1014**	± **0.4325**	0.0137	± 0.0593	**4.6575**	± **1.2868**	-0.0448	± 0.1980
Mn	**0.02203**	± **0.00093**	-0.00548	± 0.00059	0.07812	± 0.38578	-0.00135	± 0.09969
Na	**0.2721**	± **0.0873**	**0.1541**	± **0.0382**	0.4287	± 1.8771	0.1789	± 0.3999
Sb	**0.008293**	± **0.002128**	**0.011649**	± **0.001177**	-0.005925	± 0.044564	0.012497	± 0.009495
Sc	**0.000245**	± **0.000083**	-0.000013	± 0.000023	0.000915	± 0.000871	-0.000011	± 0.000186
V	**0.002171**	± **0.000707**	-0.000469	± 0.000255	0.008276	± 0.016179	-0.000329	± 0.003447
Zn	**0.2439**	± **0.1172**	-0.0425	± 0.0382	0.9699	± 1.2139	-0.0375	± 0.2586

Table 4.7: Size-Segregated Aerosol Emissions on a Gasoline-Equivalent Fuel Basis in the Caldecott Tunnel (mg l^{-1})

	Measured		Calculated	
	Bore 1 (LDV and HDV)	Bore 2 ("LDV Only")	100% HDV	100% LDV
$D_a = 1.8 - 1.0\mu m$				
Mass	**12.38 ± 3.25**	-0.64 ± 1.85	47.85 ± 29.25	-0.80 ± 6.23
Organic Compounds	**5.84 ± 2.09**	0.36 ± 1.14	**21.37 ± 6.58**	0.20 ± 1.40
Elemental Carbon	**7.98 ± 0.83**	0.27 ± 0.38	**29.93 ± 8.16**	0.02 ± 1.74
$D_a = 1.0 - 0.56\mu m$				
Mass	5.80 ± 3.29	-1.21 ± 1.99	**25.51 ± 10.53**	-1.39 ± 2.24
Organic Compounds	**9.87 ± 2.13**	1.32 ± 1.15	32.93 ± 21.32	1.25 ± 4.54
Elemental Carbon	**7.94 ± 0.81**	0.72 ± 0.38	**29.02 ± 2.91**	0.41 ± 0.62
$D_a = 0.56 - 0.32\mu m$				
Mass	**24.10 ± 3.35**	2.90 ± 1.91	**84.68 ± 21.74**	2.19 ± 4.63
Organic Compounds	**10.83 ± 2.21**	**2.48 ± 1.15**	**34.14 ± 13.58**	2.29 ± 2.89
Elemental Carbon	**22.25 ± 1.18**	**2.16 ± 0.40**	**80.25 ± 14.25**	1.39 ± 3.04
$D_a = 0.32 - 0.18\mu m$				
Mass	**33.54 ± 3.21**	**4.31 ± 1.94**	**117.18 ± 28.43**	3.31 ± 6.06
Organic Compounds	**9.65 ± 2.11**	**2.44 ± 1.16**	**29.82 ± 11.18**	2.26 ± 2.38
Elemental Carbon	**25.75 ± 1.28**	**3.17 ± 0.43**	**91.28 ± 12.72**	2.25 ± 2.71
$D_a = 0.18 - 0.1\mu m$				
Mass	**58.59 ± 3.25**	**12.64 ± 1.88**	**191.21 ± 32.27**	10.89 ± 6.88
Organic Compounds	**14.66 ± 2.29**	**5.99 ± 1.25**	**39.42 ± 10.65**	**5.70 ± 2.27**
Elemental Carbon	**42.70 ± 1.78**	**6.15 ± 0.50**	**148.02 ± 27.08**	4.78 ± 5.77
$D_a = 0.1 - 0.056\mu m$				
Mass	**39.83 ± 3.36**	**5.46 ± 1.90**	**138.71 ± 27.04**	4.20 ± 5.76
Organic Compounds	**11.30 ± 2.17**	**4.03 ± 1.25**	**32.38 ± 8.60**	**3.73 ± 1.83**
Elemental Carbon	**28.11 ± 1.33**	**2.94 ± 0.43**	**101.32 ± 12.43**	1.89 ± 2.65
$D_a < 0.056\mu m$				
Mass	-	-	-	-
Organic Compounds	**18.90 ± 2.41**	**5.65 ± 1.13**	**56.86 ± 12.15**	**5.19 ± 2.59**
Elemental Carbon	**13.75 ± 1.09**	0.74 ± 0.44	**50.65 ± 15.06**	0.35 ± 3.21

Table 4.8: PM_{10} Emissions on a Distance Driven Basis in the Caldecott Tunnel (mg km^{-1})

	Measured				Calculated			
	Bore 1 (LDV and HDV)		Bore 2 ("LDV Only")		100% HDV		100% LDV	
Mass	**49.29** ± **2.68**		**6.23** ± **0.80**		**755.96** ± **52.28**		**4.40** ± **1.55**	
Organic Compounds	**17.31** ± **3.94**		**3.78** ± **1.12**		**238.72** ± **2.75**		**3.21** ± **0.08**	
Elemental Carbon	**27.96** ± **2.55**		**3.64** ± **0.73**		**427.04** ± **18.06**		**2.61** ± **0.53**	
NH_4^+	**2.09** ± **0.11**		**0.81** ± **0.03**		**22.95** ± **1.25**		**0.76** ± **0.04**	
NO_3^-	0.28 ± 0.45		0.09 ± 0.14		**3.33** ± **1.04**		**0.08** ± **0.03**	
$SO_4^=$	**1.21** ± **0.33**		0.15 ± 0.10		**18.53** ± **2.85**		0.11 ± 0.08	
Al	0.2867 ± 0.3995		0.0465 ± 0.1200		**4.2258** ± **0.6612**		0.0363 ± 0.0196	
Ba	-		**0.0449** ± **0.0107**		-		-	
Cr	**0.0308** ± **0.0056**		0.0012 ± 0.0014		**0.5183** ± **0.1792**		-0.0001 ± 0.0053	
Fe	-		**0.4077** ± **0.1511**		-		-	
Hg	0.000018 ± 0.000077		**0.000073** ± **0.000026**		-		-	
La	0.000407 ± 0.000427		0.000103 ± 0.000133		**0.005374** ± **0.000331**		**0.000091** ± **0.000010**	
Mg	0.1478 ± 0.1183		0.0430 ± 0.0327		**1.8577** ± **0.0679**		**0.0386** ± **0.0020**	
Mn	0.01631 ± 0.00836		0.00389 ± 0.00260		**0.21938** ± **0.06266**		0.00337 ± 0.00186	
Na	0.0401 ± 0.0536		**0.0602** ± **0.0138**		-0.3140 ± 0.3771		**0.0611** ± **0.0112**	
Sb	**0.009864** ± **0.001492**		**0.004212** ± **0.000457**		0.101483 ± 0.072032		0.003973 ± 0.002133	
Sc	0.000032 ± 0.000069		0.000012 ± 0.000020		**0.000354** ± **0.000118**		**0.000011** ± **0.000003**	
V	0.000599 ± 0.001358		0.000308 ± 0.000381		**0.005276** ± **0.001333**		**0.000296** ± **0.000039**	
Zn	**0.7421** ± **0.2072**		0.0152 ± 0.0577		**12.7063** ± **3.4676**		-0.0158 ± 0.1027	

Table 4.9: Fine Particle Emissions on a Distance Driven Basis in the Caldecott Tunnel (mg km^{-1})

	Measured				Calculated			
	Bore 1 (LDV and HDV)		Bore 2 ("LDV Only")		100% HDV		100% LDV	
Mass	**32.20**	± **1.21**	**5.49**	± **0.40**	**429.54**	± **79.21**	4.70	± 3.25
Organic Compounds	**13.07**	± **1.27**	**2.80**	± **0.38**	**165.27**	± **34.98**	2.51	± 1.43
Elemental Carbon	**18.21**	± **0.97**	**1.28**	± **0.24**	**263.42**	± **111.07**	0.98	± 4.56
NH_4^+	**0.30**	± **0.02**	**0.13**	± **0.01**	2.80	± 2.68	0.13	± 0.11
NO_3^-	**0.62**	± **0.09**	0.03	± 0.04	**9.66**	± **0.88**	0.01	± 0.04
$SO_4^=$	**0.72**	± **0.06**	**0.08**	± **0.03**	**10.16**	± **2.10**	0.06	± 0.09
Al	**0.1107**	± **0.0158**	-0.0135	± 0.0064	1.7343	± 2.4803	-0.0104	± 0.1017
Ba	**0.0425**	± **0.0055**	-0.0042	± 0.0021		-		-
Cr	-0.0113	± 0.0017	-0.0008	± 0.0003	-0.1729	± 0.0146	-0.0003	± 0.0006
Fe	0.0025	± 0.0888	**0.1467**	± **0.0202**	-2.3705	± 2.6352	0.1599	± 0.1311
Hg	**0.000134**	± **0.000026**	0.000007	± 0.000008	0.001826	± 0.002245	0.000010	± 0.000092
La	**0.000098**	± **0.000028**	0.000013	± 0.000009	0.001303	± 0.001443	0.000013	± 0.000072
Mg	**0.1431**	± **0.0562**	0.0014	± 0.0061	**2.4743**	± **0.6836**	-0.0046	± 0.0202
Mn	**0.00286**	± **0.00012**	-0.00057	± 0.00006	0.04150	± 0.20494	-0.00014	± 0.01020
Na	**0.0354**	± **0.0113**	**0.0159**	± **0.0039**	0.2278	± 0.9972	0.0183	± 0.0409
Sb	**0.001078**	± **0.000277**	**0.001204**	± **0.000122**	-0.003147	± 0.023674	0.001278	± 0.000971
Sc	**0.000032**	± **0.000011**	-0.000001	± 0.000002	0.000486	± 0.000463	-0.000001	± 0.000019
V	**0.000282**	± **0.000092**	-0.000048	± 0.000026	0.004397	± 0.008595	-0.000034	± 0.000353
Zn	**0.0317**	± **0.0152**	-0.0044	± 0.0039	0.5152	± 0.6449	-0.0038	± 0.0265

Table 4.10: Size-Segregated Aerosol Emissions on a Distance Driven Basis in the Caldecott Tunnel (mg km^{-1})

	Measured		Calculated	
	Bore 1 (LDV and HDV)	Bore 2 ("LDV Only")	100% HDV	100% LDV
$D_a = 1.8 - 1.0\mu m$				
Mass	**1.61 ± 0.42**	-0.07 ± 0.19	25.42 ± 15.54	-0.08 ± 0.64
Organic Compounds	**0.76 ± 0.27**	0.04 ± 0.12	**11.35 ± 3.50**	0.02 ± 0.14
Elemental Carbon	**1.04 ± 0.11**	0.03 ± 0.04	**15.90 ± 4.33**	0.00 ± 0.18
$D_a = 1.0 - 0.56\mu m$				
Mass	0.75 ± 0.43	-0.13 ± 0.21	**13.55 ± 5.59**	-0.14 ± 0.23
Organic Compounds	**1.28 ± 0.28**	0.14 ± 0.12	17.49 ± 11.33	0.13 ± 0.46
Elemental Carbon	**1.03 ± 0.11**	0.07 ± 0.04	**15.42 ± 1.54**	0.04 ± 0.06
$D_a = 0.56 - 0.32\mu m$				
Mass	**3.13 ± 0.44**	0.30 ± 0.20	**44.99 ± 11.55**	0.22 ± 0.47
Organic Compounds	**1.41 ± 0.29**	**0.26 ± 0.12**	**18.14 ± 7.21**	0.23 ± 0.30
Elemental Carbon	**2.89 ± 0.15**	**0.22 ± 0.04**	**42.63 ± 7.57**	0.14 ± 0.31
$D_a = 0.32 - 0.18\mu m$				
Mass	**4.36 ± 0.42**	**0.45 ± 0.20**	**62.25 ± 15.10**	0.34 ± 0.62
Organic Compounds	**1.25 ± 0.27**	**0.25 ± 0.12**	**15.84 ± 5.94**	0.23 ± 0.24
Elemental Carbon	**3.35 ± 0.17**	**0.33 ± 0.04**	**48.49 ± 6.76**	0.23 ± 0.28
$D_a = 0.18 - 0.1\mu m$				
Mass	**7.61 ± 0.42**	**1.31 ± 0.19**	**101.58 ± 17.14**	1.11 ± 0.70
Organic Compounds	**1.91 ± 0.30**	**0.62 ± 0.13**	**20.94 ± 5.66**	**0.58 ± 0.23**
Elemental Carbon	**5.55 ± 0.23**	**0.64 ± 0.05**	**78.63 ± 14.39**	0.49 ± 0.59
$D_a = 0.1 - 0.056\mu m$				
Mass	**5.18 ± 0.44**	**0.56 ± 0.20**	**73.69 ± 14.36**	0.43 ± 0.59
Organic Compounds	**1.47 ± 0.28**	**0.42 ± 0.13**	**17.20 ± 4.57**	**0.38 ± 0.19**
Elemental Carbon	**3.65 ± 0.17**	**0.30 ± 0.04**	**53.82 ± 6.60**	0.19 ± 0.27
$D_a < 0.056\mu m$				
Mass	-	-	-	-
Organic Compounds	**2.46 ± 0.31**	**0.58 ± 0.12**	**30.21 ± 6.46**	**0.53 ± 0.26**
Elemental Carbon	**1.79 ± 0.14**	0.08 ± 0.05	**26.91 ± 8.00**	0.04 ± 0.33

Table 4.11: PM_{10} Emissions on a Gasoline-Equivalent Fuel Basis in the Caldecott Tunnel (mg l^{-1})

	Calculated					
	100% Diesel			0% Diesel		
Mass	**1928.58**	±	**139.57**	**47.22**	±	**15.16**
Organic Compounds	**602.52**	±	**6.62**	**32.62**	±	**0.72**
Elemental Carbon	**1089.07**	±	**46.36**	**27.85**	±	**5.03**
NH_4^+	**56.33**	±	**3.24**	**7.49**	±	**0.35**
NO_3^-	**8.28**	±	**2.73**	**0.80**	±	**0.30**
$SO_4^=$	**47.28**	±	**7.46**	1.17	±	0.81
Al	**10.7386**	±	**1.7508**	0.3778	±	0.1901
Ba		-			-	
Cr	**1.3332**	±	**0.4730**	0.0023	±	0.0514
Fe		-			-	
Hg		-			-	
La	**0.013499**	±	**0.000885**	**0.000913**	±	**0.000096**
Mg	**4.6397**	±	**0.1833**	**0.3868**	±	**0.0199**
Mn	**0.55214**	±	**0.16541**	0.03408	±	0.01796
Na	-1.0264	±	0.9938	**0.5942**	±	**0.1079**
Sb	0.246730	±	0.189722	0.039312	±	0.020603
Sc	**0.000871**	±	**0.000311**	**0.000110**	±	**0.000034**
V	**0.012508**	±	**0.003517**	**0.002916**	±	**0.000382**
Zn	**32.7354**	±	**9.1580**	-0.0814	±	0.9945

Table 4.12: Fine Particle Emissions on a Gasoline-Equivalent Fuel Basis in the Caldecott Tunnel (mg l^{-1})

	Calculated					
	100% Diesel			0% Diesel		
Mass	**1089.31**	±	**210.44**	48.16	±	31.23
Organic Compounds	**416.62**	±	**93.01**	25.37	±	13.80
Elemental Carbon	**675.08**	±	**295.93**	10.99	±	43.92
NH_4^+	6.76	±	7.16	1.24	±	1.06
NO_3^-	**24.84**	±	**2.38**	0.13	±	0.35
$SO_4^=$	**25.95**	±	**5.58**	0.65	±	0.83
Al	4.5108	±	6.6191	-0.0921	±	0.9823
Ba		-			-	
Cr	-0.4441	±	0.0395	-0.0041	±	0.0059
Fe	-6.6709	±	7.1618	1.5441	±	1.2701
Hg	0.004674	±	0.005991	0.000103	±	0.000889
La	0.003310	±	0.003902	0.000136	±	0.000692
Mg	**6.3810**	±	**1.7914**	-0.0307	±	0.1945
Mn	0.10775	±	0.55518	-0.00117	±	0.09846
Na	0.5241	±	2.6627	0.1792	±	0.3952
Sb	-0.012617	±	0.063250	0.012433	±	0.009386
Sc	0.001257	±	0.001235	-0.000008	±	0.000183
V	0.011470	±	0.022940	-0.000307	±	0.003404
Zn	1.3426	±	1.7206	-0.0347	±	0.2553

Table 4.13: Size-Segregated Aerosol Emissions on a Gasoline-Equivalent Fuel Basis in the Caldecott Tunnel (mg l^{-1})

	Calculated	
	100% Diesel	0% Diesel
$D_a = 1.8 - 1.0\mu m$		
Mass	65.80 ± 41.42	-0.66 ± 6.15
Organic Compounds	**29.16** ± **9.30**	0.26 ± 1.38
Elemental Carbon	**40.94** ± **11.53**	0.11 ± 1.71
$D_a = 1.0 - 0.56\mu m$		
Mass	**35.42** ± **14.90**	-1.31 ± 2.21
Organic Compounds	44.62 ± 30.20	1.34 ± 4.48
Elemental Carbon	**39.55** ± **4.08**	0.49 ± 0.61
$D_a = 0.56 - 0.32\mu m$		
Mass	**115.06** ± **30.73**	2.43 ± 4.56
Organic Compounds	**45.88** ± **19.21**	2.38 ± 2.85
Elemental Carbon	**109.27** ± **20.11**	1.63 ± 2.98
$D_a = 0.32 - 0.18\mu m$		
Mass	**159.10** ± **40.16**	3.65 ± 5.96
Organic Compounds	**39.98** ± **15.83**	2.34 ± 2.35
Elemental Carbon	**124.04** ± **17.93**	2.52 ± 2.66
$D_a = 0.18 - 0.1\mu m$		
Mass	**257.57** ± **45.54**	11.42 ± 6.76
Organic Compounds	**51.83** ± **15.07**	**5.80** ± **2.24**
Elemental Carbon	**200.74** ± **38.22**	5.21 ± 5.67
$D_a = 0.1 - 0.056\mu m$		
Mass	**188.22** ± **38.17**	4.60 ± 5.66
Organic Compounds	**42.93** ± **12.17**	**3.82** ± **1.81**
Elemental Carbon	**137.90** ± **17.49**	2.19 ± 2.60
$D_a < 0.056\mu m$		
Mass	-	-
Organic Compounds	**75.88** ± **17.17**	**5.34** ± **2.55**
Elemental Carbon	**69.18** ± **21.30**	0.49 ± 3.16

Table 4.14: PM_{10} Emissions on a Distance Driven Basis in the Caldecott Tunnel (mg km^{-1})

	Calculated					
	100% Diesel			0% Diesel		
Mass	**1098.13**	±	**79.47**	**4.85**	±	**1.56**
Organic Compounds	**343.07**	±	**3.77**	**3.35**	±	**0.07**
Elemental Carbon	**620.12**	±	**26.40**	**2.86**	±	**0.52**
NH_4^+	**32.07**	±	**1.85**	**0.77**	±	**0.04**
NO_3^-	**4.71**	±	**1.56**	**0.08**	±	**0.03**
$SO_4^=$	**26.92**	±	**4.25**	0.12	±	0.08
Al	**6.1146**	±	**0.9969**	0.0388	±	0.0195
Ba		-			-	
Cr	**0.7591**	±	**0.2693**	0.0002	±	0.0053
Fe		-			-	
Hg		-			-	
La	**0.007686**	±	**0.000504**	**0.000094**	±	**0.000010**
Mg	**2.6419**	±	**0.1043**	**0.0397**	±	**0.0020**
Mn	**0.31439**	±	**0.09418**	0.00350	±	0.00185
Na	-0.5844	±	0.5659	**0.0611**	±	**0.0111**
Sb	0.140488	±	0.108028	0.004039	±	0.002117
Sc	**0.000496**	±	**0.000177**	**0.000011**	±	**0.000003**
V	**0.007122**	±	**0.002002**	**0.000300**	±	**0.000039**
Zn	**18.6395**	±	**5.2145**	-0.0084	±	0.1022

Table 4.15: Fine Particle Emissions on a Distance Driven Basis in the Caldecott Tunnel (mg km^{-1})

	Calculated					
	100% Diesel			0% Diesel		
Mass	**620.25**	±	**119.82**	4.95	±	3.21
Organic Compounds	**237.22**	±	**52.96**	2.61	±	1.42
Elemental Carbon	**384.39**	±	**168.50**	1.13	±	4.51
NH_4^+	3.85	±	4.07	0.13	±	0.11
NO_3^-	**14.15**	±	**1.35**	0.01	±	0.04
$SO_4^=$	**14.78**	±	**3.18**	0.07	±	0.09
Al	2.5684	±	3.7689	-0.0095	±	0.1009
Ba		-			-	
Cr	-0.2529	±	0.0225	-0.0004	±	0.0006
Fe	-3.7984	±	4.0779	0.1586	±	0.1305
Hg	0.002661	±	0.003411	0.000011	±	0.000091
La	0.001885	±	0.002222	0.000014	±	0.000071
Mg	**3.6334**	±	**1.0200**	-0.0032	±	0.0200
Mn	0.06135	±	0.31612	-0.00012	±	0.01012
Na	0.2984	±	1.5162	0.0184	±	0.0406
Sb	-0.007184	±	0.036015	0.001277	±	0.000964
Sc	0.000716	±	0.000703	-0.000001	±	0.000019
V	0.006531	±	0.013062	-0.000032	±	0.000350
Zn	0.7645	±	0.9797	-0.0036	±	0.0262

Table 4.16: Size-Segregated Aerosol Emissions on a Distance Driven Basis in the Caldecott Tunnel (mg km^{-1})

	Calculated	
	100% Diesel	0% Diesel
$D_a = 1.8 - 1.0\mu m$		
Mass	37.47 ± 23.58	-0.07 ± 0.63
Organic Compounds	**16.60** ± **5.30**	0.03 ± 0.14
Elemental Carbon	**23.31** ± **6.57**	0.01 ± 0.18
$D_a = 1.0 - 0.56\mu m$		
Mass	**20.17** ± **8.48**	-0.14 ± 0.23
Organic Compounds	25.41 ± 17.20	0.14 ± 0.46
Elemental Carbon	**22.52** ± **2.32**	0.05 ± 0.06
$D_a = 0.56 - 0.32\mu m$		
Mass	**65.52** ± **17.50**	0.25 ± 0.47
Organic Compounds	**26.13** ± **10.94**	0.24 ± 0.29
Elemental Carbon	**62.22** ± **11.45**	0.17 ± 0.31
$D_a = 0.32 - 0.18\mu m$		
Mass	**90.59** ± **22.87**	0.37 ± 0.61
Organic Compounds	**22.76** ± **9.01**	0.24 ± 0.24
Elemental Carbon	**70.63** ± **10.21**	0.26 ± 0.27
$D_a = 0.18 - 0.1\mu m$		
Mass	**146.66** ± **25.93**	1.17 ± 0.69
Organic Compounds	**29.51** ± **8.58**	**0.60** ± **0.23**
Elemental Carbon	**114.30** ± **21.76**	0.54 ± 0.58
$D_a = 0.1 - 0.056\mu m$		
Mass	**107.17** ± **21.73**	0.47 ± 0.58
Organic Compounds	**24.44** ± **6.93**	**0.39** ± **0.19**
Elemental Carbon	**78.52** ± **9.96**	0.22 ± 0.27
$D_a < 0.056\mu m$		
Mass	-	-
Organic Compounds	**43.21** ± **9.78**	**0.55** ± **0.26**
Elemental Carbon	**39.39** ± **12.13**	0.05 ± 0.32

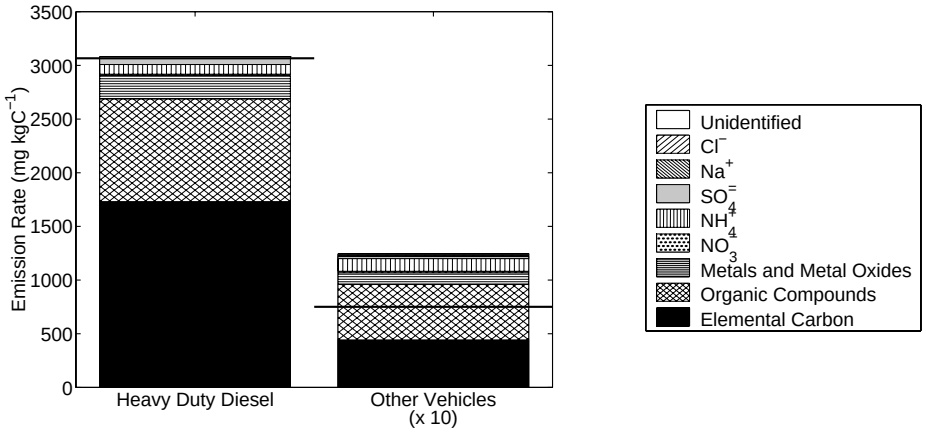

Figure 4.8: Mass balance on PM_{10} emissions for the heavy-duty diesel fleet and the other vehicles

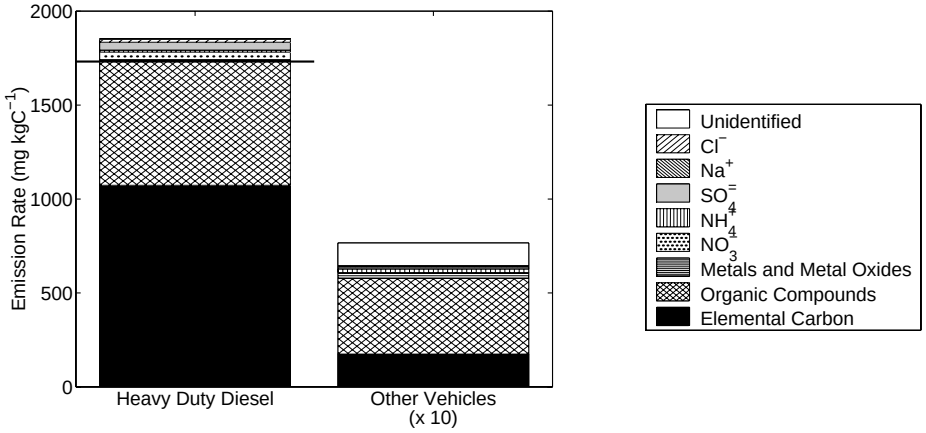

Figure 4.9: Mass balance on fine particle emissions for the heavy-duty diesel fleet and the other vehicles

fleet is carbonaceous (see Figures 4.8 and 4.9). Elemental carbon is the largest component, and organic matter is the second largest component of these emissions. Size-resolved aerosol emissions extrapolated to the condition of a 100% heavy-duty diesel fleet show a broad peak (0.056–0.56 μm particle diameter) which is composed mainly of elemental carbon with lesser amounts of organic material; ammonium and sulfate ions are present in most of the size fractions (see Figure 4.10).

4.3.3 Comparison of Aerosol Emissions Measured in Other Studies

Pierson et al. report estimated "gasoline" and "diesel" emissions on a mg km^{-1} basis estimated from the 1977 measurements in the Tuscarora Mountain Tunnel [39]. A comparison of these data with PM_{10} emissions from the present study (see Table 4.14) show that mass emissions are approximately equal for heavy-duty diesel vehicles; 865 mg km^{-1} in the Tuscarora Tunnel, and 1098 mg km^{-1} in the present

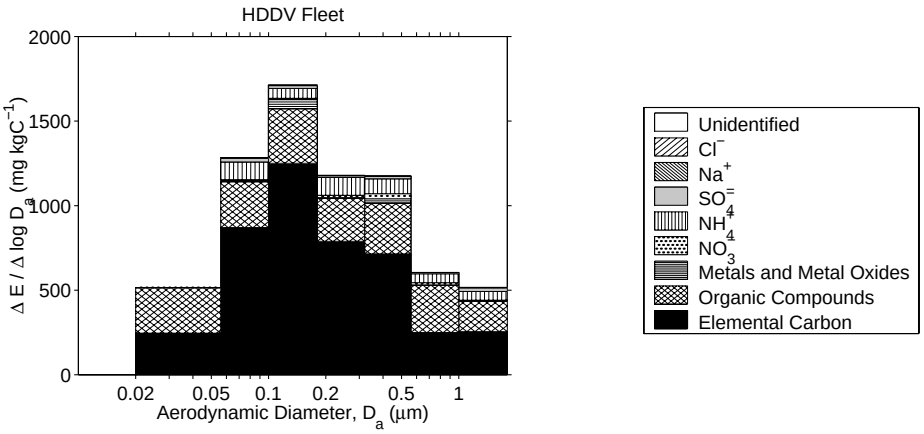

Figure 4.10: Mass balance on size-segregated aerosol emissions estimated for the heavy-duty diesel vehicle fleet in the Caldecott Tunnel

study (see Table 4.14). Emission rates for light-duty vehicles, however, have been reduced substantially, from 51 to less than 5 mg km^{-1} for light-duty vehicles. These reductions in light-duty vehicle emissions are observed even though the Caldecott Tunnel has a 4.2% grade and the Tuscarora Mountain Tunnel is essentially flat.

Weingartner et al. report fine particulate matter emissions ($D_a < 3.0$ μm) in the Gubrist Tunnel near Zurich, Switzerland, [40] to be 383.5 mg km^{-1} for heavy-duty vehicles, and 8.53 mg km^{-1} for light-duty vehicles. These HDV fine mass emission factors are equal within experimental uncertainty to those measured here for $PM_{1.9}$ (see Table 4.9). The LDV emissions measured here are nominally half of those measured in the Gubrist Tunnel, although again error bounds on the LDV emissions measured in these two studies overlap.

Emission rates measured in the Los Angeles area Van Nuys Tunnel [28] are for a mixed fleet of heavy- and light-duty vehicles; these are most closely comparable with Bore 1 emission rates. Fine particle mass emission rates in the Van Nuys Tunnel were 491 mg l^{-1} of fuel burned in the tunnel. This is substantially greater than the $PM_{1.9}$ emission rates reported here for Bore 1 (see Table 4.6). Fine elemental carbon and organic matter emission factors are equivalent between these studies within experimental error. Higher "emissions" of NO_3^- and NH_4^+ were observed in the Van Nuys Tunnel. Therefore the mass emission factors agree with the exception that a greater quantity of secondary aerosol, primarily NH_4NO_3, was formed in the Van Nuys Tunnel as compared to the Caldecott Tunnel.

Kirchstetter et al. report emissions of fine ($D_a < 2.5$ μm) particulate matter to be 1850 $\pm$ 148 and 81.4 $\pm$ 7.4 mg l^{-1} for heavy-duty diesel trucks and other vehicles on a gasoline-equivalent fuel

Table 4.17: Gas-Phase Pollutant Concentrations in the Caldecott Tunnel

		Bore 1 (LDV and HDV)		Bore 2 ("LDV only")	
		17 Nov 97	18 Nov 97	19 Nov 97	20 Nov 97
CO_2	ppmv	**411.9 ± 13.5**	**459.2 ± 14.3**	**707.5 ± 13.2**	**768.6 ± 19.1**
CO	ppmv	**17.42 ± 0.66**	**19.22 ± 0.72**	**25.06 ± 0.65**	**26.71 ± 0.95**
CH_4	ppmv	0.16 ± 0.91	0.15 ± 0.91	0.23 ± 0.78	0.22 ± 0.91
NMHC	ppbC	**1431.7 ± 16.3**	**1868.1 ± 21.0**	**2033.1 ± 15.8**	**2579.8 ± 28.1**
HNO_3	μg m^{-3}	**2.13 ± 1.05**	0.80 ± 0.84	0.04 ± 1.03	-0.08 ± 1.03
NH_3	μg m^{-3}	**99.1 ± 2.7**	**91.2 ± 2.3**	**100.2 ± 2.8**	**134.9 ± 2.8**

basis. Their estimates for the heavy duty diesel trucks are significantly higher than the $PM_{1.9}$ emissions reported here (see Table 4.12). Background-subtracted fine particle mass concentrations reported by Kirchstetter et al. were 31% greater than those reported for Bore 1 and 26% higher for Bore 2 than in the present study. Similarly, the fine particle elemental carbon and organic carbon emission rates estimated by Kirchstetter et al. are significantly higher than the $PM_{1.9}$ emissions reported here. Since traffic densities during the two studies were comparable, this comparison suggests that a systematic difference in measurement techniques led to higher concentration values in the Kirchstetter et al. study. One systematic difference was that Kirchstetter et al. collected $PM_{2.5}$, not $PM_{1.9}$. Comparison of PM_{10} data to $PM_{1.9}$ data from the present study in Tables 4.2 and 4.3 shows a large quantity of particulate matter present in the tunnel in particles between 1.9 and 10 μm aerodynamic diameter due to the heavy-duty diesel trucks; a portion of these emissions are in the 1.9 to 2.5 μm size range.

4.3.4 Gas Phase Emissions

Concentrations of ammonia in the gas phase within the Caldecott Tunnel substantially exceeded those in the outdoor air during all the sampling events (see Table 4.17). The average NH_3 concentrations before background subtraction were 103, 124, and 7 μg m^{-3} in Bore 1 (LDV and HDV), Bore 2 ("LDV Only"), and at the outdoor background site, respectively. These observations confirm the findings of an experiment in the Los Angeles area Van Nuys Tunnel by Fraser and Cass that the in-use vehicle fleet emits substantial amounts of ammonia [4]. The elevated ammonia emissions most likely are due to 3-way catalyst-equipped autos and light trucks that are running rich either because they are running under load or are poorly maintained [4, 50].

The average emission rates of NH_3 were 266.9 and 194.4 mg l^{-1} of fuel burned in Bores 1 and 2, respectively. While ammonia emissions are significantly higher in Bore 1 than in Bore 2, extrapolation of the data to the condition of 100% LDV and 100% HDV fleets shows that both the HDV and LDV fleet emissions are significantly different from zero, but that the uncertainty of the HDV emission rate is

Table 4.18: Gas-Phase Pollutant Emission Rates on a Fuel Consumption Basis (mg l^{-1}) in the Caldecott Tunnel

	Measured		Calculated	
	Bore 1 (LDV and HDV)	Bore 2 ("LDV Only")	100% HDV	100% LDV
HNO_3	**4.20 ± 1.91**	-0.03 ± 1.22	15.54 ± 11.12	-0.06 ± 2.37
NH_3	**266.9 ± 5.0**	**194.4 ± 3.3**	**466.5 ± 175.9**	**193.2 ± 37.5**

Table 4.19: Gas-Phase Pollutant Emission Rates on a Distance Traveled Basis (mg km^{-1}) in the Caldecott Tunnel

	Measured		Calculated	
	Bore 1 (LDV and HDV)	Bore 2 ("LDV Only")	100% HDV	100% LDV
HNO_3	**0.55 ± 0.25**	-0.00 ± 0.13	8.26 ± 5.91	-0.01 ± 0.24
NH_3	**34.7 ± 0.7**	**20.1 ± 0.3**	**247.8 ± 93.5**	**19.8 ± 3.8**

relatively large.

The NH_3 emission rates of 194–267 mg l^{-1} observed in the Caldecott Tunnel are slightly lower than the 380 mg l^{-1} measured in 1993 the Los Angeles area Van Nuys Tunnel [4]. In addition to increased gas phase NH_3, Fraser and Cass reported apparent emission rates of 21.0 mg l^{-1} for aerosol NH_4^+, and 61.9 mg l^{-1} for aerosol NO_3^- in the Van Nuys Tunnel. These "emissions" likely result from the formation of secondary particulate matter within the tunnel from the reaction of gas phase NH_3 and HNO_3. Thus, when the aerosol plus gas phase data are combined, the total NH_3 emission rate in the Van Nuys Tunnel in 1993 was 400 mg l^{-1}. In contrast to the Caldecott Tunnel, the Van Nuys Tunnel is more nearly flat and traffic runs more slowly, suggesting that increased load on the engines is not a cause of the higher NH_3 emissions in the Van Nuys Tunnel. Thus, the higher emissions of NH_3, CO, and NMHC measured in the Van Nuys Tunnel are likely due to an older and possibly more poorly maintained vehicle fleet at that location when compared to the long distance commuter fleet that uses the Caldecott Tunnel.

Chapter 5

Conclusions and Recommendations

5.1 Summary of Findings

The Vehicle-Oriented Trajectory Study, the Nitrate-Oriented Trajectory Study, and the Caldecott Tunnel Study were undertaken as part of the the Aerosol Project of the 1997 Southern California Ozone Study—North American Research Strategy for Tropospheric Ozone (SCOS97). The objective of the trajectory experiments was to observe single air parcels at several locations as they are transported across the South Coast Air Basin (SoCAB) and by comparison to document the effects of emissions, chemical reactions, deposition, and other processes on the particle population. The Vehicle-Oriented Trajectory Study was conducted at sites heavily influenced by primary particle emissions from motor vehicles. The Nitrate-Oriented Trajectory Study was conducted at sites influenced by the Chino dairy area, a large source of gas-phase ammonia. The objective of the Caldecott Tunnel Study was to determine aerosol emission rates for the California in-use heavy-duty and light-duty vehicle fleets.

The sample collection phase of these experiments took place in the summer and fall of 1997. Samples were collected for the Vehicle-Oriented Trajectory Study at the Central Los Angeles, Azusa, and Riverside sites in two 48-h experiments on August 21–23 and August 27–29, 1997. Samples were collected for the Nitrate-Oriented Trajectory Study at the Diamond Bar, Mira Loma, and Riverside sites in one 48-h experiment on October 31 to November 2, 1997. Additional aerosol nitrate measurements were made for the Nitrate-Oriented Calibration Study at Mira Loma on September 27–30, 1997. At the Caldecott Tunnel, samples were collected in four experiments on November 17–20, 1997. More samples were collected than were called for in the project research proposal; specifically, the Nitrate-Oriented

Calibration Study and two of the experiments in the Caldecott Tunnel were in addition to those called for in the research proposal. A total of 1600 samples were successfully collected during ambient and tunnel sampling.

In each study, aerosol samples were collected using filter samplers, cascade impactors, and electronic particle size distribution monitors. Two sets of filter samples were collected, one for particles smaller than 1.9 μm aerodynamic diameter ($PM_{1.9}$) and another for particles smaller than 10 μm aerodynamic diameter (PM_{10}). Using the impactors, size-segregated fine particle samples were collected in 6 size ranges below 1.8 μm aerodynamic diameter (D_a) with lower D_a cutoffs at 1.0, 0.56, 0.32, 0.18, 0.1, and 0.056 μm plus an afterfilter. The filter and impactor samples were analyzed for aerosol mass and for the major aerosol chemical components including organic carbon (OC), elemental carbon (EC), and sulfate, nitrate and ammonium ions by ion chromatography. In addition, aerosol concentrations of the trace elements Al, As, Au, Ba, Br, Cd, Ce, Cl, Co, Cr, Cs, Eu, Fe, Ga, Hg, In, K, La, Lu, Mg, Mn, Mo, Na, Nd, Rb, Sb, Sc, Se, Sm, Sr, Th, Ti, U, V, Yb, and Zn were measured by instrumental neutron activation analysis (INAA). Several of the analysis methods produce data on multiple chemical species; in total, more than 21,000 chemical and physical pollutant concentrations measurements were made.

5.1.1 Vehicle-Oriented Trajectory Study

The Vehicle-Oriented Trajectory Study samples were collected in two 48-h events in August of 1997 at three sites in Southern California. The monitoring sites were located at Central Los Angeles, near the highest density of vehicle traffic in the Los Angeles area, at Azusa, which is often downwind of Central Los Angeles, and at Riverside. The objective of the experiment was to use trajectory-oriented sampling to observe single air parcels that are heavily influenced by primary particle emissions from motor vehicles at several locations along the air parcel trajectory and by comparison to document the effects of emissions, chemical reactions, deposition, and other processes on the particle population.

Weather conditions were similar during both sampling events. Air parcels arriving at Central Los Angeles and Azusa generally approached from the southwest, having crossed the coastline near Hawthorne. Air stagnation at Central Los Angeles and Azusa occurred daily beginning between 1800 and 2200 PDT in the evening and ending between 1000 and 1200 PDT the following morning. The prevailing wind patterns advected air parcels past both the Central Los Angeles and Azusa monitoring sites in succession. For example, air sampled in the morning of August 28 at Azusa stagnated over the ocean on the evening of August 26-27, crossed the coastline at approximately 1400 PDT August

27, passed near the Central Los Angeles site, and proceeded to Azusa, where stagnation occurred overnight on August 27-28. Photochemical oxidant formation was generally low during the sampling periods when compared to historical conditions in Southern California. Daily peak concentrations of hourly-averaged ozone ranged between 50 and 70 ppb at Central Los Angeles and between 70 and 100 ppb at Azusa over the August 21-23 and August 27-29 sampling events. California air quality standards specify that the hourly average ozone concentration should not exceed 90 ppb. This standard was exceeded during two hours of the sampling events in this study at Azusa; the standard was not exceeded at the other two sites. In general, the smog season of 1997 was mild in comparison with previous years; there was only one Stage One ozone episode during the entire year (hourly average O_3 concentration $>$ 200 ppb), in contrast to 41, 24, 23, 14, and 7 such episodes over the 5 consecutive years 1992-1996, respectively [9].

Fine particle mass concentrations measured at Central Los Angeles were in the range 13.6–54.9 μg m^{-3}, concentrations in excess of the proposed Federal annual standard of 15 μg m^{-3} but below the proposed 24-h average standard of 65 μg m^{-3}. The largest component of fine particle mass at Central Los Angeles was organic compounds, measured to be 5.3–35.9 μg m^{-3}. Other important contributors to fine particle mass at this site were elemental carbon (0.1–5.2 μg m^{-3}), nitrate ion (0.4–7.6 μg m^{-3}), sulfate ion (1.3–6.3 μg m^{-3}), and ammonium ion (1.0–4.4 μg m^{-3}). Concentrations of organic compounds and elemental carbon exhibited strong diurnal cycles with maxima between the hours 0600 and 1400 PDT. These cycles suggest that organic compounds and elemental carbon are strongly influenced by local traffic emissions. Concentrations of nitrate, sulfate, and ammonium ions also exhibited some diurnal variation but were generally more constant with time than the carbonaceous species.

Aerosol composition as a function of particle size was measured. At the Central Los Angeles site, the reduction in elemental carbon concentration between the morning traffic rush hour period (0600–1000 PDT) and the afternoon period (1400–1800 PDT) is accompanied by a shift in size from an EC concentration peak in the 0.1–0.18 μm particle size range during the morning traffic peak to a relatively even distribution of EC between 0.1 and 0.56 μm diameter particles later in the day. The OC concentration reduction over this same pair of time periods is likewise accompanied by a shift of the peak in the OC size distribution to larger particles. The EC concentration peaks during the morning in the 0.10–0.18 μm particle size range occur in the same size range as the predominant fine particle emissions from vehicles measured in the Caldecott Tunnel. The appearance of EC and OC in larger particle sizes late in the day could result from advection into Central Los Angeles of aged aerosol having accumulated coatings of gas-to-particle conversion products over time. Alternatively, additional

sources may contribute to the afternoon aerosol. NO_3^-, Cl^-, and Na at Central Los Angeles are found in significant quantities only in the largest size range measured by the impactor ($1.0 < D_a < 1.8$ μm); sodium nitrate is associated with sea salt or transformed sea salt, which is generally found in particle sizes larger than 1 μm in diameter.

Gas phase ammonia at Central LA had a nearly constant baseline concentration of 8 to 9.5 μg m^{-3} (11.4–13.6 ppb) with a near doubling of ammonia concentrations during those hours when the elemental carbon concentrations were highest, consistent with a traffic-derived source of NH_3 emissions as measured in the Caldecott Tunnel Study. Nitric acid concentrations showed a strong diurnal profile, with the peak concentrations during daylight hours of 5 to 11 μg m^{-3} (2.1–4.2 ppb) and nearly zero concentrations at night. Fine particle nitrate levels at Central LA were generally low throughout this experiment; the highest aerosol nitrate levels occurred overnight and during the 0600–1000 PDT period on August 21, a period in which overnight fog turned to haze later in the morning. Aerosol sulfate concentrations were only marginally higher, and at times lower, than marine fine particle sulfate background levels recently reported for Santa Catalina Island (4.51 μg m^{-3}).

Fine particle mass concentrations measured at Azusa were in the range 12.8–42.5 μg m^{-3}. As at the Central Los Angeles site, the largest component of fine particle mass at Azusa was organic compounds, measured to be 9.0–34.2 μg m^{-3}. Other important contributors to fine particle mass at this site were elemental carbon (1.1–6.2 μg m^{-3}), nitrate ion (0.3–4.8 μg m^{-3}), sulfate ion (0.6–5.2 μg m^{-3}), and ammonium ion (1.1–3.6 μg m^{-3}). Concentrations of organic compounds exhibited diurnal cycles with maxima between the hours 0600 and 1800 PDT; these cycles were broader and extended later into the day than at Central Los Angeles, possibly reflecting contributions from both early morning local traffic emissions and transport of organic aerosol to Azusa in the afternoon. Elemental carbon concentrations were highest in the early morning, suggesting that considerable diesel truck traffic occurs near the Azusa monitoring site. Concentrations of nitrate, sulfate, and ammonium ions were variable and did not exhibit pronounced diurnal cycles.

Nitric acid vapor concentrations at Azusa showed the strong diurnal cycle expected for a photochemically generated pollutant. Gaseous ammonia concentrations at Azusa did not show a diurnal variation that peaked during the early morning traffic peak, suggesting less influence of local vehicle emissions than observed at Central LA.

Two air parcels were identified that passed near both the Central Los Angeles and Azusa monitoring sites in succession. Both of the air parcels passed near Central Los Angeles in the afternoon and

progressed to the Azusa area where they stagnated overnight. Along these trajectories, the particle chemical composition and concentration changed very little between Central Los Angeles and Azusa. With the onset of the morning traffic peak in Azusa, however, fine particle elemental and organic carbon concentrations increased substantially within these air parcels, as did NO and NO_2 concentrations. In both cases, on the second morning of each experiment the particle population changed noticeably during the morning traffic peak period when the air mass motion was relatively stagnant. There were increases in aerosol elemental carbon (65–258% increase), organic matter (21–146% increase), metals and metal oxides (138–538% increase), nitrate (17–84% increase), ammonium (6–25% increase), and fine aerosol mass (27–75% increase). HNO_3 concentrations in these air parcels remained relatively small when compared to other nitrogen-containing pollutant species, and there was little particulate ammonium nitrate formation, which together indicate that nitric acid production was effectively balanced by dry deposition within the air parcels studied.

5.1.2 Nitrate-Oriented Trajectory Study

In September and October of 1997, samples were collected for the Nitrate-Oriented Trajectory Study at three Southern California sites. These sites were located in Diamond Bar, Mira Loma, and Riverside, sites which were upwind of, within, and downwind of the Chino dairy area, a large source of gas-phase ammonia. This was the first time that air monitoring stations have been placed to observe the effects on ambient aerosol of a major source of ammonia emissions at close range.

Samples for the Nitrate-Oriented Calibration Study were collected at Mira Loma over September 27-30. Fine particle mass concentrations were high, averaging 81.9 μg m^{-3}, 63.9 μg m^{-3} and 58.2 μg m^{-3} on September 27 (after 1400 PDT), September 28, and September 29, respectively. By comparison, the recently proposed Federal $PM_{2.5}$ air quality standard limits 24-h average fine particle concentrations to not more than 65 μg m^{-3}. The fine particle mass concentration at Mira Loma on these days was dominated by ammonium nitrate aerosol, with significant quantities of organic aerosol also present.

September 27, 28, and 29 fell on Saturday, Sunday, and Monday, respectively, and it is interesting to note the differences between species concentration patterns on a weekend and a weekday. For example, Monday, September 29 exhibits a strong peak in the elemental carbon concentration during the 0600–1000 PDT time period. However, this pattern does not appear on Sunday, September 28.

Samples for the Nitrate-Oriented Trajectory Study were collected at all three monitoring stations from October 31 through November 2. All three sites had periods of relatively high pollutant concen-

trations on Friday, October 31. On the morning of November 1, wind patterns changed and all three sites experienced drastic reductions in particle concentrations. During the period of clean air at the end of the day on November 1, incoming air parcels at Mira Loma and Riverside approached from the mountains to the north and northeast instead of from urban and agricultural areas to the west.

At Diamond Bar fine particulate mass, NO_3^-, and NH_4^+ concentrations are essentially constant for the first half of the day on October 31. These concentrations are relatively high, an average of 98.6 μg m^{-3} fine particle mass, containing 40.8 μg m^{-3} fine particle NO_3^- and 10.5 μg m^{-3} fine particle NH_4^+. The air parcels reaching Diamond Bar during this night and morning period of low-to-stagnant wind speeds approached Diamond Bar from the northeast during a condition of mild off-shore wind flow, after having crossed the Pacific Coast along the Santa Monica Bay two to three days earlier. In contrast, air parcels arriving during the 1400–1800 time period were transported by on-shore winds after stagnating only once overnight near Fullerton; these air parcels had been over the urban area for a much shorter time, and there are minima in the fine particulate NO_3^- (18.0 μg m^{-3}), NH_4^+ (6.0 μg m^{-3}), and mass (59.9 μg m^{-3}) concentrations.

At Mira Loma gas phase NH_3 concentrations between 1000 PST and 0100 PST October 31-November 1 were among the highest concentrations measured during the study, peaking at 123.9 μg m^{-3} (180 ppb). Fine elemental carbon and organic compound concentrations peaked at 9.7 and 46.9 μg m^{-3} during the 0600–1000 PST peak traffic period on Friday, October 31. Other fine particulate species remained relatively constant from 0100 through 1000 hours PST on October 31. Air parcel trajectories arriving at Mira Loma changed around 1100 hours PST from a pattern which approached Mira Loma from the north to one which approached Mira Loma from the west. Air parcels arriving after 1100 hours PST contained higher concentrations of fine particulate NO_3^- (71.0 μg m^{-3} mean) and NH_4^- (17.8 μg m^{-3} mean), and gas-phase NH_3 (94.7 μg m^{-3} mean), and lower concentrations of EC (3.6 μg m^{-3} mean). The center of the Chino dairy area is located to the west of Mira Loma, and thus it is not surprising that the highest ammonia concentrations recorded occur at this time. Overnight between October 31 and November 1 the air stagnated at Mira Loma and concentrations of all species remained relatively high.

Sharp increases in concentrations of gas-phase ammonia and fine particulate mass, NO_3^-, NH_4^+ and organic matter occurred at Riverside in the 1400–1800 PST period of October 31. Maximum concentrations reached during this time period were 128 μg m^{-3} fine particulate mass, 62.9 μg m^{-3} fine particulate NO_3^-, 15.6 μg m^{-3} fine particulate NH_4^+, and 32.3 μg m^{-3} fine particulate organic matter; concentrations of these species stayed relatively high through 0600 PST on November 1 as a result of

overnight air stagnation. Fine particulate elemental carbon concentrations stayed relatively constant throughout October 31 at Riverside, and showed no significant traffic-associated peak. The largest components of fine particulate mass at Riverside, as at Diamond Bar and Mira Loma, were nitrate and ammonium ions.

Size-segregated aerosol samples collected at Diamond Bar, Mira Loma, and Riverside on October 31 show that aerosol nitrate accumulation occurred mainly on particles in the range 0.32–1.8 μm aerodynamic diameter. Since particles of this size efficiently scatter light, the aerosol ammonium nitrate has a strong effect on visibility.

Air parcel trajectories were identified that passed successively over two air monitoring sites during the first day of this experiment. One of these air parcel trajectories passed the Diamond Bar air monitoring site in the morning, and stagnated near Mira Loma in the evening of the same day. Between Diamond Bar and Mira Loma, NO was oxidized to NO_2, and ammonia concentration increased by a factor of 5. A second air parcel trajectory which stagnated near the Mira Loma site during the early morning hours and passed near the Riverside site approximately 24 hours later showed a decrease in ammonia concentration over time that is consistent with dilution as the air mass moves downwind from the virtual point source of ammonia in the dairy area. The particulate ammonium nitrate concentration in that air parcel remained approximately constant over time, consistent with a continued excess of NH_3 relative to HNO_3 and a widespread mass of air containing inorganic nitrate downwind of the dairy area.

A nitrogen balance on the air masses over consecutive time periods at all three air monitoring sites over the October 31–November 2 sampling period shows that NO and NO_2 concentrations were generally much higher than either HNO_3 concentrations or aerosol nitrate concentrations. Thus the precursor gases needed for more HNO_3 production are available in abundance. Excess ammonia is present at most times, thus any HNO_3 formed usually will be driven quickly into the aerosol phase. Although the aerosol nitrate concentrations are small relative to the total nitrogen burden in the atmosphere, the resulting NH_4NO_3 aerosol is large in comparison to both other aerosol species as well as the fine particle air quality standards recently proposed by the U.S. EPA.

5.1.3 Caldecott Tunnel Study

In November 1997, the Caldecott Tunnel Study was conducted to measure direct aerosol emissions from the in-use vehicle fleet traveling through the Caldecott Tunnel that connects Berkeley, CA, and Orinda,

CA. Bore 1 of the tunnel carries light-duty vehicles (LDVs) and heavy-duty vehicles (HDVs) while Bore 2 carries only LDVs plus a few stray HDVs that defy the rules. Approximately 37500 vehicles traveled through the tunnel during four experiments, each of 3-hours duration. Aerosol concentrations were measured in two tunnel bores and at a background site. Particle mass concentrations measured inside the tunnel were significantly elevated relative to background concentrations in all the samples. These measurements provide a complete set of size-segregated data on the chemical composition of fine particles emitted by in-use vehicles.

The majority of the PM_{10} and $PM_{1.9}$ mass in the tunnel was carbonaceous. Elemental carbon was the largest contributor to PM_{10} and $PM_{1.9}$ in Bore 1 (HDV and LDV) and organic carbon was the largest contributor to PM_{10} and $PM_{1.9}$ in Bore 2 ("LDV Only"). Other important contributors to particle mass were NH_4^+, $SO_4^=$, Fe, and Zn. Size-resolved aerosol mass concentrations in both Bore 1 (HDV and LDV) and Bore 2 ("LDV Only") had peaks at 0.1–0.18 μm particle aerodynamic diameter. In Bore 1, the peak is comparatively broader (0.056–0.56 μm) and composed mainly of elemental carbon with lesser amounts of organic material; ammonium and sulfate ions are present in most of the size fractions. In Bore 2, the peak is narrower and contains more organic material than elemental carbon.

Aerosol concentration measurements were used to calculate emission rates from the vehicle fleet in the tunnel. Using the assumption that the differences in emission rates between Bores 1 and 2 are due entirely to the differences in the fraction of HDVs, emission rates of aerosol mass and chemical components of the aerosol were extrapolated to the conditions of 100% LDV and 100% HDV fleets. The measured and extrapolated emission rates for aerosol mass show the expected strong influence of HDVs on emissions. The 100% LDV fleet emission rates are generally not greater than zero with 95% confidence. However, the emission rates in Bore 2 which carries very little HDV traffic generally agree with the 100% LDV fleet emission rate estimates and are more accurate; these values can be used to place an upper limit on the LDV fleet emissions in place of the extrapolated values.

Heavy-duty and light-duty vehicles emitted 809 and 46 mg of $PM_{1.9}$ mass per liter of gasoline-equivalent fuel burned, respectively. The majority of PM_{10} and $PM_{1.9}$ mass emitted by the HDV fleet was carbonaceous. Elemental carbon was the largest component and organic compounds the second largest component of these emissions. Other significant contributors to PM_{10} and $PM_{1.9}$ emissions by the HDV fleet are NH_4^+, NO_3^-, $SO_4^=$, Al, Cr, Mg, and Zn. Size-resolved aerosol emissions extrapolated to the condition of a 100% HDV fleet show a relatively broad peak (0.056–0.56 μm) which was composed mainly of elemental carbon with lesser amounts of organic material; ammonium and sulfate ions are

present in most of the size fractions. The largest component of LDV fleet emissions was organic compounds.

Emission rates can also be extrapolated to a fleet composed of 100% heavy-duty diesel powered vehicles and another fleet composed of all other vehicles. As for the HDV fleet overall, the majority of PM_{10} and $PM_{1.9}$ mass emitted by the heavy-duty diesel fleet is carbonaceous. Elemental carbon is the largest component and organic compounds the second largest component of these emissions. Size-resolved aerosol emissions extrapolated to the condition of a 100% heavy-duty diesel fleet show a broad peak (0.056–0.56 μm particle diameter) which is composed mainly of elemental carbon with lesser amounts of organic material; ammonium and sulfate ions are present in most of the size fractions.

Concentrations of ammonia in the gas phase within the Caldecott Tunnel substantially exceeded those in the outdoor air, confirming the findings of an experiment in the Los Angeles area Van Nuys Tunnel by Fraser and Cass that the in-use vehicle fleet emits substantial amounts of ammonia [4]. The elevated ammonia emissions most likely are due to 3-way catalyst-equipped autos and light trucks that are running rich either because they are running under load or are poorly maintained [4, 50]. The average emission rates of NH_3 were 266.9 and 194.4 mg per liter of fuel burned in Bores 1 and 2, respectively.

5.2 Recommendations

5.2.1 Control of Ambient $PM_{2.5}$

The Vehicle-Oriented Trajectory Study samples were collected during a time period when the ambient PM_{10} concentrations were slightly elevated above the average values for the summer and fall of 1997. Ambient fine particle concentrations exceeded the level of the annual average $PM_{2.5}$ air quality standard that has been proposed by the U. S. EPA. The most important contributors to fine particle mass were organic compounds, the concentration of which often exceeded 15 $\mu g\ m^{-3}$. Because the highest concentrations of organic compounds were observed in the morning and early afternoon and because photochemical oxidant formation during this study was generally low when compared to historical conditions in Southern California, the largest quantity of the organic compounds observed in this study was likely due to primary particles directly emitted from sources. The most important sources of these primary organic aerosols are vehicles and cooking operations [45].

The Nitrate-Oriented Trajectory Study samples were collected when ambient $PM_{1.9}$ concentrations exceeded the proposed 24-h average $PM_{2.5}$ air quality standard. Thus, data from these experiments can be helpful to the design of control strategies for 24-h averaged $PM_{2.5}$. The high aerosol concentrations were observed in the eastern part of the SoCAB during a time of low wind velocity. In contrast to the Vehicle-Oriented Trajectory experiment, the most important contributors to fine particle mass were nitrate and ammonium ions. These are secondary aerosol components formed from NO_x and NH_3 originally emitted in the gas phase.

Concentrations of NO_x upwind of the dairy area were high and relatively constant during the experiment, with concentrations during October 31 in the range 82–223 ppb. The air parcels studied spent approximately 2.5 days over the western SoCAB and accumulated substantial aerosol nitrate concentrations even before reaching the Chino dairy area. NH_3 emitted in the dairy area reacted with photochemically produced HNO_3 to form additional particulate NH_4NO_3. Consistent with this explanation, HNO_3 concentrations were higher upwind of the dairy area (1.1–78.4 μg m^{-3}) and lower in and downwind of the dairy area (0.8–11.1 μg m^{-3}). Gas phase ammonia concentrations were also high in the dairy area (40.5–124 μg m^{-3}). These conditions suggest that secondary aerosol nitrate formation in the eastern SoCAB was limited by the rate of HNO_3 formation.

Based on our measurements, the molar concentration of NH_3 is generally higher than that of HNO_3 in both the western and eastern parts of the SoCAB, indicating that NH_3 is generally not the limiting reagent in the formation of aerosol NH_4NO_3 at the present time. However, we did observe molar concentrations of NH_3 which were lower than those of HNO_3 at Diamond Bar on the afternoon and evening of October 31, 1997 (see Figure 3.13). The addition of NH_3 from agricultural sources downwind of Diamond Bar probably increased the downwind aerosol concentrations in this case.

From observations of the Chino dairy area, it is apparent that land use patterns are undergoing a change as the dairy farms and other agricultural operations are replaced by light industry and residential construction. These land use changes are expected to reduce local NH_3 emissions and increase local NO_x emissions. At some point in the future NH_3 may be the limiting reagent in the formation of particulate NH_4NO_3, at which point further reductions in NH_3 emissions will directly decrease fine particulate matter concentrations. Long-term measurements of gas phase NO_x, HNO_3, and NH_3 in or directly downwind of the Chino dairy area are recommended to determine when NH_3 becomes the limiting reagent. Such measurements will be particularly useful if the substantial emissions of NH_3 from motor vehicles, which is an unintended side effect of the current 3-way catalyst technology, are

reduced through further development of the underlying control technology or through better vehicle maintenance.

Although the ammonia emissions in the Chino dairy area clearly lead to conditions that favor essentially complete conversion of HNO_3 to aerosol nitrate, displacement of the dairy operations from the Chino area will not by itself solve the aerosol nitrate problem in the SoCAB. The days studied here show very long air parcel retention times and considerable aerosol nitrate production even before air parcels reached the dairy area. Sources of both NH_3 and NO_x in the western SoCAB will need to be reduced if the nitrate concentrations measured at Diamond Bar (upwind of the dairy area) are to be reduced. Motor vehicle exhaust is a major source of NO_x emissions. Both the Caldecott Tunnel Study and the ambient data at Central Los Angeles show significant emissions of NH_3 from motor vehicles as well.

5.2.2 Vehicle Emissions

The fine particle emission rates determined from the Caldecott Tunnel Study for HDVs (809 mg l^{-1}) were comparable with those measured in other tunnel studies from the 1970s up to the most recent studies. Since the earlier measurements were made in flat tunnels and the Caldecott Tunnel has a 4.2% grade, this comparison may obscure substantial reductions in HDV fleet emissions over this time. Periodic measurements of HDV fleet emissions in the same tunnel will be useful to assess the impact of the diesel engine emission control rules recently proposed by the U.S. EPA.

The fine particle emission rates measured for LDVs (approximately 5 mg km^{-1}) are approximately 10 times lower than those measured in the 1970s in a flat tunnel, confirming the substantial reductions in LDV fleet emission rates. The LDV fleet emission rates are comparable to emissions measurements made in the 1990s by other investigators. These fine particle mass emission rates are within a factor of two of those measured from LDVs driven over the Federal Test Procedure (FTP) using a dilution sampler.

The present study confirmed that vehicles emit NH_3 (194–267 mg l^{-1}) as was measured earlier in the Los Angeles area Van Nuys Tunnel. The NH_3 emission rate was lower than that measured in Van Nuys Tunnel, likely due to a newer, better maintained vehicle fleet in the Caldecott Tunnel as compared with that in the Van Nuys Tunnel. NH_3 emissions were higher in Bore 1 (HDV and LDV) than in Bore 2 ("LDV Only") of the Caldecott Tunnel. This observation may be due to a higher fraction of older LDVs in Bore 1 in the early afternoon as compared to Bore 2 in the late afternoon. An area for future research

is to investigate the effect of vehicle maintenance and driving conditions on NH_3 emissions.

Another explanation for the higher NH_3 emissions in Bore 1 could be the presence of more catalyst-equipped gasoline-powered trucks in Bore 1. An inventory of these vehicles, including the type of catalyst if any, would support or refute this hypothesis. At present, there are little or no laboratory-based measurement of NH_3 emissions from gasoline-powered trucks, which leaves open the possibility that they are an important class of contributor to the NH_3 emissions for the vehicle fleet.

5.2.3 Aerosol Sampling Protocols

The SCOS97 field sampling during the Vehicle-Oriented Trajectory Study was originally scheduled for a two week period and completed as planned. The fine aerosol concentrations measured during this period were in the range 8–55 μg m^{-3}; concentrations were generally above the proposed annual standard of 15 μg m^{-3} but below the proposed 24-h average standard of 65 μg m^{-3}. These data are useful for understanding aerosol sources and evolution during moderately polluted episodes, but do not capture severe episodes during which the proposed 24-h standard for $PM_{2.5}$ would be exceeded.

Field sampling for the Nitrate-Oriented Trajectory Study was also originally scheduled for a two week period. Because of unusually low concentrations of atmospheric particulate matter, the SCOS97 managers decided to postpone the second nitrate-oriented sample collection until after the planned end of the experiments on September 15. We kept our sampling equipment in the field longer than originally proposed in an effort to sample air with high particulate nitrate concentrations. A one site study was performed at Mira Loma on September 27–29. The second nitrate-oriented sample collection was on October 31 and November 1 at all three of the planned sites. In both cases, the sampled $PM_{2.5}$ concentrations were the highest observed in the late summer/early fall of 1997.

This experience demonstrates that future field studies in the SoCAB should be designed with a sampling window sufficiently long to include at least two events that will exhibit high aerosol concentrations with high probability. Since exceedences of ozone and PM standards in SoCAB have become increasingly infrequent, historical experimental designs are of limited utility in designing studies. Based on the present study, the sampling window should be 4–8 weeks. If high nitrate concentrations are sought, the experiments should take place in the October–December time period when lower temperatures and long air parcel retention times favor aerosol nitrate accumulation. Since it may be impractical to man an array of air sampling stations for such an extended period, as a practical matter future studies should be designed with forward positioning of sampling stations and rapid manning of the stations

based on meteorological predictions.

The SCOS97 Aerosol Program was designed to use data collected as part of the main Southern California Ozone Study. Coupling ozone and aerosol sampling studies has the potential to reduce the cost and increase the scientific value of both studies, however, the SCOS97 ozone and aerosol studies had different goals and time scales so that the respective intensive operating periods (IOPs) did not always coincide. As a result, some data important to understanding ambient aerosols (e.g., mixing heights, and NO_x and VOC concentrations) which were to be collected by ozone study participants were not measured during all the aerosol program IOPs. Measurements required for the aerosol program which were part of the ozone study design should have been directly attached to the aerosol study as well. These measurement should have been made during aerosol IOPs regardless of whether or not those days were targeted for the ozone study.

5.2.4 Tunnel Sampling Protocols

An important goal of traffic tunnel sampling is to estimate vehicle fleet emission rates which can be compared with laboratory measurements of emissions from individual vehicles driven over the Federal Test Procedure on a chassis dynamometer. These comparisons require a detailed breakdown of the vehicle fleet by vehicle type, engine type, and vehicle age. Future tunnel studies should include detailed characterization of the vehicle fleet either by license plate survey or expert identification of vehicles into classes and model years. We were fortunate to have had access to the extensive vehicle fleet composition data from Prof. Harley's experiments in the Caldecott Tunnel to supplement the HDV and LDV vehicle count data alone that was collected as part of this Caldecott Tunnel Study.

One example where more detailed vehicle fleet composition data would have been useful is in the explanation of NH_3 emissions which were higher in Bore 1 (HDV and LDV) than in Bore 2 ("LDV Only") of the Caldecott Tunnel. This observation could be explained by 1) a higher fraction of older LDVs in Bore 1 in the early afternoon as compared to Bore 2 in the late afternoon, or 2) the presence of more catalyst-equipped gasoline-powered trucks in Bore 1. With more detailed fleet composition data, we might have been able to recommend one of these hypotheses.

Comparisons of emissions measured in a tunnel with those measured in the laboratory also require an understanding of the driving conditions in the tunnel. Again, we were fortunate to have access to extensive vehicle driving condition data from Prof. Harley's experiments. Future tunnel studies should measure the distribution of vehicle speeds and the air flow rate through the tunnel, as these are data

needed to estimate the relative fuel consumption in the tunnel compared with that for the FTP cycle.

5.3 Future Research

5.3.1 Comparison with Single Particle Measurements

Prof. Kimberly Prather of the University of California, Riverside, and her research group sampled ambient aerosols during SCOS97 with aerosol time-of-flight mass spectrometry (ATOFMS) instruments. These instruments simultaneously measure the size and composition of individual airborne particles. During the SCOS97 experiments, three ATOFMS instruments collected particle size and chemical composition data on more than 350,000 ambient particles during time periods also sampled by our research group. We are in the process of comparing the ATOFMS data with the measurements reported here.

The quantity of ATOFMS data collected during SCOS97 is too large for *ad hoc* data analysis techniques. Therefore, as a first step in comparing ATOFMS and impactor sample data, we developed YAADA, an object-oriented toolkit of functions written for the Matlab programming environment. ATOFMS data are stored in YAADA in a hierarchical database implemented as a collection of table, column, and unique identifier objects. The data structure has four tables to store data on 1) instrument operating conditions, 2) particle time of acquisition and size, 3) mass spectra, and 4) peaks which make up the mass spectra.

We are in the process of comparing ambient aerosol mass and composition measurements made during intensive operating periods of SCOS97, using ATOFMS instruments, cascade impactors, and fine particle filter samplers. The particle detection efficiencies of the ATOFMS instruments are being determined as a function of particle size from comparisons of data from the ATOFMS instruments and colocated cascade impactors. Our approach is similar to the one used previously to determine the ATOFMS instrument particle detection efficiencies during the 1996 field study [45]. Using these calibration functions, the ATOFMS data are scaled up to estimate aerosol mass concentrations over the entire 48-h sampling periods of each trajectory-oriented experiment reported in Chapters 2 and 3.

In addition to particle size, the ATOFMS instruments record the mass spectra, i.e., chemical composition, of the single particles. The particle detection efficiency calibration functions developed are applied to increase the concentration of individual particles in proportion to the extent to which they were initially undercounted by the ATOFMS instruments. Then mass spectra of the particles containing

specific chemical substances, e.g. ammonium and nitrate, are compared to the chemical composition of cascade impactor samples. From this comparison, the chemical sensitivities of the ATOFMS instruments for these chemical species are determined and then used to construct continuous time series of aerosol chemical composition data from the ATOFMS data. The methods and results of this work will be submitted for publication in peer-reviewed journals.

5.3.2 Single-Particle Level Air Quality Modeling

The present studies were undertaken to broaden the range of aerosol observations in order to enhance our understanding of the origin of PM in the SoCAB. Our understanding of the processes leading to the formation of particulate matter in the SoCAB is expressed in air quality models. These models will be refined and tested using the novel measurements reported here. Such models provide the means to evaluate proposed control strategies in advance of their adoption.

Recently we and others have developed air quality models which treat PM as an ensemble of chemically complex particles emitted from a range of sources. To develop and test these models, we require detailed size-segregated aerosol composition data like those collected in the present studies.

In future research, we intend to model the results of the SCOS97 studies. Our approach to this research will be similar to our approach in the 1996 trajectory study. In that study we sampled air parcels along the Long Beach—Fullerton—Riverside trajectory [3, 13]. We then ran our single-particle level air quality model for the meteorological conditions observed and compared the model results with the observations [5]. Using the model we determined, for example, that the particles which made the largest contribution to visibility reduction in Riverside were background sulfate-containing particles which accumulated organic matter and ammonium nitrate over the SoCAB. The SCOS97 data will permit similar analyses in other parts of the air basin and under different meteorological conditions.

Bibliography

[1] Christoforou, C. S., L. G. Salmon, M. P. Hannigan, P. A. Solomon, and G. R. Cass. Trends in fine particle concentration and chemical composition in Southern California. J. Air and Waste Management Assoc., 50:43–53, 2000.

[2] Motallebi, N., J. Pederson, B. E. Croes, T. VanCuren, S. V. Hering, K. A. Prather, and M. A. Allan. The 1997 Southern California Ozone Study-NARSTO: Aerosol Program and Radiation Study. Air & Waste Management Assoc., 1999. Paper 98-WP75.04, Air and Waste Management Association 91st Annual Meeting, June 14-18, 1998, San Diego, California.

[3] Hughes, L. S., J. O. Allen, M. J. Kleeman, R. J. Johnson, G. R. Cass, D. S. Gross, E. E. Gard, M. E. Gälli, B. D. Morrical, D. P. Fergenson, T. Dienes, C. A. Noble, D. Y. Liu, P. J. Silva, and K. A. Prather. The size and composition distribution of atmospheric particles in Southern California. Environ. Sci. Technol., 33:3506–3515, 1999.

[4] Fraser, M. P. and G. R. Cass. Detection of excess ammonia emissions from in-use vehicles and the implications for fine particle control. Environ. Sci. Technol., 32:1053–1057, 1998.

[5] Kleeman, M. J., L. S. Hughes, J. O. Allen, and G. R. Cass. Source contributions to the size and composition distribution of atmospheric particles: Southern California in September 1996. Environ. Sci. Technol., 33:4331–4341, 1999.

[6] Kleeman, M. J. and G. R. Cass. Source contributions to the size and composition distribution of urban particulate air-pollution. Atmos. Environ., 32:2803–2816, 1998.

[7] Fujita, E. M., G. Green, R. Keislar, D. Koracin, H. Moosmuller, and J. Watson. SCOS97-NARSTO 1997 Southern California Ozone Study and Aerosol Study, Volume I: Operational program plan. Technical report, Air Resources Board, Sacramento, CA, 1999.

[8] Fujita, E. M., G. Green, R. Keislar, D. Koracin, H. Moosmuller, and J. Watson. SCOS97-NARSTO 1997 Southern California Ozone Study and Aerosol Study, Volume II: Quality assurance plan. Technical report, Air Resources Board, Sacramento, CA, 1999.

[9] Fujita, E. M., G. Green, R. Keislar, D. Koracin, H. Moosmuller, and J. Watson. SCOS97-NARSTO 1997 Southern California Ozone Study and Aerosol Study, Volume III: Summary of field study. Technical report, Air Resources Board, Sacramento, CA, 1999.

[10] Hering, S. V., M. Stolzenburg, and N. Kreisberg. Automated nitrate and $PM_{2.5}$ FRM measurements for method evaluation and secondary aerosol characterization during SCOS97. Technical report, Aerosol Dynamics, Inc., 1999.

[11] Russell, A. G. and G. R. Cass. Acquisition of regional air quality model validation data for nitrate, sulfate, ammonium ion and their precursors. Atmos. Environ., 18:1815–1827, 1984.

[12] Hildemann, L. M., A. G. Russell, and G. R. Cass. Ammonia and nitric acid concentrations in equilibrium with atmospheric aerosols - experiment vs. theory. Atmos. Environ., 18:1737–1750, 1984.

[13] Hughes, L. S., D. Y. Liu, J. O. Allen, D. P. Fergenson, M. J. Kleeman, B. D. Morrical, K. A. Prather, and G. R. Cass. Evolution of atmospheric particles along trajectories crossing the Los Angeles basin. Environ. Sci. Technol., 34:3058–3068, 2000.

[14] Hering, S. V. 1998. Aerosol Dynamics, Inc., Berkeley, CA. Personal communication.

[15] Gard, E. E., J. E. Mayer, B. D. Morrical, T. Dienes, D. P. Fergenson, and K. A. Prather. Real-time analysis of individual atmospheric aerosol-particles - design and performance of a portable ATOFMS. Anal. Chem., 69:4083–4091, 1997.

[16] Noble, C. A. and K. A. Prather. Profiles of individual atmospheric aerosol particles. Environ. Sci. Technol., 30:2667–2680, 1996.

[17] Solomon, P. A., T. Fall, L. Salmon, and G. R. Cass. Chemical characteristics of PM10 aerosols collected in the Los Angeles area. J. Air Pollut. Control Assoc., 39:154–163, 1989.

[18] John, W. and G. Reischl. A cyclone for size-selective sampling of ambient air. J. Air Pollut. Control Assoc., 30:872–876, 1980.

[19] Marple, V. A., K. L. Rubow, and S. M. Behm. A microorifice uniform deposit impactor (MOUDI): Description, calibration and use. Aerosol Sci. Technol., 14:434–446, 1991.

[20] Huntzicker, J. J., R. L. Johnson, J. J. Shah, and R. A. Cary. In G. T. Wolff and R. L. Klimisch, eds., *Particulate Carbon, Atmospheric Life Cycle*, pages 79–88. Plenum, New York, 1982.

[21] Birch, M. E. and R. A. Cary. Elemental carbon-based method for monitoring occupational exposures to particulate diesel exhaust. Aerosol Sci. Technol., 25:221–241, 1996.

[22] Gray, H. A., G. R. Cass, J. J. Huntzicker, E. K. Heyerdahl, and J. A. Rau. Characteristics of atmospheric organic and elemental carbon particle concentrations in Los Angeles. Environ. Sci. Technol., 20:580–589, 1986.

[23] Mulik, J., R. Puckett, D. Willims, and E. Sawicki. Ion chromatographic analysis of sulfate and nitrate in ambient aerosols. Anal. Letters, 9:653–663, 1976.

[24] Bolleter, W. T., C. T. Bushman, and P. W. Tidwell. Spectrophotometric determinations of ammonium as indophenol. Anal. Chem., 33:592–594, 1961.

[25] Solomon, P. A., L. G. Salmon, and G. R. Cass. Spatial and temporal distribution of atmospheric nitric acid and particulate nitrate concentrations in the Los Angeles area. Environ. Sci. Technol., 26:1594–1601, 1992.

[26] Olmez, I. Instrumental neutron activation analysis of atmospheric particulate matter. In J. P. Lodge, Jr., ed., *Methods of Air Sampling and Analysis, 3rd Edition*, pages 143–150. Lewis Publishers, Inc., Chelsea, MI, 1989.

[27] Goodin, W. R., G. J. McRae, and J. H. Seinfeld. A comparison of interpolation methods for sparse data: Application to wind and concentration fields. J. Applied Meteor., 18:761–771, 1979.

[28] Fraser, M. P., G. R. Cass, and B. R. T. Simoneit. Gas-phase and particle-phase organic compounds emitted from motor vehicle traffic in a Los Angeles roadway tunnel. Environ. Sci. Technol., 32:2051–2060, 1998.

[29] Russell, A. G. and G. R. Cass. Verification of a mathematical-model for aerosol nitrate and nitric acid formulation and its use for control measure evaluation. Atmos. Environ., 20:2011–2025, 1986.

[30] Russell, A. G., K. F. McCue, and G. R. Cass. Mathematical modeling of the formation of nitrogen-containing pollutants 1. Evaluation of an Eularian photochemical model. Environ. Sci. Technol., 22:263–270, 1988.

[31] Russell, A. G., K. F. McCue, and G. R. Cass. Mathematical modeling of the formation of nitrogen-containing pollutants 2. Evaluation of the effect of emission controls. Environ. Sci. Technol., 22:1336–1347, 1988.

[32] Kleeman, M. J., J. J. Schauer, and G. R. Cass. Size and composition distribution of fine particulate matter emitted from motor vehicles. Environ. Sci. Technol., 34:1132–1142, 2000.

[33] Vogt, R., C. Elliott, H. C. Allen, J. M. Laux, J. C. Hemminger, and B. J. Finlayson-Pitts. Some new laboratory approaches to studying tropospheric heterogeneous reactions. Atmos. Environ., 30:1729–1737, 1996.

[34] Beichert, P. and B. J. Finlayson-Pitts. Knudsen cell studies of the uptake of gaseous HNO_3 and other oxides of nitrogen on solid NaCl: The role of surface-adsorbed water. J. Phys. Chem., 100(37):15218–15228, 1996.

[35] Leu, M. T., R. S. Timonen, L. F. Keyser, and Y. L. Yung. Heterogeneous reactions of HNO_3(g)+NaCl(s) –> HCl(g)+$NaNO_3$(s) and N_2O_5(g)+NaCl(s) –> $ClNO_2$(g)+$NaNO_3$(s). J. Phys. Chem., 99(35):13203–13212, 1995.

[36] Fenter, F. F., F. Caloz, and M. J. Rossi. Kinetics of nitric acid uptake by salt. J. Phys. Chem., 98(29):9801–9810, 1994.

[37] Laux, J. M., J. C. Hemminger, and B. J. Finlayson-Pitts. X-ray photoelectron spectroscopic studies of the heterogenous reaction of gaseous nitric acid with sodium chloride - kinetics and contribution to the chemistry of the marine troposphere. Geophys. Res. Letters, 21(15):1623–1626, 1994.

[38] Mamane, Y. and J. Gottlieb. Heterogeneous reaction of nitrogen oxides on sea salt and mineral particles - a single-particle approach. J. Aerosol Sci., 21:S225–S228, 1990.

[39] Pierson, W. R. and W. W. Brachaczek. Particulate matter associated with vehicles on the road. II. Aerosol Sci. Technol., 2:1–40, 1983.

[40] Weingartner, E., C. Keller, W. A. Stahel, H. Burtscher, and U. Baltensperger. Aerosol emissions in a road tunnel. Atmos. Environ., 31:451–462, 1997.

[41] Kirchstetter, T. W., R. A. Harley, N. M. Kreisberg, M. R. Stolzenburg, and S. V. Hering. On-road measurement of fine particle and nitrogen oxide emissions from light- and heavy-duty motor vehicles. Atmos. Environ., 33:2955–2968, 1999.

[42] Gross, D. S., M. E. Gälli, P. J. Silva, S. H. Wood, D. Y. Liu, and K. A. Prather. Single particle characterization of automobile and diesel truck emissions in the Caldecott Tunnel. Aerosol Sci. Technol., 32:152–163, 2000.

[43] Kirchstetter, T. W., B. C. Singer, R. A. Harley, G. R. Kendall, and W. Chan. Impact of oxygenated gasoline use on California light-duty vehicle emissions. Environ. Sci. Technol., 30:661–670, 1996.

[44] Solomon, P. A., S. M. Larson, T. Fall, and G. R. Cass. Basinwide nitric acid and related species concentrations observed during the Claremont Nitrogen Species Comparison Study. Atmos. Environ., 22:1587–1594, 1988.

[45] Kleeman, M. J., J. J. Schauer, and G. R. Cass. Size and composition determination of fine particulate matter emitted from wood burning, meat charbroiling, and cigarettes. Environ. Sci. Technol., 33:3516–3523, 1999.

[46] Singer, B. C. and R. A. Harley. A fuel-based motor vehicle emission inventory. J. Air and Waste Management Assoc., 46:581–593, 1996.

[47] Kirchstetter, T. W., B. C. Singer, R. A. Harley, G. R. Kendall, and M. Traverse. Impact of California reformulated gasoline on motor vehicle emissions. 1. Mass emission rates. Environ. Sci. Technol., 33:318–328, 1999.

[48] California Air Resources Board, Mobile Source Emission Inventory Branch, Sacramento, CA. *Methodology for estimating emissions from on-road motor vehicles*, November 1996.

[49] Pierson, W. R., A. W. Gertler, N. F. Robinson, J. C. Sagebiel, B. Zielinska, G. A. Bishop, D. H. Stedman, R. B. Zweidinger, and W. D. Ray. Real-world automotive emissions — Summary of studies in the Fort McHenry and Tuscarora Mountain Tunnels. Atmos. Environ., 30:2233–2256, 1996.

[50] Cadle, S. H. and P. A. Mulawa. Low molecular weight aliphatic amines in exhaust from catalyst-equipped cars. Environ. Sci. Technol., 14:718–723, 1980.

Appendix A

Quality Assurance/Quality Control

Quality assurance/quality control (QA/QC) procedures were used to ensure the validity and quality of data produced by our laboratory for this study. A complete QA/QC plan was presented to the study management in July 1997, prior to the beginning of the study. That plan included detailed internal procedures followed in the preparation, collection, and analysis of samples and the cleaning, adjustment, and operation of sampling instruments. This section summarizes those procedures, and reports on QA/QC implementation and the validation of the final data.

A.1 Filter Samplers

A.1.1 Sampler Cleaning

The filter samplers at each site consisted of four sampling assemblies (see Figure 2.3). These were cleaned and assembled in the laboratory before the study began and again before the Caldecott Tunnel experiments began. All components of the samplers were cleaned by successive washes with a detergent solution, deionized water, methanol, and hexane. They were then assembled, checked for leaks, and sealed for transport. The glass inlets were washed with a dilute HCl solution, and sealed in the laboratory for transport.

Filter holders were washed in the field with methanol whenever they became visibly dirty.

A.1.2 Sampler Air Flows

The air flow through each filter was controlled by a critical orifice downstream of the filter holder. The orifices were machined at Caltech to consistently produce air flow rates equal to the nominal flow rates for the filter samplers.

The air flow rate through each filter holder was measured before and after each sampling event using a rotameter with a precision of 1% of full scale. Prior to the study, these rotameters were calibrated against the primary flow rate measurement of a Gilibrator (Gilian Instrument Corp., Wayne, NJ) to determine the actual flow rate. Multiple flow rate measurements ensured that any filter holder leaks or clogged filters would not go undetected; no such leaks or clogs occurred during the study. The flow rate for each sample is taken to be the average of the flows measured before and after sample collection.

On August 18 and 19, 1997, Fred Rogers and John Bowen of the Desert Research Institute conducted a flow audit of our samplers [8]. They measured the flow rate for the fine and PM_{10} filter samplers with a Gilibrator. (Note: This instrument was different from the one used to calibrate the rotameters.) In all cases the auditors' primary flow rate measurements agreed with the flow rates as measured with the calibrated rotameter to within 5%, the auditors' criterion for agreement between measurements.

A.1.3 Sample Storage

Prior to sample collection, sampling media were stored in sealed, prelabeled containers. PTFE, nylon, and glass fiber filters were stored in petri dishes sealed with Teflon tape. Quartz fiber filters were stored in petri dishes lined with heat-treated aluminum foil and sealed with Teflon tape. After sample collection, sampling media were placed back in their original petri dishes and sealed with Teflon tape. All samples were stored temporarily at the field sampling sites in refrigerators at approximately 5°C. Immediately after each sampling event, the samples were transferred to the laboratory in coolers. Samples were stored in the laboratory in a freezer at -20°C until analysis.

A.2 Micro-orifice Impactors

A.2.1 Sampler Cleaning

The impactor samplers at each site consisted of two MOIs and their associated cyclones. These were cleaned and assembled in the laboratory before the study began and again before the Caldecott Tunnel experiments began. The cyclones and inlet lines were cleaned with successive washes with a detergent solution, deionized water, methanol, and hexane. The MOIs were cleaned with successive washes with deionized water, methanol, and hexane. They were then assembled, checked for leaks, and sealed for transport.

A.2.2 Sampler Air Flows

The sampling flow rate in each impactor was monitored by measuring the pressure drop across impaction stages 1–6 of the impactor; the flow rate is directly related to the value of this pressure drop. Air flow was adjusted using a valve between the impactor and vacuum pump so that the pressure drop across stages 1–6 matched the manufacturer's specification. The manufacturer calibrated the pressure drop set point of each impactor to correspond to a flow of 30 lpm. The specified pressure drops vary between 20.5 and 21.5 inches H_2O among the 6 impactors used in this study. The flow rates were checked and adjusted if necessary approximately hourly during sampling events. Pressure drops across impaction stages 7–10 were also monitored to detect leaks or impactor jet clogging. The measured pressure drops were recorded at the beginning and end of each sampling event in the standard log sheet folder at each site. Pressure gages used to measure the pressure drops across stages 1–6 had a precision of 0.5 inches H_2O; those used to measure the pressure drops across stages 7–10 had a precision of 5 inches H_2O.

The impactor sampling flow rates were measured in the laboratory after the field sampling work was completed using a calibrated orifice flow meter from MSP Corp. (part number MDI-090). This orifice was calibrated such that a 30 lpm flow corresponded to a pressure drop of 2.60 inches H_2O across the orifice. Since the flow through an orifice flow meter varies as the square root of the pressure drop across it, for pressure drops near 2.60 inches H_2O, the flow rate (Q) in lpm depends on the pressure drop (dP) in inches H_2O as

$$Q = 18.605\sqrt{(dP)} \tag{A.1}$$

Table A.1: MOI Flow Rate Calibrations

Serial Number	Design Stage 6 dP	Flow Rate (lpm) at Design dP	A (inches H_20)	B (lpm)
MDI-071	21.10	28.5	12.67	0.7490
MDI-072	21.50	29.2	13.41	0.7348
MDI-107	21.00	28.4	13.12	0.7266
MDI-108	21.25	28.3	13.38	0.7044
MDI-109	20.75	28.3	13.25	0.7249
MDI-110	20.50	28.4	13.46	0.7274

This calibration is expected to be accurate to within a few percent. Pressure drops over the orifice were measured using a water manometer with an accuracy of 0.1 cm.

The flow rate into the impactors was measured for both aluminum and PTFE impaction substrates and at a range of pressure drops. The impactor pressure drop at stage 6 was determined to be an accurate measure of the flow rate. Flow rates through the impactor varied linearly with stage 6 dP. Correlations of the form

$$Q = A + B \times dP \tag{A.2}$$

were developed for each impactor from lab measurements. From these correlations, the actual flow through each impactor when stage 6 dP was set to the manufacturer's recommended value was calculated (see Table A.1). All impactor air flow rates used in reducing the field data were calculated using these correlations and the actual stage 6 dP values.

On August 18 and 19, 1997, Fred Rogers and John Bowen of the Desert Research Institute conducted a flow audit of the MOI samplers [8]. They measured air flow rates through the MOIs with a rotameter while the stage 6 pressure drop was controlled to meet the manufacturer's specifications. They observed that the MOI flow rates were 5–12% below the nominal flow rate of 30 lpm (see Table A.2).

Based on the MOI flow rate calibrations described above, we can calculate the actual flow rate for the impactors during the flow audit. The calculated flow rates are less than 30 lpm and in qualitative agreement with the auditors' results. The agreement is generally within the auditors' criterion of 5%, except in two cases where the two values differ by -6.5 and -5.6% (see Table A.2). There are several possible reasons for discrepancies. The calibrated orifice used to develop the impactor flow correlation to stage 6 dP was designed for use with these samplers and does not cause a measurable change in the pressure at stage 6; the rotameter used by the auditors may either have had small leaks at the sampler inlet interface or caused a small additional pressure drop at stage 6. If either was the case, the audit-measured flow rate would be lower than the actual flow rate, as seen in Table A.2.

Table A.2: Field Audit of MOI Flow Rates

Serial Number	Flow Rate at Design dP	Audit Flow[a] (lpm)	Difference (%)
MDI-071	28.5	26.7	-6.5
MDI-072	29.2	27.6	-5.6
MDI-107	28.4	27.6	-2.9
MDI-108	28.3	27.6	-2.5
MDI-109	28.3	27.2	-4.0
MDI-110	28.4	28.5	0.4

[a]As measured by Rogers and Bowen [8]

A.2.3 Sample Storage

Impactor samples were stored in the same manner as filter samples. Prior to sample collection, impaction substrates and afterfilters were stored in sealed, prelabeled containers. PTFE membrane substrates were stored in petri dishes sealed with Teflon tape. Aluminum impaction substrates and quartz fiber afterfilters were stored in petri dishes lined with heat-treated aluminum foil and sealed with Teflon tape. After sample collection, sampling media were placed back in their original petri dishes and sealed with Teflon tape. All samples were stored temporarily at the field sampling sites in refrigerators at approximately 5°C. Immediately after each sampling event, the samples were transferred to the laboratory in coolers. Samples were stored in the laboratory in a freezer at -20°C until analysis.

A.3 Electronic Instruments

All three of the EAAs and the two Caltech OPCs (i.e. those not stationed at Riverside) were tested and calibrated before the study began. All station operators were fully trained and had experience with the relevant sampling instruments prior to the study. Size distributions from the OPCs were corrected as suggested by Hering [14] to take into account the difference in the refractive index between the polystyrene latex (PSL) spheres used to calibrate the instruments and typical Los Angeles area atmospheric aerosols.

A.4 Sampling Interruptions

The impactor with PTFE substrates sampling on August 21, 1997, 0600 PDT at the Central Los Angeles site experienced problems which prevented the collection of size-segregated particle samples during that time period. The pressure drop across impaction stages 7–10 were in excess of the manufacturer's specifications, indicating that there was a great deal of flow resistance in the lower half of the impactor. It was determined that the PTFE filters used as the impactor afterfilters were not sufficiently porous for the 30 lpm flow rate. This set of impactor samples (S97-V11b-LA-MX*) was not analyzed. For the remainder of the ambient air quality study, PTFE afterfilters were not used in any of the impactors.

A.5 Sample Analyses

A.5.1 Mass

Atmospheric particle mass concentrations were measured gravimetrically by weighing PTFE filters and PTFE and aluminum foil substrates at least twice before and twice after sample collection with a Mettler Instruments mechanical microgram balance, model M-55-A. Filters and substrates were allowed to equilibrate in a temperature- and humidity-controlled environment of 22.9 ± 0.3°C and 48 ± 3% RH before they were weighed in the same room. Unexposed PTFE filters and substrates were equilibrated for at least 24 hours prior to weighing, while filters and substrates with collected particle samples were equilibrated for about 4 hours prior to weighing; the shorter equilibration time for collected samples avoids loss of collected aerosol species that are prone to volatilization. A set of control filters was weighed during each daily weighing period to verify the consistency of the microbalance calibration between the initial and final weighings.

The Mettler microbalance has 1 μg sensitivity, and the standard weighing method yielded an average uncertainty of 2.5 μg/filter for aluminum substrates and 2.4 μg/filter for PTFE media. The precision estimate for each filter or substrate was determined by repeated weighings.

A.5.2 Ionic species

PTFE membrane filters and substrates were extracted in deionized water and subjected to two methods of ion analysis; SO_4^{-2}, NO_3^-, and Cl^- quantities were determined using a Dionex Model 2020i ion chro-

matograph [23], and ammonium ion (NH_4^+) quantities were determined by an indophenol colorimetric procedure [24] employed by a rapid flow analyzer (Alpkem Corp., RFA-300).

Nylon filters were extracted in a carbonate/sodium bicarbonate eluent before analyzed by ion chromatography [25]. Measurement of NO_3^- and Cl^- concentrations on the denuded and undenuded Nylon filter pairs by ion chromatography allowed determination of ambient gas-phase nitric acid and hydrochloric acid concentrations by the denuder difference method. Gas-phase ammonia concentrations were determined from oxalic acid-impregnated glass fiber filters by using the Alpkem indophenol colorimetric procedure described above for aerosol NH_4^+ measurement.

PTFE filters and substrates were subject to ion chromatography analysis, indophenol colorimetry, and instrumental neutron activation analysis (INAA). A single extract can be used for both ion chromatography and indophenol colorimetry, however neutron activation requires a dry PTFE filter membrane separated from its support ring and sealed in a cleaned plastic sample bag. Where redundant PTFE samples were available, e.g. fine particle samples, one filter was extracted and subject to ion chromatography and indophenol colorimetry, while the other was separated from its filter ring, rolled, bagged, and sealed for neutron activation analysis. For PM_{10} and impactor samples, a single filter or substrate was cut in half using a scalpel and cutting template. Impactor substrates with a small number (< 40) of impaction dots were cut such that each of the two sections to be analyzed included a known number of the dots equal to close to half of the total number of discrete dots.

The concentrations of all chemical species analyzed by ion chromatography or indophenol colorimetry were determined relative to laboratory standards of known concentration. Aqueous standards were prepared weekly by dilution of concentrated ACS grade analytical reagents. The matrices of the daily standards and the sample extracts matched that of the leaching solution. Standard log sheets were completed each time standards or reagents were prepared.

Uncertainties in ionic species measurements were determined by both repeated analysis of a fraction of the samples and by the consistency of repeated analysis of the set of standards.

A.5.3 Carbon

Elemental carbon (EC) and organic carbon (OC) concentrations in the aerosol samples were be determined by thermal-optical measurement of samples collected on quartz fiber filters and aluminum foil impaction substrates[20, 21]. Prior to sample collection, quartz fiber filters were heat treated at $550°C$

in air for 8 hours to lower their carbon blank levels; aluminum foil impaction substrates were similarly heat treated at 550°C in air for 48 hours. All quartz filters and aluminum substrates were stored sealed in annealed foil-lined petri dishes.

Organic carbon concentrations and total carbon (TC) concentrations were determined relative to at least four sucrose laboratory standards of known concentration. No elemental carbon standards exist that mimic atmospheric EC samples, and for that reason it is difficult to quantify uncertainties in the division of TC into EC and OC. Standards were prepared weekly, and standard log sheets were completed each time standards were prepared.

A.5.4 INAA

The bulk concentrations of 34 major and minor trace elements were measured by neutron activation analysis at the Nuclear Reactor Lab at the Massachussetts Institute of Technology; this analysis was performed on PTFE membrane filters and impaction substrates. The elements measured were: Al, As, Au, Ba, Br, Cd, Ce, Cl, Co, Cr, Cs, Eu, Fe, Ga, Hg, In, K, La, Lu, Mg, Mn, Mo, Na, Nd, Rb, Sb, Sc, Se, Sm, Sr, Th, Ti, U, V, Yb, and Zn. The neutron activation analyses was performed by Dr. Michael Ames at the Nuclear Reactor Lab, Massachusetts Institute of Technology (MIT).

Before the samples were sent to MIT, they were cut, bagged, sealed, and labeled in our lab. PTFE membrane filters were cut from their edge support rings using a scalpel on a clean surface. Where it was necessary to cut a sample in half to be used for both neutron activation and ion analysis/indophenol colorimetry, the membrane was cut in half using a template to insure accuracy, and one half was sent to MIT. The membrane was folded in upon itself to prevent any particles from being rubbed off. The bag was heat sealed into a small labeled plastic bag, supplied from the Nuclear Reactor Lab with a precleaned inner surface.

Data and uncertainties were reported by the Nuclear Reactor Lab, and some data points were flagged as below detection limits.

A.5.5 Field Blanks

Field blanks, equal in number to 12% of the number of actual ambient or tunnel samples used in the study, were taken at each site during the study. Field blanks were obtained by loading filters and impactor substrates into their respective sampling instruments and turning the instruments on for

one minute. Field blanks were handled, stored, and analyzed in exactly the same manner as normal samples.

A.6 Data Reduction

Field blanks of the same media type and instrument type (e.g. PM_{10}, fine, MOI) for the entire study were grouped together. Blank values for mass and each analyzed chemical species were averaged together for each group, and these average blank value corrections were applied only to samples of the same group. Extreme outlier blank values, defined to be $> 3\sigma$ from the means of their respective groups of blank values, were considered contaminated and disregarded. Uncertainties in blank values, samples, and air flow rates were propagated through in the calculation of blank-corrected concentrations.

Organic matter concentrations were estimated from measured organic carbon concentrations by multiplying by a factor of 1.4 to account for the additional mass of associated H, O, N, and S present in typical atmospheric organic aerosols [22].

Fine particle NO_3^- concentrations were determined from the samples collected on the denuded nylon fine particle filters. The difference between the concentrations of fine particle NO_3^- as measured on a simultaneously collected denuded nylon filter sample and fine particle PTFE filter indicates the NO_3^- portion of the amount of NH_4NO_3 volatilized from the PTFE filter. The equivalent amount of NH_4NO_3 is added to the mass, NO_3^-, and NH_4^+ concentrations measured on the PTFE fine particle and PM_{10} filters. In addition, because the oxalic filters, on which gas-phase NH_3 is collected, were located downstream of a PTFE pre-filter from which NH_4NO_3 volatilized, adding NH_3 to the airstream, an amount of NH_3 equivalent to the NH_4^+ volatilized was subtracted from the measured NH_3 result.

Trace element oxide concentrations were estimated by converting INAA-obtained elemental concentrations to the equivalent mass of their most common oxides, where appropriate. Conversion factors and oxide species are shown in Table A.3.

A.7 Data Checking

The combination of measurements made on the quartz fiber and Teflon filters allows a nearly complete material balance on the chemical composition of the fine particles to be obtained. Similarly, the combination of measurements made on the aluminum and Teflon impaction media allows a nearly

Table A.3: Common Oxide Forms of Measured Elements and Mass Conversion Factors.

Element	Oxide	Conversion Factor
Al	Al_2O_3	1.9
Fe	Fe_2O_3	1.43
Ba	BaO	1.12
Cd	CdO	1.14
Cr	CrO_3	1.92
In	In_2O_3	1.2
K	K_2O	1.2
Mn	Mn_2O_7	2.02
Sb	Sb_2O_5	1.33
Ti	TiO_2	1.67
V	V_2O_5	1.78
Ga	Ga_2O_3	1.69
As	As_2O_5	1.53
Se	SeO_3	1.61
Hg	HgO	1.08
Mo	MoO_3	1.5
Zn	ZnO	1.24

complete material balance on the chemical composition of the size-segregated fine particles, as well as two measurements of total mass. These data sets were checked for internal consistency by comparing the sum of the analytes to the total mass measurements (see figures in main text and in Appendix C.

The study design includes numerous complementary measurements of aerosol composition and size distribution. For example, colocated impactor and fine particle filter samples were independently analyzed for aerosol mass, ionic species, trace elements, organic carbon and elemental carbon. The impactor measurements summed over the corresponding stages were compared to the fine particle filter measurements. Real-time aerosol size distribution data were collected using EAAs and OPCs. These data were combined to estimate fine particle mass concentrations integrated over the impactor size bins and sampling times. The fine particle masses as estimated from EAA/OPC data were compared to the fine filter mass data. In addition, ion balances were constructed for each sample; an ion balance would be expected to yield about equal equivalents of the negative species measured (NO_3^-, $SO_4^=$, Cl^-) and the positive species measured (NH_4^+, and Mg^{+2}, Na^+, and K^+). Note that Cl^-, Mg^{+2}, Na^+, and K^+ are measured as elemental, not ionic, concentrations. Data points found to be suspect on the basis of the above consistency checks were designated as outliers, and were disregarded.

Appendix B

Aerosol Sampling

Aerosol sampling for the SCOS97 aerosol study consisted of 3 separate experiments, as described previously in this report: the Vehicle-Oriented Trajectory Study, the Nitrate-Oriented Trajectory Study, and the Tunnel Study. In each of these studies a number of filter samplers, cascade impactors, and continuous size distribution instruments were employed at a number of sites. This appendix details the sampling sites, events, and instruments used in these experiments. The sample labeling system used to identify the time, date, location, and particle size range of a sample also is explained.

B.1 Vehicle-Oriented Trajectory Study

B.1.1 Sampling Sites

A three station air monitoring network was established in the SoCAB to measure the impact of primary vehicle emissions on ambient particulate matter concentrations. These sites were at Central Los Angeles, Azusa, and Riverside (see Figure 1.1). The sampling sites were chosen to study motor vehicle-derived aerosol: Central LA because of its proximity to the highest traffic densities in the SoCAB and Azusa because it is usually directly downwind of Central LA. The Riverside site was chosen primarily because one ATOFMS instrument permanently resides there; this site often receives air parcels advected westward across the basin south of Central LA and Azusa. The objectives and results from this experiment are described in detail in Chapter 2 of this report. Table B.1 lists the location details of the sampling sites. Table B.2 lists aerosol sampling equipment operated by our group and by other

Table B.1: Vehicle-Oriented Trajectory Study Sampling Sites.

Name	SCOS97 Code	Address	Latitude	Longitude
Central LA	LANM	1630 N. Main Street, Los Angeles	34^o 4' 1"	118^o 13' 36"
Azusa	AZSP	Hunt & Sons Plumbing 780 N. Todd Ave, Azusa	34^o 8' 10"	117^o 56' 28"
UC-Riverside	RIVR	Pierce Hall roof	33^o 58' 26"	117^o 19' 40"
UC-Riverside	RIVC	Pierce Hall, 2nd floor	33^o 58' 23"	117^o 19' 35"

research groups at these sampling sites.

B.1.2 Sampling Times

This experiment was run during two two-day sampling events: August 21, 1997, 0120 PDT–August 23, 1997, 0100 PDT and August 27, 1997 0120 PDT–August 29, 1997 0100 PDT. Five sets of filter samples per day were collected during these events on the schedule: 0120–0600 hours PDT, 0620–1000 hours PDT, 1020–1400 hours PDT, 1420–1800 hours PDT, and 1820 to 0100 hours PDT the following day. Impactor samples were collected during one or two of these sampling intervals per site per sampling day. The continuous size distribution samplers (EAA and OPC) were operated at the three sampling sites throughout the sampling events, except for the period after August 27, 1930 PDT, when the EAA at the Central LA was not in operation. An ATOFMS instrument located at each sampling station operated throughout both two-day sampling events. The results of the ATOFMS instrument measurements will be reported separately by Kimberly Prather's research group, UC-Riverside. Sampling times for impactors and bulk particle samplers during this study are presented in Figure 2.2.

B.2 Nitrate-Oriented Trajectory Study

B.2.1 Sampling Sites

A three station air monitoring network was established in the SoCAB to examine the formation of fine nitrate particles. One station was located to the west of the Chino dairy production area at Diamond Bar, one station in the midst of the dairy area at Mira Loma, and one station at Riverside, which is often downwind of Diamond Bar and Mira Loma. The three sites are labeled on the map in Figure 1.1. The objectives and results from this experiment are described in detail in Chapter 3 of this report. Table B.3 lists the location details of the sampling sites. Table B.4 lists aerosol sampling equipment operated by

Table B.2: Aerosol Sampling Instruments at Each Vehicle-Oriented Trajectory Study Sampling Site.

Site	Group	Sampling Equipment
Central LA (roof)	Caltech (Cass)	Fine Filter Samplers FTQ,FTNN,FQQ
	Caltech (Cass)	PM_{10} Filter Sampler
	Caltech (Cass)	2 micro-orifice impactors (MOIs)
	SCAQMD	Federal Reference Method sampler (FRM)
Central LA (2nd floor)	Caltech (Cass)	EAA, OPC
	UCR (Prather)	Transportable ATOFMS
Azusa	Caltech (Cass)	Fine Filter Samplers FTQ,FTNN,FQQ
	Caltech (Cass)	PM_{10} Filter Sampler
	Caltech (Cass)	EAA, OPC
	Caltech (Cass)	2 MOIs
	UCR (Prather)	Transportable ATOFMS
UC-Riverside (roof)	Caltech (Cass)	Fine Filter Samplers FTQ, FTNN, FQQ
	Caltech (Cass)	PM_{10} Filter Sampler
	Caltech (Cass)	2 MOIs
	SCAQMD	FRM
UC-Riverside (2nd floor)	UCR (Prather)	ATOFMS
	Caltech (Cass)	EAA, OPC

Table B.3: Nitrate-Oriented Trajectory Study Sampling Sites.

Name	SCOS97 Code	Address	Latitude	Longitude
Diamond Bar	DIAM	SCAQMD HQ parking lot 21865 E. Copley Dr.	33^o 59' 59"	117^o 49' 56"
Mira Loma	CHIM	Chino-Mira Loma-Union Pacific Auto Yard 4500 Etiwanda, Mira Loma	34^o 0' 20"	117^o 30' 49"
UC-Riverside	RIVR	Pierce Hall roof	33^o 58' 26"	117^o 19' 40"
UC-Riverside	RIVC	Pierce Hall, 2nd floor	33^o 58' 23"	117^o 19' 35"

our group and by other research groups at these sampling sites. Non-Caltech sampling instruments listed for the Diamond Bar and Mira Loma sites were not in operation during the October 31–November 2, 1997 sampling event.

B.2.2 Sampling Times

This experiment was intended to have been run during two two-day high particulate matter concentration episodes between August 31 and September 15, 1997. Due to generally low particulate matter concentrations during this period, the time frame for the experiment was extended until November 1, 1997, and a third sampling event was added. The second sampling event (S97-N2) was conducted from September 27, 1997, 1400 PDT through September 30, 1997, 0100 PDT at Mira Loma only, and its purpose was to collect samples for the calibration of the ATOFMS instrument and ADI continuous

Table B.4: Aerosol Sampling Instruments at Each Nitrate-Oriented Trajectory Study Sampling Site.

Site	Group	Sampling Equipment
Diamond Bar	Caltech (Cass)	Fine Filter Samplers FTQ,FTNN,FQQ
	Caltech (Cass)	PM_{10} Filter Sampler
	Caltech (Cass)	2 micro-orifice impactors (MOIs)
	SCAQMD	Federal Reference Method sampler (FRM)
	Caltech (Cass)	EAA, OPC
Mira Loma	Caltech (Cass)	Fine Filter Samplers FTQ,FTNN,FQQ
	Caltech (Cass)	PM_{10} Filter Sampler
	Caltech (Cass)	EAA, OPC
	Caltech (Cass)	2 MOIs
	UCR (Prather)	Transportable ATOFMS
	ADI (Hering)	Continuous NO_3^- Sampler
	ADI (Hering)	FRM sampler
UC-Riverside (roof)	Caltech (Cass)	Fine Filter Samplers FTQ, FTNN, FQQ
	Caltech (Cass)	PM_{10} Filter Sampler
	Caltech (Cass)	2 MOIs
	SCAQMD	FRM
UC-Riverside (2nd floor)	UCR (Prather)	ATOFMS
	Caltech (Cass)	EAA, OPC

nitrate analyzer during a high particle matter concentration episode. The third sampling event was conducted from October 31, 1997, 0120 PST to November 2, 1997, 0100 PST at all three sampling sites.

Due to budgetary constraints, samples from only two of these three events were analyzed. Samples from the first sampling event (S97-N1, September 4–6, 1997) were not analyzed because there were relatively low particulate matter concentrations during that event, and because a power outage at Mira Loma interrupted sample collection.

ATOFMS instruments operated during the second sampling event at Mira Loma, and during the third sampling event at Riverside. The results of the ATOFMS instrument measurements will be reported separately by Kimberly Prather's research group, UC-Riverside. Sampling times for impactors and bulk particle samplers during this study are presented in Figure 3.2.

B.3 Tunnel Study

B.3.1 Sampling Sites

The Caldecott Tunnel, in Northern California, was the site of the tunnel study sample collection. This is an ideal location to investigate differences in emissions from light duty vehicles (LDV) and heavy

duty vehicles (HDV), because of the segregated traffic there. The tunnel consists of three two-lane bores, running east—west between Berkeley, CA and Orinda, CA, on a major commuting corridor into San Francisco. The tunnel is approximately 1.1 km in length, and slopes upward from west to east at a grade of 4.2% [43]. Bore 1 carries mixed LDV and HDV traffic from west to east, and Bore 3 carries mixed LDV and HDV traffic from east to west. In contrast, only light-duty vehicles (and those few medium- and heavy-duty vehicles which disregard the traffic restrictions) travel through Bore 2. Travel in Bore 2 is only in the direction of the prevailing flow of traffic, i.e. during morning rush hour vehicles only travel west, whereas during afternoon rush hour vehicles travel from west to east. Thus in the afternoon the eastbound traffic, which is under load, was segregated by vehicle type in Bore 1 and Bore 2, such that Bore 1 contained a mix of emissions from LDVs and HDVs, whereas Bore 2 was almost exclusively LDVs. From the difference between Bores 1 and 2, the contribution of HDVs to the emissions in Bore 1 can be determined.

Aerosol samples were collected from the ventilation shafts directly above the traffic bores. Filter and impactor samplers were positioned at exhaust vents directly over the traffic bores. Continuous samplers were positioned in the East Fan Room, and a sampling line (copper, 150' length, 0.25" i.d.) brought aerosol to the instruments from a vent in the roof of the tunnel to a plenum from which the continuous samplers drew aerosol samples. The sampling line inlet was colocated with filter and impactor samplers located in the ventilation duct. In addition, background aerosol samples were collected with samplers positioned directly north of the East Fan Room. Continuous size distribution measurements of background aerosol were made from the ventilated north side of the East Fan Room.

A transportable ATOFMS instrument was located in the East Fan Room, directly above the eastern exit of the Caldecott Tunnel. The results of the ATOFMS instrument measurements will be reported separately by Kimberly Prather's research group, UC-Riverside.

B.3.2 Sampling Times

Particles were sampled from Bore 1 of the tunnel (LDVs and HDVs) during the period of highest expected HDV traffic, between 1200 and 1500 hours PST, on November 17 and 18, 1997. Particles were sampled from Bore 2 of the tunnel ("LDV only") during the period of highest expected LDV traffic, between 1530 and 1830 hours PST, on November 19 and 20, 1997.

The complete set of background samplers was operated only on November 17 and 19, 1997. On November 18, only fine particle samplers were operated at the background site. On November 20, all

instruments except impactors were operated at the background site.

B.4 Filter Samplers

Four filter sampling systems were operated at each air monitoring station, one to collect PM_{10} samples and three to collect fine particle samples. The PM_{10} sampler and two of the fine particle samplers were used to collect consecutive short time average samples for bulk and elemental analysis. Five sets of filter samples per day were collected during these events on the schedule: 0120–0600 hours, 0620–1000 hours, 1020–1400 hours, 1420–1800 hours, and 1820 to 0100 hours the following day, local time. These sampling times were essentially those used during the SCAQS experiments and provide fine temporal resolution for comparison with the ATOFMS data and for later modeling studies. The third fine particle sampler was used to collect samples from 0120 hours to 0100 hours on the following day. These samples, containing larger aerosol mass, were composited and will be used for for organic compound analysis by GC/MS.

Figure B.1 shows the filter sampler designs. The nominal flow rates to each filter are shown; actual flow rates were measured and used to calculate aerosol concentrations. The filter samplers were designed to collect aerosol on substrates for analysis to determine the concentration of a variety of aerosol species. See Appendix A for details of the chemical analysis procedures performed.

The filter substrates used to collect particulate matter were chosen to be compatible with particular chemical analysis procedures. Heat treated quartz fiber filters collected samples for determination of organic species in the aerosol. Polytetrafluoroethylene (PTFE) filters (47 mm diameter, Gelman Teflo, 1.0 μm pore size) were used to collect atmospheric particulate matter samples for mass concentration determination and for subsequent measurement of trace elements and water soluble ions. The combination of measurements made on the quartz fiber and PTFE filters allows a nearly complete material balance on the chemical composition of the fine particles to be obtained. Nylon filters were used for HNO_3 and aerosol nitrate collection, as they are a nearly perfect sink for small quantities of HNO_3. Oxalic acid impregnated glass fiber filters, downstream of a PTFE pre-filter, were used for ammonia collection, as oxalic acid reacts with and retains ammonia.

The PM_{10} samplers CTQ were of similar design to those used by Solomon et al. to collect the PM_{10} database used for regulatory purposes in Los Angeles from 1987 to 1995 [17]. In the PM_{10} samplers, air was drawn through an EPA-approved low volume PM_{10} inlet [17] and distributed between two filter

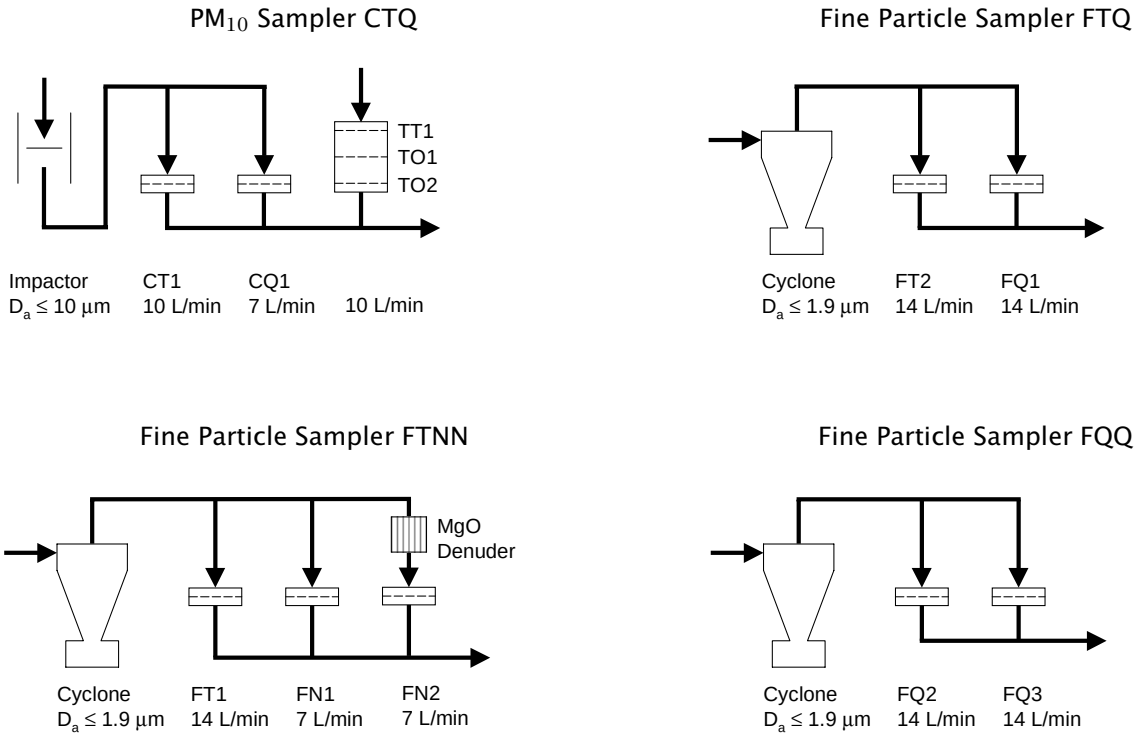

Figure B.1: Schematic diagram of the particulate matter sampling systems used in this study

samplers (see Figure B.1). The flow to each filter was controlled by a critical orifice downstream of the filter. A PTFE filter, designated CT1, was used to collect aerosol particles for gravimetric and inorganic analyses. A quartz filter, designated CQ1, was used to collect aerosol particles for carbon and organic species analyses. This sampler also housed the open face filter pack which consisted of a PTFE filter (TT1) to remove aerosol particles, upstream of two glass fiber filters pre-treated with oxalic acid (TO1 and TO2), which were used for the measurement of gas-phase ammonia.

In the fine particle samplers ambient air was drawn under a stainless steel rain cap and pulled at a nominal flow rate of 28 lpm through an acid-washed Pyrex glass inlet line (1/2" ID x 40" long) that was shaded from the sun. The air then passed through a Teflon-coated AIHL-design cyclone separator which, when operated at flow rate of 28 lpm, removed coarse particles with aerodynamic diameters larger than 1.9 μm. Following the cyclone, the airstream containing only fine particles and gases entered a sampling manifold where it was split and ducted via short lengths of Teflon tubing to separate low-volume filter holder assemblies. The flow rate through each filter holder was controlled by a critical orifice downstream of the filter.

Three fine particle filter samplers designated FTQ, FTNN, and FQQ were deployed at each sampling

site. The FTQ sampler was used to collect fine particles on PTFE and quartz fiber filters for subsequent chemical analysis. The FTNN sampler was used to collect fine particles on another PTFE filter for subsequent chemical analysis. In addition, two filter holders loaded with nylon filters were used as a denuder difference system for nitric acid measurement based on use of a MgO coated tubular HNO_3 denuder that was shown in the Claremont HNO_3 intercomparison study to lead to accurate HNO_3 determinations. The FQQ sampler was used to collect 24-h samples to be analyzed for organic tracer compounds by GC/MS.

B.5 Impactors

Two cascade impactors were placed at each sampling site. These were 10 stage micro-orifice impactors (MOI) manufactured by MSP Corporation (Minneapolis, MN) [19]. Note that the MOI are micro-orifice uniform deposit impactors (MOUDI) which were not rotated. The impactor inlets were equipped with cyclones to remove coarse particles which may have introduced particle bounce artifacts. One MOI was operated with PTFE substrates to collect samples for mass, ionic species and trace element analyses; the other impactor was operated with aluminum substrates to collect samples for mass, organic carbon, and elemental carbon analyses.

Ambient air was drawn through an AIHL-design cyclone separator at the inlet of the impactor sampling system at a nominal flow rate of 30 lpm, which removed particles with aerodynamic diameter larger than 1.8 μm. Particles were collected in size-segregated samples on the last six stages of the impactor. Pressures at impactor stages 6 and 10 were monitored and the flow rate controlled to maintain the pressure at these stages within the instrument design values. The pressure drop checks also ensured that impactors did not leak or become clogged during sampling.

Because sampling with impactors generates a large number of samples, impactor samples were collected only during one or two sampling periods per site per each intensive sampling day. The specific sampling times chosen can be seen in Figures 2.2 and 3.2.

B.6 Continuous Sampling Instruments

Continuous particle sampling instruments used in the Vehicle-Oriented Trajectory portion of this study included electrical aerosol analyzers (EAAs) and optical particle counters (OPCs). The electrical aerosol

analyzers (EAA) were TSI (Minneapolis, MN) Model 3030. The OPC at Riverside was a Particle Measuring Systems (Boulder, CO) model LAS-X 16 channel unit; the OPCs at all other sites were Particle Measuring Systems model ASASP-X 31 channel units.

B.7 Sample Identification Codes

Tables of detailed information about samples collected and the concentration data obtained from those samples are presented in Appendix D. The samples are designated by labels which specify the sampling event during which the sample was collected, the date and time of day of sample collection, the monitoring site where collection occurred, and the sampling instrument which collected the sample. These five elements uniquely identify each sample. This section provides an explanation of the internal system used to construct these labels, in order to facilitate their interpretation and use.

Each label begins with a sampling event code, which specifies a 2-3 day experiment or a single tunnel sampling session. The sampling event codes are:

Event Code	Event Description	Date(s)
S97-V1	First vehicle-oriented trajectory experiment	August 21-23, 1997
S97-V2	Second vehicle-oriented trajectory experiment	August 27-29, 1997
S97-N2	Nitrate-oriented calibration experiment	September 27-30, 1997
S97-N3	Nitrate-oriented trajectory experiment	October 31 - November 2, 1997
S97-T1	First tunnel experiment (Mixed LDV+HDV Tunnel)	Nov 17, 1997
S97-T2	Second tunnel experiment (Mixed LDV+HDV Tunnel)	Nov 18, 1997
S97-T3	Third tunnel experiment (“LDV only” Tunnel)	Nov 19, 1997
S97-T4	Fourth tunnel experiment (“LDV only” Tunnel)	Nov 20, 1997
S97-B	Field blank	

A digit following the event code in the label simply indicates on which day of a multi-day event the sample was taken. For single-day events such as the tunnel experiments, the day is always “1”. For example, a label beginning with “S97-V12” took place on the second day of sampling within event “S97-V1”, or August 22, 1997.

A single letter following the day digit indicates the time of day during which the sample was collected. Local time was always used in this study, therefore the listed time periods are in Pacific Daylight Time for all sampling events before October 26, 1997 (S97-V1, S97-V2, and S97-N2), and Pacific Standard Time for all sampling events after that date (S97-N3). Tunnel samples and field blanks were not taken on the same sampling schedule, and their time of day codes do not describe the time of day when they were collected. Tunnel samples were arbitrarily assigned the time of day code "B", and field blanks

were assigned the time of day code "A". See Chapter 4 or Section B.3.2for the times when samples were taken in each bore of the Caldecott Tunnel.

Code	Time of Day	Sampling Duration
A	0120 - 0600	4 hrs 40 min
B	0620 - 1000	3 hrs 40 min
C	1020 - 1400	3 hrs 40 min
D	1420 - 1800	3 hrs 40 min
E	1820 - 0100 (next day)	6 hrs 40 min
F	0120 - 0100 (next day)	23 hrs 40 min

Between sampling periods, it was necessary to measure air flows, retrieve used filters, and load clean filters into samplers. These tasks normally took about 20 minutes, but actual starting and stopping times varied slightly according to how quickly this work could be done. Actual starting and stopping times were recorded in log sheets in the field, and actual sampling durations were used in calculating sampled air volume.

The sampling sites used in these experiments were described in detail in Tables B.1 and B.3. A code indicating the site of sample collection is included in each sample label, as follows:

Code	Sampling Site
LA	Central Los Angeles
AZ	Azusa
RV	UC-Riverside
DB	Diamond Bar
ML	Mira Loma
TI	Caldecott Tunnel (Inside)
TO	Caldecott Tunnel (Background)

The final piece of information in a label is the sampler code, indicating the size range of the collected material and the sampler used in its collection. Sampler codes for this study are:

Code	Sample Description	Size Range
CX	PM_{10} filter sample	$D_a < 10\ \mu m$
FX	Fine particle filter sample	$D_a < 1.9\ \mu m$
FY	Fine particle quartz filter sample (24-h)	$D_a < 1.9\ \mu m$
GX	Gas phase sample	N/A
MX5	Microorifice impactor, stage 5	$1.0 < D_a < 1.8\ \mu m$
MX6	Microorifice impactor, stage 6	$0.56 < D_a < 1.0\ \mu m$
MX7	Microorifice impactor, stage 7	$0.32 < D_a < 0.56\ \mu m$
MX8	Microorifice impactor, stage 8	$0.18 < D_a < 0.32\ \mu m$
MX9	Microorifice impactor, stage 9	$0.10 < D_a < 0.18\ \mu m$
MX10	Microorifice impactor, stage 10	$0.56 < D_a < 0.10\ \mu m$

Sample labels are constructed by concatenation of the above codes with dashes between the time of

day and sampling site codes, and between the sampling site and sampler codes. Thus, "S97-V12E-AZ-CX" is the designation for the PM_{10} sample collected at Azusa on the second day of the S97-V1 event, from 1820 hours PDT on August 22, 1997 until 0100 hours PDT on August 23, 1997.

B.7.1 Sample Consolidation

In order to obtain a nearly complete material balance on the chemical composition of the particles in a given size range, several media types were used in parallel to collect samples for analysis by a range of procedures. In reporting the data from this study in Appendix D, concentrations obtained from the various different media which apply to the same sampling time, location, and instrument have been consolidated together under one identifying label. For example, fine particle elemental and organic carbon concentrations, both obtained from a quartz fiber filter sample, and ionic species concentrations, measured from a PTFE filter sample, are reported together as data for a sample with the sampler code "FX". Where there are redundant measurements, as with mass measurements of parallel fine particle PTFE filters or of aluminum and PTFE substrate impactor pairs, then the redundant measurements are averaged, and uncertainties are propagated through the calculation.

Appendix C

Graphical Presentation of Data

All of the data collected by the Caltech group during the SCOS97 studies are presented in graphical form in this appendix. Some of the plots are duplicates of those presented in the body of this report; they are included here for completeness.

The continuous particle size distribution data are presented as differential mass concentrations. These mass concentrations were calculated from the number concentration data assuming spherical particles, each with a physical diameter equal to the log mean diameter of the relevant size bin and an assumed density of 1.3 g cm^{-3}. The continuous particle size distribution measurements are considered unreliable for the Nitrate Calibration and Nitrate-Oriented Trajectory experiments. These data are not presented here.

C.1 First Vehicle-Oriented Trajectory Study

C.1.1 Particle Concentration Time Series Data at Central Los Angeles

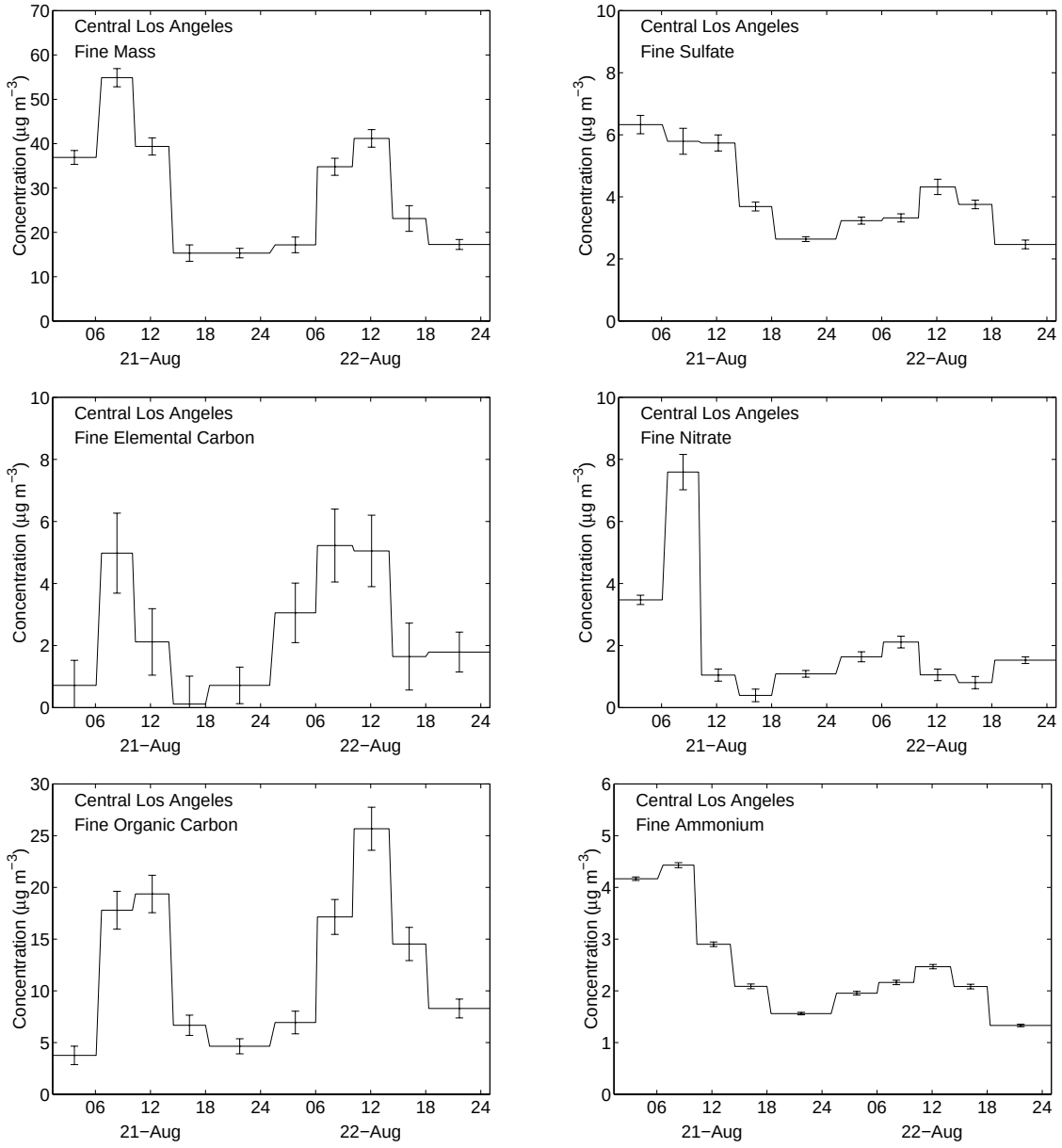

Figure C.1: Fine particle concentrations during the First Vehicle-Oriented Trajectory Experiment at Central Los Angeles

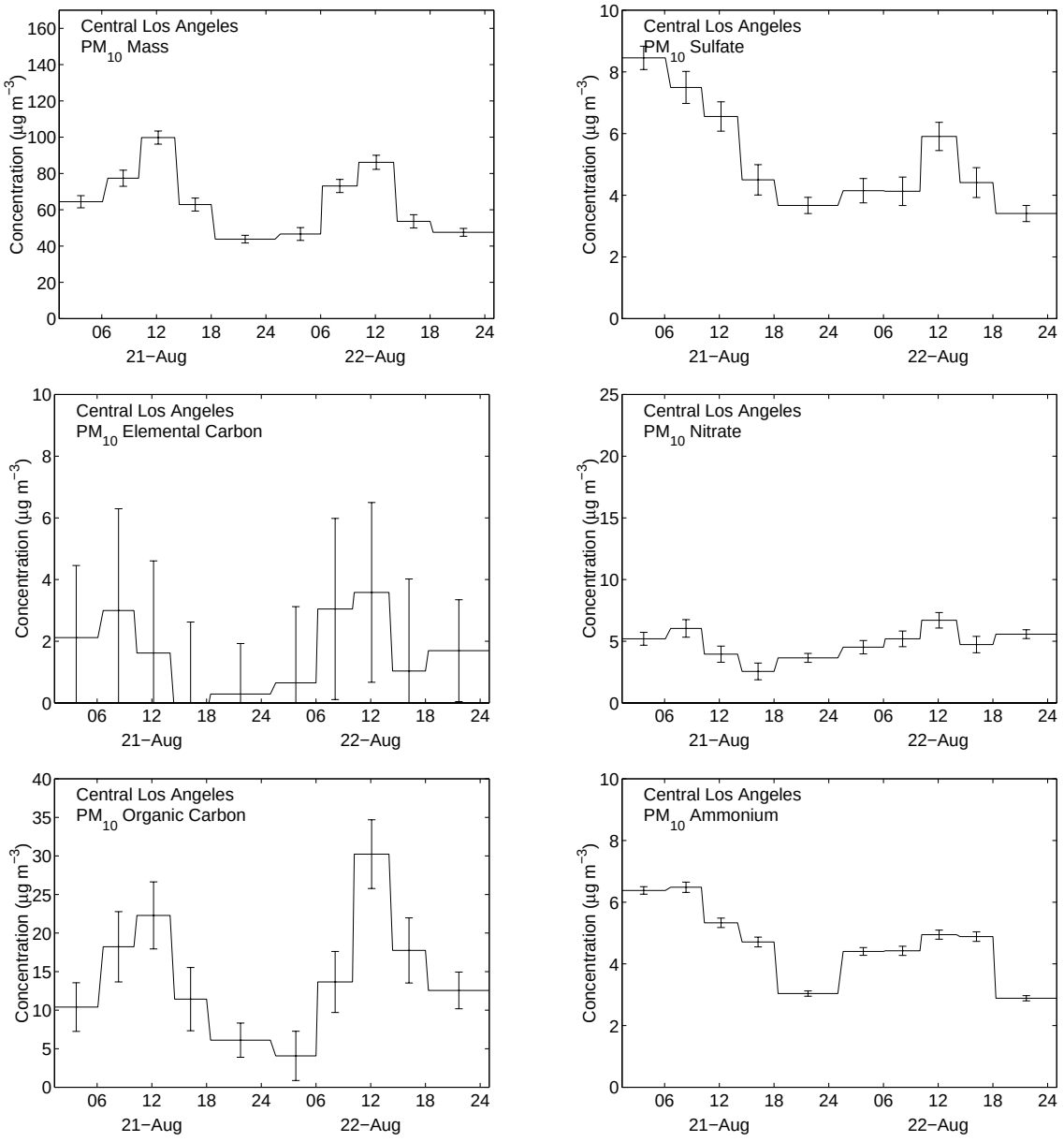

Figure C.2: PM_{10} concentrations during the First Vehicle-Oriented Trajectory Experiment at Central Los Angeles

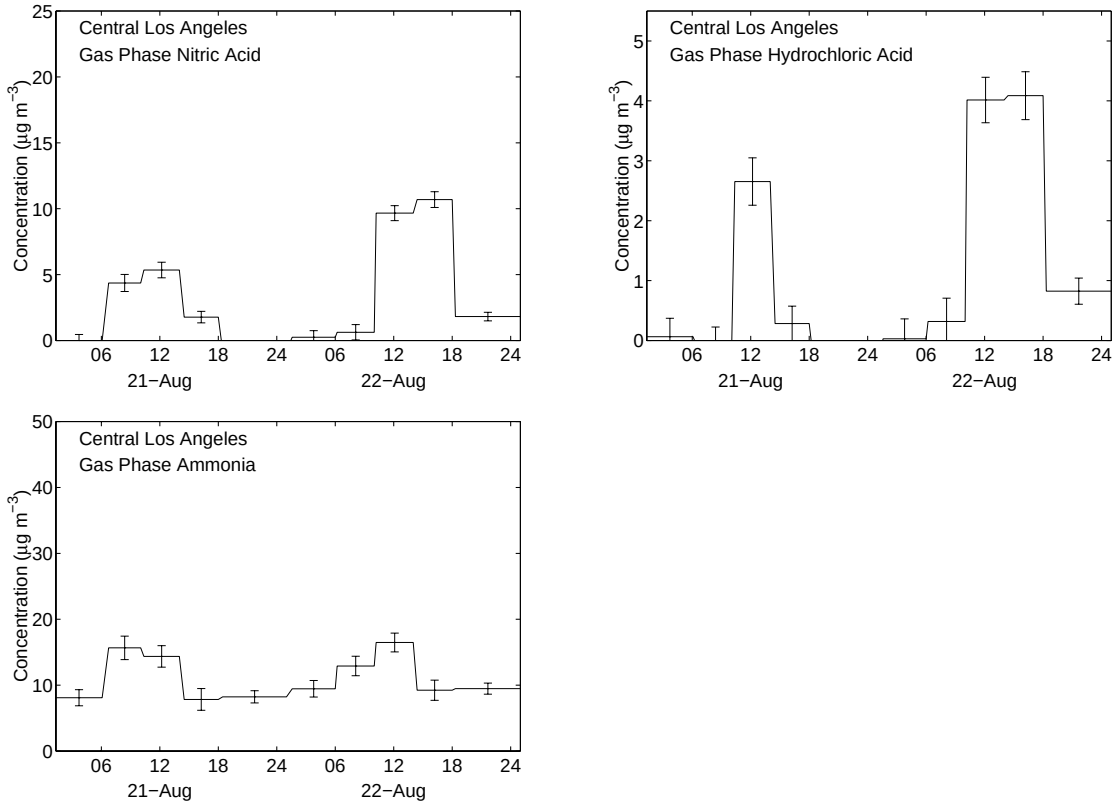

Figure C.3: Gas phase concentrations during the First Vehicle-Oriented Trajectory Experiment at Central Los Angeles

C.1.2 Particle Concentration Time Series Data at Azusa

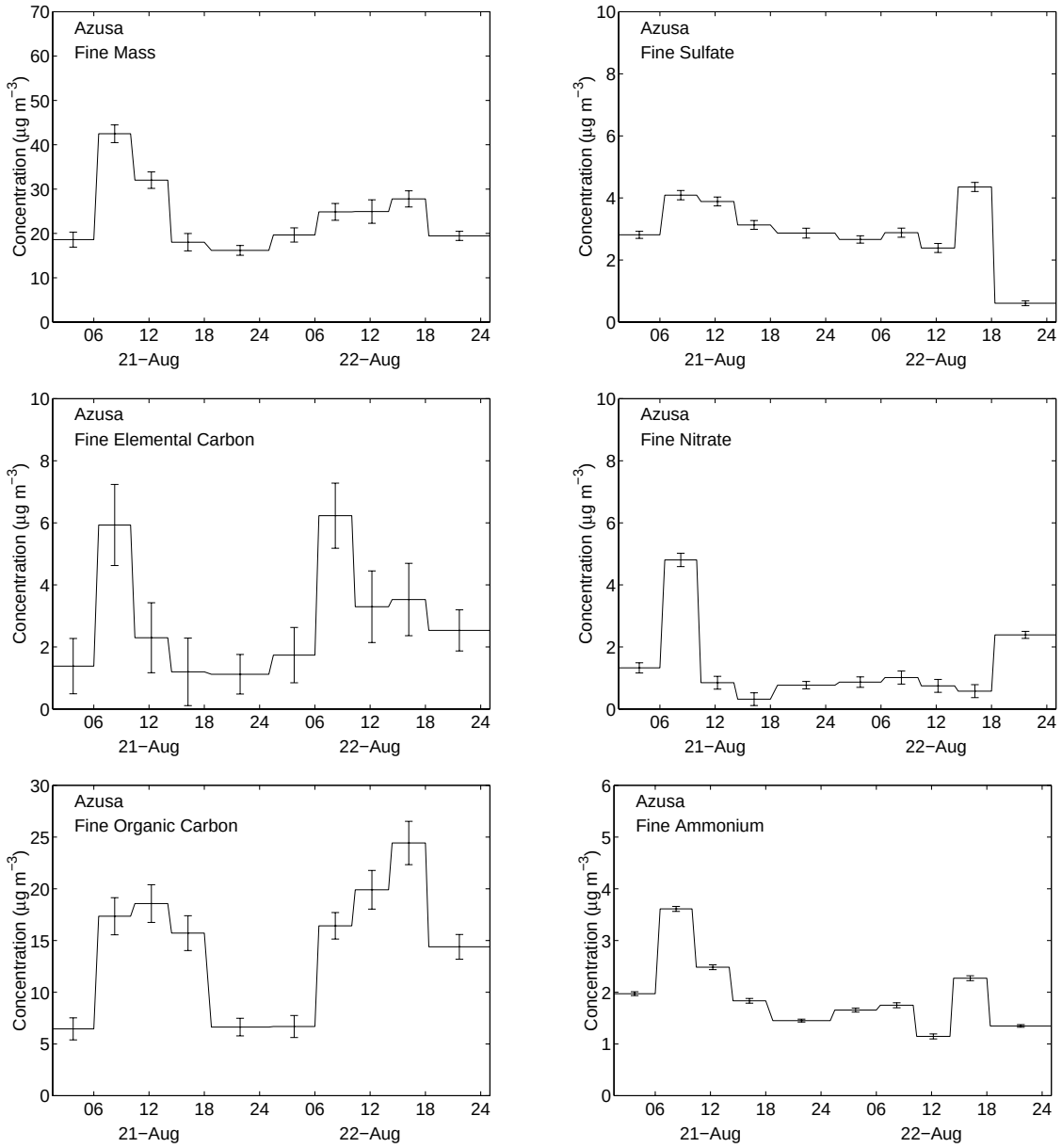

Figure C.4: Fine particle concentrations during the First Vehicle-Oriented Trajectory Experiment at Azusa

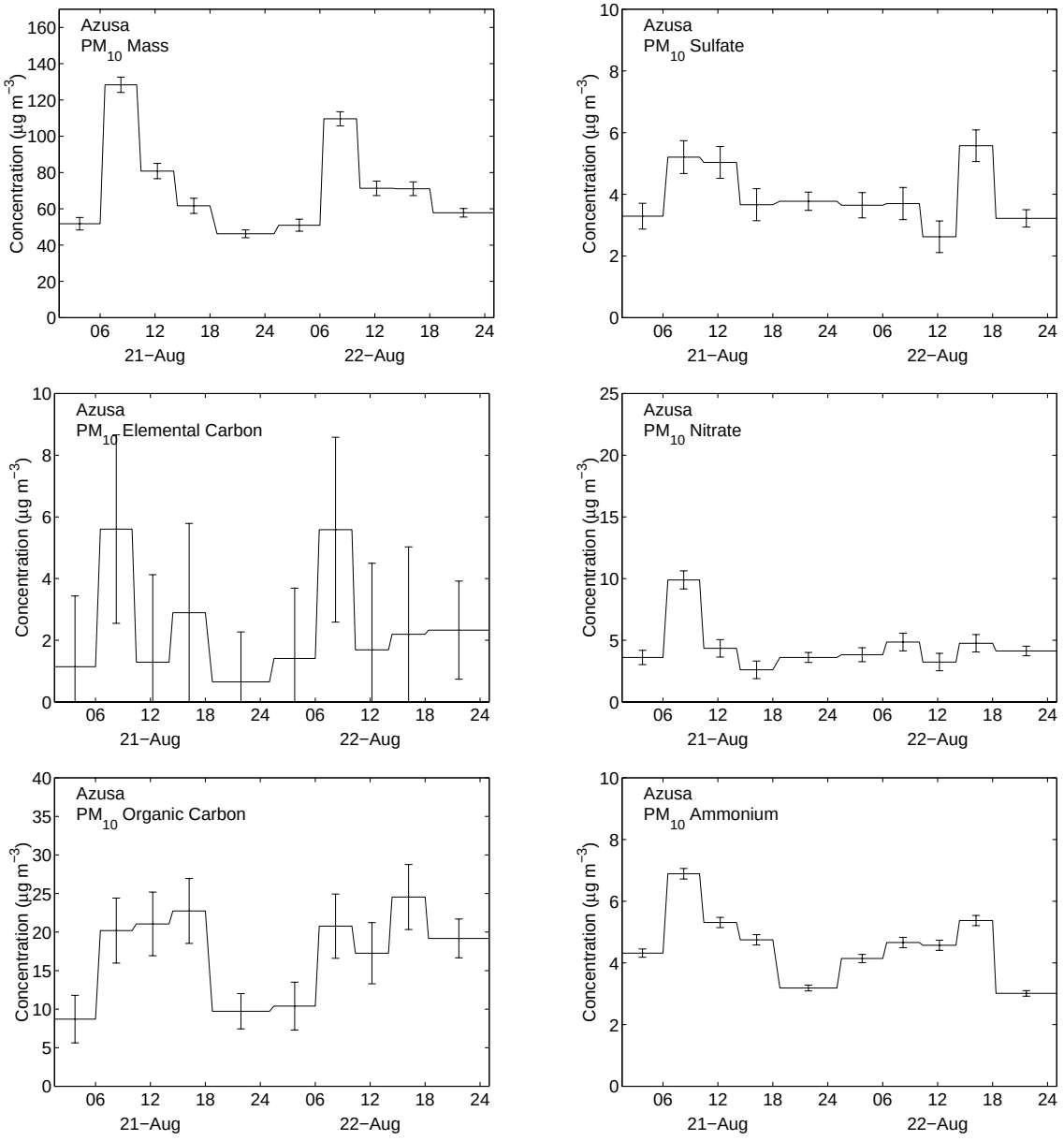

Figure C.5: PM_{10} concentrations during the First Vehicle-Oriented Trajectory Experiment at Azusa

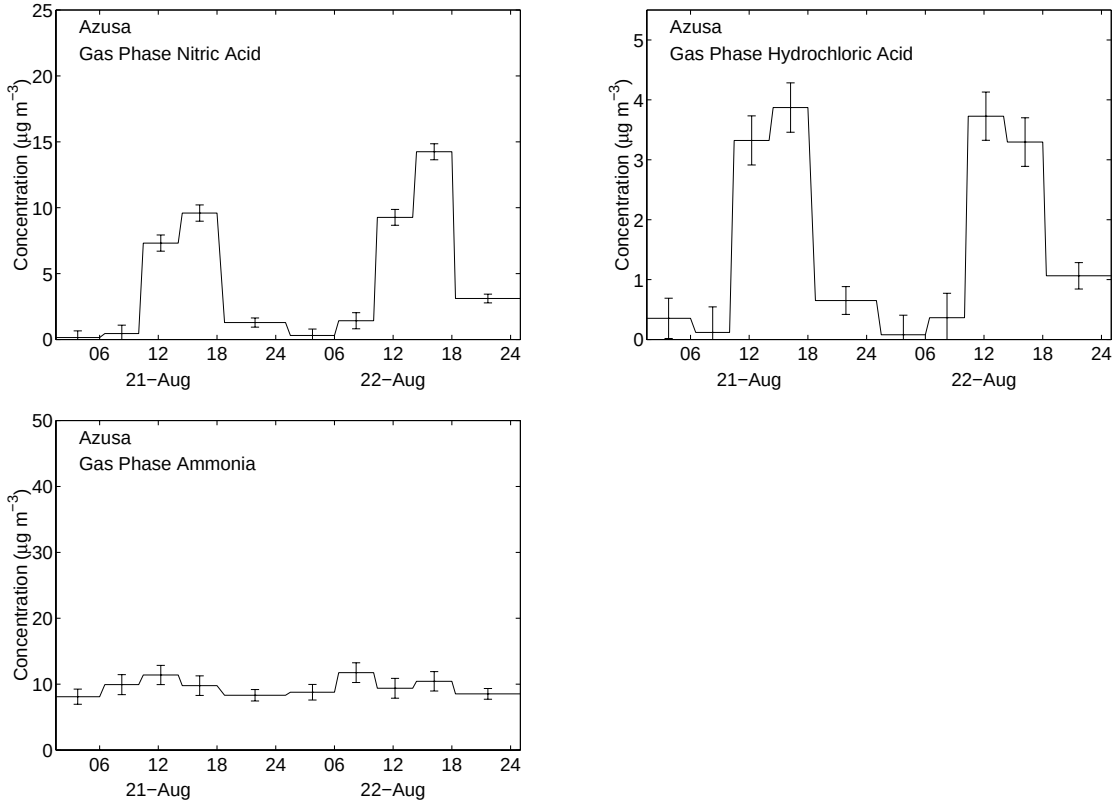

Figure C.6: Gas phase concentrations during the First Vehicle-Oriented Trajectory Experiment at Azusa

C.1.3 Particle Concentration Time Series Data at Riverside

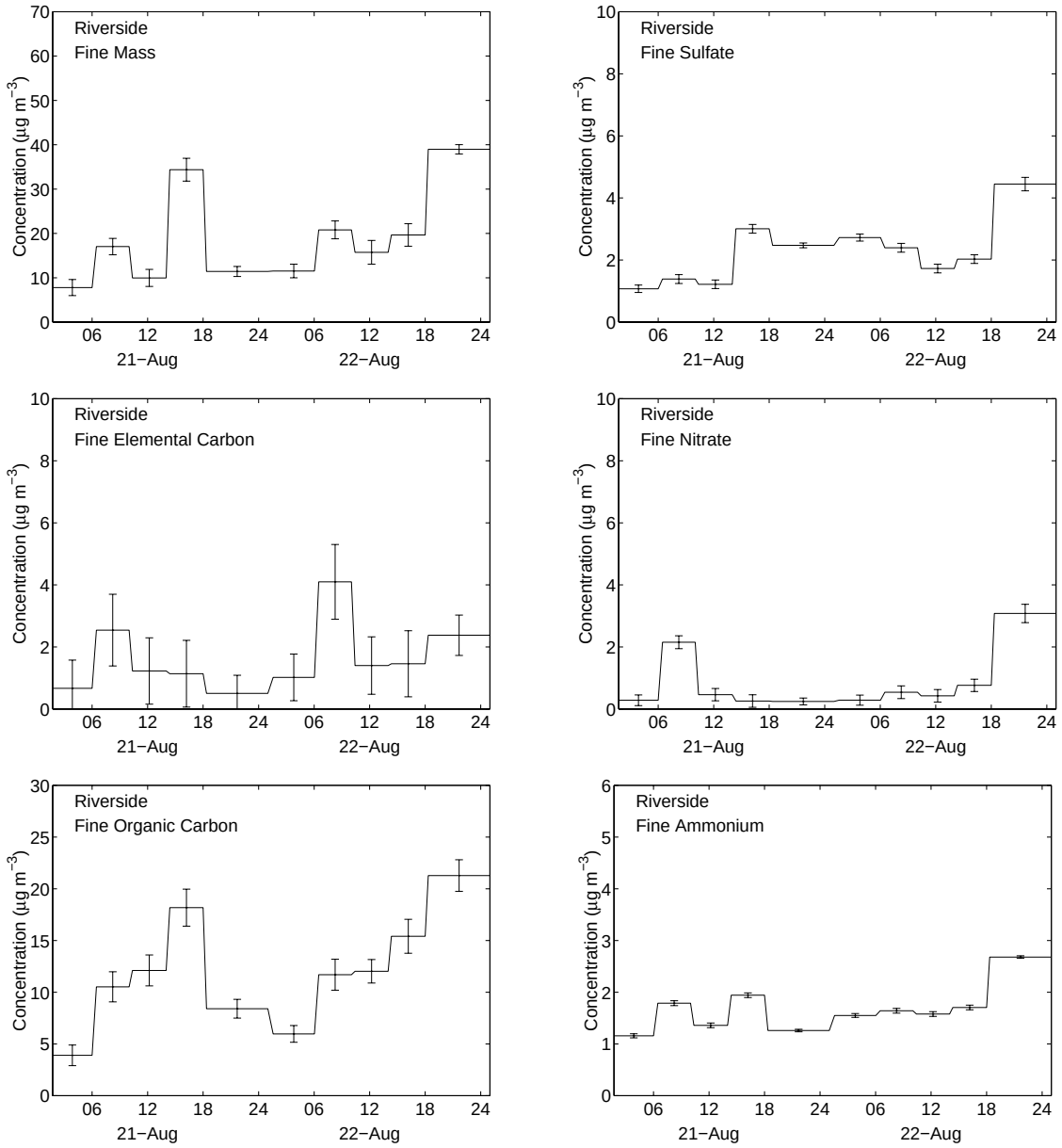

Figure C.7: Fine particle concentrations during the First Vehicle-Oriented Trajectory Experiment at Riverside

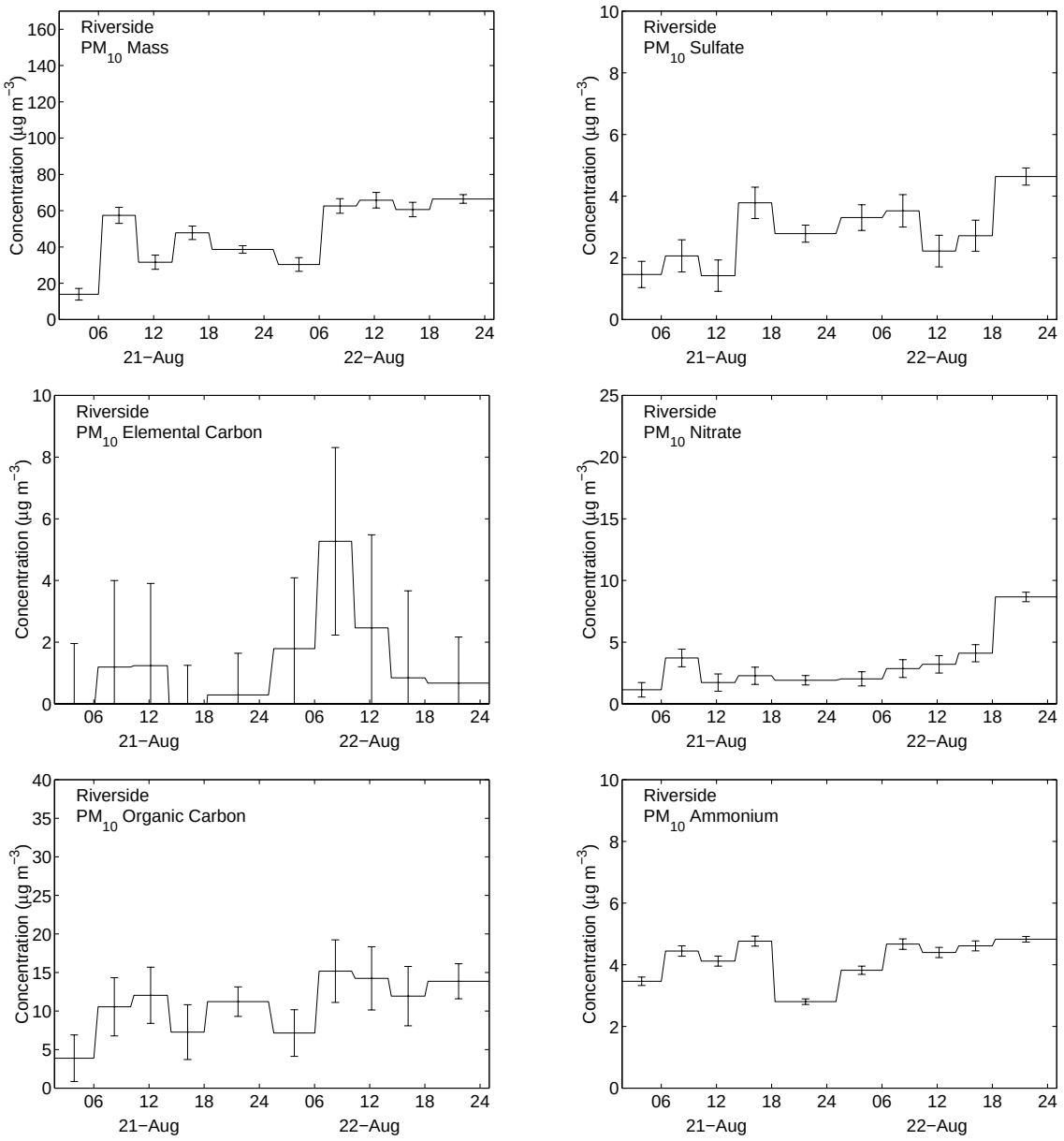

Figure C.8: PM_{10} concentrations during the First Vehicle-Oriented Trajectory Experiment at Riverside

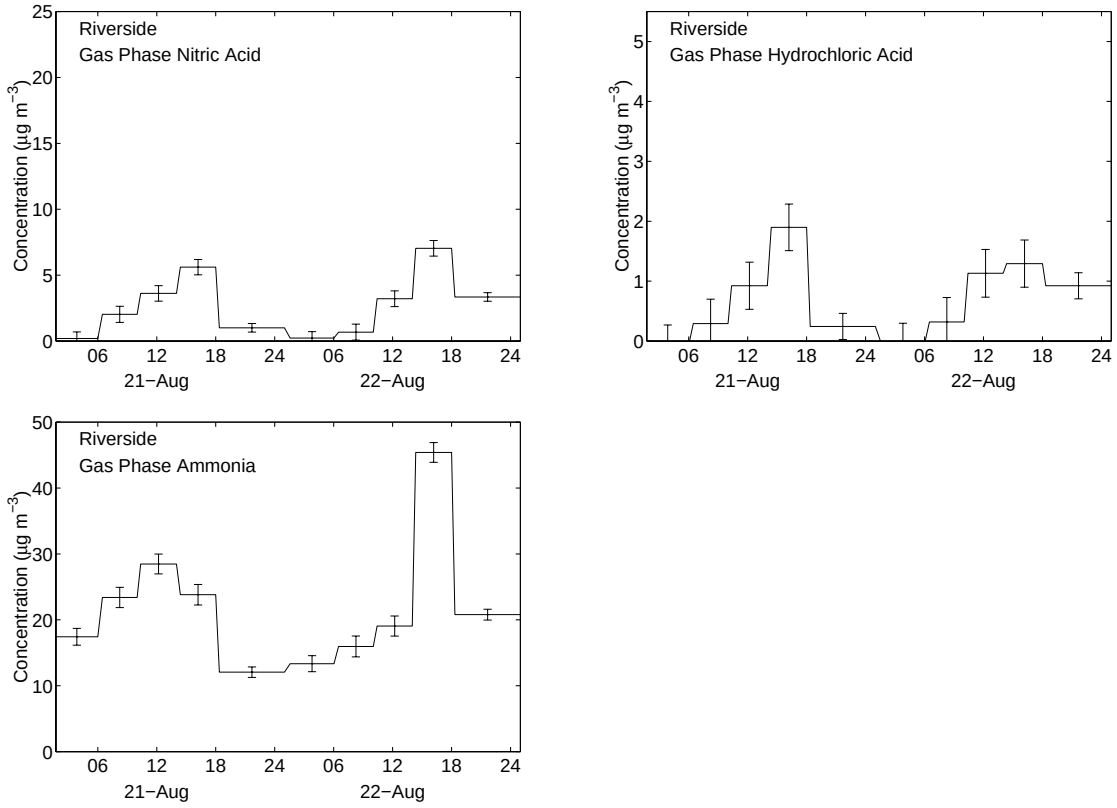

Figure C.9: Gas phase concentrations during the First Vehicle-Oriented Trajectory Experiment at Riverside

C.1.4 Mass Balances at All Sites

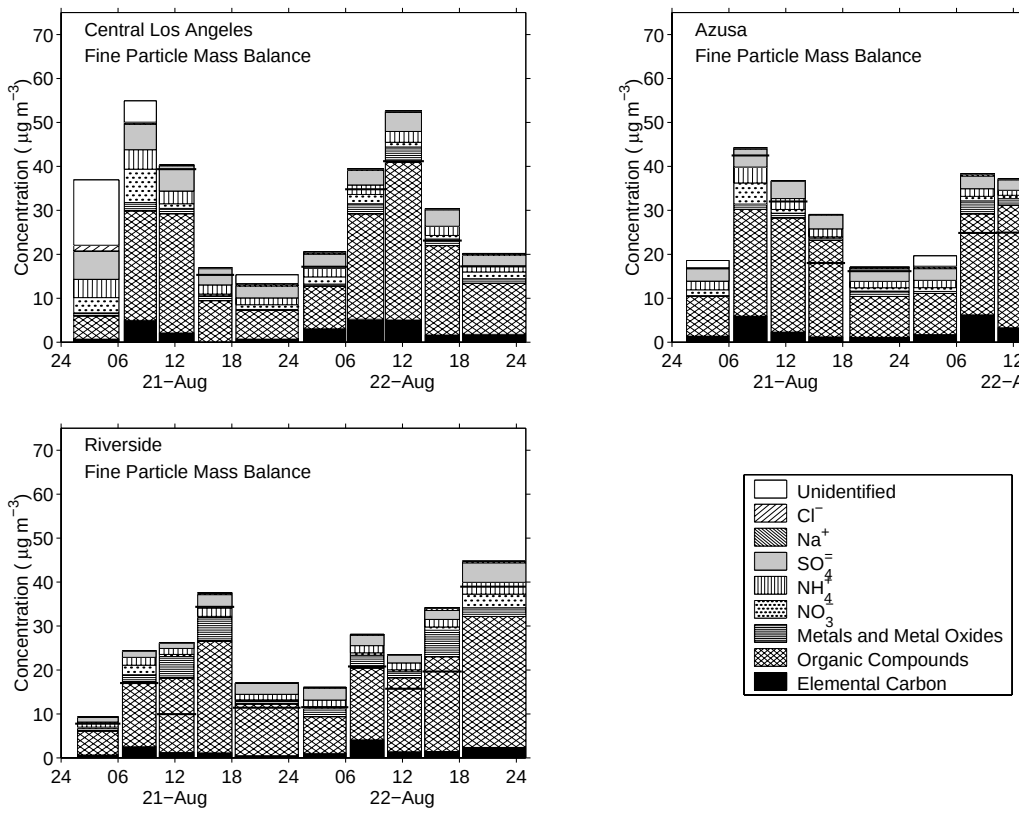

Figure C.10: Fine particle mass balances during the First Vehicle-Oriented Trajectory Experiment

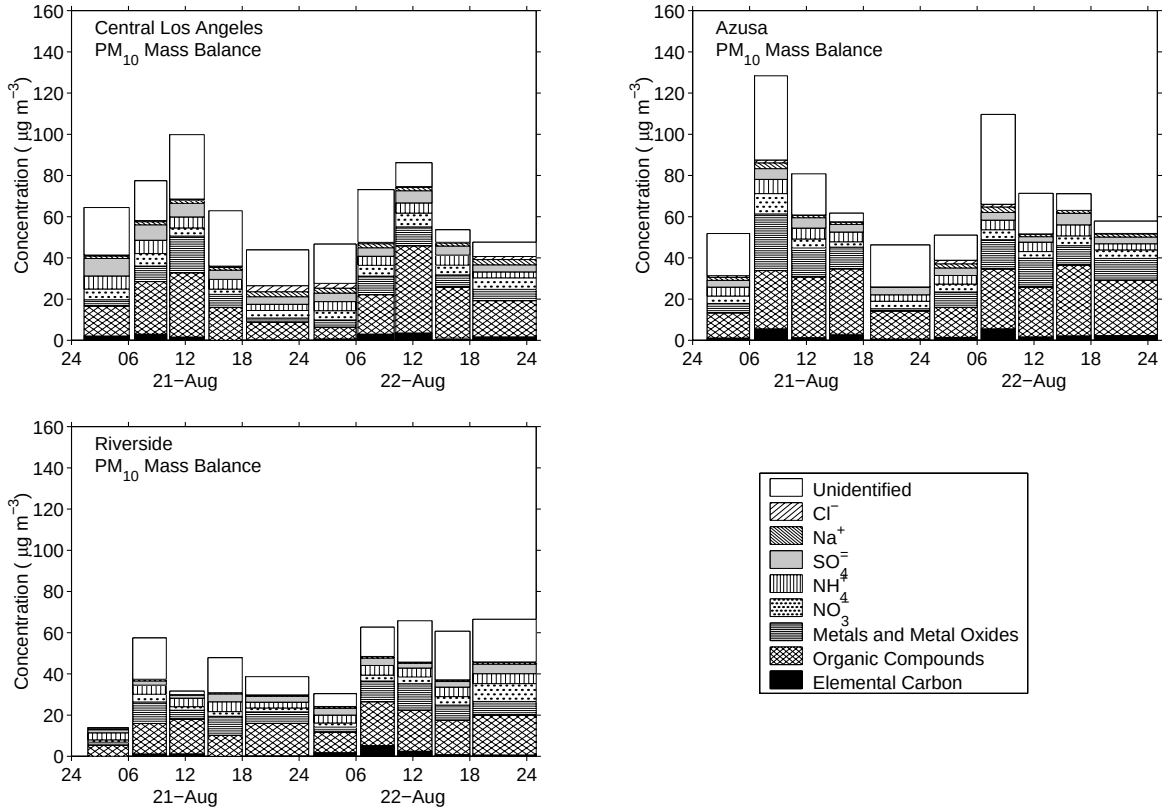

Figure C.11: PM_{10} mass balances during the First Vehicle-Oriented Trajectory Experiment

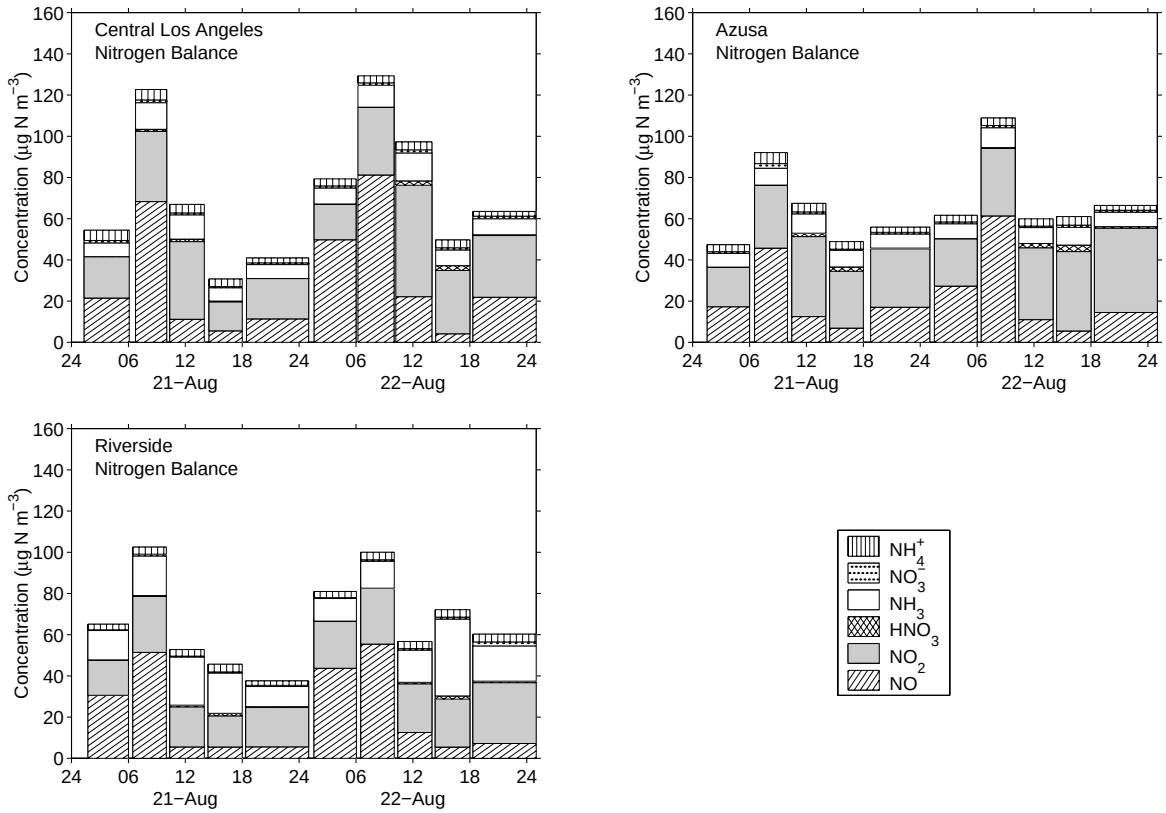

Figure C.12: Nitrogen balances during the First Vehicle-Oriented Trajectory Experiment

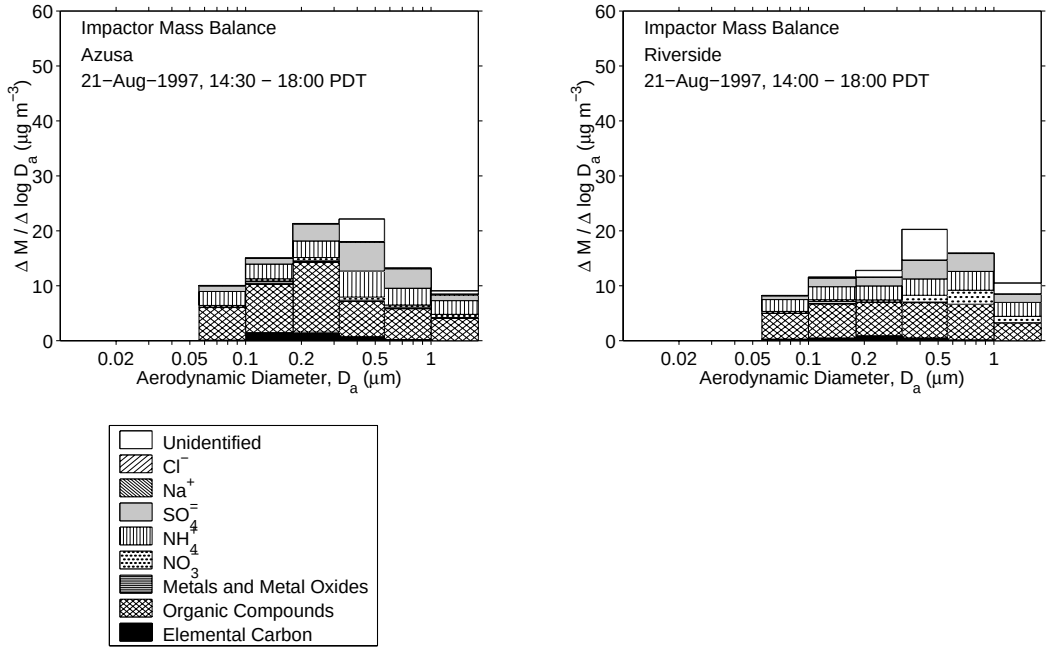

Figure C.13: Impactor mass balances during the first day of the First Vehicle-Oriented Trajectory Experiment

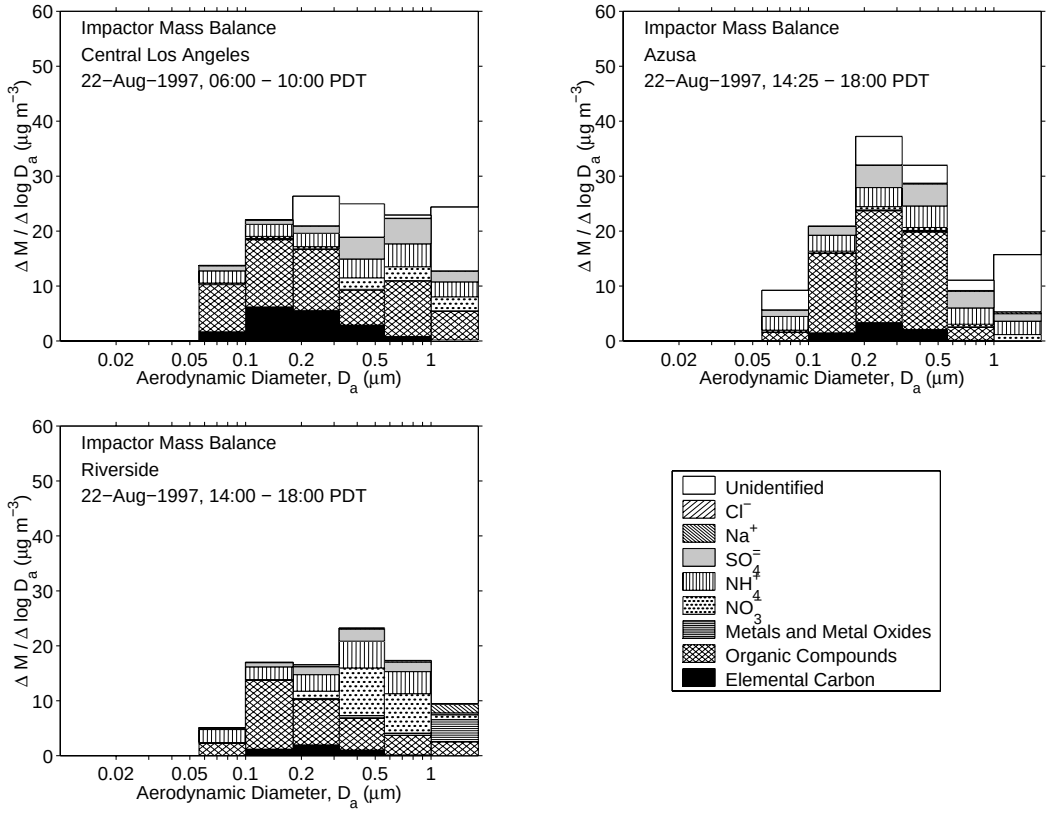

Figure C.14: Impactor mass balances during the second day of the First Vehicle-Oriented Trajectory Experiment

C.1.5 Electronic Instrument Data at Central Los Angeles

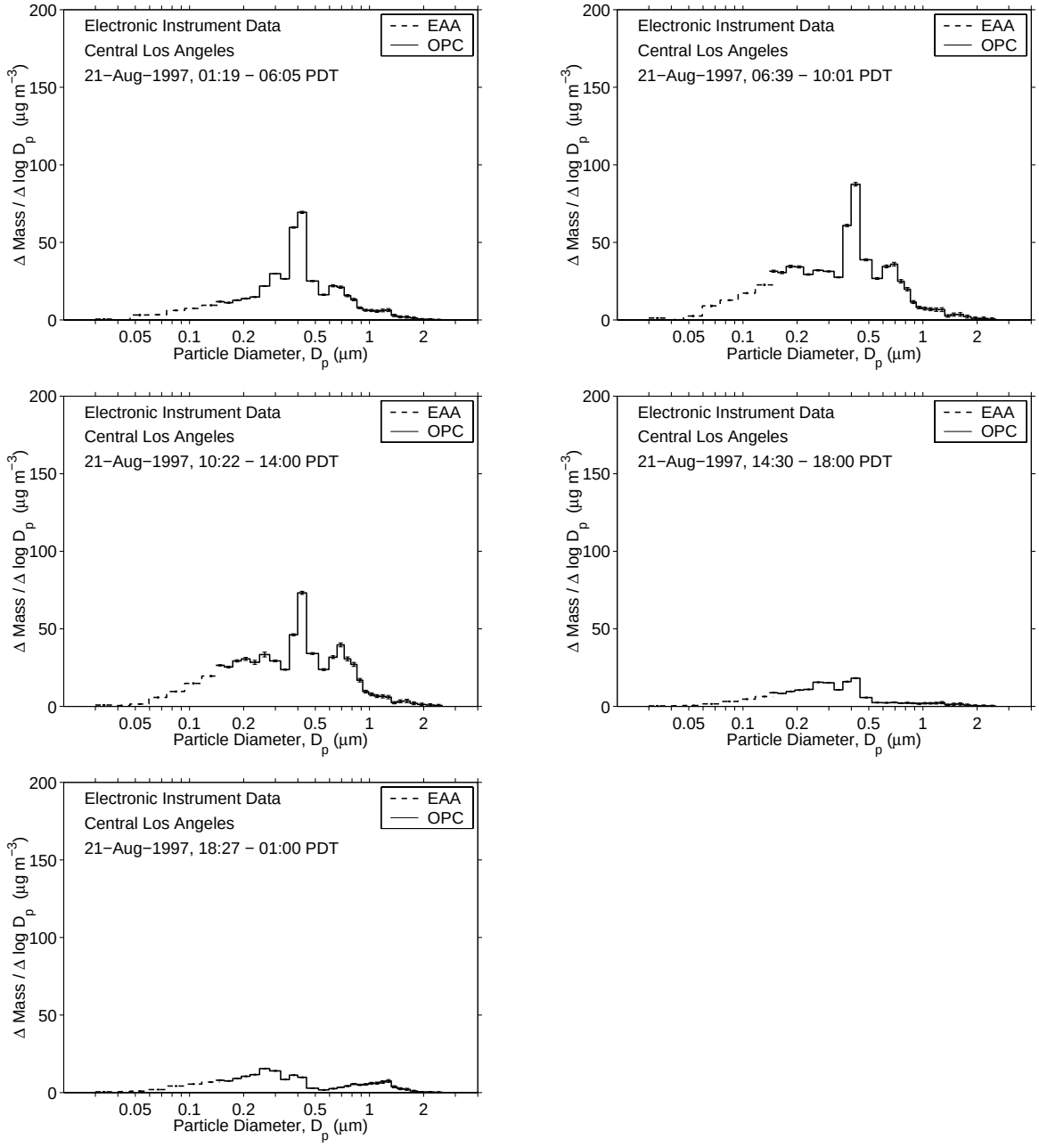

Figure C.15: Particle mass concentration during the first day of the First Vehicle-Oriented Trajectory Experiment at Central Los Angeles

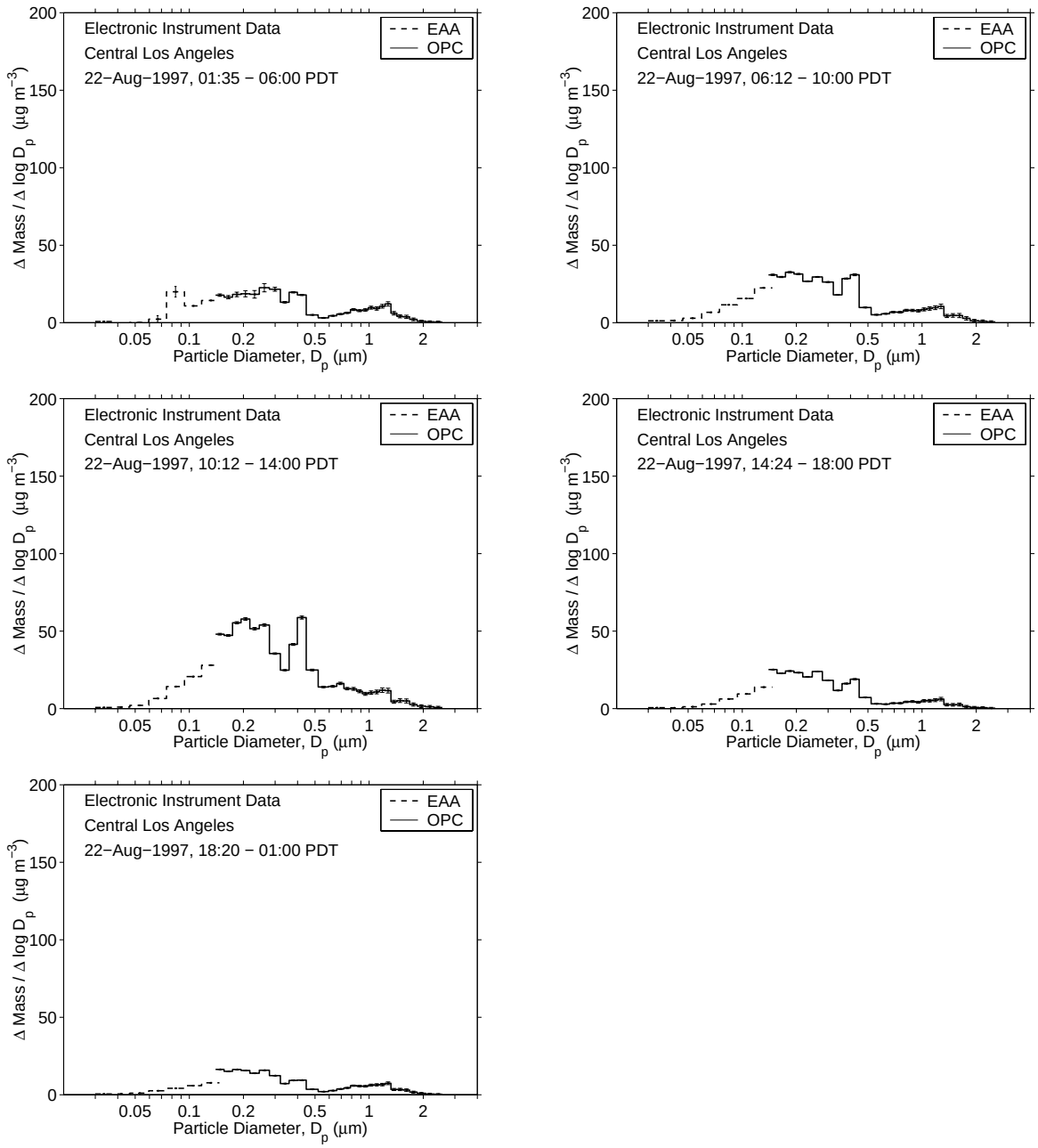

Figure C.16: Particle mass concentration during the second day of the First Vehicle-Oriented Trajectory Experiment at Central Los Angeles

C.1.6 Electronic Instrument Data at Azusa

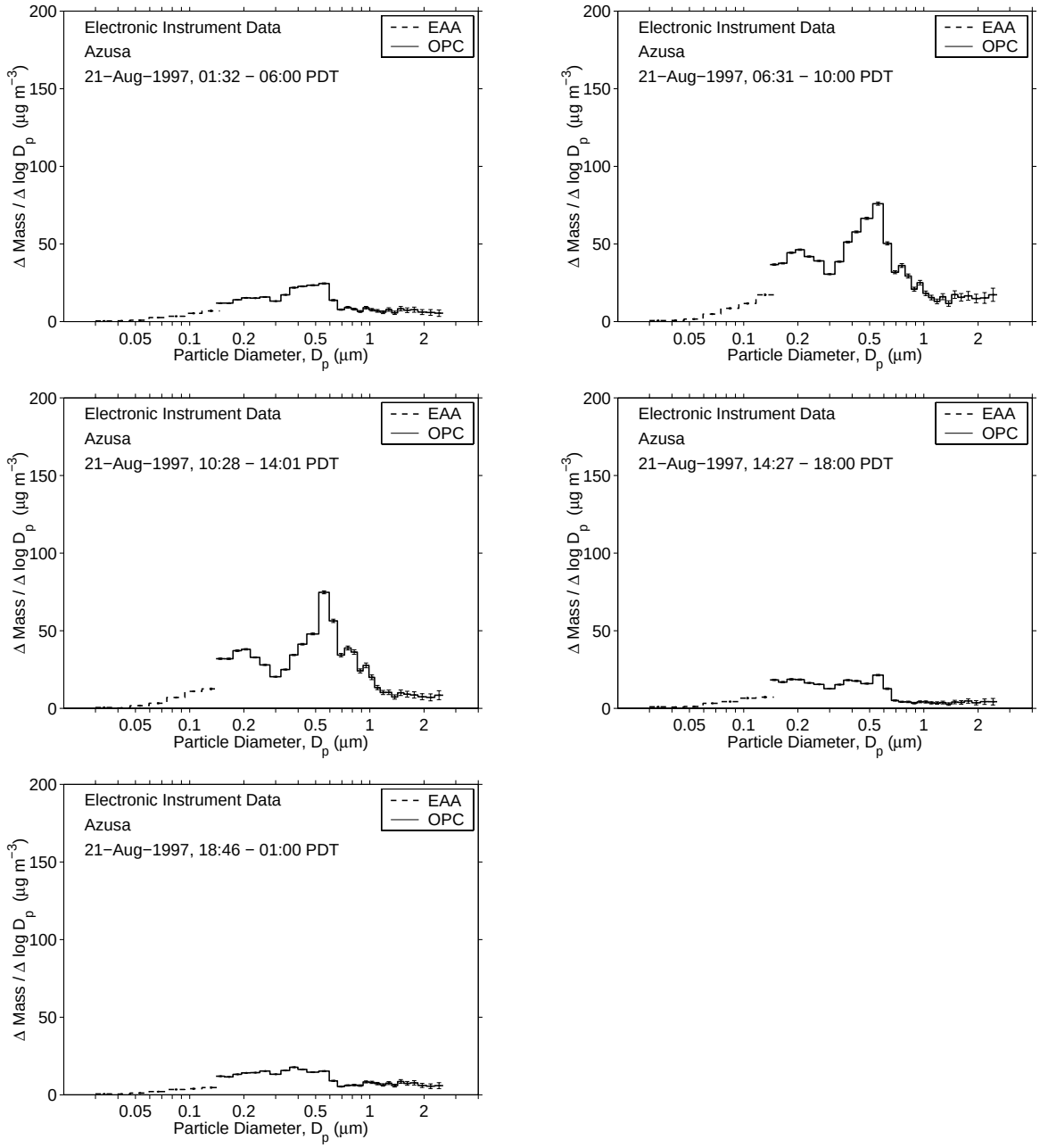

Figure C.17: Particle mass concentration during the first day of the First Vehicle-Oriented Trajectory Experiment at Azusa

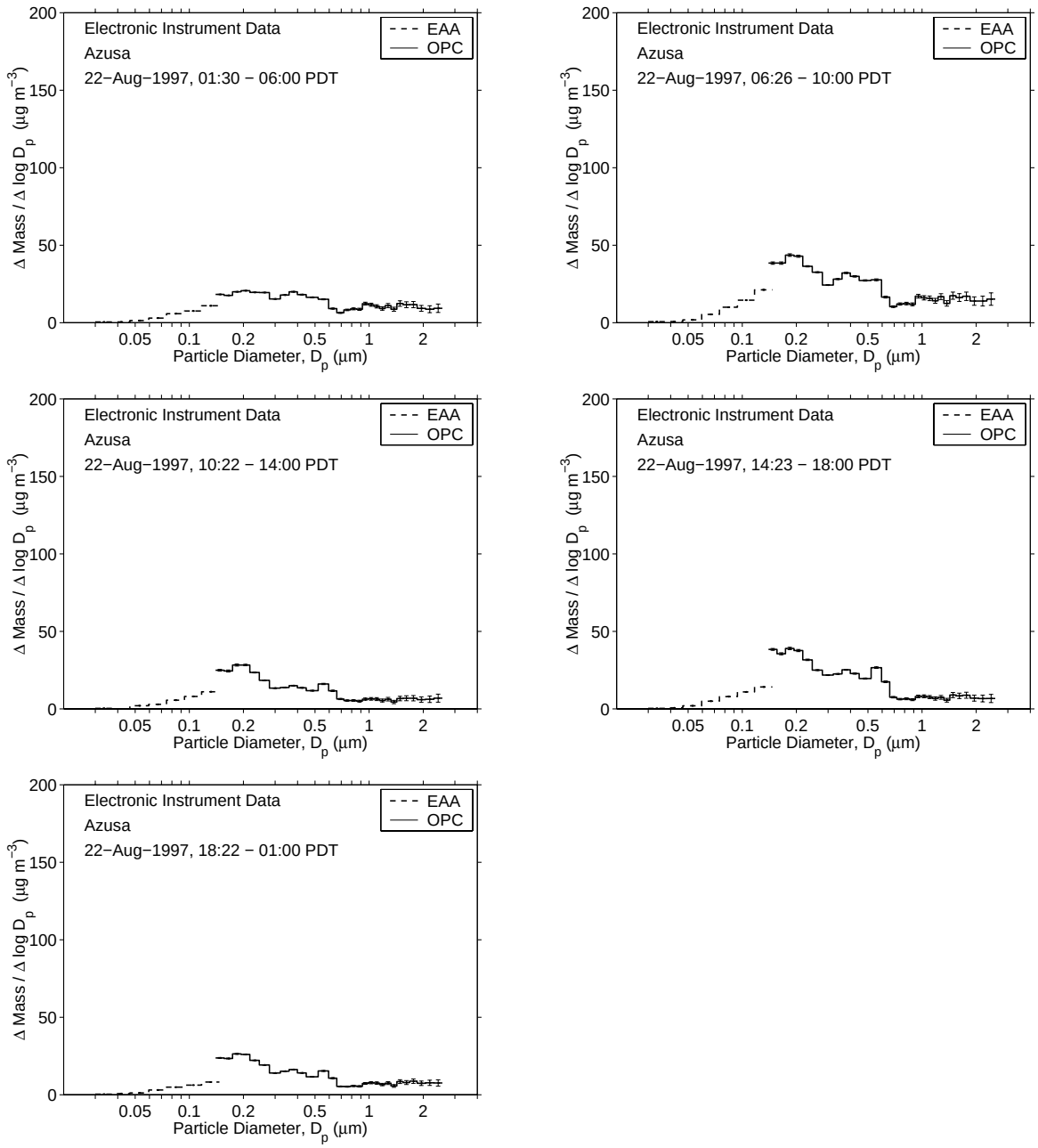

Figure C.18: Particle mass concentration during the second day of the First Vehicle-Oriented Trajectory Experiment at Azusa

C.1.7 Electronic Instrument Data at Riverside

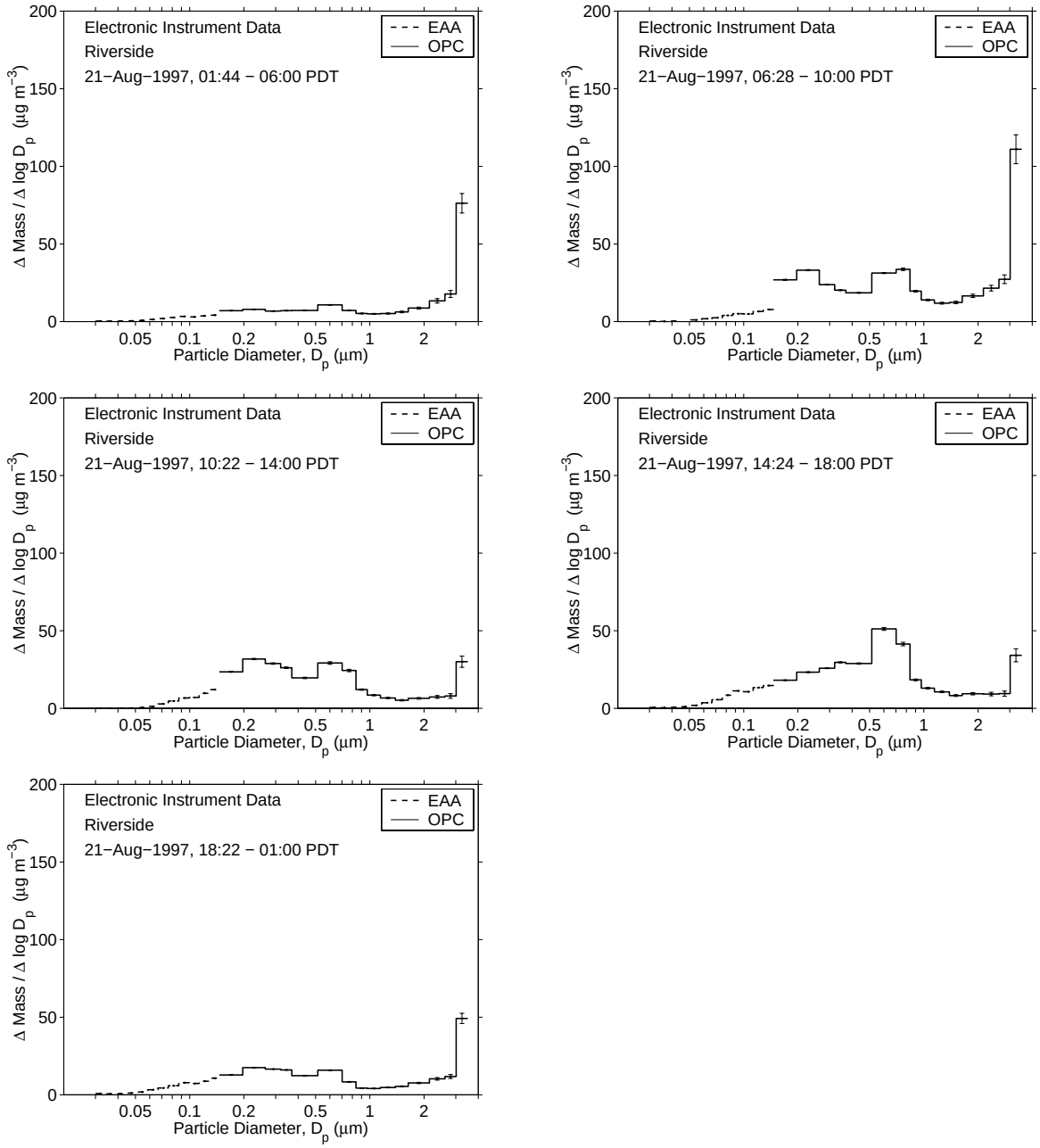

Figure C.19: Particle mass concentration during the first day of the First Vehicle-Oriented Trajectory Experiment at Riverside

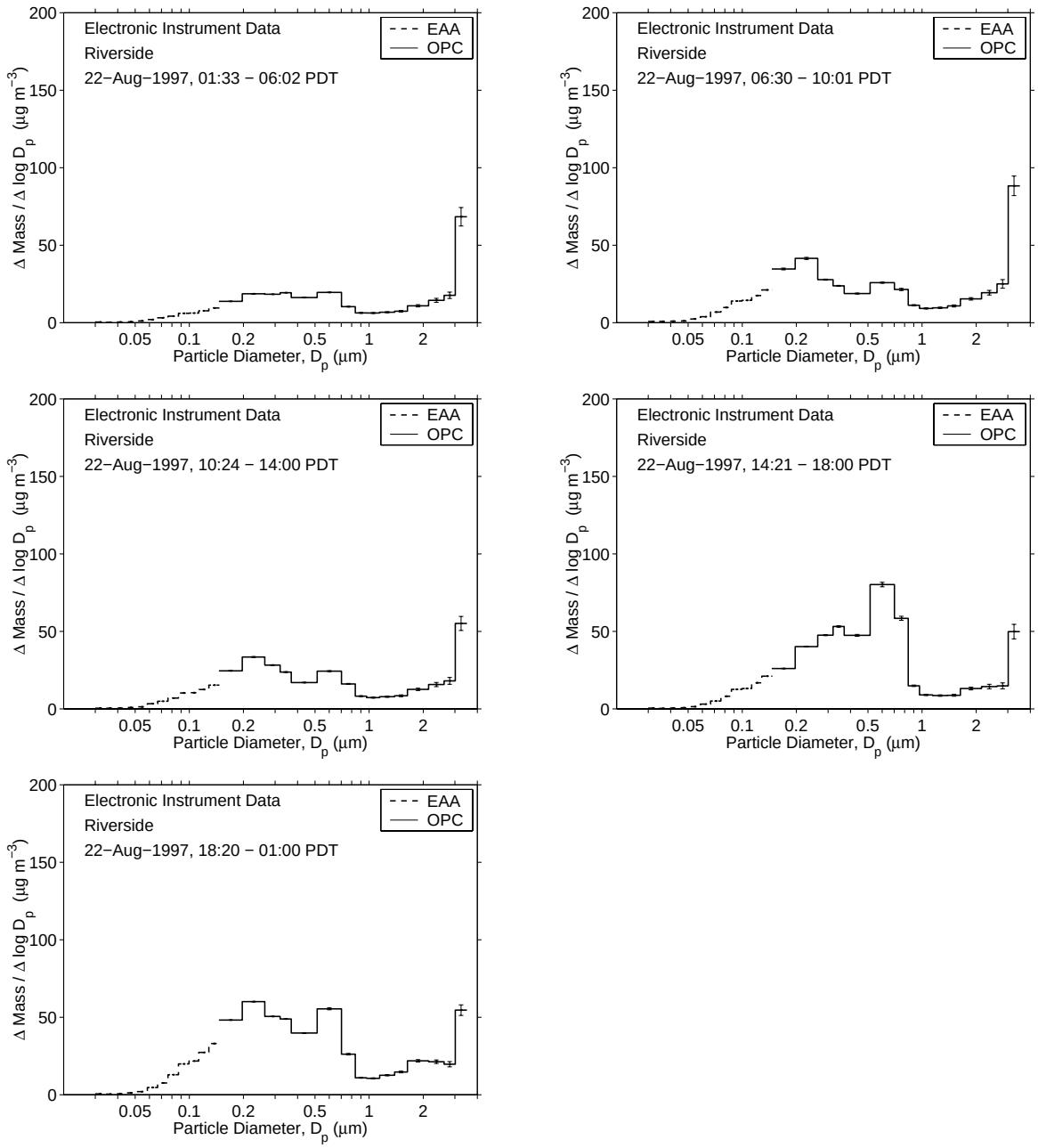

Figure C.20: Particle mass concentration during the second day of the First Vehicle-Oriented Trajectory Experiment at Riverside

C.2 Second Vehicle-Oriented Trajectory Study

C.2.1 Particle Concentration Time Series Data at Central Los Angeles

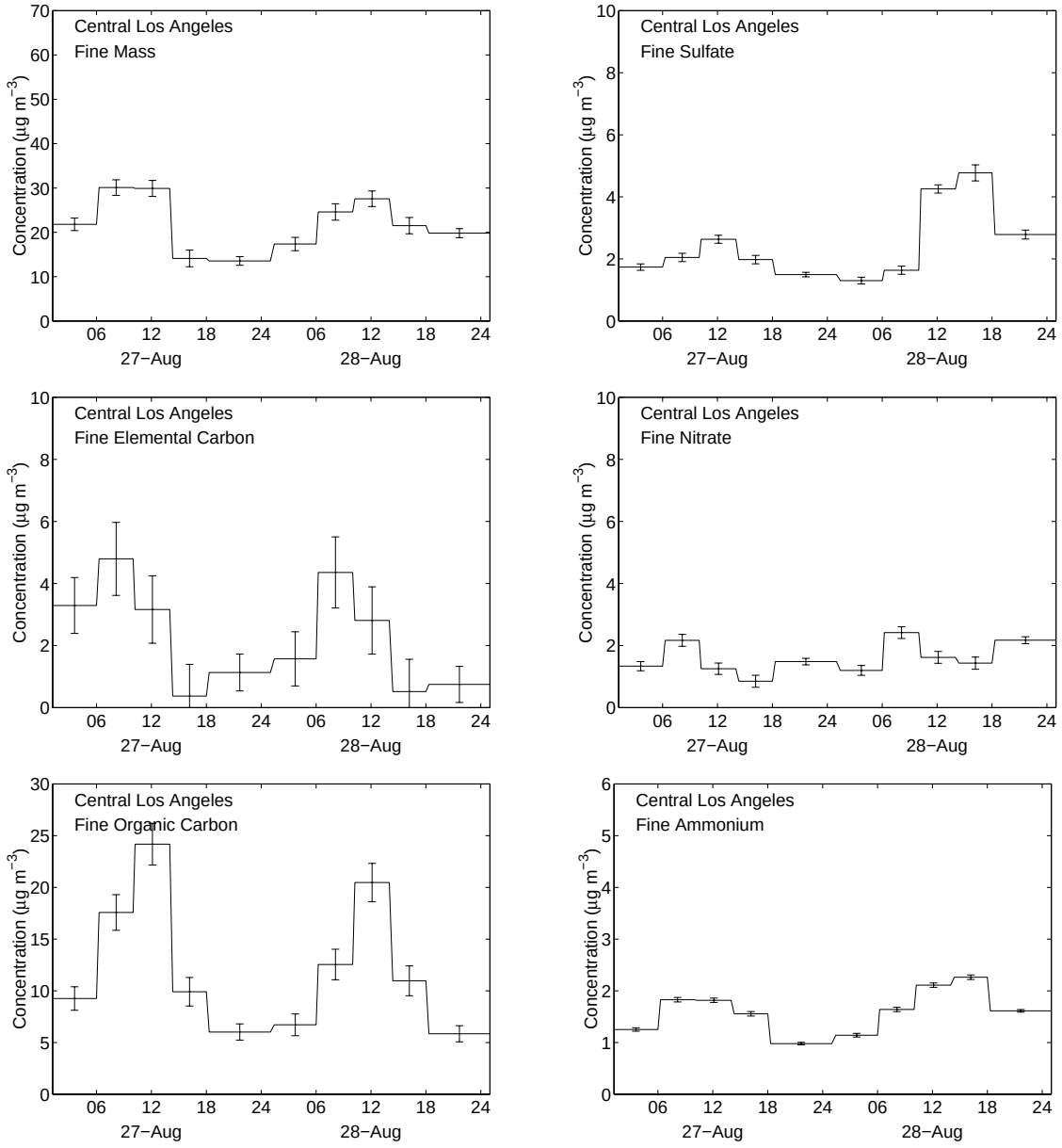

Figure C.21: Fine particle concentrations during the Second Vehicle-Oriented Trajectory Experiment at Central Los Angeles

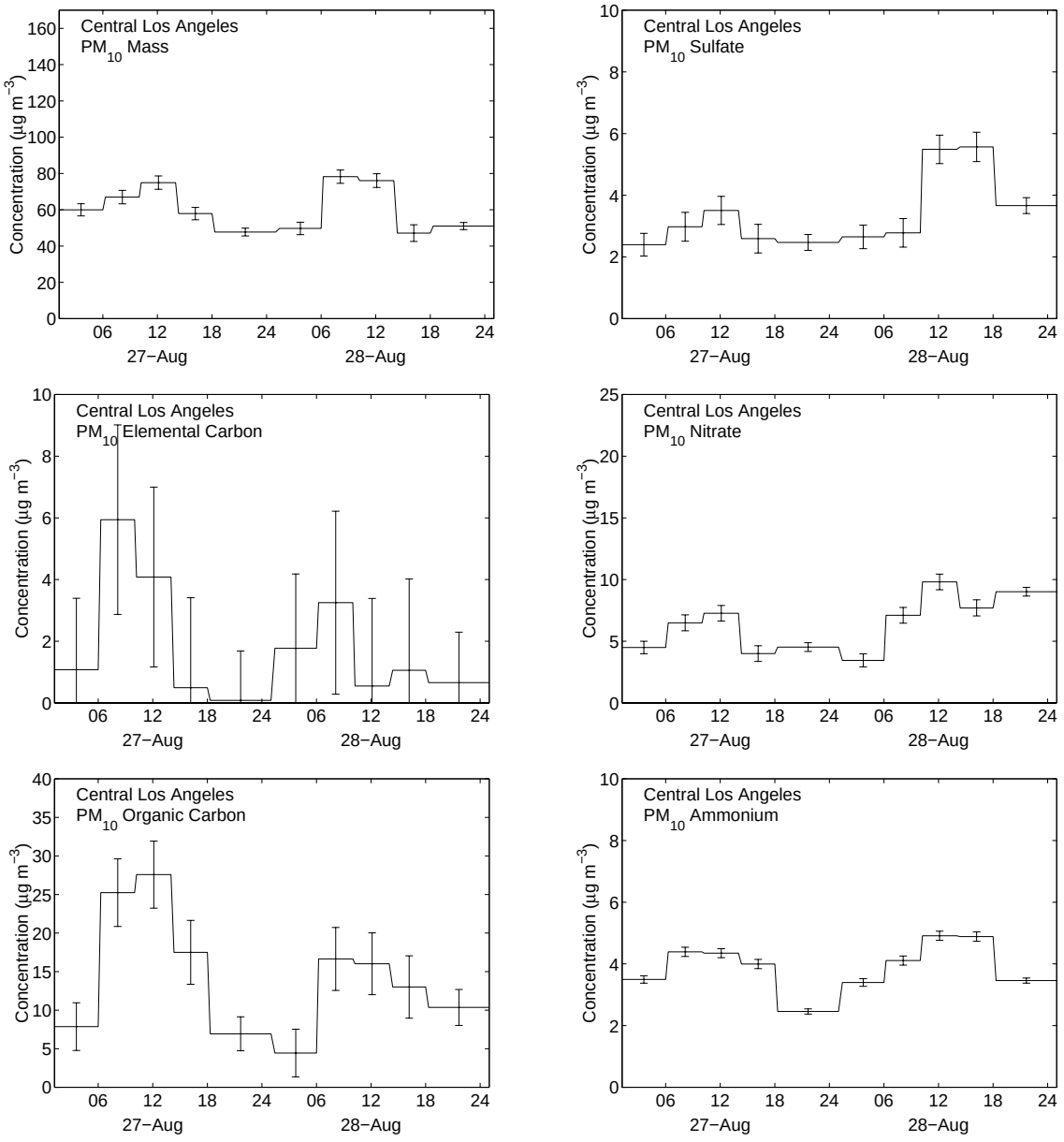

Figure C.22: PM_{10} concentrations during the Second Vehicle-Oriented Trajectory Experiment at Central Los Angeles

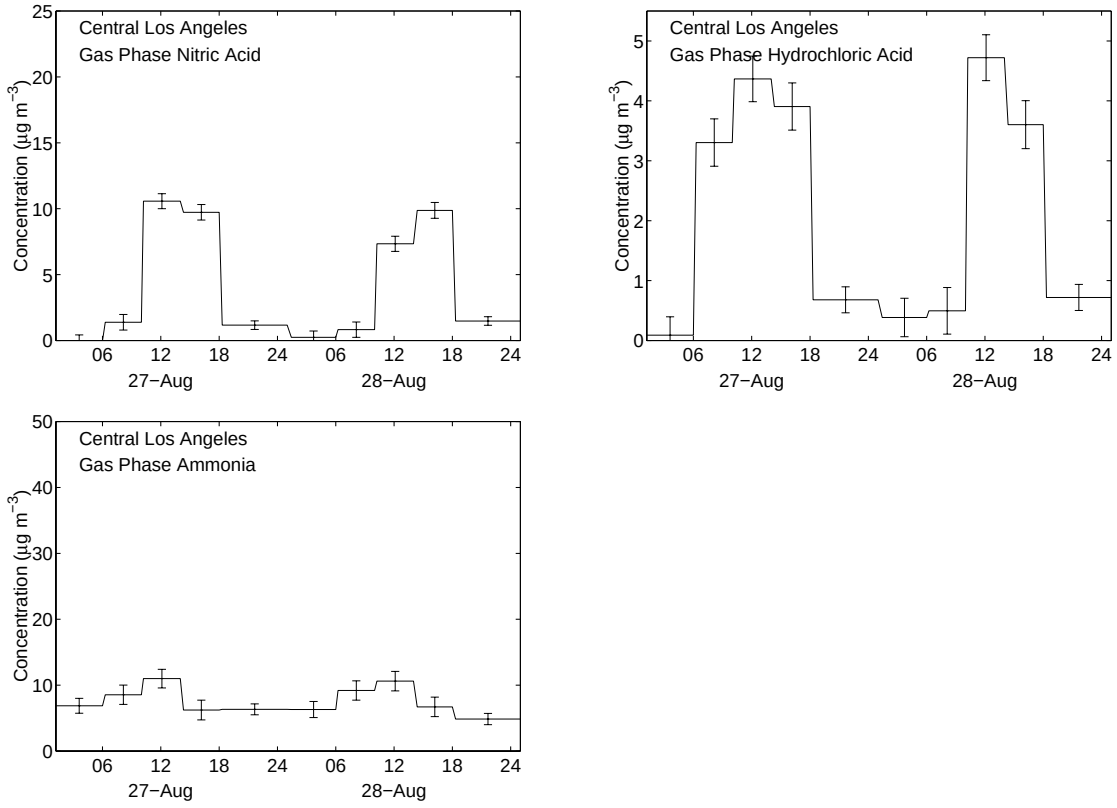

Figure C.23: Gas phase concentrations during the Second Vehicle-Oriented Trajectory Experiment at Central Los Angeles

C.2.2 Particle Concentration Time Series Data at Azusa

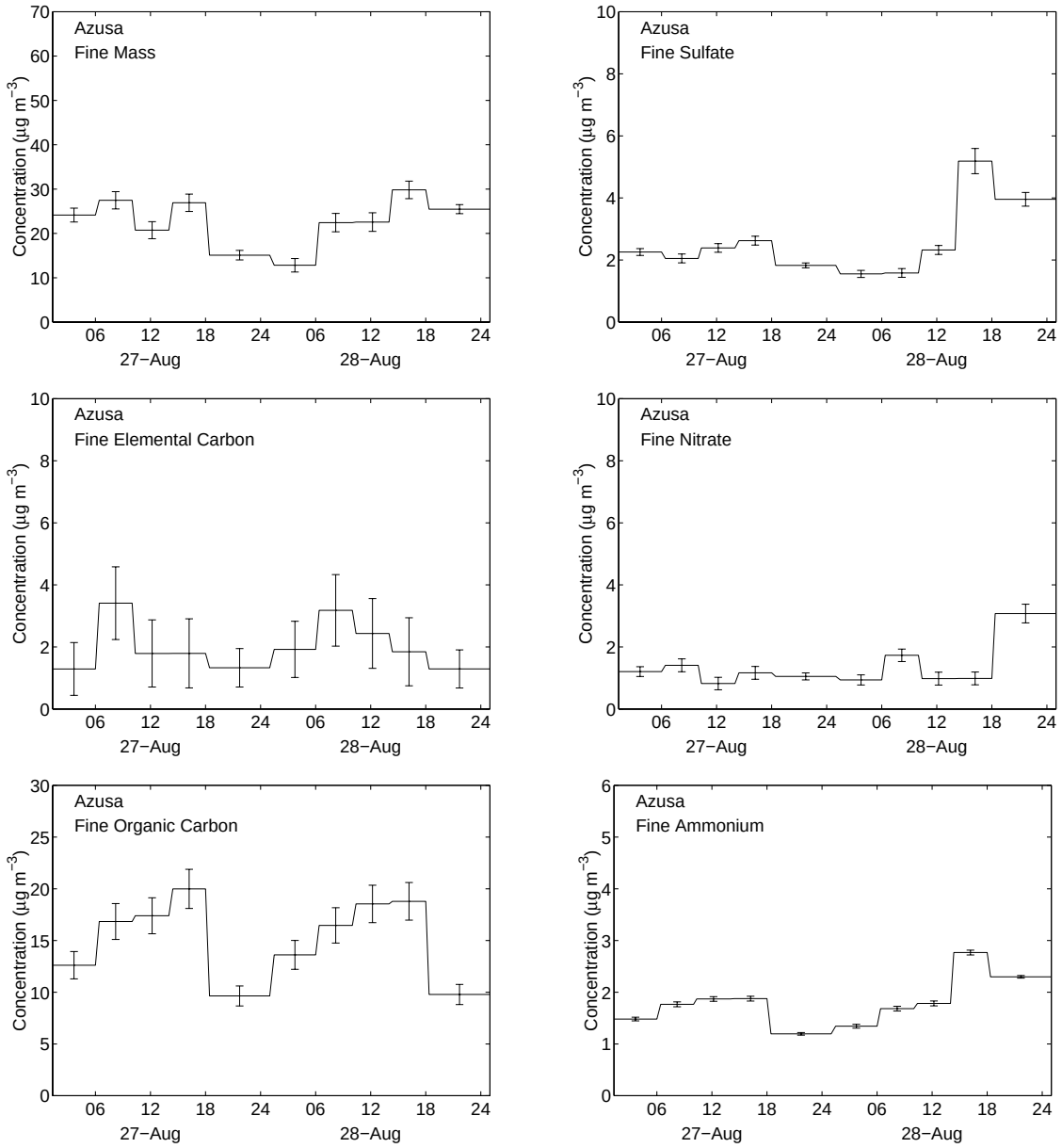

Figure C.24: Fine particle concentrations during the Second Vehicle-Oriented Trajectory Experiment at Azusa

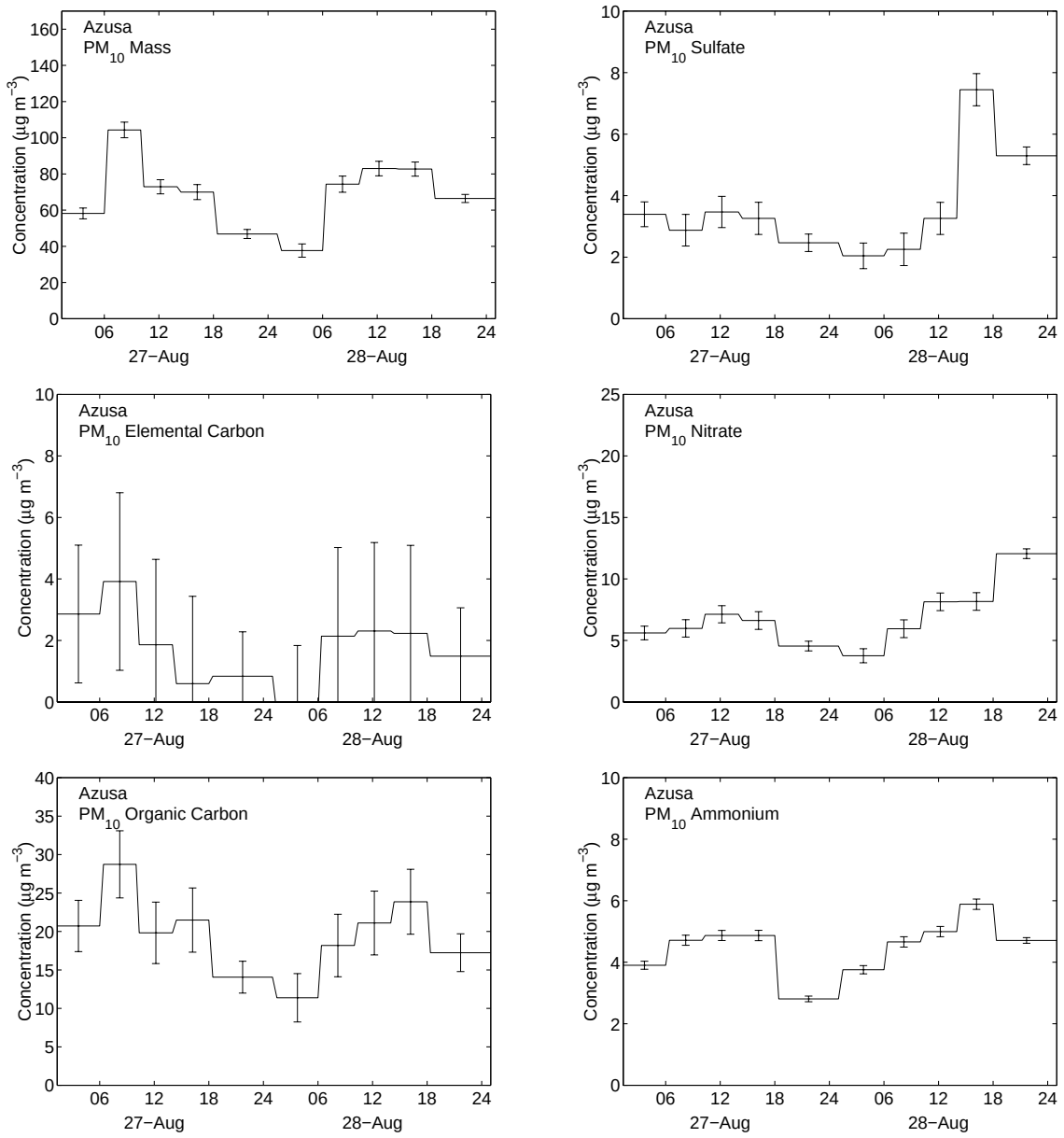

Figure C.25: PM_{10} concentrations during the Second Vehicle-Oriented Trajectory Experiment at Azusa

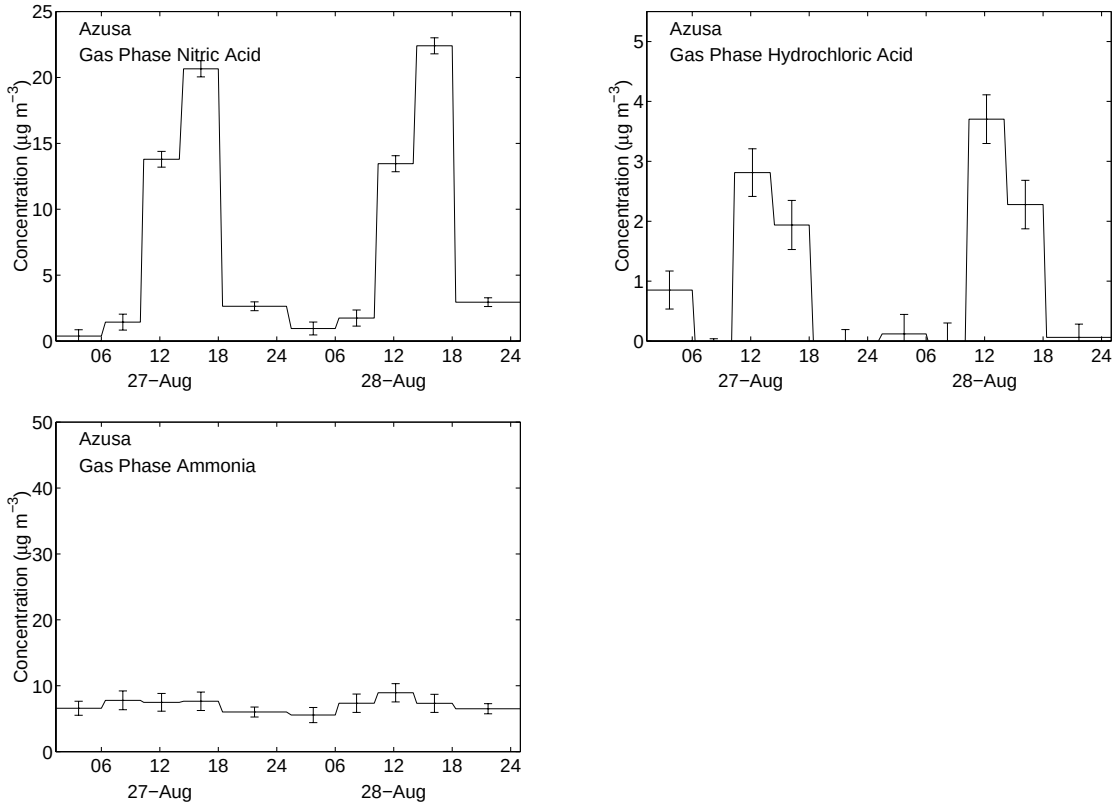

Figure C.26: Gas phase concentrations during the Second Vehicle-Oriented Trajectory Experiment at Azusa

C.2.3 Particle Concentration Time Series Data at Riverside

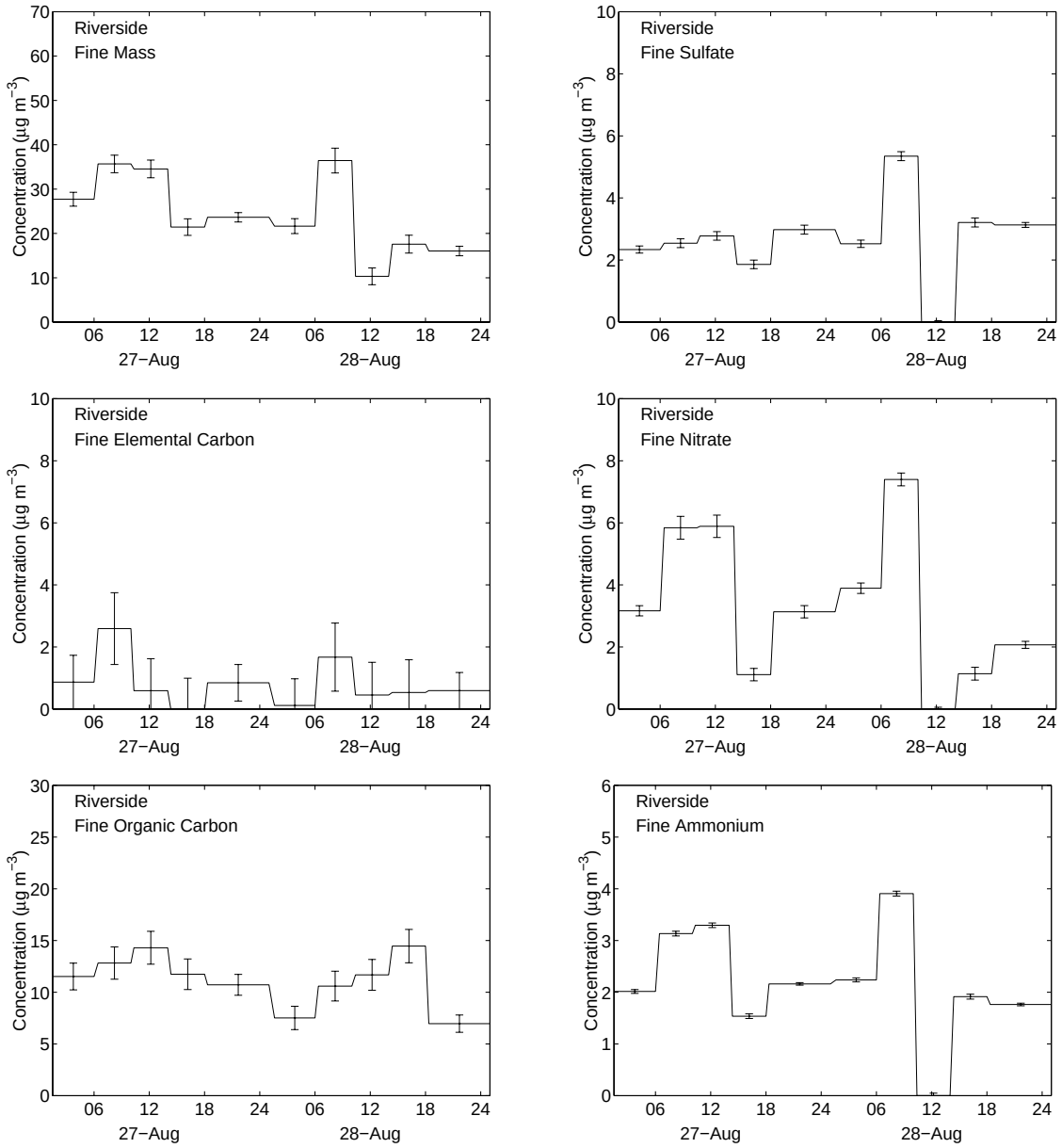

Figure C.27: Fine particle concentrations during the Second Vehicle-Oriented Trajectory Experiment at Riverside

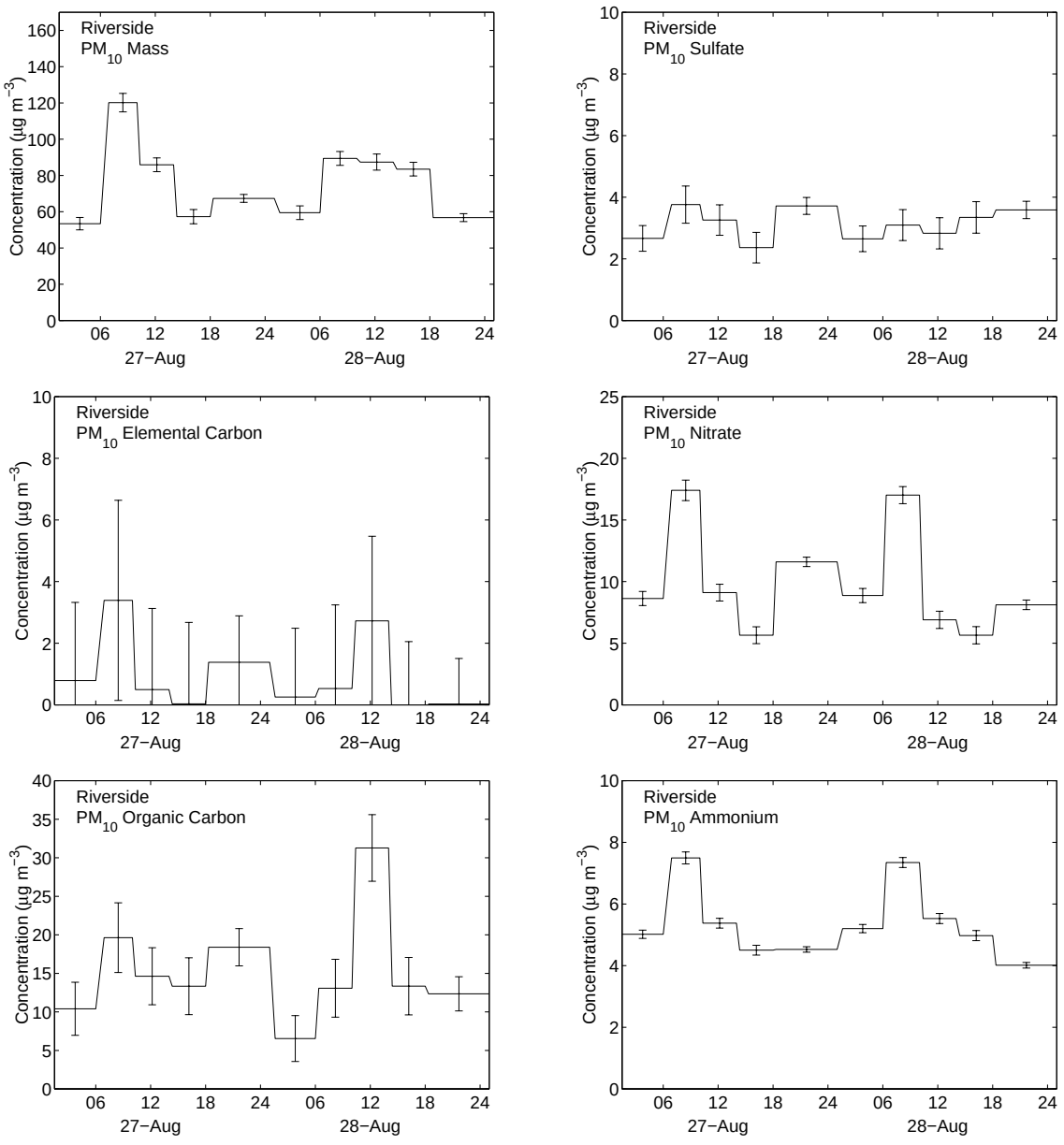

Figure C.28: PM_{10} concentrations during the Second Vehicle-Oriented Trajectory Experiment at Riverside

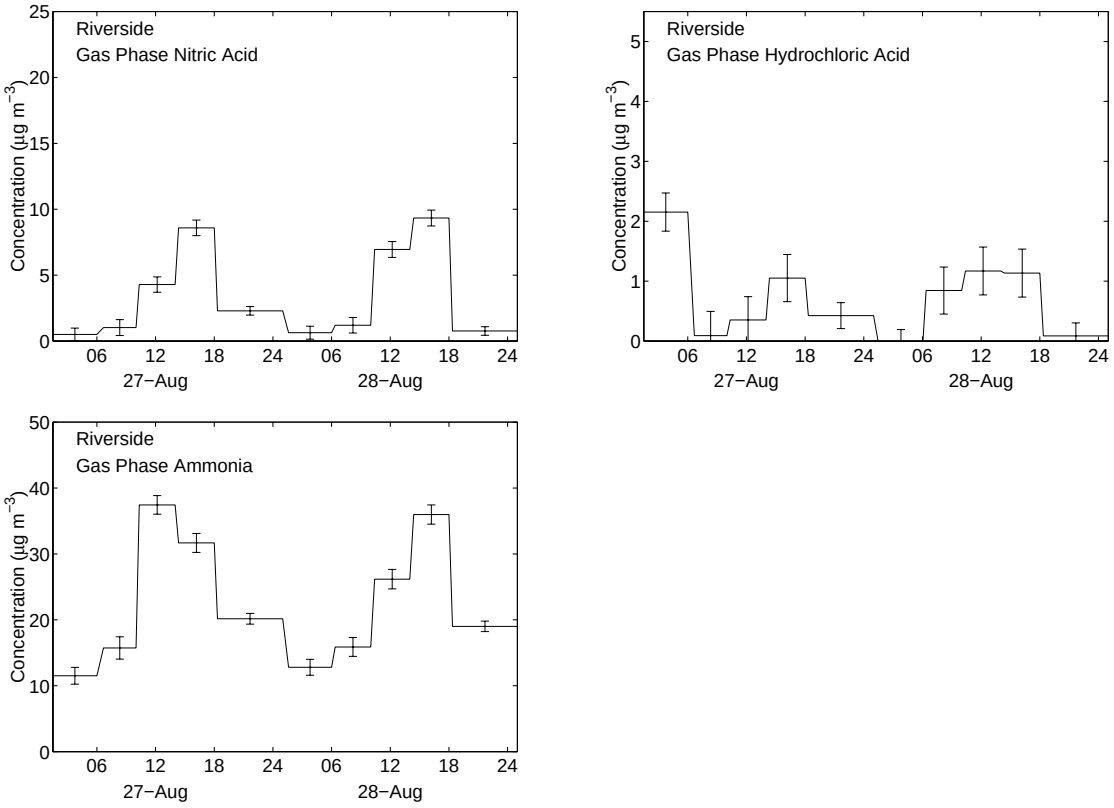

Figure C.29: Gas phase concentrations during the Second Vehicle-Oriented Trajectory Experiment at Riverside

C.2.4 Mass Balances at All Sites

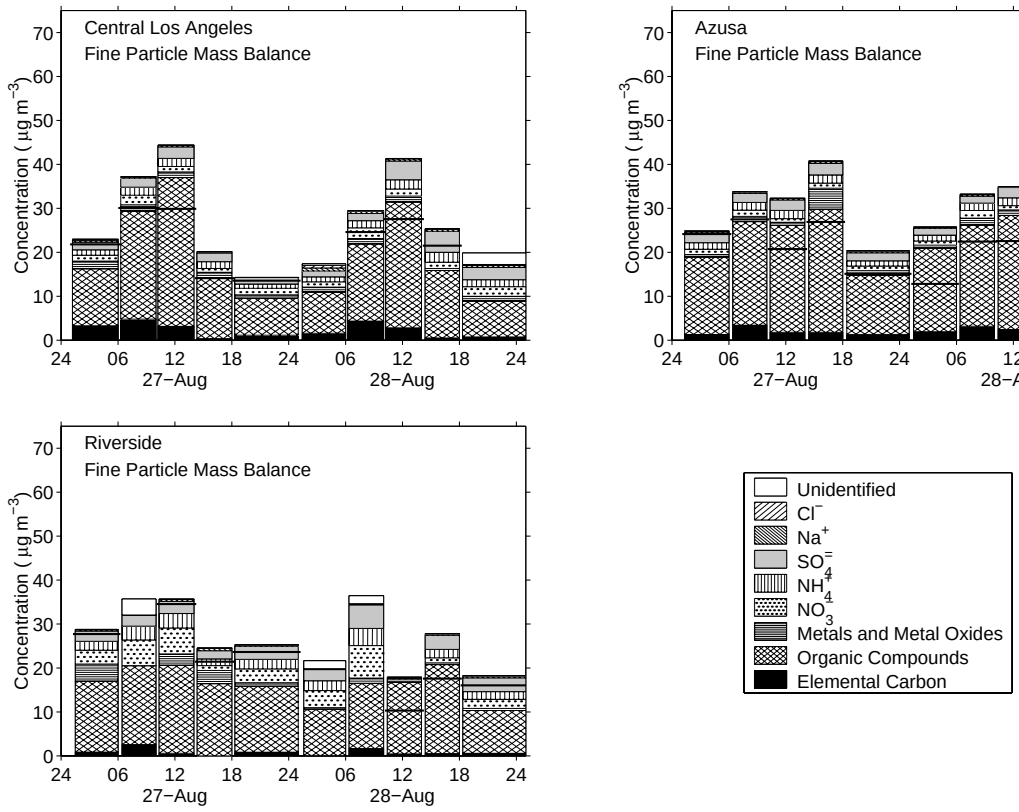

Figure C.30: Fine particle mass balances during the Second Vehicle-Oriented Trajectory Experiment

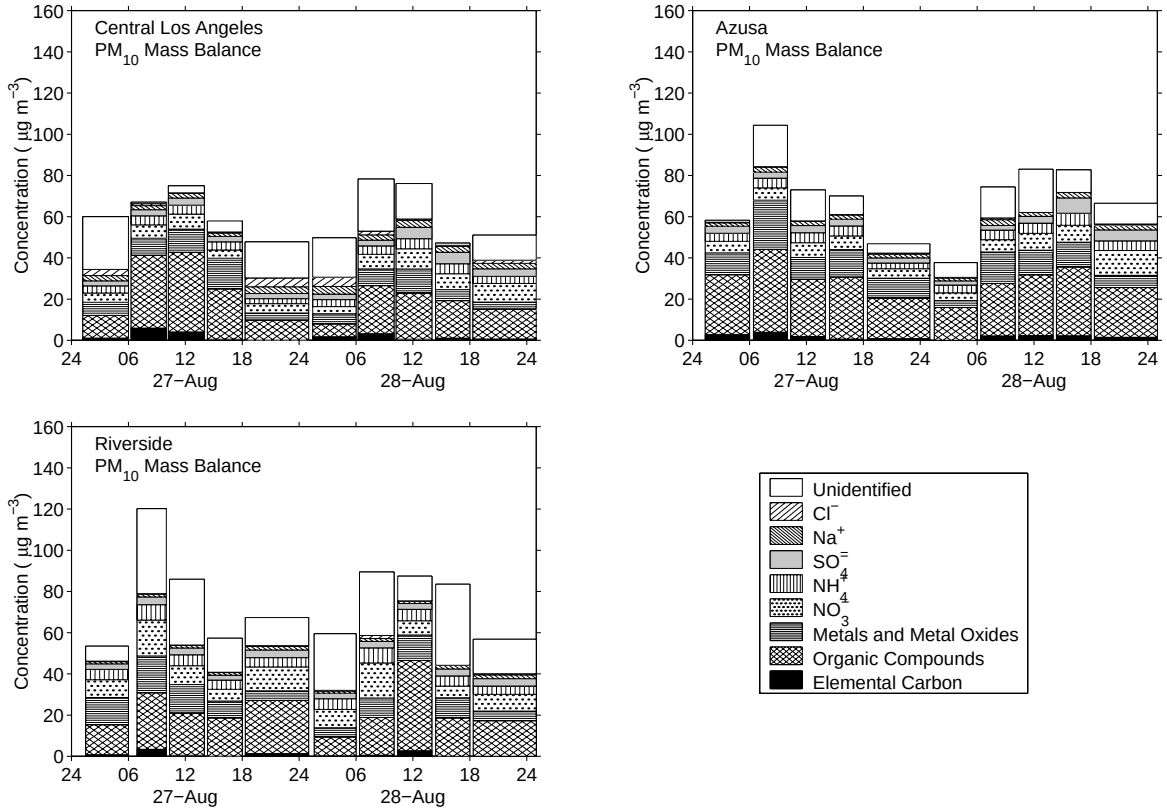

Figure C.31: PM_{10} mass balances during the Second Vehicle-Oriented Trajectory Experiment

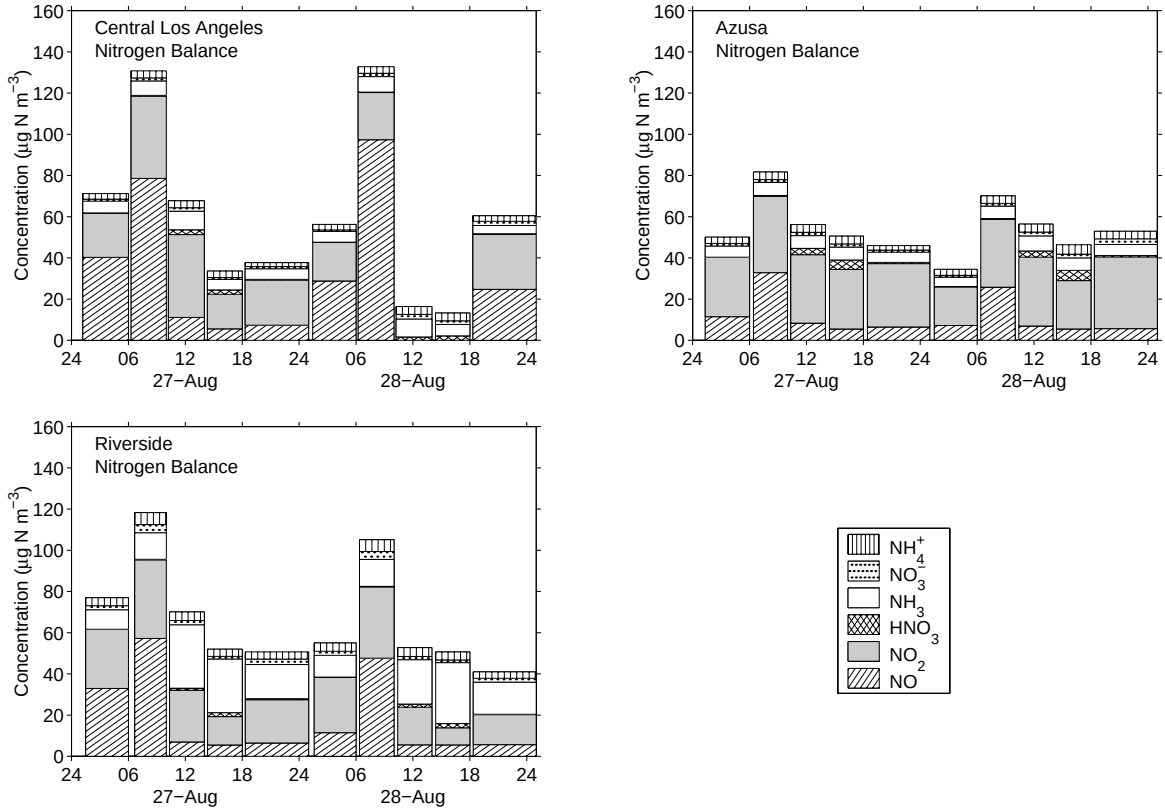

Figure C.32: Nitrogen balances during the Second Vehicle-Oriented Trajectory Experiment

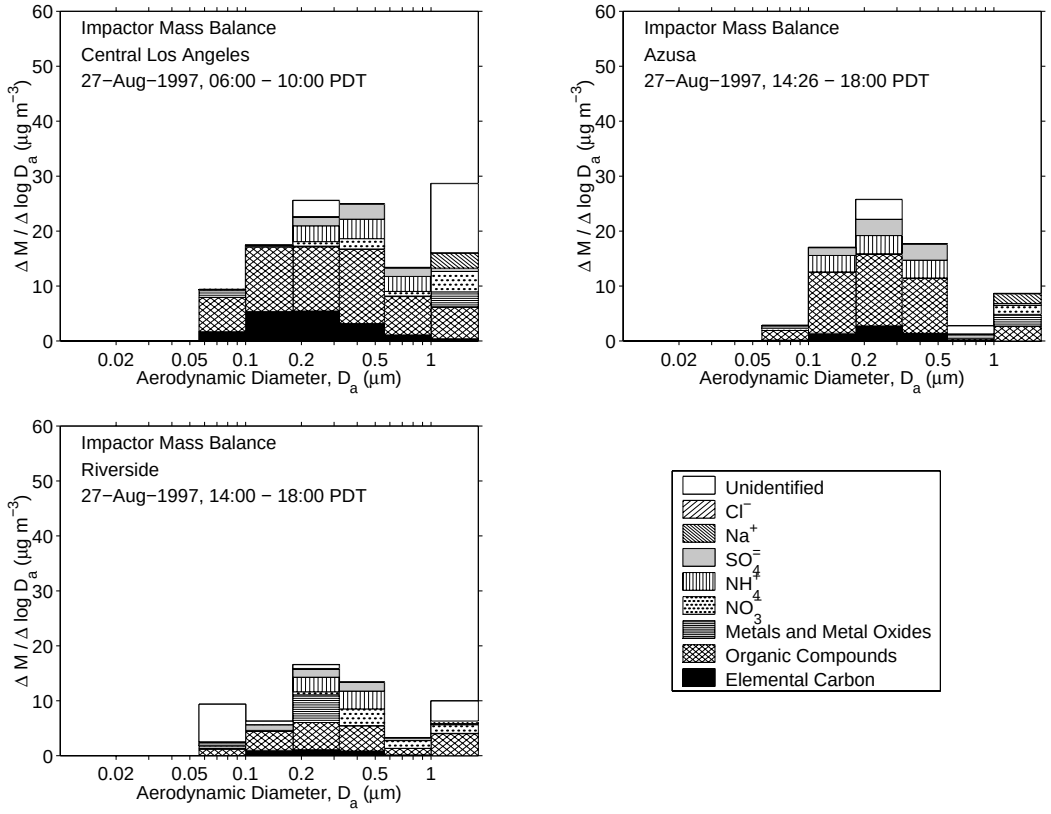

Figure C.33: Impactor mass balances during the first day of the Second Vehicle-Oriented Trajectory Experiment

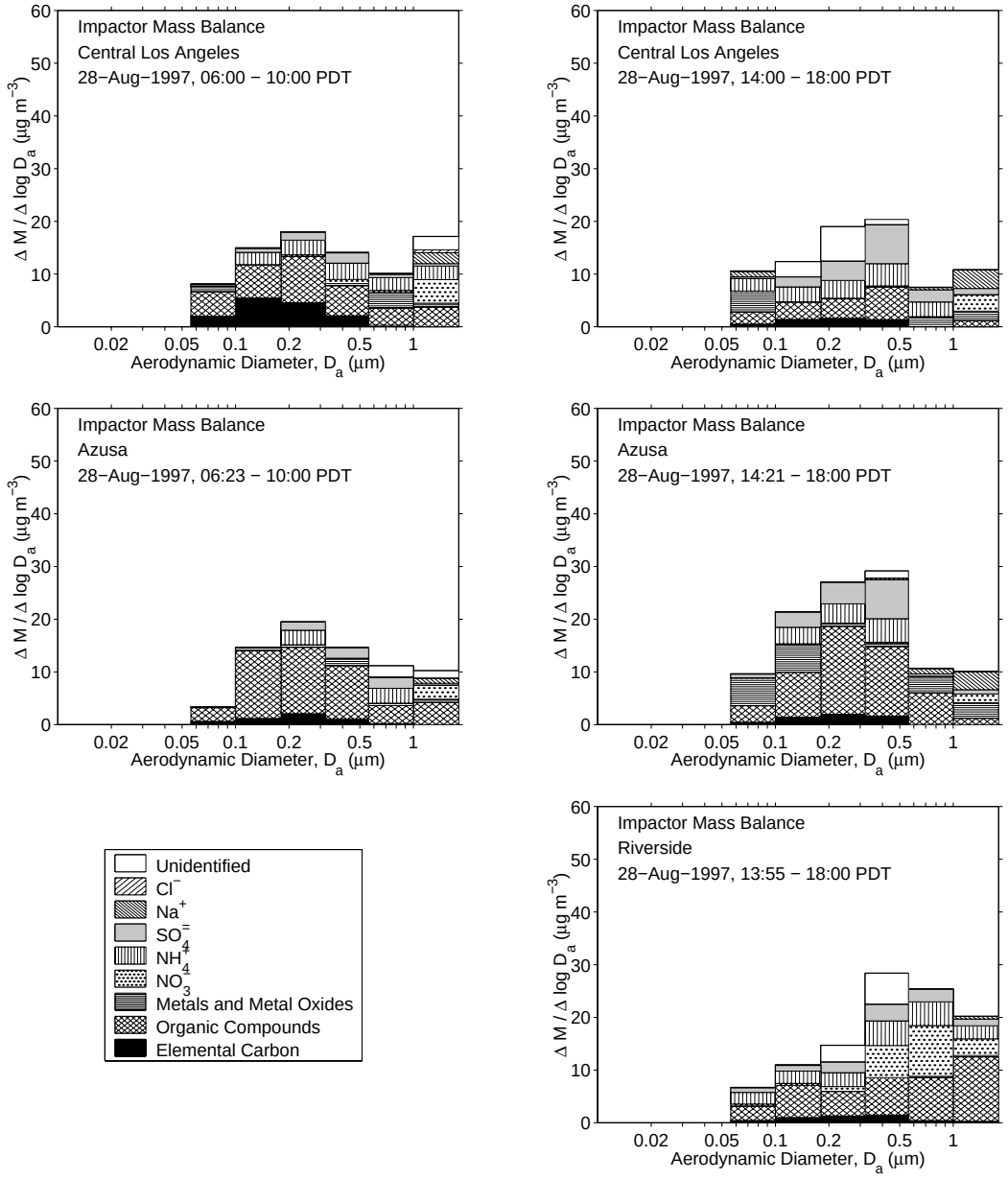

Figure C.34: Impactor mass balances during the second day of the Second Vehicle-Oriented Trajectory Experiment

C.2.5 Electronic Instrument Data at Central Los Angeles

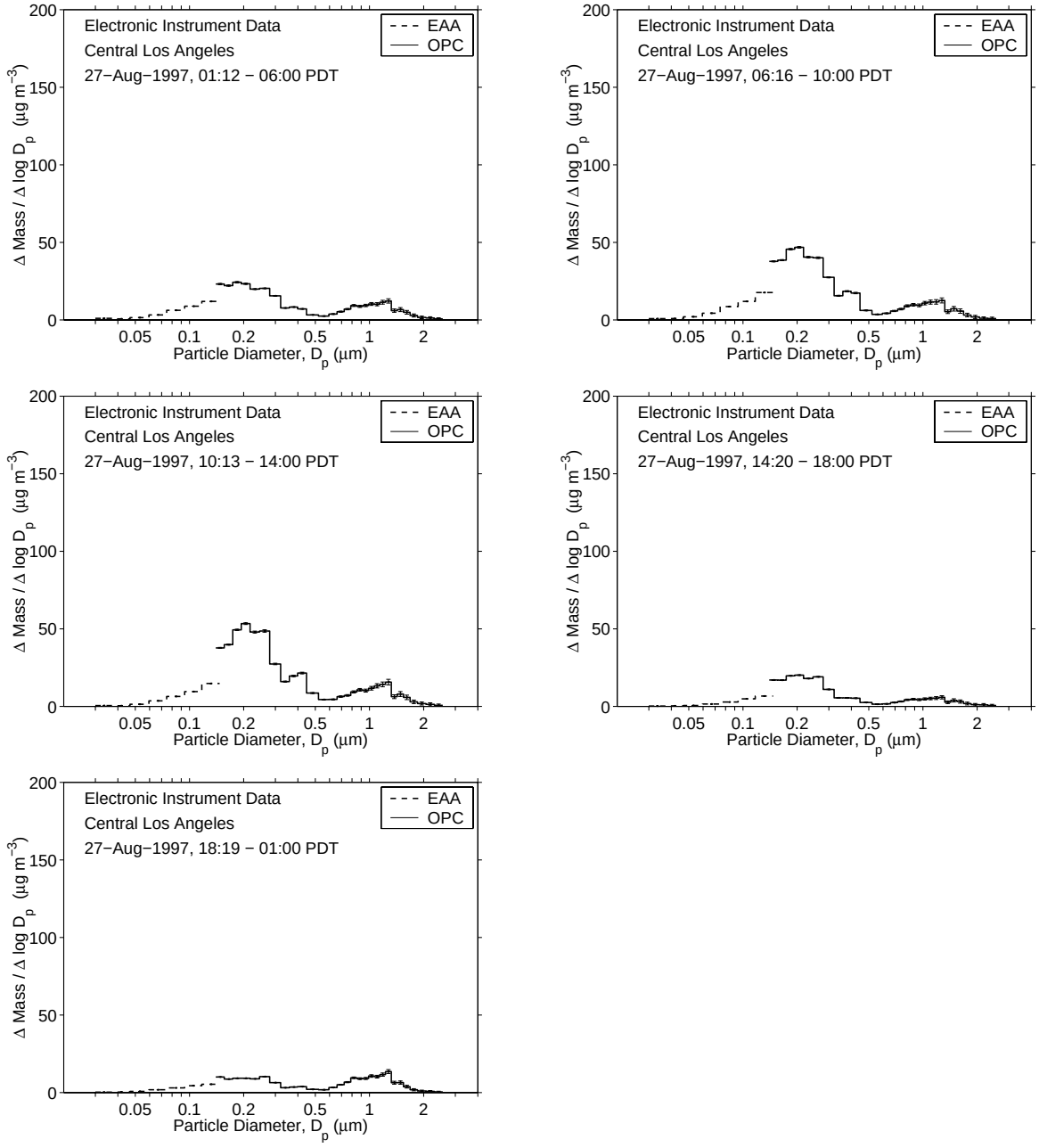

Figure C.35: Particle mass concentration during the first day of the Second Vehicle-Oriented Trajectory Experiment at Central Los Angeles

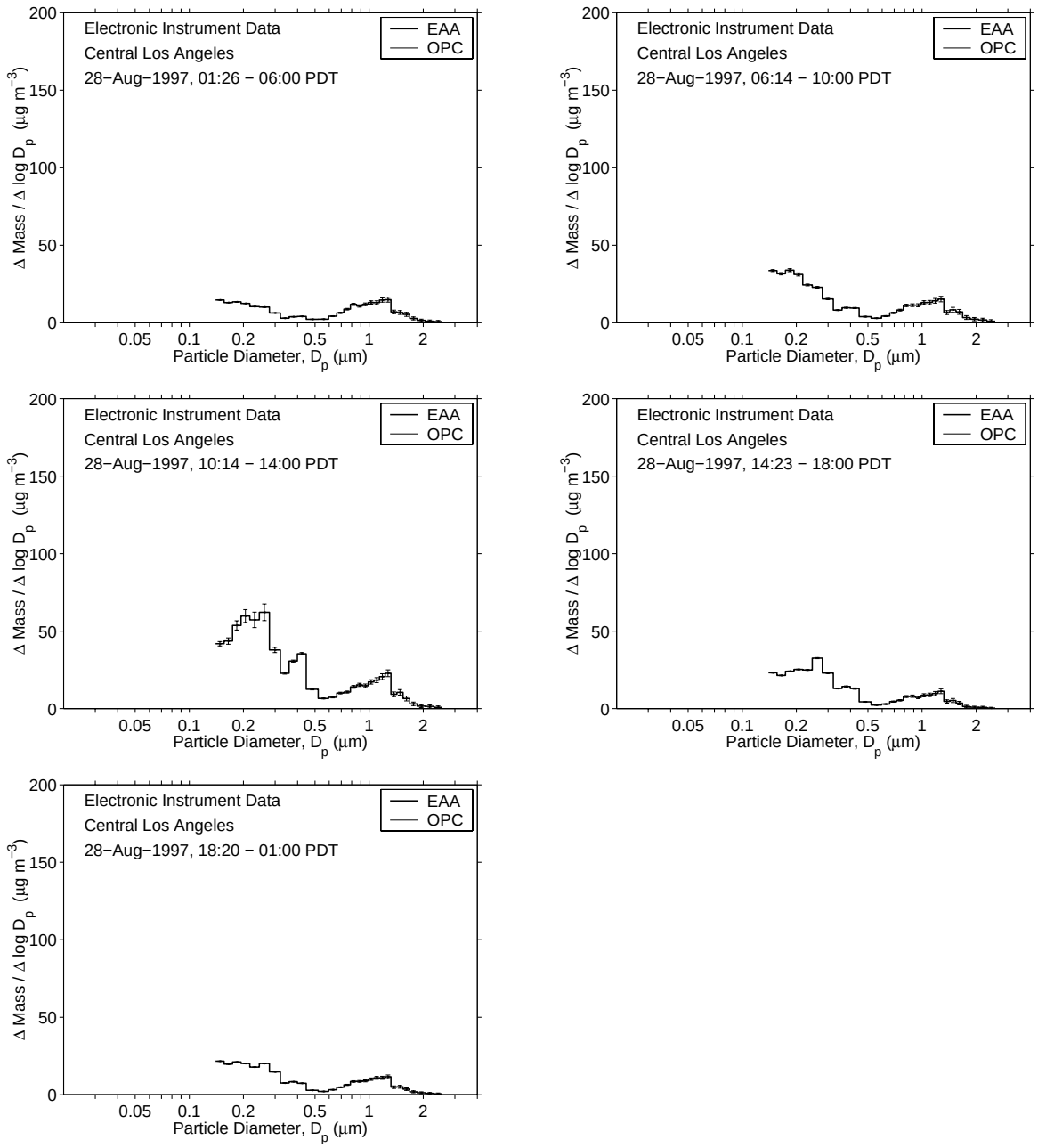

Figure C.36: Particle mass concentration during the second day of the Second Vehicle-Oriented Trajectory Experiment at Central Los Angeles

C.2.6 Electronic Instrument Data at Azusa

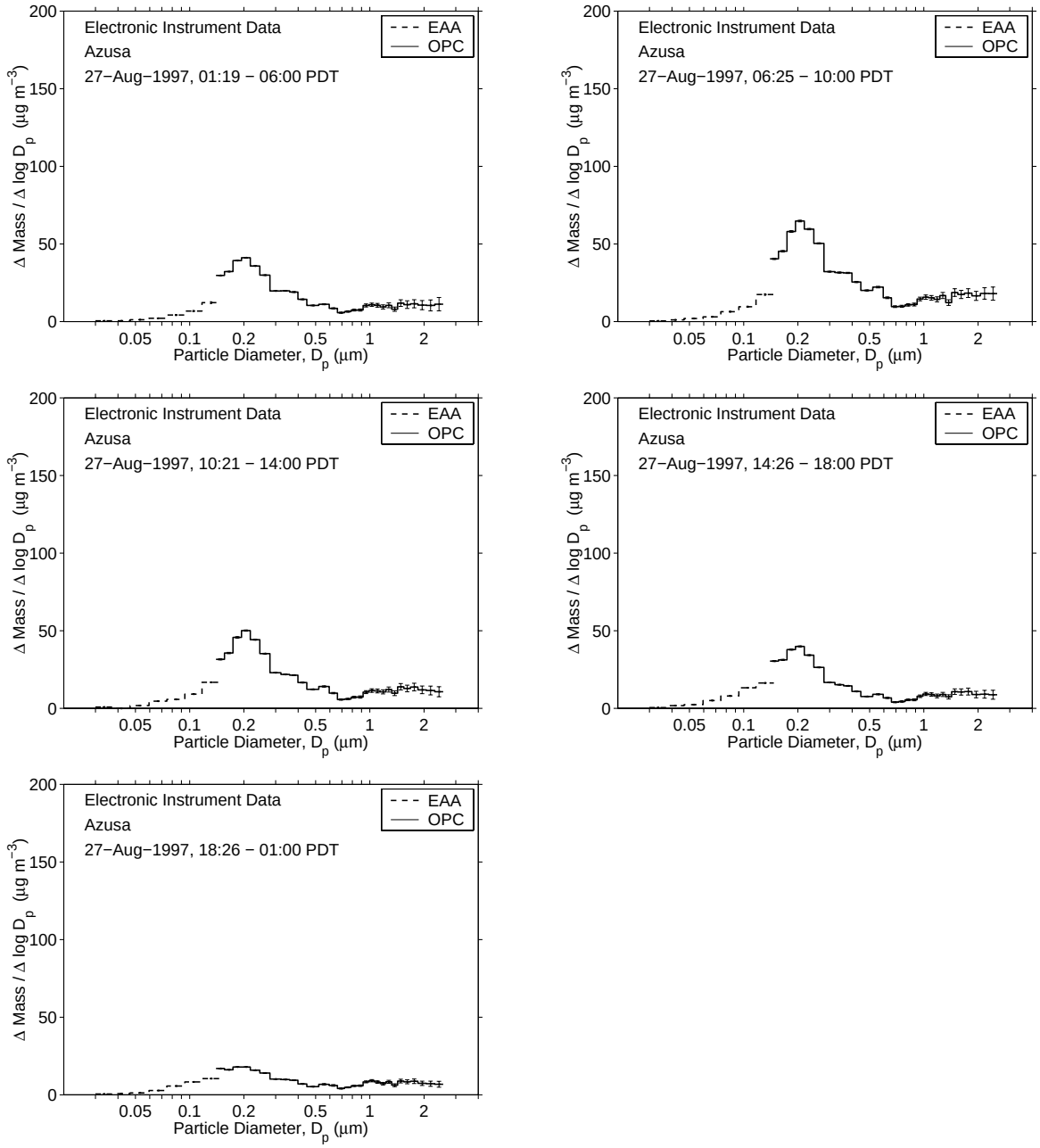

Figure C.37: Particle mass concentration during the first day of the Second Vehicle-Oriented Trajectory Experiment at Azusa

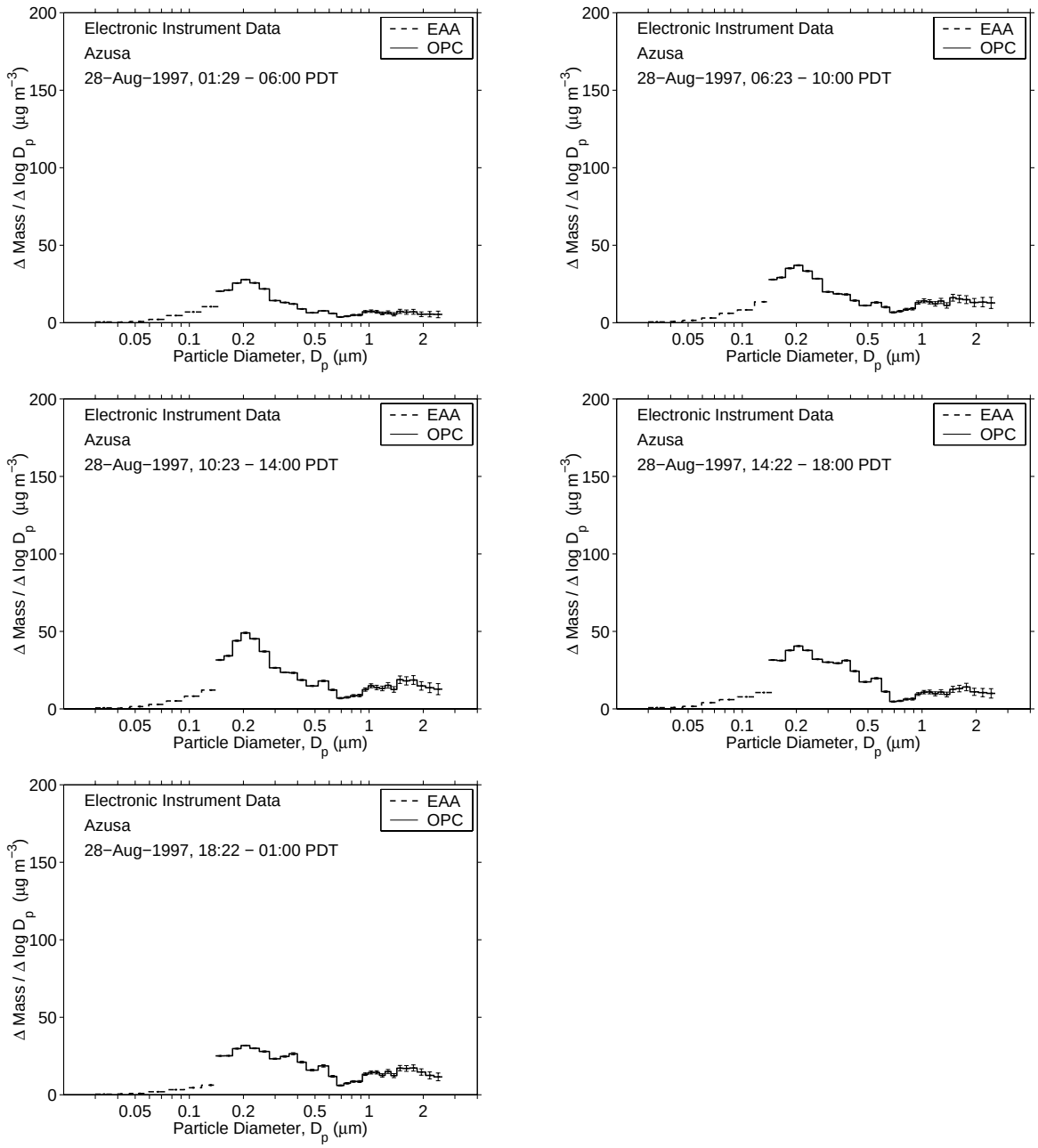

Figure C.38: Particle mass concentration during the second day of the Second Vehicle-Oriented Trajectory Experiment at Azusa

C.2.7 Electronic Instrument Data at Riverside

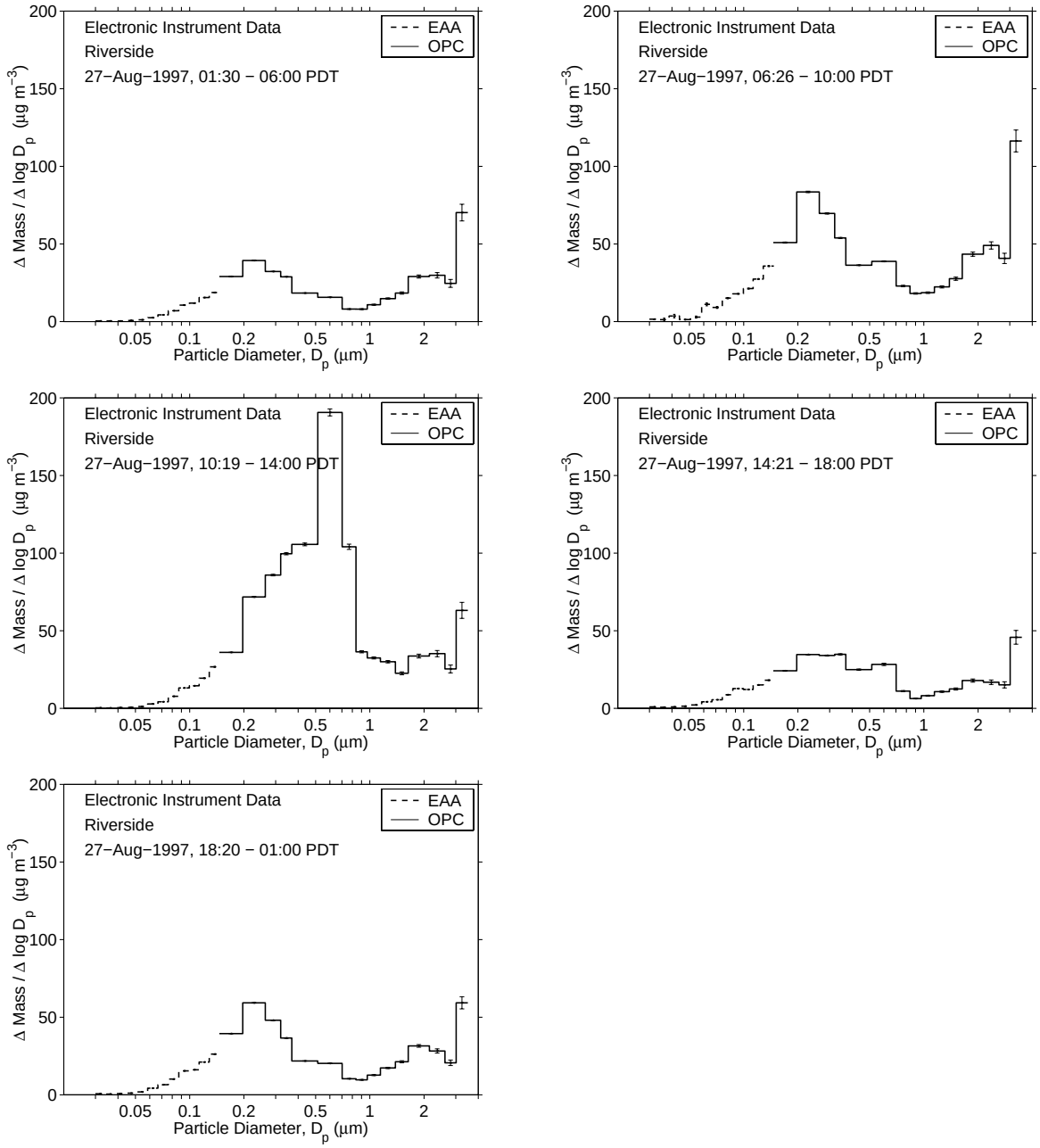

Figure C.39: Particle mass concentration during the first day of the Second Vehicle-Oriented Trajectory Experiment at Riverside

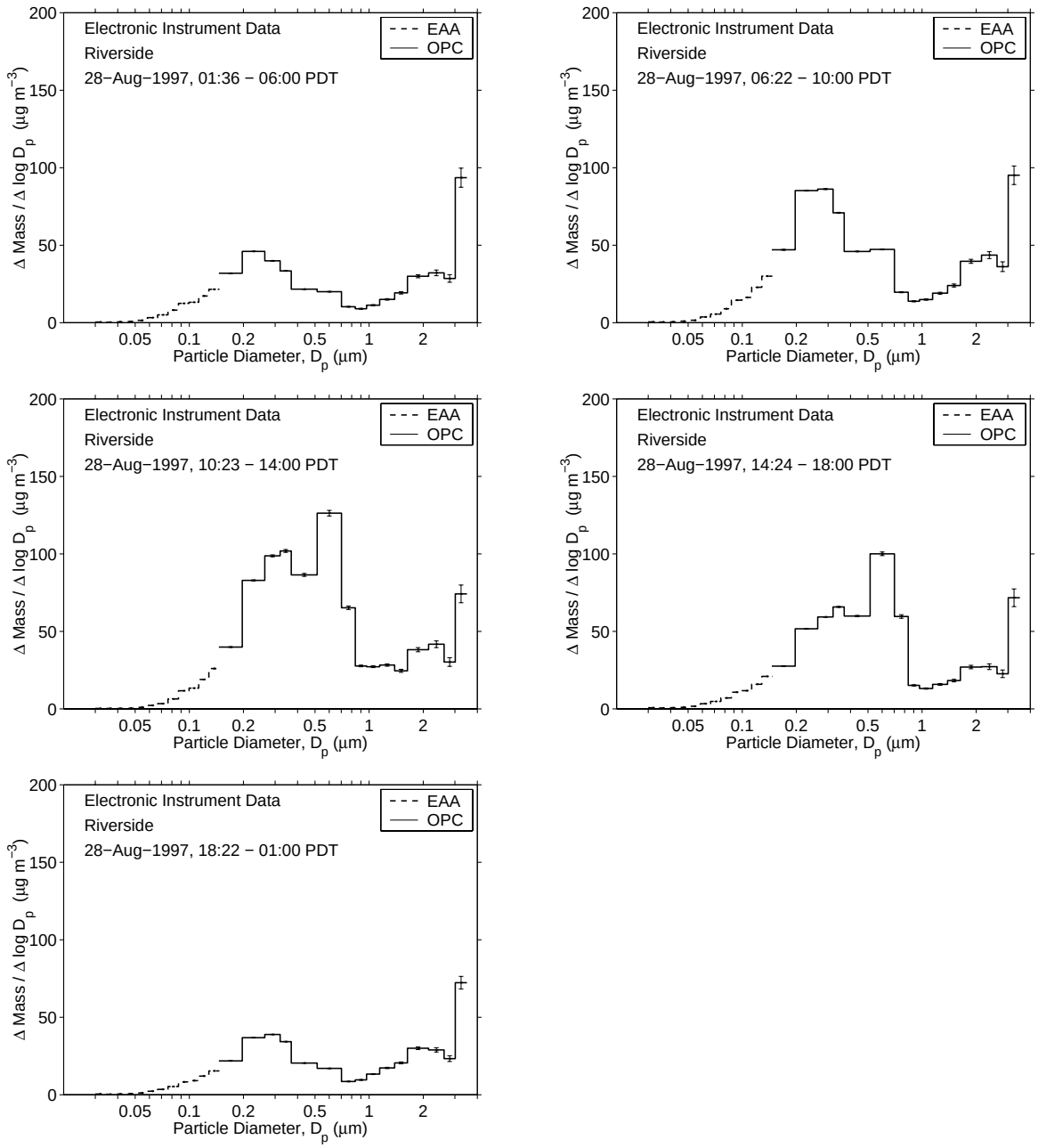

Figure C.40: Particle mass concentration during the second day of the Second Vehicle-Oriented Trajectory Experiment at Riverside

C.3 Nitrate-Oriented Calibration Study

C.3.1 Particle Concentration Time Series Data at Mira Loma

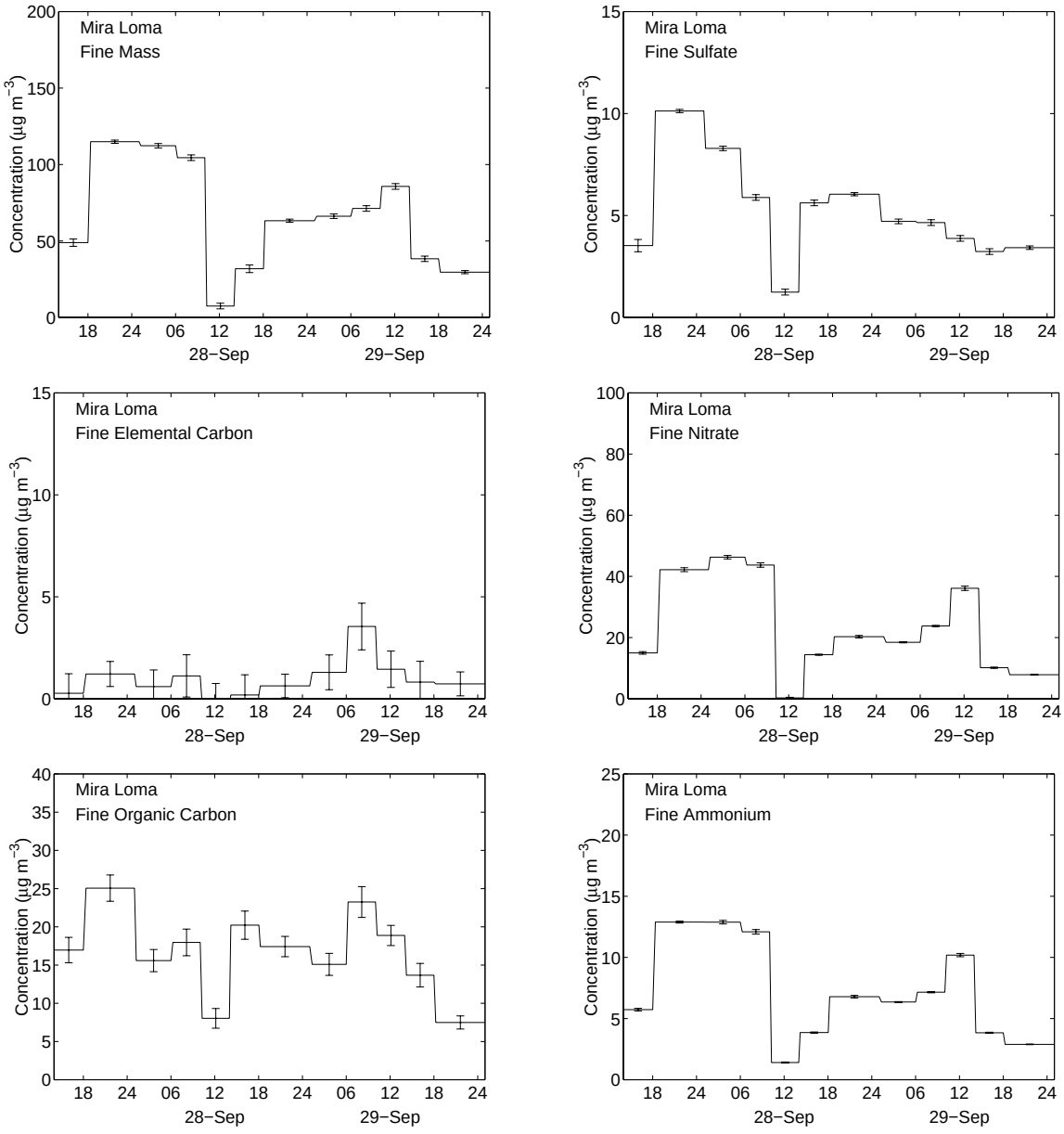

Figure C.41: Fine particle concentrations during the Nitrate-Oriented Calibration Experiment at Mira Loma

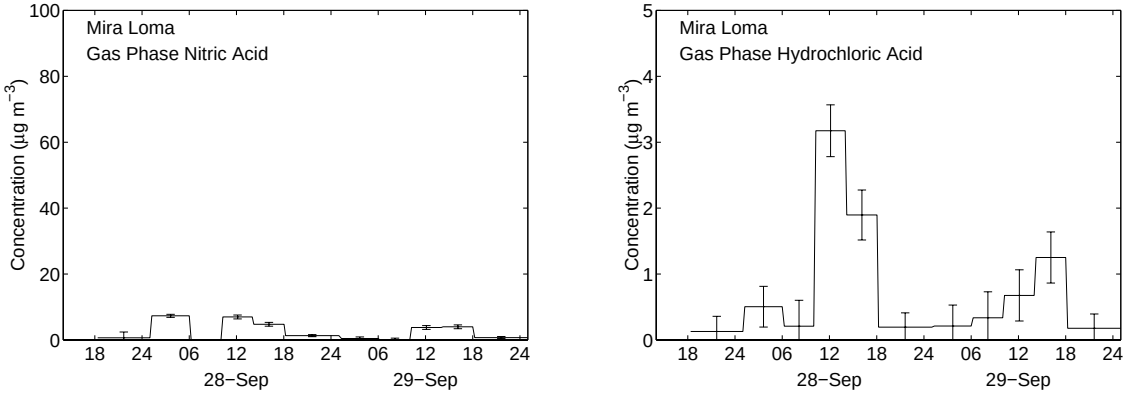

Figure C.42: Gas phase concentrations during the Nitrate-Oriented Calibration Experiment at Mira Loma

C.3.2 Mass Balances at Mira Loma

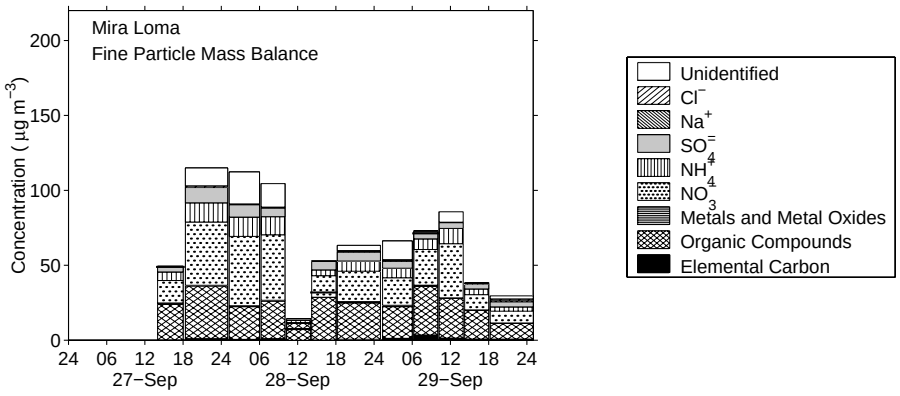

Figure C.43: Fine particle mass balances during the Nitrate-Oriented Calibration Experiment at Mira Loma

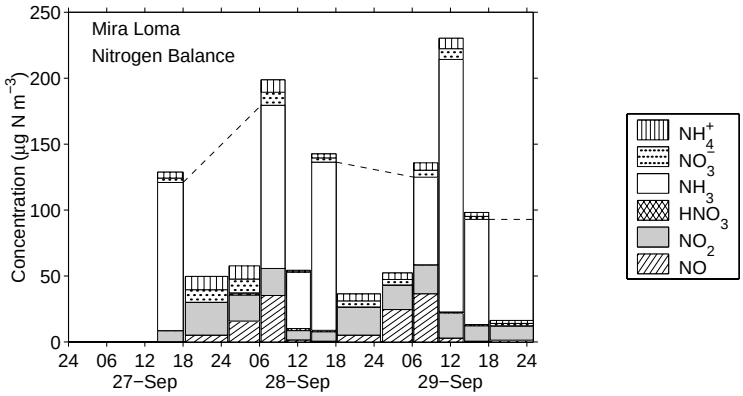

Figure C.44: Nitrogen balances during the Nitrate-Oriented Calibration Experiment at Mira Loma

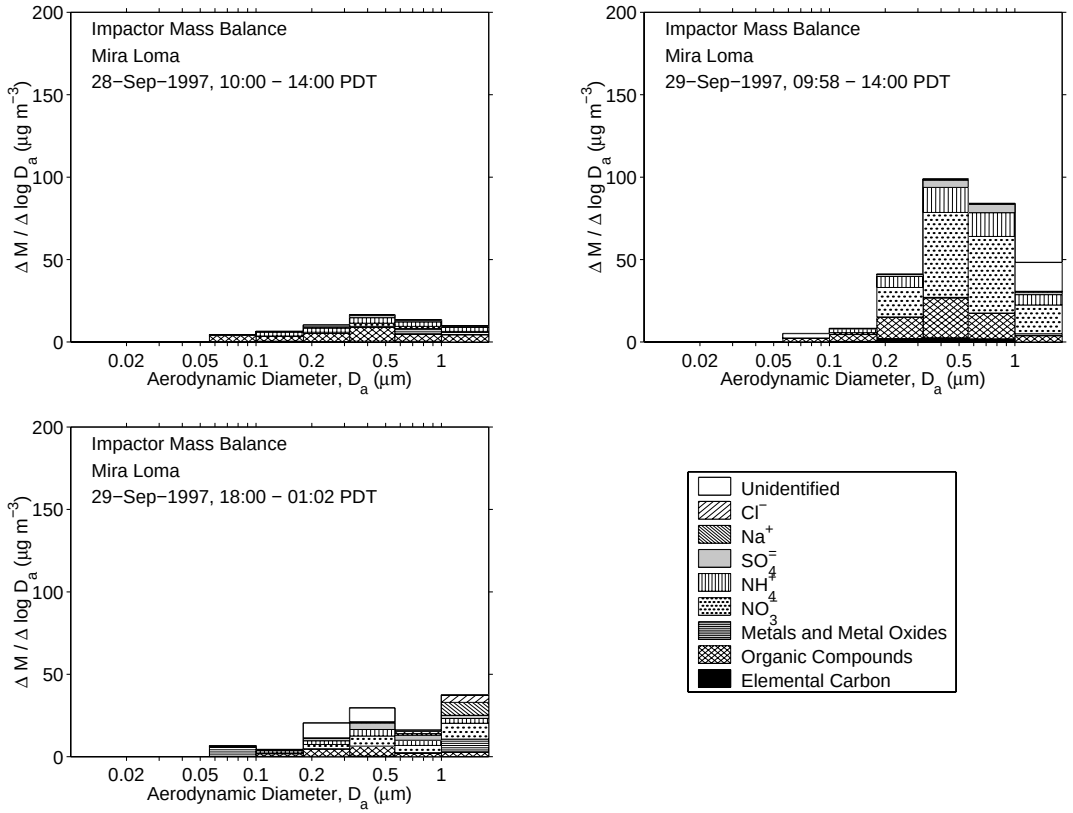

Figure C.45: Impactor mass balances during the Nitrate-Oriented Calibration Experiment at Mira Loma

C.4 Nitrate-Oriented Trajectory Study

C.4.1 Particle Concentration Time Series Data at Diamond Bar

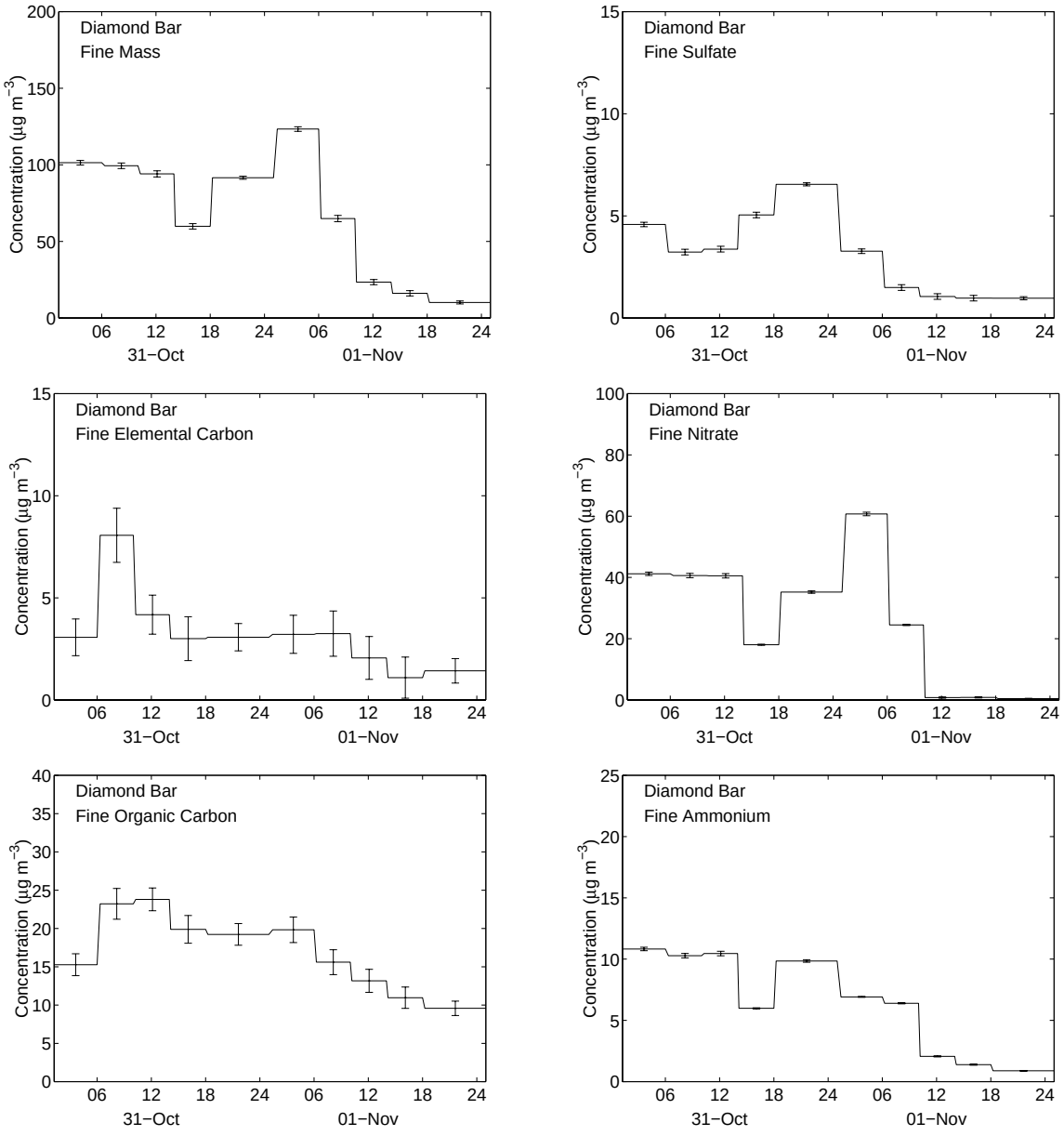

Figure C.46: Fine particle concentrations during the Nitrate-Oriented Trajectory Experiment at Diamond Bar

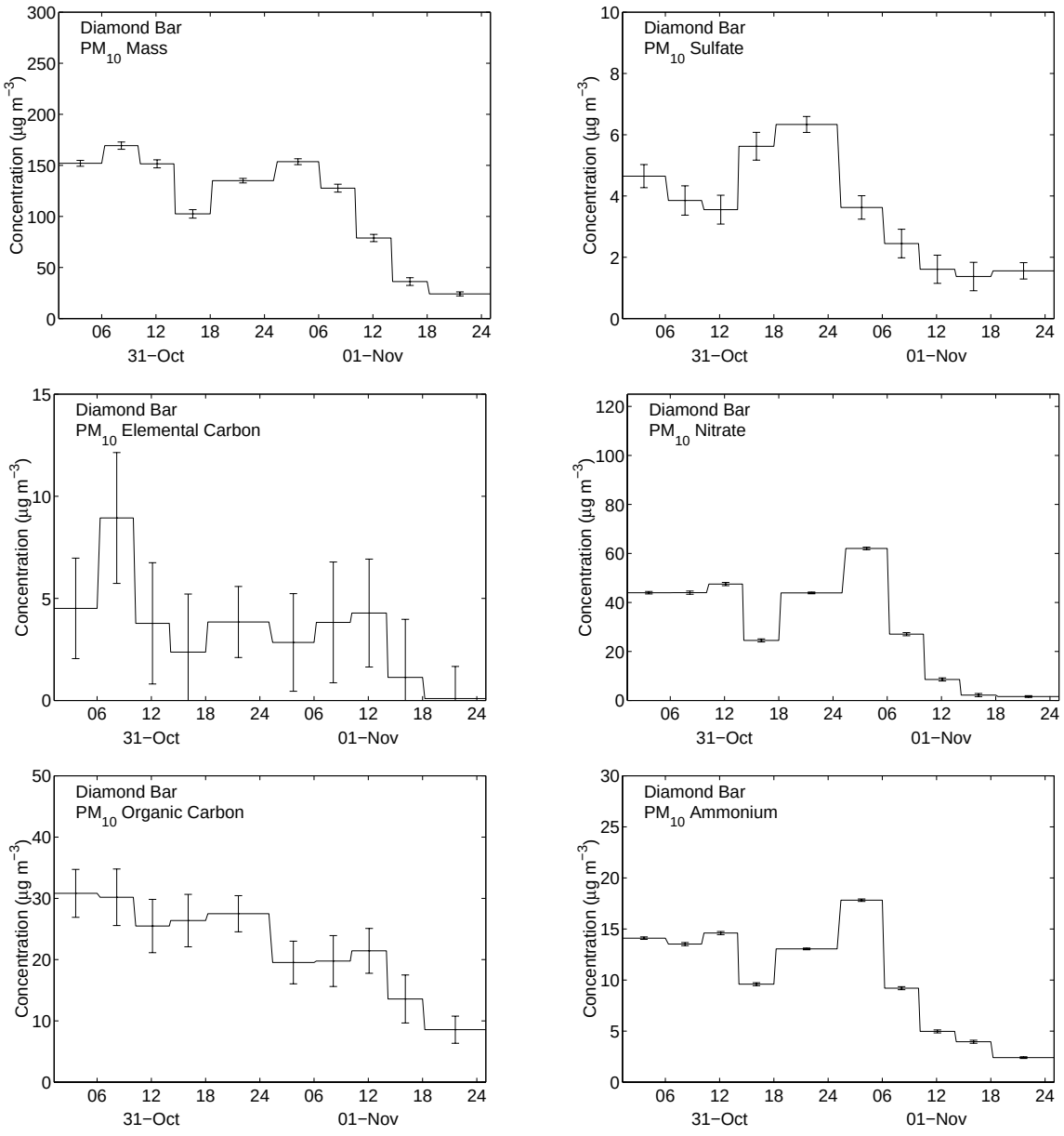

Figure C.47: PM_{10} concentrations during the First Vehicle-Oriented Sampling Experiment at Diamond Bar

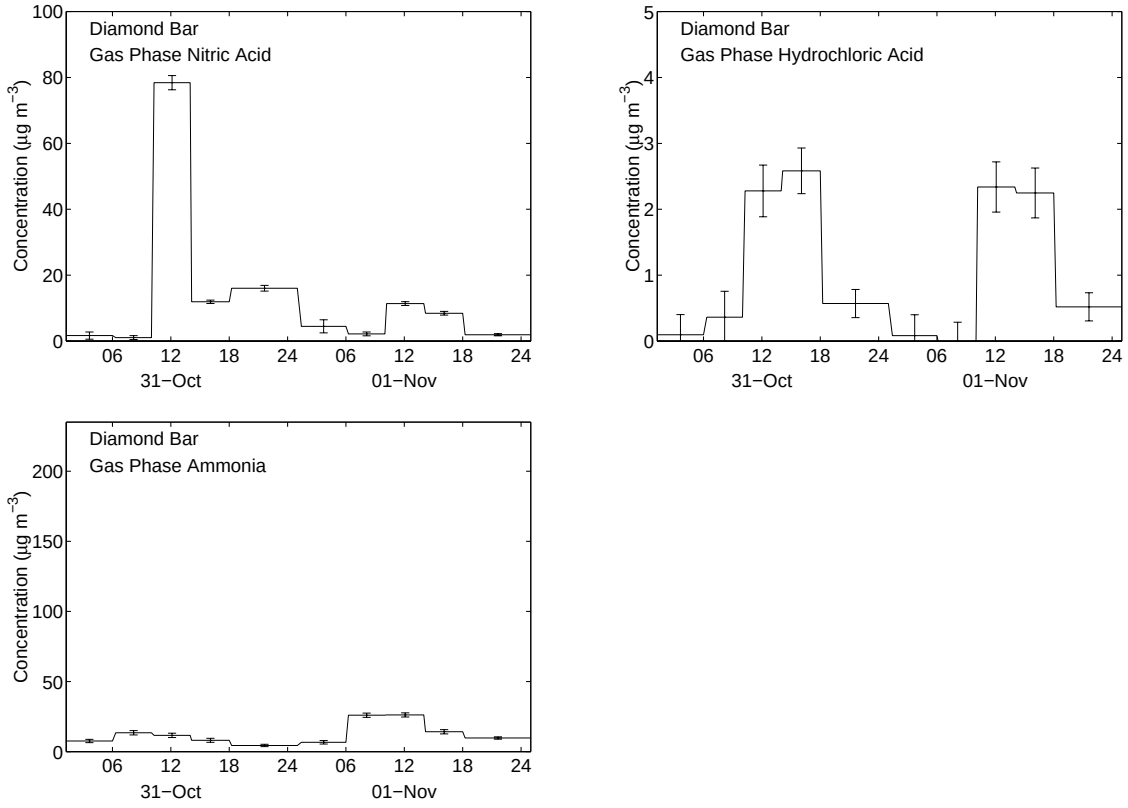

Figure C.48: Gas phase concentrations during the Nitrate-Oriented Trajectory Experiment at Diamond Bar

C.4.2 Particle Concentration Time Series Data at Mira Loma

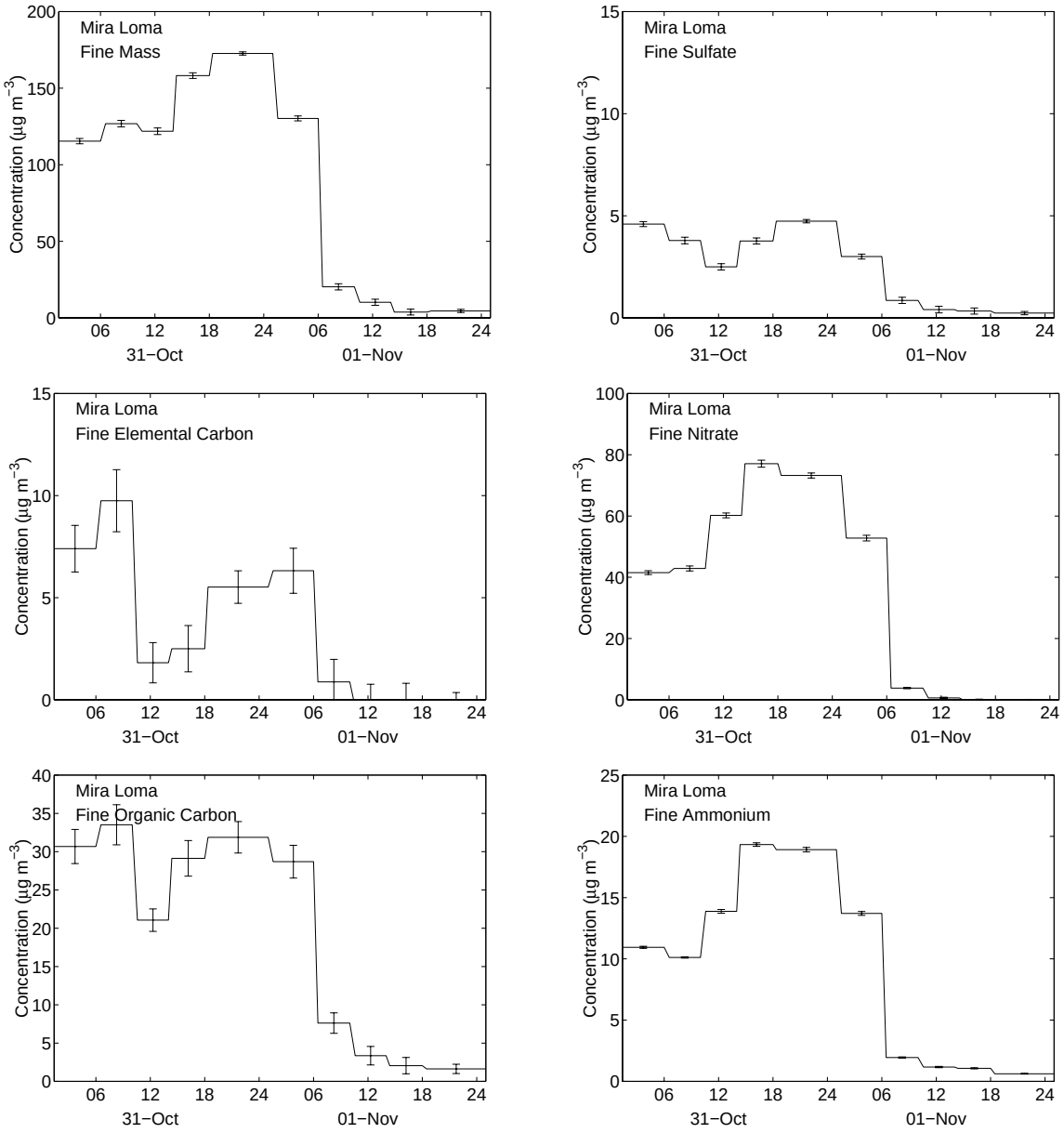

Figure C.49: Fine particle concentrations during the Nitrate-Oriented Trajectory Experiment at Mira Loma

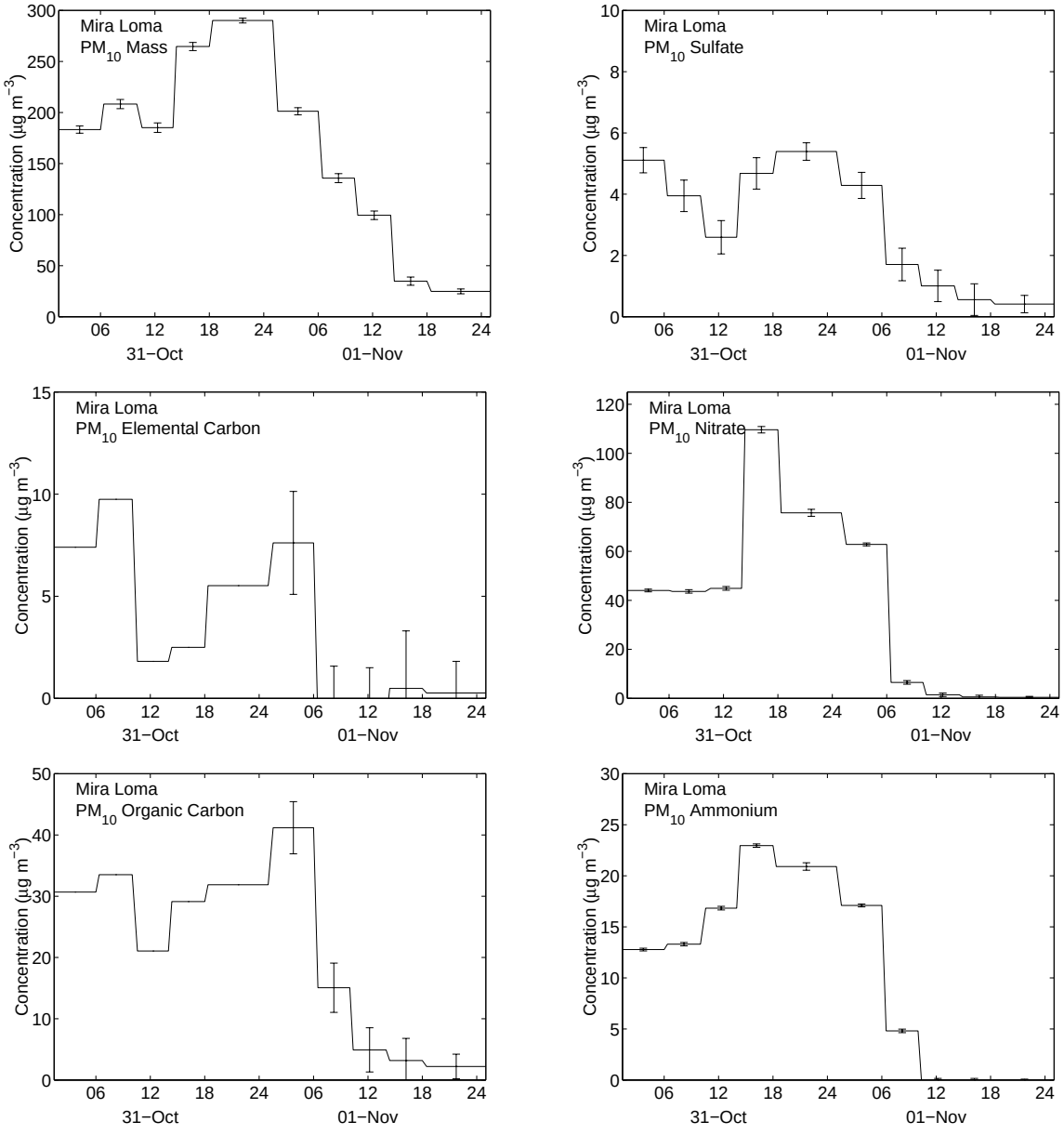

Figure C.50: PM_{10} concentrations during the Nitrate-Oriented Trajectory Experiment at Mira Loma. PM_{10} elemental and organic carbon data are missing for October 31, 1997; $PM_{1.9}$ elemental and organic carbon data are shown in place of PM_{10} concentrations for this day.

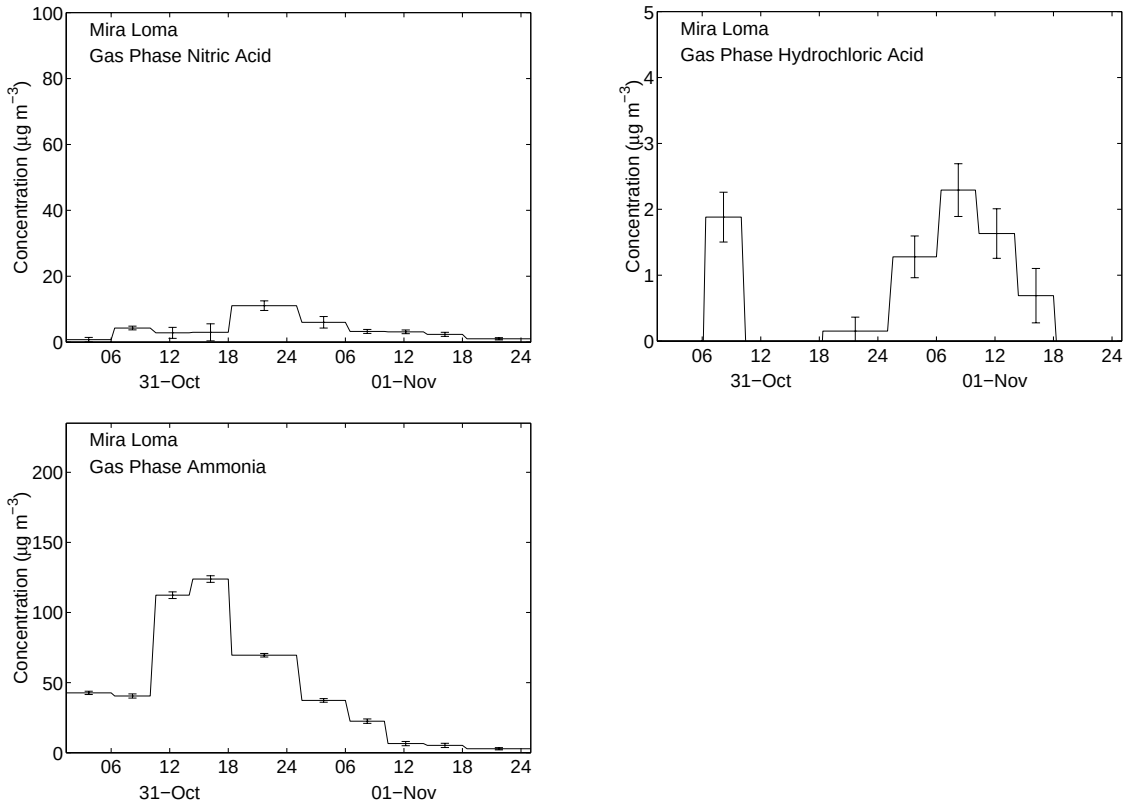

Figure C.51: Gas phase concentrations during the Nitrate-Oriented Trajectory Experiment at Mira Loma

C.4.3 Particle Concentration Time Series Data at Riverside

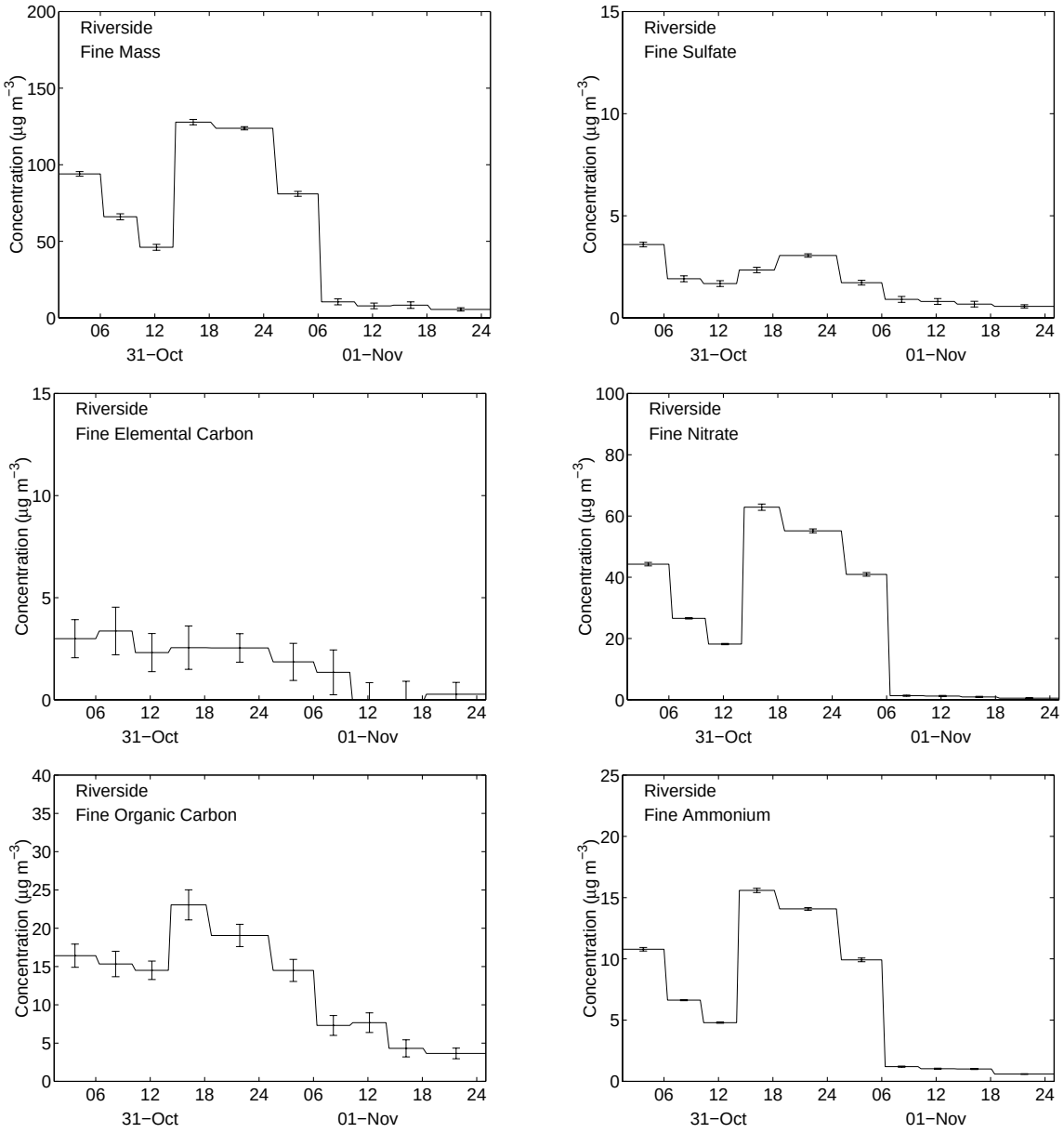

Figure C.52: Fine particle concentrations during the Nitrate-Oriented Trajectory Experiment at Riverside

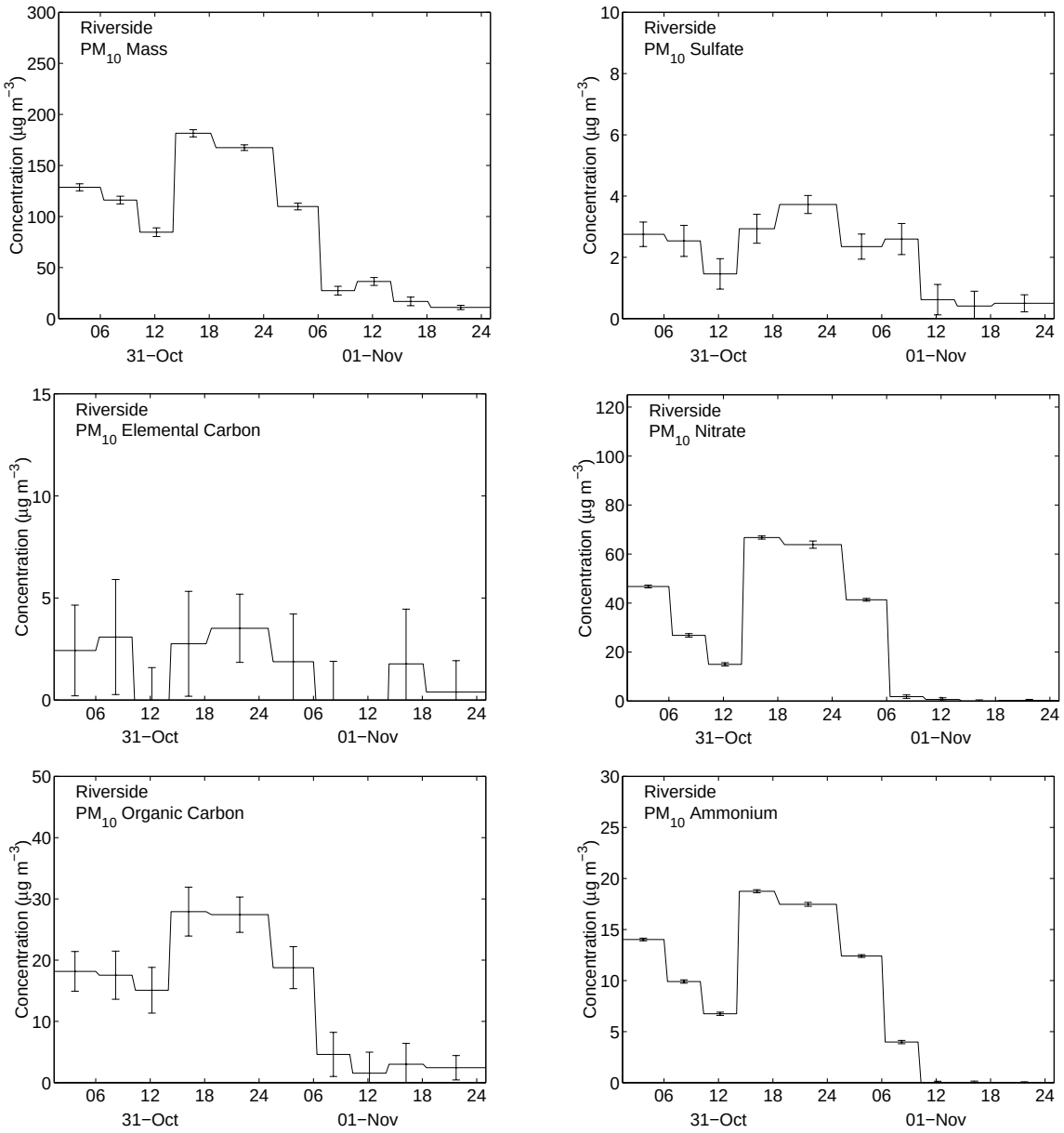

Figure C.53: PM_{10} concentrations during the Nitrate-Oriented Trajectory Experiment at Riverside

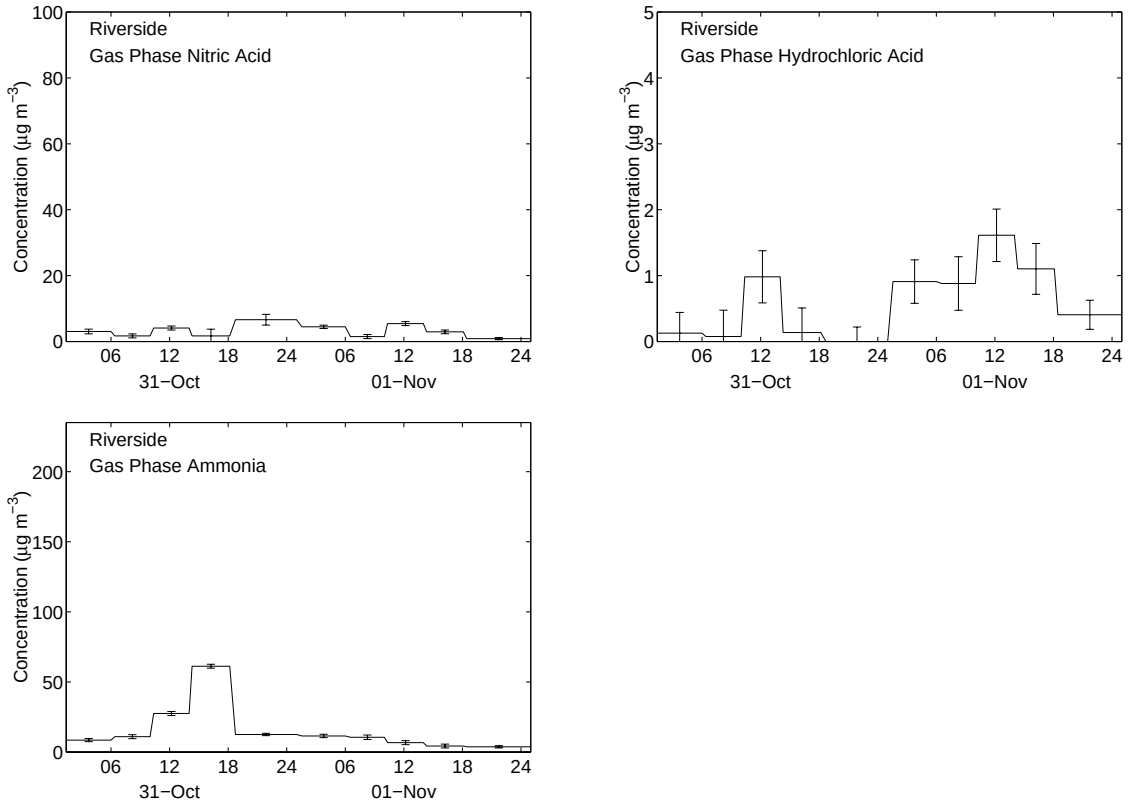

Figure C.54: Gas phase concentrations during the Nitrate-Oriented Trajectory Experiment at Riverside

C.4.4 Mass Balances at All Sites

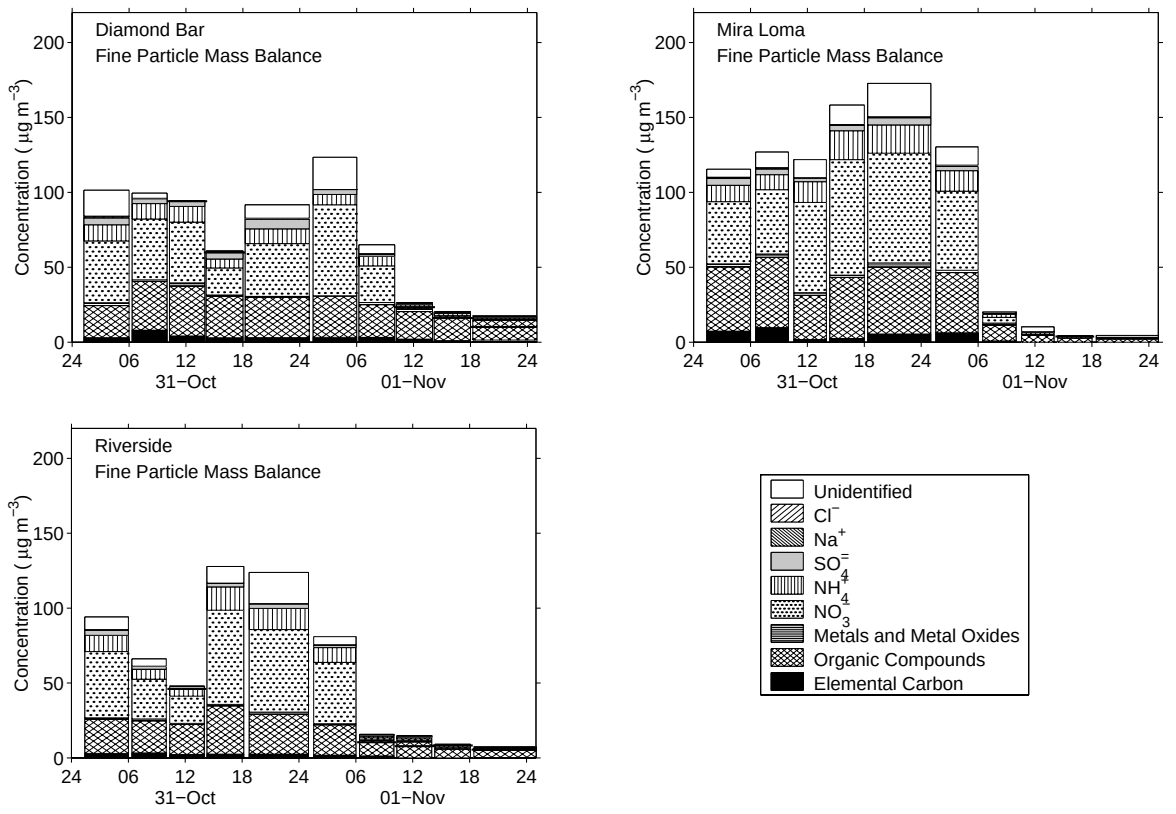

Figure C.55: Fine particle mass balances during the Nitrate-Oriented Trajectory Study

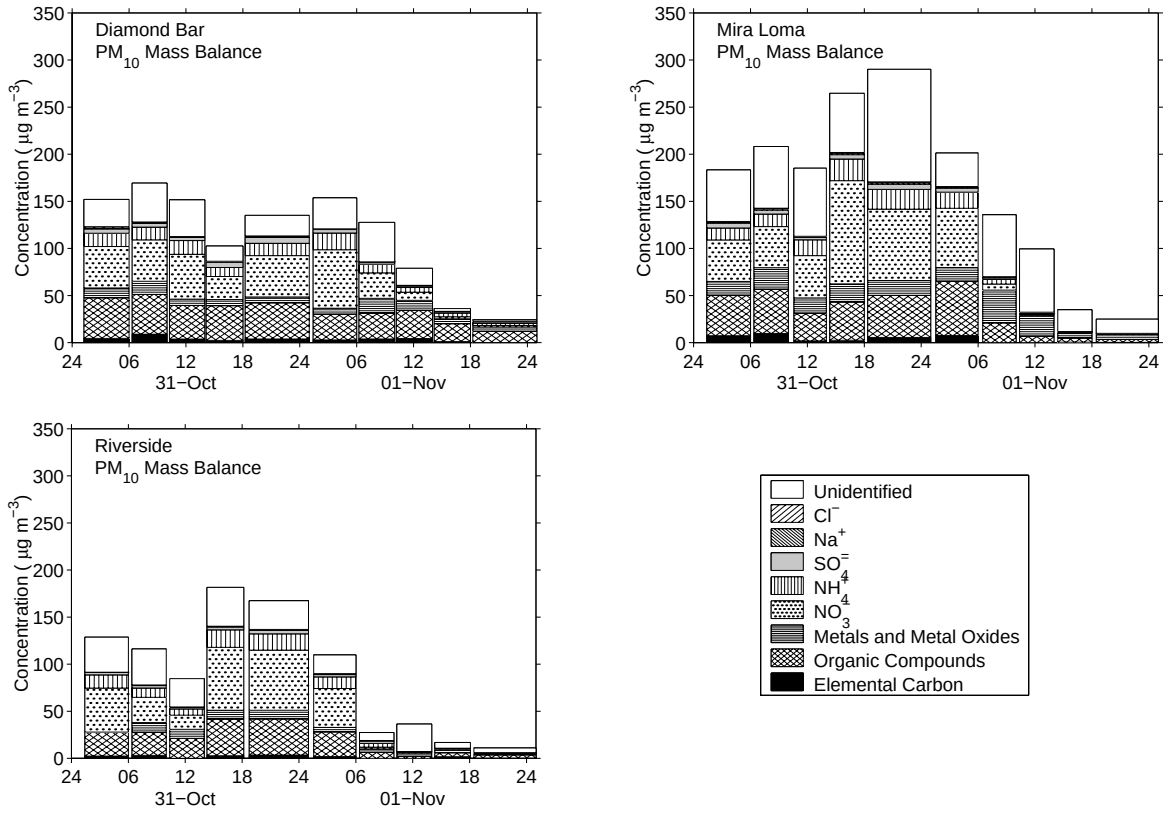

Figure C.56: PM_{10} mass balances during the Nitrate-Oriented Trajectory Study. PM_{10} elemental and organic carbon data are missing for Mira Loma on October 31, 1997; $PM_{1.9}$ elemental and organic carbon data are shown in place of PM_{10} concentrations Mira Loma on this day.

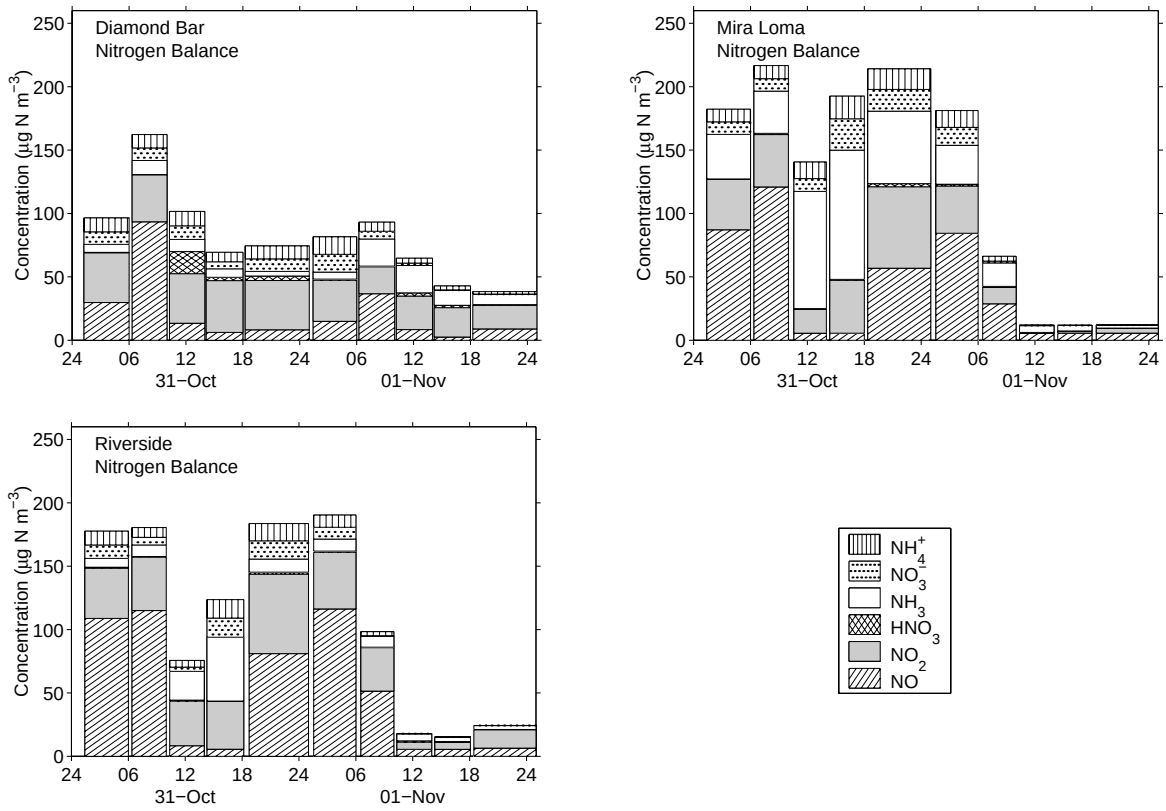

Figure C.57: Nitrogen balances during the Nitrate-Oriented Trajectory Experiment

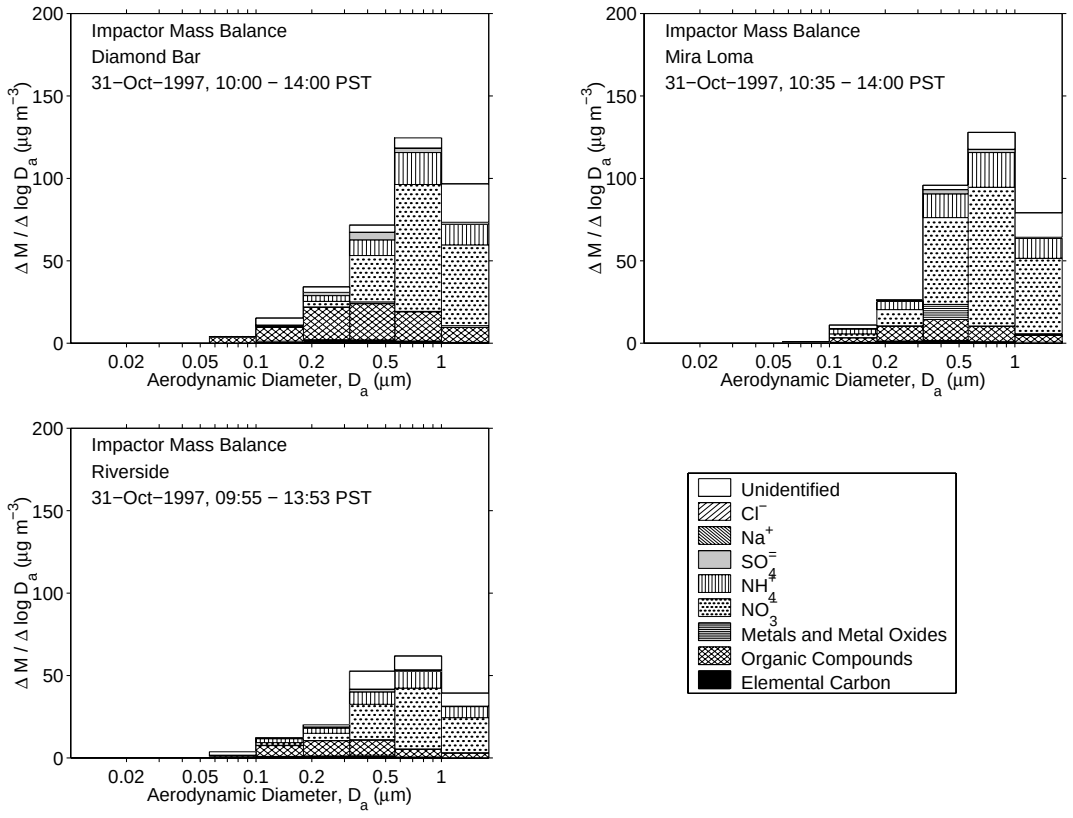

Figure C.58: Impactor mass balances during the first day of the Nitrate-Oriented Trajectory Study, 10:00-14:00 PST

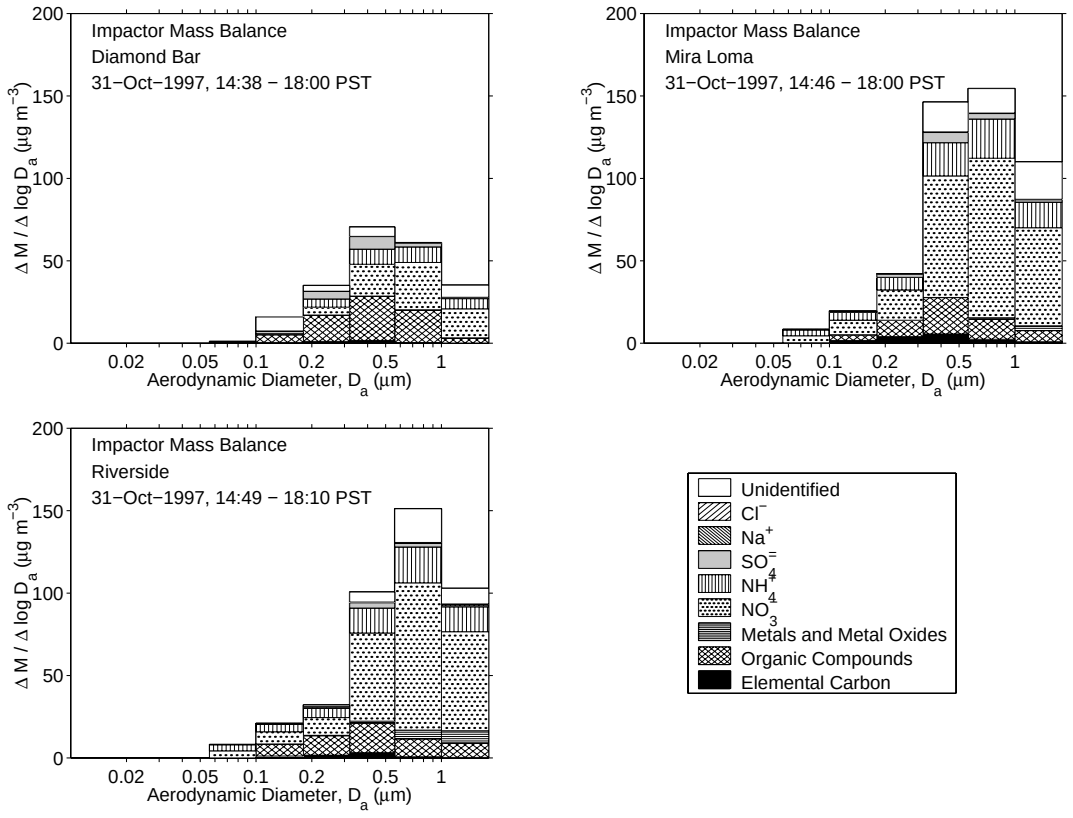

Figure C.59: Impactor mass balances during the first day of the Nitrate-Oriented Trajectory Study, 14:00-18:00 PST

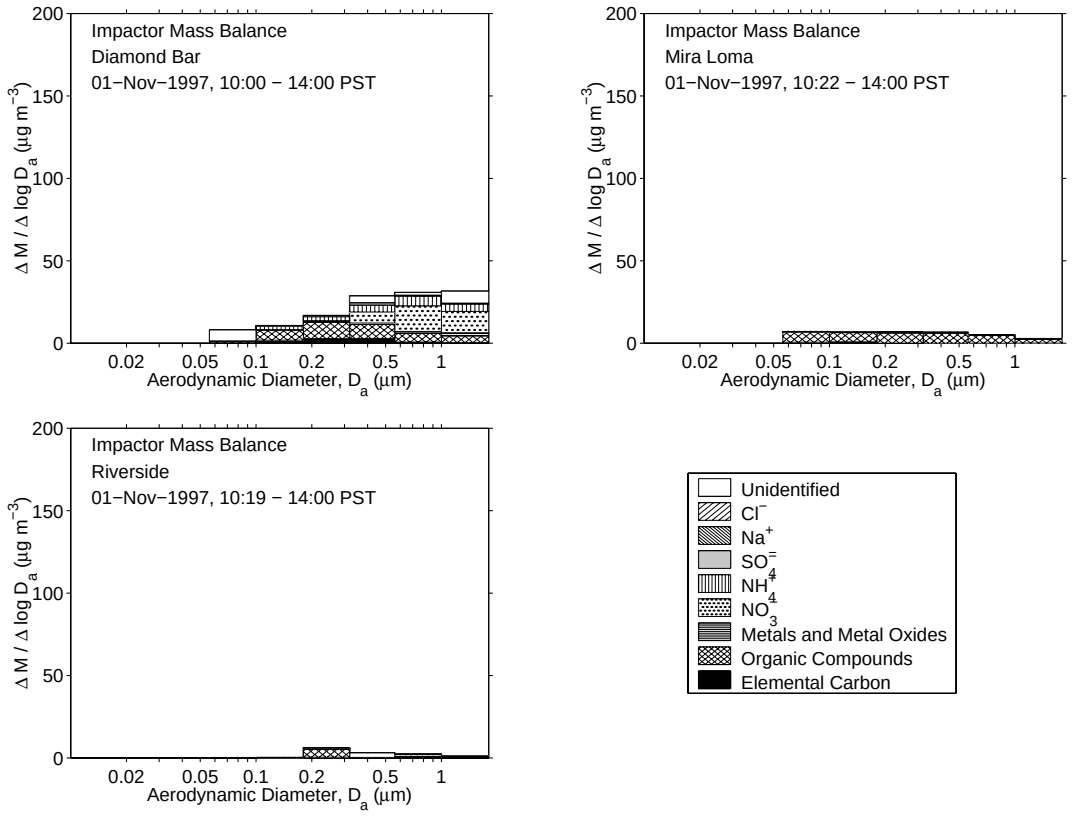

Figure C.60: Impactor mass balances during the second day of the Nitrate-Oriented Trajectory Study, 10:00-14:00 PST

C.5 Tunnel Study

C.5.1 Particle and Gas-Phase Concentrations

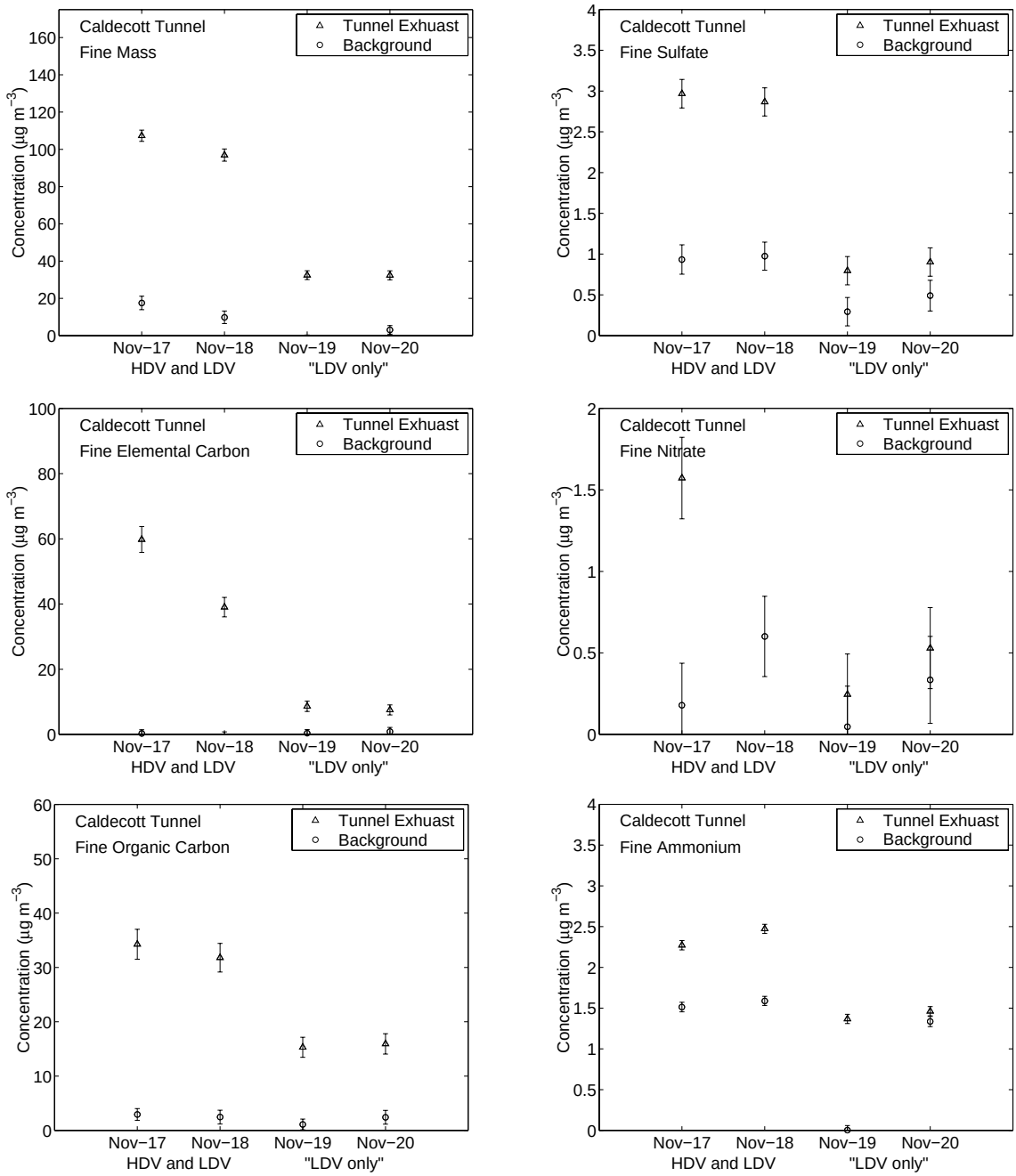

Figure C.61: Fine particle concentrations in the Caldecott Tunnel

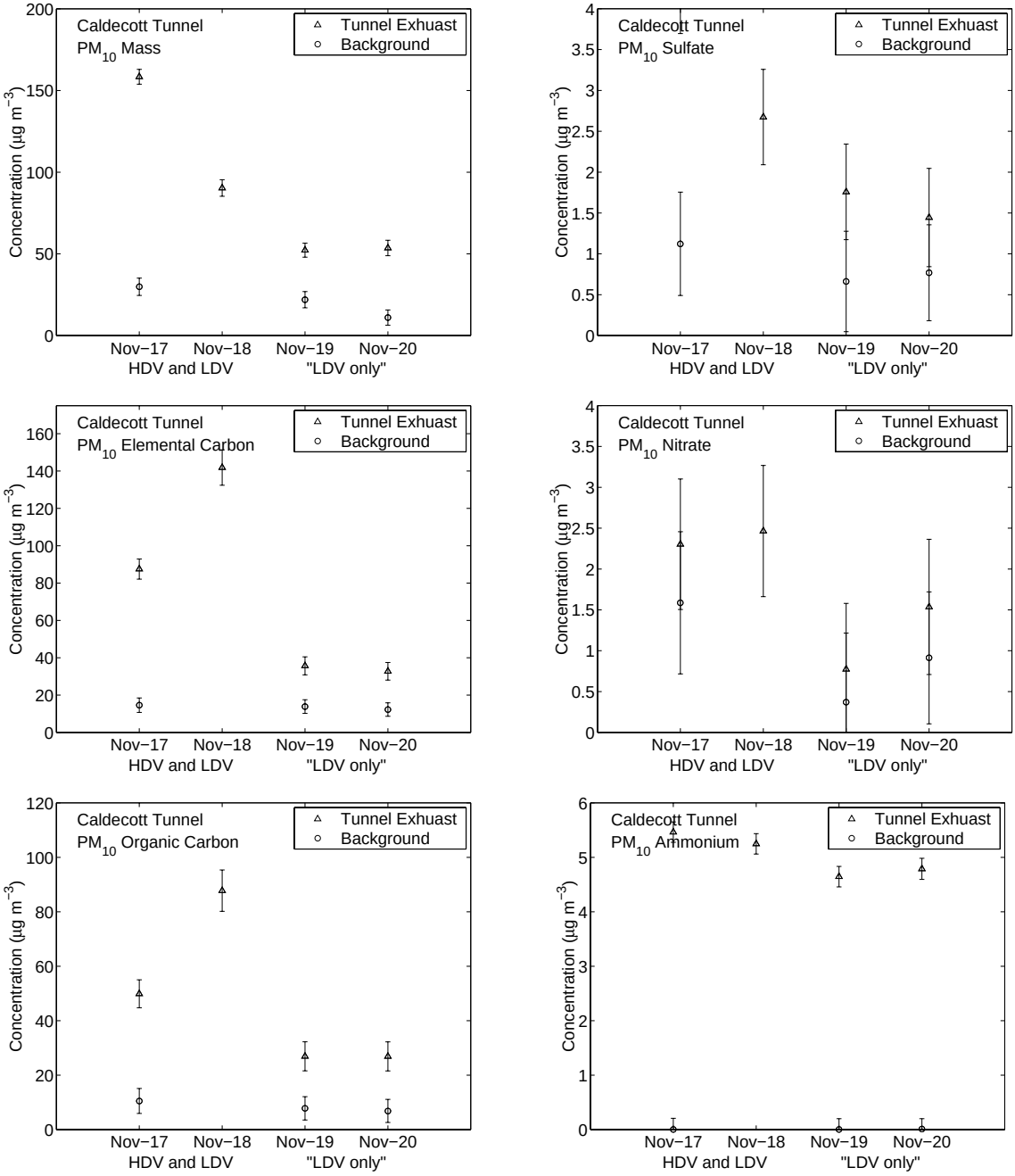

Figure C.62: PM_{10} concentrations in the Caldecott Tunnel

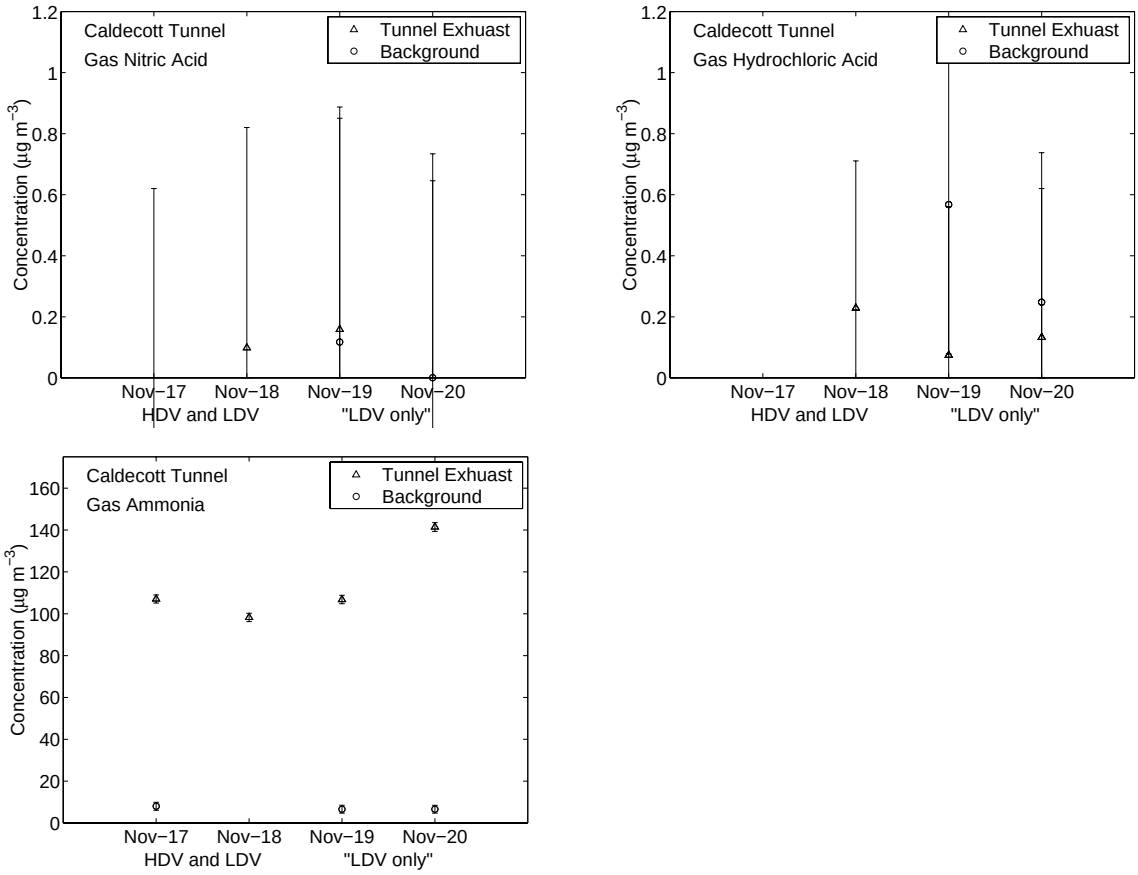

Figure C.63: Gas phase concentrations in the Caldecott Tunnel

C.5.2 Mass Balances

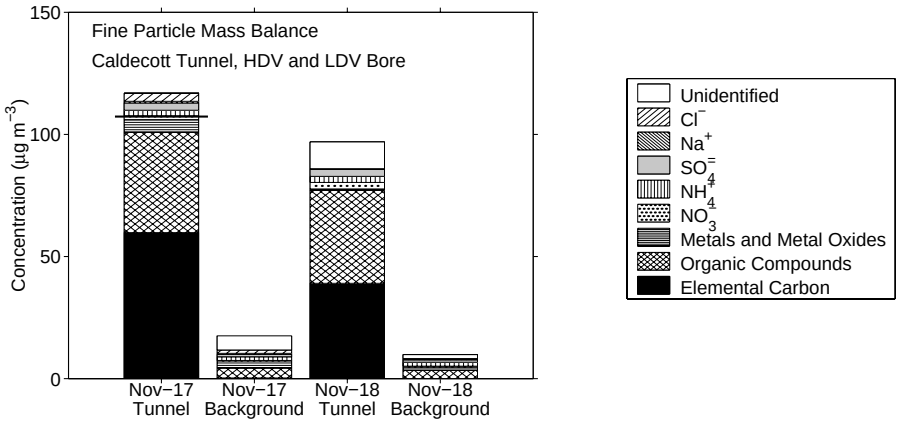

Figure C.64: Fine particle mass balances from the LDV+HDV bore of the Caldecott Tunnel

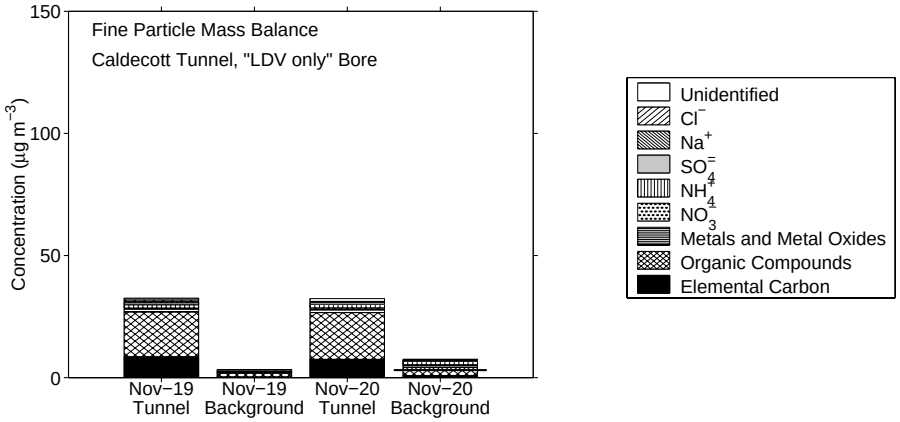

Figure C.65: Fine particle mass balances from the "LDV only" bore of the Caldecott Tunnel

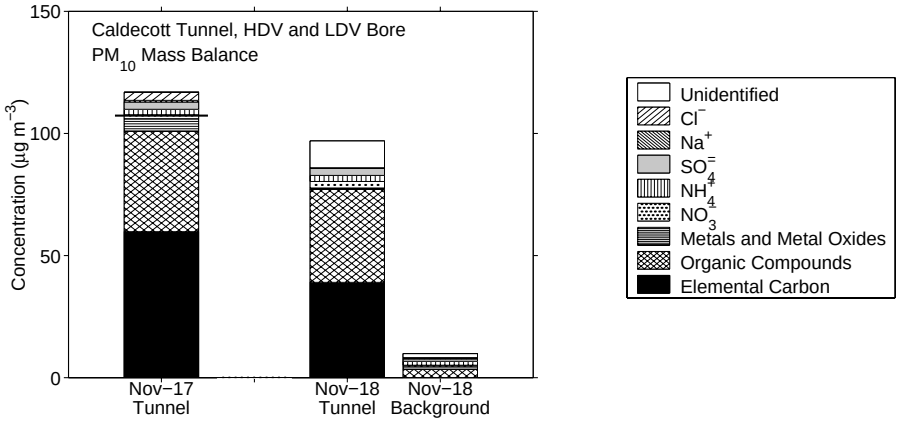

Figure C.66: PM_{10} mass balances from the LDV+HDV bore of the Caldecott Tunnel

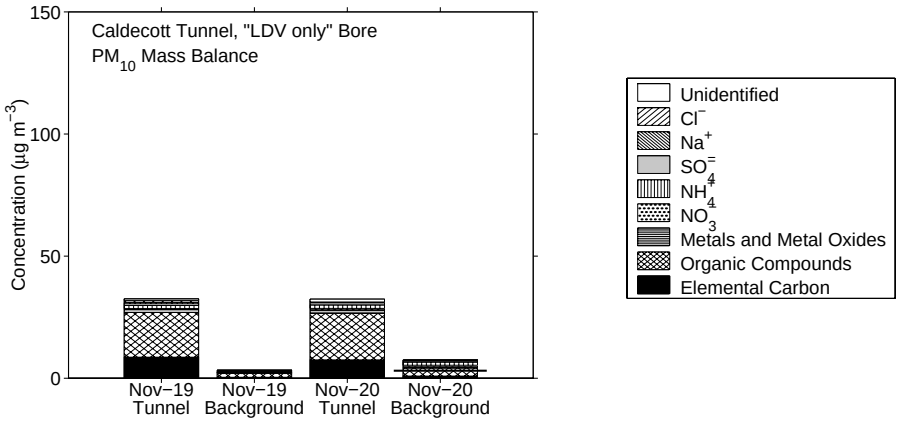

Figure C.67: PM_{10} mass balances from the "LDV only" bore of the Caldecott Tunnel

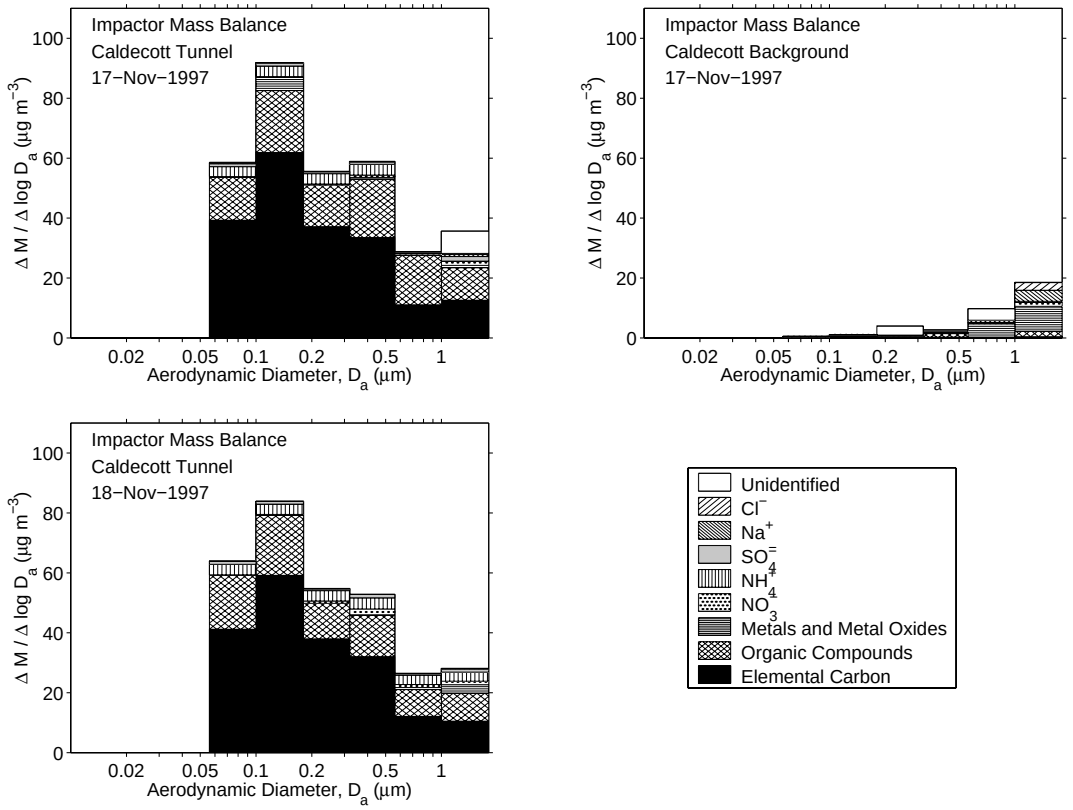

Figure C.68: Impactor mass balances from the LDV+HDV bore of the Caldecott Tunnel

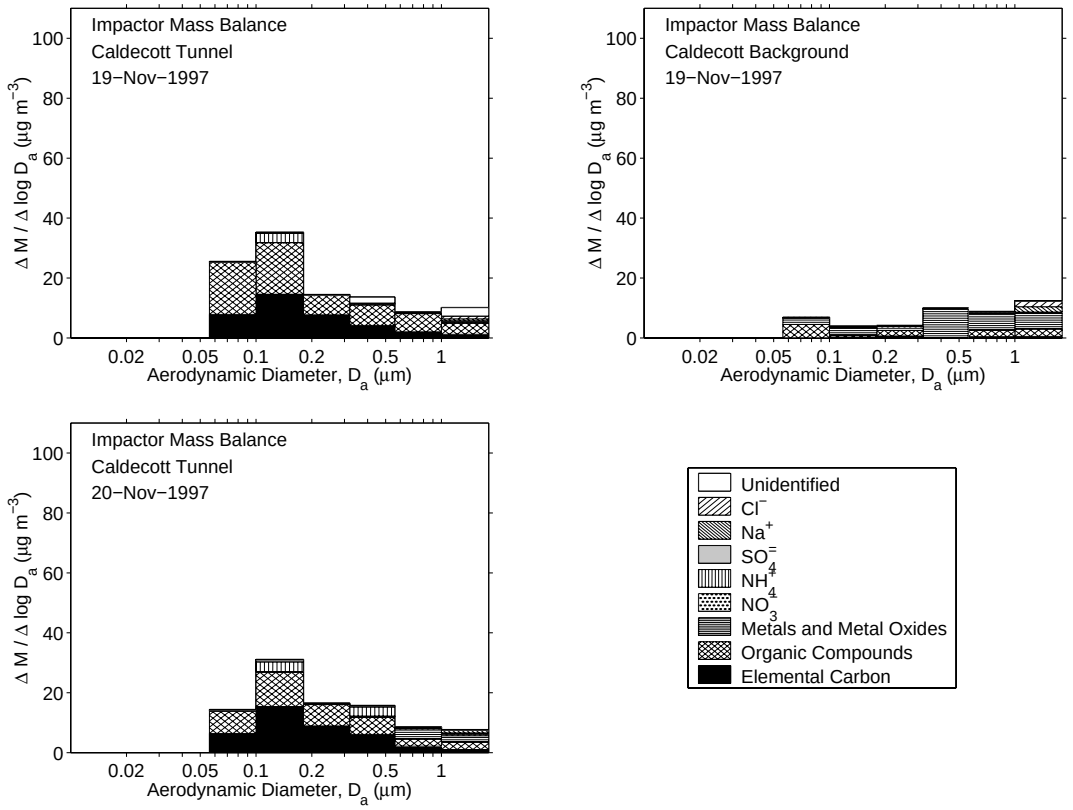

Figure C.69: Impactor mass balances from the "LDV only" bore of the Caldecott Tunnel

Appendix D

Tabulated Data

The data generated from analyses of the samples are presented here in tabular form. For information on how to interpret the sample labels and obtain information about a sample's location, date, time of operation, and size range, see Section B.7.

D.1 Mass and Aerosol Carbon Concentration Data

Table D.1: Mass and Carbon Aerosol Concentration Data

Sample	Aerosol Concentration (μg m^{-3})		
	Mass	Elemental Carbon	Organic Carbon
S97-V11A-LA-CX	64.45 ± 3.35	2.118 ± 2.339	10.403 ± 3.155
S97-V11A-LA-FX	36.90 ± 1.56	0.717 ± 0.809	3.763 ± 0.894
S97-V11B-LA-CX	77.39 ± 4.44	2.996 ± 3.301	18.219 ± 4.557
S97-V11B-LA-FX	54.89 ± 2.05	4.978 ± 1.290	17.791 ± 1.832
S97-V11C-LA-CX	99.79 ± 3.61	1.619 ± 2.986	22.287 ± 4.345
S97-V11C-LA-FX	39.37 ± 1.94	2.118 ± 1.071	19.366 ± 1.811
S97-V11D-LA-CX	62.88 ± 3.60	-0.380 ± 3.004	11.431 ± 4.103
S97-V11D-LA-FX	15.31 ± 1.85	0.114 ± 0.901	6.672 ± 0.976
S97-V11E-LA-CX	43.81 ± 2.12	0.288 ± 1.640	6.106 ± 2.219
S97-V11E-LA-FX	15.31 ± 1.07	0.717 ± 0.589	4.641 ± 0.730
S97-V11F-LA-FY	-	1.958 ± 0.252	8.445 ± 0.583
S97-V12A-LA-CX	46.64 ± 3.53	0.652 ± 2.470	4.068 ± 3.198
S97-V12A-LA-FX	17.16 ± 1.77	3.055 ± 0.960	6.939 ± 1.094
S97-V12B-LA-CX	73.11 ± 3.61	3.047 ± 2.935	13.655 ± 3.963
S97-V12B-LA-FX	34.79 ± 1.92	5.223 ± 1.176	17.144 ± 1.689
S97-V12B-LA-MX5	6.21 ± 1.20	0.046 ± 0.194	0.961 ± 0.472
S97-V12B-LA-MX6	5.76 ± 0.94	0.208 ± 0.202	1.823 ± 0.498
S97-V12B-LA-MX7	6.07 ± 0.92	0.705 ± 0.225	1.113 ± 0.476
S97-V12B-LA-MX8	6.58 ± 0.96	1.390 ± 0.258	1.991 ± 0.503
S97-V12B-LA-MX9	3.88 ± 0.91	1.581 ± 0.267	2.234 ± 0.511
S97-V12B-LA-MX10	1.25 ± 0.90	0.421 ± 0.212	1.547 ± 0.489
S97-V12B-LA-MX11	-	0.268 ± 0.235	2.117 ± 0.391
S97-V12C-LA-CX	86.16 ± 3.87	3.584 ± 2.913	30.228 ± 4.457
S97-V12C-LA-FX	41.19 ± 1.98	5.050 ± 1.151	25.672 ± 2.083
S97-V12D-LA-CX	53.64 ± 3.66	1.035 ± 2.984	17.745 ± 4.218
S97-V12D-LA-FX	23.12 ± 2.89	1.646 ± 1.078	14.530 ± 1.604
S97-V12E-LA-CX	47.58 ± 2.18	1.695 ± 1.650	12.560 ± 2.381
S97-V12E-LA-FX	17.26 ± 1.12	1.791 ± 0.642	8.296 ± 0.910
S97-V12F-LA-FY	-	3.310 ± 0.311	10.449 ± 0.676
S97-V11A-AZ-CX	51.81 ± 3.44	1.143 ± 2.297	8.709 ± 3.087
S97-V11A-AZ-FX	18.60 ± 1.68	1.382 ± 0.891	6.459 ± 1.068
S97-V11B-AZ-CX	128.36 ± 4.22	5.605 ± 3.054	20.186 ± 4.217
S97-V11B-AZ-FX	42.48 ± 2.00	5.930 ± 1.307	17.347 ± 1.792
S97-V11C-AZ-CX	80.81 ± 4.22	1.291 ± 2.836	21.057 ± 4.131
S97-V11C-AZ-FX	32.03 ± 1.86	2.298 ± 1.129	18.573 ± 1.819
S97-V11D-AZ-CX	61.67 ± 4.18	2.894 ± 2.894	22.733 ± 4.202
S97-V11D-AZ-FX	18.02 ± 1.96	1.198 ± 1.088	15.715 ± 1.684

Table D.1: Mass and Carbon Aerosol Concentration Data (continued)

Sample	Aerosol Concentration (μg m^{-3})		
	Mass	Elemental Carbon	Organic Carbon
S97-V11D-AZ-MX5	2.31 ± 1.51	-0.002 ± 0.220	0.746 ± 0.530
S97-V11D-AZ-MX6	3.04 ± 1.03	0.054 ± 0.222	1.011 ± 0.538
S97-V11D-AZ-MX7	5.37 ± 0.99	0.182 ± 0.228	1.116 ± 0.541
S97-V11D-AZ-MX8	5.15 ± 1.05	0.387 ± 0.238	2.278 ± 0.576
S97-V11D-AZ-MX9	3.55 ± 0.99	0.380 ± 0.238	1.607 ± 0.556
S97-V11D-AZ-MX10	1.21 ± 1.03	0.027 ± 0.221	1.068 ± 0.540
S97-V11D-AZ-MX11	-	0.308 ± 0.270	2.677 ± 0.459
S97-V11E-AZ-CX	46.24 ± 2.16	0.651 ± 1.620	9.730 ± 2.290
S97-V11E-AZ-FX	16.17 ± 1.10	1.121 ± 0.639	6.630 ± 0.853
S97-V11F-AZ-FY	-	2.950 ± 0.286	9.322 ± 0.613
S97-V12A-AZ-CX	50.96 ± 3.33	1.413 ± 2.278	10.397 ± 3.103
S97-V12A-AZ-FX	19.65 ± 1.60	1.738 ± 0.892	6.688 ± 1.066
S97-V12B-AZ-CX	109.61 ± 3.89	5.586 ± 2.997	20.764 ± 4.166
S97-V12B-AZ-FX	24.85 ± 1.90	6.231 ± 1.048	16.422 ± 1.280
S97-V12C-AZ-CX	71.30 ± 3.99	1.690 ± 2.808	17.255 ± 3.962
S97-V12C-AZ-FX	24.94 ± 2.65	3.296 ± 1.153	19.904 ± 1.870
S97-V12D-AZ-CX	71.07 ± 3.77	2.194 ± 2.834	24.542 ± 4.213
S97-V12D-AZ-FX	27.78 ± 1.82	3.528 ± 1.166	24.428 ± 2.090
S97-V12D-AZ-MX5	4.01 ± 1.30	-0.033 ± 0.213	-0.280 ± 0.492
S97-V12D-AZ-MX6	2.78 ± 1.04	0.034 ± 0.216	0.425 ± 0.510
S97-V12D-AZ-MX7	7.76 ± 1.02	0.511 ± 0.239	3.084 ± 0.592
S97-V12D-AZ-MX8	9.29 ± 0.99	0.835 ± 0.254	3.636 ± 0.611
S97-V12D-AZ-MX9	5.32 ± 1.17	0.379 ± 0.232	2.649 ± 0.577
S97-V12D-AZ-MX10	2.31 ± 1.23	0.020 ± 0.216	0.276 ± 0.506
S97-V12D-AZ-MX11	-	0.131 ± 0.255	2.044 ± 0.424
S97-V12E-AZ-CX	57.81 ± 2.36	2.329 ± 1.591	19.174 ± 2.517
S97-V12E-AZ-FX	19.45 ± 1.03	2.534 ± 0.662	14.389 ± 1.193
S97-V12F-AZ-FY	-	3.844 ± 0.325	11.453 ± 0.713
S97-V11A-RV-CX	13.95 ± 3.23	-0.349 ± 2.306	3.880 ± 3.019
S97-V11A-RV-FX	7.79 ± 1.82	0.668 ± 0.910	3.901 ± 0.995
S97-V11B-RV-CX	57.43 ± 4.42	1.193 ± 2.805	10.548 ± 3.776
S97-V11B-RV-FX	17.04 ± 1.85	2.543 ± 1.156	10.523 ± 1.457
S97-V11C-RV-CX	31.61 ± 3.91	1.238 ± 2.666	12.043 ± 3.643
S97-V11C-RV-FX	9.96 ± 1.92	1.227 ± 1.069	12.109 ± 1.497
S97-V11D-RV-CX	47.82 ± 3.70	-1.383 ± 2.631	7.269 ± 3.553
S97-V11D-RV-FX	34.37 ± 2.58	1.138 ± 1.075	18.180 ± 1.791
S97-V11D-RV-MX5	2.67 ± 0.86	-0.014 ± 0.191	0.597 ± 0.461
S97-V11D-RV-MX6	3.83 ± 0.88	0.038 ± 0.194	1.159 ± 0.477
S97-V11D-RV-MX7	4.92 ± 1.05	0.126 ± 0.198	1.115 ± 0.476
S97-V11D-RV-MX8	3.19 ± 0.93	0.227 ± 0.202	1.083 ± 0.475
S97-V11D-RV-MX9	1.64 ± 1.09	0.131 ± 0.198	1.131 ± 0.477
S97-V11D-RV-MX10	1.33 ± 0.87	0.077 ± 0.195	0.846 ± 0.468

Table D.1: Mass and Carbon Aerosol Concentration Data (continued)

Sample	Aerosol Concentration (μg m^{-3})		
	Mass	Elemental Carbon	Organic Carbon
S97-V11D-RV-MX11	-	0.229 ± 0.233	2.413 ± 0.404
S97-V11E-RV-CX	38.63 ± 2.08	0.288 ± 1.353	11.220 ± 1.917
S97-V11E-RV-FX	11.42 ± 1.14	0.506 ± 0.581	8.407 ± 0.905
S97-V12A-RV-CX	30.36 ± 3.77	1.791 ± 2.298	7.146 ± 3.022
S97-V12A-RV-FX	11.53 ± 1.54	1.020 ± 0.751	5.971 ± 0.809
S97-V12B-RV-CX	62.62 ± 4.02	5.270 ± 3.040	15.176 ± 4.057
S97-V12B-RV-FX	20.80 ± 2.02	4.098 ± 1.204	11.695 ± 1.500
S97-V12C-RV-CX	65.78 ± 4.29	2.463 ± 3.017	14.238 ± 4.103
S97-V12C-RV-FX	15.74 ± 2.67	1.401 ± 0.925	12.029 ± 1.134
S97-V12D-RV-CX	60.65 ± 3.99	0.844 ± 2.820	11.938 ± 3.846
S97-V12D-RV-FX	19.65 ± 2.54	1.459 ± 1.065	15.408 ± 1.640
S97-V12D-RV-MX5	2.35 ± 0.91	0.004 ± 0.192	0.460 ± 0.458
S97-V12D-RV-MX6	4.03 ± 0.90	0.036 ± 0.193	0.642 ± 0.463
S97-V12D-RV-MX7	5.36 ± 0.96	0.254 ± 0.204	1.008 ± 0.473
S97-V12D-RV-MX8	4.13 ± 0.91	0.491 ± 0.215	1.472 ± 0.487
S97-V12D-RV-MX9	0.78 ± 0.91	0.305 ± 0.206	2.286 ± 0.513
S97-V12D-RV-MX10	-0.06 ± 0.94	0.007 ± 0.192	0.407 ± 0.456
S97-V12D-RV-MX11	-	0.338 ± 0.239	2.383 ± 0.402
S97-V12E-RV-CX	66.47 ± 2.38	0.673 ± 1.494	13.858 ± 2.269
S97-V12E-RV-FX	38.97 ± 1.05	2.378 ± 0.651	21.281 ± 1.525
S97-V12F-RV-FY	-	2.242 ± 0.255	9.689 ± 0.633
S97-V21A-LA-CX	59.97 ± 3.36	1.077 ± 2.317	7.867 ± 3.091
S97-V21A-LA-FX	21.81 ± 1.41	3.292 ± 0.900	9.260 ± 1.136
S97-V21B-LA-CX	66.99 ± 3.70	5.942 ± 3.072	25.240 ± 4.393
S97-V21B-LA-FX	30.10 ± 1.76	4.794 ± 1.176	17.575 ± 1.726
S97-V21B-LA-MX5	7.31 ± 1.34	0.105 ± 0.197	1.047 ± 0.474
S97-V21B-LA-MX6	3.04 ± 0.98	0.280 ± 0.205	1.255 ± 0.481
S97-V21B-LA-MX7	5.69 ± 1.34	0.772 ± 0.228	2.347 ± 0.515
S97-V21B-LA-MX8	6.39 ± 0.97	1.365 ± 0.257	2.088 ± 0.507
S97-V21B-LA-MX9	3.45 ± 0.97	1.374 ± 0.257	2.150 ± 0.509
S97-V21B-LA-MX10	2.04 ± 0.93	0.424 ± 0.212	1.123 ± 0.477
S97-V21B-LA-MX11	-	-0.006 ± 0.223	1.642 ± 0.371
S97-V21C-LA-CX	74.96 ± 3.69	4.083 ± 2.915	27.577 ± 4.349
S97-V21C-LA-FX	29.90 ± 1.80	3.161 ± 1.087	24.180 ± 2.021
S97-V21D-LA-CX	57.90 ± 3.41	0.495 ± 2.916	17.502 ± 4.144
S97-V21D-LA-FX	14.11 ± 1.88	0.374 ± 1.023	9.915 ± 1.382
S97-V21E-LA-CX	47.73 ± 2.14	0.085 ± 1.602	6.934 ± 2.202
S97-V21E-LA-FX	13.55 ± 0.98	1.134 ± 0.594	6.019 ± 0.783
S97-V21F-LA-FY	-	2.539 ± 0.266	7.826 ± 0.538
S97-V22A-LA-CX	49.73 ± 3.42	1.772 ± 2.410	4.441 ± 3.092

Table D.1: Mass and Carbon Aerosol Concentration Data (continued)

Sample	Aerosol Concentration (μg m^{-3})		
	Mass	Elemental Carbon	Organic Carbon
S97-V22A-LA-FX	17.36 ± 1.50	1.572 ± 0.872	6.716 ± 1.055
S97-V22B-LA-CX	78.24 ± 3.66	3.251 ± 2.967	16.642 ± 4.084
S97-V22B-LA-FX	24.60 ± 1.85	4.357 ± 1.146	12.547 ± 1.476
S97-V22B-LA-MX5	4.37 ± 0.93	-0.002 ± 0.189	0.687 ± 0.457
S97-V22B-LA-MX6	1.83 ± 0.88	0.069 ± 0.192	0.594 ± 0.455
S97-V22B-LA-MX7	3.32 ± 0.96	0.506 ± 0.213	0.993 ± 0.466
S97-V22B-LA-MX8	4.12 ± 0.85	1.140 ± 0.243	1.570 ± 0.483
S97-V22B-LA-MX9	2.55 ± 0.89	1.394 ± 0.255	1.143 ± 0.471
S97-V22B-LA-MX10	0.89 ± 0.89	0.505 ± 0.213	0.833 ± 0.462
S97-V22B-LA-MX11	-	0.041 ± 0.221	2.256 ± 0.392
S97-V22C-LA-CX	76.08 ± 3.76	0.550 ± 2.840	16.014 ± 4.002
S97-V22C-LA-FX	27.57 ± 1.76	2.810 ± 1.084	20.474 ± 1.852
S97-V22D-LA-CX	47.16 ± 4.60	1.061 ± 2.958	13.006 ± 4.043
S97-V22D-LA-FX	21.52 ± 1.84	0.517 ± 1.043	10.971 ± 1.443
S97-V22D-LA-MX5	2.75 ± 0.88	-0.002 ± 0.191	0.212 ± 0.449
S97-V22D-LA-MX6	1.19 ± 0.96	0.009 ± 0.191	-0.199 ± 0.438
S97-V22D-LA-MX7	4.95 ± 0.89	0.325 ± 0.206	1.072 ± 0.472
S97-V22D-LA-MX8	4.74 ± 0.87	0.403 ± 0.210	0.660 ± 0.461
S97-V22D-LA-MX9	3.15 ± 0.93	0.360 ± 0.208	0.603 ± 0.459
S97-V22D-LA-MX10	0.47 ± 0.88	0.127 ± 0.197	0.415 ± 0.454
S97-V22D-LA-MX11	-	0.015 ± 0.222	1.940 ± 0.382
S97-V22E-LA-CX	51.03 ± 1.98	0.660 ± 1.636	10.356 ± 2.328
S97-V22E-LA-FX	19.82 ± 1.01	0.748 ± 0.583	5.851 ± 0.778
S97-V22F-LA-FY	-	2.452 ± 0.270	8.842 ± 0.597
S97-V21A-AZ-CX	58.20 ± 2.99	2.860 ± 2.239	20.711 ± 3.334
S97-V21A-AZ-FX	24.15 ± 1.57	1.292 ± 0.851	12.612 ± 1.321
S97-V21B-AZ-CX	104.33 ± 4.30	3.917 ± 2.886	28.728 ± 4.359
S97-V21B-AZ-FX	27.48 ± 1.95	3.412 ± 1.171	16.838 ± 1.736
S97-V21C-AZ-CX	72.92 ± 3.91	1.861 ± 2.776	19.821 ± 3.998
S97-V21C-AZ-FX	20.73 ± 1.92	1.791 ± 1.082	17.394 ± 1.738
S97-V21D-AZ-CX	69.98 ± 4.18	0.596 ± 2.841	21.486 ± 4.174
S97-V21D-AZ-FX	26.91 ± 1.96	1.794 ± 1.114	19.992 ± 1.890
S97-V21D-AZ-MX5	1.91 ± 1.13	-0.025 ± 0.215	0.488 ± 0.514
S97-V21D-AZ-MX6	0.69 ± 1.05	0.000 ± 0.216	0.031 ± 0.502
S97-V21D-AZ-MX7	3.74 ± 1.37	0.342 ± 0.232	1.732 ± 0.550
S97-V21D-AZ-MX8	6.43 ± 1.05	0.684 ± 0.248	2.323 ± 0.569
S97-V21D-AZ-MX9	3.21 ± 1.12	0.357 ± 0.232	2.032 ± 0.559
S97-V21D-AZ-MX10	-0.04 ± 1.06	0.039 ± 0.217	0.315 ± 0.509
S97-V21D-AZ-MX11	-	0.241 ± 0.262	2.947 ± 0.464
S97-V21E-AZ-CX	46.84 ± 2.50	0.838 ± 1.443	14.057 ± 2.074
S97-V21E-AZ-FX	15.10 ± 1.08	1.329 ± 0.618	9.642 ± 0.969
S97-V21F-AZ-FY	-	2.437 ± 0.258	11.269 ± 0.703

Table D.1: Mass and Carbon Aerosol Concentration Data (continued)

Sample	Aerosol Concentration (μg m^{-3})		
	Mass	Elemental Carbon	Organic Carbon
S97-V22A-AZ-CX	37.67 ± 3.65	-0.401 ± 2.239	11.376 ± 3.146
S97-V22A-AZ-FX	12.82 ± 1.53	1.922 ± 0.905	13.609 ± 1.395
S97-V22B-AZ-CX	74.35 ± 4.48	2.140 ± 2.881	18.179 ± 4.065
S97-V22B-AZ-FX	22.44 ± 2.07	3.181 ± 1.153	16.462 ± 1.709
S97-V22B-AZ-MX5	2.61 ± 1.01	-0.015 ± 0.212	0.769 ± 0.515
S97-V22B-AZ-MX6	2.80 ± 1.05	0.047 ± 0.215	0.615 ± 0.510
S97-V22B-AZ-MX7	2.95 ± 1.03	0.268 ± 0.225	1.752 ± 0.544
S97-V22B-AZ-MX8	4.59 ± 1.03	0.519 ± 0.237	2.249 ± 0.559
S97-V22B-AZ-MX9	2.00 ± 0.94	0.302 ± 0.227	2.350 ± 0.563
S97-V22B-AZ-MX10	-0.36 ± 1.00	0.156 ± 0.220	0.469 ± 0.506
S97-V22B-AZ-MX11	-	0.276 ± 0.260	1.721 ± 0.407
S97-V22C-AZ-CX	82.98 ± 4.04	2.309 ± 2.874	21.099 ± 4.145
S97-V22C-AZ-FX	22.56 ± 2.10	2.435 ± 1.125	18.540 ± 1.809
S97-V22D-AZ-CX	82.71 ± 3.90	2.233 ± 2.859	23.864 ± 4.219
S97-V22D-AZ-FX	29.82 ± 1.97	1.845 ± 1.097	18.788 ± 1.816
S97-V22D-AZ-MX5	1.87 ± 0.97	-0.035 ± 0.210	0.221 ± 0.498
S97-V22D-AZ-MX6	1.21 ± 0.97	0.006 ± 0.212	1.079 ± 0.521
S97-V22D-AZ-MX7	7.08 ± 1.15	0.394 ± 0.230	2.294 ± 0.559
S97-V22D-AZ-MX8	6.07 ± 0.98	0.494 ± 0.235	2.980 ± 0.581
S97-V22D-AZ-MX9	4.45 ± 1.04	0.364 ± 0.171	1.553 ± 0.483
S97-V22D-AZ-MX10	0.88 ± 1.06	0.114 ± 0.217	0.564 ± 0.507
S97-V22D-AZ-MX11	-	-0.212 ± 0.236	1.633 ± 0.402
S97-V22E-AZ-CX	66.45 ± 2.25	1.490 ± 1.573	17.239 ± 2.455
S97-V22E-AZ-FX	25.47 ± 1.02	1.293 ± 0.614	9.786 ± 0.972
S97-V22F-AZ-FY	-	2.150 ± 0.245	10.772 ± 0.679
S97-V21A-RV-CX	53.42 ± 3.41	0.790 ± 2.535	10.402 ± 3.446
S97-V21A-RV-FX	27.71 ± 1.57	0.868 ± 0.865	11.522 ± 1.296
S97-V21B-RV-CX	120.16 ± 5.09	3.391 ± 3.246	19.632 ± 4.520
S97-V21B-RV-FX	35.68 ± 1.98	2.592 ± 1.156	12.826 ± 1.562
S97-V21C-RV-CX	85.89 ± 3.80	0.497 ± 2.632	14.629 ± 3.703
S97-V21C-RV-FX	34.55 ± 1.99	0.591 ± 1.032	14.302 ± 1.587
S97-V21D-RV-CX	57.29 ± 3.95	0.033 ± 2.642	13.330 ± 3.692
S97-V21D-RV-FX	21.43 ± 1.86	-0.030 ± 1.022	11.741 ± 1.479
S97-V21D-RV-MX5	2.54 ± 0.95	-0.003 ± 0.192	0.733 ± 0.465
S97-V21D-RV-MX6	0.25 ± 1.16	0.034 ± 0.193	0.216 ± 0.451
S97-V21D-RV-MX7	2.89 ± 0.89	0.210 ± 0.202	0.798 ± 0.467
S97-V21D-RV-MX8	4.14 ± 1.02	0.271 ± 0.204	0.884 ± 0.469
S97-V21D-RV-MX9	1.60 ± 0.89	0.248 ± 0.203	0.636 ± 0.462
S97-V21D-RV-MX10	2.36 ± 1.04	0.007 ± 0.192	0.216 ± 0.451
S97-V21D-RV-MX11	-	0.119 ± 0.228	2.656 ± 0.414
S97-V21E-RV-CX	67.35 ± 2.17	1.382 ± 1.508	18.390 ± 2.422
S97-V21E-RV-FX	23.64 ± 1.06	0.847 ± 0.589	10.715 ± 1.010

Table D.1: Mass and Carbon Aerosol Concentration Data (continued)

Sample	Aerosol Concentration (μg m^{-3})		
	Mass	Elemental Carbon	Organic Carbon
S97-V21F-RV-FY	-	1.397 ± 0.213	8.906 ± 0.590
S97-V22A-RV-CX	59.47 ± 3.77	0.254 ± 2.233	6.542 ± 2.978
S97-V22A-RV-FX	21.65 ± 1.69	0.115 ± 0.859	7.516 ± 1.130
S97-V22B-RV-CX	89.42 ± 3.82	0.532 ± 2.711	13.067 ± 3.753
S97-V22B-RV-FX	36.44 ± 2.80	1.673 ± 1.097	10.595 ± 1.437
S97-V22B-RV-MX5	3.01 ± 0.89	0.035 ± 0.193	1.901 ± 0.500
S97-V22B-RV-MX6	3.72 ± 0.92	0.172 ± 0.200	2.043 ± 0.505
S97-V22B-RV-MX7	8.76 ± 0.99	0.656 ± 0.223	2.650 ± 0.525
S97-V22B-RV-MX8	8.27 ± 0.91	1.013 ± 0.240	2.841 ± 0.531
S97-V22B-RV-MX9	2.26 ± 0.95	0.813 ± 0.230	1.330 ± 0.483
S97-V22B-RV-MX10	0.40 ± 0.90	0.088 ± 0.196	0.106 ± 0.448
S97-V22B-RV-MX11	-	-0.046 ± 0.220	1.455 ± 0.363
S97-V22C-RV-CX	87.38 ± 4.44	2.726 ± 2.743	31.272 ± 4.320
S97-V22C-RV-FX	10.32 ± 1.89	0.452 ± 1.054	11.679 ± 1.489
S97-V22D-RV-CX	83.49 ± 3.78	-0.598 ± 2.651	13.339 ± 3.725
S97-V22D-RV-FX	17.58 ± 2.02	0.535 ± 1.053	14.461 ± 1.615
S97-V22D-RV-MX5	4.19 ± 0.94	0.075 ± 0.191	2.231 ± 0.502
S97-V22D-RV-MX6	5.11 ± 0.89	0.102 ± 0.193	1.467 ± 0.478
S97-V22D-RV-MX7	6.89 ± 0.85	0.356 ± 0.204	1.232 ± 0.471
S97-V22D-RV-MX8	3.67 ± 0.88	0.325 ± 0.203	0.833 ± 0.459
S97-V22D-RV-MX9	2.45 ± 0.88	0.256 ± 0.200	1.109 ± 0.467
S97-V22D-RV-MX10	0.39 ± 0.86	0.111 ± 0.193	0.497 ± 0.450
S97-V22D-RV-MX11	-	0.199 ± 0.227	2.913 ± 0.419
S97-V22E-RV-CX	56.76 ± 2.19	0.028 ± 1.478	12.342 ± 2.219
S97-V22E-RV-FX	16.04 ± 1.08	0.593 ± 0.585	6.962 ± 0.837
S97-V22F-RV-FY	-	1.500 ± 0.216	8.551 ± 0.571
S97-N21D-ML-FX	48.94 ± 2.39	0.268 ± 0.959	16.962 ± 1.658
S97-N21E-ML-FX	114.92 ± 1.08	1.214 ± 0.615	25.058 ± 1.719
S97-N22A-ML-FX	112.28 ± 1.45	0.595 ± 0.815	15.582 ± 1.452
S97-N22B-ML-FX	104.49 ± 1.83	1.119 ± 1.038	17.958 ± 1.748
S97-N22C-ML-FX	7.46 ± 1.85	-0.242 ± 0.992	8.030 ± 1.288
S97-N22C-ML-MX5	0.18 ± 0.98	-0.014 ± 0.192	0.802 ± 0.468
S97-N22C-ML-MX6	1.02 ± 1.24	0.089 ± 0.196	0.800 ± 0.468
S97-N22C-ML-MX7	3.12 ± 1.03	0.106 ± 0.197	1.478 ± 0.488
S97-N22C-ML-MX8	2.55 ± 0.90	0.063 ± 0.195	0.909 ± 0.471
S97-N22C-ML-MX9	1.39 ± 1.01	0.118 ± 0.198	0.549 ± 0.461
S97-N22C-ML-MX10	0.85 ± 0.90	0.065 ± 0.195	0.677 ± 0.465
S97-N22C-ML-MX11	-	0.174 ± 0.231	2.914 ± 0.426
S97-N22D-ML-FX	31.86 ± 2.49	0.184 ± 0.989	20.216 ± 1.843
S97-N22E-ML-FX	63.26 ± 1.05	0.629 ± 0.577	17.416 ± 1.331

Table D.1: Mass and Carbon Aerosol Concentration Data (continued)

Sample	Aerosol Concentration (μg m^{-3})		
	Mass	Elemental Carbon	Organic Carbon
S97-N22F-ML-FY	-	0.926 ± 0.186	11.570 ± 0.713
S97-N23A-ML-FX	66.19 ± 1.47	1.295 ± 0.855	15.090 ± 1.441
S97-N23B-ML-FX	71.28 ± 1.81	3.543 ± 1.146	23.248 ± 2.015
S97-N23C-ML-FX	85.69 ± 1.87	1.447 ± 0.890	18.870 ± 1.321
S97-N23C-ML-MX5	12.31 ± 0.89	0.003 ± 0.191	0.699 ± 0.462
S97-N23C-ML-MX6	13.81 ± 0.88	0.483 ± 0.213	2.808 ± 0.528
S97-N23C-ML-MX7	21.00 ± 0.91	0.626 ± 0.220	4.205 ± 0.578
S97-N23C-ML-MX8	9.82 ± 0.90	0.519 ± 0.215	2.324 ± 0.512
S97-N23C-ML-MX9	1.88 ± 0.96	0.094 ± 0.195	0.762 ± 0.464
S97-N23C-ML-MX10	1.28 ± 0.96	0.027 ± 0.192	0.414 ± 0.454
S97-N23C-ML-MX11	-	0.112 ± 0.227	2.760 ± 0.417
S97-N23D-ML-FX	38.35 ± 1.74	0.817 ± 1.022	13.671 ± 1.541
S97-N23E-ML-FX	29.63 ± 1.00	0.728 ± 0.587	7.490 ± 0.859
S97-N23E-ML-MX5	7.07 ± 0.54	0.028 ± 0.111	0.484 ± 0.267
S97-N23E-ML-MX6	4.03 ± 0.75	-0.004 ± 0.109	0.391 ± 0.265
S97-N23E-ML-MX7	7.16 ± 0.75	0.096 ± 0.114	1.042 ± 0.284
S97-N23E-ML-MX8	5.09 ± 0.56	0.053 ± 0.112	0.816 ± 0.277
S97-N23E-ML-MX9	1.10 ± 0.54	0.051 ± 0.112	0.313 ± 0.262
S97-N23E-ML-MX10	-0.11 ± 0.49	0.053 ± 0.112	0.002 ± 0.254
S97-N23E-ML-MX11	-	0.040 ± 0.129	1.502 ± 0.236
S97-N23F-ML-FY	-	1.681 ± 0.219	10.440 ± 0.659
S97-N31A-DB-CX	152.01 ± 2.85	4.511 ± 2.462	30.817 ± 3.905
S97-N31A-DB-FX	101.40 ± 1.50	3.069 ± 0.899	15.271 ± 1.428
S97-N31B-DB-CX	169.30 ± 3.54	8.937 ± 3.204	30.180 ± 4.610
S97-N31B-DB-FX	99.41 ± 1.82	8.064 ± 1.325	23.219 ± 2.008
S97-N31C-DB-CX	151.50 ± 3.92	3.777 ± 2.969	25.486 ± 4.354
S97-N31C-DB-FX	94.11 ± 2.00	4.177 ± 0.957	23.801 ± 1.485
S97-N31C-DB-MX5	24.65 ± 0.90	0.128 ± 0.146	1.652 ± 0.435
S97-N31C-DB-MX6	31.37 ± 0.98	0.339 ± 0.153	3.197 ± 0.465
S97-N31C-DB-MX7	17.39 ± 0.92	0.494 ± 0.158	3.819 ± 0.478
S97-N31C-DB-MX8	8.51 ± 1.30	0.540 ± 0.159	3.507 ± 0.472
S97-N31C-DB-MX9	3.86 ± 0.89	0.311 ± 0.152	1.572 ± 0.434
S97-N31C-DB-MX10	0.29 ± 0.92	0.058 ± 0.144	0.617 ± 0.419
S97-N31C-DB-MX11	-	0.130 ± 0.168	1.997 ± 0.305
S97-N31D-DB-CX	102.49 ± 4.15	2.370 ± 2.842	26.375 ± 4.279
S97-N31D-DB-FX	59.86 ± 1.78	3.004 ± 1.074	19.887 ± 1.808
S97-N31D-DB-MX5	8.99 ± 1.13	0.023 ± 0.228	0.570 ± 0.542
S97-N31D-DB-MX6	14.50 ± 1.16	0.111 ± 0.232	3.513 ± 0.633
S97-N31D-DB-MX7	17.14 ± 1.12	0.405 ± 0.246	4.667 ± 0.675
S97-N31D-DB-MX8	8.75 ± 1.11	0.281 ± 0.240	2.841 ± 0.611
S97-N31D-DB-MX9	4.07 ± 1.17	0.116 ± 0.232	0.870 ± 0.550
S97-N31D-DB-MX10	-0.66 ± 1.05	0.082 ± 0.230	0.015 ± 0.527

Table D.1: Mass and Carbon Aerosol Concentration Data (continued)

Sample	Aerosol Concentration (μg m^{-3})		
	Mass	Elemental Carbon	Organic Carbon
S97-N31D-DB-MX11	-	0.251 ± 0.275	3.142 ± 0.490
S97-N31E-DB-CX	135.04 ± 2.21	3.845 ± 1.738	27.493 ± 2.953
S97-N31E-DB-FX	91.58 ± 1.00	3.073 ± 0.669	19.227 ± 1.416
S97-N31F-DB-FY	-	3.443 ± 0.313	16.290 ± 0.959
S97-N32A-DB-CX	153.61 ± 2.87	2.843 ± 2.391	19.529 ± 3.480
S97-N32A-DB-FX	123.38 ± 1.48	3.215 ± 0.933	19.835 ± 1.673
S97-N32B-DB-CX	127.66 ± 3.86	3.825 ± 2.958	19.769 ± 4.151
S97-N32B-DB-FX	64.93 ± 2.03	3.249 ± 1.110	15.600 ± 1.627
S97-N32C-DB-CX	78.88 ± 3.55	4.282 ± 2.644	21.431 ± 3.662
S97-N32C-DB-FX	23.45 ± 1.69	2.059 ± 1.050	13.165 ± 1.500
S97-N32C-DB-MX5	8.05 ± 0.90	0.094 ± 0.195	0.753 ± 0.463
S97-N32C-DB-MX6	7.75 ± 0.88	0.177 ± 0.199	0.966 ± 0.469
S97-N32C-DB-MX7	6.96 ± 0.91	0.680 ± 0.223	1.520 ± 0.486
S97-N32C-DB-MX8	3.30 ± 0.91	0.698 ± 0.224	1.778 ± 0.494
S97-N32C-DB-MX9	2.08 ± 0.85	0.470 ± 0.213	1.140 ± 0.474
S97-N32C-DB-MX10	2.02 ± 0.91	0.149 ± 0.198	0.121 ± 0.446
S97-N32C-DB-MX11	-	-0.011 ± 0.221	2.437 ± 0.403
S97-N32D-DB-CX	36.20 ± 3.80	1.130 ± 2.844	13.581 ± 3.914
S97-N32D-DB-FX	16.15 ± 1.72	1.094 ± 1.006	10.960 ± 1.391
S97-N32E-DB-CX	24.11 ± 1.98	0.096 ± 1.572	8.568 ± 2.214
S97-N32E-DB-FX	10.16 ± 0.96	1.428 ± 0.600	9.575 ± 0.945
S97-N32F-DB-FY	-	2.787 ± 0.283	10.121 ± 0.657
S97-N31A-ML-CX	183.29 ± 3.58	-	-
S97-N31A-ML-FX	115.39 ± 1.75	7.400 ± 1.140	30.674 ± 2.231
S97-N31B-ML-CX	208.26 ± 4.49	-	-
S97-N31B-ML-FX	126.84 ± 2.12	9.750 ± 1.521	33.516 ± 2.619
S97-N31C-ML-CX	185.16 ± 4.66	-	-
S97-N31C-ML-FX	121.88 ± 2.15	1.815 ± 0.986	21.060 ± 1.465
S97-N31C-ML-MX5	20.17 ± 1.11	0.144 ± 0.174	0.803 ± 0.501
S97-N31C-ML-MX6	32.19 ± 1.08	0.277 ± 0.178	1.653 ± 0.514
S97-N31C-ML-MX7	23.27 ± 1.13	0.409 ± 0.183	2.209 ± 0.524
S97-N31C-ML-MX8	6.29 ± 1.08	0.337 ± 0.180	1.640 ± 0.514
S97-N31C-ML-MX9	2.78 ± 1.07	0.151 ± 0.174	0.509 ± 0.496
S97-N31C-ML-MX10	0.12 ± 1.01	0.067 ± 0.172	-0.055 ± 0.488
S97-N31C-ML-MX11	-	0.165 ± 0.200	2.813 ± 0.375
S97-N31D-ML-CX	264.64 ± 3.96	-	-
S97-N31D-ML-FX	158.20 ± 1.82	2.501 ± 1.134	29.130 ± 2.325
S97-N31D-ML-MX5	28.09 ± 1.14	0.229 ± 0.249	1.237 ± 0.586
S97-N31D-ML-MX6	38.90 ± 1.19	0.598 ± 0.266	2.191 ± 0.615
S97-N31D-ML-MX7	35.56 ± 1.18	1.371 ± 0.303	3.829 ± 0.670
S97-N31D-ML-MX8	10.06 ± 1.05	0.997 ± 0.285	1.760 ± 0.602
S97-N31D-ML-MX9	2.67 ± 1.22	0.423 ± 0.258	0.638 ± 0.570

Table D.1: Mass and Carbon Aerosol Concentration Data (continued)

Sample	Aerosol Concentration (μg m^{-3})		
	Mass	Elemental Carbon	Organic Carbon
S97-N31D-ML-MX10	0.83 ± 1.10	0.064 ± 0.241	-0.131 ± 0.550
S97-N31D-ML-MX11	-	0.347 ± 0.293	3.210 ± 0.510
S97-N31E-ML-CX	290.11 ± 2.41	-	-
S97-N31E-ML-FX	172.67 ± 1.04	5.519 ± 0.796	31.876 ± 2.059
S97-N31F-ML-FY	-	4.284 ± 0.349	23.272 ± 1.301
S97-N32A-ML-CX	201.23 ± 3.48	7.615 ± 2.519	41.183 ± 4.259
S97-N32A-ML-FX	130.23 ± 1.60	6.320 ± 1.102	28.695 ± 2.140
S97-N32B-ML-CX	135.75 ± 4.41	-1.254 ± 2.831	15.068 ± 4.023
S97-N32B-ML-FX	20.27 ± 2.02	0.876 ± 1.103	7.615 ± 1.333
S97-N32C-ML-CX	99.38 ± 4.18	-1.226 ± 2.728	4.920 ± 3.608
S97-N32C-ML-FX	10.20 ± 1.99	-0.367 ± 1.128	3.352 ± 1.210
S97-N32C-ML-MX5	0.70 ± 0.98	0.016 ± 0.212	0.453 ± 0.504
S97-N32C-ML-MX6	-0.58 ± 0.96	-0.108 ± 0.207	0.893 ± 0.516
S97-N32C-ML-MX7	0.87 ± 1.03	0.003 ± 0.212	1.096 ± 0.522
S97-N32C-ML-MX8	1.63 ± 1.04	-0.028 ± 0.210	1.141 ± 0.523
S97-N32C-ML-MX9	0.58 ± 1.03	0.210 ± 0.221	1.025 ± 0.520
S97-N32C-ML-MX10	0.48 ± 1.05	0.150 ± 0.219	1.139 ± 0.523
S97-N32C-ML-MX11	-	-0.043 ± 0.244	1.752 ± 0.407
S97-N32D-ML-CX	34.86 ± 4.03	0.491 ± 2.812	3.184 ± 3.612
S97-N32D-ML-FX	3.79 ± 1.92	-0.231 ± 1.038	2.054 ± 1.065
S97-N32E-ML-CX	24.82 ± 2.36	0.265 ± 1.549	2.214 ± 2.002
S97-N32E-ML-FX	4.53 ± 1.02	-0.218 ± 0.571	1.628 ± 0.610
S97-N32F-ML-FY	-	1.869 ± 0.237	7.344 ± 0.518
S97-N31A-RV-CX	128.59 ± 3.44	2.431 ± 2.223	18.170 ± 3.244
S97-N31A-RV-FX	94.02 ± 1.50	2.991 ± 0.931	16.418 ± 1.514
S97-N31B-RV-CX	116.10 ± 3.81	3.089 ± 2.818	17.545 ± 3.933
S97-N31B-RV-FX	66.02 ± 1.98	3.369 ± 1.167	15.332 ± 1.663
S97-N31C-RV-CX	84.60 ± 4.27	-1.011 ± 2.606	15.091 ± 3.734
S97-N31C-RV-FX	46.09 ± 1.91	2.312 ± 0.934	14.505 ± 1.201
S97-N31C-RV-MX5	10.00 ± 0.89	0.035 ± 0.147	0.536 ± 0.428
S97-N31C-RV-MX6	15.53 ± 1.00	0.144 ± 0.150	0.838 ± 0.432
S97-N31C-RV-MX7	12.76 ± 0.90	0.397 ± 0.158	1.623 ± 0.445
S97-N31C-RV-MX8	5.02 ± 0.93	0.297 ± 0.155	1.668 ± 0.446
S97-N31C-RV-MX9	1.89 ± 0.85	0.240 ± 0.153	1.201 ± 0.438
S97-N31C-RV-MX10	0.94 ± 0.83	0.071 ± 0.148	0.118 ± 0.422
S97-N31C-RV-MX11	-	0.229 ± 0.175	2.827 ± 0.333
S97-N31D-RV-CX	181.51 ± 3.48	2.759 ± 2.570	27.924 ± 3.991
S97-N31D-RV-FX	127.82 ± 1.76	2.551 ± 1.061	23.049 ± 1.964
S97-N31D-RV-MX5	26.26 ± 1.08	0.082 ± 0.234	1.581 ± 0.579
S97-N31D-RV-MX6	38.07 ± 1.26	0.173 ± 0.238	1.970 ± 0.590
S97-N31D-RV-MX7	24.46 ± 1.08	0.775 ± 0.266	3.135 ± 0.628
S97-N31D-RV-MX8	8.02 ± 1.10	0.426 ± 0.250	2.110 ± 0.595

Table D.1: Mass and Carbon Aerosol Concentration Data (continued)

Sample	Aerosol Concentration (μg m^{-3})		
	Mass	Elemental Carbon	Organic Carbon
S97-N31D-RV-MX9	4.09 ± 1.28	0.292 ± 0.244	1.331 ± 0.571
S97-N31D-RV-MX10	1.93 ± 1.16	-0.032 ± 0.229	-0.019 ± 0.534
S97-N31D-RV-MX11	-	0.313 ± 0.282	2.566 ± 0.470
S97-N31E-RV-CX	167.40 ± 2.76	3.519 ± 1.669	27.425 ± 2.882
S97-N31E-RV-FX	123.83 ± 1.04	2.539 ± 0.699	19.059 ± 1.452
S97-N31F-RV-FY	-	2.709 ± 0.273	14.789 ± 0.879
S97-N32A-RV-CX	109.80 ± 3.31	1.880 ± 2.337	18.776 ± 3.423
S97-N32A-RV-FX	80.99 ± 1.59	1.856 ± 0.908	14.487 ± 1.441
S97-N32B-RV-CX	27.39 ± 4.27	-0.840 ± 2.742	4.613 ± 3.606
S97-N32B-RV-FX	10.46 ± 1.93	1.344 ± 1.098	7.305 ± 1.299
S97-N32C-RV-CX	36.36 ± 3.87	-4.063 ± 2.579	1.556 ± 3.426
S97-N32C-RV-FX	7.85 ± 1.84	-0.172 ± 1.012	7.666 ± 1.287
S97-N32C-RV-MX5	-0.01 ± 1.03	-0.063 ± 0.206	-0.093 ± 0.484
S97-N32C-RV-MX6	-0.85 ± 0.94	0.125 ± 0.215	0.028 ± 0.487
S97-N32C-RV-MX7	0.74 ± 1.00	-0.026 ± 0.208	-0.026 ± 0.485
S97-N32C-RV-MX8	-0.70 ± 0.97	0.105 ± 0.214	0.908 ± 0.510
S97-N32C-RV-MX9	-0.32 ± 0.94	0.005 ± 0.209	-0.167 ± 0.482
S97-N32C-RV-MX10	0.02 ± 0.93	-0.055 ± 0.207	-0.357 ± 0.477
S97-N32C-RV-MX11	-	0.324 ± 0.258	2.038 ± 0.415
S97-N32D-RV-CX	16.83 ± 4.18	1.774 ± 2.683	3.008 ± 3.400
S97-N32D-RV-FX	8.33 ± 2.13	-0.083 ± 0.989	4.312 ± 1.113
S97-N32E-RV-CX	10.92 ± 2.07	0.396 ± 1.537	2.440 ± 1.988
S97-N32E-RV-FX	5.54 ± 1.07	0.271 ± 0.582	3.646 ± 0.693
S97-N32F-RV-FY	-	0.760 ± 0.183	4.215 ± 0.362
S97-T11B-TI-CX	158.40 ± 4.56	87.517 ± 5.399	49.887 ± 5.139
S97-T11B-TI-FX	107.32 ± 3.02	59.807 ± 3.973	34.265 ± 2.747
S97-T11B-TI-FY	-	73.903 ± 4.700	42.204 ± 3.310
S97-T11B-TI-MX5	9.09 ± 1.23	3.217 ± 0.410	2.312 ± 0.660
S97-T11B-TI-MX6	4.97 ± 1.19	2.785 ± 0.389	3.462 ± 0.698
S97-T11B-TI-MX7	9.76 ± 1.18	8.151 ± 0.652	3.941 ± 0.714
S97-T11B-TI-MX8	13.59 ± 1.19	9.279 ± 0.708	2.876 ± 0.678
S97-T11B-TI-MX9	20.72 ± 1.13	15.799 ± 1.032	4.399 ± 0.730
S97-T11B-TI-MX10	14.74 ± 1.25	9.891 ± 0.738	3.009 ± 0.683
S97-T11B-TI-MX11	-	5.588 ± 0.568	7.542 ± 0.733
S97-T11B-TO-CX	29.87 ± 5.30	14.597 ± 3.867	10.514 ± 4.593
S97-T11B-TO-FX	17.53 ± 3.62	0.301 ± 1.146	2.938 ± 1.084
S97-T11B-TO-FY	-	0.908 ± 1.270	4.379 ± 1.641
S97-T11B-TO-MX5	3.12 ± 1.28	0.110 ± 0.277	0.327 ± 0.639
S97-T11B-TO-MX6	2.45 ± 1.23	0.060 ± 0.274	-0.375 ± 0.622
S97-T11B-TO-MX7	0.64 ± 1.31	0.071 ± 0.275	0.207 ± 0.636
S97-T11B-TO-MX8	0.98 ± 1.23	0.184 ± 0.280	-0.315 ± 0.623
S97-T11B-TO-MX9	-0.34 ± 1.32	0.262 ± 0.284	-0.078 ± 0.629
S97-T11B-TO-MX10	0.13 ± 1.30	0.096 ± 0.276	-0.239 ± 0.625

Table D.1: Mass and Carbon Aerosol Concentration Data (continued)

Sample	Aerosol Concentration (μg m^{-3})		
	Mass	Elemental Carbon	Organic Carbon
S97-T11B-TO-MX11	-	0.157 ± 0.323	1.493 ± 0.491
S97-T21B-TI-CX	90.34 ± 5.07	141.887 ± 9.490	87.764 ± 7.581
S97-T21B-TI-FX	96.93 ± 3.27	39.052 ± 2.977	31.790 ± 2.636
S97-T21B-TI-FY	-	36.938 ± 2.895	33.587 ± 2.905
S97-T21B-TI-MX5	5.42 ± 1.18	2.687 ± 0.233	1.981 ± 0.402
S97-T21B-TI-MX6	3.55 ± 1.31	3.047 ± 0.243	1.885 ± 0.400
S97-T21B-TI-MX7	8.69 ± 1.32	7.792 ± 0.378	2.806 ± 0.416
S97-T21B-TI-MX8	11.56 ± 1.23	9.490 ± 0.427	2.466 ± 0.410
S97-T21B-TI-MX9	20.42 ± 1.22	15.108 ± 0.587	4.252 ± 0.444
S97-T21B-TI-MX10	13.78 ± 1.26	10.371 ± 0.455	3.775 ± 0.436
S97-T21B-TI-MX11	-	4.449 ± 0.308	7.226 ± 0.432
S97-T21B-TO-FX	9.82 ± 3.38	-0.449 ± 1.232	2.454 ± 1.271
S97-T31B-TI-CX	52.29 ± 4.32	35.668 ± 4.828	26.923 ± 5.338
S97-T31B-TI-FX	32.46 ± 2.38	8.626 ± 1.582	15.297 ± 1.845
S97-T31B-TI-FY	-	8.227 ± 1.526	13.770 ± 1.969
S97-T31B-TI-MX5	2.58 ± 1.16	0.309 ± 0.271	0.811 ± 0.617
S97-T31B-TI-MX6	1.19 ± 1.23	0.515 ± 0.280	1.281 ± 0.631
S97-T31B-TI-MX7	3.31 ± 1.21	1.015 ± 0.304	1.394 ± 0.634
S97-T31B-TI-MX8	3.14 ± 1.30	1.928 ± 0.348	1.363 ± 0.633
S97-T31B-TI-MX9	6.72 ± 1.20	3.727 ± 0.435	3.667 ± 0.706
S97-T31B-TI-MX10	3.20 ± 1.21	1.982 ± 0.350	3.659 ± 0.706
S97-T31B-TI-MX11	-	0.398 ± 0.316	4.500 ± 0.595
S97-T31B-TO-CX	21.97 ± 4.96	13.864 ± 3.655	7.807 ± 4.280
S97-T31B-TO-FX	-2.00 ± 2.33	0.405 ± 1.098	1.098 ± 0.990
S97-T31B-TO-MX5	2.30 ± 1.18	0.136 ± 0.262	0.454 ± 0.606
S97-T31B-TO-MX6	1.51 ± 1.36	0.109 ± 0.261	0.401 ± 0.605
S97-T31B-TO-MX7	0.65 ± 1.23	-0.097 ± 0.251	-0.020 ± 0.594
S97-T31B-TO-MX8	-0.41 ± 1.17	0.163 ± 0.263	0.330 ± 0.603
S97-T31B-TO-MX9	-0.38 ± 1.18	0.083 ± 0.260	0.121 ± 0.598
S97-T31B-TO-MX10	-0.16 ± 1.22	0.015 ± 0.257	0.800 ± 0.616
S97-T31B-TO-MX11	-	0.080 ± 0.301	1.582 ± 0.470
S97-T41B-TI-CX	53.61 ± 4.71	32.745 ± 4.716	26.871 ± 5.337
S97-T41B-TI-FX	32.37 ± 2.40	7.527 ± 1.536	15.930 ± 1.875
S97-T41B-TI-FY	-	8.557 ± 1.579	17.603 ± 2.180
S97-T41B-TI-MX5	1.61 ± 1.19	0.277 ± 0.143	0.532 ± 0.343
S97-T41B-TI-MX6	0.81 ± 1.21	0.545 ± 0.149	0.513 ± 0.341
S97-T41B-TI-MX7	1.41 ± 1.20	1.483 ± 0.173	1.163 ± 0.352
S97-T41B-TI-MX8	1.85 ± 1.27	2.229 ± 0.191	1.492 ± 0.356
S97-T41B-TI-MX9	7.77 ± 1.20	3.932 ± 0.232	2.461 ± 0.370
S97-T41B-TI-MX10	3.19 ± 1.20	1.614 ± 0.175	1.585 ± 0.357
S97-T41B-TI-MX11	-	0.704 ± 0.176	4.809 ± 0.327
S97-T41B-TO-CX	10.99 ± 4.67	12.259 ± 3.602	6.855 ± 4.255
S97-T41B-TO-FX	3.08 ± 2.28	0.873 ± 1.285	2.420 ± 1.274
S97-T41B-TO-FY	-	0.298 ± 1.177	0.565 ± 1.419

Table D.1: Mass and Carbon Aerosol Concentration Data (continued)

Sample	Aerosol Concentration (μg m^{-3})		
	Mass	Elemental Carbon	Organic Carbon
S97-B11A-AZ-MX5	14.83 ± 2.00	0.675 ± 1.234	7.119 ± 1.556
S97-B11A-AZ-MX6	16.46 ± 3.20	-0.264 ± 1.187	6.988 ± 1.549
S97-B11A-AZ-MX7	18.50 ± 3.08	0.526 ± 1.226	5.867 ± 1.493
S97-B11A-AZ-MX8	9.42 ± 1.99	0.284 ± 1.214	7.520 ± 1.576
S97-B11A-AZ-MX9	6.64 ± 6.50	0.570 ± 1.228	11.063 ± 1.753
S97-B11A-AZ-MX10	7.75 ± 4.21	0.310 ± 1.215	7.607 ± 1.580
S97-B11A-AZ-MX11	-	-0.034 ± 1.412	5.004 ± 1.664
S97-B11A-DB-CX	16.33 ± 3.51	-0.109 ± 2.145	1.927 ± 2.246
S97-B11A-DB-FX	4.42 ± 2.41	0.754 ± 1.547	3.441 ± 1.642
S97-B11A-DB-FY	-	2.333 ± 2.267	7.888 ± 2.544
S97-B11A-DB-MX5	-3.49 ± 4.00	-0.425 ± 1.179	7.023 ± 1.551
S97-B11A-DB-MX6	4.00 ± 2.58	0.030 ± 1.201	5.768 ± 1.488
S97-B11A-DB-MX7	3.96 ± 3.22	-0.084 ± 1.196	8.847 ± 1.642
S97-B11A-DB-MX8	9.33 ± 2.08	0.048 ± 1.202	5.509 ± 1.475
S97-B11A-DB-MX9	4.92 ± 3.57	-0.162 ± 1.192	8.765 ± 1.638
S97-B11A-DB-MX10	4.83 ± 2.58	-0.039 ± 1.198	5.887 ± 1.494
S97-B11A-DB-MX11	-	-0.130 ± 1.408	1.563 ± 1.492
S97-B11A-ML-CX	8.00 ± 2.65	0.499 ± 2.175	3.203 ± 2.310
S97-B11A-ML-FX	4.58 ± 3.35	2.496 ± 2.275	5.083 ± 2.404
S97-B11A-ML-FY	-	-0.654 ± 2.117	3.176 ± 2.309
S97-B11A-RV-CX	28.33 ± 3.79	-	16.050 ± 2.952
S97-B11A-RV-FX	9.33 ± 2.89	1.250 ± 2.213	6.693 ± 2.485
S97-B11A-RV-FY	-	3.120 ± 2.306	7.800 ± 2.540
S97-B11A-RV-MX5	9.33 ± 2.65	-0.286 ± 1.186	4.530 ± 1.427
S97-B11A-RV-MX6	5.33 ± 3.68	-0.339 ± 1.183	3.865 ± 1.393
S97-B11A-RV-MX7	7.67 ± 3.43	-0.709 ± 1.165	4.446 ± 1.422
S97-B11A-RV-MX8	6.83 ± 2.50	0.123 ± 1.206	6.856 ± 1.543
S97-B11A-RV-MX9	1.33 ± 2.52	0.700 ± 0.873	6.090 ± 1.068
S97-B11A-RV-MX10	1.83 ± 5.88	0.677 ± 0.872	7.773 ± 1.123
S97-B11A-RV-MX11	-	-0.032 ± 1.412	2.718 ± 1.550
S97-B11A-TI-CX	3.67 ± 3.37	-	3.628 ± 2.331
S97-B11A-TI-FX	-5.67 ± 2.31	0.701 ± 2.185	5.343 ± 2.417
S97-B11A-TI-MX5	-2.08 ± 2.26	-0.165 ± 1.192	2.981 ± 1.349
S97-B11A-TI-MX6	-4.50 ± 2.33	1.224 ± 1.261	6.230 ± 1.511
S97-B11A-TI-MX7	-5.67 ± 2.47	-0.576 ± 1.171	3.897 ± 1.395
S97-B11A-TI-MX8	-7.50 ± 3.66	0.102 ± 1.205	8.843 ± 1.642
S97-B11A-TI-MX9	-8.67 ± 2.24	0.097 ± 1.205	6.164 ± 1.508
S97-B11A-TI-MX10	-1.33 ± 1.68	1.108 ± 1.255	13.247 ± 1.862
S97-B11A-TI-MX11	-	1.025 ± 1.465	2.316 ± 1.530
S97-B21A-DB-CX	14.00 ± 4.00	2.885 ± 2.294	4.550 ± 2.378
S97-B21A-DB-FX	11.30 ± 2.52	4.964 ± 2.398	6.949 ± 2.497
S97-B21A-DB-FY	-	4.076 ± 2.354	8.042 ± 2.552
S97-B21A-DB-MX5	-5.87 ± 3.88	-	-
S97-B21A-DB-MX6	7.08 ± 1.81	0.786 ± 1.239	5.610 ± 1.480
S97-B21A-DB-MX7	3.33 ± 2.27	0.000 ± 1.200	3.408 ± 1.370

Table D.1: Mass and Carbon Aerosol Concentration Data (continued)

Sample	Aerosol Concentration (μg m^{-3})		
	Mass	Elemental Carbon	Organic Carbon
S97-B21A-DB-MX8	9.75 ± 4.77	-0.082 ± 1.196	2.113 ± 1.306
S97-B21A-DB-MX9	1.67 ± 2.77	0.439 ± 1.222	5.615 ± 1.481
S97-B21A-DB-MX10	0.25 ± 2.20	1.235 ± 1.262	8.123 ± 1.606
S97-B21A-ML-CX	11.33 ± 4.65	8.380 ± 2.569	5.985 ± 2.449
S97-B21A-ML-FX	8.58 ± 1.86	6.424 ± 2.471	8.837 ± 2.592
S97-B21A-ML-FY	-	0.000 ± 2.150	2.482 ± 2.274
S97-B21A-ML-MX5	11.33 ± 3.61	0.634 ± 1.232	8.494 ± 1.625
S97-B21A-ML-MX6	12.67 ± 1.89	0.036 ± 1.202	12.326 ± 1.816
S97-B21A-ML-MX7	6.42 ± 2.75	0.647 ± 1.232	8.342 ± 1.617
S97-B21A-ML-MX8	7.46 ± 2.77	0.027 ± 1.201	-
S97-B21A-ML-MX9	6.97 ± 2.96	0.377 ± 1.219	10.832 ± 1.742
S97-B21A-ML-MX10	3.42 ± 2.95	0.070 ± 1.204	6.657 ± 1.533
S97-B21A-ML-MX11	-	-0.058 ± 1.411	1.270 ± 1.478
S97-B21A-RV-CX	15.33 ± 5.97	0.315 ± 2.166	6.724 ± 2.486
S97-B21A-RV-FX	9.67 ± 3.96	1.827 ± 1.585	5.872 ± 1.728
S97-B21A-RV-FY	-	0.529 ± 2.176	5.280 ± 2.414
S97-B21A-RV-MX5	-1.83 ± 2.38	0.248 ± 1.212	3.285 ± 1.364
S97-B21A-RV-MX6	2.17 ± 1.63	-0.045 ± 1.198	4.371 ± 1.419
S97-B21A-RV-MX7	5.50 ± 1.98	-0.014 ± 1.199	2.323 ± 1.316
S97-B21A-RV-MX8	-1.75 ± 2.21	0.356 ± 1.218	4.343 ± 1.417
S97-B21A-RV-MX9	2.58 ± 1.67	1.168 ± 1.258	8.426 ± 1.621
S97-B21A-RV-MX10	-0.17 ± 1.91	0.879 ± 1.244	3.287 ± 1.364
S97-B21A-RV-MX11	-	0.804 ± 1.454	3.608 ± 1.594

D.2 Ionic Aerosol Concentration Data

Table D.2: Ionic Species Aerosol Concentration Data

Sample	Aerosol Concentration (μg m^{-3})			
	Cl^-	NO_3^-	$SO_4^=$	NH_4^+
S97-V11A-LA-CX	2.880 ± 0.274	5.201 ± 0.520	8.455 ± 0.378	6.381 ± 0.122
S97-V11A-LA-FX	1.465 ± 0.085	3.473 ± 0.151	6.329 ± 0.296	4.167 ± 0.034
S97-V11B-LA-CX	0.553 ± 0.376	6.043 ± 0.714	7.495 ± 0.520	6.484 ± 0.167
S97-V11B-LA-FX	0.431 ± 0.120	7.592 ± 0.569	5.792 ± 0.418	4.430 ± 0.048
S97-V11C-LA-CX	0.517 ± 0.344	3.954 ± 0.654	6.555 ± 0.476	5.331 ± 0.153
S97-V11C-LA-FX	0.127 ± 0.111	1.050 ± 0.196	5.737 ± 0.260	2.901 ± 0.044
S97-V11D-LA-CX	3.660 ± 0.356	2.555 ± 0.676	4.500 ± 0.491	4.710 ± 0.158
S97-V11D-LA-FX	0.065 ± 0.114	0.395 ± 0.203	3.688 ± 0.141	2.087 ± 0.046
S97-V11E-LA-CX	3.342 ± 0.191	3.655 ± 0.363	3.670 ± 0.264	3.038 ± 0.085
S97-V11E-LA-FX	0.418 ± 0.062	1.090 ± 0.110	2.638 ± 0.076	1.561 ± 0.025
S97-V12A-LA-CX	2.785 ± 0.286	4.520 ± 0.543	4.148 ± 0.395	4.403 ± 0.127
S97-V12A-LA-FX	0.499 ± 0.092	1.639 ± 0.163	3.232 ± 0.113	1.954 ± 0.037
S97-V12B-LA-CX	0.866 ± 0.334	5.196 ± 0.634	4.130 ± 0.461	4.423 ± 0.149
S97-V12B-LA-FX	0.578 ± 0.106	2.114 ± 0.188	3.323 ± 0.131	2.162 ± 0.042
S97-V12B-LA-MX5	0.090 ± 0.098	0.652 ± 0.172	0.514 ± 0.136	0.697 ± 0.321
S97-V12B-LA-MX6	-0.015 ± 0.099	0.635 ± 0.173	1.157 ± 0.136	1.050 ± 0.321
S97-V12B-LA-MX7	-0.018 ± 0.093	0.510 ± 0.163	0.954 ± 0.130	0.837 ± 0.320
S97-V12B-LA-MX8	-0.018 ± 0.094	0.099 ± 0.164	0.339 ± 0.130	0.608 ± 0.320
S97-V12B-LA-MX9	-0.018 ± 0.093	0.093 ± 0.164	0.204 ± 0.130	0.561 ± 0.320
S97-V12B-LA-MX10	-0.018 ± 0.093	0.061 ± 0.163	0.235 ± 0.130	0.561 ± 0.320
S97-V12C-LA-CX	0.349 ± 0.332	6.700 ± 0.630	5.907 ± 0.458	4.948 ± 0.147
S97-V12C-LA-FX	0.117 ± 0.105	1.056 ± 0.186	4.322 ± 0.247	2.467 ± 0.042
S97-V12D-LA-CX	0.334 ± 0.350	4.731 ± 0.664	4.411 ± 0.483	4.883 ± 0.155
S97-V12D-LA-FX	0.022 ± 0.111	0.807 ± 0.197	3.756 ± 0.137	2.083 ± 0.044
S97-V12E-LA-CX	1.684 ± 0.189	5.576 ± 0.359	3.409 ± 0.261	2.886 ± 0.084
S97-V12E-LA-FX	0.384 ± 0.060	1.529 ± 0.106	2.467 ± 0.141	1.331 ± 0.024
S97-V11A-AZ-CX	1.360 ± 0.303	3.608 ± 0.576	3.291 ± 0.419	4.316 ± 0.135
S97-V11A-AZ-FX	0.231 ± 0.092	1.327 ± 0.164	2.812 ± 0.114	1.972 ± 0.037
S97-V11B-AZ-CX	1.554 ± 0.385	9.894 ± 0.732	5.205 ± 0.532	6.891 ± 0.171
S97-V11B-AZ-FX	0.153 ± 0.121	4.806 ± 0.216	4.092 ± 0.150	3.611 ± 0.049
S97-V11C-AZ-CX	0.010 ± 0.372	4.348 ± 0.708	5.034 ± 0.515	5.310 ± 0.166
S97-V11C-AZ-FX	-0.017 ± 0.116	0.848 ± 0.206	3.886 ± 0.144	2.484 ± 0.047
S97-V11D-AZ-CX	0.119 ± 0.376	2.608 ± 0.714	3.663 ± 0.520	4.748 ± 0.167
S97-V11D-AZ-FX	0.002 ± 0.115	0.319 ± 0.205	3.131 ± 0.143	1.835 ± 0.046
S97-V11D-AZ-MX5	-0.021 ± 0.107	0.147 ± 0.187	0.250 ± 0.149	0.640 ± 0.365
S97-V11D-AZ-MX6	-0.021 ± 0.106	0.105 ± 0.185	0.891 ± 0.148	0.769 ± 0.365
S97-V11D-AZ-MX7	0.056 ± 0.106	0.136 ± 0.186	1.284 ± 0.148	1.155 ± 0.365

Table D.2: Ionic Species Aerosol Concentration Data (continued)

Sample	Aerosol Concentration (μg m^{-3})			
	Cl^-	NO_3^-	$SO_4^=$	NH_4^+
S97-V11D-AZ-MX8	0.039 ± 0.107	0.150 ± 0.187	0.762 ± 0.149	0.757 ± 0.365
S97-V11D-AZ-MX9	-0.021 ± 0.107	0.110 ± 0.187	0.267 ± 0.149	0.685 ± 0.365
S97-V11D-AZ-MX10	-0.021 ± 0.106	0.073 ± 0.186	0.262 ± 0.148	0.640 ± 0.365
S97-V11E-AZ-CX	2.760 ± 0.213	3.609 ± 0.405	3.776 ± 0.295	3.186 ± 0.095
S97-V11E-AZ-FX	0.144 ± 0.067	0.768 ± 0.120	2.867 ± 0.158	1.452 ± 0.027
S97-V12A-AZ-CX	1.867 ± 0.297	3.832 ± 0.565	3.646 ± 0.411	4.142 ± 0.132
S97-V12A-AZ-FX	0.247 ± 0.095	0.868 ± 0.169	2.662 ± 0.118	1.656 ± 0.039
S97-V12B-AZ-CX	1.258 ± 0.378	4.857 ± 0.717	3.699 ± 0.522	4.661 ± 0.168
S97-V12B-AZ-FX	0.052 ± 0.119	1.015 ± 0.211	2.882 ± 0.148	1.748 ± 0.048
S97-V12C-AZ-CX	0.307 ± 0.371	3.237 ± 0.704	2.623 ± 0.512	4.571 ± 0.165
S97-V12C-AZ-FX	0.058 ± 0.118	0.747 ± 0.208	2.387 ± 0.146	1.146 ± 0.048
S97-V12D-AZ-CX	0.248 ± 0.371	4.761 ± 0.704	5.575 ± 0.512	5.373 ± 0.165
S97-V12D-AZ-FX	-0.000 ± 0.117	0.577 ± 0.208	4.355 ± 0.146	2.271 ± 0.047
S97-V12D-AZ-MX5	-0.020 ± 0.104	0.280 ± 0.183	0.345 ± 0.145	0.625 ± 0.356
S97-V12D-AZ-MX6	-0.020 ± 0.104	0.120 ± 0.182	0.768 ± 0.145	0.749 ± 0.356
S97-V12D-AZ-MX7	0.202 ± 0.104	0.130 ± 0.183	0.974 ± 0.145	0.954 ± 0.356
S97-V12D-AZ-MX8	-0.020 ± 0.104	0.149 ± 0.182	1.019 ± 0.145	0.866 ± 0.356
S97-V12D-AZ-MX9	-0.020 ± 0.104	0.081 ± 0.182	0.405 ± 0.145	0.742 ± 0.356
S97-V12D-AZ-MX10	0.211 ± 0.106	0.090 ± 0.185	0.304 ± 0.147	0.626 ± 0.356
S97-V12E-AZ-CX	0.182 ± 0.204	4.133 ± 0.387	3.220 ± 0.281	3.011 ± 0.091
S97-V12E-AZ-FX	0.017 ± 0.064	2.389 ± 0.114	0.607 ± 0.080	1.349 ± 0.026
S97-V11A-RV-CX	0.333 ± 0.307	1.141 ± 0.586	1.461 ± 0.426	3.465 ± 0.137
S97-V11A-RV-FX	0.027 ± 0.097	0.283 ± 0.172	1.073 ± 0.120	1.158 ± 0.039
S97-V11B-RV-CX	0.289 ± 0.378	3.718 ± 0.717	2.064 ± 0.521	4.446 ± 0.168
S97-V11B-RV-FX	-0.011 ± 0.117	2.153 ± 0.207	1.387 ± 0.144	1.789 ± 0.047
S97-V11C-RV-CX	-0.026 ± 0.368	1.725 ± 0.700	1.423 ± 0.509	4.119 ± 0.164
S97-V11C-RV-FX	0.012 ± 0.112	0.463 ± 0.198	1.217 ± 0.138	1.360 ± 0.045
S97-V11D-RV-CX	0.128 ± 0.368	2.280 ± 0.699	3.785 ± 0.509	4.766 ± 0.164
S97-V11D-RV-FX	-0.069 ± 0.114	0.257 ± 0.202	3.006 ± 0.141	1.942 ± 0.046
S97-V11D-RV-MX5	-0.017 ± 0.091	0.294 ± 0.159	0.377 ± 0.126	0.648 ± 0.311
S97-V11D-RV-MX6	-0.017 ± 0.091	0.644 ± 0.159	0.820 ± 0.127	0.862 ± 0.311
S97-V11D-RV-MX7	-0.017 ± 0.091	0.298 ± 0.159	0.827 ± 0.127	0.727 ± 0.311
S97-V11D-RV-MX8	-0.017 ± 0.091	0.099 ± 0.159	0.402 ± 0.126	0.637 ± 0.311
S97-V11D-RV-MX9	-0.017 ± 0.091	0.085 ± 0.159	0.407 ± 0.127	0.606 ± 0.311
S97-V11D-RV-MX10	-0.017 ± 0.091	0.080 ± 0.160	0.177 ± 0.127	0.546 ± 0.311
S97-V11E-RV-CX	0.212 ± 0.201	1.911 ± 0.382	2.785 ± 0.278	2.804 ± 0.090
S97-V11E-RV-FX	-0.020 ± 0.062	0.245 ± 0.111	2.473 ± 0.077	1.260 ± 0.025
S97-V12A-RV-CX	0.346 ± 0.301	2.027 ± 0.572	3.306 ± 0.416	3.822 ± 0.134
S97-V12A-RV-FX	0.039 ± 0.092	0.286 ± 0.163	2.723 ± 0.113	1.551 ± 0.037
S97-V12B-RV-CX	0.230 ± 0.381	2.860 ± 0.724	3.525 ± 0.526	4.671 ± 0.169
S97-V12B-RV-FX	0.049 ± 0.116	0.542 ± 0.205	2.394 ± 0.143	1.642 ± 0.046

Table D.2: Ionic Species Aerosol Concentration Data (continued)

Sample	Aerosol Concentration (μg m^{-3})			
	Cl^-	NO_3^-	$SO_4^=$	NH_4^+
S97-V12C-RV-CX	0.141 ± 0.372	3.206 ± 0.706	2.222 ± 0.513	4.397 ± 0.165
S97-V12C-RV-FX	-0.054 ± 0.114	0.426 ± 0.203	1.726 ± 0.141	1.578 ± 0.046
S97-V12D-RV-CX	0.115 ± 0.365	4.107 ± 0.693	2.720 ± 0.504	4.613 ± 0.162
S97-V12D-RV-FX	-0.011 ± 0.112	0.764 ± 0.199	2.030 ± 0.139	1.705 ± 0.045
S97-V12D-RV-MX5	0.000 ± 0.096	0.230 ± 0.167	0.086 ± 0.132	-0.170 ± 0.311
S97-V12D-RV-MX6	0.033 ± 0.095	1.807 ± 0.167	0.435 ± 0.132	1.013 ± 0.311
S97-V12D-RV-MX7	-0.014 ± 0.096	2.103 ± 0.167	0.539 ± 0.132	1.184 ± 0.311
S97-V12D-RV-MX8	0.096 ± 0.096	0.331 ± 0.167	0.358 ± 0.132	0.753 ± 0.311
S97-V12D-RV-MX9	0.010 ± 0.096	0.020 ± 0.168	0.192 ± 0.133	0.591 ± 0.312
S97-V12D-RV-MX10	0.033 ± 0.096	0.017 ± 0.168	0.065 ± 0.132	0.593 ± 0.312
S97-V12E-RV-CX	0.154 ± 0.202	8.667 ± 0.383	4.637 ± 0.279	4.828 ± 0.090
S97-V12E-RV-FX	0.059 ± 0.062	3.080 ± 0.295	4.447 ± 0.217	2.681 ± 0.025
S97-V21A-LA-CX	2.776 ± 0.267	4.496 ± 0.506	2.397 ± 0.368	3.495 ± 0.119
S97-V21A-LA-FX	0.418 ± 0.084	1.337 ± 0.149	1.736 ± 0.104	1.252 ± 0.034
S97-V21B-LA-CX	0.878 ± 0.339	6.492 ± 0.643	2.979 ± 0.468	4.390 ± 0.151
S97-V21B-LA-FX	0.181 ± 0.108	2.169 ± 0.192	2.047 ± 0.134	1.828 ± 0.043
S97-V21B-LA-MX5	0.034 ± 0.097	0.945 ± 0.170	0.154 ± 0.135	-0.107 ± 0.321
S97-V21B-LA-MX6	0.028 ± 0.099	0.209 ± 0.172	0.373 ± 0.136	0.690 ± 0.321
S97-V21B-LA-MX7	0.019 ± 0.099	0.456 ± 0.173	0.664 ± 0.136	0.863 ± 0.321
S97-V21B-LA-MX8	0.077 ± 0.098	0.202 ± 0.172	0.386 ± 0.136	0.721 ± 0.321
S97-V21B-LA-MX9	0.031 ± 0.098	-0.026 ± 0.172	0.067 ± 0.136	-0.179 ± 0.321
S97-V21B-LA-MX10	0.248 ± 0.099	-0.023 ± 0.173	0.009 ± 0.136	-0.181 ± 0.321
S97-V21C-LA-CX	0.400 ± 0.330	7.271 ± 0.627	3.508 ± 0.456	4.347 ± 0.147
S97-V21C-LA-FX	0.116 ± 0.104	1.254 ± 0.185	2.634 ± 0.128	1.817 ± 0.042
S97-V21D-LA-CX	0.721 ± 0.336	4.002 ± 0.639	2.593 ± 0.465	3.996 ± 0.150
S97-V21D-LA-FX	0.047 ± 0.109	0.851 ± 0.194	1.978 ± 0.135	1.556 ± 0.044
S97-V21E-LA-CX	4.359 ± 0.187	4.529 ± 0.356	2.471 ± 0.259	2.458 ± 0.083
S97-V21E-LA-FX	0.618 ± 0.060	1.485 ± 0.106	1.495 ± 0.074	0.980 ± 0.024
S97-V22A-LA-CX	5.416 ± 0.278	3.450 ± 0.527	2.651 ± 0.383	3.397 ± 0.124
S97-V22A-LA-FX	0.808 ± 0.089	1.200 ± 0.158	1.302 ± 0.110	1.142 ± 0.036
S97-V22B-LA-CX	1.796 ± 0.336	7.103 ± 0.638	2.781 ± 0.464	4.108 ± 0.149
S97-V22B-LA-FX	0.213 ± 0.106	2.418 ± 0.188	1.636 ± 0.131	1.641 ± 0.042
S97-V22B-LA-MX5	0.080 ± 0.098	1.141 ± 0.171	0.122 ± 0.135	0.657 ± 0.319
S97-V22B-LA-MX6	0.031 ± 0.098	0.103 ± 0.171	0.156 ± 0.136	0.614 ± 0.319
S97-V22B-LA-MX7	0.016 ± 0.098	0.189 ± 0.171	0.472 ± 0.136	0.754 ± 0.319
S97-V22B-LA-MX8	0.025 ± 0.098	0.073 ± 0.171	0.380 ± 0.136	0.693 ± 0.319
S97-V22B-LA-MX9	0.056 ± 0.098	-0.013 ± 0.171	0.192 ± 0.135	0.590 ± 0.319
S97-V22B-LA-MX10	0.135 ± 0.098	-0.019 ± 0.171	0.069 ± 0.135	-0.172 ± 0.319
S97-V22C-LA-CX	0.780 ± 0.334	9.810 ± 0.634	5.488 ± 0.461	4.912 ± 0.149
S97-V22C-LA-FX	0.105 ± 0.107	1.619 ± 0.191	4.255 ± 0.133	2.110 ± 0.043
S97-V22D-LA-CX	0.528 ± 0.344	7.704 ± 0.653	5.568 ± 0.475	4.885 ± 0.153
S97-V22D-LA-FX	0.072 ± 0.110	1.434 ± 0.195	4.773 ± 0.258	2.264 ± 0.044

Table D.2: Ionic Species Aerosol Concentration Data (continued)

Sample	Aerosol Concentration (μg m^{-3})			
	Cl^-	NO_3^-	$SO_4^=$	NH_4^+
S97-V22D-LA-MX5	0.013 ± 0.097	0.800 ± 0.170	0.297 ± 0.134	-0.171 ± 0.317
S97-V22D-LA-MX6	-0.015 ± 0.097	0.011 ± 0.170	0.581 ± 0.135	0.702 ± 0.317
S97-V22D-LA-MX7	-0.009 ± 0.097	0.029 ± 0.170	1.790 ± 0.135	1.029 ± 0.317
S97-V22D-LA-MX8	-0.003 ± 0.097	0.020 ± 0.170	0.921 ± 0.134	0.843 ± 0.317
S97-V22D-LA-MX9	-0.018 ± 0.097	-0.016 ± 0.170	0.484 ± 0.135	0.724 ± 0.317
S97-V22D-LA-MX10	-0.018 ± 0.097	-0.038 ± 0.170	0.075 ± 0.134	0.603 ± 0.317
S97-V22E-LA-CX	1.581 ± 0.187	9.018 ± 0.355	3.664 ± 0.258	3.458 ± 0.083
S97-V22E-LA-FX	0.257 ± 0.062	2.174 ± 0.110	2.786 ± 0.145	1.613 ± 0.025
S97-V21A-AZ-CX	0.504 ± 0.292	5.610 ± 0.554	3.395 ± 0.403	3.902 ± 0.130
S97-V21A-AZ-FX	0.125 ± 0.089	1.206 ± 0.158	2.258 ± 0.110	1.482 ± 0.036
S97-V21B-AZ-CX	0.201 ± 0.372	5.981 ± 0.706	2.877 ± 0.513	4.715 ± 0.165
S97-V21B-AZ-FX	0.131 ± 0.117	1.409 ± 0.207	2.052 ± 0.144	1.766 ± 0.047
S97-V21C-AZ-CX	0.151 ± 0.367	7.130 ± 0.698	3.470 ± 0.508	4.869 ± 0.163
S97-V21C-AZ-FX	-0.030 ± 0.113	0.822 ± 0.201	2.389 ± 0.140	1.870 ± 0.045
S97-V21D-AZ-CX	0.168 ± 0.379	6.623 ± 0.719	3.262 ± 0.523	4.868 ± 0.168
S97-V21D-AZ-FX	-0.051 ± 0.116	1.166 ± 0.206	2.624 ± 0.143	1.876 ± 0.046
S97-V21D-AZ-MX5	-0.020 ± 0.110	0.422 ± 0.192	0.088 ± 0.152	-0.200 ± 0.358
S97-V21D-AZ-MX6	-0.010 ± 0.110	0.068 ± 0.193	0.158 ± 0.152	-0.202 ± 0.358
S97-V21D-AZ-MX7	-0.010 ± 0.110	0.016 ± 0.193	0.706 ± 0.152	0.787 ± 0.358
S97-V21D-AZ-MX8	-0.010 ± 0.110	0.030 ± 0.193	0.736 ± 0.152	0.827 ± 0.358
S97-V21D-AZ-MX9	0.004 ± 0.110	-0.001 ± 0.192	0.364 ± 0.152	0.763 ± 0.358
S97-V21D-AZ-MX10	0.004 ± 0.110	-0.032 ± 0.193	0.109 ± 0.152	-0.201 ± 0.358
S97-V21E-AZ-CX	2.009 ± 0.206	4.548 ± 0.392	2.469 ± 0.285	2.808 ± 0.092
S97-V21E-AZ-FX	0.062 ± 0.063	1.051 ± 0.113	1.827 ± 0.078	1.196 ± 0.025
S97-V22A-AZ-CX	0.404 ± 0.301	3.761 ± 0.573	2.044 ± 0.417	3.758 ± 0.134
S97-V22A-AZ-FX	0.051 ± 0.093	0.939 ± 0.164	1.553 ± 0.114	1.343 ± 0.037
S97-V22B-AZ-CX	1.159 ± 0.381	5.954 ± 0.724	2.255 ± 0.527	4.661 ± 0.170
S97-V22B-AZ-FX	0.065 ± 0.114	1.731 ± 0.202	1.583 ± 0.141	1.683 ± 0.046
S97-V22B-AZ-MX5	-0.020 ± 0.109	0.685 ± 0.190	0.084 ± 0.150	-0.198 ± 0.353
S97-V22B-AZ-MX6	-0.020 ± 0.109	0.019 ± 0.190	0.518 ± 0.150	0.713 ± 0.353
S97-V22B-AZ-MX7	-0.020 ± 0.109	0.016 ± 0.190	0.478 ± 0.150	-0.131 ± 0.353
S97-V22B-AZ-MX8	-0.020 ± 0.109	-0.011 ± 0.190	0.387 ± 0.150	0.689 ± 0.353
S97-V22B-AZ-MX9	-0.020 ± 0.109	-0.028 ± 0.190	0.139 ± 0.150	-0.199 ± 0.353
S97-V22B-AZ-MX10	-0.020 ± 0.108	-0.005 ± 0.189	0.023 ± 0.150	-0.196 ± 0.353
S97-V22C-AZ-CX	0.119 ± 0.377	8.145 ± 0.716	3.261 ± 0.521	4.996 ± 0.168
S97-V22C-AZ-FX	0.037 ± 0.117	0.981 ± 0.208	2.324 ± 0.145	1.783 ± 0.047
S97-V22D-AZ-CX	0.144 ± 0.378	8.168 ± 0.718	7.445 ± 0.523	5.885 ± 0.168
S97-V22D-AZ-FX	0.026 ± 0.116	0.986 ± 0.207	5.187 ± 0.406	2.768 ± 0.047
S97-V22D-AZ-MX5	0.078 ± 0.108	0.425 ± 0.189	0.205 ± 0.149	-0.197 ± 0.352
S97-V22D-AZ-MX6	-0.020 ± 0.107	0.022 ± 0.187	0.109 ± 0.148	-0.189 ± 0.352
S97-V22D-AZ-MX7	-0.016 ± 0.108	0.026 ± 0.189	1.796 ± 0.149	1.091 ± 0.352
S97-V22D-AZ-MX8	-0.020 ± 0.108	0.026 ± 0.189	1.031 ± 0.149	0.915 ± 0.352
S97-V22D-AZ-MX9	-0.020 ± 0.108	0.039 ± 0.189	0.738 ± 0.149	0.803 ± 0.352

Table D.2: Ionic Species Aerosol Concentration Data (continued)

Sample	Aerosol Concentration (μg m^{-3})			
	Cl^-	NO_3^-	$SO_4^=$	NH_4^+
S97-V22D-AZ-MX10	0.041 ± 0.108	-0.032 ± 0.189	0.174 ± 0.149	-0.196 ± 0.352
S97-V22E-AZ-CX	0.599 ± 0.208	12.054 ± 0.395	5.297 ± 0.287	4.708 ± 0.092
S97-V22E-AZ-FX	0.115 ± 0.063	3.076 ± 0.301	3.956 ± 0.221	2.299 ± 0.025
S97-V21A-RV-CX	0.231 ± 0.302	8.631 ± 0.573	2.665 ± 0.417	5.018 ± 0.134
S97-V21A-RV-FX	0.122 ± 0.092	3.166 ± 0.164	2.338 ± 0.114	2.015 ± 0.037
S97-V21B-RV-CX	0.250 ± 0.437	17.400 ± 0.830	3.761 ± 0.603	7.495 ± 0.194
S97-V21B-RV-FX	0.075 ± 0.114	5.842 ± 0.368	2.542 ± 0.141	3.134 ± 0.046
S97-V21C-RV-CX	0.044 ± 0.358	9.106 ± 0.680	3.259 ± 0.495	5.378 ± 0.159
S97-V21C-RV-FX	-0.007 ± 0.111	5.889 ± 0.360	2.777 ± 0.138	3.295 ± 0.045
S97-V21D-RV-CX	0.159 ± 0.359	5.653 ± 0.682	2.365 ± 0.496	4.502 ± 0.160
S97-V21D-RV-FX	-0.069 ± 0.112	1.109 ± 0.199	1.859 ± 0.138	1.537 ± 0.045
S97-V21D-RV-MX5	-0.017 ± 0.096	0.407 ± 0.168	0.047 ± 0.133	-0.176 ± 0.312
S97-V21D-RV-MX6	-0.017 ± 0.096	0.360 ± 0.168	0.098 ± 0.133	-0.121 ± 0.312
S97-V21D-RV-MX7	-0.009 ± 0.095	0.734 ± 0.167	0.390 ± 0.132	0.791 ± 0.311
S97-V21D-RV-MX8	-0.017 ± 0.096	0.137 ± 0.167	0.362 ± 0.132	0.663 ± 0.311
S97-V21D-RV-MX9	-0.011 ± 0.096	0.035 ± 0.167	0.266 ± 0.132	-0.175 ± 0.311
S97-V21D-RV-MX10	0.018 ± 0.096	-0.010 ± 0.167	0.116 ± 0.132	-0.175 ± 0.311
S97-V21E-RV-CX	0.440 ± 0.199	11.600 ± 0.379	3.718 ± 0.276	4.526 ± 0.089
S97-V21E-RV-FX	0.130 ± 0.114	3.134 ± 0.199	2.978 ± 0.145	2.162 ± 0.025
S97-V22A-RV-CX	0.464 ± 0.302	8.871 ± 0.574	2.651 ± 0.418	5.203 ± 0.134
S97-V22A-RV-FX	0.128 ± 0.095	3.893 ± 0.169	2.524 ± 0.118	2.238 ± 0.039
S97-V22B-RV-CX	0.395 ± 0.364	17.012 ± 0.691	3.097 ± 0.503	7.345 ± 0.162
S97-V22B-RV-FX	0.013 ± 0.116	7.398 ± 0.206	5.346 ± 0.144	3.907 ± 0.047
S97-V22B-RV-MX5	-0.017 ± 0.091	0.944 ± 0.159	0.264 ± 0.127	0.707 ± 0.311
S97-V22B-RV-MX6	-0.017 ± 0.091	1.464 ± 0.159	0.481 ± 0.126	0.970 ± 0.311
S97-V22B-RV-MX7	0.028 ± 0.091	2.658 ± 0.160	0.762 ± 0.127	1.383 ± 0.311
S97-V22B-RV-MX8	-0.017 ± 0.091	1.884 ± 0.159	0.804 ± 0.126	1.123 ± 0.311
S97-V22B-RV-MX9	-0.017 ± 0.091	0.159 ± 0.159	0.241 ± 0.127	0.581 ± 0.311
S97-V22B-RV-MX10	-0.017 ± 0.091	0.068 ± 0.159	0.142 ± 0.127	0.546 ± 0.311
S97-V22C-RV-CX	0.257 ± 0.367	6.898 ± 0.697	2.830 ± 0.507	5.527 ± 0.163
S97-V22C-RV-FX	0.014 ± 0.118	-0.150 ± 0.209	-0.098 ± 0.146	0.002 ± 0.048
S97-V22D-RV-CX	0.507 ± 0.369	5.650 ± 0.702	3.345 ± 0.510	4.975 ± 0.164
S97-V22D-RV-FX	0.007 ± 0.116	1.139 ± 0.206	3.209 ± 0.144	1.915 ± 0.047
S97-V22D-RV-MX5	0.025 ± 0.089	0.803 ± 0.156	0.328 ± 0.124	0.635 ± 0.305
S97-V22D-RV-MX6	-0.017 ± 0.089	2.425 ± 0.156	0.596 ± 0.124	1.132 ± 0.305
S97-V22D-RV-MX7	-0.017 ± 0.089	1.483 ± 0.156	0.770 ± 0.124	1.133 ± 0.305
S97-V22D-RV-MX8	-0.017 ± 0.089	0.225 ± 0.156	0.514 ± 0.124	0.660 ± 0.305
S97-V22D-RV-MX9	-0.017 ± 0.089	0.097 ± 0.156	0.274 ± 0.124	0.595 ± 0.305
S97-V22D-RV-MX10	-0.017 ± 0.089	0.088 ± 0.155	0.230 ± 0.124	0.556 ± 0.305
S97-V22E-RV-CX	0.502 ± 0.204	8.115 ± 0.386	3.587 ± 0.281	4.014 ± 0.091
S97-V22E-RV-FX	0.091 ± 0.064	2.069 ± 0.113	3.131 ± 0.079	1.763 ± 0.026

Table D.2: Ionic Species Aerosol Concentration Data (continued)

Sample	Aerosol Concentration (μg m^{-3})			
	Cl^-	NO_3^-	$SO_4^=$	NH_4^+
S97-N21D-ML-FX	0.004 ± 0.236	14.987 ± 0.413	3.523 ± 0.302	5.730 ± 0.103
S97-N21E-ML-FX	0.998 ± 0.065	42.205 ± 0.649	10.125 ± 0.081	12.887 ± 0.079
S97-N22A-ML-FX	0.492 ± 0.090	46.285 ± 0.570	8.292 ± 0.111	12.879 ± 0.145
S97-N22B-ML-FX	0.480 ± 0.113	43.730 ± 0.716	5.884 ± 0.140	12.093 ± 0.182
S97-N22C-ML-FX	-0.001 ± 0.115	0.265 ± 0.203	1.244 ± 0.142	1.408 ± 0.046
S97-N22C-ML-MX5	-0.006 ± 0.098	-0.032 ± 0.172	0.097 ± 0.136	0.661 ± 0.320
S97-N22C-ML-MX6	-0.018 ± 0.099	0.335 ± 0.172	0.246 ± 0.136	0.697 ± 0.320
S97-N22C-ML-MX7	-0.018 ± 0.098	0.476 ± 0.172	0.384 ± 0.136	0.820 ± 0.320
S97-N22C-ML-MX8	-0.006 ± 0.098	0.070 ± 0.172	0.162 ± 0.136	0.655 ± 0.320
S97-N22C-ML-MX9	0.037 ± 0.098	-0.017 ± 0.171	0.079 ± 0.135	0.608 ± 0.320
S97-N22C-ML-MX10	0.031 ± 0.098	-0.032 ± 0.172	0.024 ± 0.136	-0.180 ± 0.320
S97-N22D-ML-FX	0.172 ± 0.112	14.393 ± 0.198	5.618 ± 0.138	3.856 ± 0.045
S97-N22E-ML-FX	0.810 ± 0.064	20.286 ± 0.405	6.044 ± 0.079	6.788 ± 0.103
S97-N23A-ML-FX	0.775 ± 0.092	18.445 ± 0.162	4.713 ± 0.114	6.352 ± 0.037
S97-N23B-ML-FX	0.375 ± 0.115	23.787 ± 0.203	4.655 ± 0.142	7.154 ± 0.046
S97-N23C-ML-FX	0.085 ± 0.113	36.121 ± 0.716	3.877 ± 0.140	10.189 ± 0.137
S97-N23C-ML-MX5	-0.015 ± 0.098	4.447 ± 0.171	0.388 ± 0.135	1.613 ± 0.317
S97-N23C-ML-MX6	3.302 ± 0.757	11.705 ± 1.319	1.284 ± 0.135	3.638 ± 0.317
S97-N23C-ML-MX7	0.089 ± 0.097	12.515 ± 0.988	1.102 ± 0.135	3.702 ± 0.317
S97-N23C-ML-MX8	-0.018 ± 0.098	4.457 ± 0.171	0.304 ± 0.135	1.671 ± 0.317
S97-N23C-ML-MX9	-0.012 ± 0.097	0.270 ± 0.170	0.008 ± 0.134	0.628 ± 0.317
S97-N23C-ML-MX10	-0.006 ± 0.097	-0.022 ± 0.170	-0.004 ± 0.135	-0.178 ± 0.317
S97-N23D-ML-FX	0.095 ± 0.112	10.146 ± 0.199	3.232 ± 0.139	3.839 ± 0.045
S97-N23E-ML-FX	1.029 ± 0.069	7.853 ± 0.122	3.423 ± 0.086	2.891 ± 0.028
S97-N23E-ML-MX5	0.422 ± 0.056	2.464 ± 0.098	0.501 ± 0.077	0.733 ± 0.182
S97-N23E-ML-MX6	-	1.100 ± 0.098	0.790 ± 0.077	0.795 ± 0.182
S97-N23E-ML-MX7	0.202 ± 0.056	1.498 ± 0.097	0.984 ± 0.077	0.952 ± 0.182
S97-N23E-ML-MX8	0.067 ± 0.056	0.641 ± 0.098	0.348 ± 0.077	0.586 ± 0.182
S97-N23E-ML-MX9	0.006 ± 0.056	0.088 ± 0.098	0.054 ± 0.077	0.356 ± 0.182
S97-N23E-ML-MX10	0.009 ± 0.056	0.005 ± 0.098	0.003 ± 0.077	-0.100 ± 0.182
S97-N31A-DB-CX	1.743 ± 0.273	43.977 ± 0.519	4.649 ± 0.378	14.105 ± 0.122
S97-N31A-DB-FX	1.010 ± 0.087	41.203 ± 0.555	4.581 ± 0.108	10.826 ± 0.141
S97-N31B-DB-CX	0.921 ± 0.347	44.008 ± 0.659	3.854 ± 0.479	13.522 ± 0.154
S97-N31B-DB-FX	0.160 ± 0.112	40.617 ± 0.713	3.229 ± 0.139	10.281 ± 0.182
S97-N31C-DB-CX	0.086 ± 0.341	47.517 ± 0.647	3.555 ± 0.471	14.603 ± 0.151
S97-N31C-DB-FX	0.519 ± 0.113	40.541 ± 0.716	3.373 ± 0.140	10.456 ± 0.182
S97-N31C-DB-MX5	0.022 ± 0.099	12.514 ± 0.173	0.324 ± 0.137	3.177 ± 0.323
S97-N31C-DB-MX6	0.000 ± 0.099	19.380 ± 0.173	0.638 ± 0.137	4.878 ± 0.323
S97-N31C-DB-MX7	0.187 ± 0.099	6.836 ± 0.173	1.067 ± 0.137	2.328 ± 0.323
S97-N31C-DB-MX8	-0.012 ± 0.099	0.846 ± 0.173	0.468 ± 0.137	0.886 ± 0.323
S97-N31C-DB-MX9	-0.018 ± 0.099	0.129 ± 0.173	0.142 ± 0.137	-0.122 ± 0.323

Table D.2: Ionic Species Aerosol Concentration Data (continued)

Sample	Aerosol Concentration (μg m^{-3})			
	Cl^-	NO_3^-	$SO_4^=$	NH_4^+
S97-N31C-DB-MX10	-0.015 ± 0.099	0.052 ± 0.173	0.008 ± 0.137	-0.181 ± 0.323
S97-N31D-DB-CX	0.230 ± 0.329	24.513 ± 0.625	5.624 ± 0.454	9.594 ± 0.146
S97-N31D-DB-FX	0.038 ± 0.108	18.031 ± 0.192	5.045 ± 0.134	5.986 ± 0.044
S97-N31D-DB-MX5	-0.021 ± 0.117	4.486 ± 0.205	0.175 ± 0.162	1.590 ± 0.381
S97-N31D-DB-MX6	-0.007 ± 0.117	7.222 ± 0.791	0.617 ± 0.162	2.383 ± 0.381
S97-N31D-DB-MX7	0.059 ± 0.117	4.680 ± 0.204	1.853 ± 0.162	2.243 ± 0.381
S97-N31D-DB-MX8	-0.003 ± 0.117	1.188 ± 0.205	1.160 ± 0.162	1.246 ± 0.381
S97-N31D-DB-MX9	0.001 ± 0.117	0.141 ± 0.204	0.409 ± 0.162	-
S97-N31D-DB-MX10	-0.021 ± 0.117	0.021 ± 0.204	0.141 ± 0.162	-0.212 ± 0.381
S97-N31E-DB-CX	0.712 ± 0.188	43.889 ± 0.358	6.335 ± 0.260	13.053 ± 0.084
S97-N31E-DB-FX	0.492 ± 0.062	35.230 ± 0.391	6.546 ± 0.076	9.848 ± 0.100
S97-N32A-DB-CX	1.052 ± 0.276	62.048 ± 0.525	3.626 ± 0.382	17.821 ± 0.123
S97-N32A-DB-FX	0.891 ± 0.091	60.728 ± 0.581	3.271 ± 0.113	6.915 ± 0.037
S97-N32B-DB-CX	0.344 ± 0.337	27.065 ± 0.641	2.448 ± 0.466	9.202 ± 0.150
S97-N32B-DB-FX	0.052 ± 0.112	24.489 ± 0.199	1.493 ± 0.139	6.396 ± 0.045
S97-N32C-DB-CX	0.255 ± 0.333	8.587 ± 0.633	1.609 ± 0.460	4.973 ± 0.148
S97-N32C-DB-FX	-0.007 ± 0.111	0.782 ± 0.196	1.053 ± 0.137	2.061 ± 0.045
S97-N32C-DB-MX5	-0.018 ± 0.099	3.291 ± 0.173	0.080 ± 0.137	1.172 ± 0.319
S97-N32C-DB-MX6	-0.018 ± 0.099	3.927 ± 0.172	0.123 ± 0.136	1.486 ± 0.321
S97-N32C-DB-MX7	-0.018 ± 0.099	1.622 ± 0.172	0.342 ± 0.136	1.028 ± 0.321
S97-N32C-DB-MX8	-0.015 ± 0.099	0.122 ± 0.172	0.144 ± 0.136	0.629 ± 0.321
S97-N32C-DB-MX9	-0.018 ± 0.098	-0.007 ± 0.172	0.036 ± 0.136	0.559 ± 0.321
S97-N32C-DB-MX10	-0.018 ± 0.099	0.011 ± 0.173	0.021 ± 0.137	-0.177 ± 0.321
S97-N32D-DB-CX	0.709 ± 0.336	2.206 ± 0.637	1.372 ± 0.464	3.956 ± 0.149
S97-N32D-DB-FX	0.163 ± 0.110	0.842 ± 0.194	0.973 ± 0.136	1.384 ± 0.044
S97-N32E-DB-CX	0.394 ± 0.192	1.604 ± 0.365	1.557 ± 0.266	2.406 ± 0.086
S97-N32E-DB-FX	0.011 ± 0.062	0.437 ± 0.110	0.970 ± 0.077	0.885 ± 0.025
S97-N31A-ML-CX	0.931 ± 0.300	44.035 ± 0.569	5.110 ± 0.414	12.777 ± 0.133
S97-N31A-ML-FX	0.756 ± 0.098	41.514 ± 0.624	4.594 ± 0.122	10.943 ± 0.084
S97-N31B-ML-CX	1.145 ± 0.372	43.646 ± 0.707	3.948 ± 0.514	13.306 ± 0.166
S97-N31B-ML-FX	0.762 ± 0.129	42.875 ± 0.822	3.790 ± 0.160	10.113 ± 0.052
S97-N31C-ML-CX	0.528 ± 0.394	44.893 ± 0.747	2.595 ± 0.544	16.833 ± 0.175
S97-N31C-ML-FX	0.341 ± 0.125	60.196 ± 0.792	2.499 ± 0.155	13.881 ± 0.151
S97-N31C-ML-MX5	-	11.670 ± 0.201	0.164 ± 0.159	3.075 ± 0.374
S97-N31C-ML-MX6	0.119 ± 0.114	21.185 ± 0.200	0.475 ± 0.158	5.314 ± 0.374
S97-N31C-ML-MX7	-	12.793 ± 0.201	0.614 ± 0.159	3.512 ± 0.374
S97-N31C-ML-MX8	0.065 ± 0.115	2.460 ± 0.201	0.186 ± 0.159	1.235 ± 0.374
S97-N31C-ML-MX9	-0.007 ± 0.115	0.588 ± 0.201	0.071 ± 0.159	0.754 ± 0.374
S97-N31C-ML-MX10	-0.021 ± 0.115	0.139 ± 0.201	-0.026 ± 0.159	-0.209 ± 0.374
S97-N31D-ML-CX	0.735 ± 0.371	109.628 ± 1.317	4.679 ± 0.512	22.955 ± 0.165
S97-N31D-ML-FX	0.386 ± 0.120	77.084 ± 1.142	3.766 ± 0.149	19.328 ± 0.146
S97-N31D-ML-MX5	-	15.189 ± 0.212	0.390 ± 0.168	3.961 ± 0.395

Table D.2: Ionic Species Aerosol Concentration Data (continued)

Sample	Aerosol Concentration (μg m^{-3})			
	Cl^-	NO_3^-	$SO_4^=$	NH_4^+
S97-N31D-ML-MX6	0.162 ± 0.088	24.366 ± 0.155	0.839 ± 0.129	6.000 ± 0.395
S97-N31D-ML-MX7	-	17.911 ± 0.212	1.489 ± 0.168	4.917 ± 0.395
S97-N31D-ML-MX8	0.039 ± 0.121	4.603 ± 0.212	0.511 ± 0.168	1.907 ± 0.395
S97-N31D-ML-MX9	-0.022 ± 0.122	2.249 ± 0.213	0.193 ± 0.168	1.207 ± 0.395
S97-N31D-ML-MX10	0.004 ± 0.121	1.067 ± 0.212	0.063 ± 0.168	0.912 ± 0.395
S97-N31E-ML-CX	1.055 ± 0.206	75.725 ± 1.434	5.393 ± 0.284	20.909 ± 0.366
S97-N31E-ML-FX	0.745 ± 0.066	73.233 ± 0.829	4.736 ± 0.081	18.913 ± 0.186
S97-N32A-ML-CX	1.222 ± 0.308	62.838 ± 0.585	4.288 ± 0.425	17.095 ± 0.137
S97-N32A-ML-FX	0.591 ± 0.097	52.793 ± 0.925	3.004 ± 0.121	13.708 ± 0.158
S97-N32B-ML-CX	0.257 ± 0.384	6.521 ± 0.730	1.706 ± 0.531	4.812 ± 0.171
S97-N32B-ML-FX	0.053 ± 0.122	3.805 ± 0.216	0.857 ± 0.151	1.947 ± 0.049
S97-N32C-ML-CX	0.677 ± 0.371	1.477 ± 0.705	1.006 ± 0.513	-0.010 ± 0.165
S97-N32C-ML-FX	0.046 ± 0.131	0.616 ± 0.231	0.406 ± 0.162	1.168 ± 0.053
S97-N32C-ML-MX5	0.055 ± 0.108	-0.015 ± 0.189	-0.018 ± 0.150	-0.192 ± 0.352
S97-N32C-ML-MX6	0.011 ± 0.108	-0.018 ± 0.189	-0.008 ± 0.149	-0.191 ± 0.352
S97-N32C-ML-MX7	0.034 ± 0.108	-0.015 ± 0.189	0.053 ± 0.149	-0.191 ± 0.352
S97-N32C-ML-MX8	0.048 ± 0.108	-0.032 ± 0.189	0.098 ± 0.150	-0.194 ± 0.352
S97-N32C-ML-MX9	-0.006 ± 0.108	-0.025 ± 0.189	0.016 ± 0.149	-0.190 ± 0.352
S97-N32C-ML-MX10	0.027 ± 0.108	-0.032 ± 0.188	-0.011 ± 0.149	-0.188 ± 0.352
S97-N32D-ML-CX	0.407 ± 0.375	0.577 ± 0.711	0.558 ± 0.517	-0.009 ± 0.167
S97-N32D-ML-FX	-0.053 ± 0.120	0.009 ± 0.213	0.335 ± 0.149	1.065 ± 0.049
S97-N32E-ML-CX	0.362 ± 0.206	0.423 ± 0.391	0.413 ± 0.285	-0.001 ± 0.092
S97-N32E-ML-FX	-0.029 ± 0.066	0.014 ± 0.117	0.235 ± 0.082	0.621 ± 0.027
S97-N31A-RV-CX	0.258 ± 0.289	46.762 ± 0.550	2.752 ± 0.400	14.026 ± 0.129
S97-N31A-RV-FX	0.389 ± 0.090	44.279 ± 0.573	3.590 ± 0.112	10.786 ± 0.146
S97-N31B-RV-CX	0.622 ± 0.367	26.829 ± 0.698	2.537 ± 0.507	9.908 ± 0.163
S97-N31B-RV-FX	0.544 ± 0.115	26.575 ± 0.204	1.915 ± 0.143	6.633 ± 0.047
S97-N31C-RV-CX	0.033 ± 0.360	14.996 ± 0.683	1.458 ± 0.497	6.750 ± 0.160
S97-N31C-RV-FX	0.013 ± 0.116	18.191 ± 0.205	1.680 ± 0.144	4.789 ± 0.047
S97-N31C-RV-MX5	-0.003 ± 0.096	5.420 ± 0.490	0.050 ± 0.133	1.711 ± 0.314
S97-N31C-RV-MX6	0.010 ± 0.097	9.294 ± 0.816	0.205 ± 0.133	2.580 ± 0.314
S97-N31C-RV-MX7	-0.003 ± 0.097	5.220 ± 0.491	0.395 ± 0.133	1.838 ± 0.314
S97-N31C-RV-MX8	-0.009 ± 0.097	1.096 ± 0.169	0.153 ± 0.134	0.810 ± 0.314
S97-N31C-RV-MX9	-0.018 ± 0.096	0.409 ± 0.169	0.084 ± 0.133	0.616 ± 0.314
S97-N31C-RV-MX10	0.013 ± 0.096	0.174 ± 0.169	-0.013 ± 0.133	-0.175 ± 0.314
S97-N31D-RV-CX	0.119 ± 0.342	66.734 ± 0.649	2.933 ± 0.472	18.748 ± 0.152
S97-N31D-RV-FX	0.097 ± 0.108	62.880 ± 1.023	2.348 ± 0.134	15.588 ± 0.174
S97-N31D-RV-MX5	-0.014 ± 0.114	15.332 ± 0.200	0.228 ± 0.158	3.868 ± 0.374
S97-N31D-RV-MX6	0.020 ± 0.084	22.503 ± 0.147	0.575 ± 0.122	5.475 ± 0.374
S97-N31D-RV-MX7	0.072 ± 0.114	13.005 ± 0.200	0.801 ± 0.158	3.672 ± 0.374
S97-N31D-RV-MX8	-0.014 ± 0.115	2.699 ± 0.201	0.258 ± 0.159	1.378 ± 0.374
S97-N31D-RV-MX9	-0.021 ± 0.115	1.891 ± 0.201	0.132 ± 0.159	1.151 ± 0.374

Table D.2: Ionic Species Aerosol Concentration Data (continued)

Sample	Aerosol Concentration (μg m^{-3})			
	Cl^-	NO_3^-	$SO_4^=$	NH_4^+
S97-N31D-RV-MX10	-0.003 ± 0.115	1.083 ± 0.201	0.039 ± 0.159	0.935 ± 0.374
S97-N31E-RV-CX	0.217 ± 0.213	63.839 ± 1.484	3.724 ± 0.294	17.469 ± 0.189
S97-N31E-RV-FX	0.074 ± 0.067	55.145 ± 0.636	3.054 ± 0.083	14.074 ± 0.108
S97-N32A-RV-CX	0.361 ± 0.297	41.333 ± 0.565	2.350 ± 0.411	12.403 ± 0.132
S97-N32A-RV-FX	0.147 ± 0.094	40.934 ± 0.595	1.725 ± 0.116	9.920 ± 0.151
S97-N32B-RV-CX	0.104 ± 0.367	1.815 ± 0.697	2.597 ± 0.507	3.980 ± 0.163
S97-N32B-RV-FX	-0.037 ± 0.116	1.331 ± 0.205	0.905 ± 0.144	1.202 ± 0.047
S97-N32C-RV-CX	0.391 ± 0.360	0.670 ± 0.684	0.618 ± 0.497	-0.015 ± 0.160
S97-N32C-RV-FX	0.033 ± 0.113	1.220 ± 0.201	0.804 ± 0.140	1.032 ± 0.046
S97-N32C-RV-MX5	0.024 ± 0.105	-0.017 ± 0.183	-0.024 ± 0.145	-0.188 ± 0.340
S97-N32C-RV-MX6	-0.019 ± 0.105	-0.011 ± 0.183	-0.011 ± 0.145	-0.187 ± 0.340
S97-N32C-RV-MX7	-0.016 ± 0.104	-0.027 ± 0.182	0.071 ± 0.144	-0.185 ± 0.340
S97-N32C-RV-MX8	-0.016 ± 0.105	-0.027 ± 0.183	0.150 ± 0.144	-0.186 ± 0.338
S97-N32C-RV-MX9	0.086 ± 0.105	-0.011 ± 0.183	0.052 ± 0.145	-0.187 ± 0.340
S97-N32C-RV-MX10	0.043 ± 0.104	-0.027 ± 0.183	-0.024 ± 0.144	-0.185 ± 0.340
S97-N32D-RV-CX	-0.024 ± 0.350	-0.157 ± 0.666	0.409 ± 0.484	0.003 ± 0.156
S97-N32D-RV-FX	0.029 ± 0.111	0.932 ± 0.197	0.675 ± 0.138	1.014 ± 0.045
S97-N32E-RV-CX	0.051 ± 0.201	0.303 ± 0.382	0.500 ± 0.278	-0.004 ± 0.089
S97-N32E-RV-FX	0.069 ± 0.064	0.520 ± 0.113	0.563 ± 0.079	0.597 ± 0.026
S97-T11B-TI-CX	2.032 ± 0.420	2.304 ± 0.799	4.277 ± 0.581	5.463 ± 0.187
S97-T11B-TI-FX	1.024 ± 0.141	1.573 ± 0.250	2.967 ± 0.175	2.272 ± 0.057
S97-T11B-TI-MX5	0.120 ± 0.131	0.360 ± 0.230	0.389 ± 0.181	-0.232 ± 0.427
S97-T11B-TI-MX6	0.210 ± 0.131	0.089 ± 0.230	0.073 ± 0.182	-0.233 ± 0.427
S97-T11B-TI-MX7	0.009 ± 0.132	0.184 ± 0.230	0.205 ± 0.182	0.876 ± 0.427
S97-T11B-TI-MX8	0.046 ± 0.132	0.089 ± 0.230	0.164 ± 0.182	0.867 ± 0.427
S97-T11B-TI-MX9	0.009 ± 0.131	0.040 ± 0.230	0.241 ± 0.182	0.894 ± 0.427
S97-T11B-TI-MX10	-0.016 ± 0.132	0.048 ± 0.230	0.250 ± 0.182	0.839 ± 0.427
S97-T11B-TO-CX	2.377 ± 0.458	1.586 ± 0.870	1.123 ± 0.633	0.003 ± 0.204
S97-T11B-TO-FX	1.947 ± 0.145	0.179 ± 0.258	0.933 ± 0.180	1.513 ± 0.059
S97-T11B-TO-MX5	0.197 ± 0.139	0.368 ± 0.243	0.060 ± 0.192	-0.249 ± 0.451
S97-T11B-TO-MX6	0.096 ± 0.139	0.046 ± 0.243	0.043 ± 0.192	-0.249 ± 0.451
S97-T11B-TO-MX7	0.035 ± 0.138	0.046 ± 0.242	0.077 ± 0.191	-0.251 ± 0.451
S97-T11B-TO-MX8	-0.021 ± 0.139	0.012 ± 0.243	0.038 ± 0.192	-0.254 ± 0.451
S97-T11B-TO-MX9	0.188 ± 0.139	-0.014 ± 0.243	-0.014 ± 0.192	-0.257 ± 0.451
S97-T11B-TO-MX10	-0.008 ± 0.139	-0.032 ± 0.243	-0.053 ± 0.192	-0.254 ± 0.451
S97-T21B-TI-CX	0.092 ± 0.422	2.465 ± 0.803	2.674 ± 0.584	5.248 ± 0.188
S97-T21B-TI-FX	0.556 ± 0.139	2.667 ± 0.247	2.866 ± 0.173	2.473 ± 0.056
S97-T21B-TI-MX5	-	0.298 ± 0.229	0.261 ± 0.181	0.770 ± 0.426
S97-T21B-TI-MX6	0.046 ± 0.131	0.257 ± 0.229	0.126 ± 0.181	0.789 ± 0.426
S97-T21B-TI-MX7	-0.020 ± 0.131	0.473 ± 0.229	0.269 ± 0.181	0.900 ± 0.424
S97-T21B-TI-MX8	-0.024 ± 0.131	0.191 ± 0.229	0.155 ± 0.181	0.873 ± 0.426
S97-T21B-TI-MX9	0.013 ± 0.131	0.064 ± 0.229	0.228 ± 0.181	0.882 ± 0.426
S97-T21B-TI-MX10	0.025 ± 0.131	-0.001 ± 0.229	0.261 ± 0.181	0.882 ± 0.426

Table D.2: Ionic Species Aerosol Concentration Data (continued)

Sample	Aerosol Concentration (μg m^{-3})			
	Cl^-	NO_3^-	$SO_4^=$	NH_4^+
S97-T21B-TO-FX	0.871 ± 0.139	0.601 ± 0.246	0.975 ± 0.172	1.589 ± 0.056
S97-T31B-TI-CX	2.634 ± 0.424	0.774 ± 0.805	1.759 ± 0.585	4.645 ± 0.188
S97-T31B-TI-FX	0.749 ± 0.140	0.246 ± 0.248	0.796 ± 0.173	1.367 ± 0.057
S97-T31B-TI-MX5	0.336 ± 0.131	0.064 ± 0.228	0.093 ± 0.181	-0.231 ± 0.426
S97-T31B-TI-MX6	0.066 ± 0.131	0.015 ± 0.229	0.024 ± 0.181	-0.233 ± 0.426
S97-T31B-TI-MX7	0.078 ± 0.131	-0.030 ± 0.229	0.052 ± 0.181	-0.232 ± 0.426
S97-T31B-TI-MX8	0.037 ± 0.130	-0.042 ± 0.228	0.048 ± 0.180	-0.229 ± 0.426
S97-T31B-TI-MX9	0.033 ± 0.131	-0.010 ± 0.228	0.068 ± 0.181	0.789 ± 0.426
S97-T31B-TI-MX10	0.042 ± 0.131	-0.030 ± 0.229	0.048 ± 0.181	-0.231 ± 0.426
S97-T31B-TO-CX	1.738 ± 0.445	0.371 ± 0.845	0.662 ± 0.614	0.002 ± 0.198
S97-T31B-TO-FX	0.541 ± 0.141	0.047 ± 0.249	0.293 ± 0.174	0.003 ± 0.057
S97-T31B-TO-MX5	0.115 ± 0.130	0.027 ± 0.227	0.019 ± 0.180	-0.233 ± 0.422
S97-T31B-TO-MX6	0.013 ± 0.130	-0.017 ± 0.228	-0.013 ± 0.180	-0.234 ± 0.422
S97-T31B-TO-MX7	0.033 ± 0.130	-0.018 ± 0.227	-0.042 ± 0.180	-0.232 ± 0.422
S97-T31B-TO-MX8	-0.011 ± 0.130	-0.030 ± 0.227	0.028 ± 0.180	-0.233 ± 0.422
S97-T31B-TO-MX9	0.054 ± 0.130	-0.038 ± 0.228	-0.001 ± 0.180	-0.234 ± 0.422
S97-T31B-TO-MX10	-0.024 ± 0.130	-0.050 ± 0.227	-0.046 ± 0.180	-0.232 ± 0.422
S97-T41B-TI-CX	0.375 ± 0.435	1.536 ± 0.827	1.445 ± 0.602	4.788 ± 0.194
S97-T41B-TI-FX	0.135 ± 0.140	0.529 ± 0.249	0.902 ± 0.174	1.462 ± 0.057
S97-T41B-TI-MX5	-0.024 ± 0.131	0.163 ± 0.229	0.077 ± 0.181	-0.233 ± 0.424
S97-T41B-TI-MX6	-0.024 ± 0.131	0.019 ± 0.229	0.032 ± 0.181	-0.232 ± 0.426
S97-T41B-TI-MX7	0.091 ± 0.131	0.052 ± 0.229	0.081 ± 0.181	0.743 ± 0.426
S97-T41B-TI-MX8	-0.024 ± 0.131	-0.001 ± 0.229	0.073 ± 0.181	-0.232 ± 0.426
S97-T41B-TI-MX9	0.025 ± 0.131	0.015 ± 0.229	0.187 ± 0.181	0.831 ± 0.426
S97-T41B-TI-MX10	0.005 ± 0.131	-0.014 ± 0.230	0.085 ± 0.182	-0.236 ± 0.426
S97-T41B-TO-CX	0.284 ± 0.425	0.913 ± 0.808	0.769 ± 0.587	0.011 ± 0.189
S97-T41B-TO-FX	0.239 ± 0.151	0.334 ± 0.267	0.490 ± 0.188	1.336 ± 0.062
S97-B11A-AZ-MX5	0.000 ± 0.616	0.656 ± 1.074	0.000 ± 0.795	0.434 ± 0.276
S97-B11A-AZ-MX6	0.000 ± 0.616	0.000 ± 1.073	0.000 ± 0.795	0.434 ± 0.275
S97-B11A-AZ-MX7	0.000 ± 0.617	0.000 ± 1.074	0.975 ± 0.796	0.434 ± 0.276
S97-B11A-AZ-MX8	0.000 ± 0.615	0.774 ± 1.072	0.853 ± 0.794	0.434 ± 0.275
S97-B11A-AZ-MX9	0.000 ± 0.618	0.757 ± 1.076	1.554 ± 0.797	0.435 ± 0.276
S97-B11A-AZ-MX10	0.000 ± 0.612	0.711 ± 1.067	0.849 ± 0.790	0.432 ± 0.274
S97-B11A-DB-CX	0.000 ± 0.776	1.026 ± 1.352	0.000 ± 1.001	-7.898 ± 0.347
S97-B11A-DB-FX	0.148 ± 0.329	0.456 ± 0.573	0.000 ± 0.424	-2.866 ± 0.147
S97-B11A-DB-MX5	-	0.755 ± 1.133	0.000 ± 0.839	-4.485 ± 0.291
S97-B11A-DB-MX6	0.336 ± 0.651	0.839 ± 1.133	0.462 ± 0.839	-4.486 ± 0.291
S97-B11A-DB-MX7	0.000 ± 0.651	0.084 ± 1.134	0.000 ± 0.840	-4.616 ± 0.291
S97-B11A-DB-MX8	0.168 ± 0.651	0.042 ± 1.134	0.252 ± 0.840	-4.615 ± 0.291
S97-B11A-DB-MX9	0.126 ± 0.650	0.042 ± 1.133	0.000 ± 0.839	-4.613 ± 0.291
S97-B11A-DB-MX10	0.042 ± 0.652	0.063 ± 1.135	0.000 ± 0.841	-4.622 ± 0.291
S97-B11A-ML-CX	0.000 ± 0.775	0.000 ± 1.350	0.575 ± 1.000	-7.888 ± 0.347
S97-B11A-ML-FX	-	0.391 ± 0.571	0.349 ± 0.423	-2.858 ± 0.147

Table D.2: Ionic Species Aerosol Concentration Data (continued)

Sample	Aerosol Concentration (μg m^{-3})			
	Cl^-	NO_3^-	$SO_4^=$	NH_4^+
S97-B11A-RV-CX	0.000 ± 0.776	0.000 ± 1.352	0.000 ± 1.002	-7.899 ± 0.347
S97-B11A-RV-FX	0.254 ± 0.328	0.423 ± 0.571	0.349 ± 0.423	-2.860 ± 0.147
S97-B11A-RV-MX5	0.000 ± 0.650	0.000 ± 1.132	0.021 ± 0.838	-4.608 ± 0.291
S97-B11A-RV-MX6	0.210 ± 0.651	0.168 ± 1.133	0.105 ± 0.840	-4.614 ± 0.291
S97-B11A-RV-MX7	0.000 ± 0.651	0.126 ± 1.135	0.021 ± 0.841	-4.619 ± 0.291
S97-B11A-RV-MX8	0.000 ± 0.651	0.000 ± 1.134	0.000 ± 0.840	-4.616 ± 0.291
S97-B11A-RV-MX9	0.000 ± 0.651	0.000 ± 1.134	0.000 ± 0.840	-4.617 ± 0.291
S97-B11A-RV-MX10	0.000 ± 0.643	0.000 ± 1.120	0.062 ± 0.829	-4.558 ± 0.287
S97-B11A-TI-CX	0.000 ± 0.778	0.000 ± 1.355	0.000 ± 1.004	-7.916 ± 0.348
S97-B11A-TI-FX	0.000 ± 0.327	0.000 ± 0.570	0.359 ± 0.422	-2.853 ± 0.146
S97-B11A-TI-MX5	0.000 ± 0.649	0.000 ± 1.131	0.168 ± 0.838	-4.571 ± 0.290
S97-B11A-TI-MX6	0.000 ± 0.650	0.042 ± 1.133	0.168 ± 0.839	-4.583 ± 0.291
S97-B11A-TI-MX7	0.000 ± 0.650	0.063 ± 1.133	0.063 ± 0.839	-4.579 ± 0.291
S97-B11A-TI-MX8	0.000 ± 0.653	0.126 ± 1.138	0.506 ± 0.843	-4.600 ± 0.292
S97-B11A-TI-MX9	0.630 ± 0.651	0.273 ± 1.135	0.231 ± 0.840	-4.586 ± 0.291
S97-B11A-TI-MX10	0.000 ± 0.651	0.021 ± 1.135	0.252 ± 0.840	-4.586 ± 0.291
S97-B21A-DB-CX	-	0.000 ± 1.351	0.775 ± 1.000	-7.890 ± 0.347
S97-B21A-DB-FX	-	0.581 ± 0.570	0.275 ± 0.422	-2.854 ± 0.146
S97-B21A-DB-MX5	0.273 ± 0.650	0.063 ± 1.133	0.168 ± 0.839	-4.579 ± 0.291
S97-B21A-DB-MX6	0.126 ± 0.651	0.252 ± 1.134	0.042 ± 0.840	-4.585 ± 0.291
S97-B21A-DB-MX7	0.168 ± 0.652	0.273 ± 1.135	0.000 ± 0.841	-4.622 ± 0.291
S97-B21A-DB-MX8	0.294 ± 0.651	0.189 ± 1.134	0.000 ± 0.840	-4.616 ± 0.291
S97-B21A-DB-MX9	-	-	-	-4.616 ± 0.291
S97-B21A-DB-MX10	0.400 ± 0.652	0.021 ± 1.136	0.042 ± 0.842	-4.625 ± 0.292
S97-B21A-ML-CX	0.150 ± 0.776	0.000 ± 1.351	0.000 ± 1.001	-7.893 ± 0.347
S97-B21A-ML-FX	0.424 ± 0.328	-	0.498 ± 0.424	-2.863 ± 0.147
S97-B21A-ML-MX5	0.419 ± 0.649	0.063 ± 1.130	0.042 ± 0.837	-4.569 ± 0.290
S97-B21A-ML-MX6	0.273 ± 0.651	0.189 ± 1.134	0.189 ± 0.840	-4.586 ± 0.291
S97-B21A-ML-MX7	0.231 ± 0.650	0.671 ± 1.133	0.000 ± 0.839	-4.486 ± 0.291
S97-B21A-ML-MX8	0.210 ± 0.650	0.126 ± 1.133	0.000 ± 0.839	-4.579 ± 0.291
S97-B21A-ML-MX9	0.126 ± 0.651	0.063 ± 1.133	0.189 ± 0.840	-4.582 ± 0.291
S97-B21A-ML-MX10	0.084 ± 0.653	0.189 ± 1.137	0.063 ± 0.842	-4.627 ± 0.292
S97-B21A-RV-CX	0.175 ± 0.776	1.426 ± 1.351	0.851 ± 1.001	-7.893 ± 0.347
S97-B21A-RV-FX	0.232 ± 0.327	0.908 ± 0.570	0.274 ± 0.422	-2.853 ± 0.146
S97-B21A-RV-MX5	0.000 ± 0.615	0.000 ± 1.071	0.754 ± 0.793	0.433 ± 0.275
S97-B21A-RV-MX6	0.496 ± 0.615	0.714 ± 1.071	0.754 ± 0.794	0.433 ± 0.275
S97-B21A-RV-MX7	0.252 ± 0.650	0.776 ± 1.132	0.482 ± 0.838	-4.481 ± 0.291
S97-B21A-RV-MX8	0.000 ± 0.615	0.734 ± 1.072	0.734 ± 0.794	0.433 ± 0.275
S97-B21A-RV-MX9	0.042 ± 0.650	0.042 ± 1.133	0.063 ± 0.839	-4.613 ± 0.291
S97-B21A-RV-MX10	0.000 ± 0.616	0.716 ± 1.074	1.352 ± 0.795	0.434 ± 0.276

D.3 Gas-Phase Pollutant Concentration Data

Table D.3: Gas-Phase Pollutant Concentration Data

Sample	Gas Concentration (μg m^{-3})		
	HNO_3	HCl	NH_3
S97-V11A-LA-GX	0.00 ± 0.46	0.06 ± 0.31	8.095 ± 1.220
S97-V11B-LA-GX	4.37 ± 0.64	-0.21 ± 0.43	15.662 ± 1.781
S97-V11C-LA-GX	5.35 ± 0.59	2.65 ± 0.40	14.363 ± 1.629
S97-V11D-LA-GX	1.78 ± 0.44	0.28 ± 0.29	7.837 ± 1.646
S97-V11E-LA-GX	-0.77 ± 0.33	-0.34 ± 0.22	8.234 ± 0.925
S97-V12A-LA-GX	0.25 ± 0.50	0.03 ± 0.33	9.454 ± 1.256
S97-V12B-LA-GX	0.63 ± 0.58	0.32 ± 0.39	12.911 ± 1.476
S97-V12C-LA-GX	9.67 ± 0.57	4.01 ± 0.38	16.478 ± 1.430
S97-V12D-LA-GX	10.69 ± 0.60	4.09 ± 0.40	9.234 ± 1.533
S97-V12E-LA-GX	1.82 ± 0.33	0.82 ± 0.22	9.481 ± 0.841
S97-V11A-AZ-GX	0.15 ± 0.50	0.35 ± 0.34	8.103 ± 1.154
S97-V11B-AZ-GX	0.45 ± 0.64	0.12 ± 0.43	9.935 ± 1.518
S97-V11C-AZ-GX	7.32 ± 0.61	3.32 ± 0.41	11.397 ± 1.460
S97-V11D-AZ-GX	9.60 ± 0.62	3.87 ± 0.41	9.778 ± 1.482
S97-V11E-AZ-GX	1.29 ± 0.35	0.65 ± 0.23	8.319 ± 0.867
S97-V12A-AZ-GX	0.31 ± 0.49	0.08 ± 0.33	8.784 ± 1.182
S97-V12B-AZ-GX	1.43 ± 0.61	0.36 ± 0.41	11.753 ± 1.499
S97-V12C-AZ-GX	9.27 ± 0.60	3.73 ± 0.40	9.380 ± 1.502
S97-V12D-AZ-GX	14.25 ± 0.61	3.30 ± 0.41	10.439 ± 1.470
S97-V12E-AZ-GX	3.11 ± 0.33	1.06 ± 0.22	8.536 ± 0.814
S97-V11A-RV-GX	0.20 ± 0.50	-0.07 ± 0.33	17.431 ± 1.279
S97-V11B-RV-GX	2.03 ± 0.61	0.29 ± 0.41	23.395 ± 1.541
S97-V11C-RV-GX	3.62 ± 0.59	0.92 ± 0.39	28.476 ± 1.510
S97-V11D-RV-GX	5.61 ± 0.58	1.90 ± 0.39	23.813 ± 1.555
S97-V11E-RV-GX	1.01 ± 0.33	0.24 ± 0.22	12.060 ± 0.795
S97-V12A-RV-GX	0.23 ± 0.48	-0.03 ± 0.32	13.345 ± 1.215
S97-V12B-RV-GX	0.68 ± 0.61	0.32 ± 0.41	15.960 ± 1.584
S97-V12C-RV-GX	3.21 ± 0.60	1.13 ± 0.40	19.055 ± 1.523
S97-V12D-RV-GX	7.04 ± 0.59	1.29 ± 0.39	45.403 ± 1.495
S97-V12E-RV-GX	3.35 ± 0.33	0.92 ± 0.22	20.790 ± 0.819
S97-V21A-LA-GX	-0.03 ± 0.46	0.09 ± 0.31	6.871 ± 1.129
S97-V21B-LA-GX	1.38 ± 0.59	3.30 ± 0.40	8.549 ± 1.465
S97-V21C-LA-GX	10.57 ± 0.57	4.37 ± 0.38	10.995 ± 1.410
S97-V21D-LA-GX	9.73 ± 0.59	3.91 ± 0.39	6.231 ± 1.493
S97-V21E-LA-GX	1.17 ± 0.32	0.68 ± 0.22	6.331 ± 0.828
S97-V22A-LA-GX	0.25 ± 0.48	0.38 ± 0.32	6.307 ± 1.224
S97-V22B-LA-GX	0.83 ± 0.58	0.50 ± 0.39	9.196 ± 1.469
S97-V22C-LA-GX	7.34 ± 0.57	4.72 ± 0.38	10.614 ± 1.476
S97-V22D-LA-GX	9.87 ± 0.60	3.60 ± 0.40	6.707 ± 1.475
S97-V22E-LA-GX	1.48 ± 0.33	0.72 ± 0.22	4.865 ± 0.857

Table D.3: Gas-Phase Pollutant Concentration Data (continued)

Sample	Gas Concentration (μg m^{-3})		
	HNO_3	HCl	NH_3
S97-V21A-AZ-GX	0.38 ± 0.48	0.85 ± 0.32	6.586 ± 1.069
S97-V21B-AZ-GX	1.44 ± 0.61	-0.37 ± 0.40	7.783 ± 1.428
S97-V21C-AZ-GX	13.79 ± 0.60	2.81 ± 0.40	7.483 ± 1.347
S97-V21D-AZ-GX	20.66 ± 0.61	1.94 ± 0.41	7.647 ± 1.399
S97-V21E-AZ-GX	2.64 ± 0.34	-0.03 ± 0.22	6.014 ± 0.760
S97-V22A-AZ-GX	0.95 ± 0.49	0.12 ± 0.33	5.559 ± 1.150
S97-V22B-AZ-GX	1.75 ± 0.61	-0.11 ± 0.41	7.353 ± 1.393
S97-V22C-AZ-GX	13.46 ± 0.61	3.70 ± 0.41	8.934 ± 1.386
S97-V22D-AZ-GX	22.40 ± 0.61	2.28 ± 0.41	7.334 ± 1.373
S97-V22E-AZ-GX	2.95 ± 0.33	0.06 ± 0.22	6.510 ± 0.771
S97-V21A-RV-GX	0.51 ± 0.48	2.15 ± 0.32	11.513 ± 1.278
S97-V21B-RV-GX	1.03 ± 0.61	0.09 ± 0.40	15.733 ± 1.690
S97-V21C-RV-GX	4.29 ± 0.58	0.35 ± 0.39	37.439 ± 1.409
S97-V21D-RV-GX	8.59 ± 0.59	1.05 ± 0.39	31.671 ± 1.436
S97-V21E-RV-GX	2.29 ± 0.33	0.43 ± 0.22	20.166 ± 0.817
S97-V22A-RV-GX	0.64 ± 0.49	-0.14 ± 0.33	12.806 ± 1.210
S97-V22B-RV-GX	1.20 ± 0.59	0.84 ± 0.39	15.884 ± 1.424
S97-V22C-RV-GX	6.95 ± 0.60	1.17 ± 0.40	26.171 ± 1.479
S97-V22D-RV-GX	9.34 ± 0.60	1.13 ± 0.40	35.975 ± 1.465
S97-V22E-RV-GX	0.77 ± 0.33	0.09 ± 0.22	19.012 ± 0.799
S97-N21D-ML-GX	-	-	136.588 ± 0.000
S97-N21E-ML-GX	0.65 ± 1.76	0.13 ± 0.23	-
S97-N22A-ML-GX	7.33 ± 0.46	0.51 ± 0.31	-
S97-N22B-ML-GX	-0.62 ± 0.59	0.21 ± 0.39	150.540 ± 11.046
S97-N22C-ML-GX	6.99 ± 0.59	3.17 ± 0.39	52.281 ± 22.085
S97-N22D-ML-GX	4.76 ± 0.57	1.90 ± 0.38	155.098 ± 9.001
S97-N22E-ML-GX	1.31 ± 0.32	0.19 ± 0.22	-
S97-N23A-ML-GX	0.44 ± 0.48	0.21 ± 0.32	-
S97-N23B-ML-GX	-0.04 ± 0.59	0.34 ± 0.39	80.740 ± 0.000
S97-N23C-ML-GX	3.78 ± 0.58	0.68 ± 0.39	232.908 ± 6.325
S97-N23D-ML-GX	3.99 ± 0.58	1.25 ± 0.39	96.994 ± 29.359
S97-N23E-ML-GX	0.72 ± 0.32	0.18 ± 0.22	-
S97-N31A-DB-GX	1.67 ± 1.08	0.10 ± 0.31	7.593 ± 1.197
S97-N31B-DB-GX	1.06 ± 0.59	0.36 ± 0.39	13.469 ± 1.569
S97-N31C-DB-GX	78.42 ± 2.17	2.28 ± 0.39	11.618 ± 1.522
S97-N31D-DB-GX	11.92 ± 0.50	2.58 ± 0.35	8.108 ± 1.424
S97-N31E-DB-GX	16.03 ± 0.86	0.57 ± 0.21	4.410 ± 0.825
S97-N32A-DB-GX	4.47 ± 1.98	0.08 ± 0.32	6.689 ± 1.227
S97-N32B-DB-GX	2.18 ± 0.58	-0.10 ± 0.39	25.997 ± 1.517
S97-N32C-DB-GX	11.38 ± 0.57	2.34 ± 0.38	26.186 ± 1.459
S97-N32D-DB-GX	8.45 ± 0.57	2.25 ± 0.38	14.201 ± 1.517
S97-N32E-DB-GX	1.93 ± 0.32	0.52 ± 0.21	9.733 ± 0.843
S97-N31A-ML-GX	0.77 ± 0.68	-0.86 ± 0.31	42.707 ± 1.172

Table D.3: Gas-Phase Pollutant Concentration Data (continued)

Sample	Gas Concentration (μg m^{-3})		
	HNO_3	HCl	NH_3
S97-N31B-ML-GX	4.30 ± 0.57	1.88 ± 0.38	40.490 ± 1.484
S97-N31C-ML-GX	2.84 ± 1.67	-0.55 ± 0.40	112.346 ± 2.361
S97-N31D-ML-GX	2.99 ± 2.60	-0.96 ± 0.38	123.885 ± 2.350
S97-N31E-ML-GX	11.07 ± 1.46	0.15 ± 0.21	69.544 ± 1.260
S97-N32A-ML-GX	6.03 ± 1.75	1.28 ± 0.32	37.312 ± 1.319
S97-N32B-ML-GX	3.26 ± 0.60	2.29 ± 0.40	22.507 ± 1.583
S97-N32C-ML-GX	3.14 ± 0.56	1.63 ± 0.38	6.526 ± 1.498
S97-N32D-ML-GX	2.37 ± 0.62	0.69 ± 0.41	5.233 ± 1.496
S97-N32E-ML-GX	1.03 ± 0.34	-0.42 ± 0.23	2.812 ± 0.803
S97-N31A-RV-GX	3.06 ± 0.71	0.13 ± 0.31	8.521 ± 1.126
S97-N31B-RV-GX	1.71 ± 0.60	0.08 ± 0.40	11.021 ± 1.420
S97-N31C-RV-GX	4.10 ± 0.59	0.98 ± 0.40	27.541 ± 1.463
S97-N31D-RV-GX	1.71 ± 2.06	0.14 ± 0.37	61.241 ± 1.395
S97-N31E-RV-GX	6.63 ± 1.63	-0.01 ± 0.24	12.567 ± 0.846
S97-N32A-RV-GX	4.46 ± 0.49	0.91 ± 0.33	11.496 ± 1.207
S97-N32B-RV-GX	1.51 ± 0.61	0.88 ± 0.41	10.595 ± 1.587
S97-N32C-RV-GX	5.44 ± 0.60	1.61 ± 0.40	6.724 ± 1.421
S97-N32D-RV-GX	2.93 ± 0.58	1.10 ± 0.39	4.327 ± 1.383
S97-N32E-RV-GX	0.87 ± 0.33	0.41 ± 0.22	3.738 ± 0.804
S97-T11B-TI-GX	-0.11 ± 0.73	-1.64 ± -0.35	107.070 ± 1.937
S97-T11B-TO-GX	-2.23 ± 0.76	-0.75 ± 0.51	7.981 ± 1.913
S97-T21B-TI-GX	0.10 ± 0.72	0.23 ± 0.48	98.243 ± 1.998
S97-T31B-TI-GX	0.16 ± 0.73	0.07 ± 0.49	106.785 ± 2.019
S97-T31B-TO-GX	0.12 ± 0.73	0.57 ± 0.49	6.600 ± 1.875
S97-T41B-TI-GX	-0.08 ± 0.73	0.13 ± 0.49	141.452 ± 2.085
S97-T41B-TO-GX	0.00 ± 0.73	0.25 ± 0.49	6.576 ± 1.855
S97-B11A-DB-GX	0.58 ± 0.56	0.77 ± 0.32	-12.966 ± 0.378
S97-B11A-ML-GX	-0.37 ± 0.79	-0.32 ± 0.46	-12.991 ± 0.379
S97-B11A-RV-GX	0.06 ± 0.79	-0.04 ± 0.46	-12.966 ± 0.378
S97-B11A-TI-GX	-0.48 ± 0.79	0.41 ± 0.46	0.249 ± 0.189
S97-B21A-DB-GX	0.17 ± 0.68	0.92 ± 0.32	-12.968 ± 0.379
S97-B21A-ML-GX	-0.09 ± 0.79	-0.31 ± 0.46	-12.945 ± 0.378
S97-B21A-RV-GX	-0.01 ± 0.79	0.11 ± 0.46	-12.961 ± 0.378

D.4 Trace Elements Aerosol Concentration Data (Al, As, Au, Ba)

Table D.4: Trace Metals Aerosol Concentration Data (Al, As, Au, Ba)

Sample	Aerosol Concentration (ng m^{-3})			
	Al	As	Au	Ba
S97-V11A-LA-CX	577.26 ± 442.02	0.0513 ± 0.2060	-0.002048 ± 0.004911	56.89 ± 58.07
S97-V11A-LA-FX	136.21 ± 23.21	0.0261 ± 0.2274	0.001586 ± 0.001061	4.22 ± 4.15
S97-V11B-LA-CX	1370.57 ± 609.16	0.8501 ± 0.3416	-0.002592 ± 0.006750	5.00 ± 38.43
S97-V11B-LA-FX	159.42 ± 103.25	0.8120 ± 0.3428	0.007588 ± 0.004100	17.11 ± 5.98
S97-V11C-LA-CX	2492.38 ± 569.92	2.1917 ± 0.4198	0.006051 ± 0.007599	42.54 ± 39.30
S97-V11C-LA-FX	47.21 ± 28.81	0.5992 ± 0.3051	0.008671 ± 0.004777	7.71 ± 5.11
S97-V11D-LA-CX	933.33 ± 575.82	0.0486 ± 0.2944	-0.002255 ± 0.006397	1.09 ± 39.38
S97-V11D-LA-FX	161.09 ± 31.06	-0.1427 ± 0.3079	0.005046 ± 0.002860	1.09 ± 5.25
S97-V11E-LA-CX	354.45 ± 308.39	0.2807 ± 0.1605	-0.001451 ± 0.003432	16.74 ± 20.58
S97-V11E-LA-FX	5.11 ± 16.06	0.1046 ± 0.1698	0.000393 ± 0.000425	3.26 ± 3.03
S97-V12A-LA-CX	820.33 ± 460.62	0.7906 ± 0.2921	-0.002243 ± 0.005116	40.29 ± 30.95
S97-V12A-LA-FX	18.72 ± 23.59	0.2056 ± 0.2478	-	12.88 ± 4.82
S97-V12B-LA-CX	1896.45 ± 543.73	-	-0.002461 ± 0.005978	120.40 ± 39.70
S97-V12B-LA-FX	99.05 ± 27.82	1.2920 ± 0.4017	0.018778 ± 0.009951	18.17 ± 5.74
S97-V12B-LA-MX5	-29.45 ± 62.69	-	0.000707 ± 0.000573	-
S97-V12B-LA-MX6	-15.06 ± 62.70	0.0137 ± 0.1078	-	0.59 ± 2.52
S97-V12B-LA-MX7	-27.69 ± 62.70	-	0.000487 ± 0.000424	-
S97-V12B-LA-MX8	-28.87 ± 62.69	0.0196 ± 0.1003	-	-
S97-V12B-LA-MX9	-29.75 ± 62.70	0.0490 ± 0.0949	-0.000012 ± 0.000244	-
S97-V12B-LA-MX10	-30.63 ± 62.70	0.0460 ± 0.1038	-	-
S97-V12C-LA-CX	1632.07 ± 538.59	2.2761 ± 0.4035	-0.000885 ± 0.006019	68.88 ± 37.01
S97-V12C-LA-FX	120.59 ± 28.07	0.9943 ± 0.3125	0.005538 ± 0.003345	21.57 ± 5.76
S97-V12D-LA-CX	1095.96 ± 565.48	0.1641 ± 0.2852	0.000946 ± 0.006552	24.35 ± 38.32
S97-V12D-LA-FX	31.74 ± 29.14	-	0.041276 ± 0.021557	5.56 ± 5.23
S97-V12E-LA-CX	930.28 ± 307.44	0.2917 ± 0.1970	0.000366 ± 0.003525	39.26 ± 21.31
S97-V12E-LA-FX	24.27 ± 16.00	0.1903 ± 0.1697	0.002854 ± 0.001709	4.08 ± 2.99
S97-V11A-AZ-CX	1338.36 ± 492.24	0.5227 ± 0.2439	-0.002366 ± 0.005442	26.55 ± 31.66
S97-V11A-AZ-FX	62.44 ± 23.87	0.1798 ± 0.2447	0.000054 ± 0.000392	3.22 ± 4.10
S97-V11B-AZ-CX	6351.59 ± 679.92	4.8282 ± 0.7022	-0.002663 ± 0.006934	169.27 ± 44.03
S97-V11B-AZ-FX	380.11 ± 35.73	1.2868 ± 0.3495	0.000580 ± 0.000752	18.11 ± 5.72
S97-V11C-AZ-CX	3176.10 ± 617.01	1.8950 ± 0.3892	0.001869 ± 0.007111	77.59 ± 39.84
S97-V11C-AZ-FX	159.49 ± 30.46	0.7138 ± 0.3205	-0.000240 ± 0.000403	10.21 ± 5.12
S97-V11D-AZ-CX	2615.02 ± 615.73	1.1359 ± 0.4049	-0.001962 ± 0.006748	77.95 ± 39.71
S97-V11D-AZ-FX	97.55 ± 29.93	0.2244 ± 0.3055	0.002713 ± 0.001739	9.24 ± 5.07
S97-V11D-AZ-MX5	5.92 ± 71.50	-	0.000742 ± 0.000613	1.78 ± 2.97
S97-V11D-AZ-MX6	4.58 ± 71.47	-	0.000635 ± 0.000524	1.78 ± 3.05
S97-V11D-AZ-MX7	3.91 ± 71.47	-	0.000672 ± 0.000532	-
S97-V11D-AZ-MX8	-13.48 ± 71.47	0.0758 ± 0.1089	-0.000004 ± 0.000274	-
S97-V11D-AZ-MX9	-31.21 ± 71.42	-	0.000371 ± 0.000447	0.41 ± 2.93
S97-V11D-AZ-MX10	-19.16 ± 71.43	-	-	-
S97-V11E-AZ-CX	-	1.1390 ± 0.2227	-0.001259 ± 0.003839	-
S97-V11E-AZ-FX	85.99 ± 17.50	0.6913 ± 0.1928	0.027806 ± 0.014063	6.24 ± 3.15

Table D.4: Trace Metals Aerosol Concentration Data (Al, As, Au, Ba) (continued)

Sample	Aerosol Concentration (ng m^{-3})			
	Al	As	Au	Ba
S97-V12A-AZ-CX	1693.99 ± 526.94	1.0536 ± 0.2796	-0.000795 ± 0.005405	32.14 ± 31.51
S97-V12A-AZ-FX	81.89 ± 25.24	0.3704 ± 0.2808	0.001150 ± 0.001033	8.09 ± 4.49
S97-V12B-AZ-CX	-	2.1103 ± 0.3802	0.011460 ± 0.010065	97.82 ± 48.36
S97-V12B-AZ-FX	346.92 ± 39.60	1.4781 ± 0.3542	0.004214 ± 0.002556	21.32 ± 6.21
S97-V12C-AZ-CX	3529.31 ± 721.38	2.1639 ± 0.4284	-0.001652 ± 0.006680	62.74 ± 39.51
S97-V12C-AZ-FX	267.61 ± 35.51	0.7899 ± 0.3218	0.000565 ± 0.000732	15.65 ± 5.73
S97-V12D-AZ-CX	1918.19 ± 640.67	1.5005 ± 0.3601	0.019766 ± 0.013171	57.05 ± 39.84
S97-V12D-AZ-FX	151.46 ± 32.09	0.3928 ± 0.3131	0.001690 ± 0.001249	13.66 ± 5.91
S97-V12D-AZ-MX5	-0.75 ± 69.80	-0.0396 ± 0.1061	0.000415 ± 0.000458	2.07 ± 2.81
S97-V12D-AZ-MX6	-6.30 ± 69.78	-	0.000405 ± 0.000477	0.92 ± 2.78
S97-V12D-AZ-MX7	-23.95 ± 69.76	-0.0109 ± 0.1093	0.000219 ± 0.000348	-1.01 ± 2.79
S97-V12D-AZ-MX8	-27.21 ± 69.76	-	0.000366 ± 0.000428	-
S97-V12D-AZ-MX9	-	-0.0109 ± 0.1053	0.000075 ± 0.000304	-0.97 ± 2.73
S97-V12D-AZ-MX10	-34.92 ± 69.75	-0.0435 ± 0.1047	-0.000023 ± 0.000263	-
S97-V12E-AZ-CX	2039.36 ± 410.83	1.8623 ± 0.2860	0.004083 ± 0.004663	62.99 ± 22.67
S97-V12E-AZ-FX	96.53 ± 17.93	0.8889 ± 0.2005	0.002911 ± 0.001849	16.61 ± 3.83
S97-V11A-RV-CX	492.90 ± 505.28	0.1391 ± 0.2430	-0.002485 ± 0.005627	13.81 ± 32.02
S97-V11A-RV-FX	33.50 ± 25.53	-0.0714 ± 0.2619	0.000340 ± 0.000531	1.49 ± 4.30
S97-V11B-RV-CX	2626.01 ± 620.35	0.9479 ± 0.3539	-0.002876 ± 0.006758	41.65 ± 40.88
S97-V11B-RV-FX	117.24 ± 30.80	0.1134 ± 0.3058	-	15.46 ± 6.23
S97-V11C-RV-CX	682.51 ± 593.75	0.0879 ± 0.2786	-0.002200 ± 0.006619	14.33 ± 38.45
S97-V11C-RV-FX	482.77 ± 36.02	0.0128 ± 0.2960	0.000564 ± 0.000694	5.71 ± 5.03
S97-V11D-RV-CX	1339.96 ± 595.21	-	-0.000700 ± 0.006692	25.59 ± 39.90
S97-V11D-RV-FX	1028.80 ± 53.14	0.2100 ± 0.3000	0.001153 ± 0.000936	31.10 ± 5.71
S97-V11D-RV-MX5	-16.35 ± 60.94	-	-	0.67 ± 2.27
S97-V11D-RV-MX6	-20.06 ± 60.92	0.0590 ± 0.0922	0.000647 ± 0.000513	0.15 ± 2.42
S97-V11D-RV-MX7	-25.19 ± 60.94	0.2530 ± 0.1008	0.003255 ± 0.001697	1.23 ± 2.61
S97-V11D-RV-MX8	-26.62 ± 60.93	0.4527 ± 0.1062	0.000285 ± 0.000336	-
S97-V11D-RV-MX9	44.42 ± 61.12	0.4527 ± 0.1124	0.002228 ± 0.001246	-
S97-V11D-RV-MX10	-29.19 ± 60.92	0.1902 ± 0.0955	-0.000112 ± 0.000218	-
S97-V11E-RV-CX	987.98 ± 326.11	-0.0702 ± 0.1659	-0.001049 ± 0.003609	31.94 ± 21.97
S97-V11E-RV-FX	73.17 ± 16.22	0.0624 ± 0.1632	0.000106 ± 0.000289	7.92 ± 2.92
S97-V12A-RV-CX	635.38 ± 485.73	0.0102 ± 0.2337	-0.002339 ± 0.005405	24.83 ± 31.25
S97-V12A-RV-FX	77.23 ± 23.64	0.0070 ± 0.2412	0.001450 ± 0.001050	3.70 ± 4.13
S97-V12B-RV-CX	2070.44 ± 621.56	1.0560 ± 0.3244	-0.002743 ± 0.006833	61.61 ± 41.34
S97-V12B-RV-FX	190.58 ± 31.24	0.8520 ± 0.3269	0.000430 ± 0.000729	21.50 ± 7.42
S97-V12C-RV-CX	1733.85 ± 603.41	0.3929 ± 0.4151	-0.000232 ± 0.006814	23.95 ± 41.06
S97-V12C-RV-FX	290.71 ± 32.09	0.1558 ± 0.3014	0.001538 ± 0.001177	18.65 ± 5.53
S97-V12D-RV-CX	1515.54 ± 591.11	0.7310 ± 0.3205	-0.001720 ± 0.006569	12.32 ± 39.23
S97-V12D-RV-FX	577.66 ± 38.80	0.2817 ± 0.3027	-0.000465 ± 0.000364	34.08 ± 7.40
S97-V12D-RV-MX5	149.70 ± 62.69	0.1332 ± 0.0965	-	21.20 ± 3.88
S97-V12D-RV-MX6	29.87 ± 61.12	0.4527 ± 0.1076	0.000077 ± 0.000259	10.36 ± 3.65
S97-V12D-RV-MX7	9.90 ± 61.39	0.6524 ± 0.1158	0.000174 ± 0.000285	3.23 ± 3.32
S97-V12D-RV-MX8	18.46 ± 61.06	-	0.006679 ± 0.003715	-
S97-V12D-RV-MX9	-12.64 ± 60.95	1.7651 ± 0.2671	-	1.80 ± 3.05
S97-V12D-RV-MX10	-7.22 ± 60.99	0.4812 ± 0.1092	0.000174 ± 0.000306	-

Table D.4: Trace Metals Aerosol Concentration Data (Al, As, Au, Ba) (continued)

Sample	Aerosol Concentration (ng m^{-3})			
	Al	As	Au	Ba
S97-V12E-RV-CX	1200.66 ± 329.43	0.8696 ± 134.3254	-0.001144 ± 0.003630	34.72 ± 23.51
S97-V12E-RV-FX	59.11 ± 35.10	0.8531 ± 0.2327	0.002672 ± 0.001532	29.20 ± 3.80
S97-V21A-LA-CX	1380.84 ± 433.79	0.6026 ± 0.2637	-0.001804 ± 0.004785	47.89 ± 29.76
S97-V21A-LA-FX	57.58 ± 22.16	-	0.001666 ± 0.001120	11.17 ± 4.75
S97-V21B-LA-CX	1668.66 ± 550.80	0.4278 ± 0.2931	-0.002518 ± 0.006080	122.46 ± 37.47
S97-V21B-LA-FX	89.28 ± 29.88	0.2434 ± 0.2933	0.000868 ± 0.000821	27.62 ± 5.89
S97-V21B-LA-MX5	104.16 ± 63.43	-	0.000472 ± 0.000442	45.02 ± 6.05
S97-V21B-LA-MX6	-20.64 ± 62.84	-	-0.000041 ± 0.000239	4.50 ± 2.58
S97-V21B-LA-MX7	-4.49 ± 62.72	-	-0.000103 ± 0.000230	-0.67 ± 2.52
S97-V21B-LA-MX8	7.25 ± 62.74	-0.0098 ± 0.1003	0.000038 ± 0.000271	-
S97-V21B-LA-MX9	-27.69 ± 62.69	-0.0409 ± 0.0942	-0.000100 ± 0.000229	-
S97-V21B-LA-MX10	-	0.1664 ± 0.1003	-	-
S97-V21C-LA-CX	1622.31 ± 535.37	1.1664 ± 0.3747	0.002999 ± 0.006569	59.19 ± 36.08
S97-V21C-LA-FX	111.18 ± 27.99	0.4485 ± 0.3462	0.012759 ± 0.006644	17.28 ± 5.29
S97-V21D-LA-CX	1570.69 ± 546.14	0.2870 ± 0.3006	-0.001157 ± 0.006086	-0.69 ± 36.52
S97-V21D-LA-FX	-	-0.0443 ± 0.2955	0.005986 ± 0.003429	0.71 ± 4.98
S97-V21E-LA-CX	635.26 ± 469.37	0.1407 ± 0.1648	-0.000309 ± 0.003412	15.45 ± 20.93
S97-V21E-LA-FX	13.58 ± 15.66	-	0.010756 ± 0.005700	1.95 ± 2.86
S97-V22A-LA-CX	863.97 ± 445.63	0.2141 ± 0.2314	-0.001534 ± 0.004960	12.14 ± 29.43
S97-V22A-LA-FX	96.76 ± 29.54	-0.0263 ± 0.2408	0.000487 ± 0.000588	6.97 ± 4.47
S97-V22B-LA-CX	1483.10 ± 545.36	0.4072 ± 0.2954	-0.002377 ± 0.006033	87.06 ± 38.72
S97-V22B-LA-FX	82.60 ± 28.45	0.1128 ± 0.2872	-0.000029 ± 0.000449	24.69 ± 5.67
S97-V22B-LA-MX5	13.04 ± 62.37	-	-	15.27 ± 3.27
S97-V22B-LA-MX6	-14.38 ± 62.31	0.0807 ± 0.0962	-	1.84 ± 2.70
S97-V22B-LA-MX7	-24.60 ± 62.30	-	-	-
S97-V22B-LA-MX8	-17.59 ± 62.31	0.0253 ± 0.0962	-	-0.72 ± 2.40
S97-V22B-LA-MX9	-7.09 ± 62.36	0.1012 ± 0.0947	0.000294 ± 0.000354	-
S97-V22B-LA-MX10	30.55 ± 62.49	-	-	-
S97-V22C-LA-CX	3015.75 ± 817.65	0.4307 ± 0.3037	-0.001834 ± 0.006015	37.83 ± 35.68
S97-V22C-LA-FX	11.75 ± 32.97	0.5129 ± 0.2947	0.006478 ± 0.003665	6.17 ± 5.32
S97-V22D-LA-CX	810.83 ± 553.11	0.0204 ± 0.2722	0.002156 ± 0.006624	5.44 ± 36.03
S97-V22D-LA-FX	21.66 ± 28.62	-0.1271 ± 0.2938	0.018079 ± 0.009787	2.30 ± 4.91
S97-V22D-LA-MX5	53.55 ± 62.32	-	-	7.34 ± 4.42
S97-V22D-LA-MX6	10.06 ± 62.05	-0.0300 ± 0.0966	0.007077 ± 0.003776	2.99 ± 3.55
S97-V22D-LA-MX7	-27.05 ± 61.90	-	-	-0.98 ± 2.39
S97-V22D-LA-MX8	-15.45 ± 61.91	-	0.002641 ± 0.001466	-0.57 ± 2.45
S97-V22D-LA-MX9	-23.86 ± 61.91	-	0.002728 ± 0.001581	-0.37 ± 2.46
S97-V22D-LA-MX10	24.56 ± 61.98	0.0628 ± 0.1195	-	18.94 ± 3.94
S97-V22E-LA-CX	820.72 ± 301.99	0.0920 ± 0.1459	-0.001401 ± 0.003337	30.09 ± 20.57
S97-V22E-LA-FX	81.92 ± 16.23	-0.0245 ± 0.1596	0.001935 ± 0.001197	6.90 ± 3.26
S97-V21A-AZ-CX	2692.78 ± 483.48	0.8792 ± 0.2637	-0.002068 ± 0.005210	60.33 ± 31.80
S97-V21A-AZ-FX	87.66 ± 66.77	0.2482 ± 0.2461	0.003094 ± 0.001857	3.59 ± 3.85
S97-V21B-AZ-CX	6109.61 ± 661.99	3.0275 ± 0.4373	-0.002819 ± 0.006667	143.80 ± 41.49
S97-V21B-AZ-FX	235.31 ± 156.67	0.3232 ± 0.3098	0.001115 ± 0.001020	13.19 ± 5.46
S97-V21C-AZ-CX	3121.46 ± 828.77	0.9234 ± 0.3125	-0.002708 ± 0.006584	54.65 ± 39.15
S97-V21C-AZ-FX	169.94 ± 128.63	0.1887 ± 0.3007	0.000002 ± 0.000462	13.59 ± 5.74

Table D.4: Trace Metals Aerosol Concentration Data (Al, As, Au, Ba) (continued)

Sample	Aerosol Concentration (ng m^{-3})			
	Al	As	Au	Ba
S97-V21D-AZ-CX	2729.60 ± 619.96	0.5831 ± 0.3609	-0.002972 ± 0.006775	78.49 ± 40.63
S97-V21D-AZ-FX	1863.01 ± 531.35	0.0023 ± 0.3256	0.000400 ± 0.000650	15.02 ± 6.99
S97-V21D-AZ-MX5	139.40 ± 71.11	-	-	21.11 ± 4.73
S97-V21D-AZ-MX6	-7.32 ± 70.10	-0.0142 ± 0.1058	-0.000169 ± 0.000249	2.07 ± 2.87
S97-V21D-AZ-MX7	-20.78 ± 70.08	-0.0415 ± 0.1065	-	-0.91 ± 2.71
S97-V21D-AZ-MX8	-27.34 ± 70.08	-0.0559 ± 0.1054	-0.000190 ± 0.000249	-1.17 ± 2.70
S97-V21D-AZ-MX9	-29.31 ± 70.09	-	-	-
S97-V21D-AZ-MX10	54.06 ± 70.20	-	-0.000056 ± 0.000259	-
S97-V21E-AZ-CX	1596.82 ± 339.80	0.6776 ± 0.1874	-0.001544 ± 0.003702	32.84 ± 22.60
S97-V21E-AZ-FX	128.65 ± 92.22	-0.0623 ± 0.1704	0.000146 ± 0.000313	8.40 ± 3.46
S97-V22A-AZ-CX	1099.64 ± 488.46	0.6049 ± 0.2459	-0.002065 ± 0.005416	14.05 ± 31.29
S97-V22A-AZ-FX	73.25 ± 25.59	0.2332 ± 0.2477	0.000711 ± 0.000698	1.92 ± 4.21
S97-V22B-AZ-CX	3926.69 ± 640.32	1.8377 ± 0.4336	-0.002941 ± 0.006840	69.48 ± 42.16
S97-V22B-AZ-FX	210.51 ± 31.72	0.3912 ± 0.3112	0.000760 ± 0.000816	6.36 ± 5.40
S97-V22B-AZ-MX5	43.60 ± 69.23	-	-0.000152 ± 0.000247	3.02 ± 2.82
S97-V22B-AZ-MX6	11.23 ± 69.15	-0.0302 ± 0.1041	-0.000146 ± 0.000247	2.37 ± 2.87
S97-V22B-AZ-MX7	20.94 ± 69.19	0.1252 ± 0.1095	-0.000029 ± 0.000259	-0.67 ± 2.79
S97-V22B-AZ-MX8	-5.60 ± 69.13	0.0928 ± 0.1057	-0.000143 ± 0.000247	-
S97-V22B-AZ-MX9	-22.11 ± 69.11	0.0086 ± 0.1044	-	-
S97-V22B-AZ-MX10	-31.82 ± 69.11	-0.0205 ± 0.1050	-0.000177 ± 0.000245	-
S97-V22C-AZ-CX	3298.00 ± 884.57	1.3324 ± 0.3418	-0.002893 ± 0.006752	78.21 ± 40.16
S97-V22C-AZ-FX	88.96 ± 33.36	0.5255 ± 0.3220	0.001161 ± 0.001000	6.06 ± 5.56
S97-V22D-AZ-CX	3885.64 ± 630.90	2.5910 ± 1.3798	-0.002891 ± 0.006769	68.75 ± 40.59
S97-V22D-AZ-FX	58.15 ± 29.70	-0.0498 ± 0.3028	-	4.65 ± 5.39
S97-V22D-AZ-MX5	169.06 ± 69.46	-	-	9.77 ± 3.42
S97-V22D-AZ-MX6	123.95 ± 69.25	-	-	16.54 ± 3.92
S97-V22D-AZ-MX7	-18.78 ± 68.80	-	0.000196 ± 0.000355	-
S97-V22D-AZ-MX8	-27.48 ± 68.79	0.7368 ± 0.1413	0.001872 ± 0.001122	0.23 ± 3.12
S97-V22D-AZ-MX9	-23.94 ± 68.80	-	0.001807 ± 0.001060	-
S97-V22D-AZ-MX10	-26.84 ± 68.79	-	0.001807 ± 0.001060	-
S97-V22E-AZ-CX	1396.08 ± 340.21	0.2731 ± 0.2093	-0.001539 ± 0.003730	48.52 ± 22.37
S97-V22E-AZ-FX	69.57 ± 16.81	0.1230 ± 0.1715	0.001326 ± 0.000953	8.29 ± 3.17
S97-V21A-RV-CX	711.19 ± 485.14	0.6029 ± 0.2778	-0.001935 ± 0.005401	2.46 ± 32.64
S97-V21A-RV-FX	465.05 ± 30.89	0.1245 ± 0.2392	0.001024 ± 0.000868	8.26 ± 4.30
S97-V21B-RV-CX	3042.84 ± 716.47	1.9920 ± 0.4795	-0.002663 ± 0.007842	101.87 ± 49.23
S97-V21C-RV-CX	1849.62 ± 580.91	0.8072 ± 0.3089	-0.002105 ± 0.006417	20.29 ± 38.42
S97-V21C-RV-FX	604.38 ± 47.18	0.2479 ± 0.2968	0.000254 ± 0.000568	23.40 ± 5.61
S97-V21D-RV-CX	1591.30 ± 585.40	0.4645 ± 0.3447	-0.002228 ± 0.006479	30.64 ± 39.50
S97-V21D-RV-FX	776.99 ± 45.58	-0.0299 ± 0.2992	0.001094 ± 0.000911	21.62 ± 5.69
S97-V21D-RV-MX5	-1.51 ± 60.93	-	-	1.52 ± 2.57
S97-V21D-RV-MX6	-19.49 ± 60.92	-0.0266 ± 0.0928	-0.000148 ± 0.000216	-0.17 ± 2.39
S97-V21D-RV-MX7	-28.90 ± 60.91	-	-	-1.05 ± 2.36
S97-V21D-RV-MX8	309.47 ± 62.82	0.2530 ± 0.0965	-0.000158 ± 0.000216	-
S97-V21D-RV-MX9	-25.19 ± 60.91	0.0675 ± 0.0930	-	-
S97-V21D-RV-MX10	-25.48 ± 60.92	-	-	6.37 ± 2.40
S97-V21E-RV-CX	1289.60 ± 326.71	0.5535 ± 0.1727	-0.001468 ± 0.003582	36.38 ± 21.86

Table D.4: Trace Metals Aerosol Concentration Data (Al, As, Au, Ba) (continued)

Sample	Aerosol Concentration (ng m^{-3})			
	Al	As	Au	Ba
S97-V21E-RV-FX	136.13 ± 17.09	0.3084 ± 0.1658	0.000225 ± 0.000339	8.85 ± 2.95
S97-V22A-RV-CX	459.84 ± 646.30	0.1264 ± 0.2537	-0.002256 ± 0.005427	10.22 ± 31.79
S97-V22A-RV-FX	32.34 ± 25.13	0.1613 ± 0.2601	-0.000246 ± 0.000353	3.10 ± 4.50
S97-V22B-RV-CX	-	0.5345 ± 0.3254	-0.002772 ± 0.006536	51.47 ± 41.52
S97-V22B-RV-FX	135.56 ± 31.65	0.5201 ± 0.3186	0.000494 ± 0.000697	13.86 ± 5.68
S97-V22B-RV-MX5	13.61 ± 60.99	-	0.000311 ± 0.000381	5.80 ± 2.46
S97-V22B-RV-MX6	-18.34 ± 60.92	-	-	0.23 ± 2.37
S97-V22B-RV-MX7	-26.05 ± 60.93	0.3386 ± 0.1008	-	31.19 ± 5.36
S97-V22B-RV-MX8	-30.70 ± 60.91	0.6895 ± 0.1213	0.000399 ± 0.000407	-0.75 ± 2.34
S97-V22B-RV-MX9	-	0.0789 ± 0.0926	-	-
S97-V22B-RV-MX10	-26.90 ± 60.91	0.0561 ± 0.0928	-	-
S97-V22C-RV-CX	869.47 ± 906.18	0.4359 ± 0.2884	0.034681 ± 0.019942	17.13 ± 41.91
S97-V22C-RV-FX	76.47 ± 31.26	0.0292 ± 0.3125	0.000304 ± 0.000687	6.48 ± 5.50
S97-V22D-RV-CX	1063.50 ± 1046.19	-	-0.002643 ± 0.006635	3.97 ± 39.14
S97-V22D-RV-FX	55.14 ± 30.10	0.0284 ± 0.3094	0.001473 ± 0.001234	0.42 ± 5.11
S97-V22D-RV-MX5	-7.63 ± 59.71	-	0.000631 ± 0.000510	1.21 ± 2.48
S97-V22D-RV-MX6	-28.87 ± 59.67	-	-	-0.40 ± 2.36
S97-V22D-RV-MX7	-29.74 ± 59.68	0.0913 ± 0.0922	-0.000006 ± 0.000241	-0.58 ± 2.47
S97-V22D-RV-MX8	-29.65 ± 59.68	0.1137 ± 0.0922	0.000050 ± 0.000238	-0.39 ± 2.46
S97-V22D-RV-MX9	-26.91 ± 59.79	0.1081 ± 0.0933	0.002350 ± 0.001303	-
S97-V22D-RV-MX10	-25.24 ± 59.68	-	-	-0.41 ± 2.46
S97-V22E-RV-CX	531.69 ± 544.60	0.4067 ± 0.2268	-0.001497 ± 0.003640	14.12 ± 21.48
S97-V22E-RV-FX	51.31 ± 16.99	0.1424 ± 0.1712	0.001159 ± 0.000787	5.48 ± 3.04
S97-N21D-ML-FX	178.41 ± 122.17	0.3001 ± 0.3286	0.000210 ± 0.000649	-1.58 ± 4.60
S97-N21E-ML-FX	-	2.8432 ± 0.3401	0.001142 ± 0.000815	6.53 ± 3.50
S97-N22A-ML-FX	39.86 ± 23.23	1.8559 ± 0.3819	0.000091 ± 0.000292	5.38 ± 4.55
S97-N22B-ML-FX	59.12 ± 29.31	-	0.002596 ± 0.001757	7.69 ± 5.56
S97-N22C-ML-FX	31.37 ± 29.31	0.2976 ± 0.3367	-0.000284 ± 0.000417	-
S97-N22C-ML-MX5	215.02 ± 66.93	-0.0185 ± 0.0965	-	10.63 ± 6.57
S97-N22C-ML-MX6	405.25 ± 67.03	-0.0244 ± 0.1000	-0.000169 ± 0.000222	-
S97-N22C-ML-MX7	-4.77 ± 62.67	0.0722 ± 0.0966	0.000500 ± 0.000415	0.01 ± 2.34
S97-N22C-ML-MX8	-26.13 ± 62.50	-0.0244 ± 0.0949	0.000793 ± 0.000545	0.97 ± 2.54
S97-N22C-ML-MX9	-26.72 ± 62.51	-	0.001554 ± 0.000906	-0.99 ± 2.46
S97-N22C-ML-MX10	-26.43 ± 62.49	-	-	-
S97-N22D-ML-FX	59.07 ± 28.56	0.1816 ± 0.2944	0.000046 ± 0.000474	1.41 ± 4.81
S97-N22E-ML-FX	67.53 ± 17.95	1.3999 ± 0.2198	0.000612 ± 0.000543	6.88 ± 3.43
S97-N23A-ML-FX	61.46 ± 24.34	1.3589 ± 0.2867	-	3.65 ± 4.33
S97-N23B-ML-FX	70.07 ± 29.43	1.7327 ± 0.3568	-	10.41 ± 5.55
S97-N23C-ML-FX	53.39 ± 29.29	0.5853 ± 0.3069	-0.000152 ± 0.000430	5.76 ± 5.13
S97-N23C-ML-MX5	1.36 ± 62.03	0.0048 ± 0.1038	-0.000093 ± 0.000223	4.45 ± 2.66
S97-N23C-ML-MX6	-25.63 ± 61.97	-0.0300 ± 0.0944	-	-
S97-N23C-ML-MX7	-28.82 ± 61.96	0.1964 ± 0.1014	-	-
S97-N23C-ML-MX8	-25.34 ± 61.97	0.0513 ± 0.0970	-	-
S97-N23C-ML-MX9	-31.26 ± 61.96	-0.0439 ± 0.0930	-	-
S97-N23C-ML-MX10	-30.88 ± 61.96	-0.0436 ± 0.0930	-	-

Table D.4: Trace Metals Aerosol Concentration Data (Al, As, Au, Ba) (continued)

Sample	Aerosol Concentration (ng m^{-3})			
	Al	As	Au	Ba
S97-N23D-ML-FX	36.43 ± 28.93	-	0.001019 ± 0.000990	-
S97-N23E-ML-FX	27.44 ± 16.48	0.3740 ± 0.1809	-	3.38 ± 3.39
S97-N23E-ML-MX5	746.46 ± 49.84	0.0843 ± 0.0814	-	12.87 ± 4.05
S97-N23E-ML-MX6	14.10 ± 37.45	-	-	-
S97-N23E-ML-MX7	-17.03 ± 35.54	0.0577 ± 0.0543	-0.000091 ± 0.000126	-
S97-N23E-ML-MX8	0.78 ± 35.67	-	-	1.39 ± 1.69
S97-N23E-ML-MX9	-18.21 ± 35.53	0.0061 ± 0.0536	-0.000088 ± 0.000126	-
S97-N23E-ML-MX10	796.39 ± 51.02	0.0910 ± 0.1059	-	-
S97-N31A-DB-CX	2538.84 ± 558.08	1.3194 ± 0.3975	0.005504 ± 0.006285	77.90 ± 30.87
S97-N31A-DB-FX	122.25 ± 24.75	1.3479 ± 0.3170	0.007642 ± 0.004651	5.97 ± 4.39
S97-N31B-DB-CX	3041.85 ± 696.91	1.2289 ± 0.3947	0.012310 ± 0.009857	160.98 ± 39.56
S97-N31B-DB-FX	187.65 ± 32.21	1.8735 ± 0.3892	0.003025 ± 0.001975	47.19 ± 6.27
S97-N31C-DB-CX	1677.42 ± 586.20	1.1188 ± 0.3614	0.003101 ± 0.006792	70.79 ± 37.31
S97-N31C-DB-FX	196.90 ± 32.41	0.7928 ± 0.3212	0.005389 ± 0.003113	26.87 ± 6.72
S97-N31C-DB-MX5	63.51 ± 63.32	0.0020 ± 0.0964	0.000417 ± 0.000371	0.15 ± 2.59
S97-N31C-DB-MX6	-4.53 ± 63.17	0.1469 ± 0.1086	-0.000065 ± 0.000232	21.10 ± 3.53
S97-N31C-DB-MX7	-1.57 ± 63.42	-	0.000535 ± 0.000471	6.01 ± 2.71
S97-N31C-DB-MX8	-26.41 ± 63.15	0.0049 ± 0.0962	0.000180 ± 0.000303	-
S97-N31C-DB-MX9	-27.89 ± 63.15	-0.0246 ± 0.0966	0.000065 ± 0.000265	-0.97 ± 2.41
S97-N31C-DB-MX10	-26.12 ± 63.15	-0.0187 ± 0.0962	-	-
S97-N31D-DB-CX	1452.37 ± 586.38	0.9126 ± 0.2990	0.000806 ± 0.006165	50.71 ± 34.36
S97-N31D-DB-FX	78.96 ± 28.07	0.6863 ± 0.3029	0.002398 ± 0.001577	11.55 ± 5.43
S97-N31D-DB-MX5	-26.27 ± 74.55	0.1035 ± 0.1281	0.000492 ± 0.000466	-
S97-N31D-DB-MX6	-5.34 ± 74.52	0.0547 ± 0.1192	-	5.35 ± 3.54
S97-N31D-DB-MX7	-23.13 ± 74.49	0.1210 ± 0.1138	0.000422 ± 0.000429	0.01 ± 2.93
S97-N31D-DB-MX8	-31.16 ± 74.48	0.0337 ± 0.1138	0.000387 ± 0.000438	-
S97-N31D-DB-MX9	-31.50 ± 74.48	-	-	-1.88 ± 2.80
S97-N31D-DB-MX10	-33.25 ± 74.49	-0.0256 ± 0.1122	-0.000095 ± 0.000277	-1.07 ± 2.88
S97-N31E-DB-CX	1073.26 ± 329.92	0.8123 ± 0.1932	0.000462 ± 0.003531	101.92 ± 21.49
S97-N31E-DB-FX	88.45 ± 16.83	0.6944 ± 0.1869	0.001806 ± 0.001088	15.23 ± 3.29
S97-N32A-DB-CX	1430.93 ± 449.42	1.1901 ± 0.4509	-0.002131 ± 0.004956	22.06 ± 28.11
S97-N32A-DB-FX	-14.29 ± 22.75	-	-	-
S97-N32B-DB-CX	4081.96 ± 572.25	2.2322 ± 0.6855	-0.002388 ± 0.006060	-
S97-N32B-DB-FX	186.68 ± 29.94	-	0.000461 ± 0.000748	21.11 ± 6.49
S97-N32C-DB-CX	3416.36 ± 554.71	1.1744 ± 0.2869	-0.002608 ± 0.005951	77.43 ± 35.69
S97-N32C-DB-FX	168.38 ± 29.21	0.3735 ± 0.2932	0.001012 ± 0.000879	25.78 ± 6.11
S97-N32C-DB-MX5	104.16 ± 63.30	-	-0.000146 ± 0.000223	10.37 ± 3.04
S97-N32C-DB-MX6	13.13 ± 62.84	0.0578 ± 0.1308	-0.000138 ± 0.000223	8.61 ± 3.04
S97-N32C-DB-MX7	-22.11 ± 62.71	0.0578 ± 0.0968	-0.000149 ± 0.000223	-
S97-N32C-DB-MX8	-27.10 ± 62.69	0.0137 ± 0.0964	-	-
S97-N32C-DB-MX9	-	-0.0010 ± 0.0959	-0.000169 ± 0.000222	-
S97-N32C-DB-MX10	-28.87 ± 62.70	-	-0.000147 ± 0.000223	-0.11 ± 2.34
S97-N32D-DB-CX	1565.00 ± 544.40	0.6721 ± 0.2812	-0.002659 ± 0.006014	39.64 ± 34.59
S97-N32D-DB-FX	99.80 ± 28.11	0.0387 ± 0.2833	0.000967 ± 0.000861	12.82 ± 5.26
S97-N32E-DB-CX	702.02 ± 311.96	0.6819 ± 0.1841	-0.001496 ± 0.003456	64.68 ± 29.82
S97-N32E-DB-FX	45.41 ± 15.75	0.2768 ± 0.1827	0.001263 ± 0.000824	-0.74 ± 2.55

Table D.4: Trace Metals Aerosol Concentration Data (Al, As, Au, Ba) (continued)

Sample	Aerosol Concentration (ng m^{-3})			
	Al	As	Au	Ba
S97-N31A-ML-CX	2916.55 ± 589.30	2.3516 ± 0.3448	-0.000110 ± 0.005484	130.57 ± 33.61
S97-N31A-ML-FX	514.51 ± 45.04	0.4480 ± 0.2582	0.001940 ± 0.001336	20.79 ± 5.99
S97-N31B-ML-CX	4102.77 ± 750.06	2.5460 ± 0.4073	-0.000800 ± 0.006748	143.46 ± 42.26
S97-N31B-ML-FX	317.12 ± 40.02	-	0.002506 ± 0.001689	36.33 ± 7.18
S97-N31C-ML-CX	3434.95 ± 763.61	1.0867 ± 0.3445	-0.002923 ± 0.007034	48.35 ± 41.20
S97-N31C-ML-FX	336.13 ± 40.22	1.4727 ± 0.4301	0.003484 ± 0.002390	13.47 ± 6.28
S97-N31C-ML-MX5	25.60 ± 73.22	-0.0217 ± 0.1119	-0.000176 ± 0.000260	0.93 ± 3.07
S97-N31C-ML-MX6	18.74 ± 73.24	0.0331 ± 0.1113	-0.000187 ± 0.000260	1.14 ± 2.97
S97-N31C-ML-MX7	-24.43 ± 73.15	0.0400 ± 0.1241	-0.000158 ± 0.000261	-
S97-N31C-ML-MX8	-32.65 ± 73.15	-0.0114 ± 0.1102	-	-
S97-N31C-ML-MX9	-33.68 ± 73.15	-0.0217 ± 0.1143	-	-
S97-N31C-ML-MX10	-35.74 ± 73.15	-	-	1.48 ± 3.14
S97-N31D-ML-CX	4102.77 ± 750.06	2.0716 ± 0.4289	0.000433 ± 0.006867	96.02 ± 39.89
S97-N31D-ML-FX	296.19 ± 40.67	1.1340 ± 0.3520	0.001977 ± 0.001392	20.86 ± 6.38
S97-N31D-ML-MX5	30.67 ± 77.86	0.0097 ± 0.1171	-0.000142 ± 0.000277	6.63 ± 3.63
S97-N31D-ML-MX6	-5.54 ± 77.33	0.0712 ± 0.1427	-0.000174 ± 0.000276	1.56 ± 3.26
S97-N31D-ML-MX7	-26.54 ± 77.30	0.1545 ± 0.1201	-0.000134 ± 0.000277	-0.46 ± 3.18
S97-N31D-ML-MX8	-38.92 ± 77.29	0.0024 ± 0.1166	-0.000167 ± 0.000275	-1.15 ± 2.98
S97-N31D-ML-MX9	-	-0.0302 ± 0.1164	-0.000204 ± 0.000274	-
S97-N31D-ML-MX10	-35.95 ± 77.30	-	-	-
S97-N31E-ML-CX	-139.86 ± 330.25	3.6719 ± 0.4766	-0.000181 ± 0.003759	184.66 ± 26.31
S97-N31E-ML-FX	389.76 ± 32.18	1.9126 ± 0.2646	0.003187 ± 0.001835	44.25 ± 4.58
S97-N32A-ML-CX	3172.54 ± 515.12	3.1404 ± 0.4271	-0.002210 ± 0.005528	-
S97-N32A-ML-FX	350.08 ± 30.27	0.7892 ± 0.2733	0.007765 ± 0.004357	33.70 ± 5.76
S97-N32B-ML-CX	9489.52 ± 739.58	2.2514 ± 0.4232	-0.002893 ± 0.006913	89.93 ± 42.20
S97-N32B-ML-FX	335.07 ± 35.17	-	0.000493 ± 0.000789	1.83 ± 5.42
S97-N32C-ML-CX	6474.87 ± 660.44	1.0279 ± 0.3065	-0.002878 ± 0.006651	62.81 ± 39.56
S97-N32C-ML-FX	-13.12 ± 29.90	0.0957 ± 0.3360	0.001412 ± 0.001358	3.77 ± 5.17
S97-N32C-ML-MX5	-4.93 ± 68.81	-0.0268 ± 0.1036	-	-1.57 ± 2.59
S97-N32C-ML-MX6	-12.98 ± 68.80	-0.0491 ± 0.1033	-	-0.64 ± 2.67
S97-N32C-ML-MX7	-11.05 ± 68.82	-0.0458 ± 0.1037	-0.000187 ± 0.000244	-
S97-N32C-ML-MX8	-16.53 ± 68.81	-	-	-0.99 ± 2.66
S97-N32C-ML-MX9	-9.76 ± 68.80	-	-	-
S97-N32C-ML-MX10	-36.41 ± 68.78	-	-0.000182 ± 0.000244	-1.51 ± 2.63
S97-N32D-ML-CX	1746.70 ± 607.34	1.4204 ± 0.3343	-0.002929 ± 0.006713	4.02 ± 38.78
S97-N32D-ML-FX	-22.66 ± 30.17	-	-	-2.60 ± 5.10
S97-N32E-ML-CX	1226.30 ± 337.42	0.1020 ± 0.1637	-0.001479 ± 0.003700	14.88 ± 21.67
S97-N32E-ML-FX	73.74 ± 17.26	-	-0.000017 ± 0.000293	-1.52 ± 2.79
S97-N31A-RV-CX	-	-0.2099 ± 0.2129	-0.002148 ± 0.005204	-
S97-N31A-RV-FX	95.44 ± 26.36	0.5950 ± 0.2497	0.007564 ± 0.004068	14.12 ± 4.59
S97-N31B-RV-CX	2280.26 ± 743.62	1.3013 ± 0.4400	-0.001170 ± 0.006657	95.20 ± 40.26
S97-N31B-RV-FX	172.06 ± 31.22	0.4467 ± 0.3115	0.000818 ± 0.000800	27.32 ± 5.67
S97-N31C-RV-CX	1958.81 ± 626.90	0.3350 ± 0.2747	-0.001977 ± 0.006487	61.05 ± 38.77
S97-N31C-RV-FX	144.05 ± 30.52	0.1869 ± 0.3035	0.000549 ± 0.000681	10.95 ± 5.04
S97-N31C-RV-MX5	15.74 ± 61.50	-0.0484 ± 0.0924	-0.000153 ± 0.000218	3.54 ± 2.62
S97-N31C-RV-MX6	1.35 ± 61.45	-0.0067 ± 0.0937	0.000031 ± 0.000246	1.24 ± 2.46

Table D.4: Trace Metals Aerosol Concentration Data (Al, As, Au, Ba) (continued)

Sample	Aerosol Concentration (ng m^{-3})			
	Al	As	Au	Ba
S97-N31C-RV-MX7	-15.33 ± 61.45	0.0422 ± 0.0933	-0.000142 ± 0.000218	-
S97-N31C-RV-MX8	-22.24 ± 61.43	-	-	0.15 ± 2.39
S97-N31C-RV-MX9	21.49 ± 61.49	-0.0240 ± 0.0924	-0.000038 ± 0.000232	-0.60 ± 2.49
S97-N31C-RV-MX10	9.98 ± 61.61	-0.0268 ± 0.0924	-0.000164 ± 0.000218	-
S97-N31D-RV-CX	2286.30 ± 614.19	1.1181 ± 0.3549	0.000572 ± 0.006328	79.46 ± 37.64
S97-N31D-RV-FX	137.10 ± 28.61	0.7844 ± 0.3304	0.001282 ± 0.001009	14.91 ± 4.88
S97-N31D-RV-MX5	645.26 ± 83.84	0.1837 ± 0.1292	-0.000194 ± 0.000259	62.76 ± 8.98
S97-N31D-RV-MX6	337.13 ± 80.14	-	-0.000144 ± 0.000262	35.37 ± 9.64
S97-N31D-RV-MX7	107.74 ± 73.51	0.0468 ± 0.1110	0.000174 ± 0.000387	-1.19 ± 2.93
S97-N31D-RV-MX8	-	-0.0398 ± 0.1103	0.000174 ± 0.000353	-
S97-N31D-RV-MX9	-36.63 ± 73.09	-0.0473 ± 0.1098	0.000058 ± 0.000320	-
S97-N31D-RV-MX10	-34.34 ± 73.09	-	-	-
S97-N31E-RV-CX	2193.06 ± 427.53	1.8439 ± 0.2725	0.000467 ± 0.003973	98.75 ± 24.02
S97-N31E-RV-FX	196.53 ± 20.11	0.7873 ± 0.1993	0.002554 ± 0.001507	17.50 ± 3.49
S97-N32A-RV-CX	1084.01 ± 481.52	0.5963 ± 0.2459	-0.002279 ± 0.005336	32.89 ± 31.05
S97-N32A-RV-FX	112.39 ± 24.95	0.2873 ± 0.2530	0.000247 ± 0.000499	9.67 ± 4.67
S97-N32B-RV-CX	1052.79 ± 591.15	0.1342 ± 0.2871	-0.002866 ± 0.006566	-6.37 ± 37.43
S97-N32B-RV-FX	63.59 ± 32.57	0.3772 ± 0.4145	0.001027 ± 0.000984	1.82 ± 5.15
S97-N32C-RV-CX	940.88 ± 579.47	-0.0521 ± 0.2816	-0.002732 ± 0.006441	-8.09 ± 36.49
S97-N32C-RV-FX	225.67 ± 35.26	-0.0171 ± 0.3031	-0.000160 ± 0.000449	-0.75 ± 5.11
S97-N32C-RV-MX5	-13.79 ± 66.47	-0.0496 ± 0.0998	-0.000157 ± 0.000236	-
S97-N32C-RV-MX6	-16.59 ± 66.46	-0.0104 ± 0.1075	-0.000147 ± 0.000237	-
S97-N32C-RV-MX7	-20.32 ± 66.47	-	-	-
S97-N32C-RV-MX9	-28.10 ± 66.46	-0.0536 ± 0.0998	-	-
S97-N32C-RV-MX10	-28.10 ± 66.45	-	-0.000147 ± 0.000237	-0.15 ± 2.82
S97-N32D-RV-CX	1189.50 ± 567.58	3.3091 ± 1.6374	-0.002698 ± 0.006298	0.18 ± 35.97
S97-N32D-RV-FX	95.67 ± 31.06	-0.0703 ± 0.2922	-0.000112 ± 0.000432	-1.14 ± 4.78
S97-N32E-RV-CX	372.40 ± 324.00	-0.0086 ± 0.1712	-0.001524 ± 0.003606	4.73 ± 21.44
S97-N32E-RV-FX	-12.56 ± 16.23	-0.0221 ± 0.1686	-	-0.20 ± 2.79
S97-T11B-TI-CX	717.19 ± 688.73	0.5976 ± 0.3351	-0.002888 ± 0.007577	314.53 ± 51.48
S97-T11B-TI-FX	823.31 ± 55.07	0.8652 ± 0.4010	0.004082 ± 0.002512	114.71 ± 12.32
S97-T11B-TI-MX5	-6.38 ± 87.04	-0.0052 ± 0.1295	-0.000215 ± 0.000297	44.37 ± 4.98
S97-T11B-TI-MX6	25.33 ± 94.03	-	-0.000215 ± 0.000297	-
S97-T11B-TI-MX7	60.57 ± 106.85	-0.0052 ± 0.1261	-0.000224 ± 0.000296	4.43 ± 3.60
S97-T11B-TI-MX8	-22.83 ± 84.58	-0.0604 ± 0.1254	-0.000071 ± 0.000313	-0.15 ± 3.31
S97-T11B-TI-MX9	581.31 ± 324.19	-0.0557 ± 0.1271	-	0.17 ± 3.39
S97-T11B-TI-MX10	-22.83 ± 84.64	-0.0620 ± 0.1256	-0.000067 ± 0.000315	-
S97-T11B-TO-CX	-30.54 ± 781.61	-	-0.001578 ± 0.008313	-
S97-T11B-TO-FX	220.58 ± 38.76	1.3019 ± 0.6630	0.002816 ± 0.002028	3.82 ± 7.21
S97-T11B-TO-MX5	696.08 ± 96.71	-	-	37.32 ± 15.23
S97-T11B-TO-MX6	572.12 ± 94.94	-	-	4.26 ± 6.30
S97-T11B-TO-MX7	-24.50 ± 88.22	-	-	2.61 ± 3.53
S97-T11B-TO-MX8	-41.03 ± 88.21	-	-	-
S97-T11B-TO-MX9	-31.94 ± 88.21	-0.0753 ± 0.1323	-	-
S97-T11B-TO-MX10	-40.20 ± 88.21	-	-	-

Table D.4: Trace Metals Aerosol Concentration Data (Al, As, Au, Ba) (continued)

Sample	Aerosol Concentration (ng m^{-3})			
	Al	As	Au	Ba
S97-T21B-TI-CX	471.24 ± 686.96	0.2316 ± 0.4055	-0.002469 ± 0.007631	240.18 ± 46.91
S97-T21B-TI-FX	28.12 ± 39.07	-0.1126 ± 0.3691	-	-
S97-T21B-TI-MX5	-9.87 ± 83.39	-0.0052 ± 0.1270	-0.000160 ± 0.000298	48.12 ± 4.90
S97-T21B-TI-MX6	-32.11 ± 83.33	-	-	14.95 ± 3.61
S97-T21B-TI-MX7	-37.58 ± 83.33	-	-0.000141 ± 0.000300	-0.23 ± 3.31
S97-T21B-TI-MX8	-37.97 ± 83.51	-	-0.000164 ± 0.000298	-1.05 ± 3.35
S97-T21B-TI-MX9	-32.50 ± 83.32	-0.0169 ± 0.1379	-	-
S97-T21B-TI-MX10	-38.75 ± 83.31	-0.0501 ± 0.1261	-0.000184 ± 0.000297	-
S97-T21B-TO-FX	56.48 ± 35.78	-0.0051 ± 0.3632	0.000041 ± 0.000798	0.11 ± 6.39
S97-T31B-TI-CX	26.06 ± 682.98	-	-0.003033 ± 0.007615	120.74 ± 45.65
S97-T31B-TI-FX	22.86 ± 37.04	-	0.000347 ± 0.000747	63.41 ± 8.83
S97-T31B-TI-MX5	-25.48 ± 83.32	-0.0286 ± 0.1259	-	15.73 ± 3.69
S97-T31B-TI-MX6	-13.77 ± 83.33	-	-	3.64 ± 3.37
S97-T31B-TI-MX7	-29.38 ± 83.32	-	-0.000220 ± 0.000296	-
S97-T31B-TI-MX9	-32.89 ± 83.32	-0.0524 ± 0.1252	-0.000223 ± 0.000296	-
S97-T31B-TI-MX10	-	-0.0661 ± 0.1250	-0.000210 ± 0.000296	-
S97-T31B-TO-CX	-177.83 ± 716.22	-	-0.002945 ± 0.007998	-
S97-T31B-TO-FX	58.99 ± 35.35	-	0.000240 ± 0.000704	-
S97-T31B-TO-MX5	535.30 ± 94.67	-	-	5.54 ± 7.26
S97-T31B-TO-MX6	689.93 ± 94.67	-	-	-
S97-T31B-TO-MX7	1192.49 ± 107.95	-	-0.000201 ± 0.000293	-
S97-T31B-TO-MX8	171.91 ± 84.34	-	-	-
S97-T31B-TO-MX9	307.22 ± 85.52	-0.0508 ± 0.1245	-0.000212 ± 0.000293	-
S97-T31B-TO-MX10	253.10 ± 86.38	-	-	-
S97-T41B-TI-CX	115.98 ± 703.76	0.0260 ± 0.3287	-0.003194 ± 0.007819	246.69 ± 48.18
S97-T41B-TI-FX	19.09 ± 36.81	-0.1199 ± 0.3862	-0.000615 ± 0.000478	84.84 ± 8.53
S97-T41B-TI-MX5	146.22 ± 85.30	0.1392 ± 0.1633	-	102.75 ± 9.50
S97-T41B-TI-MX6	138.41 ± 86.22	-	-	59.83 ± 8.77
S97-T41B-TI-MX7	9.64 ± 83.83	-	-	6.76 ± 5.62
S97-T41B-TI-MX8	-2.07 ± 83.63	-	-	-
S97-T41B-TI-MX9	-	0.0533 ± 0.1308	-	-
S97-T41B-TI-MX10	-36.02 ± 83.31	-0.0536 ± 0.1255	-	-
S97-T41B-TO-CX	-225.96 ± 686.99	-0.2256 ± 0.3163	-0.003322 ± 0.007652	-24.12 ± 43.07
S97-T41B-TO-FX	143.78 ± 39.94	-0.0369 ± 0.3680	0.000276 ± 0.000714	110.13 ± 9.36
S97-B11A-AZ-MX5	48.00 ± 12.20	-	0.002400 ± 0.001200	-
S97-B11A-AZ-MX6	34.00 ± 7.40	-	0.000600 ± 0.000360	-
S97-B11A-AZ-MX7	30.00 ± 10.80	-	0.001300 ± 0.000760	-
S97-B11A-AZ-MX8	24.00 ± 5.20	-	-	7.20 ± 5.00
S97-B11A-AZ-MX9	44.00 ± 6.80	0.1000 ± 0.0500	0.001560 ± 0.001020	-
S97-B11A-AZ-MX10	18.60 ± 5.20	-	0.000960 ± 0.000700	13.00 ± 5.60
S97-B11A-DB-CX	3400.00 ± 460.00	1.7400 ± 0.2000	0.038000 ± 0.019000	200.00 ± 32.00
S97-B11A-DB-FX	9.30 ± 2.10	-	0.000850 ± 0.000610	-
S97-B11A-DB-MX5	260.00 ± 162.00	0.0560 ± 0.0380	0.000740 ± 0.000420	-
S97-B11A-DB-MX6	220.00 ± 136.00	-	-	11.00 ± 6.00

Table D.4: Trace Metals Aerosol Concentration Data (Al, As, Au, Ba) (continued)

Sample	Aerosol Concentration (ng m^{-3})			
	Al	As	Au	Ba
S97-B11A-DB-MX7	400.00 ± 260.00	-	-	-
S97-B11A-DB-MX8	96.00 ± 62.00	-	-	-
S97-B11A-DB-MX9	200.00 ± 126.00	0.3200 ± 0.3000	-	-
S97-B11A-DB-MX10	380.00 ± 360.00	-	-	5.80 ± 5.40
S97-B11A-ML-CX	112.00 ± 18.40	-	0.000540 ± 0.000420	4.00 ± 3.40
S97-B11A-ML-FX	2.10 ± 0.20	0.0450 ± 0.0430	0.001070 ± 0.000590	-
S97-B11A-RV-CX	80.00 ± 14.00	-	0.001780 ± 0.001100	24.00 ± 7.00
S97-B11A-RV-FX	171.00 ± 13.00	0.1000 ± 0.0000	0.001400 ± 0.001200	-
S97-B11A-RV-MX5	36.00 ± 6.20	0.2400 ± 0.1220	-	-
S97-B11A-RV-MX6	74.00 ± 11.20	-	0.000166 ± 0.000104	-
S97-B11A-RV-MX7	50.00 ± 6.20	0.0860 ± 0.0340	-	-
S97-B11A-RV-MX8	13.80 ± 4.60	-	-	3.80 ± 2.00
S97-B11A-RV-MX9	108.00 ± 7.40	0.0400 ± 0.0140	-	3.60 ± 2.40
S97-B11A-RV-MX10	320.00 ± 19.00	-	-	3.40 ± 1.94
S97-B11A-TI-CX	26.00 ± 0.56	-	-	-
S97-B11A-TI-FX	234.00 ± 18.00	-	0.004000 ± 0.002000	6.00 ± 4.00
S97-B11A-TI-MX5	1300.00 ± 680.00	-	-	-
S97-B11A-TI-MX6	580.00 ± 540.00	-	0.002200 ± 0.001220	6.60 ± 5.00
S97-B11A-TI-MX7	128.00 ± 120.00	0.1820 ± 0.1120	-	-
S97-B11A-TI-MX8	92.00 ± 88.00	0.0360 ± 0.0220	0.000520 ± 0.000320	-
S97-B11A-TI-MX9	118.00 ± 100.00	-	-	-
S97-B11A-TI-MX10	112.00 ± 106.00	0.2200 ± 0.0540	0.000340 ± 0.000280	-
S97-B21A-DB-CX	106.00 ± 40.00	-	0.002800 ± 0.001460	-
S97-B21A-DB-FX	23.00 ± 3.20	-	-	9.30 ± 0.53
S97-B21A-DB-MX5	1520.00 ± 100.00	0.5600 ± 0.2000	0.000132 ± 0.000116	-
S97-B21A-DB-MX6	2000.00 ± 192.00	-	-	-
S97-B21A-DB-MX7	14.40 ± 2.60	-	-	-
S97-B21A-DB-MX9	32.00 ± 5.20	3.4000 ± 0.5800	-	-
S97-B21A-DB-MX10	22.00 ± 5.60	0.4000 ± 0.0600	-	-
S97-B21A-ML-CX	68.00 ± 14.00	-	-	8.80 ± 3.80
S97-B21A-ML-FX	38.00 ± 17.00	-	0.000670 ± 0.000510	45.40 ± 5.50
S97-B21A-ML-MX5	1.04 ± 0.20	-	0.000030 ± 0.000024	-
S97-B21A-ML-MX6	86.00 ± 7.40	-	0.000072 ± 0.000046	-
S97-B21A-ML-MX7	18.60 ± 3.80	-	0.000060 ± 0.000036	-
S97-B21A-ML-MX8	34.00 ± 5.20	-	-	3.80 ± 2.40
S97-B21A-ML-MX9	100.00 ± 24.00	0.6200 ± 0.2400	0.000020 ± 0.000034	5.80 ± 3.40
S97-B21A-ML-MX10	15.40 ± 3.20	-	-	-
S97-B21A-RV-CX	72.00 ± 12.20	-	0.000052 ± 0.000042	-
S97-B21A-RV-FX	92.00 ± 9.00	-	0.002100 ± 0.001200	-
S97-B21A-RV-MX5	50.00 ± 14.80	0.2200 ± 0.1800	0.003200 ± 0.001800	-
S97-B21A-RV-MX6	36.00 ± 10.00	-	0.000980 ± 0.000740	7.20 ± 4.20
S97-B21A-RV-MX7	-	-	-	-
S97-B21A-RV-MX8	90.00 ± 20.00	-	0.000162 ± 0.000158	12.60 ± 6.80
S97-B21A-RV-MX9	460.00 ± 64.00	0.3200 ± 0.2400	-	-

Table D.4: Trace Metals Aerosol Concentration Data (Al, As, Au, Ba) (continued)

Sample	Aerosol Concentration (ng m^{-3})			
	Al	As	Au	Ba
S97-B21A-RV-MX10	58.00 ± 12.40	0.0300 ± 0.0240	0.000520 ± 0.000420	5.20 ± 3.60

D.5 Trace Elements Aerosol Concentration Data (Br, Cd, Ce, Cl)

Table D.5: Trace Metals Aerosol Concentration Data (Br, Cd, Ce, Cl)

Sample	Aerosol Concentration (ng m^{-3})			
	Br	Cd	Ce	Cl
S97-V11A-LA-CX	4.911 ± 1.915	-	-	473.58 ± 213.81
S97-V11A-LA-FX	7.360 ± 7.205	0.044 ± 0.651	-	1277.10 ± 77.24
S97-V11B-LA-CX	8.479 ± 1.780	-	0.7686 ± 1.1838	525.51 ± 268.53
S97-V11B-LA-FX	8.908 ± 9.907	-0.313 ± 0.672	-	274.84 ± 28.58
S97-V11C-LA-CX	14.130 ± 4.261	-	-	543.66 ± 247.35
S97-V11C-LA-FX	3.235 ± 8.883	-0.356 ± 0.679	-0.0699 ± 0.3453	15.23 ± 20.95
S97-V11D-LA-CX	5.933 ± 2.422	0.745 ± 1.129	-	661.72 ± 256.09
S97-V11D-LA-FX	-1.620 ± 9.057	-0.413 ± 0.676	-0.3165 ± 0.2664	38.88 ± 21.98
S97-V11E-LA-CX	3.187 ± 1.301	0.645 ± 0.743	0.7337 ± 0.9047	2925.66 ± 218.25
S97-V11E-LA-FX	0.568 ± 4.926	-	-	273.99 ± 20.67
S97-V12A-LA-CX	5.627 ± 2.109	-	0.3639 ± 0.8156	2317.94 ± 244.62
S97-V12A-LA-FX	3.184 ± 7.346	0.073 ± 0.647	-	271.15 ± 23.69
S97-V12B-LA-CX	10.241 ± 3.337	-	1.4484 ± 1.0178	661.71 ± 240.08
S97-V12B-LA-FX	3.371 ± 8.449	-0.422 ± 0.657	-	131.99 ± 22.45
S97-V12B-LA-MX5	0.121 ± 0.224	-	-	-1.67 ± 3.82
S97-V12B-LA-MX6	0.579 ± 0.279	-	-	1.00 ± 3.89
S97-V12B-LA-MX7	0.461 ± 0.244	-0.088 ± 0.364	-	1.59 ± 3.77
S97-V12B-LA-MX8	0.784 ± 0.301	0.406 ± 0.705	-	0.80 ± 3.77
S97-V12B-LA-MX9	0.209 ± 0.205	0.230 ± 0.458	-	-1.70 ± 3.77
S97-V12B-LA-MX10	-0.029 ± 0.193	-0.070 ± 0.380	-	-2.02 ± 3.77
S97-V12C-LA-CX	10.188 ± 3.168	1.117 ± 1.361	-	327.43 ± 235.89
S97-V12C-LA-FX	7.922 ± 8.810	0.024 ± 0.651	-	99.20 ± 21.71
S97-V12D-LA-CX	13.440 ± 3.991	0.284 ± 0.990	0.7150 ± 1.1327	300.85 ± 248.69
S97-V12D-LA-FX	4.886 ± 9.083	-0.264 ± 0.654	0.4761 ± 0.4025	41.16 ± 21.85
S97-V12E-LA-CX	6.290 ± 1.979	-	-	1438.93 ± 159.37
S97-V12E-LA-FX	1.258 ± 4.874	-0.126 ± 0.354	0.0490 ± 0.1953	118.66 ± 14.28
S97-V11A-AZ-CX	1.405 ± 1.475	-	0.3870 ± 1.3723	912.94 ± 222.12
S97-V11A-AZ-FX	-1.416 ± 7.185	-0.361 ± 0.534	-0.1413 ± 0.2669	117.20 ± 19.00
S97-V11B-AZ-CX	8.216 ± 3.098	1.599 ± 2.780	7.4141 ± 1.8270	1360.49 ± 286.84
S97-V11B-AZ-FX	0.063 ± 9.368	0.129 ± 0.863	-	125.02 ± 23.98
S97-V11C-AZ-CX	8.609 ± 3.074	0.685 ± 1.788	2.3874 ± 1.2396	-3.82 ± 264.17
S97-V11C-AZ-FX	5.936 ± 9.316	-0.392 ± 0.680	-	0.64 ± 21.43
S97-V11D-AZ-CX	3.561 ± 2.092	0.016 ± 1.296	1.2466 ± 1.0921	44.16 ± 265.46
S97-V11D-AZ-FX	-0.494 ± 8.996	-0.507 ± 0.644	-	-11.45 ± 21.35
S97-V11D-AZ-MX5	-	0.395 ± 0.688	-0.3715 ± 0.6292	0.04 ± 4.33
S97-V11D-AZ-MX6	-	0.085 ± 0.506	-	-0.60 ± 4.35
S97-V11D-AZ-MX7	0.191 ± 0.237	0.061 ± 0.423	-	9.84 ± 4.32
S97-V11D-AZ-MX8	0.027 ± 0.220	-	-	0.56 ± 4.30
S97-V11D-AZ-MX9	0.659 ± 0.338	0.124 ± 0.475	-	-0.68 ± 4.30
S97-V11D-AZ-MX10	0.024 ± 0.220	-0.153 ± 0.399	-	0.81 ± 4.30
S97-V11E-AZ-CX	4.325 ± 1.624	-	0.4913 ± 0.8044	-
S97-V11E-AZ-FX	3.222 ± 5.321	0.933 ± 0.737	0.6150 ± 0.4552	102.73 ± 14.15

Table D.5: Trace Metals Aerosol Concentration Data (Br, Cd, Ce, Cl) (continued)

Sample	Aerosol Concentration (ng m^{-3})			
	Br	Cd	Ce	Cl
S97-V12A-AZ-CX	2.826 ± 1.660	-	-0.1230 ± 0.9158	1733.60 ± 235.81
S97-V12A-AZ-FX	-1.018 ± 7.344	-	-	183.72 ± 23.66
S97-V12B-AZ-CX	8.612 ± 3.029	84.882 ± 60.899	8.0212 ± 4.9442	1330.00 ± 280.41
S97-V12B-AZ-FX	31.734 ± 13.206	1.172 ± 1.383	0.7682 ± 0.4007	49.51 ± 25.60
S97-V12C-AZ-CX	1.905 ± 1.835	3.902 ± 3.770	2.1784 ± 1.0843	72.03 ± 262.30
S97-V12C-AZ-FX	-2.255 ± 9.083	-	-0.0728 ± 0.3059	9.91 ± 21.78
S97-V12D-AZ-CX	5.506 ± 2.379	1.059 ± 2.124	-	5.69 ± 262.07
S97-V12D-AZ-FX	2.709 ± 9.226	-0.239 ± 0.764	0.0596 ± 0.3250	6.93 ± 21.78
S97-V12D-AZ-MX5	-0.045 ± 0.218	-	-0.2583 ± 0.6328	-2.74 ± 4.20
S97-V12D-AZ-MX6	0.301 ± 0.262	0.226 ± 0.638	-0.3825 ± 0.6137	-1.95 ± 4.22
S97-V12D-AZ-MX7	1.350 ± 0.445	0.092 ± 0.468	-	14.00 ± 4.42
S97-V12D-AZ-MX8	2.147 ± 0.624	0.027 ± 0.435	-	2.26 ± 4.20
S97-V12D-AZ-MX9	1.428 ± 0.456	-0.055 ± 0.404	-	-1.95 ± 4.20
S97-V12D-AZ-MX10	0.229 ± 0.229	-0.169 ± 0.385	-0.3073 ± 0.6225	-1.01 ± 4.20
S97-V12E-AZ-CX	4.527 ± 1.629	-	1.5064 ± 0.6443	185.02 ± 144.65
S97-V12E-AZ-FX	0.580 ± 5.042	-	-	59.83 ± 12.46
S97-V11A-RV-CX	0.570 ± 1.463	-	-0.2179 ± 0.9418	77.07 ± 222.08
S97-V11A-RV-FX	-1.246 ± 7.758	-0.441 ± 0.577	-0.0056 ± 0.2202	6.48 ± 18.53
S97-V11B-RV-CX	1.938 ± 1.883	-	3.2763 ± 1.4856	25.06 ± 266.88
S97-V11B-RV-FX	-1.475 ± 8.983	-0.412 ± 0.694	-	15.67 ± 22.20
S97-V11C-RV-CX	2.366 ± 1.872	-	-	-31.11 ± 260.50
S97-V11C-RV-FX	-1.318 ± 8.736	-0.293 ± 0.662	-	26.90 ± 21.03
S97-V11D-RV-CX	3.020 ± 2.108	-	0.2810 ± 1.0967	15.06 ± 260.11
S97-V11D-RV-FX	-0.260 ± 8.809	-	0.6968 ± 0.2621	34.50 ± 21.32
S97-V11D-RV-MX5	-0.056 ± 0.186	-	-0.2969 ± 0.5316	-2.33 ± 3.67
S97-V11D-RV-MX6	-0.023 ± 0.184	-	-	-1.58 ± 3.67
S97-V11D-RV-MX7	0.032 ± 0.189	-	-	-0.68 ± 3.66
S97-V11D-RV-MX8	0.180 ± 0.199	-0.076 ± 0.368	-	-0.58 ± 3.67
S97-V11D-RV-MX9	-	0.252 ± 0.456	-	21.66 ± 3.76
S97-V11D-RV-MX10	-0.054 ± 0.184	-	-0.2056 ± 0.5503	-1.96 ± 3.66
S97-V11E-RV-CX	0.981 ± 0.951	0.984 ± 0.497	0.5128 ± 0.5752	126.32 ± 142.46
S97-V11E-RV-FX	-0.282 ± 4.813	-	0.1363 ± 0.1749	6.63 ± 11.51
S97-V12A-RV-CX	5.714 ± 2.228	-	1.3098 ± 1.5527	143.42 ± 213.59
S97-V12A-RV-FX	0.565 ± 7.150	-0.355 ± 0.515	-0.0310 ± 0.2960	38.26 ± 17.42
S97-V12B-RV-CX	3.519 ± 2.068	-	2.3381 ± 1.2539	122.82 ± 270.09
S97-V12B-RV-FX	-0.433 ± 9.071	-0.435 ± 0.655	1.1132 ± 0.5274	45.43 ± 23.64
S97-V12C-RV-CX	1.911 ± 1.845	-	-	81.75 ± 262.91
S97-V12C-RV-FX	2.939 ± 8.937	-0.103 ± 0.722	-	6.06 ± 21.08
S97-V12D-RV-CX	4.302 ± 2.151	-	1.4918 ± 2.2868	14.93 ± 257.96
S97-V12D-RV-FX	-0.258 ± 8.757	-	0.1525 ± 0.4542	31.11 ± 21.57
S97-V12D-RV-MX5	-	1.279 ± 1.079	-	20.66 ± 4.66
S97-V12D-RV-MX6	0.277 ± 0.213	-0.134 ± 0.341	-	-0.77 ± 3.73
S97-V12D-RV-MX7	1.161 ± 0.388	-0.156 ± 0.341	-	0.98 ± 3.78
S97-V12D-RV-MX8	1.361 ± 0.465	-	-	-1.96 ± 3.69
S97-V12D-RV-MX9	0.137 ± 0.273	0.080 ± 0.476	-	-0.77 ± 3.70
S97-V12D-RV-MX10	0.137 ± 0.202	-	0.3764 ± 0.6173	-2.36 ± 3.68

Table D.5: Trace Metals Aerosol Concentration Data (Br, Cd, Ce, Cl) (continued)

Sample	Aerosol Concentration (ng m^{-3})			
	Br	Cd	Ce	Cl
S97-V12E-RV-CX	7.238 ± 2.208	-	-	101.26 ± 143.15
S97-V12E-RV-FX	6.666 ± 5.298	-	1.4628 ± 0.1826	50.26 ± 12.25
S97-V21A-LA-CX	4.987 ± 1.918	-	1.4999 ± 0.9500	2985.45 ± 258.75
S97-V21A-LA-FX	3.664 ± 6.824	-	0.0434 ± 0.3864	274.56 ± 23.80
S97-V21B-LA-CX	9.549 ± 3.163	-	0.8660 ± 1.1109	933.20 ± 246.84
S97-V21B-LA-FX	2.223 ± 8.601	-0.038 ± 0.714	-	-
S97-V21B-LA-MX5	0.162 ± 0.205	1.492 ± 1.195	-	17.74 ± 6.49
S97-V21B-LA-MX6	0.403 ± 0.230	-	-0.3203 ± 0.5551	-0.17 ± 3.93
S97-V21B-LA-MX7	-	-	-0.3320 ± 0.5516	-1.73 ± 3.88
S97-V21B-LA-MX8	0.726 ± 0.303	-	-0.1705 ± 0.5747	20.68 ± 4.35
S97-V21B-LA-MX9	0.344 ± 0.222	-	-	-1.55 ± 3.81
S97-V21B-LA-MX10	0.226 ± 0.212	0.494 ± 0.490	1.0922 ± 0.6076	-0.79 ± 3.99
S97-V21C-LA-CX	8.440 ± 2.928	-	4.1305 ± 1.9162	342.34 ± 234.58
S97-V21C-LA-FX	5.485 ± 8.591	0.205 ± 0.766	-0.1267 ± 0.2597	53.67 ± 20.40
S97-V21D-LA-CX	12.064 ± 3.681	-	1.2905 ± 1.0675	539.06 ± 241.05
S97-V21D-LA-FX	0.368 ± 8.557	-0.255 ± 0.666	-0.0682 ± 0.4176	33.47 ± 20.68
S97-V21E-LA-CX	4.083 ± 1.464	-	-0.0007 ± 0.6532	4258.71 ± 278.26
S97-V21E-LA-FX	0.378 ± 4.783	0.100 ± 0.449	0.3418 ± 0.2326	-
S97-V22A-LA-CX	1.136 ± 1.333	-	1.5519 ± 1.0877	4500.55 ± 325.87
S97-V22A-LA-FX	-0.821 ± 7.029	-0.082 ± 0.682	0.0715 ± 0.3442	571.85 ± 39.46
S97-V22B-LA-CX	11.192 ± 3.521	-	-	1785.91 ± 262.55
S97-V22B-LA-FX	1.287 ± 8.522	-0.130 ± 0.744	0.4335 ± 0.3895	134.65 ± 22.20
S97-V22B-LA-MX5	-	-	-	145.14 ± 13.65
S97-V22B-LA-MX6	0.076 ± 0.196	-0.107 ± 0.352	0.3849 ± 0.5904	-1.40 ± 3.84
S97-V22B-LA-MX7	0.896 ± 0.344	-0.058 ± 0.369	-	-0.46 ± 3.91
S97-V22B-LA-MX8	0.038 ± 0.192	-0.145 ± 0.356	-	1.00 ± 3.93
S97-V22B-LA-MX9	1.071 ± 0.397	-	-	2.75 ± 3.85
S97-V22B-LA-MX10	0.134 ± 0.202	0.257 ± 0.601	2.3399 ± 0.5916	15.88 ± 4.16
S97-V22C-LA-CX	7.454 ± 2.682	-	0.5978 ± 1.0609	715.43 ± 241.63
S97-V22C-LA-FX	5.530 ± 8.678	0.450 ± 1.041	-	105.79 ± 21.58
S97-V22D-LA-CX	5.713 ± 2.332	-	-	452.80 ± 244.70
S97-V22D-LA-FX	2.583 ± 8.807	-0.070 ± 0.801	-	-14.53 ± 21.18
S97-V22D-LA-MX5	-	-	-0.0814 ± 0.5730	2.15 ± 3.93
S97-V22D-LA-MX6	0.252 ± 0.222	-	-	-1.97 ± 3.75
S97-V22D-LA-MX7	0.890 ± 0.330	-	-	-0.17 ± 3.87
S97-V22D-LA-MX8	0.600 ± 0.269	0.021 ± 0.435	-0.2989 ± 0.5507	-1.79 ± 3.81
S97-V22D-LA-MX9	0.658 ± 0.277	0.111 ± 0.444	-	0.99 ± 3.91
S97-V22D-LA-MX10	0.513 ± 0.271	0.082 ± 0.383	0.2665 ± 0.6425	25.35 ± 5.30
S97-V22E-LA-CX	5.717 ± 1.863	-	-	1511.95 ± 159.56
S97-V22E-LA-FX	7.905 ± 5.350	-0.021 ± 0.424	-	211.88 ± 17.01
S97-V21A-AZ-CX	2.088 ± 1.497	-	0.8163 ± 0.9894	234.80 ± 206.37
S97-V21A-AZ-FX	0.550 ± 6.952	-	-0.1911 ± 0.2210	22.11 ± 16.77
S97-V21B-AZ-CX	2.197 ± 1.867	-	3.2322 ± 1.6069	157.88 ± 263.68
S97-V21B-AZ-FX	-0.332 ± 9.021	-	-	48.44 ± 22.15
S97-V21C-AZ-CX	3.766 ± 2.047	-	-	127.71 ± 260.44
S97-V21C-AZ-FX	3.275 ± 8.986	-0.232 ± 0.708	0.0900 ± 0.4072	21.84 ± 21.44

Table D.5: Trace Metals Aerosol Concentration Data (Br, Cd, Ce, Cl) (continued)

Sample	Aerosol Concentration (ng m^{-3})			
	Br	Cd	Ce	Cl
S97-V21D-AZ-CX	8.709 ± 3.191	-	2.2217 ± 1.1159	131.45 ± 267.59
S97-V21D-AZ-FX	7.357 ± 9.541	0.424 ± 0.931	0.0928 ± 0.3723	135.26 ± 26.08
S97-V21D-AZ-MX5	0.010 ± 0.220	-	-	3.42 ± 4.75
S97-V21D-AZ-MX6	-0.046 ± 0.213	-0.144 ± 0.405	-0.2661 ± 0.6404	0.47 ± 4.30
S97-V21D-AZ-MX7	1.763 ± 0.535	-0.163 ± 0.395	-	1.12 ± 4.29
S97-V21D-AZ-MX8	-0.046 ± 0.212	-	-0.3219 ± 0.6194	-0.19 ± 4.29
S97-V21D-AZ-MX9	0.778 ± 0.324	-	-	0.47 ± 4.31
S97-V21D-AZ-MX10	0.548 ± 0.275	-0.134 ± 0.398	-	4.40 ± 4.35
S97-V21E-AZ-CX	5.286 ± 1.788	-	1.0553 ± 0.8137	568.18 ± 150.42
S97-V21E-AZ-FX	1.123 ± 5.049	-	-	37.75 ± 12.44
S97-V22A-AZ-CX	2.633 ± 1.638	16.848 ± 17.000	0.0761 ± 0.9284	298.08 ± 214.83
S97-V22A-AZ-FX	2.152 ± 7.334	0.310 ± 0.858	0.2576 ± 0.5641	25.75 ± 17.48
S97-V22B-AZ-CX	2.254 ± 1.929	-	0.4865 ± 1.3966	854.82 ± 275.94
S97-V22B-AZ-FX	-0.268 ± 9.084	-0.399 ± 0.690	-	75.13 ± 22.48
S97-V22B-AZ-MX5	-	-	-0.0585 ± 0.6844	12.11 ± 4.63
S97-V22B-AZ-MX6	-	-0.051 ± 0.418	-	-1.03 ± 4.35
S97-V22B-AZ-MX7	0.670 ± 0.298	-	-0.3531 ± 0.6108	0.78 ± 4.44
S97-V22B-AZ-MX8	0.508 ± 0.269	-0.216 ± 0.382	-	0.46 ± 4.26
S97-V22B-AZ-MX9	0.152 ± 0.219	-0.226 ± 0.380	-	-1.19 ± 4.18
S97-V22B-AZ-MX10	2.159 ± 0.619	-0.207 ± 0.381	-	-1.61 ± 4.20
S97-V22C-AZ-CX	7.426 ± 2.783	-	4.5257 ± 2.1047	5.78 ± 266.40
S97-V22C-AZ-FX	-0.501 ± 9.120	0.026 ± 0.732	-	4.29 ± 21.90
S97-V22D-AZ-CX	-	-	2.6058 ± 1.9444	34.76 ± 267.02
S97-V22D-AZ-FX	2.014 ± 9.041	-0.072 ± 0.769	-	-2.62 ± 21.34
S97-V22D-AZ-MX5	-0.048 ± 0.211	-	-	8.83 ± 5.45
S97-V22D-AZ-MX6	0.094 ± 0.217	-	-	7.55 ± 4.91
S97-V22D-AZ-MX7	1.730 ± 0.526	0.123 ± 0.538	-	7.22 ± 4.55
S97-V22D-AZ-MX8	2.343 ± 0.707	-	-	-0.51 ± 4.37
S97-V22D-AZ-MX9	0.699 ± 0.304	3.248 ± 2.191	-	-1.06 ± 4.22
S97-V22D-AZ-MX10	0.699 ± 0.304	3.248 ± 2.191	-	2.39 ± 4.32
S97-V22E-AZ-CX	4.687 ± 1.712	-	2.9255 ± 1.6463	519.27 ± 151.30
S97-V22E-AZ-FX	3.434 ± 5.104	0.605 ± 0.584	-	69.44 ± 12.85
S97-V21A-RV-CX	6.319 ± 2.349	-	1.4613 ± 1.3004	258.61 ± 213.77
S97-V21A-RV-FX	-1.384 ± 7.022	-	0.5574 ± 0.3445	62.64 ± 17.52
S97-V21B-RV-CX	25.703 ± 7.304	-	2.7910 ± 2.8380	163.09 ± 309.51
S97-V21C-RV-CX	11.889 ± 3.823	0.198 ± 1.310	-0.8969 ± 0.9863	69.45 ± 252.86
S97-V21C-RV-FX	2.894 ± 8.793	-	0.2457 ± 0.4243	21.40 ± 20.94
S97-V21D-RV-CX	3.424 ± 2.012	-	-	134.76 ± 255.60
S97-V21D-RV-FX	-0.261 ± 8.857	-0.200 ± 0.742	0.3791 ± 0.3116	28.25 ± 21.42
S97-V21D-RV-MX5	0.017 ± 0.187	-	-	-0.74 ± 3.92
S97-V21D-RV-MX6	-0.034 ± 0.185	-	-0.3141 ± 0.5379	-1.68 ± 3.78
S97-V21D-RV-MX7	-	-	-	-1.85 ± 3.69
S97-V21D-RV-MX8	0.057 ± 0.188	-0.139 ± 0.340	-0.2684 ± 0.5379	10.68 ± 3.97
S97-V21D-RV-MX9	0.534 ± 0.253	-0.099 ± 0.351	-0.1714 ± 0.5489	-1.36 ± 3.70
S97-V21D-RV-MX10	-	-	-	4.97 ± 3.84
S97-V21E-RV-CX	10.735 ± 3.144	1.439 ± 1.882	2.0941 ± 1.3445	411.81 ± 144.05

Table D.5: Trace Metals Aerosol Concentration Data (Br, Cd, Ce, Cl) (continued)

Sample	Aerosol Concentration (ng m^{-3})			
	Br	Cd	Ce	Cl
S97-V21E-RV-FX	1.931 ± 4.842	-0.195 ± 0.364	0.0483 ± 0.1596	42.80 ± 11.82
S97-V22A-RV-CX	4.807 ± 1.999	0.246 ± 0.935	1.7794 ± 0.9635	345.27 ± 215.56
S97-V22A-RV-FX	0.601 ± 7.618	-0.281 ± 0.608	-	53.03 ± 18.83
S97-V22B-RV-CX	9.333 ± 3.238	5.424 ± 3.709	-	1469.38 ± 277.12
S97-V22B-RV-FX	0.717 ± 9.041	0.976 ± 1.432	-	115.33 ± 25.42
S97-V22B-RV-MX5	-	-	-	-1.58 ± 3.68
S97-V22B-RV-MX6	0.163 ± 0.232	-	-	-0.32 ± 3.70
S97-V22B-RV-MX7	0.933 ± 0.329	-	-	12.90 ± 3.69
S97-V22B-RV-MX8	1.561 ± 0.465	0.135 ± 0.476	-	2.43 ± 3.73
S97-V22B-RV-MX9	0.260 ± 0.206	-0.196 ± 0.334	-	-1.80 ± 3.68
S97-V22B-RV-MX10	-0.011 ± 0.185	-	-	-0.17 ± 3.66
S97-V22C-RV-CX	12.242 ± 3.766	28.998 ± 13.194	-	5.65 ± 260.11
S97-V22C-RV-FX	-1.617 ± 9.238	-	0.2956 ± 0.5089	34.25 ± 23.23
S97-V22D-RV-CX	12.310 ± 3.958	2.760 ± 3.857	0.9448 ± 1.2998	90.83 ± 261.81
S97-V22D-RV-FX	3.004 ± 9.115	-0.072 ± 0.873	-	1.62 ± 21.74
S97-V22D-RV-MX5	-0.014 ± 0.185	0.417 ± 0.523	-	-1.62 ± 3.61
S97-V22D-RV-MX6	0.112 ± 0.210	-	-	-1.92 ± 3.61
S97-V22D-RV-MX7	0.858 ± 0.309	0.358 ± 0.530	-0.1623 ± 0.5325	0.76 ± 3.59
S97-V22D-RV-MX8	0.299 ± 0.207	-	-0.3076 ± 0.5303	1.00 ± 3.60
S97-V22D-RV-MX9	0.635 ± 0.269	-0.061 ± 0.368	-	-0.38 ± 3.62
S97-V22D-RV-MX10	-	1.253 ± 1.004	-0.3048 ± 0.5288	-2.09 ± 3.59
S97-V22E-RV-CX	4.159 ± 1.542	-	1.0896 ± 0.9595	558.69 ± 147.90
S97-V22E-RV-FX	0.576 ± 5.014	-	-0.1483 ± 0.1452	62.40 ± 18.11
S97-N21D-ML-FX	1.129 ± 8.252	-	0.0715 ± 0.2964	41.11 ± 20.13
S97-N21E-ML-FX	8.817 ± 5.825	-	-	956.65 ± 76.94
S97-N22A-ML-FX	4.325 ± 7.275	-	-0.1076 ± 0.2515	420.24 ± 38.16
S97-N22B-ML-FX	18.762 ± 10.595	0.476 ± 1.670	-	409.75 ± 44.24
S97-N22C-ML-FX	-0.621 ± 8.934	-0.104 ± 0.824	-0.2985 ± 0.2606	-6.83 ± 21.28
S97-N22C-ML-MX5	-	-	-0.0822 ± 0.5957	4.51 ± 4.76
S97-N22C-ML-MX6	0.030 ± 0.197	-	-	8.32 ± 5.35
S97-N22C-ML-MX7	0.176 ± 0.205	0.024 ± 0.364	-	-2.25 ± 3.87
S97-N22C-ML-MX8	-0.061 ± 0.189	0.317 ± 0.419	-0.3426 ± 0.5616	-3.27 ± 3.77
S97-N22C-ML-MX9	0.313 ± 0.223	2.951 ± 1.051	-	-2.04 ± 3.81
S97-N22C-ML-MX10	-	-	-0.2344 ± 0.5765	0.71 ± 3.81
S97-N22D-ML-FX	0.940 ± 8.707	-	0.0252 ± 0.2468	44.05 ± 23.75
S97-N22E-ML-FX	13.157 ± 6.321	0.248 ± 0.572	-	521.33 ± 100.46
S97-N23A-ML-FX	7.490 ± 7.563	-	0.1494 ± 0.2529	638.36 ± 61.31
S97-N23B-ML-FX	5.379 ± 9.095	-	-	318.84 ± 37.19
S97-N23C-ML-FX	4.128 ± 9.007	-0.487 ± 0.660	0.2499 ± 0.2511	64.69 ± 26.32
S97-N23C-ML-MX5	0.108 ± 0.197	0.314 ± 0.485	-0.3340 ± 0.5441	6.80 ± 3.98
S97-N23C-ML-MX6	0.659 ± 0.278	-	-0.3050 ± 0.5472	71.81 ± 6.18
S97-N23C-ML-MX7	5.129 ± 1.176	-	-	83.42 ± 8.16
S97-N23C-ML-MX8	0.340 ± 0.221	-	-	7.96 ± 3.98
S97-N23C-ML-MX9	0.029 ± 0.189	-	-0.1424 ± 0.5599	0.41 ± 3.79
S97-N23C-ML-MX10	-0.080 ± 0.186	-	-	-1.79 ± 3.77

Table D.5: Trace Metals Aerosol Concentration Data (Br, Cd, Ce, Cl) (continued)

Sample	Aerosol Concentration (ng m^{-3})			
	Br	Cd	Ce	Cl
S97-N23D-ML-FX	0.059 ± 8.767	-	-	116.92 ± 20.81
S97-N23E-ML-FX	0.378 ± 5.001	0.177 ± 0.605	0.4307 ± 0.1453	921.41 ± 176.65
S97-N23E-ML-MX5	0.245 ± 0.162	-	-	1113.09 ± 70.77
S97-N23E-ML-MX6	0.378 ± 0.191	-	-	330.80 ± 21.74
S97-N23E-ML-MX7	0.628 ± 0.212	-0.018 ± 0.206	-0.1399 ± 0.3211	131.06 ± 8.27
S97-N23E-ML-MX8	0.228 ± 0.175	-	-	71.14 ± 6.21
S97-N23E-ML-MX9	0.047 ± 0.110	0.014 ± 0.217	-	-1.40 ± 2.15
S97-N23E-ML-MX10	-	-	-0.0950 ± 0.3688	-
S97-N31A-DB-CX	7.713 ± 2.494	-	0.9798 ± 0.7847	1524.43 ± 216.88
S97-N31A-DB-FX	3.239 ± 6.897	-	-	958.80 ± 79.02
S97-N31B-DB-CX	5.073 ± 2.230	1.348 ± 1.503	1.7755 ± 1.0354	751.58 ± 251.03
S97-N31B-DB-FX	9.925 ± 9.404	1.043 ± 1.651	-	141.92 ± 36.67
S97-N31C-DB-CX	5.501 ± 2.252	3.677 ± 3.127	1.3937 ± 1.0808	74.98 ± 241.19
S97-N31C-DB-FX	7.710 ± 9.202	0.216 ± 0.942	-0.0701 ± 0.2947	127.81 ± 25.62
S97-N31C-DB-MX5	0.317 ± 0.224	0.083 ± 0.438	-0.0535 ± 0.5602	-
S97-N31C-DB-MX6	0.701 ± 0.290	-	-	9.88 ± 4.37
S97-N31C-DB-MX7	0.133 ± 0.204	-	0.0649 ± 0.5799	5.45 ± 3.95
S97-N31C-DB-MX8	0.583 ± 0.266	-	-	-0.47 ± 3.87
S97-N31C-DB-MX9	0.258 ± 0.218	-	-	-
S97-N31C-DB-MX10	-0.032 ± 0.193	-	-0.2398 ± 0.5577	-
S97-N31D-DB-CX	3.294 ± 1.836	-0.070 ± 0.974	1.6837 ± 1.1784	47.18 ± 233.05
S97-N31D-DB-FX	4.253 ± 8.578	-	-	56.85 ± 20.74
S97-N31D-DB-MX5	3.723 ± 1.070	-	-	6.77 ± 4.66
S97-N31D-DB-MX6	-	-	0.7045 ± 0.7548	1.19 ± 4.65
S97-N31D-DB-MX7	3.374 ± 0.968	-0.048 ± 0.471	-	8.87 ± 4.69
S97-N31D-DB-MX8	1.385 ± 0.475	-	-	2.94 ± 4.60
S97-N31D-DB-MX9	0.011 ± 0.231	0.004 ± 0.510	-	-1.70 ± 4.52
S97-N31D-DB-MX10	0.063 ± 0.231	-	-	1.54 ± 4.57
S97-N31E-DB-CX	9.656 ± 2.739	1.263 ± 1.684	1.6884 ± 0.8530	519.26 ± 137.71
S97-N31E-DB-FX	14.588 ± 6.427	0.065 ± 0.439	0.2386 ± 0.1598	356.97 ± 65.29
S97-N32A-DB-CX	5.804 ± 2.157	-0.059 ± 0.876	-	4.24 ± 195.29
S97-N32A-DB-FX	-2.413 ± 6.957	-	-	-13.20 ± 16.55
S97-N32B-DB-CX	3.465 ± 1.991	-	3.1959 ± 1.0798	-106.02 ± 238.59
S97-N32B-DB-FX	-2.815 ± 8.569	-	-	175.52 ± 25.48
S97-N32C-DB-CX	2.555 ± 1.754	-0.427 ± 0.776	0.2535 ± 1.1716	13.58 ± 234.82
S97-N32C-DB-FX	1.868 ± 8.530	-0.252 ± 0.679	-0.0982 ± 0.2684	36.20 ± 22.29
S97-N32C-DB-MX5	-0.020 ± 0.202	-	-0.1970 ± 0.5524	3.35 ± 4.04
S97-N32C-DB-MX6	0.109 ± 0.203	-	-	0.12 ± 3.87
S97-N32C-DB-MX7	0.226 ± 0.209	-0.126 ± 0.363	-0.3614 ± 0.5496	1.30 ± 3.89
S97-N32C-DB-MX8	0.050 ± 0.193	-	-	-0.76 ± 3.84
S97-N32C-DB-MX9	0.100 ± 0.199	-	0.1231 ± 0.5477	-0.85 ± 3.84
S97-N32C-DB-MX10	0.176 ± 0.204	0.053 ± 0.389	-	-1.64 ± 3.82
S97-N32D-DB-CX	1.381 ± 1.620	-	1.3716 ± 1.1681	-12.01 ± 237.10
S97-N32D-DB-FX	0.696 ± 8.421	0.268 ± 0.923	-	9.12 ± 20.45
S97-N32E-DB-CX	1.139 ± 0.970	-0.105 ± 0.443	1.6755 ± 0.5578	-33.03 ± 136.23
S97-N32E-DB-FX	0.669 ± 4.773	0.014 ± 0.448	0.0138 ± 0.1592	8.09 ± 11.80

Table D.5: Trace Metals Aerosol Concentration Data (Br, Cd, Ce, Cl) (continued)

Sample	Aerosol Concentration (ng m^{-3})			
	Br	Cd	Ce	Cl
S97-N31A-ML-CX	13.736 ± 4.040	1.615 ± 2.218	3.8124 ± 1.7333	820.66 ± 218.84
S97-N31A-ML-FX	1.377 ± 7.360	0.074 ± 0.765	0.3399 ± 0.2778	577.78 ± 50.84
S97-N31B-ML-CX	7.600 ± 2.818	2.388 ± 2.942	4.7428 ± 1.3394	1115.83 ± 271.99
S97-N31B-ML-FX	9.944 ± 9.734	0.718 ± 1.183	0.2240 ± 0.2881	728.99 ± 64.31
S97-N31C-ML-CX	2.618 ± 2.002	0.218 ± 1.355	2.2056 ± 1.4760	186.59 ± 278.05
S97-N31C-ML-FX	0.066 ± 9.704	2.208 ± 5.670	0.0281 ± 0.3455	65.75 ± 26.03
S97-N31C-ML-MX5	0.148 ± 0.237	-	-0.3669 ± 0.6445	0.83 ± 4.67
S97-N31C-ML-MX6	0.298 ± 0.247	-	-	2.88 ± 4.70
S97-N31C-ML-MX7	0.607 ± 0.306	-	-	9.74 ± 4.76
S97-N31C-ML-MX8	0.110 ± 0.228	-	-	-1.40 ± 4.60
S97-N31C-ML-MX9	0.059 ± 0.230	-	-	-0.88 ± 4.50
S97-N31C-ML-MX10	-0.034 ± 0.224	-	-	-1.71 ± 4.47
S97-N31D-ML-CX	7.126 ± 2.742	0.965 ± 1.360	3.8889 ± 1.1493	726.81 ± 267.14
S97-N31D-ML-FX	7.763 ± 9.664	-	0.0603 ± 0.2688	195.17 ± 30.82
S97-N31D-ML-MX5	0.185 ± 0.249	-	-0.0654 ± 0.7833	7.75 ± 4.96
S97-N31D-ML-MX6	1.474 ± 0.493	-	-	38.89 ± 5.68
S97-N31D-ML-MX7	1.438 ± 0.461	-	-	64.60 ± 6.61
S97-N31D-ML-MX8	0.714 ± 0.320	-	-0.1994 ± 0.7206	9.93 ± 4.86
S97-N31D-ML-MX9	0.011 ± 0.236	0.102 ± 0.494	-	5.58 ± 4.79
S97-N31D-ML-MX10	-0.032 ± 0.235	-	-0.1379 ± 0.7033	-
S97-N31E-ML-CX	10.521 ± 3.035	0.903 ± 0.612	7.3079 ± 0.7064	1091.57 ± 160.47
S97-N31E-ML-FX	28.207 ± 9.391	-	0.5119 ± 0.2054	491.27 ± 94.86
S97-N32A-ML-CX	18.929 ± 5.307	-	3.7044 ± 1.0228	848.32 ± 224.77
S97-N32A-ML-FX	23.423 ± 10.200	0.743 ± 1.408	0.4975 ± 0.4789	505.95 ± 59.07
S97-N32B-ML-CX	3.165 ± 2.092	-	6.7036 ± 1.9855	134.10 ± 273.37
S97-N32B-ML-FX	-2.139 ± 9.498	-	-0.2421 ± 0.3419	-3.20 ± 22.74
S97-N32C-ML-CX	0.674 ± 1.721	-	2.0861 ± 1.6772	72.11 ± 262.75
S97-N32C-ML-FX	-2.932 ± 9.150	-	0.2601 ± 0.3534	-5.02 ± 21.81
S97-N32C-ML-MX5	-0.055 ± 0.208	-	-	0.78 ± 4.23
S97-N32C-ML-MX6	-	-0.183 ± 0.386	-	-3.02 ± 4.22
S97-N32C-ML-MX7	-0.048 ± 0.208	-	-0.3676 ± 0.6090	-1.83 ± 4.19
S97-N32C-ML-MX8	-0.029 ± 0.213	-0.135 ± 0.391	-	-1.38 ± 4.17
S97-N32C-ML-MX9	0.200 ± 0.234	0.510 ± 0.611	-	-1.35 ± 4.21
S97-N32C-ML-MX10	0.032 ± 0.216	-0.022 ± 0.433	-0.3933 ± 0.6037	3.68 ± 4.25
S97-N32D-ML-CX	-0.556 ± 1.686	-	-0.3270 ± 1.1472	-49.80 ± 264.57
S97-N32D-ML-FX	-3.313 ± 9.231	-	-	-7.56 ± 22.04
S97-N32E-ML-CX	0.955 ± 1.009	-	-	-2.11 ± 145.86
S97-N32E-ML-FX	-1.384 ± 5.089	-0.078 ± 0.428	-	-1.22 ± 12.18
S97-N31A-RV-CX	-0.690 ± 1.299	-0.173 ± 0.732	-0.6766 ± 0.8078	-88.33 ± 204.98
S97-N31A-RV-FX	4.311 ± 7.289	0.226 ± 0.721	-0.0308 ± 0.2374	143.54 ± 32.62
S97-N31B-RV-CX	1.891 ± 1.817	0.298 ± 1.509	1.3156 ± 1.1803	52.68 ± 260.24
S97-N31B-RV-FX	1.773 ± 9.139	-0.402 ± 0.679	-	34.22 ± 23.49
S97-N31C-RV-CX	0.931 ± 1.683	-	0.9209 ± 1.4884	23.98 ± 255.02
S97-N31C-RV-FX	-0.199 ± 8.928	-0.298 ± 0.702	-0.0065 ± 0.3853	25.25 ± 22.62
S97-N31C-RV-MX5	-	-	-	2.13 ± 3.91
S97-N31C-RV-MX6	0.279 ± 0.216	-	-	3.57 ± 3.87

Table D.5: Trace Metals Aerosol Concentration Data (Br, Cd, Ce, Cl) (continued)

Sample	Aerosol Concentration (ng m^{-3})			
	Br	Cd	Ce	Cl
S97-N31C-RV-MX7	1.142 ± 0.366	-	-0.1786 ± 0.5482	5.87 ± 3.90
S97-N31C-RV-MX8	-	-	-	-0.46 ± 3.79
S97-N31C-RV-MX9	0.538 ± 0.249	-	-	-1.78 ± 3.75
S97-N31C-RV-MX10	-0.026 ± 24.168	-	-	-1.81 ± 3.73
S97-N31D-RV-CX	4.191 ± 2.066	-	2.6127 ± 1.0476	118.50 ± 241.28
S97-N31D-RV-FX	4.182 ± 8.613	0.238 ± 0.837	-0.1283 ± 0.2825	24.12 ± 21.56
S97-N31D-RV-MX5	0.264 ± 0.294	-	-0.0276 ± 0.6915	8.36 ± 7.02
S97-N31D-RV-MX6	0.011 ± 0.241	-	0.5201 ± 0.7979	40.20 ± 8.14
S97-N31D-RV-MX7	1.394 ± 0.466	-	-	53.89 ± 6.02
S97-N31D-RV-MX8	0.055 ± 0.225	-	-	1.51 ± 4.49
S97-N31D-RV-MX9	0.028 ± 0.224	-	0.2805 ± 0.7979	-2.32 ± 4.55
S97-N31D-RV-MX10	-0.031 ± 0.224	-	-	-2.29 ± 4.43
S97-N31E-RV-CX	4.910 ± 1.799	0.609 ± 1.222	1.9612 ± 0.6783	161.32 ± 151.31
S97-N31E-RV-FX	9.234 ± 6.034	-	0.5699 ± 0.2423	79.16 ± 14.94
S97-N32A-RV-CX	3.890 ± 1.805	-	0.3034 ± 0.9834	293.84 ± 211.69
S97-N32A-RV-FX	-2.258 ± 7.495	-0.176 ± 0.625	-	49.83 ± 20.82
S97-N32B-RV-CX	0.009 ± 1.664	-	-	43.09 ± 258.96
S97-N32B-RV-FX	-1.033 ± 9.134	0.756 ± 1.275	1.0882 ± 0.3946	-5.33 ± 21.79
S97-N32C-RV-CX	-0.349 ± 1.619	-	0.5500 ± 1.0890	-67.07 ± 253.83
S97-N32C-RV-FX	-2.883 ± 8.874	-	-	25.54 ± 21.39
S97-N32C-RV-MX5	-0.088 ± 0.200	-	-	-1.55 ± 4.03
S97-N32C-RV-MX6	0.137 ± 0.214	-	-	1.06 ± 4.09
S97-N32C-RV-MX7	0.240 ± 0.230	-	-	-
S97-N32C-RV-MX9	-0.081 ± 0.200	-	-	0.75 ± 4.08
S97-N32C-RV-MX10	0.150 ± 0.218	-0.071 ± 0.411	-0.0874 ± 0.6064	-
S97-N32D-RV-CX	0.997 ± 1.656	-	0.0886 ± 0.9932	-55.70 ± 248.18
S97-N32D-RV-FX	-2.304 ± 8.646	-0.259 ± 0.697	0.1827 ± 0.2470	4.71 ± 21.08
S97-N32E-RV-CX	0.519 ± 0.945	-	-	49.38 ± 142.26
S97-N32E-RV-FX	-1.286 ± 4.970	-0.276 ± 0.369	-	28.42 ± 13.67
S97-T11B-TI-CX	5.735 ± 2.561	10.604 ± 4.934	7.2352 ± 3.0406	1810.27 ± 321.03
S97-T11B-TI-FX	6.974 ± 11.405	4.123 ± 3.931	3.2408 ± 1.0501	3318.23 ± 263.62
S97-T11B-TI-MX5	0.243 ± 0.281	0.893 ± 0.939	-	96.87 ± 8.98
S97-T11B-TI-MX6	0.118 ± 0.264	-	-	2.12 ± 5.22
S97-T11B-TI-MX7	0.192 ± 0.268	-0.128 ± 0.503	-	4.86 ± 5.29
S97-T11B-TI-MX8	0.149 ± 0.262	-	-0.4192 ± 0.7370	0.56 ± 5.13
S97-T11B-TI-MX9	0.419 ± 0.290	-	-0.4740 ± 0.7321	28.75 ± 6.62
S97-T11B-TI-MX10	0.263 ± 0.272	-	-	-0.23 ± 5.15
S97-T11B-TO-CX	-0.446 ± 2.069	20.926 ± 14.124	-	1733.52 ± 341.45
S97-T11B-TO-FX	4.841 ± 11.451	2.638 ± 3.276	-	1380.06 ± 113.51
S97-T11B-TO-MX5	0.025 ± 0.275	0.406 ± 0.720	-	655.88 ± 49.86
S97-T11B-TO-MX6	-	-	-	22.90 ± 8.16
S97-T11B-TO-MX7	-	-0.028 ± 0.592	-	-2.22 ± 5.37
S97-T11B-TO-MX8	-	-	-	-1.85 ± 5.37
S97-T11B-TO-MX9	-0.119 ± 0.265	-	-0.3846 ± 0.7810	-1.48 ± 5.36
S97-T11B-TO-MX10	-	-	-	-2.14 ± 5.36

Table D.5: Trace Metals Aerosol Concentration Data (Br, Cd, Ce, Cl) (continued)

Sample	Aerosol Concentration (ng m^{-3})			
	Br	Cd	Ce	Cl
S97-T21B-TI-CX	2.291 ± 2.112	-	2.1701 ± 1.5189	60.81 ± 300.25
S97-T21B-TI-FX	-3.269 ± 10.919	1.185 ± 2.029	-	179.87 ± 31.76
S97-T21B-TI-MX5	0.082 ± 0.260	-0.050 ± 0.498	-0.3398 ± 0.7461	6.80 ± 5.35
S97-T21B-TI-MX6	-	-	-0.3671 ± 0.7335	0.16 ± 5.24
S97-T21B-TI-MX7	0.535 ± 0.337	0.422 ± 0.624	-	0.16 ± 5.32
S97-T21B-TI-MX8	0.418 ± 0.317	-	-	-3.54 ± 5.03
S97-T21B-TI-MX9	0.574 ± 0.320	-0.148 ± 0.493	-0.3320 ± 0.7404	0.55 ± 5.10
S97-T21B-TI-MX10	0.418 ± 0.291	-0.054 ± 0.508	-	-2.22 ± 5.06
S97-T21B-TO-FX	-3.831 ± 10.716	-	-	384.56 ± 63.14
S97-T31B-TI-CX	1.422 ± 2.026	3.602 ± 2.638	3.6902 ± 1.4027	2579.89 ± 336.15
S97-T31B-TI-FX	-2.511 ± 11.277	-	0.1561 ± 0.3797	701.46 ± 63.06
S97-T31B-TI-MX5	-0.050 ± 0.254	-	-	237.03 ± 15.65
S97-T31B-TI-MX6	-0.019 ± 0.254	-0.140 ± 0.501	-	21.63 ± 5.53
S97-T31B-TI-MX7	-0.007 ± 0.253	-	-	-1.01 ± 5.16
S97-T31B-TI-MX9	0.149 ± 0.262	-	-	-2.49 ± 5.14
S97-T31B-TI-MX10	0.192 ± 0.266	-	-	1.72 ± 5.09
S97-T31B-TO-CX	-0.262 ± 2.013	-	-	1796.56 ± 334.77
S97-T31B-TO-FX	-3.934 ± 10.669	0.420 ± 1.396	-	502.52 ± 53.81
S97-T31B-TO-MX5	-	-	-	497.69 ± 36.68
S97-T31B-TO-MX6	-	-	-	31.09 ± 7.93
S97-T31B-TO-MX7	-	-0.049 ± 0.477	-	7.89 ± 7.34
S97-T31B-TO-MX8	-0.065 ± 0.250	-	-0.2786 ± 0.7366	6.73 ± 6.79
S97-T31B-TO-MX9	0.004 ± 0.253	-	-0.1858 ± 0.7543	19.49 ± 6.79
S97-T31B-TO-MX10	-	-	-	10.21 ± 6.13
S97-T41B-TI-CX	3.357 ± 2.247	3.588 ± 2.604	3.4556 ± 2.1523	307.81 ± 309.63
S97-T41B-TI-FX	0.485 ± 11.296	-	0.2782 ± 0.3577	118.20 ± 35.70
S97-T41B-TI-MX5	1.237 ± 0.497	-	1.9976 ± 0.7412	14.99 ± 6.60
S97-T41B-TI-MX6	-	-	0.5538 ± 0.9842	5.24 ± 5.82
S97-T41B-TI-MX7	-0.035 ± 0.261	-	-	-1.28 ± 6.07
S97-T41B-TI-MX8	-	-	-	2.89 ± 5.45
S97-T41B-TI-MX9	0.418 ± 0.301	-	-0.1486 ± 0.7766	-1.12 ± 5.10
S97-T41B-TI-MX10	0.340 ± 0.280	-	-	4.46 ± 5.36
S97-T41B-TO-CX	-0.382 ± 1.920	0.128 ± 1.184	-	6.55 ± 301.64
S97-T41B-TO-FX	2.096 ± 11.006	-0.365 ± 0.859	-	175.21 ± 45.68
S97-B11A-AZ-MX5	-	-	-	9.00 ± 0.40
S97-B11A-AZ-MX6	1.200 ± 0.400	2.600 ± 1.400	-	6.08 ± 0.40
S97-B11A-AZ-MX7	-	-	-	19.00 ± 1.20
S97-B11A-AZ-MX8	-	-	-	12.00 ± 0.60
S97-B11A-AZ-MX9	-	1.980 ± 1.460	-	17.00 ± 0.60
S97-B11A-AZ-MX10	1.740 ± 0.580	-	-	3.96 ± 0.40
S97-B11A-DB-CX	9.800 ± 2.600	2.800 ± 2.600	-	1500.00 ± 70.00
S97-B11A-DB-FX	0.150 ± 0.071	0.610 ± 0.580	-	14.85 ± 2.40
S97-B11A-DB-MX5	0.178 ± 0.090	-	0.7600 ± 0.6600	17.80 ± 4.40
S97-B11A-DB-MX6	0.240 ± 0.166	2.800 ± 1.260	0.9200 ± 0.7000	22.00 ± 5.20

Table D.5: Trace Metals Aerosol Concentration Data (Br, Cd, Ce, Cl) (continued)

Sample	Aerosol Concentration (ng m^{-3})			
	Br	Cd	Ce	Cl
S97-B11A-DB-MX7	0.340 ± 0.128	1.280 ± 0.980	-	20.00 ± 4.80
S97-B11A-DB-MX8	0.980 ± 0.280	-	-	10.60 ± 3.40
S97-B11A-DB-MX9	0.540 ± 0.360	-	-	11.80 ± 5.20
S97-B11A-DB-MX10	0.050 ± 0.032	-	-	48.00 ± 7.40
S97-B11A-ML-CX	0.122 ± 0.112	1.440 ± 1.060	0.6800 ± 0.5400	30.00 ± 6.60
S97-B11A-ML-FX	73.000 ± 0.068	0.330 ± 0.240	0.3200 ± 0.2400	14.43 ± 2.10
S97-B11A-RV-CX	0.480 ± 0.240	-	1.3400 ± 0.8200	42.00 ± 7.20
S97-B11A-RV-FX	0.000 ± 0.000	-	-	71.00 ± 10.00
S97-B11A-RV-MX5	0.220 ± 0.134	1.560 ± 1.080	2.2000 ± 0.1040	16.40 ± 3.20
S97-B11A-RV-MX6	0.260 ± 0.176	1.360 ± 1.000	-	18.60 ± 4.40
S97-B11A-RV-MX7	0.100 ± 0.080	-	-	38.00 ± 6.80
S97-B11A-RV-MX8	-	-	-	10.80 ± 3.40
S97-B11A-RV-MX9	0.540 ± 0.160	-	1.2600 ± 0.7800	20.00 ± 3.80
S97-B11A-RV-MX10	-	-	-	10.00 ± 4.00
S97-B11A-TI-CX	0.520 ± 0.280	-	1.3200 ± 0.5600	20.00 ± 5.60
S97-B11A-TI-FX	0.000 ± 0.000	1.100 ± 0.800	0.8000 ± 0.6000	199.00 ± 8.00
S97-B11A-TI-MX5	0.166 ± 0.088	4.600 ± 3.800	1.4600 ± 1.3400	54.00 ± 15.60
S97-B11A-TI-MX6	-	-	1.5600 ± 1.1800	146.00 ± 12.60
S97-B11A-TI-MX7	-	3.800 ± 2.400	1.6200 ± 0.9400	17.00 ± 4.00
S97-B11A-TI-MX8	0.076 ± 0.026	-	-	-
S97-B11A-TI-MX9	0.400 ± 0.192	-	-	22.00 ± 5.60
S97-B11A-TI-MX10	0.460 ± 0.126	1.300 ± 1.100	1.7800 ± 0.9800	12.60 ± 2.80
S97-B21A-DB-CX	1.940 ± 0.560	5.600 ± 2.400	0.9400 ± 0.5600	62.00 ± 9.40
S97-B21A-DB-FX	-	2.010 ± 1.750	-	21.10 ± 3.76
S97-B21A-DB-MX5	0.800 ± 0.340	-	-	80.00 ± 22.00
S97-B21A-DB-MX6	-	-	-	60.00 ± 38.00
S97-B21A-DB-MX7	0.160 ± 0.120	-	-	16.60 ± 3.20
S97-B21A-DB-MX9	8.000 ± 2.400	14.000 ± 6.400	-	32.00 ± 5.20
S97-B21A-DB-MX10	-	1.060 ± 0.700	24.0000 ± 3.2000	22.00 ± 5.80
S97-B21A-ML-CX	0.700 ± 0.200	-	1.3400 ± 0.9200	36.00 ± 7.40
S97-B21A-ML-FX	0.200 ± 0.100	-	1.4000 ± 0.6000	42.00 ± 4.00
S97-B21A-ML-MX5	0.158 ± 0.096	-	-	13.40 ± 3.80
S97-B21A-ML-MX6	-	-	-	13.60 ± 4.20
S97-B21A-ML-MX7	-	-	1.6000 ± 0.5200	9.80 ± 4.60
S97-B21A-ML-MX8	-	-	1.5600 ± 0.8600	12.40 ± 3.00
S97-B21A-ML-MX9	1.680 ± 0.340	-	-	13.80 ± 5.00
S97-B21A-ML-MX10	-	-	-	-
S97-B21A-RV-CX	-	-	-	46.00 ± 9.00
S97-B21A-RV-FX	1.000 ± 1.000	4.200 ± 3.600	-	72.00 ± 6.00
S97-B21A-RV-MX5	-	3.000 ± 2.200	0.6800 ± 0.5600	51.00 ± 1.40
S97-B21A-RV-MX6	0.154 ± 0.114	-	-	-
S97-B21A-RV-MX7	-	-	8.0000 ± 3.8000	34.00 ± 13.20
S97-B21A-RV-MX8	-	-	-	28.60 ± 1.60
S97-B21A-RV-MX9	-	-	-	48.00 ± 15.60

Table D.5: Trace Metals Aerosol Concentration Data (Br, Cd, Ce, Cl) (continued)

Sample	Aerosol Concentration (ng m^{-3})			
	Br	Cd	Ce	Cl
S97-B21A-RV-MX10	0.160 ± 0.060	-	0.8000 ± 0.5000	11.88 ± 1.00

D.6 Trace Elements Aerosol Concentration Data (Co, Cr, Cs, Eu)

Table D.6: Trace Metals Aerosol Concentration Data (Co, Cr, Cs, Eu)

Sample	Aerosol Concentration (ng m^{-3})			
	Co	Cr	Cs	Eu
S97-V11A-LA-CX	3.16 ± 1.14	33.80 ± 6.13	-	-
S97-V11A-LA-FX	0.70 ± 0.55	39.90 ± 1.91	-	-
S97-V11B-LA-CX	2.61 ± 1.25	24.30 ± 6.79	-0.315 ± 0.851	-0.0896 ± 0.1249
S97-V11B-LA-FX	10.06 ± 0.93	406.05 ± 8.92	-	-
S97-V11C-LA-CX	3.19 ± 1.22	92.00 ± 6.42	-0.183 ± 0.813	-0.1299 ± 0.0846
S97-V11C-LA-FX	-0.30 ± 0.59	5.61 ± 1.42	0.360 ± 0.111	-
S97-V11D-LA-CX	1.02 ± 1.22	79.52 ± 8.03	-	-
S97-V11D-LA-FX	1.14 ± 0.59	67.14 ± 1.85	-0.055 ± 0.115	0.0963 ± 0.0280
S97-V11E-LA-CX	-0.34 ± 0.77	8.44 ± 3.72	-	-
S97-V11E-LA-FX	0.37 ± 0.37	0.14 ± 0.74	0.060 ± 0.152	-
S97-V12A-LA-CX	1.69 ± 0.92	24.99 ± 5.08	-0.224 ± 0.599	-0.0826 ± 0.0738
S97-V12A-LA-FX	0.51 ± 0.54	7.49 ± 1.42	-	-
S97-V12B-LA-CX	2.23 ± 1.10	18.11 ± 5.88	-0.296 ± 0.734	0.1252 ± 0.1226
S97-V12B-LA-FX	4.99 ± 0.66	251.25 ± 6.71	0.493 ± 0.254	0.0579 ± 0.0389
S97-V12B-LA-MX5	-1.30 ± 6.85	-0.58 ± 1.37	-0.098 ± 0.244	-
S97-V12B-LA-MX6	-0.95 ± 6.85	-0.17 ± 1.39	-0.187 ± 0.243	0.0367 ± 0.0646
S97-V12B-LA-MX7	-0.53 ± 6.85	-	-	-
S97-V12B-LA-MX8	-1.21 ± 6.85	-	-0.113 ± 0.245	-0.0073 ± 0.0600
S97-V12B-LA-MX9	-1.30 ± 6.85	-	-0.172 ± 0.245	-0.0429 ± 0.0614
S97-V12B-LA-MX10	-1.27 ± 6.85	4.85 ± 1.40	-0.037 ± 0.248	0.0367 ± 0.0661
S97-V12C-LA-CX	3.24 ± 1.50	24.81 ± 7.82	-	0.7693 ± 0.3814
S97-V12C-LA-FX	5.01 ± 0.85	143.28 ± 4.36	-	-
S97-V12D-LA-CX	1.18 ± 1.15	15.44 ± 6.17	-0.168 ± 0.775	0.0330 ± 0.1287
S97-V12D-LA-FX	3.08 ± 0.72	110.56 ± 4.02	0.783 ± 0.289	0.1808 ± 0.1041
S97-V12E-LA-CX	0.54 ± 0.86	7.85 ± 4.23	-	-
S97-V12E-LA-FX	0.33 ± 0.37	28.65 ± 1.37	0.094 ± 0.192	0.0721 ± 0.0480
S97-V11A-AZ-CX	1.80 ± 1.26	5.62 ± 6.09	-	-
S97-V11A-AZ-FX	-0.06 ± 0.48	3.31 ± 1.01	-	-
S97-V11B-AZ-CX	8.62 ± 2.31	29.90 ± 8.64	-	-
S97-V11B-AZ-FX	0.87 ± 0.80	2.60 ± 1.68	-	0.2589 ± 0.1978
S97-V11C-AZ-CX	4.89 ± 1.56	16.48 ± 6.91	-	-
S97-V11C-AZ-FX	-0.30 ± 0.60	5.11 ± 1.42	0.060 ± 0.186	0.0170 ± 0.0299
S97-V11D-AZ-CX	8.37 ± 1.85	5.03 ± 6.53	-	-0.1768 ± 0.0888
S97-V11D-AZ-FX	-0.21 ± 0.60	1.10 ± 1.25	-	-
S97-V11D-AZ-MX5	-1.21 ± 7.80	-0.16 ± 1.55	-	-0.0635 ± 0.0679
S97-V11D-AZ-MX6	-0.60 ± 7.80	0.31 ± 1.57	-0.095 ± 0.281	-0.0388 ± 0.0693
S97-V11D-AZ-MX7	-0.61 ± 7.80	5.86 ± 1.71	-	-
S97-V11D-AZ-MX8	-1.48 ± 7.80	2.11 ± 1.61	-	-
S97-V11D-AZ-MX9	-1.56 ± 7.80	2.52 ± 1.62	-	0.0291 ± 0.0748
S97-V11D-AZ-MX10	-0.71 ± 7.80	-	-	-
S97-V11E-AZ-CX	0.88 ± 1.05	3.96 ± 4.29	-	-
S97-V11E-AZ-FX	0.97 ± 0.44	70.06 ± 2.52	-	0.0191 ± 0.0533

Table D.6: Trace Metals Aerosol Concentration Data (Co, Cr, Cs, Eu) (continued)

Sample	Aerosol Concentration (ng m^{-3})			
	Co	Cr	Cs	Eu
S97-V12A-AZ-CX	0.24 ± 0.96	2.24 ± 5.18	-0.470 ± 0.620	0.2718 ± 0.4098
S97-V12A-AZ-FX	-0.09 ± 0.47	8.19 ± 1.23	0.007 ± 0.103	-
S97-V12B-AZ-CX	2.53 ± 1.86	47.60 ± 12.41	2.168 ± 1.715	0.3449 ± 0.5200
S97-V12B-AZ-FX	-0.04 ± 0.62	13.03 ± 1.79	0.076 ± 0.204	-
S97-V12C-AZ-CX	0.30 ± 1.16	4.97 ± 6.34	-0.225 ± 0.745	0.1107 ± 0.1050
S97-V12C-AZ-FX	0.52 ± 0.61	1.21 ± 1.33	-	-
S97-V12D-AZ-CX	2.48 ± 1.61	1.08 ± 6.86	-	0.4898 ± 0.3431
S97-V12D-AZ-FX	1.11 ± 0.64	4.85 ± 1.33	-	-
S97-V12D-AZ-MX5	-1.11 ± 7.62	-	-	-
S97-V12D-AZ-MX6	1.30 ± 7.62	-0.74 ± 1.52	0.067 ± 0.278	-0.0601 ± 0.0670
S97-V12D-AZ-MX7	-1.12 ± 7.62	0.69 ± 1.55	-	-0.0245 ± 0.0711
S97-V12D-AZ-MX8	-0.59 ± 7.62	-	-	-
S97-V12D-AZ-MX9	-1.43 ± 7.62	-0.78 ± 1.51	-	0.0082 ± 0.0689
S97-V12D-AZ-MX10	-1.25 ± 7.62	0.14 ± 1.52	-0.178 ± 0.279	-0.0245 ± 0.0663
S97-V12E-AZ-CX	0.99 ± 0.66	4.28 ± 3.51	-0.321 ± 0.421	0.0088 ± 0.0747
S97-V12E-AZ-FX	0.25 ± 0.38	2.30 ± 0.84	-	-
S97-V11A-RV-CX	-0.07 ± 1.02	-1.25 ± 5.41	-	-0.0748 ± 0.0776
S97-V11A-RV-FX	-0.35 ± 0.50	0.98 ± 1.05	-	-0.0023 ± 0.0240
S97-V11B-RV-CX	1.07 ± 1.48	6.02 ± 7.01	0.331 ± 1.126	0.5368 ± 0.3958
S97-V11B-RV-FX	-0.37 ± 0.59	1.20 ± 1.27	0.109 ± 0.102	-
S97-V11C-RV-CX	1.33 ± 1.25	3.34 ± 6.56	-	0.2233 ± 0.1908
S97-V11C-RV-FX	-0.41 ± 0.58	3.92 ± 1.39	-	0.0441 ± 0.0531
S97-V11D-RV-CX	0.01 ± 1.17	26.58 ± 6.49	0.134 ± 0.814	-0.0312 ± 0.1426
S97-V11D-RV-FX	0.09 ± 0.56	4.37 ± 1.13	-0.136 ± 0.099	0.0134 ± 0.0181
S97-V11D-RV-MX5	-1.71 ± 6.65	-	-0.197 ± 0.232	-0.0656 ± 0.0580
S97-V11D-RV-MX6	0.05 ± 6.65	4.87 ± 1.36	-	-0.0385 ± 0.0580
S97-V11D-RV-MX7	-1.06 ± 6.65	-0.17 ± 1.36	-0.130 ± 0.248	-
S97-V11D-RV-MX8	-0.80 ± 6.65	-0.11 ± 1.36	-	0.0014 ± 0.0720
S97-V11D-RV-MX9	-0.38 ± 6.65	-	-	-
S97-V11D-RV-MX10	-1.18 ± 6.65	-	-0.119 ± 0.244	-0.0214 ± 0.0604
S97-V11E-RV-CX	0.47 ± 0.64	23.23 ± 3.59	-0.204 ± 0.418	0.0703 ± 0.0699
S97-V11E-RV-FX	0.17 ± 0.31	9.03 ± 0.75	-	-
S97-V12A-RV-CX	-0.07 ± 1.26	13.30 ± 7.21	-	-
S97-V12A-RV-FX	-0.09 ± 0.50	1.20 ± 1.21	-	0.1014 ± 0.0888
S97-V12B-RV-CX	4.89 ± 1.32	4.04 ± 6.70	-0.348 ± 0.839	-0.0323 ± 0.1328
S97-V12B-RV-FX	0.55 ± 0.70	-	-	0.2147 ± 0.1851
S97-V12C-RV-CX	3.82 ± 1.36	165.63 ± 13.87	-0.416 ± 0.740	0.0445 ± 0.1517
S97-V12C-RV-FX	0.66 ± 0.64	2.13 ± 1.37	-	-
S97-V12D-RV-CX	3.75 ± 1.59	46.89 ± 9.27	0.133 ± 1.154	-0.1690 ± 0.0866
S97-V12D-RV-FX	0.47 ± 0.67	-	1.250 ± 0.517	0.2452 ± 0.0840
S97-V12D-RV-MX5	-0.09 ± 6.66	-	-	-0.0214 ± 0.0642
S97-V12D-RV-MX6	-0.38 ± 6.66	1.29 ± 1.42	-0.070 ± 0.247	-
S97-V12D-RV-MX7	-0.40 ± 6.66	-0.48 ± 1.42	0.218 ± 0.285	-
S97-V12D-RV-MX8	-0.40 ± 6.66	2.15 ± 1.70	-	-
S97-V12D-RV-MX9	-0.52 ± 6.65	2.43 ± 1.45	0.161 ± 0.261	0.0328 ± 0.0659
S97-V12D-RV-MX10	-0.35 ± 6.66	-	0.247 ± 0.354	0.1384 ± 0.0774

Table D.6: Trace Metals Aerosol Concentration Data (Co, Cr, Cs, Eu) (continued)

Sample	Aerosol Concentration (ng m^{-3})			
	Co	Cr	Cs	Eu
S97-V12E-RV-CX	1.82 ± 1.03	11.49 ± 5.77	-	-0.0910 ± 0.0484
S97-V12E-RV-FX	0.40 ± 2.64	4.30 ± 0.65	0.020 ± 0.066	-
S97-V21A-LA-CX	-0.19 ± 0.95	20.63 ± 5.47	-	-
S97-V21A-LA-FX	4.48 ± 0.66	203.56 ± 4.66	-	-
S97-V21B-LA-CX	2.53 ± 1.29	15.82 ± 6.21	0.384 ± 0.901	-0.0201 ± 0.2150
S97-V21B-LA-FX	1.38 ± 0.62	72.27 ± 2.53	-	-
S97-V21B-LA-MX5	0.26 ± 6.85	2.21 ± 1.36	-	-
S97-V21B-LA-MX6	-1.21 ± 6.85	0.18 ± 1.39	-0.134 ± 0.246	-
S97-V21B-LA-MX7	-1.18 ± 6.85	-0.55 ± 1.36	-0.037 ± 0.245	-0.0014 ± 0.0646
S97-V21B-LA-MX8	-1.00 ± 6.85	-0.05 ± 1.37	-0.113 ± 0.250	-
S97-V21B-LA-MX9	-1.26 ± 6.85	-0.55 ± 1.36	-0.125 ± 0.242	-0.0461 ± 0.0607
S97-V21B-LA-MX10	0.29 ± 6.86	14.84 ± 2.10	-0.002 ± 0.262	-
S97-V21C-LA-CX	3.98 ± 1.43	26.34 ± 6.24	-	-0.1586 ± 0.0781
S97-V21C-LA-FX	0.32 ± 0.53	28.25 ± 1.33	-	-0.0024 ± 0.0188
S97-V21D-LA-CX	0.70 ± 1.11	14.85 ± 6.01	-0.419 ± 0.745	0.2298 ± 0.3201
S97-V21D-LA-FX	1.38 ± 0.73	50.74 ± 3.02	-	-
S97-V21E-LA-CX	1.97 ± 0.81	6.35 ± 3.84	-	-
S97-V21E-LA-FX	1.31 ± 0.33	74.87 ± 2.16	0.179 ± 0.111	-
S97-V22A-LA-CX	2.41 ± 1.10	9.35 ± 5.08	-	-0.1293 ± 0.0654
S97-V22A-LA-FX	1.68 ± 0.56	62.26 ± 2.32	-	-
S97-V22B-LA-CX	2.85 ± 2.39	13.11 ± 11.05	-	-
S97-V22B-LA-FX	1.99 ± 0.67	53.39 ± 2.29	0.626 ± 0.131	-
S97-V22B-LA-MX5	-	-	-	-
S97-V22B-LA-MX6	0.40 ± 6.82	1.03 ± 1.65	0.398 ± 0.317	-
S97-V22B-LA-MX7	-1.00 ± 6.81	0.21 ± 1.42	-0.171 ± 0.240	-
S97-V22B-LA-MX8	-1.17 ± 6.81	0.33 ± 1.37	-	-
S97-V22B-LA-MX9	-0.18 ± 6.81	2.49 ± 1.45	0.001 ± 0.263	-0.0335 ± 0.0656
S97-V22B-LA-MX10	0.99 ± 6.81	-	-	0.3662 ± 0.0940
S97-V22C-LA-CX	2.92 ± 1.22	31.02 ± 6.38	-	-0.0112 ± 0.0799
S97-V22C-LA-FX	3.82 ± 0.90	104.49 ± 4.09	-	-
S97-V22D-LA-CX	2.91 ± 1.55	7.23 ± 6.89	-	-
S97-V22D-LA-FX	-0.07 ± 0.60	27.66 ± 1.84	-	-
S97-V22D-LA-MX5	0.08 ± 6.77	3.34 ± 2.07	-0.013 ± 0.307	-
S97-V22D-LA-MX6	-0.50 ± 6.76	-	-	-0.0043 ± 0.0656
S97-V22D-LA-MX7	-0.88 ± 6.76	-0.43 ± 1.39	-	0.0392 ± 0.0868
S97-V22D-LA-MX8	-1.17 ± 6.76	-0.52 ± 1.34	-0.202 ± 0.237	-0.0043 ± 0.0625
S97-V22D-LA-MX9	-1.75 ± 6.76	-0.52 ± 1.38	-0.086 ± 0.269	-
S97-V22D-LA-MX10	0.98 ± 6.79	0.44 ± 1.45	0.338 ± 0.293	-
S97-V22E-LA-CX	2.01 ± 0.99	34.87 ± 4.69	-	-0.0862 ± 0.0443
S97-V22E-LA-FX	1.30 ± 0.35	63.95 ± 2.30	0.263 ± 0.068	-
S97-V21A-AZ-CX	1.50 ± 1.00	4.64 ± 5.15	-	0.0274 ± 0.1637
S97-V21A-AZ-FX	0.90 ± 0.46	3.69 ± 1.01	-	-
S97-V21B-AZ-CX	6.39 ± 1.55	11.64 ± 7.04	1.467 ± 1.436	-
S97-V21B-AZ-FX	0.74 ± 0.69	6.76 ± 1.74	0.339 ± 0.341	-
S97-V21C-AZ-CX	-0.46 ± 1.53	11.50 ± 8.40	-	-
S97-V21C-AZ-FX	0.79 ± 0.63	2.46 ± 1.36	-	-

Table D.6: Trace Metals Aerosol Concentration Data (Co, Cr, Cs, Eu) (continued)

Sample	Aerosol Concentration (ng m^{-3})			
	Co	Cr	Cs	Eu
S97-V21D-AZ-CX	2.82 ± 1.29	7.00 ± 6.50	-0.432 ± 0.780	0.0840 ± 0.2218
S97-V21D-AZ-FX	2.01 ± 0.67	64.21 ± 2.13	-	0.0206 ± 0.0428
S97-V21D-AZ-MX5	-	-	-	-
S97-V21D-AZ-MX6	-1.16 ± 7.66	-	-	-
S97-V21D-AZ-MX7	-0.93 ± 7.66	-0.16 ± 1.60	-0.146 ± 0.290	0.0443 ± 0.0679
S97-V21D-AZ-MX8	-1.45 ± 7.65	-0.81 ± 1.52	-	-
S97-V21D-AZ-MX9	-0.79 ± 7.66	-	-	-0.0410 ± 0.0692
S97-V21D-AZ-MX10	-1.16 ± 7.66	0.01 ± 1.54	-0.169 ± 0.277	0.0411 ± 0.0743
S97-V21E-AZ-CX	1.91 ± 0.80	6.46 ± 3.82	-	-
S97-V21E-AZ-FX	-0.01 ± 0.34	1.75 ± 0.80	0.001 ± 0.100	0.0294 ± 0.0303
S97-V22A-AZ-CX	2.10 ± 1.31	-	-	-0.0179 ± 0.0819
S97-V22A-AZ-FX	0.10 ± 0.74	3.59 ± 1.78	-	-
S97-V22B-AZ-CX	3.72 ± 1.66	14.87 ± 7.27	-	-
S97-V22B-AZ-FX	0.45 ± 0.65	2.85 ± 1.43	-	0.0930 ± 0.1034
S97-V22B-AZ-MX5	-1.01 ± 7.55	0.56 ± 1.59	-	-
S97-V22B-AZ-MX6	-1.24 ± 7.55	-0.06 ± 1.53	0.176 ± 0.305	-
S97-V22B-AZ-MX7	-1.04 ± 7.55	0.27 ± 1.51	-0.147 ± 0.271	0.0049 ± 0.0720
S97-V22B-AZ-MX8	-1.17 ± 7.55	-0.32 ± 1.55	-	-0.0511 ± 0.0711
S97-V22B-AZ-MX9	-1.37 ± 7.55	0.10 ± 1.50	-	-0.0602 ± 0.0671
S97-V22B-AZ-MX10	-1.27 ± 7.55	-0.74 ± 1.49	-0.141 ± 0.269	-0.0482 ± 0.0680
S97-V22C-AZ-CX	3.29 ± 1.93	7.94 ± 7.72	3.701 ± 1.885	-0.1610 ± 0.0901
S97-V22C-AZ-FX	1.05 ± 0.62	3.20 ± 1.36	-0.065 ± 0.136	0.0702 ± 0.0521
S97-V22D-AZ-CX	4.36 ± 1.78	6.99 ± 8.14	-	-
S97-V22D-AZ-FX	0.38 ± 0.71	3.14 ± 1.78	-	-
S97-V22D-AZ-MX5	-1.59 ± 7.52	-	-	-
S97-V22D-AZ-MX6	-1.26 ± 7.52	-	-	-
S97-V22D-AZ-MX7	-1.52 ± 7.51	-	-	-0.0306 ± 0.0686
S97-V22D-AZ-MX8	-0.91 ± 7.51	4.68 ± 1.57	0.826 ± 0.341	0.2755 ± 0.0964
S97-V22D-AZ-MX9	2.47 ± 7.52	-0.41 ± 1.55	-	0.5010 ± 0.1013
S97-V22D-AZ-MX10	0.90 ± 7.52	-0.41 ± 1.55	-	0.5010 ± 0.1013
S97-V22E-AZ-CX	1.98 ± 1.20	4.92 ± 4.94	1.459 ± 1.140	-
S97-V22E-AZ-FX	1.03 ± 0.48	14.62 ± 1.90	-	0.3064 ± 0.1613
S97-V21A-RV-CX	2.17 ± 1.11	40.21 ± 6.88	-	0.3208 ± 0.4445
S97-V21A-RV-FX	0.38 ± 0.47	3.49 ± 1.05	-0.050 ± 0.135	-
S97-V21B-RV-CX	6.49 ± 2.80	99.69 ± 19.35	-	-0.1856 ± 0.1039
S97-V21C-RV-CX	5.95 ± 1.55	95.26 ± 10.96	0.587 ± 1.123	-
S97-V21C-RV-FX	0.05 ± 0.63	1.47 ± 1.51	0.061 ± 0.298	-
S97-V21D-RV-CX	1.58 ± 1.43	75.91 ± 14.30	-	-
S97-V21D-RV-FX	-0.17 ± 0.58	1.82 ± 1.22	-0.034 ± 0.142	-
S97-V21D-RV-MX5	-1.32 ± 6.66	-0.37 ± 1.39	-	0.0385 ± 0.0813
S97-V21D-RV-MX6	-1.18 ± 6.65	-	-	-
S97-V21D-RV-MX7	-1.15 ± 6.65	-0.31 ± 1.32	-0.059 ± 0.235	-0.0385 ± 0.0583
S97-V21D-RV-MX8	-1.12 ± 6.65	11.28 ± 1.40	-0.093 ± 0.242	-
S97-V21D-RV-MX9	-1.00 ± 6.66	-0.05 ± 1.42	-	-0.0014 ± 0.0645
S97-V21D-RV-MX10	-0.55 ± 6.65	-	-0.107 ± 0.237	-0.0459 ± 0.0585
S97-V21E-RV-CX	-	-	-	-

Table D.6: Trace Metals Aerosol Concentration Data (Co, Cr, Cs, Eu) (continued)

Sample	Aerosol Concentration (ng m^{-3})			
	Co	Cr	Cs	Eu
S97-V21E-RV-FX	0.05 ± 0.32	1.15 ± 0.68	-0.037 ± 0.080	-
S97-V22A-RV-CX	2.10 ± 1.03	1.50 ± 5.28	-	0.0440 ± 0.1173
S97-V22A-RV-FX	0.18 ± 0.49	2.65 ± 1.10	0.007 ± 0.141	-
S97-V22B-RV-CX	1.69 ± 1.43	54.30 ± 7.27	-	-
S97-V22B-RV-FX	0.97 ± 0.66	23.48 ± 1.74	-	-
S97-V22B-RV-MX5	-1.07 ± 6.65	-0.49 ± 1.35	-0.044 ± 0.246	-0.0548 ± 0.0592
S97-V22B-RV-MX6	-0.95 ± 6.65	-0.51 ± 1.32	-0.093 ± 0.238	-0.0328 ± 0.0587
S97-V22B-RV-MX7	-1.07 ± 6.65	-0.65 ± 1.33	-	-0.0405 ± 0.0600
S97-V22B-RV-MX8	-0.81 ± 6.65	-	-0.176 ± 0.234	-0.0485 ± 0.0582
S97-V22B-RV-MX9	-1.36 ± 6.65	-	-0.123 ± 0.236	-0.0299 ± 0.0584
S97-V22B-RV-MX10	-0.86 ± 6.65	-0.19 ± 1.36	-	-
S97-V22C-RV-CX	1.80 ± 1.88	40.69 ± 10.82	-	0.4864 ± 0.2864
S97-V22C-RV-FX	0.39 ± 0.66	1.23 ± 1.78	-	-
S97-V22D-RV-CX	1.43 ± 1.30	10.64 ± 6.74	-	-
S97-V22D-RV-FX	-0.17 ± 0.62	0.22 ± 1.31	-	-
S97-V22D-RV-MX5	-1.21 ± 6.52	-	-0.032 ± 0.235	-
S97-V22D-RV-MX6	-1.64 ± 6.52	1.22 ± 1.37	-	0.0042 ± 0.0624
S97-V22D-RV-MX7	-1.07 ± 6.52	-	-0.043 ± 0.259	-
S97-V22D-RV-MX8	-1.04 ± 6.52	-	-0.049 ± 0.237	0.0014 ± 0.0568
S97-V22D-RV-MX9	-0.87 ± 6.52	-0.37 ± 1.30	-	-0.0349 ± 0.0600
S97-V22D-RV-MX10	-1.15 ± 6.52	-	-	-0.0265 ± 0.0623
S97-V22E-RV-CX	0.16 ± 0.68	3.24 ± 3.60	-	0.0347 ± 0.0707
S97-V22E-RV-FX	-0.13 ± 0.32	1.93 ± 0.65	-0.030 ± 0.059	-0.0069 ± 0.0089
S97-N21D-ML-FX	2.67 ± 0.61	5.26 ± 1.49	-	0.0632 ± 0.0385
S97-N21E-ML-FX	1.86 ± 0.59	9.16 ± 1.82	0.809 ± 0.486	-
S97-N22A-ML-FX	0.12 ± 0.47	18.12 ± 1.40	-0.122 ± 0.097	0.0389 ± 0.0307
S97-N22B-ML-FX	-	0.18 ± 1.28	-	-
S97-N22C-ML-FX	-0.43 ± 0.58	3.91 ± 1.21	-	-
S97-N22C-ML-MX5	-1.35 ± 6.83	-0.49 ± 1.36	-	0.0395 ± 0.0651
S97-N22C-ML-MX6	-1.26 ± 6.83	-	-	-0.0161 ± 0.0605
S97-N22C-ML-MX7	-1.47 ± 6.83	2.49 ± 1.44	0.312 ± 0.270	-
S97-N22C-ML-MX8	-1.50 ± 6.83	0.59 ± 1.45	0.633 ± 0.295	-0.0161 ± 0.0656
S97-N22C-ML-MX9	0.02 ± 6.83	-	-	-
S97-N22C-ML-MX10	-0.62 ± 6.83	-0.49 ± 1.38	-0.089 ± 0.245	-0.0424 ± 0.0610
S97-N22D-ML-FX	-0.07 ± 0.57	-0.61 ± 1.16	-	-
S97-N22E-ML-FX	-0.02 ± 0.39	38.59 ± 1.90	0.161 ± 0.222	-
S97-N23A-ML-FX	0.76 ± 0.47	6.50 ± 1.02	-0.099 ± 0.114	0.0366 ± 0.0263
S97-N23B-ML-FX	0.89 ± 0.64	-0.72 ± 1.41	-	0.1801 ± 0.0272
S97-N23C-ML-FX	-0.78 ± 0.58	6.07 ± 1.39	-	0.0807 ± 0.0566
S97-N23C-ML-MX5	-1.14 ± 6.77	-0.34 ± 1.34	-0.086 ± 0.240	0.0247 ± 0.0613
S97-N23C-ML-MX6	-1.49 ± 6.77	-0.83 ± 1.34	-	0.0740 ± 0.0632
S97-N23C-ML-MX7	-1.34 ± 6.77	-0.11 ± 1.39	-	0.1553 ± 0.2311
S97-N23C-ML-MX8	-1.67 ± 6.77	-	-	-
S97-N23C-ML-MX9	-1.08 ± 6.77	-0.60 ± 1.37	-	-
S97-N23C-ML-MX10	-1.20 ± 6.77	0.01 ± 1.37	-	-

Table D.6: Trace Metals Aerosol Concentration Data (Co, Cr, Cs, Eu) (continued)

Sample	Aerosol Concentration (ng m^{-3})			
	Co	Cr	Cs	Eu
S97-N23D-ML-FX	-0.20 ± 0.56	16.10 ± 1.46	-0.119 ± 0.109	-0.0216 ± 0.0296
S97-N23E-ML-FX	0.08 ± 0.37	0.12 ± 0.84	0.111 ± 0.178	0.0456 ± 0.0443
S97-N23E-ML-MX5	-0.09 ± 3.89	-	0.444 ± 0.269	-
S97-N23E-ML-MX6	-0.25 ± 3.88	-	-0.016 ± 0.157	0.0941 ± 0.0536
S97-N23E-ML-MX7	-0.59 ± 3.88	-	-0.084 ± 0.145	0.0441 ± 0.0392
S97-N23E-ML-MX8	-0.32 ± 3.88	-0.35 ± 0.77	0.144 ± 0.172	0.0341 ± 0.0463
S97-N23E-ML-MX9	-0.69 ± 3.88	-	-0.077 ± 0.143	-0.0281 ± 0.0356
S97-N23E-ML-MX10	-0.52 ± 3.88	-	0.144 ± 0.192	0.0142 ± 0.0430
S97-N31A-DB-CX	1.27 ± 0.87	304.92 ± 4.76	-0.488 ± 0.557	0.1379 ± 0.0954
S97-N31A-DB-FX	0.97 ± 0.46	87.62 ± 4.75	-	-
S97-N31B-DB-CX	1.35 ± 1.12	9.99 ± 6.00	0.011 ± 0.732	0.0416 ± 0.1277
S97-N31B-DB-FX	0.21 ± 0.58	36.17 ± 2.21	-	0.0038 ± 0.0180
S97-N31C-DB-CX	3.41 ± 1.16	6.31 ± 5.95	-	-0.1387 ± 0.0840
S97-N31C-DB-FX	2.06 ± 0.61	76.08 ± 3.38	-0.050 ± 1.072	-0.0217 ± 0.0156
S97-N31C-DB-MX5	-1.28 ± 6.90	-0.20 ± 1.37	-0.161 ± 0.246	-
S97-N31C-DB-MX6	-0.95 ± 6.90	-0.41 ± 1.41	-0.079 ± 0.260	-
S97-N31C-DB-MX7	-1.37 ± 6.90	-0.32 ± 1.44	-	0.0015 ± 0.0683
S97-N31C-DB-MX8	-1.01 ± 6.90	-	-	-0.0429 ± 0.0663
S97-N31C-DB-MX9	-1.10 ± 6.90	9.92 ± 1.41	-0.067 ± 0.246	-0.0340 ± 0.0626
S97-N31C-DB-MX10	-0.89 ± 6.90	-0.74 ± 1.36	-	-
S97-N31D-DB-CX	1.19 ± 1.37	6.10 ± 6.17	-	0.7640 ± 0.3295
S97-N31D-DB-FX	1.36 ± 0.78	38.64 ± 2.51	-	-
S97-N31D-DB-MX5	-1.61 ± 8.14	0.01 ± 1.64	-0.054 ± 0.295	-0.0296 ± 0.0770
S97-N31D-DB-MX6	-1.65 ± 8.14	-	0.546 ± 0.402	-
S97-N31D-DB-MX7	-1.05 ± 8.14	-0.55 ± 1.62	-	-
S97-N31D-DB-MX8	-1.19 ± 8.14	-	0.057 ± 0.342	0.0332 ± 0.0902
S97-N31D-DB-MX9	-1.44 ± 8.14	-0.27 ± 1.62	-0.159 ± 0.288	-0.0052 ± 0.0760
S97-N31D-DB-MX10	-1.37 ± 8.14	-0.34 ± 1.61	-0.037 ± 0.292	-0.0527 ± 0.0723
S97-N31E-DB-CX	1.99 ± 0.85	7.36 ± 3.62	-	-
S97-N31E-DB-FX	0.51 ± 0.31	7.36 ± 0.69	-	-
S97-N32A-DB-CX	0.43 ± 0.88	11.48 ± 4.79	-0.238 ± 0.571	-0.0376 ± 0.0768
S97-N32A-DB-FX	-0.34 ± 0.45	-0.75 ± 0.91	-0.022 ± 0.094	0.0081 ± 0.0187
S97-N32B-DB-CX	0.44 ± 1.08	30.45 ± 6.04	-0.058 ± 0.722	0.1183 ± 0.1242
S97-N32B-DB-FX	1.96 ± 0.70	80.51 ± 3.19	-	-
S97-N32C-DB-CX	0.35 ± 1.31	-0.81 ± 6.02	-	0.1586 ± 0.2343
S97-N32C-DB-FX	0.24 ± 0.55	29.54 ± 1.43	-	-
S97-N32C-DB-MX5	-1.09 ± 6.85	-0.05 ± 1.35	-0.134 ± 0.240	-0.0014 ± 0.0607
S97-N32C-DB-MX6	-1.12 ± 6.85	-0.32 ± 1.35	-0.104 ± 0.241	-0.0279 ± 0.0603
S97-N32C-DB-MX7	-1.15 ± 6.85	-0.58 ± 1.36	-0.072 ± 0.245	-0.0161 ± 0.0619
S97-N32C-DB-MX8	-1.18 ± 6.85	-0.02 ± 1.42	-	-
S97-N32C-DB-MX9	-0.95 ± 6.85	0.74 ± 1.41	-0.013 ± 0.255	0.0279 ± 0.0678
S97-N32C-DB-MX10	-1.39 ± 6.85	-0.35 ± 1.38	-	-0.0014 ± 0.0708
S97-N32D-DB-CX	0.96 ± 1.21	2.01 ± 6.11	-	0.0402 ± 0.1813
S97-N32D-DB-FX	-0.19 ± 0.61	22.01 ± 2.35	-	0.0768 ± 0.0656
S97-N32E-DB-CX	0.35 ± 0.61	3.57 ± 3.29	-0.255 ± 0.388	0.0231 ± 0.0603
S97-N32E-DB-FX	-0.07 ± 0.31	1.20 ± 0.65	0.044 ± 0.062	0.0245 ± 0.0132

Table D.6: Trace Metals Aerosol Concentration Data (Co, Cr, Cs, Eu) (continued)

Sample	Aerosol Concentration (ng m^{-3})			
	Co	Cr	Cs	Eu
S97-N31A-ML-CX	1.00 ± 1.35	19.25 ± 6.03	-	-
S97-N31A-ML-FX	0.44 ± 0.50	37.88 ± 1.84	0.248 ± 0.165	-0.0074 ± 0.0150
S97-N31B-ML-CX	1.53 ± 1.24	19.21 ± 6.57	-0.405 ± 0.813	0.1299 ± 0.1754
S97-N31B-ML-FX	0.12 ± 0.58	11.75 ± 1.32	-0.097 ± 0.119	-0.0059 ± 0.0161
S97-N31C-ML-CX	4.13 ± 1.63	2.15 ± 6.70	-	0.2075 ± 0.2487
S97-N31C-ML-FX	-0.72 ± 0.64	31.54 ± 2.44	-	0.0007 ± 0.0199
S97-N31C-ML-MX5	-1.45 ± 7.99	0.08 ± 1.62	-	-
S97-N31C-ML-MX6	-1.48 ± 7.99	-0.78 ± 1.61	-	-
S97-N31C-ML-MX7	-1.24 ± 7.99	-0.27 ± 1.60	-0.156 ± 0.292	0.0394 ± 0.0755
S97-N31C-ML-MX8	-1.72 ± 7.99	-	-	-
S97-N31C-ML-MX9	-1.38 ± 7.99	1.00 ± 1.65	0.022 ± 0.280	-0.0291 ± 0.0791
S97-N31C-ML-MX10	-1.41 ± 7.99	-	-	-0.0051 ± 0.0826
S97-N31D-ML-CX	1.44 ± 1.19	11.62 ± 6.39	0.230 ± 0.782	-0.0694 ± 0.1084
S97-N31D-ML-FX	0.52 ± 0.60	7.92 ± 1.21	-0.122 ± 0.110	-0.0161 ± 0.0164
S97-N31D-ML-MX5	-1.31 ± 8.45	-	0.168 ± 0.408	-
S97-N31D-ML-MX6	-1.56 ± 8.44	-0.79 ± 1.71	-0.064 ± 0.304	-0.0416 ± 0.0776
S97-N31D-ML-MX7	-1.56 ± 8.44	-0.17 ± 1.68	-0.016 ± 0.307	-0.0380 ± 0.0761
S97-N31D-ML-MX8	-1.53 ± 8.45	-	-	-
S97-N31D-ML-MX9	-1.56 ± 8.44	-0.79 ± 1.68	-0.154 ± 0.303	0.0163 ± 0.0799
S97-N31D-ML-MX10	-1.53 ± 8.44	-0.75 ± 1.72	-0.118 ± 0.315	-
S97-N31E-ML-CX	2.27 ± 0.68	19.06 ± 3.55	0.075 ± 0.424	0.0930 ± 0.0629
S97-N31E-ML-FX	-0.36 ± 0.33	10.25 ± 0.98	-	-
S97-N32A-ML-CX	1.51 ± 1.04	11.23 ± 5.40	-0.258 ± 0.668	0.0448 ± 0.1258
S97-N32A-ML-FX	0.16 ± 0.53	13.49 ± 1.73	-0.073 ± 0.207	0.0361 ± 0.0274
S97-N32B-ML-CX	2.38 ± 1.61	20.95 ± 7.58	-	0.5392 ± 0.3856
S97-N32B-ML-FX	-0.05 ± 0.62	12.73 ± 1.61	-	-
S97-N32C-ML-CX	3.14 ± 1.44	5.92 ± 6.90	0.420 ± 1.018	0.0539 ± 0.1041
S97-N32C-ML-FX	0.10 ± 0.60	2.96 ± 1.30	-	-
S97-N32C-ML-MX5	-1.49 ± 7.51	-	-0.224 ± 0.263	-0.0467 ± 0.0667
S97-N32C-ML-MX6	-1.49 ± 7.51	0.17 ± 1.50	-	-
S97-N32C-ML-MX7	-1.20 ± 7.51	-	-	-
S97-N32C-ML-MX8	-1.42 ± 7.51	-0.61 ± 1.49	-0.156 ± 0.268	-
S97-N32C-ML-MX9	-1.39 ± 7.51	-0.28 ± 1.50	-0.118 ± 0.277	-0.0370 ± 0.0669
S97-N32C-ML-MX10	-1.55 ± 7.51	-0.80 ± 1.48	-	-
S97-N32D-ML-CX	-0.75 ± 1.21	-1.68 ± 6.47	-0.323 ± 0.812	0.1694 ± 0.1451
S97-N32D-ML-FX	-0.13 ± 0.61	1.99 ± 1.49	-0.042 ± 0.198	0.0121 ± 0.0226
S97-N32E-ML-CX	0.80 ± 0.74	6.99 ± 4.03	-	-
S97-N32E-ML-FX	-0.13 ± 0.33	2.07 ± 0.74	0.027 ± 0.056	0.0059 ± 0.0135
S97-N31A-RV-CX	1.79 ± 0.93	-3.59 ± 4.93	-	-
S97-N31A-RV-FX	-0.32 ± 0.45	2.74 ± 1.04	-	0.0339 ± 0.0380
S97-N31B-RV-CX	2.27 ± 1.18	4.93 ± 6.27	-0.439 ± 0.737	-0.0688 ± 0.0980
S97-N31B-RV-FX	-0.01 ± 0.62	5.81 ± 1.36	-	-
S97-N31C-RV-CX	2.04 ± 1.30	2.71 ± 6.57	-0.136 ± 0.763	-0.0675 ± 0.1037
S97-N31C-RV-FX	-0.08 ± 0.62	0.70 ± 1.39	-	-
S97-N31C-RV-MX5	-1.30 ± 6.71	-	0.047 ± 0.245	-0.0187 ± 0.0614
S97-N31C-RV-MX6	-1.33 ± 6.71	-0.74 ± 1.33	-0.168 ± 0.234	-0.0477 ± 0.0596

Table D.6: Trace Metals Aerosol Concentration Data (Co, Cr, Cs, Eu) (continued)

Sample	Aerosol Concentration (ng m^{-3})			
	Co	Cr	Cs	Eu
S97-N31C-RV-MX7	-1.21 ± 6.71	-0.08 ± 1.34	-0.027 ± 0.245	-
S97-N31C-RV-MX8	-0.90 ± 6.71	-	-0.131 ± 0.236	-0.0187 ± 0.0597
S97-N31C-RV-MX9	-1.36 ± 6.71	-0.78 ± 1.33	-0.189 ± 0.236	-
S97-N31C-RV-MX10	-1.19 ± 6.71	-0.54 ± 1.33	0.013 ± 0.237	-0.0244 ± 0.0585
S97-N31D-RV-CX	2.71 ± 1.11	16.77 ± 5.89	-0.268 ± 0.696	-0.1317 ± 0.0823
S97-N31D-RV-FX	-0.04 ± 0.55	0.51 ± 1.15	-0.020 ± 0.118	0.0159 ± 0.0235
S97-N31D-RV-MX5	-1.62 ± 7.99	-0.37 ± 1.61	-	-
S97-N31D-RV-MX6	0.16 ± 7.99	-	0.638 ± 0.496	0.1181 ± 0.1385
S97-N31D-RV-MX7	-0.97 ± 7.99	1.24 ± 1.74	-	-
S97-N31D-RV-MX8	-0.76 ± 7.98	0.35 ± 1.61	-0.108 ± 0.283	-0.0428 ± 0.0709
S97-N31D-RV-MX9	-1.44 ± 7.99	0.42 ± 1.65	0.570 ± 0.739	-
S97-N31D-RV-MX10	-	-	-	0.1010 ± 0.1879
S97-N31E-RV-CX	1.81 ± 0.71	3.40 ± 3.69	-	-
S97-N31E-RV-FX	1.27 ± 0.38	1.68 ± 0.83	-	-
S97-N32A-RV-CX	0.70 ± 1.06	4.75 ± 6.32	-	-
S97-N32A-RV-FX	0.31 ± 0.51	2.39 ± 1.30	0.105 ± 0.237	-
S97-N32B-RV-CX	0.58 ± 1.42	4.91 ± 7.72	-	-
S97-N32B-RV-FX	0.82 ± 0.61	44.64 ± 1.86	-	-
S97-N32C-RV-CX	0.01 ± 1.15	0.96 ± 6.25	-0.576 ± 0.717	-0.1701 ± 0.0850
S97-N32C-RV-FX	-0.01 ± 0.57	-0.60 ± 1.17	-0.160 ± 0.109	0.0039 ± 0.0248
S97-N32C-RV-MX5	-1.22 ± 7.26	-	-0.070 ± 0.260	0.0078 ± 0.0672
S97-N32C-RV-MX6	-1.03 ± 7.26	-0.27 ± 1.46	0.005 ± 0.268	-
S97-N32C-RV-MX7	0.43 ± 7.26	-0.68 ± 1.45	-	-0.0737 ± 0.0632
S97-N32C-RV-MX9	-1.10 ± 7.26	-0.62 ± 1.46	0.207 ± 0.270	0.9198 ± 0.1102
S97-N32C-RV-MX10	-1.22 ± 7.26	-	-0.148 ± 0.267	0.9198 ± 0.1179
S97-N32D-RV-CX	3.07 ± 1.22	1.39 ± 6.04	-0.384 ± 0.708	-0.1672 ± 0.0831
S97-N32D-RV-FX	-0.36 ± 0.57	3.55 ± 1.30	-	-
S97-N32E-RV-CX	0.83 ± 0.74	15.04 ± 4.27	-	-
S97-N32E-RV-FX	0.47 ± 0.34	1.81 ± 0.79	-	-
S97-T11B-TI-CX	5.20 ± 1.91	101.79 ± 11.14	-	0.0398 ± 0.1723
S97-T11B-TI-FX	3.76 ± 1.16	159.78 ± 5.83	-	-
S97-T11B-TI-MX5	-0.75 ± 9.19	-	-	-
S97-T11B-TI-MX6	-0.95 ± 9.13	0.01 ± 1.90	-	-0.0019 ± 0.0795
S97-T11B-TI-MX7	-1.50 ± 9.13	-0.07 ± 1.83	-0.206 ± 0.323	-
S97-T11B-TI-MX8	0.03 ± 9.13	2.55 ± 1.83	-0.080 ± 0.331	-0.0528 ± 0.0823
S97-T11B-TI-MX9	-0.20 ± 9.13	0.13 ± 1.82	-	-0.0622 ± 0.0808
S97-T11B-TI-MX10	-0.52 ± 9.13	-	-0.147 ± 0.331	-
S97-T11B-TO-CX	2.95 ± 1.91	21.43 ± 9.28	-	-
S97-T11B-TO-FX	3.86 ± 0.80	185.39 ± 5.24	-	-
S97-T11B-TO-MX5	-1.50 ± 9.64	3.11 ± 1.97	-	-0.0020 ± 0.0893
S97-T11B-TO-MX6	-0.63 ± 9.64	0.17 ± 2.06	0.399 ± 0.532	0.2996 ± 0.2306
S97-T11B-TO-MX7	-0.26 ± 9.64	-	0.233 ± 0.427	-
S97-T11B-TO-MX8	-1.83 ± 9.64	-1.02 ± 1.91	0.109 ± 0.516	-
S97-T11B-TO-MX9	-2.07 ± 9.64	0.46 ± 1.98	-	-
S97-T11B-TO-MX10	-1.83 ± 9.64	-0.37 ± 1.98	-0.097 ± 0.341	-

Table D.6: Trace Metals Aerosol Concentration Data (Co, Cr, Cs, Eu) (continued)

Sample	Aerosol Concentration (ng m^{-3})			
	Co	Cr	Cs	Eu
S97-T21B-TI-CX	3.16 ± 1.41	12.21 ± 7.55	-	0.0292 ± 0.1645
S97-T21B-TI-FX	1.38 ± 0.87	29.40 ± 1.41	-	-
S97-T21B-TI-MX5	-1.41 ± 9.10	0.44 ± 1.87	-	1.1531 ± 0.1413
S97-T21B-TI-MX6	-1.69 ± 9.10	-0.46 ± 1.81	-0.240 ± 0.324	0.2946 ± 0.0901
S97-T21B-TI-MX7	-1.33 ± 9.10	0.20 ± 1.79	-0.221 ± 0.330	1.2312 ± 0.1512
S97-T21B-TI-MX8	-1.53 ± 9.10	-0.11 ± 1.80	-0.201 ± 0.320	0.2400 ± 0.0863
S97-T21B-TI-MX9	-1.61 ± 9.10	-0.30 ± 1.81	-0.256 ± 0.320	-0.0175 ± 0.0815
S97-T21B-TI-MX10	-0.98 ± 9.10	14.25 ± 2.20	-	1.2312 ± 0.1545
S97-T21B-TO-FX	0.42 ± 0.72	66.63 ± 4.13	0.037 ± 0.233	-
S97-T31B-TI-CX	0.99 ± 1.38	12.21 ± 7.52	0.003 ± 0.930	0.0074 ± 0.1732
S97-T31B-TI-FX	-0.34 ± 0.74	6.39 ± 1.61	-	-
S97-T31B-TI-MX5	-1.80 ± 9.10	-0.30 ± 2.00	-	-
S97-T31B-TI-MX6	-1.80 ± 9.10	-0.97 ± 1.82	-	0.0293 ± 0.1008
S97-T31B-TI-MX7	-1.41 ± 9.10	1.96 ± 1.89	-0.170 ± 0.334	-0.0292 ± 0.0901
S97-T31B-TI-MX9	-1.92 ± 9.10	0.24 ± 1.89	-0.289 ± 0.342	-
S97-T31B-TI-MX10	-1.41 ± 9.10	-	-	-
S97-T31B-TO-CX	-0.33 ± 1.42	20.80 ± 7.75	-0.635 ± 0.913	-0.0606 ± 0.1455
S97-T31B-TO-FX	-1.10 ± 0.68	9.90 ± 1.47	-	-
S97-T31B-TO-MX5	-1.90 ± 9.02	1.05 ± 1.80	-0.126 ± 0.320	-
S97-T31B-TO-MX6	-	-	-	-
S97-T31B-TO-MX7	-0.28 ± 9.02	-0.38 ± 1.82	-0.095 ± 0.324	0.0058 ± 0.0790
S97-T31B-TO-MX8	-0.86 ± 9.02	1.40 ± 1.81	-0.172 ± 0.323	-0.0174 ± 0.0842
S97-T31B-TO-MX9	-1.40 ± 9.02	-	-0.122 ± 0.364	-0.0058 ± 0.0868
S97-T31B-TO-MX10	-0.66 ± 9.02	-	-	-
S97-T41B-TI-CX	3.14 ± 1.67	22.58 ± 8.87	0.159 ± 1.107	0.2530 ± 0.2868
S97-T41B-TI-FX	-0.26 ± 0.72	2.93 ± 1.51	0.125 ± 0.155	0.0540 ± 0.0283
S97-T41B-TI-MX5	-0.87 ± 9.11	-	-	-
S97-T41B-TI-MX6	0.03 ± 9.11	-	-	0.3727 ± 0.3107
S97-T41B-TI-MX7	-0.75 ± 9.10	0.01 ± 2.00	-	0.2322 ± 0.2034
S97-T41B-TI-MX8	-0.98 ± 9.10	-	0.572 ± 0.598	0.1737 ± 0.1820
S97-T41B-TI-MX9	-1.57 ± 9.10	-0.93 ± 1.82	0.002 ± 0.357	-0.0370 ± 0.0832
S97-T41B-TI-MX10	-1.92 ± 9.10	-	-	-0.0214 ± 0.0822
S97-T41B-TO-CX	-0.31 ± 1.35	-1.04 ± 7.31	-0.641 ± 0.869	0.0075 ± 0.1314
S97-T41B-TO-FX	0.07 ± 0.86	8.55 ± 2.26	1.017 ± 0.172	-
S97-B11A-AZ-MX5	8.00 ± 0.68	3.00 ± 1.58	-	-
S97-B11A-AZ-MX6	4.80 ± 0.60	1.66 ± 1.24	1.260 ± 0.480	0.4200 ± 0.1400
S97-B11A-AZ-MX7	5.20 ± 0.60	-	1.460 ± 0.420	0.2000 ± 0.1000
S97-B11A-AZ-MX8	8.00 ± 0.80	-	1.200 ± 0.400	-
S97-B11A-AZ-MX9	4.80 ± 0.86	2.50 ± 2.08	-	0.4200 ± 0.2200
S97-B11A-AZ-MX10	6.40 ± 0.62	2.60 ± 1.86	1.640 ± 0.520	-
S97-B11A-DB-CX	11.40 ± 2.20	40.00 ± 8.80	-	0.5000 ± 0.1920
S97-B11A-DB-FX	-	7.63 ± 2.16	-	0.0680 ± 0.0380
S97-B11A-DB-MX5	8.80 ± 0.62	4.60 ± 1.32	-	0.3000 ± 0.0820
S97-B11A-DB-MX6	6.00 ± 0.46	4.20 ± 1.48	0.620 ± 0.360	0.3200 ± 0.1060

Table D.6: Trace Metals Aerosol Concentration Data (Co, Cr, Cs, Eu) (continued)

Sample	Aerosol Concentration (ng m^{-3})			
	Co	Cr	Cs	Eu
S97-B11A-DB-MX7	7.00 ± 0.78	8.20 ± 2.60	1.480 ± 0.640	0.5800 ± 0.1300
S97-B11A-DB-MX8	5.80 ± 0.94	4.20 ± 2.80	-	-
S97-B11A-DB-MX9	4.80 ± 0.46	9.20 ± 2.00	0.700 ± 0.300	0.5400 ± 0.1760
S97-B11A-DB-MX10	3.40 ± 0.96	6.00 ± 2.60	-	-
S97-B11A-ML-CX	4.60 ± 0.54	-	1.480 ± 0.480	0.3600 ± 0.1580
S97-B11A-ML-FX	3.54 ± 0.23	13.13 ± 0.72	0.580 ± 0.130	0.1200 ± 0.0230
S97-B11A-RV-CX	5.20 ± 0.62	3.20 ± 2.20	1.200 ± 0.540	0.6400 ± 0.2400
S97-B11A-RV-FX	1.40 ± 0.40	7.00 ± 2.00	-	-
S97-B11A-RV-MX5	5.60 ± 0.66	5.40 ± 1.96	1.000 ± 0.520	0.3800 ± 0.1700
S97-B11A-RV-MX6	4.80 ± 0.48	4.60 ± 1.44	1.000 ± 0.300	0.4400 ± 0.0900
S97-B11A-RV-MX7	5.60 ± 0.90	3.80 ± 1.96	4.200 ± 3.200	-
S97-B11A-RV-MX8	4.40 ± 0.60	4.20 ± 1.28	-	-
S97-B11A-RV-MX9	4.40 ± 0.74	5.40 ± 1.62	2.800 ± 2.400	0.9000 ± 0.8600
S97-B11A-RV-MX10	10.60 ± 0.98	6.40 ± 2.80	2.600 ± 0.820	-
S97-B11A-TI-CX	7.60 ± 0.54	7.40 ± 1.16	0.840 ± 0.300	0.4400 ± 0.1240
S97-B11A-TI-FX	5.50 ± 0.50	4.00 ± 1.00	-	-
S97-B11A-TI-MX5	5.00 ± 0.64	13.00 ± 2.60	1.260 ± 0.480	0.4000 ± 0.1020
S97-B11A-TI-MX6	5.00 ± 0.60	-	0.940 ± 0.500	0.4200 ± 0.1360
S97-B11A-TI-MX7	5.00 ± 0.42	4.20 ± 1.66	1.620 ± 0.940	0.3600 ± 0.0900
S97-B11A-TI-MX8	5.40 ± 0.50	5.00 ± 1.38	0.820 ± 0.400	0.2400 ± 0.0920
S97-B11A-TI-MX9	5.40 ± 0.58	3.60 ± 2.20	1.080 ± 0.900	0.4000 ± 0.1360
S97-B11A-TI-MX10	6.20 ± 0.52	3.40 ± 1.50	1.060 ± 0.500	0.3600 ± 0.0960
S97-B21A-DB-CX	5.00 ± 0.58	15.80 ± 1.96	-	0.0840 ± 0.0440
S97-B21A-DB-FX	-	2.82 ± 1.25	0.399 ± 0.234	-
S97-B21A-DB-MX5	10.00 ± 1.16	13.20 ± 3.40	-	-
S97-B21A-DB-MX6	2.60 ± 0.40	-	0.880 ± 0.440	-
S97-B21A-DB-MX7	3.60 ± 0.82	-	-	-
S97-B21A-DB-MX9	300.00 ± 5.20	60.00 ± 6.20	-	0.0780 ± 0.0160
S97-B21A-DB-MX10	-	-	9.600 ± 2.800	0.0660 ± 0.0080
S97-B21A-ML-CX	7.00 ± 0.90	4.80 ± 2.00	2.400 ± 0.840	0.2200 ± 0.0720
S97-B21A-ML-FX	4.60 ± 0.50	3.80 ± 1.60	0.720 ± 0.410	0.1600 ± 0.1500
S97-B21A-ML-MX5	5.60 ± 0.62	-	0.900 ± 0.360	-
S97-B21A-ML-MX6	3.60 ± 1.08	10.20 ± 2.80	0.660 ± 0.560	-
S97-B21A-ML-MX7	3.40 ± 0.42	1.34 ± 1.24	1.080 ± 0.300	0.5800 ± 0.1480
S97-B21A-ML-MX8	4.00 ± 0.84	9.40 ± 5.20	2.600 ± 0.840	-
S97-B21A-ML-MX9	4.00 ± 0.64	2.60 ± 1.58	1.740 ± 0.640	0.4800 ± 0.1560
S97-B21A-ML-MX10	2.20 ± 0.48	-	-	-
S97-B21A-RV-CX	5.20 ± 0.58	5.40 ± 2.20	0.980 ± 0.460	0.4600 ± 0.2000
S97-B21A-RV-FX	4.30 ± 0.30	6.00 ± 1.00	0.510 ± 0.160	0.0300 ± 0.0100
S97-B21A-RV-MX5	6.40 ± 0.58	12.40 ± 2.60	1.140 ± 0.560	0.4000 ± 0.2000
S97-B21A-RV-MX6	5.60 ± 0.80	7.40 ± 2.80	0.900 ± 0.480	-
S97-B21A-RV-MX7	-	11.00 ± 6.00	-	1.9000 ± 1.1200
S97-B21A-RV-MX8	5.00 ± 0.60	4.60 ± 1.40	1.280 ± 0.480	0.4600 ± 0.1600
S97-B21A-RV-MX9	3.60 ± 0.46	-	-	-

Table D.6: Trace Metals Aerosol Concentration Data (Co, Cr, Cs, Eu) (continued)

Sample	Aerosol Concentration (ng m^{-3})			
	Co	Cr	Cs	Eu
S97-B21A-RV-MX10	4.80 ± 0.60	5.60 ± 1.86	1.420 ± 0.520	-

D.7 Trace Elements Aerosol Concentration Data (Fe, Ga, Hg, In)

Table D.7: Trace Metals Aerosol Concentration Data (Fe, Ga, Hg, In)

Sample	Aerosol Concentration (ng m^{-3})			
	Fe	Ga	Hg	In
S97-V11A-LA-CX	305.25 ± 491.34	-	-0.02282 ± 0.06744	-
S97-V11A-LA-FX	144.46 ± 137.08	-	0.05141 ± 0.02794	0.0013 ± 0.0063
S97-V11B-LA-CX	1747.58 ± 528.48	12.28 ± 9.07	0.03410 ± 0.08936	0.0081 ± 0.0359
S97-V11B-LA-FX	177.73 ± 178.49	-	0.95617 ± 0.07219	0.0154 ± 0.0147
S97-V11C-LA-CX	2485.06 ± 537.13	30.68 ± 9.51	1.22274 ± 0.11880	0.5317 ± 0.2400
S97-V11C-LA-FX	654.96 ± 131.74	-	0.06696 ± 0.03639	0.0048 ± 0.0083
S97-V11D-LA-CX	470.05 ± 514.87	24.39 ± 9.32	1.35390 ± 0.14589	0.3941 ± 0.1756
S97-V11D-LA-FX	317.29 ± 68.18	0.34 ± 0.80	0.22115 ± 0.02862	-
S97-V11E-LA-CX	595.17 ± 382.24	-	0.03203 ± 0.07411	0.0550 ± 0.0377
S97-V11E-LA-FX	89.52 ± 64.55	-	0.02688 ± 0.02042	0.0045 ± 0.0061
S97-V12A-LA-CX	887.26 ± 383.35	-	0.04045 ± 0.06337	0.0602 ± 0.0718
S97-V12A-LA-FX	131.27 ± 115.42	-	0.03157 ± 0.03869	0.0050 ± 0.0072
S97-V12B-LA-CX	1804.11 ± 459.52	11.73 ± 7.43	0.20075 ± 0.10068	0.2835 ± 0.1727
S97-V12B-LA-FX	862.69 ± 149.72	-	0.27451 ± 0.04201	0.0106 ± 0.0103
S97-V12B-LA-MX5	-51.17 ± 66.35	-	0.02343 ± 0.07313	-
S97-V12B-LA-MX6	-	-	-0.00594 ± 0.07221	0.0004 ± 0.0018
S97-V12B-LA-MX7	-	-	-0.01387 ± 0.07149	-
S97-V12B-LA-MX8	-24.16 ± 66.74	-	-0.02503 ± 0.07068	-0.0002 ± 0.0013
S97-V12B-LA-MX9	35.45 ± 80.77	-	-0.03237 ± 0.07006	-
S97-V12B-LA-MX10	-21.81 ± 70.89	-0.11 ± 0.43	0.03811 ± 0.07191	-
S97-V12C-LA-CX	2473.30 ± 637.05	37.12 ± 11.61	0.09791 ± 0.13577	0.2226 ± 0.1054
S97-V12C-LA-FX	1712.90 ± 337.56	-	0.06378 ± 0.03467	0.0137 ± 0.0131
S97-V12D-LA-CX	999.00 ± 498.45	38.28 ± 12.25	0.04068 ± 0.08463	0.2529 ± 0.1199
S97-V12D-LA-FX	760.01 ± 177.84	-	0.07105 ± 0.03687	0.0081 ± 0.0110
S97-V12E-LA-CX	1119.68 ± 500.50	0.51 ± 2.58	-	0.0689 ± 0.0421
S97-V12E-LA-FX	571.04 ± 115.06	-	0.03341 ± 0.01745	-
S97-V11A-AZ-CX	710.88 ± 629.91	4.47 ± 4.93	0.28369 ± 0.08991	0.0298 ± 0.0429
S97-V11A-AZ-FX	-	-	0.01592 ± 0.02271	-
S97-V11B-AZ-CX	6343.40 ± 1040.70	31.40 ± 11.66	0.23277 ± 0.14128	0.0350 ± 0.0538
S97-V11B-AZ-FX	-	-	-	-
S97-V11C-AZ-CX	3741.48 ± 614.50	7.41 ± 6.50	0.05296 ± 0.09984	0.0463 ± 0.0520
S97-V11C-AZ-FX	375.17 ± 118.27	-	0.07535 ± 0.03299	-
S97-V11D-AZ-CX	2607.06 ± 538.28	-	0.07241 ± 0.09415	0.0110 ± 0.0402
S97-V11D-AZ-FX	160.86 ± 99.51	-	0.00355 ± 0.02661	0.0017 ± 0.0063
S97-V11D-AZ-MX5	-54.84 ± 75.56	-	-0.02416 ± 0.08014	0.0052 ± 0.0042
S97-V11D-AZ-MX6	-	-	-0.02081 ± 0.08151	-
S97-V11D-AZ-MX7	-	-	-0.03051 ± 0.08068	-
S97-V11D-AZ-MX8	20.98 ± 92.21	-0.29 ± 0.45	-0.00008 ± 0.08087	0.0012 ± 0.0026
S97-V11D-AZ-MX9	89.55 ± 84.95	-	-0.01212 ± 0.08252	0.0008 ± 0.0020
S97-V11D-AZ-MX10	-	-	-0.03854 ± 0.08009	0.0008 ± 0.0029
S97-V11E-AZ-CX	719.34 ± 469.55	-	0.02484 ± 0.06132	-0.0129 ± 0.0176
S97-V11E-AZ-FX	517.94 ± 135.88	-	3.92058 ± 0.07986	0.0085 ± 0.0064

Table D.7: Trace Metals Aerosol Concentration Data (Fe, Ga, Hg, In) (continued)

Sample	Aerosol Concentration (ng m^{-3})			
	Fe	Ga	Hg	In
S97-V12A-AZ-CX	1306.84 ± 427.09	8.96 ± 6.64	-	0.0110 ± 0.0329
S97-V12A-AZ-FX	129.65 ± 55.01	-	-	0.0067 ± 0.0116
S97-V12B-AZ-CX	2528.28 ± 893.44	58.73 ± 13.22	0.58519 ± 0.21639	0.6016 ± 0.2820
S97-V12B-AZ-FX	888.65 ± 124.98	0.08 ± 0.97	0.14854 ± 0.03603	0.0118 ± 0.0146
S97-V12C-AZ-CX	2384.20 ± 502.47	0.24 ± 5.29	0.10939 ± 0.09068	0.0686 ± 0.0620
S97-V12C-AZ-FX	151.06 ± 93.20	0.37 ± 0.98	0.02676 ± 0.02873	0.0116 ± 0.0114
S97-V12D-AZ-CX	2289.42 ± 747.14	-	-0.00433 ± 0.11405	0.1445 ± 0.0888
S97-V12D-AZ-FX	179.52 ± 114.03	-	-	-
S97-V12D-AZ-MX5	-	-0.34 ± 0.40	-0.02164 ± 0.07869	0.0028 ± 0.0037
S97-V12D-AZ-MX6	-12.83 ± 74.25	-	0.00646 ± 0.08264	0.0024 ± 0.0034
S97-V12D-AZ-MX7	16.90 ± 85.90	-	-	-
S97-V12D-AZ-MX8	-	-	-0.02164 ± 0.07925	-
S97-V12D-AZ-MX9	-40.60 ± 78.12	-0.42 ± 0.39	-0.03993 ± 0.07766	-
S97-V12D-AZ-MX10	-69.67 ± 74.25	-	-0.00987 ± 0.07791	0.0632 ± 0.0034
S97-V12E-AZ-CX	2190.97 ± 295.82	-	0.03400 ± 0.05327	0.0532 ± 0.0372
S97-V12E-AZ-FX	217.64 ± 74.98	-	-	0.0082 ± 0.0079
S97-V11A-RV-CX	181.20 ± 446.88	-1.00 ± 4.09	-0.03257 ± 0.07542	-
S97-V11A-RV-FX	356.43 ± 67.82	-	0.09059 ± 0.02623	0.0015 ± 0.0055
S97-V11B-RV-CX	2425.21 ± 676.12	2.18 ± 6.05	-	0.0554 ± 0.0548
S97-V11B-RV-FX	576.13 ± 110.18	-	0.03951 ± 0.02837	0.0246 ± 0.0204
S97-V11C-RV-CX	674.70 ± 524.78	-	-0.03353 ± 0.09914	0.0579 ± 0.0521
S97-V11C-RV-FX	2594.77 ± 117.92	-	0.03100 ± 0.02822	0.0038 ± 0.0068
S97-V11D-RV-CX	1238.06 ± 510.13	28.00 ± 8.86	0.33445 ± 0.14245	0.2658 ± 0.1260
S97-V11D-RV-FX	1490.30 ± 74.83	-	0.13133 ± 0.02604	0.0112 ± 0.0110
S97-V11D-RV-MX5	-	-	-	0.0016 ± 0.0030
S97-V11D-RV-MX6	-	-	-0.03516 ± 0.06820	0.0021 ± 0.0027
S97-V11D-RV-MX7	-9.21 ± 70.67	-	0.07697 ± 0.07097	0.0038 ± 0.0030
S97-V11D-RV-MX8	5.63 ± 85.31	-0.25 ± 0.41	-	0.0067 ± 0.0030
S97-V11D-RV-MX9	-	-	-0.02118 ± 0.06877	-
S97-V11D-RV-MX10	-45.16 ± 63.22	-	0.00279 ± 0.06882	-
S97-V11E-RV-CX	829.67 ± 272.25	17.85 ± 5.11	0.01819 ± 0.05005	0.1964 ± 0.0939
S97-V11E-RV-FX	308.04 ± 51.88	-	0.02287 ± 0.01424	0.0166 ± 0.0092
S97-V12A-RV-CX	-	10.61 ± 6.25	-	0.1021 ± 0.0573
S97-V12A-RV-FX	1128.06 ± 123.69	-	0.04677 ± 0.02106	0.0272 ± 0.0161
S97-V12B-RV-CX	3134.63 ± 559.20	1.03 ± 6.78	0.08327 ± 0.10384	0.0618 ± 0.0621
S97-V12B-RV-FX	1337.98 ± 312.47	-	0.56347 ± 0.04311	0.0083 ± 0.0143
S97-V12C-RV-CX	2486.43 ± 518.56	88.17 ± 17.58	0.38539 ± 0.10257	0.3350 ± 0.1644
S97-V12C-RV-FX	371.91 ± 127.05	-	0.08346 ± 0.03189	0.0080 ± 0.0083
S97-V12D-RV-CX	667.91 ± 680.60	32.44 ± 9.04	0.04239 ± 0.13335	0.2076 ± 0.1069
S97-V12D-RV-FX	2529.10 ± 245.56	-	0.05109 ± 0.02669	0.0461 ± 0.0238
S97-V12D-RV-MX5	372.54 ± 93.86	-	0.05414 ± 0.06921	-
S97-V12D-RV-MX6	-	-	-0.03088 ± 0.06778	0.0087 ± 0.0072
S97-V12D-RV-MX7	50.14 ± 91.71	-	-0.03002 ± 0.06782	0.0267 ± 0.0143
S97-V12D-RV-MX8	-	-	-0.01718 ± 0.06832	0.0124 ± 0.0080
S97-V12D-RV-MX9	-	-0.08 ± 0.43	-0.00577 ± 0.06853	0.0104 ± 0.0095
S97-V12D-RV-MX10	-	-	-	-

Table D.7: Trace Metals Aerosol Concentration Data (Fe, Ga, Hg, In) (continued)

Sample	Aerosol Concentration (ng m^{-3})			
	Fe	Ga	Hg	In
S97-V12E-RV-CX	1506.36 ± 626.71	15.89 ± 4.91	0.07513 ± 0.11083	0.0839 ± 0.0479
S97-V12E-RV-FX	761.50 ± 50.47	-	0.12932 ± 0.02585	0.0114 ± 0.0076
S97-V21A-LA-CX	1375.19 ± 426.65	3.93 ± 5.13	0.04464 ± 0.07409	0.0903 ± 0.0525
S97-V21A-LA-FX	594.14 ± 179.52	-	0.24390 ± 0.04223	0.0061 ± 0.0063
S97-V21B-LA-CX	2442.03 ± 527.83	16.27 ± 7.33	0.05675 ± 0.08890	0.1235 ± 0.0731
S97-V21B-LA-FX	576.03 ± 168.07	0.75 ± 1.35	0.07449 ± 0.03792	0.0109 ± 0.0080
S97-V21B-LA-MX5	-	-	0.04398 ± 0.07143	0.0204 ± 0.0171
S97-V21B-LA-MX6	-1.25 ± 73.49	-	-0.00888 ± 0.06997	0.0010 ± 0.0028
S97-V21B-LA-MX7	-	-	-0.01915 ± 0.07044	0.0066 ± 0.0054
S97-V21B-LA-MX8	-36.49 ± 68.13	-	-0.01857 ± 0.07198	0.0072 ± 0.0057
S97-V21B-LA-MX9	-	-	-0.02209 ± 0.06997	-
S97-V21B-LA-MX10	113.27 ± 84.00	1.12 ± 0.48	0.13501 ± 0.07278	0.0025 ± 0.0025
S97-V21C-LA-CX	2964.44 ± 704.00	51.23 ± 12.34	0.10576 ± 0.14993	0.3225 ± 0.1542
S97-V21C-LA-FX	561.70 ± 65.59	-	0.06058 ± 0.03698	0.0136 ± 0.0103
S97-V21D-LA-CX	1391.33 ± 476.04	47.15 ± 12.60	0.18551 ± 0.08715	0.3638 ± 0.1744
S97-V21D-LA-FX	732.45 ± 154.02	0.81 ± 1.38	0.06537 ± 0.03315	0.0016 ± 0.0060
S97-V21E-LA-CX	967.14 ± 360.33	19.08 ± 7.02	0.06978 ± 0.05486	0.0635 ± 0.0400
S97-V21E-LA-FX	321.53 ± 71.62	-	0.05885 ± 0.04486	0.0004 ± 0.0034
S97-V22A-LA-CX	646.36 ± 462.64	-	0.03912 ± 0.10686	0.0723 ± 0.0537
S97-V22A-LA-FX	297.04 ± 106.00	-	0.03344 ± 0.03345	-
S97-V22B-LA-CX	2766.37 ± 1201.76	29.90 ± 9.35	0.37458 ± 0.17655	0.3720 ± 0.1742
S97-V22B-LA-FX	449.66 ± 184.51	-0.05 ± 0.80	0.03409 ± 0.03288	0.0040 ± 0.0085
S97-V22B-LA-MX5	-	-	0.02036 ± 0.07628	0.0086 ± 0.0076
S97-V22B-LA-MX6	497.70 ± 207.99	-	-	-
S97-V22B-LA-MX7	57.11 ± 77.93	-	-	-
S97-V22B-LA-MX8	-	-	-0.02778 ± 0.06947	-
S97-V22B-LA-MX9	-	-	-0.01728 ± 0.06983	-
S97-V22B-LA-MX10	-	-	0.11665 ± 0.07891	0.0136 ± 0.0091
S97-V22C-LA-CX	1639.42 ± 469.89	0.05 ± 5.56	0.22715 ± 0.09722	0.2331 ± 0.1146
S97-V22C-LA-FX	383.85 ± 199.86	-	0.48977 ± 0.05045	0.0624 ± 0.0278
S97-V22D-LA-CX	1242.32 ± 746.61	11.19 ± 6.53	-	0.1425 ± 0.0797
S97-V22D-LA-FX	48.10 ± 142.25	-	0.06021 ± 0.03868	0.0101 ± 0.0108
S97-V22D-LA-MX5	158.23 ± 155.01	-	-0.02181 ± 0.06964	-
S97-V22D-LA-MX6	291.60 ± 111.59	-	-	0.0057 ± 0.0062
S97-V22D-LA-MX7	-	0.53 ± 0.72	-0.01630 ± 0.06947	-
S97-V22D-LA-MX8	-	-0.02 ± 0.43	-0.01891 ± 0.06973	0.0019 ± 0.0028
S97-V22D-LA-MX9	-	-	-0.02239 ± 0.06994	-
S97-V22D-LA-MX10	465.56 ± 121.40	-0.14 ± 0.46	0.08982 ± 0.07324	0.0007 ± 0.0025
S97-V22E-LA-CX	483.54 ± 420.41	13.21 ± 4.91	-	0.0678 ± 0.0441
S97-V22E-LA-FX	335.88 ± 74.07	0.16 ± 0.94	0.06861 ± 0.01962	0.0101 ± 0.0093
S97-V21A-AZ-CX	1869.28 ± 464.68	-	0.02632 ± 0.10002	0.1058 ± 0.0780
S97-V21A-AZ-FX	93.65 ± 65.37	-	0.07564 ± 0.02707	0.0106 ± 0.0088
S97-V21B-AZ-CX	4294.72 ± 735.40	-	0.06223 ± 0.10805	0.2496 ± 0.1739
S97-V21B-AZ-FX	-	0.79 ± 1.35	0.02975 ± 0.03173	0.0541 ± 0.0268
S97-V21C-AZ-CX	1611.17 ± 821.67	-	-	0.0774 ± 0.0432
S97-V21C-AZ-FX	164.73 ± 165.67	-	-	0.0267 ± 0.0160

Table D.7: Trace Metals Aerosol Concentration Data (Fe, Ga, Hg, In) (continued)

Sample	Aerosol Concentration (ng m^{-3})			
	Fe	Ga	Hg	In
S97-V21D-AZ-CX	3108.22 ± 541.97	1.51 ± 6.28	-0.01988 ± 0.08226	0.1087 ± 0.0709
S97-V21D-AZ-FX	484.92 ± 123.00	-	3.28620 ± 0.08617	0.1509 ± 0.0698
S97-V21D-AZ-MX5	-	1.16 ± 1.24	-	0.0136 ± 0.0086
S97-V21D-AZ-MX6	-	-	-	-
S97-V21D-AZ-MX7	-4.68 ± 93.89	-	0.00321 ± 0.07917	0.0139 ± 0.0073
S97-V21D-AZ-MX8	-	-	-0.03421 ± 0.07855	0.0176 ± 0.0086
S97-V21D-AZ-MX9	-	-	-	0.0071 ± 0.0054
S97-V21D-AZ-MX10	-	-	-0.01320 ± 0.07894	0.0005 ± 0.0017
S97-V21E-AZ-CX	2014.89 ± 381.37	6.74 ± 4.51	0.00815 ± 0.05052	-
S97-V21E-AZ-FX	319.95 ± 93.56	-	0.01286 ± 0.02211	0.0027 ± 0.0059
S97-V22A-AZ-CX	-	-	-0.03596 ± 0.07717	0.0351 ± 0.0378
S97-V22A-AZ-FX	253.01 ± 208.34	-	0.07646 ± 0.03893	0.0008 ± 0.0063
S97-V22B-AZ-CX	2942.78 ± 838.06	-	0.09312 ± 0.12044	0.2170 ± 0.1497
S97-V22B-AZ-FX	383.16 ± 65.13	-	0.01347 ± 0.03063	0.0030 ± 0.0078
S97-V22B-AZ-MX5	-94.21 ± 69.22	-	-0.02823 ± 0.07790	-
S97-V22B-AZ-MX6	-	-	0.03553 ± 0.07968	0.0018 ± 0.0028
S97-V22B-AZ-MX7	34.22 ± 77.84	-	-0.00655 ± 0.07769	0.0040 ± 0.0040
S97-V22B-AZ-MX8	-40.22 ± 82.73	0.20 ± 0.58	-0.02305 ± 0.07738	0.0018 ± 0.0025
S97-V22B-AZ-MX9	-36.99 ± 73.04	-0.29 ± 0.39	-0.03147 ± 0.07710	-
S97-V22B-AZ-MX10	-	-	-0.02241 ± 0.07730	0.0002 ± 0.0019
S97-V22C-AZ-CX	2230.50 ± 827.23	-0.91 ± 4.91	-	0.0688 ± 0.0664
S97-V22C-AZ-FX	351.82 ± 111.61	0.04 ± 0.67	0.00194 ± 0.03347	0.0070 ± 0.0089
S97-V22D-AZ-CX	1463.60 ± 768.62	6.52 ± 8.25	0.15974 ± 0.12998	0.0893 ± 0.0868
S97-V22D-AZ-FX	-75.91 ± 254.80	-	0.07189 ± 0.03481	0.0108 ± 0.0092
S97-V22D-AZ-MX5	211.28 ± 232.75	7.81 ± 5.17	0.00637 ± 0.07967	-
S97-V22D-AZ-MX6	-	-	-	0.0098 ± 0.0059
S97-V22D-AZ-MX7	-20.71 ± 75.01	1.36 ± 1.50	0.00315 ± 0.08128	0.0150 ± 0.0094
S97-V22D-AZ-MX8	56.62 ± 71.56	-	0.47034 ± 0.08423	0.0031 ± 0.0040
S97-V22D-AZ-MX9	904.01 ± 106.00	-	0.12655 ± 0.07852	-
S97-V22D-AZ-MX10	904.01 ± 106.00	-	0.08048 ± 0.10871	0.0018 ± 0.0028
S97-V22E-AZ-CX	646.81 ± 645.39	3.60 ± 4.00	0.01885 ± 0.07602	0.0348 ± 0.0468
S97-V22E-AZ-FX	1299.95 ± 306.14	-0.27 ± 0.45	0.14335 ± 0.03133	0.0049 ± 0.0063
S97-V21A-RV-CX	1474.49 ± 589.39	36.76 ± 10.53	-	0.1635 ± 0.0882
S97-V21A-RV-FX	476.25 ± 97.07	-	3.81286 ± 0.07139	0.0064 ± 0.0088
S97-V21B-RV-CX	6161.33 ± 1457.10	79.04 ± 19.58	0.35235 ± 0.29240	0.4384 ± 0.2042
S97-V21C-RV-CX	2755.89 ± 640.93	95.73 ± 22.28	0.22428 ± 0.10449	0.3129 ± 0.1491
S97-V21C-RV-FX	397.68 ± 177.10	-	0.44442 ± 0.04665	0.0142 ± 0.0108
S97-V21D-RV-CX	2137.46 ± 845.51	48.70 ± 11.75	0.25423 ± 0.15587	0.1038 ± 0.0652
S97-V21D-RV-FX	598.31 ± 108.28	0.11 ± 0.82	0.02919 ± 0.02985	0.0017 ± 0.0068
S97-V21D-RV-MX5	-	-0.14 ± 0.37	-0.02831 ± 0.06862	0.0010 ± 0.0022
S97-V21D-RV-MX6	-	-0.02 ± 0.43	-0.02432 ± 0.06887	0.0004 ± 0.0022
S97-V21D-RV-MX7	-52.57 ± 62.02	-	0.44502 ± 0.21087	0.0016 ± 0.0030
S97-V21D-RV-MX8	41.58 ± 79.75	-	0.00564 ± 0.06828	-
S97-V21D-RV-MX9	-	-	-0.00577 ± 0.06904	-
S97-V21D-RV-MX10	-4.07 ± 61.09	-	-	0.0027 ± 0.0025
S97-V21E-RV-CX	-	12.14 ± 5.55	-	0.1341 ± 0.0684

Table D.7: Trace Metals Aerosol Concentration Data (Fe, Ga, Hg, In) (continued)

Sample	Aerosol Concentration (ng m^{-3})			
	Fe	Ga	Hg	In
S97-V21E-RV-FX	235.17 ± 55.34	-	0.02949 ± 0.01604	0.0406 ± 0.0175
S97-V22A-RV-CX	708.89 ± 419.68	1.67 ± 4.86	-0.02599 ± 0.07317	0.0948 ± 0.0603
S97-V22A-RV-FX	165.31 ± 72.23	-	-0.00251 ± 0.02386	0.0207 ± 0.0119
S97-V22B-RV-CX	2438.76 ± 647.56	25.88 ± 8.78	0.00506 ± 0.11008	0.3286 ± 0.1521
S97-V22B-RV-FX	371.44 ± 122.98	1.58 ± 0.76	0.10842 ± 0.03504	0.0508 ± 0.0268
S97-V22B-RV-MX5	42.01 ± 71.51	-0.02 ± 0.46	0.07126 ± 0.07311	0.0021 ± 0.0035
S97-V22B-RV-MX6	-30.60 ± 63.85	-	0.10721 ± 0.07412	-
S97-V22B-RV-MX7	-	-	-	0.0210 ± 0.0114
S97-V22B-RV-MX8	373.96 ± 280.61	-	-0.02888 ± 0.06853	0.0190 ± 0.0092
S97-V22B-RV-MX9	-	-	-0.01176 ± 0.06798	-
S97-V22B-RV-MX10	-	-	-0.00491 ± 0.06877	0.0581 ± 0.0428
S97-V22C-RV-CX	1614.46 ± 713.59	35.53 ± 10.23	0.09921 ± 0.11909	0.1623 ± 0.0855
S97-V22C-RV-FX	340.78 ± 145.08	-	0.02044 ± 0.03850	0.0286 ± 0.0177
S97-V22D-RV-CX	1055.66 ± 570.77	15.86 ± 8.00	0.31737 ± 0.14324	0.1158 ± 0.0686
S97-V22D-RV-FX	150.55 ± 91.83	-	0.07875 ± 0.03747	0.0082 ± 0.0085
S97-V22D-RV-MX5	-61.46 ± 63.11	-0.10 ± 0.49	-0.01404 ± 0.06903	-
S97-V22D-RV-MX6	11.76 ± 59.88	-	-	-
S97-V22D-RV-MX7	-	-	-	0.0074 ± 0.0046
S97-V22D-RV-MX8	-	-0.33 ± 0.34	0.00273 ± 0.06700	-
S97-V22D-RV-MX9	-	-0.05 ± 0.42	-0.01991 ± 0.06713	-
S97-V22D-RV-MX10	-31.38 ± 63.91	-	-0.00565 ± 0.06837	-
S97-V22E-RV-CX	579.31 ± 289.05	10.26 ± 4.98	0.01320 ± 0.05975	0.0480 ± 0.0326
S97-V22E-RV-FX	84.20 ± 37.04	-	0.06528 ± 0.01570	0.0082 ± 0.0062
S97-N21D-ML-FX	239.16 ± 105.45	1.17 ± 1.44	0.09264 ± 0.04310	-
S97-N21E-ML-FX	148.00 ± 226.03	-	0.03899 ± 0.02267	0.0065 ± 0.0063
S97-N22A-ML-FX	290.79 ± 70.42	-	0.00278 ± 0.03140	0.0039 ± 0.0067
S97-N22B-ML-FX	-	-	-	-
S97-N22C-ML-FX	79.66 ± 69.61	-	0.00352 ± 0.02303	0.0017 ± 0.0084
S97-N22C-ML-MX5	-	-	-	-
S97-N22C-ML-MX6	-	-	-	0.0037 ± 0.0039
S97-N22C-ML-MX7	74.84 ± 71.77	-0.27 ± 0.33	0.03505 ± 0.07160	0.0004 ± 0.0023
S97-N22C-ML-MX8	33.87 ± 68.02	-	0.02627 ± 0.07160	-
S97-N22C-ML-MX9	-84.25 ± 62.59	-0.32 ± 0.35	0.18724 ± 0.07325	-
S97-N22C-ML-MX10	-	-0.02 ± 0.44	-0.00299 ± 0.07533	-0.0001 ± 0.0017
S97-N22D-ML-FX	-	-	0.03489 ± 0.02233	0.0048 ± 0.0082
S97-N22E-ML-FX	64.80 ± 78.13	-	0.26082 ± 0.02353	-
S97-N23A-ML-FX	266.65 ± 80.29	0.32 ± 0.82	0.02855 ± 0.03158	-
S97-N23B-ML-FX	55.27 ± 136.67	-	0.00348 ± 0.03929	-
S97-N23C-ML-FX	-	0.26 ± 1.02	0.03551 ± 0.02273	0.0016 ± 0.0062
S97-N23C-ML-MX5	155.49 ± 66.68	0.76 ± 0.40	-0.01545 ± 0.06962	0.0019 ± 0.0036
S97-N23C-ML-MX6	-	-	-0.02648 ± 0.07012	-
S97-N23C-ML-MX7	16.18 ± 79.29	0.15 ± 0.57	0.11894 ± 0.07405	0.0039 ± 0.0042
S97-N23C-ML-MX8	-	-0.22 ± 0.35	-0.01342 ± 0.07228	-
S97-N23C-ML-MX9	10.37 ± 72.64	-0.14 ± 0.36	-0.02183 ± 0.06903	0.0007 ± 0.0025
S97-N23C-ML-MX10	-	-0.14 ± 0.34	-0.01429 ± 0.06916	-

Table D.7: Trace Metals Aerosol Concentration Data (Fe, Ga, Hg, In) (continued)

Sample	Aerosol Concentration (ng m^{-3})			
	Fe	Ga	Hg	In
S97-N23D-ML-FX	54.49 ± 62.50	-	-	0.0080 ± 0.0109
S97-N23E-ML-FX	-	-	0.02006 ± 0.02219	0.0082 ± 0.0062
S97-N23E-ML-MX5	79.18 ± 101.33	-	0.15975 ± 0.06108	-
S97-N23E-ML-MX6	-	1.54 ± 1.41	0.10482 ± 0.05982	0.0079 ± 0.0078
S97-N23E-ML-MX7	-	-	-0.01485 ± 0.04000	-
S97-N23E-ML-MX8	-	-	0.15975 ± 0.15170	-
S97-N23E-ML-MX9	-22.35 ± 42.54	-	-	-
S97-N23E-ML-MX10	-	0.22 ± 0.50	-	-
S97-N31A-DB-CX	1972.59 ± 377.52	-	0.08087 ± 0.07227	0.0577 ± 0.0422
S97-N31A-DB-FX	567.84 ± 103.89	-	0.10339 ± 0.03638	0.0529 ± 0.0346
S97-N31B-DB-CX	3123.33 ± 494.55	1.21 ± 5.32	0.24469 ± 0.11174	0.0643 ± 0.0491
S97-N31B-DB-FX	-74.95 ± 59.71	-	0.09575 ± 0.04995	0.0398 ± 0.0198
S97-N31C-DB-CX	1757.38 ± 485.34	11.12 ± 7.75	0.23141 ± 0.10293	0.2375 ± 0.1252
S97-N31C-DB-FX	524.55 ± 81.36	2.50 ± 1.37	0.53583 ± 0.03909	0.0271 ± 0.0168
S97-N31C-DB-MX5	90.43 ± 69.22	-	-0.02403 ± 0.07048	0.0010 ± 0.0028
S97-N31C-DB-MX6	3.17 ± 84.62	-	-0.00007 ± 0.07182	-
S97-N31C-DB-MX7	170.30 ± 99.58	-	-	0.0013 ± 0.0026
S97-N31C-DB-MX8	-	-	-0.00007 ± 0.07385	0.0016 ± 0.0028
S97-N31C-DB-MX9	10.57 ± 72.53	-	0.00881 ± 0.07119	0.0010 ± 0.0023
S97-N31C-DB-MX10	-	-	-0.00007 ± 0.07130	-0.0004 ± 0.0015
S97-N31D-DB-CX	1866.61 ± 638.86	-	-	0.0206 ± 0.0348
S97-N31D-DB-FX	128.16 ± 184.50	-0.08 ± 0.62	0.12493 ± 0.06453	0.0076 ± 0.0104
S97-N31D-DB-MX5	-56.96 ± 87.31	-	0.03481 ± 0.08678	0.0065 ± 0.0047
S97-N31D-DB-MX6	-	5.66 ± 3.44	-	-
S97-N31D-DB-MX7	-8.47 ± 85.55	-	0.01737 ± 0.08354	0.0092 ± 0.0054
S97-N31D-DB-MX8	-	-	0.18483 ± 0.08850	0.0026 ± 0.0040
S97-N31D-DB-MX9	-	-	0.01737 ± 0.08518	-
S97-N31D-DB-MX10	-	-	0.05225 ± 0.08364	0.0009 ± 0.0024
S97-N31E-DB-CX	1889.66 ± 414.46	0.65 ± 2.79	0.02675 ± 0.06896	0.0398 ± 0.0324
S97-N31E-DB-FX	-40.72 ± 32.44	1.08 ± 0.83	0.01916 ± 0.02120	0.0303 ± 0.0141
S97-N32A-DB-CX	1495.77 ± 376.76	16.09 ± 3.03	0.01798 ± 0.08671	-
S97-N32A-DB-FX	-41.48 ± 49.00	-	0.02051 ± 0.02308	-0.0020 ± 0.0045
S97-N32B-DB-CX	3988.39 ± 495.70	-2.46 ± 3.77	0.25528 ± 0.11631	-
S97-N32B-DB-FX	296.88 ± 188.33	-	0.19080 ± 0.03830	0.0047 ± 0.0081
S97-N32C-DB-CX	1456.63 ± 595.45	9.13 ± 4.33	-	0.0165 ± 0.0416
S97-N32C-DB-FX	547.65 ± 79.80	-	0.15678 ± 0.03763	0.0139 ± 0.0133
S97-N32C-DB-MX5	148.51 ± 65.14	0.65 ± 0.40	-0.00300 ± 0.07089	0.0025 ± 0.0031
S97-N32C-DB-MX6	142.63 ± 65.63	0.13 ± 0.51	-0.00888 ± 0.07058	0.0051 ± 0.0059
S97-N32C-DB-MX7	104.46 ± 73.49	0.18 ± 0.48	-0.02914 ± 0.06992	0.0169 ± 0.0100
S97-N32C-DB-MX8	69.22 ± 76.70	-	-0.01974 ± 0.07063	0.0019 ± 0.0034
S97-N32C-DB-MX9	-	-	-0.00007 ± 0.07237	-
S97-N32C-DB-MX10	-	-	-	-
S97-N32D-DB-CX	785.69 ± 526.88	-	0.00466 ± 0.09023	0.0029 ± 0.0360
S97-N32D-DB-FX	-	1.77 ± 1.10	0.09468 ± 0.03735	0.0016 ± 0.0079
S97-N32E-DB-CX	1733.21 ± 267.26	-	0.02733 ± 0.04577	-
S97-N32E-DB-FX	-40.73 ± 32.31	-0.05 ± 0.35	0.07076 ± 0.02112	-

Table D.7: Trace Metals Aerosol Concentration Data (Fe, Ga, Hg, In) (continued)

Sample	Aerosol Concentration (ng m^{-3})			
	Fe	Ga	Hg	In
S97-N31A-ML-CX	3749.20 ± 673.55	-0.34 ± 4.16	-	0.0857 ± 0.0643
S97-N31A-ML-FX	360.19 ± 84.92	6.46 ± 1.55	2.40861 ± 0.05635	0.0545 ± 0.0295
S97-N31B-ML-CX	5992.59 ± 627.88	3.09 ± 6.09	0.22338 ± 0.10238	0.0782 ± 0.0791
S97-N31B-ML-FX	726.85 ± 82.31	-	0.22429 ± 0.04592	0.0445 ± 0.0366
S97-N31C-ML-CX	4128.88 ± 738.83	-1.85 ± 5.12	-0.03869 ± 0.10618	0.0305 ± 0.0484
S97-N31C-ML-FX	570.66 ± 103.58	-	0.08120 ± 0.03761	0.0088 ± 0.0121
S97-N31C-ML-MX5	46.51 ± 87.58	-	-0.01036 ± 0.08224	-
S97-N31C-ML-MX6	-35.73 ± 82.40	-	-0.03091 ± 0.08171	0.0002 ± 0.0023
S97-N31C-ML-MX7	1543.81 ± 129.04	-	0.00678 ± 0.09267	-
S97-N31C-ML-MX8	-	-	-	-
S97-N31C-ML-MX9	-67.93 ± 78.23	-	-	-
S97-N31C-ML-MX10	-	-	-	-
S97-N31D-ML-CX	3905.14 ± 528.20	-	0.10003 ± 0.09078	0.0687 ± 0.0612
S97-N31D-ML-FX	280.72 ± 67.78	-	0.01033 ± 0.02906	0.0118 ± 0.0145
S97-N31D-ML-MX5	400.34 ± 80.04	-	-	-
S97-N31D-ML-MX6	2.08 ± 85.47	-	-0.02724 ± 0.08783	0.0027 ± 0.0042
S97-N31D-ML-MX7	-26.89 ± 80.92	-	-0.03412 ± 0.08702	0.0023 ± 0.0035
S97-N31D-ML-MX8	9.32 ± 98.91	-0.28 ± 0.50	-0.03556 ± 0.08708	0.0009 ± 0.0025
S97-N31D-ML-MX9	-12.41 ± 77.51	-0.44 ± 0.45	-0.03158 ± 0.08660	-0.0002 ± 0.0022
S97-N31D-ML-MX10	-	-	-0.01094 ± 0.08783	-
S97-N31E-ML-CX	6580.83 ± 394.88	1.45 ± 4.72	0.10802 ± 0.05601	0.0234 ± 0.0339
S97-N31E-ML-FX	639.05 ± 67.83	-	0.07934 ± 0.01835	0.0194 ± 0.0115
S97-N32A-ML-CX	3875.57 ± 467.42	-	0.02793 ± 0.07929	0.0500 ± 0.0449
S97-N32A-ML-FX	414.00 ± 138.34	-	0.02128 ± 0.04610	0.0129 ± 0.0111
S97-N32B-ML-CX	7706.50 ± 1020.67	7.65 ± 7.26	0.36032 ± 0.15782	-
S97-N32B-ML-FX	290.38 ± 89.22	-	0.04111 ± 0.05522	0.0032 ± 0.0080
S97-N32C-ML-CX	3905.14 ± 712.57	-	0.00515 ± 0.08809	-
S97-N32C-ML-FX	7.16 ± 71.53	-0.45 ± 0.75	0.04964 ± 0.04997	0.0091 ± 0.0095
S97-N32C-ML-MX5	-56.15 ± 70.55	-	-0.03004 ± 0.07666	-0.0008 ± 0.0014
S97-N32C-ML-MX6	-36.82 ± 72.01	-	-0.03197 ± 0.07663	0.0008 ± 0.0025
S97-N32C-ML-MX7	-	-0.02 ± 0.39	-0.02230 ± 0.07680	-0.0005 ± 0.0017
S97-N32C-ML-MX8	-4.60 ± 72.20	-	-0.02810 ± 0.07796	0.0011 ± 0.0028
S97-N32C-ML-MX9	37.29 ± 76.06	-	0.00315 ± 0.07852	0.0005 ± 0.0022
S97-N32C-ML-MX10	-76.77 ± 70.34	-	-0.02005 ± 0.07711	-
S97-N32D-ML-CX	972.67 ± 529.38	-	-0.05417 ± 0.08272	0.0090 ± 0.0401
S97-N32D-ML-FX	21.84 ± 76.97	-	-	-0.0030 ± 0.0058
S97-N32E-ML-CX	905.33 ± 326.98	-	0.20866 ± 0.05621	0.0593 ± 0.0397
S97-N32E-ML-FX	-9.02 ± 45.09	-	0.04040 ± 0.02289	-
S97-N31A-RV-CX	-313.46 ± 382.28	-	-0.04645 ± 0.05895	-
S97-N31A-RV-FX	160.62 ± 79.25	0.80 ± 1.12	0.00279 ± 0.01822	0.0116 ± 0.0088
S97-N31B-RV-CX	2648.75 ± 504.04	2.31 ± 5.90	0.09918 ± 0.08733	0.0869 ± 0.0648
S97-N31B-RV-FX	364.26 ± 114.26	-	0.20110 ± 0.04037	0.0083 ± 0.0086
S97-N31C-RV-CX	2504.50 ± 634.33	-	-	0.0945 ± 0.0652
S97-N31C-RV-FX	-	-	-	0.0114 ± 0.0111
S97-N31C-RV-MX5	-	-	-0.02078 ± 0.06853	0.0024 ± 0.0039
S97-N31C-RV-MX6	-27.12 ± 64.22	0.27 ± 0.35	-0.01992 ± 0.06861	0.0013 ± 0.0028

Table D.7: Trace Metals Aerosol Concentration Data (Fe, Ga, Hg, In) (continued)

Sample	Aerosol Concentration (ng m^{-3})			
	Fe	Ga	Hg	In
S97-N31C-RV-MX7	-21.37 ± 67.32	-	-0.02193 ± 0.06864	0.0022 ± 0.0030
S97-N31C-RV-MX8	-	-	-	0.0016 ± 0.0022
S97-N31C-RV-MX9	-	-	-0.02711 ± 0.06848	-
S97-N31C-RV-MX10	-68.26 ± 63.06	-	-0.02941 ± 0.06834	0.0013 ± 0.0020
S97-N31D-RV-CX	2191.95 ± 472.35	1.01 ± 5.21	0.13543 ± 0.08286	0.1154 ± 0.0719
S97-N31D-RV-FX	209.46 ± 68.22	-	0.12554 ± 0.03747	0.0138 ± 0.0105
S97-N31D-RV-MX5	-	-	-	-
S97-N31D-RV-MX6	49.89 ± 107.52	-	-	0.0125 ± 0.0086
S97-N31D-RV-MX7	-	-	-	0.0022 ± 0.0033
S97-N31D-RV-MX8	-59.66 ± 76.33	-	-0.02404 ± 0.08234	0.0002 ± 0.0023
S97-N31D-RV-MX9	-	-	-0.01548 ± 0.08193	0.0046 ± 0.0046
S97-N31D-RV-MX10	-	-0.23 ± 0.43	0.14714 ± 0.08673	-
S97-N31E-RV-CX	2406.55 ± 320.39	-	0.06836 ± 0.05551	0.0776 ± 0.0516
S97-N31E-RV-FX	408.20 ± 82.25	-	0.00208 ± 0.01357	0.0144 ± 0.0101
S97-N32A-RV-CX	1382.20 ± 508.61	-	0.42282 ± 0.07754	0.0133 ± 0.0324
S97-N32A-RV-FX	108.07 ± 115.35	-0.18 ± 0.63	0.01382 ± 0.02713	0.0123 ± 0.0101
S97-N32B-RV-CX	764.03 ± 478.97	2.21 ± 5.05	0.00508 ± 0.12608	-0.0080 ± 0.0328
S97-N32B-RV-FX	127.56 ± 75.17	-	-	0.0050 ± 0.0086
S97-N32C-RV-CX	1025.15 ± 484.80	-	-0.01615 ± 0.08240	-0.0097 ± 0.0325
S97-N32C-RV-FX	130.84 ± 72.57	-	0.00351 ± 0.02295	-
S97-N32C-RV-MX5	176.08 ± 77.89	-	0.02483 ± 0.07491	-
S97-N32C-RV-MX6	281.90 ± 76.32	-	-0.01376 ± 0.07513	0.0014 ± 0.0027
S97-N32C-RV-MX7	-	-	-0.00318 ± 0.07513	0.0020 ± 0.0024
S97-N32C-RV-MX9	-	-0.02 ± 0.36	-0.01408 ± 0.07448	-
S97-N32C-RV-MX10	-	-	-0.00629 ± 0.07622	-
S97-N32D-RV-CX	822.69 ± 469.93	-	0.14862 ± 0.08391	-0.0032 ± 0.0339
S97-N32D-RV-FX	-	-	0.72809 ± 0.03863	0.0016 ± 0.0082
S97-N32E-RV-CX	234.40 ± 302.38	2.34 ± 2.87	0.12624 ± 0.05658	0.0069 ± 0.0200
S97-N32E-RV-FX	-	-	0.04778 ± 0.01521	-
S97-T11B-TI-CX	3689.35 ± 851.51	6.22 ± 7.10	0.14628 ± 0.14539	0.1646 ± 0.0991
S97-T11B-TI-FX	1298.53 ± 369.14	1.82 ± 1.58	1.16753 ± 0.08512	0.0181 ± 0.0250
S97-T11B-TI-MX5	-	-	-	0.0021 ± 0.0041
S97-T11B-TI-MX6	-	-	-	0.0006 ± 0.0020
S97-T11B-TI-MX7	-	-	-0.03807 ± 0.09360	-
S97-T11B-TI-MX8	-48.65 ± 89.67	-	-0.03846 ± 0.09302	-
S97-T11B-TI-MX9	-40.82 ± 87.86	-	-0.00400 ± 0.09410	0.0100 ± 0.0064
S97-T11B-TI-MX10	-	0.13 ± 0.49	-0.03298 ± 0.09392	0.0014 ± 0.0034
S97-T11B-TO-CX	-	-	0.10033 ± 0.13690	0.0968 ± 0.0728
S97-T11B-TO-FX	1100.92 ± 144.78	-	0.53381 ± 0.08642	0.0102 ± 0.0140
S97-T11B-TO-MX5	-	-	-0.02075 ± 0.09799	-
S97-T11B-TO-MX6	-34.82 ± 105.61	-	0.04536 ± 0.10802	0.0085 ± 0.0092
S97-T11B-TO-MX7	-	-	-0.00836 ± 0.10068	-
S97-T11B-TO-MX8	-	0.38 ± 0.84	-0.00009 ± 0.10014	-
S97-T11B-TO-MX9	-	-	-0.05050 ± 0.09810	-
S97-T11B-TO-MX10	-72.00 ± 92.84	-	-0.03645 ± 0.09867	0.0010 ± 0.0032

Table D.7: Trace Metals Aerosol Concentration Data (Fe, Ga, Hg, In) (continued)

Sample	Aerosol Concentration (ng m^{-3})			
	Fe	Ga	Hg	In
S97-T21B-TI-CX	2623.01 ± 600.24	-1.35 ± 5.37	-	-0.0017 ± 0.0416
S97-T21B-TI-FX	158.59 ± 237.32	-	0.24312 ± 0.04880	-
S97-T21B-TI-MX5	431.48 ± 101.93	-0.11 ± 0.67	-0.03131 ± 0.09338	0.0021 ± 0.0041
S97-T21B-TI-MX6	84.18 ± 92.12	-	0.02723 ± 0.09672	-
S97-T21B-TI-MX7	-	-	0.01162 ± 0.09718	-
S97-T21B-TI-MX8	-	-	0.03113 ± 0.09537	-
S97-T21B-TI-MX9	-	-	-	-0.0006 ± 0.0020
S97-T21B-TI-MX10	2.24 ± 95.69	-	-0.02272 ± 0.09606	0.0002 ± 0.0027
S97-T21B-TO-FX	364.46 ± 121.11	-	0.16822 ± 0.05443	0.0059 ± 0.0102
S97-T31B-TI-CX	2080.10 ± 604.45	4.08 ± 6.65	0.22306 ± 0.12100	0.0178 ± 0.0532
S97-T31B-TI-FX	711.53 ± 122.86	-	0.04553 ± 0.02914	-
S97-T31B-TI-MX5	-	-	-0.02545 ± 0.09355	0.0029 ± 0.0049
S97-T31B-TI-MX6	-	-	-	-
S97-T31B-TI-MX7	52.97 ± 109.07	-0.31 ± 0.51	-0.02662 ± 0.09310	0.0014 ± 0.0034
S97-T31B-TI-MX9	-	-	-0.02740 ± 0.09367	-0.0010 ± 0.0017
S97-T31B-TI-MX10	-44.59 ± 106.60	-	-0.03794 ± 0.09302	-
S97-T31B-TO-CX	-210.08 ± 596.27	0.52 ± 6.36	-	0.0940 ± 0.0746
S97-T31B-TO-FX	-	1.84 ± 0.88	0.00422 ± 0.04769	0.0059 ± 0.0101
S97-T31B-TO-MX5	-	-	-0.02135 ± 0.09232	-
S97-T31B-TO-MX6	-	-	-0.03952 ± 0.09279	0.0118 ± 0.0105
S97-T31B-TO-MX7	-	-	-0.02560 ± 0.09311	0.0164 ± 0.0151
S97-T31B-TO-MX8	-	0.51 ± 0.82	-0.04261 ± 0.09219	-
S97-T31B-TO-MX9	-	-	-0.00782 ± 0.09291	-
S97-T31B-TO-MX10	33.14 ± 145.59	-	-	-
S97-T41B-TI-CX	3028.67 ± 789.85	-	0.40754 ± 0.12428	0.0629 ± 0.0691
S97-T41B-TI-FX	792.15 ± 96.75	-0.11 ± 1.07	0.12716 ± 0.05016	0.0103 ± 0.0140
S97-T41B-TI-MX5	-	1.92 ± 1.55	0.28087 ± 0.13166	-
S97-T41B-TI-MX6	353.44 ± 183.91	0.87 ± 1.00	-	-
S97-T41B-TI-MX7	-	1.30 ± 0.86	0.20283 ± 0.12361	-
S97-T41B-TI-MX8	-	-	0.14820 ± 0.12892	-
S97-T41B-TI-MX9	-36.79 ± 95.69	-	0.04284 ± 0.10202	-0.0002 ± 0.0020
S97-T41B-TI-MX10	-	-	-0.03989 ± 0.09287	-
S97-T41B-TO-CX	-	-	-0.03010 ± 0.09119	0.0398 ± 0.0487
S97-T41B-TO-FX	-93.38 ± 74.39	-	0.08360 ± 0.04861	0.0100 ± 0.0103
S97-B11A-AZ-MX5	-	-	-	-
S97-B11A-AZ-MX6	-	1.20 ± 1.20	0.48000 ± 0.11000	-
S97-B11A-AZ-MX7	-	-	-	0.0200 ± 0.0060
S97-B11A-AZ-MX8	-	-	-	-
S97-B11A-AZ-MX9	-	-	0.07800 ± 0.06200	0.0120 ± 0.0080
S97-B11A-AZ-MX10	-	-	0.07800 ± 0.07000	0.0160 ± 0.0140
S97-B11A-DB-CX	3200.00 ± 840.00	12.20 ± 6.40	-	0.1780 ± 0.0800
S97-B11A-DB-FX	3.92 ± 0.56	-	0.06200 ± 0.03200	-
S97-B11A-DB-MX5	-	7.00 ± 3.40	0.05200 ± 0.05000	-
S97-B11A-DB-MX6	-	-	0.16400 ± 0.11400	-

Table D.7: Trace Metals Aerosol Concentration Data (Fe, Ga, Hg, In) (continued)

Sample	Aerosol Concentration (ng m^{-3})			
	Fe	Ga	Hg	In
S97-B11A-DB-MX7	-	2.40 ± 1.54	0.16200 ± 0.08200	-
S97-B11A-DB-MX8	-	-	0.09000 ± 0.06600	-
S97-B11A-DB-MX9	2000.00 ± 220.00	-	0.13600 ± 0.10200	-
S97-B11A-DB-MX10	-	-	-	-
S97-B11A-ML-CX	-	6.20 ± 3.00	0.16000 ± 0.06200	-
S97-B11A-ML-FX	122.37 ± 46.43	0.72 ± 0.34	0.13900 ± 0.02900	-
S97-B11A-RV-CX	-	11.60 ± 6.80	-	0.0520 ± 0.0300
S97-B11A-RV-FX	-	-	0.05000 ± 0.04000	-
S97-B11A-RV-MX5	1300.00 ± 240.00	-	-	-
S97-B11A-RV-MX6	1140.00 ± 172.00	-	0.08600 ± 0.07400	0.0180 ± 0.0160
S97-B11A-RV-MX7	-	4.00 ± 2.20	0.22000 ± 0.07000	0.0160 ± 0.0100
S97-B11A-RV-MX8	126.00 ± 70.00	1.60 ± 1.20	0.34000 ± 0.08000	0.0160 ± 0.0140
S97-B11A-RV-MX9	142.00 ± 88.00	2.20 ± 1.30	0.13600 ± 0.03800	-
S97-B11A-RV-MX10	-	-	0.12600 ± 0.05600	0.0140 ± 0.0120
S97-B11A-TI-CX	220.00 ± 92.00	2.20 ± 1.58	0.34000 ± 0.15000	-
S97-B11A-TI-FX	156.00 ± 9.00	-	0.04000 ± 0.03000	0.0100 ± 0.0100
S97-B11A-TI-MX5	440.00 ± 300.00	-	0.26000 ± 0.10800	-
S97-B11A-TI-MX6	280.00 ± 168.00	-	0.08600 ± 0.06200	0.0160 ± 0.0140
S97-B11A-TI-MX7	220.00 ± 90.00	-	0.28000 ± 0.06400	-
S97-B11A-TI-MX8	360.00 ± 160.00	-	0.04800 ± 0.03000	0.0200 ± 0.0180
S97-B11A-TI-MX9	-	-	-	0.0140 ± 0.0120
S97-B11A-TI-MX10	-	-	0.09200 ± 0.07400	-
S97-B21A-DB-CX	-	-	0.24000 ± 0.12600	0.0300 ± 0.0160
S97-B21A-DB-FX	-	-	-	0.0090 ± 0.0080
S97-B21A-DB-MX5	420.00 ± 260.00	7.20 ± 3.40	-	-
S97-B21A-DB-MX6	-	2.00 ± 0.30	0.07000 ± 0.04800	0.0340 ± 0.0700
S97-B21A-DB-MX7	-	2.80 ± 0.48	0.12000 ± 0.05000	-
S97-B21A-DB-MX9	-	-	2.60000 ± 0.22000	-
S97-B21A-DB-MX10	960.00 ± 360.00	-	0.46000 ± 0.09400	-
S97-B21A-ML-CX	-	4.60 ± 2.60	-	-
S97-B21A-ML-FX	-	-	0.10000 ± 0.00000	0.0100 ± 0.0100
S97-B21A-ML-MX5	136.00 ± 132.00	-	0.19400 ± 0.06000	0.0140 ± 0.0120
S97-B21A-ML-MX6	132.00 ± 126.00	-	0.17200 ± 0.09600	-
S97-B21A-ML-MX7	320.00 ± 118.00	-	0.26000 ± 0.06800	-
S97-B21A-ML-MX8	420.00 ± 162.00	2.40 ± 0.82	0.15600 ± 0.05400	-
S97-B21A-ML-MX9	520.00 ± 200.00	2.60 ± 0.42	0.42000 ± 0.15000	-
S97-B21A-ML-MX10	-	-	0.24000 ± 0.08400	-
S97-B21A-RV-CX	1080.00 ± 178.00	-	0.14400 ± 0.07400	-
S97-B21A-RV-FX	114.00 ± 55.00	-	0.22000 ± 0.07000	0.0200 ± 0.0100
S97-B21A-RV-MX5	236.00 ± 188.00	4.00 ± 2.00	0.14800 ± 0.11400	-
S97-B21A-RV-MX6	222.00 ± 216.00	-	0.11600 ± 0.08800	-
S97-B21A-RV-MX7	880.00 ± 460.00	-	0.50000 ± 0.40000	-
S97-B21A-RV-MX8	484.00 ± 186.00	-	0.58000 ± 0.11600	0.0200 ± 0.0140
S97-B21A-RV-MX9	-	-	-	-

Table D.7: Trace Metals Aerosol Concentration Data (Fe, Ga, Hg, In) (continued)

Sample	Aerosol Concentration (ng m^{-3})			
	Fe	Ga	Hg	In
S97-B21A-RV-MX10	-	-	0.08200 ± 0.03000	0.0160 ± 0.0100

D.8 Trace Elements Aerosol Concentration Data (K, La, Lu, Mg)

Table D.8: Trace Metals Aerosol Concentration Data (K, La, Lu, Mg)

Sample	Aerosol Concentration (ng m^{-3})			
	K	La	Lu	Mg
S97-V11A-LA-CX	-	1.85679 ± 0.50487	0.0152 ± 0.0208	31.9 ± 96.9
S97-V11A-LA-FX	-	0.49432 ± 0.02938	-	44.2 ± 32.3
S97-V11B-LA-CX	-	1.87724 ± 0.68447	-	178.6 ± 141.2
S97-V11B-LA-FX	-	0.85976 ± 0.07177	0.0028 ± 0.0076	-
S97-V11C-LA-CX	254.31 ± 254.34	1.72139 ± 0.63161	-	446.2 ± 223.8
S97-V11C-LA-FX	-	0.00871 ± 0.03318	-	41.7 ± 35.8
S97-V11D-LA-CX	16.54 ± 265.92	0.34674 ± 0.63629	-	141.8 ± 145.0
S97-V11D-LA-FX	52.75 ± 40.44	0.15079 ± 0.02579	-	49.9 ± 46.9
S97-V11E-LA-CX	-	0.18625 ± 0.34246	-	134.9 ± 74.2
S97-V11E-LA-FX	-	0.05299 ± 0.01862	-	46.6 ± 18.2
S97-V12A-LA-CX	-	0.38712 ± 0.50956	-	157.3 ± 108.2
S97-V12A-LA-FX	23.51 ± 26.96	0.07770 ± 0.02320	0.0032 ± 0.0061	13.2 ± 9.9
S97-V12B-LA-CX	126.32 ± 231.06	0.98099 ± 0.60154	-	192.3 ± 126.0
S97-V12B-LA-FX	51.23 ± 51.81	0.36992 ± 0.03632	-0.0005 ± 0.0043	99.9 ± 42.9
S97-V12B-LA-MX5	-14.78 ± 19.24	-	-0.0027 ± 0.0085	8.3 ± 10.5
S97-V12B-LA-MX6	-6.85 ± 20.23	0.01031 ± 0.01078	-0.0036 ± 0.0085	4.4 ± 9.8
S97-V12B-LA-MX7	-	-	-	-
S97-V12B-LA-MX8	8.71 ± 22.46	-	-	-
S97-V12B-LA-MX9	2.25 ± 22.84	-0.00848 ± 0.00834	-	-
S97-V12B-LA-MX10	-	-	0.0011 ± 0.0087	-
S97-V12C-LA-CX	312.28 ± 314.11	2.67240 ± 0.62666	-	174.3 ± 120.3
S97-V12C-LA-FX	102.85 ± 49.01	0.73430 ± 0.05812	-	54.9 ± 37.1
S97-V12D-LA-CX	356.49 ± 231.11	1.11963 ± 0.63019	-	130.3 ± 118.7
S97-V12D-LA-FX	-	0.68440 ± 0.05583	0.0059 ± 0.0072	45.5 ± 26.7
S97-V12E-LA-CX	124.82 ± 221.11	0.65295 ± 0.34602	-	549.0 ± 126.8
S97-V12E-LA-FX	29.76 ± 23.19	0.23234 ± 0.02562	0.0032 ± 0.0039	47.5 ± 17.2
S97-V11A-AZ-CX	378.95 ± 334.28	0.73783 ± 0.54447	-	276.0 ± 140.6
S97-V11A-AZ-FX	-	0.06997 ± 0.02047	-0.0031 ± 0.0037	-
S97-V11B-AZ-CX	1451.59 ± 551.76	2.42281 ± 0.71800	-	2111.5 ± 471.6
S97-V11B-AZ-FX	-	0.16562 ± 0.03298	-	51.5 ± 33.4
S97-V11C-AZ-CX	638.41 ± 386.38	1.57699 ± 0.67757	-	884.4 ± 250.6
S97-V11C-AZ-FX	22.85 ± 33.36	0.17867 ± 0.02985	-	42.9 ± 36.8
S97-V11D-AZ-CX	113.42 ± 253.85	1.68040 ± 0.68271	-	1090.1 ± 121.1
S97-V11D-AZ-FX	-	0.10042 ± 0.02405	-	7.0 ± 13.3
S97-V11D-AZ-MX5	15.27 ± 22.87	0.04385 ± 0.01392	-	-
S97-V11D-AZ-MX6	-3.46 ± 23.22	0.06927 ± 0.02927	-	-
S97-V11D-AZ-MX7	-	0.01442 ± 0.01206	-	-
S97-V11D-AZ-MX8	6.24 ± 26.02	-0.00398 ± 0.01025	-	14.8 ± 15.8
S97-V11D-AZ-MX9	2.23 ± 24.75	-	-	-
S97-V11D-AZ-MX10	-	0.00572 ± 0.01055	-	-
S97-V11E-AZ-CX	-	0.84767 ± 0.38881	-	-
S97-V11E-AZ-FX	-	0.10826 ± 0.01820	-	17.1 ± 9.0

Table D.8: Trace Metals Aerosol Concentration Data (K, La, Lu, Mg) (continued)

Sample	Aerosol Concentration (ng m^{-3})			
	K	La	Lu	Mg
S97-V12A-AZ-CX	965.93 ± 275.71	0.64776 ± 0.53372	-	864.9 ± 240.9
S97-V12A-AZ-FX	-	-	-	21.5 ± 17.6
S97-V12B-AZ-CX	839.12 ± 407.71	1.78857 ± 0.68949	-	1677.5 ± 507.8
S97-V12B-AZ-FX	-	1.39066 ± 0.10359	-	173.0 ± 64.2
S97-V12C-AZ-CX	1391.39 ± 350.94	1.65892 ± 0.67205	0.0120 ± 0.0199	981.4 ± 256.9
S97-V12C-AZ-FX	208.16 ± 111.18	0.20764 ± 0.03988	-	133.2 ± 53.9
S97-V12D-AZ-CX	538.44 ± 276.50	1.94323 ± 0.68055	-	791.9 ± 248.6
S97-V12D-AZ-FX	193.93 ± 69.68	0.77023 ± 0.06983	-0.0032 ± 0.0049	52.1 ± 32.2
S97-V12D-AZ-MX5	-5.34 ± 21.55	0.28459 ± 0.02582	-0.0034 ± 0.0095	-
S97-V12D-AZ-MX6	-	0.24146 ± 0.03801	-	6.2 ± 15.7
S97-V12D-AZ-MX7	13.61 ± 24.78	0.04937 ± 0.01384	-	-
S97-V12D-AZ-MX8	5.12 ± 24.37	-	-	-
S97-V12D-AZ-MX9	-14.81 ± 23.03	-0.00193 ± 0.00964	-	-2.9 ± 9.2
S97-V12D-AZ-MX10	-17.43 ± 21.26	0.00461 ± 0.00935	-0.0060 ± 0.0092	-
S97-V12E-AZ-CX	711.04 ± 205.68	1.27352 ± 0.37454	0.0030 ± 0.0111	1161.8 ± 395.3
S97-V12E-AZ-FX	73.85 ± 30.19	0.25965 ± 0.02192	-	58.3 ± 21.6
S97-V11A-RV-CX	-	0.12879 ± 0.55938	-	140.9 ± 123.0
S97-V11A-RV-FX	-	0.01339 ± 0.01980	-	8.9 ± 10.9
S97-V11B-RV-CX	171.73 ± 325.38	1.01264 ± 0.67849	-	198.1 ± 236.1
S97-V11B-RV-FX	-	0.09723 ± 0.02557	-	52.8 ± 62.7
S97-V11C-RV-CX	252.78 ± 255.44	0.09467 ± 0.65630	-	335.2 ± 177.6
S97-V11C-RV-FX	170.60 ± 47.32	0.12104 ± 0.12894	-0.0039 ± 0.0036	21.6 ± 15.8
S97-V11D-RV-CX	591.07 ± 274.54	1.08253 ± 0.66547	-	259.3 ± 177.3
S97-V11D-RV-FX	482.65 ± 80.32	0.99964 ± 0.07048	-0.0037 ± 0.0035	281.7 ± 58.1
S97-V11D-RV-MX5	-	0.00345 ± 0.01275	-	-
S97-V11D-RV-MX6	-	0.02599 ± 0.00887	-	-
S97-V11D-RV-MX7	13.31 ± 20.27	0.02029 ± 0.00976	-	-
S97-V11D-RV-MX8	-0.38 ± 22.96	-	-	-
S97-V11D-RV-MX9	0.47 ± 18.82	0.02599 ± 0.01125	-	-
S97-V11D-RV-MX10	-2.67 ± 18.69	-0.00282 ± 0.00833	-0.0044 ± 0.0082	-
S97-V11E-RV-CX	-	0.64210 ± 0.36141	-0.0017 ± 0.0104	393.1 ± 125.8
S97-V11E-RV-FX	31.46 ± 16.68	0.16209 ± 0.01696	-	6.5 ± 6.0
S97-V12A-RV-CX	-	0.31648 ± 0.53966	-	605.7 ± 169.5
S97-V12A-RV-FX	93.09 ± 29.20	0.22172 ± 0.02702	-0.0004 ± 0.0037	21.1 ± 12.7
S97-V12B-RV-CX	583.06 ± 336.86	1.21890 ± 0.68606	0.0182 ± 0.0228	-
S97-V12B-RV-FX	-	0.30545 ± 0.03969	-0.0006 ± 0.0074	66.3 ± 37.2
S97-V12C-RV-CX	730.18 ± 359.99	0.90345 ± 0.66632	0.0026 ± 0.0207	499.6 ± 193.7
S97-V12C-RV-FX	108.78 ± 51.83	0.68063 ± 0.05259	-0.0005 ± 0.0046	42.0 ± 20.2
S97-V12D-RV-CX	903.48 ± 307.57	0.98027 ± 0.65680	-	425.1 ± 175.8
S97-V12D-RV-FX	733.72 ± 133.65	0.45339 ± 0.04095	-	156.1 ± 42.1
S97-V12D-RV-MX5	-	0.10303 ± 0.01632	-	160.9 ± 43.5
S97-V12D-RV-MX6	-	0.16294 ± 0.01707	-0.0049 ± 0.0081	5.5 ± 11.7
S97-V12D-RV-MX7	-	0.05738 ± 0.01166	-0.0015 ± 0.0085	-
S97-V12D-RV-MX8	-	0.09447 ± 0.02824	-	3.2 ± 12.8
S97-V12D-RV-MX9	-	-	-	-
S97-V12D-RV-MX10	-	0.01458 ± 0.01166	-	-

Table D.8: Trace Metals Aerosol Concentration Data (K, La, Lu, Mg) (continued)

Sample	Aerosol Concentration (ng m^{-3})			
	K	La	Lu	Mg
S97-V12E-RV-CX	448.51 ± 222.47	3.53918 ± 0.43353	-	338.7 ± 105.2
S97-V12E-RV-FX	329.39 ± 50.82	2.43112 ± 0.15928	0.0032 ± 0.0025	160.8 ± 33.5
S97-V21A-LA-CX	796.95 ± 305.88	1.53532 ± 0.48990	-	201.6 ± 101.2
S97-V21A-LA-FX	-	0.60981 ± 0.04863	-	58.3 ± 23.5
S97-V21B-LA-CX	596.82 ± 321.15	1.34467 ± 0.61501	-	369.1 ± 145.1
S97-V21B-LA-FX	-	0.41055 ± 0.03987	-	43.7 ± 37.9
S97-V21B-LA-MX5	261.25 ± 121.63	0.24112 ± 0.02130	-0.0013 ± 0.0088	109.9 ± 36.1
S97-V21B-LA-MX6	-0.69 ± 17.73	0.04437 ± 0.01005	-	-
S97-V21B-LA-MX7	-	-0.00379 ± 0.00817	-	-
S97-V21B-LA-MX8	-	-	-0.0045 ± 0.0084	3.9 ± 9.8
S97-V21B-LA-MX9	-	-0.00907 ± 0.00824	-0.0048 ± 0.0082	-0.6 ± 7.9
S97-V21B-LA-MX10	85.06 ± 30.34	-	0.0078 ± 0.0096	48.2 ± 20.9
S97-V21C-LA-CX	529.65 ± 326.48	1.98188 ± 0.61232	-	510.6 ± 185.3
S97-V21C-LA-FX	-	0.55113 ± 0.04684	-	45.7 ± 34.0
S97-V21D-LA-CX	334.24 ± 283.81	0.81844 ± 0.60384	0.0144 ± 0.0206	297.5 ± 156.0
S97-V21D-LA-FX	-	0.10462 ± 0.02425	-	-
S97-V21E-LA-CX	219.82 ± 241.15	1.70350 ± 0.35781	-	271.3 ± 83.5
S97-V21E-LA-FX	-	0.55718 ± 0.05139	-0.0003 ± 0.0025	46.9 ± 15.8
S97-V22A-LA-CX	1248.06 ± 380.78	1.23555 ± 0.50198	-	385.1 ± 127.8
S97-V22A-LA-FX	-	0.41585 ± 0.03968	-	186.9 ± 71.8
S97-V22B-LA-CX	316.70 ± 244.87	1.76391 ± 0.62228	-	469.3 ± 155.8
S97-V22B-LA-FX	-	0.50038 ± 0.04229	-	120.4 ± 58.9
S97-V22B-LA-MX5	43.67 ± 33.84	-	-	82.9 ± 28.8
S97-V22B-LA-MX6	-	0.09077 ± 0.01397	0.0040 ± 0.0088	-
S97-V22B-LA-MX7	-	0.03242 ± 0.01236	-	13.2 ± 15.3
S97-V22B-LA-MX8	-	-	-	-
S97-V22B-LA-MX9	-	-	-	-
S97-V22B-LA-MX10	93.27 ± 28.72	0.02075 ± 0.01421	0.0203 ± 0.0119	-0.3 ± 8.9
S97-V22C-LA-CX	999.67 ± 324.09	2.18259 ± 0.61672	-0.0028 ± 0.0187	535.3 ± 262.8
S97-V22C-LA-FX	91.21 ± 40.28	0.70764 ± 0.05558	-	13.8 ± 16.0
S97-V22D-LA-CX	454.68 ± 310.40	1.09728 ± 0.61904	-	338.3 ± 152.8
S97-V22D-LA-FX	176.67 ± 35.62	0.45033 ± 0.04339	-0.0018 ± 0.0045	15.9 ± 12.6
S97-V22D-LA-MX5	-	0.77155 ± 0.07581	-	94.0 ± 28.0
S97-V22D-LA-MX6	-	0.33665 ± 0.02731	-	-
S97-V22D-LA-MX7	8.60 ± 19.97	0.00786 ± 0.00877	-	0.6 ± 9.7
S97-V22D-LA-MX8	-14.02 ± 19.39	0.00264 ± 0.00810	-0.0027 ± 0.0083	1.8 ± 9.7
S97-V22D-LA-MX9	-	0.02931 ± 0.00992	-0.0015 ± 0.0087	-
S97-V22D-LA-MX10	86.88 ± 18.62	-	0.0277 ± 0.0119	137.5 ± 38.5
S97-V22E-LA-CX	318.07 ± 324.11	0.69048 ± 0.33758	-	431.1 ± 112.6
S97-V22E-LA-FX	47.92 ± 36.21	0.22719 ± 0.02354	-	43.0 ± 15.2
S97-V21A-AZ-CX	793.67 ± 300.47	0.92912 ± 0.52296	-	345.9 ± 129.3
S97-V21A-AZ-FX	148.34 ± 65.68	0.18792 ± 0.02551	-	-1.7 ± 7.0
S97-V21B-AZ-CX	2062.04 ± 443.46	3.94731 ± 1.40205	-	984.9 ± 266.3
S97-V21B-AZ-FX	75.31 ± 85.54	0.17925 ± 0.03062	-	-9.0 ± 8.8
S97-V21C-AZ-CX	1003.06 ± 339.91	2.01940 ± 0.67204	-	465.3 ± 176.9
S97-V21C-AZ-FX	-	0.23062 ± 0.02918	-	16.5 ± 14.9

Table D.8: Trace Metals Aerosol Concentration Data (K, La, Lu, Mg) (continued)

Sample	Aerosol Concentration (ng m^{-3})			
	K	La	Lu	Mg
S97-V21D-AZ-CX	935.78 ± 366.05	1.88523 ± 0.68739	0.0036 ± 0.0203	479.0 ± 161.7
S97-V21D-AZ-FX	69.63 ± 80.03	0.37383 ± 0.04561	-	56.8 ± 34.2
S97-V21D-AZ-MX5	127.89 ± 31.27	0.06601 ± 0.01993	-	60.4 ± 23.4
S97-V21D-AZ-MX6	-	0.07257 ± 0.01466	-	-0.9 ± 10.4
S97-V21D-AZ-MX7	-	0.02662 ± 0.01142	-0.0001 ± 0.0102	-
S97-V21D-AZ-MX8	-18.82 ± 19.98	-	-	-
S97-V21D-AZ-MX9	-	-0.00062 ± 0.01020	-	3.6 ± 11.1
S97-V21D-AZ-MX10	-	0.00102 ± 0.01036	-	-
S97-V21E-AZ-CX	564.03 ± 241.48	1.13553 ± 0.37790	0.0189 ± 0.0159	451.8 ± 116.1
S97-V21E-AZ-FX	150.68 ± 43.81	0.14295 ± 0.01982	-	22.0 ± 10.3
S97-V22A-AZ-CX	176.18 ± 209.24	0.48683 ± 0.67504	-	359.5 ± 139.9
S97-V22A-AZ-FX	63.09 ± 45.19	0.09922 ± 0.02369	-	2.2 ± 9.9
S97-V22B-AZ-CX	261.66 ± 361.34	1.61052 ± 0.69609	-	454.3 ± 163.3
S97-V22B-AZ-FX	-	0.33865 ± 0.03444	-	8.1 ± 12.4
S97-V22B-AZ-MX5	-	0.20752 ± 0.02437	-	37.6 ± 23.0
S97-V22B-AZ-MX6	16.07 ± 29.33	0.06186 ± 0.01371	-	-
S97-V22B-AZ-MX7	35.49 ± 26.95	0.02625 ± 0.01071	-0.0056 ± 0.0092	-
S97-V22B-AZ-MX8	19.31 ± 19.07	0.00942 ± 0.01054	-0.0004 ± 0.0096	-
S97-V22B-AZ-MX9	-	-	-	-
S97-V22B-AZ-MX10	-	-0.00256 ± 0.00927	-	-4.5 ± 9.0
S97-V22C-AZ-CX	1028.84 ± 317.45	1.58970 ± 0.68302	0.0344 ± 0.0402	650.7 ± 261.1
S97-V22C-AZ-FX	119.21 ± 53.65	0.34022 ± 0.03615	-	11.7 ± 17.1
S97-V22D-AZ-CX	934.85 ± 333.69	1.78680 ± 0.69340	-	275.7 ± 139.7
S97-V22D-AZ-FX	39.06 ± 36.12	0.49717 ± 0.04477	-	9.6 ± 14.1
S97-V22D-AZ-MX5	-	0.19368 ± 0.02367	-	49.7 ± 22.9
S97-V22D-AZ-MX6	325.31 ± 45.96	0.12924 ± 0.01542	-	91.5 ± 27.8
S97-V22D-AZ-MX7	122.33 ± 40.18	0.03580 ± 0.01341	-	6.8 ± 12.2
S97-V22D-AZ-MX8	-	0.01969 ± 0.00915	0.0186 ± 0.0114	-
S97-V22D-AZ-MX9	-	0.02291 ± 0.01066	0.0244 ± 0.0114	-
S97-V22D-AZ-MX10	-	0.02291 ± 0.01066	0.0244 ± 0.0114	1.0 ± 10.2
S97-V22E-AZ-CX	408.68 ± 219.77	2.20820 ± 0.40716	-	417.9 ± 104.3
S97-V22E-AZ-FX	60.86 ± 32.54	0.45240 ± 0.03947	0.0042 ± 0.0070	14.6 ± 7.7
S97-V21A-RV-CX	183.29 ± 213.75	0.33899 ± 0.53894	-	142.8 ± 123.9
S97-V21A-RV-FX	-	0.33944 ± 0.03081	-	2163.7 ± 358.1
S97-V21B-RV-CX	724.01 ± 342.34	2.06702 ± 0.80214	0.0176 ± 0.0390	1045.0 ± 140.9
S97-V21C-RV-CX	884.73 ± 377.47	-	0.0043 ± 0.0219	653.9 ± 289.0
S97-V21C-RV-FX	318.15 ± 69.76	0.51264 ± 0.04610	-	290.3 ± 98.0
S97-V21D-RV-CX	524.41 ± 311.54	0.87727 ± 0.65278	0.0385 ± 0.0377	226.6 ± 136.4
S97-V21D-RV-FX	122.07 ± 55.22	0.58706 ± 0.04989	-	341.0 ± 74.3
S97-V21D-RV-MX5	-	-	-	5.5 ± 8.7
S97-V21D-RV-MX6	-	0.01059 ± 0.01105	-	-
S97-V21D-RV-MX7	-	-	-0.0007 ± 0.0093	-
S97-V21D-RV-MX8	316.59 ± 48.63	0.01144 ± 0.00842	-	92.5 ± 21.9
S97-V21D-RV-MX9	-	-	-	-
S97-V21D-RV-MX10	125.44 ± 31.62	-	-	-
S97-V21E-RV-CX	382.25 ± 180.73	1.35419 ± 0.37103	0.0126 ± 0.0139	886.7 ± 194.9

Table D.8: Trace Metals Aerosol Concentration Data (K, La, Lu, Mg) (continued)

Sample	Aerosol Concentration (ng m^{-3})			
	K	La	Lu	Mg
S97-V21E-RV-FX	39.70 ± 27.96	0.28090 ± 0.02225	-0.0020 ± 0.0022	90.0 ± 29.7
S97-V22A-RV-CX	308.22 ± 249.08	1.35508 ± 0.55054	-	50.7 ± 100.9
S97-V22A-RV-FX	-	0.14496 ± 0.03312	-	12.5 ± 13.0
S97-V22B-RV-CX	445.80 ± 265.39	1.16584 ± 0.65937	-	555.2 ± 175.7
S97-V22B-RV-FX	83.24 ± 61.52	0.23838 ± 0.03949	-	53.2 ± 43.4
S97-V22B-RV-MX5	-5.80 ± 17.89	0.07735 ± 0.03237	-	-
S97-V22B-RV-MX6	15.31 ± 19.96	0.03170 ± 0.02228	-0.0027 ± 0.0082	-
S97-V22B-RV-MX7	-	0.00402 ± 0.00887	-	1.7 ± 10.8
S97-V22B-RV-MX8	-	0.00802 ± 0.00914	-0.0052 ± 0.0080	-5.1 ± 7.6
S97-V22B-RV-MX9	-	-	-0.0055 ± 0.0080	-4.0 ± 7.7
S97-V22B-RV-MX10	-	0.00231 ± 0.00852	-	-
S97-V22C-RV-CX	544.02 ± 248.82	1.17663 ± 0.66227	0.0138 ± 0.0313	9.0 ± 120.6
S97-V22C-RV-FX	-	0.21076 ± 0.04048	0.0001 ± 0.0066	86.5 ± 28.5
S97-V22D-RV-CX	916.03 ± 366.35	0.80465 ± 0.66747	-0.0012 ± 0.0206	128.2 ± 125.5
S97-V22D-RV-FX	2.62 ± 27.76	0.13975 ± 0.03940	-	43.6 ± 21.9
S97-V22D-RV-MX5	44.06 ± 21.56	0.06515 ± 0.01822	-	7.9 ± 10.2
S97-V22D-RV-MX6	7.17 ± 20.18	-	-	-
S97-V22D-RV-MX7	-	0.00366 ± 0.00882	-	-
S97-V22D-RV-MX8	-6.80 ± 18.83	-	-	0.3 ± 9.7
S97-V22D-RV-MX9	0.46 ± 20.18	-0.00137 ± 0.00869	-	-
S97-V22D-RV-MX10	-	-	-0.0046 ± 0.0080	-
S97-V22E-RV-CX	237.88 ± 175.25	0.64926 ± 0.36721	-	75.6 ± 69.0
S97-V22E-RV-FX	95.87 ± 27.17	0.13158 ± 0.02180	-0.0027 ± 0.0020	90.7 ± 25.9
S97-N21D-ML-FX	-	0.19295 ± 0.03253	-0.0005 ± 0.0051	-8.6 ± 7.9
S97-N21E-ML-FX	-	0.77609 ± 0.05504	0.0086 ± 0.0082	19.5 ± 36.7
S97-N22A-ML-FX	-	0.42702 ± 0.04210	-	19.6 ± 17.9
S97-N22B-ML-FX	147.10 ± 86.33	-	-	-
S97-N22C-ML-FX	63.93 ± 27.86	0.10625 ± 0.03391	-0.0048 ± 0.0038	-7.0 ± 8.4
S97-N22C-ML-MX5	-	-	-0.0045 ± 0.0084	-
S97-N22C-ML-MX6	52.58 ± 47.15	-	-0.0036 ± 0.0083	-
S97-N22C-ML-MX7	-	-0.00114 ± 0.01019	0.0031 ± 0.0089	0.9 ± 8.3
S97-N22C-ML-MX8	-	-0.00641 ± 0.00854	-	-
S97-N22C-ML-MX9	-	0.00354 ± 0.00953	0.0368 ± 0.0131	-4.1 ± 10.3
S97-N22C-ML-MX10	-	-	-	-
S97-N22D-ML-FX	48.47 ± 25.23	0.20064 ± 0.02836	-0.0037 ± 0.0039	28.8 ± 18.8
S97-N22E-ML-FX	212.49 ± 50.90	0.43638 ± 0.03793	-	96.1 ± 31.1
S97-N23A-ML-FX	218.11 ± 76.25	0.38818 ± 0.03542	-	52.1 ± 24.3
S97-N23B-ML-FX	292.90 ± 81.49	0.43180 ± 0.04131	-	-
S97-N23C-ML-FX	176.50 ± 51.58	0.21060 ± 0.02886	-	36.0 ± 14.1
S97-N23C-ML-MX5	14.41 ± 22.39	0.13674 ± 0.01510	-	41.8 ± 14.0
S97-N23C-ML-MX6	-	0.00380 ± 0.00916	-	-
S97-N23C-ML-MX7	17.32 ± 30.95	-0.00229 ± 0.00856	-0.0027 ± 0.0088	-
S97-N23C-ML-MX8	-18.38 ± 17.67	-	-	-
S97-N23C-ML-MX9	-	-0.00810 ± 0.00814	-	-
S97-N23C-ML-MX10	-	-0.00200 ± 0.00839	-	-

Table D.8: Trace Metals Aerosol Concentration Data (K, La, Lu, Mg) (continued)

Sample	Aerosol Concentration (ng m^{-3})			
	K	La	Lu	Mg
S97-N23D-ML-FX	50.21 ± 63.43	0.07227 ± 0.02136	-	36.0 ± 20.4
S97-N23E-ML-FX	56.10 ± 42.05	0.08639 ± 0.02333	-	144.1 ± 31.1
S97-N23E-ML-MX5	-	0.04346 ± 0.01888	-	395.2 ± 81.7
S97-N23E-ML-MX6	-	0.01683 ± 0.00486	0.0054 ± 0.0071	35.6 ± 30.3
S97-N23E-ML-MX7	-	-	-	-
S97-N23E-ML-MX8	-	-	0.0099 ± 0.0072	-
S97-N23E-ML-MX9	-4.38 ± 9.80	-	-	-
S97-N23E-ML-MX10	-	0.03181 ± 0.01457	0.0068 ± 0.0068	19.0 ± 16.7
S97-N31A-DB-CX	678.25 ± 320.37	3.74831 ± 0.55169	-	242.1 ± 132.0
S97-N31A-DB-FX	-	1.01395 ± 0.07553	-	33.0 ± 23.2
S97-N31B-DB-CX	1037.77 ± 351.58	3.06533 ± 0.65630	0.0140 ± 0.0198	386.9 ± 174.1
S97-N31B-DB-FX	144.16 ± 55.65	0.67704 ± 0.06715	-	53.9 ± 20.1
S97-N31C-DB-CX	50.69 ± 225.03	1.70046 ± 0.62191	-	231.5 ± 137.6
S97-N31C-DB-FX	160.03 ± 64.27	0.58255 ± 0.19247	-	72.8 ± 49.4
S97-N31C-DB-MX5	-	0.46177 ± 0.03070	-0.0048 ± 0.0083	7.1 ± 9.7
S97-N31C-DB-MX6	-	0.12456 ± 0.01539	-	0.0 ± 8.9
S97-N31C-DB-MX7	-	0.46177 ± 0.03356	-	-
S97-N31C-DB-MX8	35.39 ± 24.01	-	-	-
S97-N31C-DB-MX9	-	-0.00677 ± 0.00863	-0.0051 ± 0.0083	-
S97-N31C-DB-MX10	-	-	-	-
S97-N31D-DB-CX	318.56 ± 277.65	2.56980 ± 0.61955	-	147.9 ± 135.6
S97-N31D-DB-FX	83.01 ± 56.18	1.15777 ± 0.08166	-	-
S97-N31D-DB-MX5	-	0.01399 ± 0.01236	-	-
S97-N31D-DB-MX6	41.75 ± 33.24	0.16436 ± 0.01995	-	9.8 ± 16.2
S97-N31D-DB-MX7	-5.70 ± 25.60	0.02132 ± 0.01055	-	-
S97-N31D-DB-MX8	-	-0.00031 ± 0.01118	-	-
S97-N31D-DB-MX9	-	-	-0.0046 ± 0.0099	-
S97-N31D-DB-MX10	-	-	-0.0057 ± 0.0098	-
S97-N31E-DB-CX	418.95 ± 166.77	2.53377 ± 0.38003	-	229.5 ± 84.0
S97-N31E-DB-FX	161.12 ± 40.35	0.88466 ± 0.05991	-	-
S97-N32A-DB-CX	755.16 ± 298.21	2.15660 ± 0.51767	-0.0023 ± 0.0148	166.5 ± 98.4
S97-N32A-DB-FX	-9.64 ± 11.81	-	-	-4.2 ± 7.5
S97-N32B-DB-CX	-154.55 ± 176.56	2.11739 ± 0.62505	0.0162 ± 0.0202	756.5 ± 182.9
S97-N32B-DB-FX	154.30 ± 80.67	0.11164 ± 0.03032	0.0041 ± 0.0078	-
S97-N32C-DB-CX	906.85 ± 286.55	0.97671 ± 0.93884	-	301.8 ± 133.5
S97-N32C-DB-FX	-	0.30304 ± 0.03207	-0.0051 ± 0.0033	6.9 ± 10.7
S97-N32C-DB-MX5	8.71 ± 27.74	0.18532 ± 0.01835	-0.0030 ± 0.0083	21.8 ± 17.4
S97-N32C-DB-MX6	-	0.00532 ± 0.01289	-0.0054 ± 0.0082	-
S97-N32C-DB-MX7	11.65 ± 34.06	0.00385 ± 0.00877	-	-
S97-N32C-DB-MX8	-	-0.00555 ± 0.00913	-0.0048 ± 0.0084	-
S97-N32C-DB-MX9	26.33 ± 23.04	-0.00731 ± 0.00857	-0.0045 ± 0.0083	-
S97-N32C-DB-MX10	-	-	-0.0033 ± 0.0087	6.2 ± 9.0
S97-N32D-DB-CX	547.53 ± 276.06	0.72967 ± 0.60259	-	124.9 ± 116.4
S97-N32D-DB-FX	35.33 ± 35.58	0.16674 ± 0.02745	-	1.0 ± 10.0
S97-N32E-DB-CX	358.97 ± 162.48	1.01084 ± 0.35167	0.0018 ± 0.0100	91.5 ± 66.9
S97-N32E-DB-FX	63.21 ± 20.79	0.22000 ± 0.02675	-0.0022 ± 0.0020	9.2 ± 7.2

Table D.8: Trace Metals Aerosol Concentration Data (K, La, Lu, Mg) (continued)

Sample	Aerosol Concentration (ng m^{-3})			
	K	La	Lu	Mg
S97-N31A-ML-CX	1043.48 ± 276.07	4.61464 ± 0.61554	-	1628.8 ± 341.8
S97-N31A-ML-FX	-	0.21971 ± 0.03200	-0.0028 ± 0.0036	75.8 ± 28.7
S97-N31B-ML-CX	2057.22 ± 408.57	4.31762 ± 0.72612	0.0026 ± 0.0207	2216.0 ± 461.7
S97-N31B-ML-FX	121.88 ± 103.12	0.73376 ± 0.10128	-0.0039 ± 0.0037	31.8 ± 19.6
S97-N31C-ML-CX	1372.52 ± 371.48	1.85635 ± 0.71343	0.0077 ± 0.0252	1339.8 ± 363.8
S97-N31C-ML-FX	-	0.39654 ± 0.04238	-	119.4 ± 43.5
S97-N31C-ML-MX5	64.98 ± 35.40	0.17855 ± 0.01960	-	-2.4 ± 10.0
S97-N31C-ML-MX6	-	0.04492 ± 0.01153	-	-
S97-N31C-ML-MX7	-	0.02779 ± 0.01585	-0.0039 ± 0.0099	0.4 ± 10.0
S97-N31C-ML-MX8	-	-	-	-0.6 ± 9.5
S97-N31C-ML-MX9	-	-	-	-6.7 ± 9.3
S97-N31C-ML-MX10	-	-0.00339 ± 0.01000	-	8.6 ± 10.5
S97-N31D-ML-CX	2436.75 ± 433.90	4.22273 ± 0.72221	0.0054 ± 0.0203	1362.1 ± 300.1
S97-N31D-ML-FX	225.66 ± 81.47	1.01360 ± 0.07064	-	53.4 ± 55.2
S97-N31D-ML-MX5	28.84 ± 37.71	0.56521 ± 0.04108	-	15.6 ± 24.4
S97-N31D-ML-MX6	148.32 ± 65.12	0.16333 ± 0.01976	-	7.6 ± 18.6
S97-N31D-ML-MX7	-	0.03299 ± 0.01142	-	6.6 ± 18.0
S97-N31D-ML-MX8	-	0.01307 ± 0.01126	-	-
S97-N31D-ML-MX9	-7.36 ± 23.72	0.00619 ± 0.01068	-	-
S97-N31D-ML-MX10	-16.42 ± 24.76	0.01235 ± 0.01110	-	-
S97-N31E-ML-CX	2559.70 ± 357.98	6.65167 ± 0.55727	0.0288 ± 0.0136	1806.4 ± 363.6
S97-N31E-ML-FX	378.59 ± 73.44	1.22036 ± 0.07469	-0.0014 ± 0.0029	197.8 ± 66.5
S97-N32A-ML-CX	920.97 ± 325.66	3.58758 ± 0.60335	0.0163 ± 0.0184	706.0 ± 206.8
S97-N32A-ML-FX	-24.18 ± 6.96	0.60069 ± 0.04744	-	-
S97-N32B-ML-CX	1644.83 ± 541.08	3.99383 ± 0.74655	0.0106 ± 0.0297	2007.1 ± 423.0
S97-N32B-ML-FX	54.31 ± 43.11	0.21012 ± 0.06972	-	47.5 ± 32.3
S97-N32C-ML-CX	1677.68 ± 459.59	2.13529 ± 0.67903	-	1172.3 ± 248.9
S97-N32C-ML-FX	68.69 ± 49.42	0.09251 ± 0.04018	-	-0.9 ± 9.0
S97-N32C-ML-MX5	-	0.00970 ± 0.01002	-0.0069 ± 0.0090	-2.9 ± 9.7
S97-N32C-ML-MX6	-	-0.00834 ± 0.00931	-	-5.9 ± 8.7
S97-N32C-ML-MX7	-8.49 ± 20.97	0.00261 ± 0.00962	-0.0046 ± 0.0092	-
S97-N32C-ML-MX8	-	0.00068 ± 0.00974	-0.0053 ± 0.0091	-
S97-N32C-ML-MX9	-3.65 ± 21.87	0.00358 ± 0.01017	-	-0.3 ± 10.7
S97-N32C-ML-MX10	-	-0.00641 ± 0.00922	-	-6.4 ± 8.7
S97-N32D-ML-CX	103.56 ± 300.73	0.38346 ± 0.66778	-0.0003 ± 0.0205	350.0 ± 151.8
S97-N32D-ML-FX	42.40 ± 35.05	0.09000 ± 0.04925	-	0.5 ± 11.5
S97-N32E-ML-CX	458.09 ± 169.78	0.44875 ± 0.37001	0.0062 ± 0.0143	546.4 ± 157.2
S97-N32E-ML-FX	-	0.06813 ± 0.01543	-	7.1 ± 13.8
S97-N31A-RV-CX	-	-0.25058 ± 0.51603	-	-
S97-N31A-RV-FX	141.24 ± 37.81	0.46673 ± 0.03758	-	-
S97-N31B-RV-CX	910.73 ± 310.03	1.45849 ± 0.66528	0.0044 ± 0.0194	259.2 ± 170.4
S97-N31B-RV-FX	130.37 ± 50.74	0.26911 ± 0.02966	-	14.6 ± 10.8
S97-N31C-RV-CX	1169.52 ± 333.82	1.15318 ± 0.64907	-	438.5 ± 160.5
S97-N31C-RV-FX	45.68 ± 37.84	0.21298 ± 0.03144	-	-
S97-N31C-RV-MX5	-	-	-0.0024 ± 0.0082	-
S97-N31C-RV-MX6	40.18 ± 19.67	0.01499 ± 0.00882	-	-2.6 ± 7.9

Table D.8: Trace Metals Aerosol Concentration Data (K, La, Lu, Mg) (continued)

Sample	Aerosol Concentration (ng m^{-3})			
	K	La	Lu	Mg
S97-N31C-RV-MX7	14.29 ± 22.57	0.00751 ± 0.00859	-0.0030 ± 0.0082	-
S97-N31C-RV-MX8	0.48 ± 20.45	-	-0.0061 ± 0.0080	-1.4 ± 9.1
S97-N31C-RV-MX9	-15.63 ± 19.53	-0.00544 ± 0.00812	-	-
S97-N31C-RV-MX10	-	-0.00544 ± 0.00799	-0.0061 ± 0.0080	-2.8 ± 8.0
S97-N31D-RV-CX	216.21 ± 248.01	1.52516 ± 0.61786	-0.0037 ± 0.0177	353.3 ± 140.2
S97-N31D-RV-FX	168.37 ± 33.31	0.09088 ± 0.02753	0.0004 ± 0.0043	67.7 ± 33.0
S97-N31D-RV-MX5	379.91 ± 105.67	0.00654 ± 0.01049	-0.0004 ± 0.0101	97.3 ± 32.1
S97-N31D-RV-MX6	266.93 ± 118.13	0.21949 ± 0.03553	-	111.0 ± 38.8
S97-N31D-RV-MX7	5.70 ± 28.26	0.00517 ± 0.01114	-	-
S97-N31D-RV-MX8	-2.17 ± 22.58	0.00312 ± 0.00999	-	-
S97-N31D-RV-MX9	-	-0.00168 ± 0.01064	-	-
S97-N31D-RV-MX10	-	-	-	-
S97-N31E-RV-CX	527.63 ± 220.38	2.04397 ± 0.40643	0.0031 ± 0.0119	242.8 ± 106.8
S97-N31E-RV-FX	185.89 ± 36.66	0.83141 ± 0.05693	0.0008 ± 0.0038	33.4 ± 19.2
S97-N32A-RV-CX	249.80 ± 244.93	0.87576 ± 0.53577	-	141.2 ± 105.3
S97-N32A-RV-FX	134.07 ± 47.40	0.20188 ± 0.02826	-	17.7 ± 18.6
S97-N32B-RV-CX	148.12 ± 273.27	0.70289 ± 0.65542	-	117.6 ± 124.2
S97-N32B-RV-FX	55.07 ± 22.85	0.18826 ± 0.06375	0.0071 ± 0.0045	-2.5 ± 11.1
S97-N32C-RV-CX	191.25 ± 231.58	0.96517 ± 0.64505	-0.0085 ± 0.0182	60.2 ± 121.8
S97-N32C-RV-FX	53.05 ± 36.52	0.05416 ± 0.02710	-0.0038 ± 0.0037	52.2 ± 46.7
S97-N32C-RV-MX5	-	-0.00152 ± 0.00891	-0.0048 ± 0.0088	-
S97-N32C-RV-MX6	-	0.00097 ± 0.00968	-0.0054 ± 0.0088	-
S97-N32C-RV-MX7	-	0.00159 ± 0.01102	-0.0032 ± 0.0087	-
S97-N32C-RV-MX9	-	-0.00619 ± 0.00918	-	-
S97-N32C-RV-MX10	-	-0.00246 ± 0.00954	-	-2.8 ± 8.9
S97-N32D-RV-CX	402.62 ± 249.49	1.21324 ± 0.63378	-0.0030 ± 0.0180	49.9 ± 115.5
S97-N32D-RV-FX	82.55 ± 20.25	0.16618 ± 0.02640	-	16.8 ± 23.5
S97-N32E-RV-CX	81.34 ± 129.64	0.33455 ± 0.36022	-	-1.8 ± 66.2
S97-N32E-RV-FX	16.30 ± 16.24	0.02144 ± 0.01381	-	2.3 ± 5.2
S97-T11B-TI-CX	-	0.69173 ± 0.75521	-	427.2 ± 264.6
S97-T11B-TI-FX	-	1.30252 ± 0.09611	-	492.7 ± 135.1
S97-T11B-TI-MX5	-	0.06699 ± 0.01659	-	1.6 ± 11.3
S97-T11B-TI-MX6	27.27 ± 26.57	0.01218 ± 0.01317	-	-
S97-T11B-TI-MX7	-	0.00004 ± 0.01131	-	-6.7 ± 11.0
S97-T11B-TI-MX8	-	-	-	-9.4 ± 10.5
S97-T11B-TI-MX9	-	-	-0.0076 ± 0.0109	-
S97-T11B-TI-MX10	-	-0.01092 ± 0.01121	-0.0068 ± 0.0111	-
S97-T11B-TO-CX	-	-0.37063 ± 0.81698	-	41.7 ± 158.9
S97-T11B-TO-FX	-	0.97629 ± 0.09758	-	119.5 ± 56.7
S97-T11B-TO-MX5	417.17 ± 203.91	0.02525 ± 0.01544	-	129.8 ± 79.3
S97-T11B-TO-MX6	-	-	-	-
S97-T11B-TO-MX7	-	-0.00822 ± 0.01345	-	-
S97-T11B-TO-MX8	-	0.00087 ± 0.01219	-	-4.9 ± 11.7
S97-T11B-TO-MX9	-	-0.00533 ± 0.01159	-	2.5 ± 12.1
S97-T11B-TO-MX10	-	-0.00987 ± 0.01206	-	-

Table D.8: Trace Metals Aerosol Concentration Data (K, La, Lu, Mg) (continued)

Sample	Aerosol Concentration (ng m^{-3})			
	K	La	Lu	Mg
S97-T21B-TI-CX	-	0.44565 ± 0.75842	-	386.0 ± 170.8
S97-T21B-TI-FX	-	0.21787 ± 0.03586	-	-
S97-T21B-TI-MX5	-	0.05506 ± 0.01313	-0.0064 ± 0.0111	16.4 ± 16.9
S97-T21B-TI-MX6	-	-	-0.0048 ± 0.0113	-
S97-T21B-TI-MX7	-	-	-0.0052 ± 0.0114	-
S97-T21B-TI-MX8	-7.55 ± 25.92	-	-0.0052 ± 0.0110	-
S97-T21B-TI-MX9	-	-	-	-
S97-T21B-TI-MX10	-	-0.00659 ± 0.01180	-	2.4 ± 11.6
S97-T21B-TO-FX	119.47 ± 129.62	0.01071 ± 0.04705	-	103.2 ± 38.0
S97-T31B-TI-CX	182.57 ± 375.23	0.23934 ± 0.75801	-	310.0 ± 174.1
S97-T31B-TI-FX	-	0.20840 ± 0.04292	-	88.9 ± 43.6
S97-T31B-TI-MX5	-4.82 ± 34.19	0.00511 ± 0.01291	-	2.4 ± 11.3
S97-T31B-TI-MX6	11.57 ± 31.94	0.01448 ± 0.01291	-	-
S97-T31B-TI-MX7	-11.06 ± 24.91	-	-0.0044 ± 0.0113	-0.3 ± 12.5
S97-T31B-TI-MX9	-	-	-	-
S97-T31B-TI-MX10	-	-	-	-
S97-T31B-TO-CX	-	-0.31186 ± 0.79305	-	74.7 ± 165.0
S97-T31B-TO-FX	-	-	-	24.3 ± 22.5
S97-T31B-TO-MX5	231.82 ± 88.03	-	-	55.7 ± 55.1
S97-T31B-TO-MX6	42.39 ± 55.15	0.00932 ± 0.01084	-	-
S97-T31B-TO-MX7	-	0.00236 ± 0.01185	-	-
S97-T31B-TO-MX8	-	-	-	-
S97-T31B-TO-MX9	77.18 ± 88.03	-	-	-
S97-T31B-TO-MX10	-	-	-	-
S97-T41B-TI-CX	332.50 ± 325.38	0.56925 ± 0.77865	-	262.7 ± 263.7
S97-T41B-TI-FX	16.36 ± 35.52	0.29348 ± 0.04275	-0.0068 ± 0.0043	39.0 ± 25.5
S97-T41B-TI-MX5	-	0.05506 ± 0.01165	-	56.2 ± 63.3
S97-T41B-TI-MX6	-	0.10969 ± 0.03975	-	-
S97-T41B-TI-MX7	-	0.00824 ± 0.01743	-	-
S97-T41B-TI-MX8	-	0.03945 ± 0.01139	-	-
S97-T41B-TI-MX9	-	-	-	-
S97-T41B-TI-MX10	-	-0.00698 ± 0.01127	-	-
S97-T41B-TO-CX	41.64 ± 256.97	-0.08686 ± 0.75931	-	-3.8 ± 139.7
S97-T41B-TO-FX	-	0.21703 ± 0.03572	-0.0046 ± 0.0054	91.4 ± 45.1
S97-B11A-AZ-MX5	-	-	-	28.0 ± 22.0
S97-B11A-AZ-MX6	-	0.03800 ± 0.02200	-	-
S97-B11A-AZ-MX7	-	-	0.0280 ± 0.0160	-
S97-B11A-AZ-MX8	-	-	-	-
S97-B11A-AZ-MX9	-	-	-	-
S97-B11A-AZ-MX10	-	-	-	-
S97-B11A-DB-CX	-	3.80000 ± 0.26000	-	-
S97-B11A-DB-FX	-	-	0.0180 ± 0.0100	-
S97-B11A-DB-MX5	-	-	-	14.8 ± 10.8
S97-B11A-DB-MX6	240.00 ± 0.06	-	-	-

Table D.8: Trace Metals Aerosol Concentration Data (K, La, Lu, Mg) (continued)

Sample	Aerosol Concentration (ng m^{-3})			
	K	La	Lu	Mg
S97-B11A-DB-MX7	240.00 ± 94.00	-	-	38.0 ± 24.0
S97-B11A-DB-MX8	-	0.03000 ± 0.01600	0.0160 ± 0.0140	-
S97-B11A-DB-MX9	-	-	-	11.2 ± 5.4
S97-B11A-DB-MX10	-	0.18200 ± 0.03200	-	-
S97-B11A-ML-CX	-	-	-	24.0 ± 18.6
S97-B11A-ML-FX	-	-	0.0060 ± 0.0030	-
S97-B11A-RV-CX	-	-	-	38.0 ± 30.0
S97-B11A-RV-FX	118.00 ± 51.00	-	-	-
S97-B11A-RV-MX5	-	0.05000 ± 0.02200	-	-
S97-B11A-RV-MX6	-	-	-	-
S97-B11A-RV-MX7	-	-	-	-
S97-B11A-RV-MX8	-	0.06800 ± 0.02400	0.0200 ± 0.0120	-
S97-B11A-RV-MX9	-	0.02400 ± 0.01000	-	-
S97-B11A-RV-MX10	-	0.11400 ± 0.02600	-	-
S97-B11A-TI-CX	-	-	-	-
S97-B11A-TI-FX	102.00 ± 51.00	0.00000 ± 0.00000	-	-
S97-B11A-TI-MX5	-	-	-	-
S97-B11A-TI-MX6	-	-	-	-
S97-B11A-TI-MX7	-	-	0.0260 ± 0.0120	-
S97-B11A-TI-MX8	-	0.03000 ± 0.01000	0.0160 ± 0.0100	-
S97-B11A-TI-MX9	-	-	0.0320 ± 0.0260	-
S97-B11A-TI-MX10	-	-	-	-
S97-B21A-DB-CX	-	0.74000 ± 0.06400	-	-
S97-B21A-DB-FX	113.00 ± 42.00	0.08400 ± 0.03900	-	-
S97-B21A-DB-MX5	-	-	-	-
S97-B21A-DB-MX6	78.00 ± 18.00	0.09600 ± 0.01800	-	-
S97-B21A-DB-MX7	-	-	0.0340 ± 0.0140	-
S97-B21A-DB-MX9	-	-	0.1020 ± 0.0420	-
S97-B21A-DB-MX10	220.00 ± 54.00	-	0.1160 ± 0.0300	200.0 ± 54.0
S97-B21A-ML-CX	-	-	0.0240 ± 0.0120	18.5 ± 15.8
S97-B21A-ML-FX	81.00 ± 30.00	-	-	-
S97-B21A-ML-MX5	-	0.02400 ± 0.01000	0.0220 ± 0.0100	-
S97-B21A-ML-MX6	-	-	-	-
S97-B21A-ML-MX7	-	0.06200 ± 0.00400	-	-
S97-B21A-ML-MX8	-	-	-	32.0 ± 30.0
S97-B21A-ML-MX9	-	-	-	-
S97-B21A-ML-MX10	-	-	-	6.6 ± 4.0
S97-B21A-RV-CX	-	0.06000 ± 0.01600	-	-
S97-B21A-RV-FX	-	0.20000 ± 0.10000	-	38.0 ± 23.0
S97-B21A-RV-MX5	-	-	0.0220 ± 0.0140	-
S97-B21A-RV-MX6	-	-	-	-
S97-B21A-RV-MX7	-	-	-	168.0 ± 70.0
S97-B21A-RV-MX8	-	-	0.0440 ± 0.0160	92.0 ± 15.0
S97-B21A-RV-MX9	-	-	-	-

Table D.8: Trace Metals Aerosol Concentration Data (K, La, Lu, Mg) (continued)

Sample	Aerosol Concentration (ng m^{-3})			
	K	La	Lu	Mg
S97-B21A-RV-MX10	-	0.00800 ± 0.00600	-	-

D.9 Trace Elements Aerosol Concentration Data (Mn, Mo, Na, Nd)

Table D.9: Trace Metals Aerosol Concentration Data (Mn, Mo, Na, Nd)

Sample	Aerosol Concentration (ng m^{-3})			
	Mn	Mo	Na	Nd
S97-V11A-LA-CX	11.846 ± 9.574	1.211 ± 1.020	1178.53 ± 84.28	-
S97-V11A-LA-FX	6.596 ± 0.176	3.187 ± 0.794	139.05 ± 11.64	0.930 ± 2.685
S97-V11B-LA-CX	9.537 ± 13.139	1.567 ± 1.118	1522.89 ± 96.60	-
S97-V11B-LA-FX	47.301 ± 0.736	27.237 ± 6.126	187.19 ± 15.65	-3.600 ± 3.575
S97-V11C-LA-CX	43.165 ± 12.070	2.761 ± 1.206	1572.97 ± 106.18	0.504 ± 3.873
S97-V11C-LA-FX	13.672 ± 0.277	0.467 ± 0.317	168.40 ± 19.78	-2.377 ± 3.350
S97-V11D-LA-CX	25.437 ± 12.450	2.578 ± 1.576	1259.88 ± 86.03	1.615 ± 4.624
S97-V11D-LA-FX	16.170 ± 0.314	4.638 ± 1.106	188.00 ± 15.16	-4.699 ± 3.411
S97-V11E-LA-CX	16.111 ± 6.690	0.063 ± 0.541	2439.16 ± 156.72	-0.601 ± 2.484
S97-V11E-LA-FX	9.986 ± 0.185	0.030 ± 0.168	331.41 ± 23.51	-1.707 ± 1.876
S97-V12A-LA-CX	13.800 ± 9.966	0.094 ± 0.597	2395.50 ± 160.68	-0.970 ± 2.868
S97-V12A-LA-FX	3.410 ± 0.152	0.306 ± 0.300	303.11 ± 21.72	-
S97-V12B-LA-CX	27.209 ± 11.650	-	1946.13 ± 128.11	1.340 ± 3.591
S97-V12B-LA-FX	20.208 ± 0.340	6.953 ± 1.577	259.27 ± 19.05	-1.984 ± 3.191
S97-V12B-LA-MX5	-2.280 ± 15.037	-	-0.76 ± 5.90	-0.636 ± 1.050
S97-V12B-LA-MX6	-1.352 ± 15.037	-	14.40 ± 6.07	-0.695 ± 1.059
S97-V12B-LA-MX7	-0.471 ± 15.037	-	8.23 ± 5.98	2.124 ± 1.122
S97-V12B-LA-MX8	-1.352 ± 15.037	-	4.41 ± 5.94	0.656 ± 1.110
S97-V12B-LA-MX9	-2.225 ± 15.037	-	1.48 ± 5.91	-0.255 ± 1.054
S97-V12B-LA-MX10	-2.380 ± 15.037	-	0.30 ± 5.90	-1.036 ± 1.040
S97-V12C-LA-CX	32.157 ± 11.592	0.873 ± 1.311	1681.49 ± 110.51	3.708 ± 5.490
S97-V12C-LA-FX	19.073 ± 0.330	4.559 ± 1.074	263.26 ± 19.41	-0.056 ± 3.342
S97-V12D-LA-CX	14.244 ± 12.225	-0.162 ± 0.814	1506.29 ± 98.79	1.318 ± 3.808
S97-V12D-LA-FX	11.920 ± 0.255	2.660 ± 0.733	222.07 ± 17.08	2.514 ± 3.602
S97-V12E-LA-CX	18.813 ± 6.609	0.207 ± 0.747	2602.39 ± 169.28	-
S97-V12E-LA-FX	4.385 ± 0.115	0.415 ± 0.198	273.10 ± 19.66	-1.205 ± 1.861
S97-V11A-AZ-CX	26.324 ± 10.606	1.730 ± 1.200	1383.59 ± 93.39	2.617 ± 4.094
S97-V11A-AZ-FX	5.508 ± 0.172	0.044 ± 0.199	125.67 ± 10.92	-3.659 ± 2.716
S97-V11B-AZ-CX	102.737 ± 13.598	22.571 ± 5.771	2849.78 ± 188.05	1.257 ± 5.563
S97-V11B-AZ-FX	10.551 ± 8.157	5.800 ± 1.408	190.38 ± 15.63	-2.849 ± 3.606
S97-V11C-AZ-CX	55.332 ± 13.082	2.321 ± 1.223	1320.76 ± 89.24	1.502 ± 4.338
S97-V11C-AZ-FX	8.177 ± 0.216	1.100 ± 0.467	140.44 ± 12.54	-0.713 ± 3.479
S97-V11D-AZ-CX	39.272 ± 13.121	-0.472 ± 0.797	1230.96 ± 854.43	-
S97-V11D-AZ-FX	3.283 ± 0.183	-	114.42 ± 11.28	-4.111 ± 3.390
S97-V11D-AZ-MX5	-1.708 ± 17.128	-	60.88 ± 7.99	1.018 ± 1.275
S97-V11D-AZ-MX6	-1.507 ± 17.128	-0.210 ± 0.642	23.76 ± 7.01	7.456 ± 1.714
S97-V11D-AZ-MX7	-1.708 ± 17.128	-	13.05 ± 6.85	2.085 ± 1.307
S97-V11D-AZ-MX8	-1.841 ± 17.128	-	-	-0.892 ± 1.208
S97-V11D-AZ-MX9	-1.942 ± 17.128	-	6.70 ± 6.77	0.881 ± 1.307
S97-V11D-AZ-MX10	-2.547 ± 17.128	-	3.02 ± 6.74	1.750 ± 1.264
S97-V11E-AZ-CX	-	-	-	-
S97-V11E-AZ-FX	9.384 ± 0.176	4.325 ± 1.037	255.04 ± 17.77	-1.853 ± 2.023

Table D.9: Trace Metals Aerosol Concentration Data (Mn, Mo, Na, Nd) (continued)

Sample	Aerosol Concentration (ng m^{-3})			
	Mn	Mo	Na	Nd
S97-V12A-AZ-CX	28.113 ± 10.408	0.783 ± 0.753	2043.05 ± 129.65	2.035 ± 3.307
S97-V12A-AZ-FX	5.622 ± 0.139	-	358.99 ± 25.05	-1.117 ± 2.812
S97-V12B-AZ-CX	66.605 ± 13.242	3.314 ± 2.311	2689.26 ± 174.18	9.058 ± 10.178
S97-V12B-AZ-FX	24.277 ± 0.380	1.405 ± 0.513	491.34 ± 33.89	2.296 ± 3.734
S97-V12C-AZ-CX	48.247 ± 12.961	0.311 ± 0.855	1310.00 ± 87.56	9.829 ± 4.353
S97-V12C-AZ-FX	7.960 ± 0.172	0.189 ± 0.258	217.85 ± 16.98	2.587 ± 3.668
S97-V12D-AZ-CX	34.979 ± 12.950	-	1404.78 ± 91.34	6.986 ± 5.264
S97-V12D-AZ-FX	6.967 ± 0.172	-0.109 ± 0.221	292.97 ± 21.54	2.917 ± 3.668
S97-V12D-AZ-MX5	-1.772 ± 16.730	-	93.77 ± 9.25	-0.375 ± 1.227
S97-V12D-AZ-MX6	-1.439 ± 16.730	-	30.39 ± 7.01	1.007 ± 1.231
S97-V12D-AZ-MX7	-0.786 ± 16.730	-	21.57 ± 6.89	0.141 ± 1.235
S97-V12D-AZ-MX8	-1.897 ± 16.730	-	8.83 ± 6.64	2.036 ± 1.277
S97-V12D-AZ-MX9	-2.452 ± 16.730	-	1.97 ± 6.60	1.154 ± 1.292
S97-V12D-AZ-MX10	0.292 ± 16.730	-	4.58 ± 6.60	-
S97-V12E-AZ-CX	38.931 ± 7.120	1.418 ± 0.613	1549.93 ± 98.85	6.430 ± 2.705
S97-V12E-AZ-FX	8.559 ± 0.205	0.577 ± 0.260	334.56 ± 22.75	0.148 ± 2.016
S97-V11A-RV-CX	4.743 ± 10.957	-0.146 ± 0.666	435.31 ± 31.26	-2.672 ± 3.291
S97-V11A-RV-FX	1.398 ± 0.151	-0.059 ± 0.203	65.02 ± 8.18	-3.892 ± 2.923
S97-V11B-RV-CX	167.652 ± 13.393	-	754.13 ± 53.66	0.165 ± 4.481
S97-V11B-RV-FX	120.638 ± 1.741	0.000 ± 0.263	81.82 ± 10.11	-4.114 ± 3.394
S97-V11C-RV-CX	14.997 ± 12.870	-	275.52 ± 22.24	-0.781 ± 4.137
S97-V11C-RV-FX	4.361 ± 0.186	0.018 ± 0.255	59.43 ± 8.83	-
S97-V11D-RV-CX	19.675 ± 12.850	-	585.54 ± 41.25	-1.627 ± 3.891
S97-V11D-RV-FX	18.875 ± 0.332	0.214 ± 0.232	338.91 ± 23.52	-4.086 ± 3.308
S97-V11D-RV-MX5	-1.930 ± 14.610	-	27.68 ± 6.16	-0.884 ± 1.013
S97-V11D-RV-MX6	-1.828 ± 14.610	-	8.00 ± 5.80	0.874 ± 1.073
S97-V11D-RV-MX7	-1.742 ± 14.610	-0.142 ± 0.543	8.28 ± 5.81	-0.333 ± 1.030
S97-V11D-RV-MX8	-1.970 ± 14.610	-	5.71 ± 5.77	0.894 ± 1.188
S97-V11D-RV-MX9	-2.178 ± 14.610	-	3.15 ± 5.79	2.064 ± 1.102
S97-V11D-RV-MX10	-2.170 ± 14.610	-	1.43 ± 5.75	-1.046 ± 1.022
S97-V11E-RV-CX	18.439 ± 7.017	0.631 ± 0.485	607.10 ± 42.33	-1.093 ± 2.044
S97-V11E-RV-FX	3.505 ± 0.110	0.519 ± 0.204	85.69 ± 7.29	-2.516 ± 1.810
S97-V12A-RV-CX	9.183 ± 10.527	-	718.87 ± 49.02	4.142 ± 5.629
S97-V12A-RV-FX	2.056 ± 0.144	0.018 ± 0.189	121.61 ± 10.57	-2.194 ± 2.722
S97-V12B-RV-CX	159.775 ± 13.524	-	743.05 ± 52.33	3.579 ± 4.643
S97-V12B-RV-FX	91.906 ± 1.361	0.484 ± 0.358	112.07 ± 11.62	-1.378 ± 3.574
S97-V12C-RV-CX	46.491 ± 12.998	9.343 ± 2.641	534.48 ± 37.95	5.106 ± 4.366
S97-V12C-RV-FX	6.415 ± 0.199	-	105.67 ± 10.80	-2.394 ± 3.351
S97-V12D-RV-CX	30.711 ± 12.750	3.386 ± 2.412	804.68 ± 54.71	19.011 ± 8.455
S97-V12D-RV-FX	20.980 ± 0.358	-	559.11 ± 38.79	-2.885 ± 3.344
S97-V12D-RV-MX5	-0.002 ± 14.610	-	396.59 ± 26.86	4.061 ± 1.309
S97-V12D-RV-MX6	0.198 ± 14.610	-	65.63 ± 7.69	2.064 ± 1.142
S97-V12D-RV-MX7	-0.059 ± 14.610	-0.027 ± 0.551	28.54 ± 6.37	2.634 ± 1.272
S97-V12D-RV-MX8	-1.514 ± 14.610	-	13.42 ± 5.96	2.634 ± 1.468
S97-V12D-RV-MX9	-1.913 ± 14.610	0.115 ± 0.603	10.56 ± 5.91	3.205 ± 1.290
S97-V12D-RV-MX10	-1.913 ± 14.610	0.400 ± 0.617	5.43 ± 5.83	0.951 ± 1.204

Table D.9: Trace Metals Aerosol Concentration Data (Mn, Mo, Na, Nd) (continued)

Sample	Aerosol Concentration (ng m^{-3})			
	Mn	Mo	Na	Nd
S97-V12E-RV-CX	21.651 ± 7.062	2.185 ± 1.486	972.45 ± 62.15	10.008 ± 5.153
S97-V12E-RV-FX	12.926 ± 0.212	0.553 ± 0.250	324.73 ± 21.32	-1.219 ± 1.829
S97-V21A-LA-CX	21.087 ± 9.320	-	2580.39 ± 170.66	4.347 ± 3.692
S97-V21A-LA-FX	20.280 ± 0.338	13.528 ± 2.899	352.33 ± 24.04	-0.527 ± 2.641
S97-V21B-LA-CX	27.674 ± 11.849	1.326 ± 1.186	1979.38 ± 130.30	2.664 ± 4.183
S97-V21B-LA-FX	10.841 ± 0.245	4.970 ± 1.220	290.82 ± 21.00	-3.583 ± 3.230
S97-V21B-LA-MX5	0.762 ± 15.037	-	701.83 ± 47.35	-0.313 ± 1.078
S97-V21B-LA-MX6	-1.264 ± 15.037	-	29.37 ± 6.41	-0.666 ± 1.043
S97-V21B-LA-MX7	-1.323 ± 15.037	-	12.93 ± 6.06	-0.372 ± 1.044
S97-V21B-LA-MX8	-1.940 ± 15.037	-	11.17 ± 6.02	-0.401 ± 1.088
S97-V21B-LA-MX9	-2.377 ± 15.037	-	0.30 ± 5.91	-0.431 ± 1.039
S97-V21B-LA-MX10	-2.295 ± 15.037	0.676 ± 0.611	-	-
S97-V21C-LA-CX	30.278 ± 11.522	2.891 ± 2.016	2177.36 ± 143.52	7.059 ± 5.732
S97-V21C-LA-FX	12.984 ± 0.340	1.680 ± 0.515	319.77 ± 21.91	-3.162 ± 3.130
S97-V21D-LA-CX	20.588 ± 11.760	0.541 ± 1.001	1620.87 ± 112.19	4.625 ± 4.205
S97-V21D-LA-FX	7.457 ± 0.203	2.068 ± 0.647	226.42 ± 17.31	-3.499 ± 3.312
S97-V21E-LA-CX	9.072 ± 6.552	-	3302.12 ± 215.95	5.936 ± 3.626
S97-V21E-LA-FX	-	5.191 ± 1.247	-	-
S97-V22A-LA-CX	10.523 ± 9.637	-	3728.53 ± 247.12	2.592 ± 3.447
S97-V22A-LA-FX	7.935 ± 0.188	4.106 ± 0.983	705.32 ± 46.36	-3.369 ± 2.665
S97-V22B-LA-CX	21.428 ± 11.750	-	2565.54 ± 172.21	23.547 ± 13.323
S97-V22B-LA-FX	9.548 ± 0.222	3.096 ± 0.820	479.74 ± 34.53	-2.686 ± 3.231
S97-V22B-LA-MX5	0.057 ± 14.942	-	522.30 ± 35.50	1.235 ± 1.338
S97-V22B-LA-MX6	-1.636 ± 14.942	-	32.10 ± 6.46	-
S97-V22B-LA-MX7	-1.781 ± 14.942	-	12.26 ± 6.02	-
S97-V22B-LA-MX8	-2.175 ± 14.942	-	5.55 ± 5.93	0.768 ± 1.154
S97-V22B-LA-MX9	-2.102 ± 14.942	-	19.56 ± 6.29	-0.982 ± 1.092
S97-V22B-LA-MX10	-2.292 ± 14.942	-	5.55 ± 6.04	2.694 ± 1.356
S97-V22C-LA-CX	28.162 ± 11.692	0.795 ± 1.095	3322.34 ± 214.07	4.597 ± 4.232
S97-V22C-LA-FX	16.434 ± 0.300	7.622 ± 1.803	474.40 ± 34.15	-2.124 ± 3.281
S97-V22D-LA-CX	9.572 ± 11.979	-	2880.25 ± 184.43	-3.535 ± 3.383
S97-V22D-LA-FX	4.118 ± 0.185	1.600 ± 0.539	523.80 ± 35.44	-2.907 ± 3.316
S97-V22D-LA-MX5	-0.929 ± 14.847	0.059 ± 0.658	895.91 ± 61.16	1.807 ± 1.471
S97-V22D-LA-MX6	-0.813 ± 14.847	-	115.98 ± 10.22	1.807 ± 1.191
S97-V22D-LA-MX7	-1.915 ± 14.847	-	12.76 ± 6.01	-1.005 ± 1.036
S97-V22D-LA-MX8	-2.165 ± 14.847	-	4.36 ± 5.86	-0.744 ± 1.038
S97-V22D-LA-MX9	-2.275 ± 14.847	-0.248 ± 0.552	5.81 ± 5.89	1.111 ± 1.147
S97-V22D-LA-MX10	0.056 ± 14.847	0.291 ± 0.584	249.35 ± 17.79	-
S97-V22E-LA-CX	17.094 ± 6.505	1.823 ± 1.047	2657.46 ± 171.43	1.224 ± 3.197
S97-V22E-LA-FX	10.278 ± 0.181	4.120 ± 0.964	438.19 ± 29.35	-0.545 ± 1.820
S97-V21A-AZ-CX	48.230 ± 10.173	16.963 ± 4.042	1695.82 ± 111.64	0.053 ± 3.160
S97-V21A-AZ-FX	12.081 ± 0.238	2.783 ± 0.720	342.00 ± 23.58	-
S97-V21B-AZ-CX	108.334 ± 13.092	8.206 ± 2.366	2551.00 ± 171.38	-
S97-V21B-AZ-FX	15.406 ± 0.307	2.118 ± 0.652	347.17 ± 25.03	-2.974 ± 3.482
S97-V21C-AZ-CX	48.746 ± 12.843	-	2143.20 ± 141.09	-0.872 ± 5.492
S97-V21C-AZ-FX	6.767 ± 0.209	0.087 ± 0.252	340.83 ± 24.57	-2.727 ± 3.358

Table D.9: Trace Metals Aerosol Concentration Data (Mn, Mo, Na, Nd) (continued)

Sample	Aerosol Concentration (ng m^{-3})			
	Mn	Mo	Na	Nd
S97-V21D-AZ-CX	24.076 ± 13.214	0.511 ± 0.992	2109.32 ± 145.22	8.092 ± 4.904
S97-V21D-AZ-FX	16.596 ± 0.322	3.007 ± 0.852	384.72 ± 26.94	-3.178 ± 3.479
S97-V21D-AZ-MX5	-0.986 ± 16.808	-	456.24 ± 31.87	-
S97-V21D-AZ-MX6	-1.413 ± 16.808	-	42.68 ± 7.34	-0.646 ± 1.194
S97-V21D-AZ-MX7	-1.151 ± 16.808	-	15.76 ± 6.76	0.076 ± 1.283
S97-V21D-AZ-MX8	-2.070 ± 16.808	-	8.21 ± 6.66	-1.305 ± 1.141
S97-V21D-AZ-MX9	-2.365 ± 16.808	-	7.23 ± 6.69	-0.974 ± 1.166
S97-V21D-AZ-MX10	-2.578 ± 16.808	-0.307 ± 0.621	12.48 ± 6.69	-0.285 ± 1.205
S97-V21E-AZ-CX	34.803 ± 7.230	2.550 ± 1.011	1733.20 ± 110.98	0.091 ± 2.547
S97-V21E-AZ-FX	10.176 ± 0.187	0.176 ± 0.189	410.33 ± 27.54	-1.831 ± 1.891
S97-V22A-AZ-CX	17.690 ± 10.546	12.223 ± 3.054	1376.30 ± 92.90	-
S97-V22A-AZ-FX	3.694 ± 0.154	3.699 ± 0.907	234.04 ± 17.11	-2.493 ± 2.837
S97-V22B-AZ-CX	65.291 ± 13.360	5.688 ± 2.240	2812.56 ± 185.59	-
S97-V22B-AZ-FX	11.224 ± 0.252	1.177 ± 0.442	349.48 ± 24.26	-0.390 ± 3.597
S97-V22B-AZ-MX5	-0.423 ± 16.575	-0.264 ± 0.619	249.25 ± 17.74	-
S97-V22B-AZ-MX6	0.484 ± 16.575	-0.031 ± 0.630	32.38 ± 7.00	-
S97-V22B-AZ-MX7	0.225 ± 16.576	-0.109 ± 0.626	14.90 ± 6.67	-0.540 ± 1.178
S97-V22B-AZ-MX8	-1.038 ± 16.575	0.163 ± 0.635	6.16 ± 6.56	-0.960 ± 1.178
S97-V22B-AZ-MX9	-2.268 ± 16.575	-0.277 ± 0.606	1.30 ± 6.52	-0.540 ± 1.144
S97-V22B-AZ-MX10	-2.611 ± 16.576	-	-2.71 ± 6.50	0.205 ± 1.178
S97-V22C-AZ-CX	46.146 ± 13.170	-	1909.32 ± 125.49	-
S97-V22C-AZ-FX	3.991 ± 0.187	-0.136 ± 0.229	195.47 ± 15.81	-3.306 ± 3.446
S97-V22D-AZ-CX	46.261 ± 13.203	-	2590.04 ± 164.36	0.455 ± 4.489
S97-V22D-AZ-FX	2.621 ± 0.179	-	244.21 ± 18.47	-1.362 ± 3.462
S97-V22D-AZ-MX5	1.803 ± 16.500	-	866.73 ± 58.36	-0.730 ± 1.205
S97-V22D-AZ-MX6	5.347 ± 16.500	-	251.32 ± 18.26	-
S97-V22D-AZ-MX7	0.256 ± 16.499	-	67.67 ± 8.27	-0.215 ± 1.183
S97-V22D-AZ-MX8	-	-	2.91 ± 6.55	1.622 ± 1.274
S97-V22D-AZ-MX9	-2.537 ± 16.499	1.064 ± 0.750	1.62 ± 6.50	1.267 ± 1.259
S97-V22D-AZ-MX10	-2.595 ± 16.499	1.064 ± 0.750	8.39 ± 6.55	1.267 ± 1.259
S97-V22E-AZ-CX	25.489 ± 7.275	1.718 ± 1.582	2331.54 ± 154.36	4.454 ± 5.014
S97-V22E-AZ-FX	3.410 ± 0.112	0.460 ± 0.256	440.38 ± 28.93	1.220 ± 2.122
S97-V21A-RV-CX	13.014 ± 10.509	-	1063.90 ± 71.11	1.517 ± 4.798
S97-V21A-RV-FX	7.173 ± 0.177	-0.023 ± 0.188	296.70 ± 20.53	-3.141 ± 2.661
S97-V21B-RV-CX	65.804 ± 15.285	-	1432.36 ± 99.87	-
S97-V21C-RV-CX	38.298 ± 12.491	1.123 ± 1.249	1354.56 ± 91.72	-
S97-V21C-RV-FX	11.356 ± 0.245	-	459.99 ± 28.32	-4.027 ± 3.300
S97-V21D-RV-CX	29.452 ± 12.610	-	1275.87 ± 86.20	11.419 ± 9.892
S97-V21D-RV-FX	12.867 ± 0.267	-	565.49 ± 39.23	-4.525 ± 3.328
S97-V21D-RV-MX5	-1.913 ± 14.610	-	119.84 ± 10.06	-0.504 ± 1.038
S97-V21D-RV-MX6	-1.942 ± 14.610	-	28.54 ± 6.19	-0.333 ± 1.047
S97-V21D-RV-MX7	-1.970 ± 14.610	2.769 ± 2.399	3.43 ± 5.76	1.778 ± 1.090
S97-V21D-RV-MX8	0.341 ± 14.610	-	25.69 ± 6.23	-0.105 ± 1.030
S97-V21D-RV-MX9	-2.241 ± 14.610	-0.250 ± 0.539	0.86 ± 5.74	-0.476 ± 1.067
S97-V21D-RV-MX10	-1.942 ± 14.610	-	42.80 ± 6.67	6.914 ± 1.928
S97-V21E-RV-CX	22.434 ± 6.984	0.577 ± 0.836	1677.02 ± 112.49	0.139 ± 2.838

Table D.9: Trace Metals Aerosol Concentration Data (Mn, Mo, Na, Nd) (continued)

Sample	Aerosol Concentration (ng m^{-3})			
	Mn	Mo	Na	Nd
S97-V21E-RV-FX	3.634 ± 0.110	0.116 ± 0.140	269.31 ± 19.39	-1.827 ± 1.796
S97-V22A-RV-CX	13.090 ± 10.570	-	1070.07 ± 73.07	-2.577 ± 3.063
S97-V22A-RV-FX	2.488 ± 0.143	-	157.84 ± 12.88	3.247 ± 3.046
S97-V22B-RV-CX	49.329 ± 12.756	2.264 ± 1.357	1381.99 ± 93.57	1.558 ± 4.092
S97-V22B-RV-FX	7.554 ± 0.170	-	162.63 ± 13.95	4.200 ± 3.763
S97-V22B-RV-MX5	-0.943 ± 14.610	-	64.20 ± 7.32	-1.137 ± 1.022
S97-V22B-RV-MX6	-0.800 ± 14.610	0.258 ± 0.548	11.70 ± 5.84	-0.775 ± 1.019
S97-V22B-RV-MX7	-1.171 ± 14.610	-	23.12 ± 6.36	0.066 ± 1.038
S97-V22B-RV-MX8	-2.027 ± 14.610	-	0.58 ± 5.75	0.805 ± 1.053
S97-V22B-RV-MX9	-2.287 ± 14.610	-0.261 ± 0.535	-0.96 ± 5.73	-1.149 ± 1.003
S97-V22B-RV-MX10	-2.281 ± 14.610	-	4.29 ± 5.76	1.151 ± 1.067
S97-V22C-RV-CX	29.084 ± 12.855	-	1300.69 ± 87.88	3.549 ± 5.159
S97-V22C-RV-FX	4.384 ± 0.175	-	252.37 ± 19.06	-1.070 ± 3.616
S97-V22D-RV-CX	33.976 ± 12.929	-	1686.33 ± 113.83	-2.960 ± 3.985
S97-V22D-RV-FX	2.960 ± 0.170	-	358.11 ± 25.31	-2.022 ± 3.519
S97-V22D-RV-MX5	-1.790 ± 14.312	-	124.10 ± 10.09	0.694 ± 1.038
S97-V22D-RV-MX6	-1.874 ± 14.312	-	17.06 ± 5.82	5.781 ± 1.503
S97-V22D-RV-MX7	-1.818 ± 14.312	-0.267 ± 0.527	6.16 ± 5.68	0.658 ± 1.048
S97-V22D-RV-MX8	-2.126 ± 14.312	-	3.92 ± 5.64	-1.047 ± 0.985
S97-V22D-RV-MX9	-2.209 ± 14.312	-	22.65 ± 6.23	0.792 ± 1.119
S97-V22D-RV-MX10	-2.221 ± 14.312	-	-0.10 ± 5.62	-
S97-V22E-RV-CX	18.126 ± 7.095	-0.141 ± 0.498	1860.03 ± 119.51	-1.261 ± 2.147
S97-V22E-RV-FX	2.723 ± 0.094	-	427.86 ± 28.70	-
S97-N21D-ML-FX	3.532 ± 0.182	-	131.22 ± 12.18	-0.532 ± 3.225
S97-N21E-ML-FX	2.935 ± 0.112	0.104 ± 0.261	216.38 ± 15.55	3.035 ± 2.248
S97-N22A-ML-FX	2.574 ± 0.144	0.205 ± 0.258	92.01 ± 9.23	-1.891 ± 2.701
S97-N22B-ML-FX	5.721 ± 0.198	-	79.28 ± 9.96	4.318 ± 3.579
S97-N22C-ML-FX	2.227 ± 0.176	0.055 ± 0.299	39.03 ± 8.33	-3.857 ± 3.367
S97-N22C-ML-MX5	0.233 ± 14.987	-	87.81 ± 9.84	-0.107 ± 1.053
S97-N22C-ML-MX6	-0.119 ± 14.987	-0.218 ± 0.566	40.98 ± 7.16	-1.152 ± 1.034
S97-N22C-ML-MX7	-2.311 ± 14.987	0.294 ± 0.575	10.84 ± 5.99	0.185 ± 1.074
S97-N22C-ML-MX8	-2.355 ± 14.987	-0.057 ± 0.554	0.01 ± 5.88	-0.517 ± 1.042
S97-N22C-ML-MX9	-	2.430 ± 0.866	0.89 ± 5.89	0.156 ± 1.131
S97-N22C-ML-MX10	-2.340 ± 14.987	-	2.06 ± 5.90	-0.605 ± 1.045
S97-N22D-ML-FX	1.342 ± 0.168	-0.085 ± 0.213	207.20 ± 16.15	-3.394 ± 3.275
S97-N22E-ML-FX	5.762 ± 0.203	2.260 ± 0.568	442.83 ± 29.59	3.562 ± 2.064
S97-N23A-ML-FX	2.210 ± 0.144	-0.108 ± 0.191	340.76 ± 23.65	2.270 ± 2.794
S97-N23B-ML-FX	9.108 ± 0.227	-0.026 ± 0.274	249.41 ± 18.77	1.736 ± 3.497
S97-N23C-ML-FX	6.234 ± 0.197	0.096 ± 0.245	239.38 ± 18.18	-1.244 ± 3.373
S97-N23C-ML-MX5	-1.017 ± 14.863	-	121.91 ± 10.23	0.068 ± 1.033
S97-N23C-ML-MX6	-0.698 ± 14.863	-	34.84 ± 6.47	-
S97-N23C-ML-MX7	-0.872 ± 14.863	-	22.07 ± 6.21	1.054 ± 1.337
S97-N23C-ML-MX8	-1.743 ± 14.863	-	4.36 ± 5.86	1.083 ± 1.224
S97-N23C-ML-MX9	-2.190 ± 14.863	-	-1.73 ± 5.83	-1.035 ± 1.043
S97-N23C-ML-MX10	-2.367 ± 14.863	-0.246 ± 0.546	1.46 ± 5.84	-0.107 ± 1.075

Table D.9: Trace Metals Aerosol Concentration Data (Mn, Mo, Na, Nd) (continued)

Sample	Aerosol Concentration (ng m^{-3})			
	Mn	Mo	Na	Nd
S97-N23D-ML-FX	4.147 ± 0.165	0.912 ± 0.398	668.97 ± 45.07	-1.647 ± 3.345
S97-N23E-ML-FX	1.377 ± 0.101	-	1000.92 ± 65.45	-1.391 ± 1.876
S97-N23E-ML-MX5	0.049 ± 8.524	-	1995.68 ± 132.20	-
S97-N23E-ML-MX6	-0.384 ± 8.524	-	231.36 ± 16.65	0.621 ± 0.820
S97-N23E-ML-MX7	-1.133 ± 8.523	-	31.63 ± 4.17	0.405 ± 0.629
S97-N23E-ML-MX8	-0.950 ± 8.523	-	8.16 ± 3.73	1.870 ± 0.920
S97-N23E-ML-MX9	-1.362 ± 8.523	-	-0.21 ± 3.34	-0.344 ± 0.587
S97-N23E-ML-MX10	-1.271 ± 8.523	0.800 ± 0.387	4.17 ± 3.81	0.239 ± 0.797
S97-N31A-DB-CX	33.563 ± 9.580	1.982 ± 0.897	828.25 ± 54.97	-1.141 ± 2.784
S97-N31A-DB-FX	18.192 ± 0.277	6.036 ± 1.384	175.23 ± 13.71	-0.291 ± 2.723
S97-N31B-DB-CX	59.441 ± 12.163	0.558 ± 0.871	819.33 ± 55.60	-2.513 ± 3.537
S97-N31B-DB-FX	16.565 ± 0.359	3.205 ± 0.880	187.54 ± 15.19	-2.605 ± 3.351
S97-N31C-DB-CX	35.666 ± 11.916	0.897 ± 0.875	638.42 ± 45.08	-0.984 ± 3.519
S97-N31C-DB-FX	17.550 ± 0.359	2.573 ± 0.665	159.16 ± 13.57	3.767 ± 3.660
S97-N31C-DB-MX5	-2.356 ± 15.147	-	-0.61 ± 5.95	-0.345 ± 1.049
S97-N31C-DB-MX6	1.063 ± 15.147	-	56.21 ± 7.24	1.311 ± 1.062
S97-N31C-DB-MX7	-1.007 ± 15.147	-	47.34 ± 6.91	-0.523 ± 1.076
S97-N31C-DB-MX8	-1.747 ± 15.147	-	13.91 ± 6.07	0.217 ± 1.170
S97-N31C-DB-MX9	-2.264 ± 15.147	-	4.15 ± 5.99	-1.218 ± 1.042
S97-N31C-DB-MX10	-2.386 ± 15.147	-	-0.70 ± 5.95	-1.301 ± 1.031
S97-N31D-DB-CX	22.669 ± 11.506	0.445 ± 0.839	911.74 ± 59.41	-
S97-N31D-DB-FX	8.746 ± 0.213	2.205 ± 0.620	142.70 ± 12.43	0.947 ± 3.370
S97-N31D-DB-MX5	-0.735 ± 17.866	0.071 ± 0.682	19.20 ± 7.22	-
S97-N31D-DB-MX6	-0.560 ± 17.866	-	20.59 ± 7.14	-
S97-N31D-DB-MX7	-1.293 ± 17.866	-	20.59 ± 7.25	0.325 ± 1.270
S97-N31D-DB-MX8	-2.409 ± 17.866	-0.257 ± 0.667	9.08 ± 7.09	-0.861 ± 1.281
S97-N31D-DB-MX9	-2.800 ± 17.866	-0.351 ± 0.661	1.40 ± 7.02	-0.721 ± 1.239
S97-N31D-DB-MX10	-2.681 ± 17.866	-	3.50 ± 7.04	-1.245 ± 1.227
S97-N31E-DB-CX	27.463 ± 6.603	0.882 ± 0.618	1004.87 ± 67.69	-1.365 ± 1.979
S97-N31E-DB-FX	7.268 ± 0.147	0.800 ± 0.258	162.38 ± 11.90	-0.602 ± 1.814
S97-N32A-DB-CX	11.954 ± 9.652	0.656 ± 0.759	765.14 ± 50.56	0.687 ± 2.950
S97-N32A-DB-FX	0.039 ± 0.132	-	-2.46 ± 5.81	-3.603 ± 2.629
S97-N32B-DB-CX	-4.227 ± 11.792	2.012 ± 1.106	-4.95 ± 7.52	1.703 ± 3.792
S97-N32B-DB-FX	21.572 ± 0.366	2.661 ± 0.748	131.59 ± 12.26	-2.744 ± 3.353
S97-N32C-DB-CX	68.691 ± 11.639	-0.061 ± 0.731	664.14 ± 46.41	2.608 ± 3.947
S97-N32C-DB-FX	12.783 ± 0.258	1.627 ± 0.484	78.35 ± 9.29	-3.248 ± 3.187
S97-N32C-DB-MX5	1.643 ± 15.037	0.001 ± 0.572	41.12 ± 6.72	0.773 ± 1.069
S97-N32C-DB-MX6	0.762 ± 15.037	-	16.16 ± 6.11	-1.238 ± 1.024
S97-N32C-DB-MX7	0.468 ± 15.037	-	14.40 ± 6.10	-1.221 ± 1.028
S97-N32C-DB-MX8	-1.558 ± 15.037	-	12.93 ± 6.04	-
S97-N32C-DB-MX9	-2.178 ± 15.037	-	7.06 ± 5.97	0.803 ± 1.134
S97-N32C-DB-MX10	-2.407 ± 15.037	-	0.89 ± 5.91	-0.049 ± 1.110
S97-N32D-DB-CX	26.520 ± 13.840	-	405.21 ± 29.25	1.348 ± 4.087
S97-N32D-DB-FX	7.335 ± 0.202	1.401 ± 0.492	57.65 ± 8.46	-1.884 ± 3.278
S97-N32E-DB-CX	31.013 ± 6.763	-	296.91 ± 24.03	1.416 ± 2.057
S97-N32E-DB-FX	2.735 ± 0.102	0.162 ± 0.166	67.39 ± 6.34	-2.271 ± 1.790

Table D.9: Trace Metals Aerosol Concentration Data (Mn, Mo, Na, Nd) (continued)

Sample	Aerosol Concentration (ng m^{-3})			
	Mn	Mo	Na	Nd
S97-N31A-ML-CX	94.505 ± 10.509	0.251 ± 0.830	901.71 ± 62.88	10.198 ± 4.577
S97-N31A-ML-FX	31.878 ± 0.549	2.939 ± 0.734	190.73 ± 15.07	-2.704 ± 2.796
S97-N31B-ML-CX	117.569 ± 13.116	1.450 ± 0.952	1121.78 ± 76.34	0.352 ± 4.036
S97-N31B-ML-FX	29.994 ± 0.371	1.341 ± 0.563	149.65 ± 13.74	-3.025 ± 3.421
S97-N31C-ML-CX	72.139 ± 13.744	-	905.15 ± 62.78	0.573 ± 4.838
S97-N31C-ML-FX	12.680 ± 0.396	1.009 ± 0.471	132.00 ± 12.68	-2.175 ± 3.786
S97-N31C-ML-MX5	-1.338 ± 17.546	-0.269 ± 0.647	25.02 ± 7.22	-0.708 ± 1.225
S97-N31C-ML-MX6	-1.270 ± 17.546	-	13.71 ± 7.04	-1.435 ± 1.203
S97-N31C-ML-MX7	-1.441 ± 17.546	-	9.60 ± 6.99	-0.229 ± 1.282
S97-N31C-ML-MX8	-2.366 ± 17.546	-	1.04 ± 6.91	-
S97-N31C-ML-MX9	-2.620 ± 17.546	-	3.09 ± 6.91	-
S97-N31C-ML-MX10	-2.743 ± 17.546	-	-0.40 ± 6.89	-
S97-N31D-ML-CX	89.104 ± 13.027	0.122 ± 0.882	1501.31 ± 95.23	-0.027 ± 3.996
S97-N31D-ML-FX	11.736 ± 0.377	-0.110 ± 0.224	140.04 ± 12.87	5.965 ± 3.844
S97-N31D-ML-MX5	-0.038 ± 18.541	-0.227 ± 0.690	47.08 ± 8.11	-0.785 ± 1.318
S97-N31D-ML-MX6	0.324 ± 18.541	-	23.54 ± 7.58	0.012 ± 1.307
S97-N31D-ML-MX7	-0.436 ± 18.541	-	18.84 ± 7.52	-0.676 ± 1.270
S97-N31D-ML-MX8	-2.247 ± 18.540	-	7.25 ± 7.35	-0.097 ± 1.302
S97-N31D-ML-MX9	-2.645 ± 18.540	-	2.18 ± 7.30	-0.821 ± 1.270
S97-N31D-ML-MX10	-2.859 ± 18.540	-0.125 ± 0.686	0.37 ± 7.28	-0.604 ± 1.291
S97-N31E-ML-CX	144.023 ± 7.478	1.067 ± 0.568	1568.09 ± 105.26	8.608 ± 2.474
S97-N31E-ML-FX	25.237 ± 0.381	0.565 ± 0.230	189.16 ± 13.73	5.858 ± 2.201
S97-N32A-ML-CX	66.942 ± 10.816	-0.269 ± 0.750	853.26 ± 56.38	4.235 ± 3.710
S97-N32A-ML-FX	15.322 ± 0.277	0.834 ± 0.391	150.15 ± 12.81	6.866 ± 3.425
S97-N32B-ML-CX	171.478 ± 13.698	0.423 ± 1.262	1165.75 ± 80.31	-0.225 ± 5.268
S97-N32B-ML-FX	7.974 ± 0.223	-	40.57 ± 8.73	-2.295 ± 3.688
S97-N32C-ML-CX	117.569 ± 13.087	-	837.13 ± 58.44	1.396 ± 4.876
S97-N32C-ML-FX	8.020 ± 0.219	-	31.11 ± 8.27	-3.436 ± 3.517
S97-N32C-ML-MX5	-1.967 ± 16.499	-	2.91 ± 6.50	0.043 ± 1.142
S97-N32C-ML-MX6	-1.967 ± 16.499	-0.353 ± 0.601	1.30 ± 6.49	-0.376 ± 1.143
S97-N32C-ML-MX7	-1.903 ± 16.499	-0.266 ± 0.604	1.62 ± 6.50	-1.220 ± 1.136
S97-N32C-ML-MX8	-1.967 ± 16.499	-0.298 ± 0.605	0.65 ± 6.50	-1.414 ± 1.118
S97-N32C-ML-MX9	-1.709 ± 16.499	-0.240 ± 0.613	1.94 ± 6.50	-0.408 ± 1.136
S97-N32C-ML-MX10	-2.399 ± 16.499	-	5.16 ± 6.52	0.011 ± 1.173
S97-N32D-ML-CX	29.599 ± 13.082	-	299.03 ± 23.49	0.356 ± 4.203
S97-N32D-ML-FX	1.734 ± 0.179	0.330 ± 0.244	13.22 ± 7.92	-3.579 ± 3.528
S97-N32E-ML-CX	18.948 ± 7.210	-	212.26 ± 15.95	-0.437 ± 2.931
S97-N32E-ML-FX	1.234 ± 0.100	0.134 ± 0.224	11.74 ± 4.44	-
S97-N31A-RV-CX	-4.388 ± 10.130	-	-7.00 ± 6.46	-3.673 ± 2.868
S97-N31A-RV-FX	6.893 ± 0.177	0.411 ± 0.244	139.26 ± 11.59	-1.871 ± 2.686
S97-N31B-RV-CX	45.068 ± 12.863	-0.472 ± 0.694	651.22 ± 44.94	-3.602 ± 3.675
S97-N31B-RV-FX	9.818 ± 0.233	0.425 ± 0.286	103.80 ± 10.88	-3.056 ± 3.434
S97-N31C-RV-CX	52.483 ± 12.618	-	500.09 ± 35.92	-2.609 ± 3.884
S97-N31C-RV-FX	8.747 ± 0.223	0.117 ± 0.272	86.26 ± 10.02	-3.915 ± 3.379
S97-N31C-RV-MX5	-0.980 ± 14.733	-	19.86 ± 6.01	-0.595 ± 1.024
S97-N31C-RV-MX6	-0.174 ± 14.733	-0.212 ± 0.542	12.38 ± 5.91	-0.422 ± 1.014

Table D.9: Trace Metals Aerosol Concentration Data (Mn, Mo, Na, Nd) (continued)

Sample	Aerosol Concentration (ng m^{-3})			
	Mn	Mo	Na	Nd
S97-N31C-RV-MX7	-0.778 ± 14.733	-0.241 ± 0.541	10.08 ± 5.88	0.182 ± 1.030
S97-N31C-RV-MX8	-1.526 ± 14.733	-0.354 ± 0.535	8.06 ± 5.86	-
S97-N31C-RV-MX9	-2.191 ± 14.733	-	3.46 ± 5.81	-0.422 ± 1.011
S97-N31C-RV-MX10	-2.309 ± 14.733	-	-0.77 ± 5.78	-0.422 ± 1.014
S97-N31D-RV-CX	48.713 ± 11.920	0.635 ± 0.786	725.16 ± 49.36	-4.033 ± 3.371
S97-N31D-RV-FX	7.588 ± 0.202	-	103.67 ± 9.45	-2.684 ± 3.196
S97-N31D-RV-MX5	7.051 ± 17.534	-0.163 ± 0.654	184.89 ± 15.63	0.388 ± 1.281
S97-N31D-RV-MX6	9.448 ± 17.534	-	78.75 ± 10.19	10.008 ± 2.954
S97-N31D-RV-MX7	-1.337 ± 17.532	-	34.25 ± 7.47	0.114 ± 1.308
S97-N31D-RV-MX8	-2.398 ± 17.532	-	5.14 ± 6.92	-0.331 ± 1.213
S97-N31D-RV-MX9	-2.672 ± 17.532	-	-0.33 ± 6.88	-0.845 ± 1.281
S97-N31D-RV-MX10	-2.761 ± 17.532	-0.101 ± 0.670	-0.64 ± 6.88	0.593 ± 1.371
S97-N31E-RV-CX	41.915 ± 7.471	0.397 ± 0.507	698.83 ± 47.64	-2.305 ± 2.147
S97-N31E-RV-FX	9.163 ± 0.174	0.120 ± 0.155	130.48 ± 10.15	5.377 ± 2.267
S97-N32A-RV-CX	22.768 ± 10.399	0.326 ± 0.702	717.29 ± 48.40	4.089 ± 4.283
S97-N32A-RV-FX	5.078 ± 0.167	0.029 ± 0.211	145.07 ± 12.03	4.669 ± 3.269
S97-N32B-RV-CX	16.774 ± 12.788	-	442.35 ± 32.83	-
S97-N32B-RV-FX	1.500 ± 0.177	2.492 ± 0.795	96.64 ± 10.49	-4.407 ± 3.456
S97-N32C-RV-CX	14.617 ± 12.545	-	158.28 ± 15.07	1.628 ± 4.032
S97-N32C-RV-FX	6.748 ± 0.204	-0.204 ± 0.209	19.82 ± 7.90	-2.777 ± 3.366
S97-N32C-RV-MX5	-2.358 ± 15.938	-0.323 ± 0.584	-1.14 ± 6.26	-0.052 ± 1.142
S97-N32C-RV-MX6	-2.274 ± 15.938	-	7.17 ± 6.32	-0.581 ± 1.111
S97-N32C-RV-MX7	-2.212 ± 15.938	-0.251 ± 0.597	1.25 ± 6.28	0.975 ± 1.262
S97-N32C-RV-MX9	-2.473 ± 15.938	-	0.01 ± 6.26	-0.986 ± 1.100
S97-N32C-RV-MX10	-2.504 ± 15.938	-0.158 ± 0.605	-0.96 ± 6.25	-
S97-N32D-RV-CX	14.292 ± 12.266	-	163.75 ± 15.50	2.131 ± 3.986
S97-N32D-RV-FX	1.995 ± 0.170	-0.009 ± 0.225	15.84 ± 7.49	-3.965 ± 3.269
S97-N32E-RV-CX	5.611 ± 7.021	-0.088 ± 0.520	206.91 ± 15.55	-
S97-N32E-RV-FX	0.839 ± 0.097	-0.085 ± 0.127	90.23 ± 7.71	0.763 ± 1.988
S97-T11B-TI-CX	44.186 ± 14.763	3.811 ± 1.867	1493.00 ± 101.95	7.962 ± 7.521
S97-T11B-TI-FX	29.429 ± 0.495	6.237 ± 1.515	670.74 ± 46.23	-0.836 ± 4.571
S97-T11B-TI-MX5	0.115 ± 20.050	-	168.37 ± 14.13	-
S97-T11B-TI-MX6	-1.764 ± 20.050	-0.226 ± 0.747	25.46 ± 8.24	-
S97-T11B-TI-MX7	-2.430 ± 20.050	-	11.36 ± 8.05	-0.692 ± 1.404
S97-T11B-TI-MX8	-2.704 ± 20.050	-0.382 ± 0.731	8.23 ± 7.96	-1.510 ± 1.370
S97-T11B-TI-MX9	-2.939 ± 20.050	-	5.10 ± 7.96	0.013 ± 1.402
S97-T11B-TI-MX10	-3.076 ± 20.050	-	-1.91 ± 7.88	-0.574 ± 1.425
S97-T11B-TO-CX	1.654 ± 16.030	-	1388.54 ± 95.66	-
S97-T11B-TO-FX	10.458 ± 0.280	7.383 ± 1.836	450.91 ± 32.30	-5.084 ± 4.280
S97-T11B-TO-MX5	1.485 ± 21.159	-	946.18 ± 66.63	-1.627 ± 1.451
S97-T11B-TO-MX6	0.080 ± 21.158	-	157.02 ± 14.91	8.360 ± 3.081
S97-T11B-TO-MX7	-2.688 ± 21.158	-	13.65 ± 8.41	1.088 ± 1.743
S97-T11B-TO-MX8	-3.068 ± 21.158	-	5.80 ± 8.36	0.551 ± 1.634
S97-T11B-TO-MX9	-3.097 ± 21.158	-	1.66 ± 8.31	0.179 ± 1.546
S97-T11B-TO-MX10	-3.312 ± 21.158	-	0.42 ± 8.31	-0.689 ± 1.546

Table D.9: Trace Metals Aerosol Concentration Data (Mn, Mo, Na, Nd) (continued)

Sample	Aerosol Concentration (ng m^{-3})			
	Mn	Mo	Na	Nd
S97-T21B-TI-CX	22.703 ± 14.826	0.248 ± 1.065	415.07 ± 30.75	1.163 ± 4.818
S97-T21B-TI-FX	3.718 ± 0.222	0.880 ± 0.495	122.30 ± 13.15	-1.108 ± 4.641
S97-T21B-TI-MX5	-0.119 ± 19.983	0.158 ± 0.760	39.03 ± 8.41	-1.431 ± 1.384
S97-T21B-TI-MX6	-1.836 ± 19.983	-0.135 ± 0.764	7.81 ± 7.91	-0.846 ± 1.397
S97-T21B-TI-MX7	-2.734 ± 19.983	0.001 ± 0.787	3.13 ± 7.87	-
S97-T21B-TI-MX8	-3.050 ± 19.983	-0.194 ± 0.760	1.18 ± 7.86	-0.182 ± 1.392
S97-T21B-TI-MX9	-2.995 ± 19.983	-	0.40 ± 7.85	0.988 ± 1.432
S97-T21B-TI-MX10	-3.089 ± 19.983	1.406 ± 0.886	-2.33 ± 7.84	-0.846 ± 1.446
S97-T21B-TO-FX	8.220 ± 0.203	3.932 ± 1.080	161.75 ± 15.00	-
S97-T31B-TI-CX	16.188 ± 14.825	-	1718.04 ± 119.80	2.901 ± 4.818
S97-T31B-TI-FX	6.096 ± 0.244	-0.004 ± 0.312	466.67 ± 33.36	-4.265 ± 4.274
S97-T31B-TI-MX5	-1.680 ± 19.983	-	163.90 ± 13.76	-
S97-T31B-TI-MX6	-2.382 ± 19.983	-	33.18 ± 8.32	-
S97-T31B-TI-MX7	-2.890 ± 19.983	-	12.11 ± 7.94	-
S97-T31B-TI-MX9	-3.058 ± 19.983	-	2.35 ± 7.88	-0.416 ± 1.460
S97-T31B-TI-MX10	-3.186 ± 19.983	-0.432 ± 0.729	0.79 ± 7.85	-1.529 ± 1.367
S97-T31B-TO-CX	-0.332 ± 15.558	0.147 ± 0.975	1347.73 ± 87.18	1.677 ± 4.674
S97-T31B-TO-FX	-	0.086 ± 0.275	310.11 ± 22.79	1.329 ± 4.136
S97-T31B-TO-MX5	-1.626 ± 19.797	-	460.04 ± 33.01	0.167 ± 1.432
S97-T31B-TO-MX6	-0.775 ± 19.796	-	92.79 ± 11.23	-
S97-T31B-TO-MX7	0.462 ± 19.797	-	50.27 ± 9.46	-0.644 ± 1.367
S97-T31B-TO-MX8	-1.201 ± 19.796	-0.354 ± 0.725	46.40 ± 9.24	-0.644 ± 1.356
S97-T31B-TO-MX9	-2.399 ± 19.796	-	42.53 ± 8.84	-
S97-T31B-TO-MX10	-2.631 ± 19.796	-	26.30 ± 8.66	1.366 ± 2.047
S97-T41B-TI-CX	25.548 ± 15.230	1.593 ± 1.428	593.60 ± 42.35	1.753 ± 5.658
S97-T41B-TI-FX	7.262 ± 0.248	0.601 ± 0.389	149.43 ± 14.43	-3.471 ± 4.262
S97-T41B-TI-MX5	5.305 ± 19.983	-	253.65 ± 20.30	2.042 ± 2.066
S97-T41B-TI-MX6	1.403 ± 19.983	-	70.25 ± 10.01	9.066 ± 3.655
S97-T41B-TI-MX7	-1.563 ± 19.983	-	27.72 ± 8.50	9.456 ± 3.119
S97-T41B-TI-MX8	-2.422 ± 19.983	-	8.99 ± 8.08	6.334 ± 3.049
S97-T41B-TI-MX9	-	-	1.57 ± 7.85	0.871 ± 1.563
S97-T41B-TI-MX10	-3.136 ± 19.983	-0.350 ± 0.730	0.79 ± 7.85	-0.026 ± 1.409
S97-T41B-TO-CX	-3.702 ± 14.897	-	264.45 ± 21.74	3.134 ± 4.514
S97-T41B-TO-FX	10.677 ± 0.273	1.368 ± 0.524	125.39 ± 13.10	-
S97-B11A-AZ-MX5	0.280 ± 0.040	-	8.00 ± 0.20	17.800 ± 2.400
S97-B11A-AZ-MX6	0.280 ± 0.060	-	7.20 ± 1.60	5.600 ± 2.000
S97-B11A-AZ-MX7	1.000 ± 0.060	-	17.00 ± 2.80	3.200 ± 2.000
S97-B11A-AZ-MX8	0.400 ± 0.040	-	8.60 ± 2.20	30.000 ± 4.400
S97-B11A-AZ-MX9	0.260 ± 0.040	-	16.60 ± 2.60	6.600 ± 2.600
S97-B11A-AZ-MX10	0.100 ± 0.040	-	9.20 ± 1.80	18.800 ± 3.600
S97-B11A-DB-CX	74.000 ± 1.220	-	-	-
S97-B11A-DB-FX	0.627 ± 0.029	-	12.00 ± 1.80	5.200 ± 1.700
S97-B11A-DB-MX5	0.320 ± 0.048	0.780 ± 0.380	18.60 ± 2.80	5.800 ± 1.020
S97-B11A-DB-MX6	0.340 ± 0.060	-	15.40 ± 3.20	7.000 ± 1.220

Table D.9: Trace Metals Aerosol Concentration Data (Mn, Mo, Na, Nd) (continued)

Sample	Aerosol Concentration (ng m^{-3})			
	Mn	Mo	Na	Nd
S97-B11A-DB-MX7	0.980 ± 0.070	-	34.00 ± 4.40	6.200 ± 1.440
S97-B11A-DB-MX8	0.156 ± 0.048	-	7.80 ± 2.40	7.200 ± 2.000
S97-B11A-DB-MX9	0.240 ± 0.046	1.500 ± 0.880	8.00 ± 2.80	7.600 ± 1.480
S97-B11A-DB-MX10	0.340 ± 0.066	1.540 ± 1.000	11.60 ± 2.60	14.800 ± 5.200
S97-B11A-ML-CX	1.460 ± 0.112	-	28.00 ± 4.60	9.200 ± 2.200
S97-B11A-ML-FX	1.008 ± 0.041	-	18.00 ± 1.90	4.690 ± 0.840
S97-B11A-RV-CX	0.620 ± 0.080	-	22.00 ± 3.60	7.600 ± 3.600
S97-B11A-RV-FX	1.000 ± 0.000	-	64.00 ± 6.00	6.000 ± 3.000
S97-B11A-RV-MX5	0.260 ± 0.040	-	12.40 ± 2.40	5.400 ± 1.680
S97-B11A-RV-MX6	0.380 ± 0.044	1.220 ± 0.780	20.00 ± 3.40	8.800 ± 1.560
S97-B11A-RV-MX7	0.540 ± 0.048	0.680 ± 0.560	24.00 ± 3.40	3.600 ± 2.600
S97-B11A-RV-MX8	0.300 ± 0.040	-	7.00 ± 2.20	10.800 ± 3.000
S97-B11A-RV-MX9	0.190 ± 0.036	1.180 ± 0.280	3.40 ± 1.80	11.400 ± 3.200
S97-B11A-RV-MX10	0.600 ± 0.048	-	7.00 ± 2.00	-
S97-B11A-TI-CX	0.400 ± 0.056	-	12.80 ± 2.60	22.000 ± 3.400
S97-B11A-TI-FX	1.000 ± 0.000	-	57.00 ± 5.00	20.000 ± 3.000
S97-B11A-TI-MX5	0.360 ± 0.068	-	10.40 ± 3.80	14.600 ± 3.800
S97-B11A-TI-MX6	0.164 ± 0.054	1.140 ± 0.840	24.00 ± 3.60	9.000 ± 3.400
S97-B11A-TI-MX7	0.260 ± 0.054	-	15.00 ± 3.20	14.000 ± 2.800
S97-B11A-TI-MX8	0.500 ± 0.050	0.460 ± 0.400	12.00 ± 4.20	16.000 ± 2.800
S97-B11A-TI-MX9	0.700 ± 0.062	-	20.00 ± 3.40	18.200 ± 5.000
S97-B11A-TI-MX10	0.168 ± 0.030	-	4.80 ± 2.40	15.600 ± 3.000
S97-B21A-DB-CX	1.800 ± 0.078	-	44.00 ± 5.60	6.600 ± 2.400
S97-B21A-DB-FX	0.490 ± 0.037	0.920 ± 0.570	26.00 ± 2.90	26.700 ± 3.900
S97-B21A-DB-MX5	-	-	260.00 ± 24.00	8.200 ± 1.820
S97-B21A-DB-MX6	-	-	-	-
S97-B21A-DB-MX7	0.360 ± 0.040	-	10.00 ± 2.40	-
S97-B21A-DB-MX9	0.620 ± 0.060	22.000 ± 5.200	26.00 ± 3.20	-
S97-B21A-DB-MX10	0.460 ± 0.080	-	26.00 ± 4.60	-
S97-B21A-ML-CX	2.400 ± 0.126	-	50.00 ± 7.20	9.200 ± 2.800
S97-B21A-ML-FX	0.510 ± 0.050	-	34.00 ± 3.00	14.700 ± 2.500
S97-B21A-ML-MX5	0.200 ± 0.040	-	5.60 ± 1.84	9.800 ± 2.200
S97-B21A-ML-MX6	0.600 ± 0.052	1.020 ± 0.980	19.80 ± 3.80	2.600 ± 2.400
S97-B21A-ML-MX7	0.092 ± 0.030	-	8.40 ± 2.60	2.800 ± 1.160
S97-B21A-ML-MX8	-	0.500 ± 0.420	8.80 ± 2.00	-
S97-B21A-ML-MX9	0.360 ± 0.040	-	-	5.200 ± 2.000
S97-B21A-ML-MX10	0.220 ± 0.034	-	9.60 ± 2.20	10.600 ± 3.200
S97-B21A-RV-CX	4.600 ± 0.440	1.340 ± 0.720	56.00 ± 10.60	22.000 ± 4.200
S97-B21A-RV-FX	2.000 ± 0.000	0.400 ± 0.500	67.00 ± 6.00	29.000 ± 4.000
S97-B21A-RV-MX5	0.560 ± 0.060	-	12.40 ± 2.80	11.800 ± 2.400
S97-B21A-RV-MX6	0.160 ± 0.040	-	5.20 ± 1.40	12.600 ± 3.200
S97-B21A-RV-MX7	0.780 ± 0.176	-	-	30.000 ± 12.200
S97-B21A-RV-MX8	0.400 ± 0.040	-	20.00 ± 2.80	2.600 ± 1.600
S97-B21A-RV-MX9	0.900 ± 0.118	-	24.00 ± 12.40	1.400 ± 0.740

Table D.9: Trace Metals Aerosol Concentration Data (Mn, Mo, Na, Nd) (continued)

Sample	Aerosol Concentration (ng m^{-3})			
	Mn	Mo	Na	Nd
S97-B21A-RV-MX10	0.800 ± 0.060	-	14.40 ± 2.00	-

D.10 Trace Elements Aerosol Concentration Data (Rb, Sb, Sc, Se)

Table D.10: Trace Metals Aerosol Concentration Data (Rb, Sb, Sc, Se)

Sample	Aerosol Concentration (ng m^{-3})			
	Rb	Sb	Sc	Se
S97-V11A-LA-CX	-	2.551 ± 1.474	-	2.922 ± 3.503
S97-V11A-LA-FX	6.79 ± 4.51	4.554 ± 0.368	-	2.417 ± 1.641
S97-V11B-LA-CX	21.01 ± 23.82	7.162 ± 2.091	0.1423 ± 0.1027	5.170 ± 4.537
S97-V11B-LA-FX	-	17.579 ± 1.294	0.0154 ± 0.0140	4.392 ± 1.480
S97-V11C-LA-CX	-	7.361 ± 1.940	0.1481 ± 0.0950	8.712 ± 3.824
S97-V11C-LA-FX	-1.00 ± 4.90	1.676 ± 0.148	0.0048 ± 0.0155	4.100 ± 1.131
S97-V11D-LA-CX	-	3.865 ± 1.925	0.1074 ± 0.0989	1.979 ± 2.773
S97-V11D-LA-FX	-3.97 ± 3.57	-	0.0017 ± 0.0099	2.938 ± 0.323
S97-V11E-LA-CX	-	3.594 ± 1.063	0.0332 ± 0.0565	-
S97-V11E-LA-FX	-	2.436 ± 0.181	-	0.519 ± 0.634
S97-V12A-LA-CX	-	3.898 ± 1.554	0.0860 ± 0.0766	2.753 ± 2.417
S97-V12A-LA-FX	-	3.834 ± 0.291	0.0152 ± 0.0207	1.858 ± 0.905
S97-V12B-LA-CX	-	4.640 ± 1.820	0.2454 ± 194.4202	1.852 ± 2.225
S97-V12B-LA-FX	-2.45 ± 4.34	7.136 ± 0.306	0.0196 ± 0.0147	9.015 ± 0.925
S97-V12B-LA-MX5	-	-0.086 ± 0.185	-0.0028 ± 0.0114	0.221 ± 0.454
S97-V12B-LA-MX6	-	0.158 ± 0.187	-0.0002 ± 0.0120	0.221 ± 0.479
S97-V12B-LA-MX7	-	0.202 ± 0.186	0.0013 ± 0.0116	-
S97-V12B-LA-MX8	-2.10 ± 2.57	0.196 ± 0.186	-0.0043 ± 0.0115	-
S97-V12B-LA-MX9	-	0.079 ± 0.185	-	0.691 ± 0.505
S97-V12B-LA-MX10	-	-0.042 ± 0.185	-0.0020 ± 0.0112	0.045 ± 0.395
S97-V12C-LA-CX	-	9.026 ± 1.918	0.1763 ± 0.0986	12.615 ± 7.308
S97-V12C-LA-FX	-	8.070 ± 0.607	-	11.771 ± 2.971
S97-V12D-LA-CX	-	3.081 ± 1.881	0.0339 ± 0.0948	1.228 ± 2.114
S97-V12D-LA-FX	-	3.113 ± 0.254	-	-
S97-V12E-LA-CX	57.46 ± 15.27	3.549 ± 1.053	0.1779 ± 0.0655	9.125 ± 6.803
S97-V12E-LA-FX	-	2.044 ± 0.161	0.0062 ± 0.0072	2.435 ± 0.935
S97-V11A-AZ-CX	-	1.429 ± 1.619	0.0992 ± 0.0895	2.462 ± 3.364
S97-V11A-AZ-FX	-	0.962 ± 0.091	0.0380 ± 0.0128	3.640 ± 0.526
S97-V11B-AZ-CX	-	12.498 ± 2.317	0.8976 ± 0.1346	-
S97-V11B-AZ-FX	-	2.167 ± 0.187	0.0561 ± 0.0195	4.727 ± 2.186
S97-V11C-AZ-CX	20.86 ± 26.44	4.434 ± 2.028	0.4852 ± 0.1082	-
S97-V11C-AZ-FX	-	3.811 ± 0.296	0.0213 ± 0.0125	4.867 ± 1.452
S97-V11D-AZ-CX	-	2.823 ± 2.007	0.3915 ± 0.1047	-
S97-V11D-AZ-FX	-	0.907 ± 0.098	0.0082 ± 0.0113	0.853 ± 0.565
S97-V11D-AZ-MX5	-	0.086 ± 0.211	-0.0076 ± 0.0126	-
S97-V11D-AZ-MX6	-2.42 ± 2.98	0.084 ± 0.211	0.0014 ± 0.0130	0.128 ± 0.466
S97-V11D-AZ-MX7	-	-0.021 ± 0.211	-0.0009 ± 0.0142	-
S97-V11D-AZ-MX8	-	0.036 ± 0.211	0.0051 ± 0.0165	-
S97-V11D-AZ-MX9	-	0.036 ± 0.211	0.0041 ± 0.0133	0.218 ± 0.463
S97-V11D-AZ-MX10	-	-0.021 ± 0.210	-0.0026 ± 0.0130	-0.076 ± 0.442
S97-V11E-AZ-CX	-	5.271 ± 1.227	0.2284 ± 0.0688	-
S97-V11E-AZ-FX	-	4.814 ± 0.358	0.0441 ± 0.0177	2.233 ± 1.076

Table D.10: Trace Metals Aerosol Concentration Data (Rb, Sb, Sc, Se) (continued)

Sample	Aerosol Concentration (ng m^{-3})			
	Rb	Sb	Sc	Se
S97-V12A-AZ-CX	-	1.326 ± 1.587	0.2345 ± 0.0826	2.644 ± 1.679
S97-V12A-AZ-FX	-	1.329 ± 0.117	0.1376 ± 0.0277	1.846 ± 0.820
S97-V12B-AZ-CX	-	7.675 ± 2.109	0.3555 ± 0.1211	12.441 ± 11.678
S97-V12B-AZ-FX	-	7.303 ± 0.542	0.0725 ± 0.0139	4.350 ± 3.040
S97-V12C-AZ-CX	-2.72 ± 6.52	3.166 ± 1.989	0.5192 ± 0.1059	1.774 ± 1.812
S97-V12C-AZ-FX	-	1.779 ± 0.145	0.0249 ± 0.0114	0.633 ± 0.696
S97-V12D-AZ-CX	14.05 ± 17.10	3.261 ± 1.992	0.3012 ± 0.1097	4.806 ± 4.467
S97-V12D-AZ-FX	-	1.812 ± 0.145	0.0149 ± 0.0114	2.287 ± 1.341
S97-V12D-AZ-MX5	-	0.349 ± 0.209	0.0053 ± 0.0136	0.478 ± 0.946
S97-V12D-AZ-MX6	-	0.316 ± 0.540	-0.0032 ± 0.0130	-
S97-V12D-AZ-MX7	-	0.336 ± 0.209	-0.0028 ± 0.0125	0.638 ± 0.590
S97-V12D-AZ-MX8	-	0.244 ± 0.208	-0.0041 ± 0.0130	1.161 ± 0.800
S97-V12D-AZ-MX9	-	0.124 ± 0.206	-0.0025 ± 0.0127	0.377 ± 0.478
S97-V12D-AZ-MX10	-2.56 ± 2.96	-0.059 ± 0.205	-0.0055 ± 0.0124	0.017 ± 0.379
S97-V12E-AZ-CX	1.99 ± 4.54	5.010 ± 1.151	0.4147 ± 0.0619	2.220 ± 1.227
S97-V12E-AZ-FX	-	2.888 ± 0.221	0.0118 ± 0.0075	2.349 ± 1.279
S97-V11A-RV-CX	-	0.836 ± 1.668	0.0866 ± 0.0853	-
S97-V11A-RV-FX	-	1.264 ± 0.113	0.0015 ± 0.0098	0.540 ± 0.436
S97-V11B-RV-CX	-	1.967 ± 2.012	0.3064 ± 0.1092	1.804 ± 2.763
S97-V11B-RV-FX	-	1.757 ± 0.152	0.0017 ± 0.0113	-
S97-V11C-RV-CX	-	0.604 ± 1.957	0.0734 ± 0.1001	-
S97-V11C-RV-FX	-	0.957 ± 0.098	0.0016 ± 0.0123	0.163 ± 0.423
S97-V11D-RV-CX	-	1.262 ± 1.959	0.1673 ± 0.1006	1.008 ± 1.932
S97-V11D-RV-FX	-4.17 ± 3.51	1.910 ± 0.161	0.1519 ± 0.0132	0.579 ± 0.223
S97-V11D-RV-MX5	-	-0.052 ± 0.179	-	-
S97-V11D-RV-MX6	-1.11 ± 2.73	0.062 ± 0.180	-	0.046 ± 0.420
S97-V11D-RV-MX7	-	0.248 ± 0.182	-0.0025 ± 0.0114	-
S97-V11D-RV-MX8	-	0.676 ± 0.189	-	0.671 ± 0.834
S97-V11D-RV-MX9	-	-0.015 ± 0.180	-0.0036 ± 0.0112	0.101 ± 0.516
S97-V11D-RV-MX10	-	-0.058 ± 0.179	0.0001 ± 0.0113	0.072 ± 0.466
S97-V11E-RV-CX	-	1.921 ± 1.081	0.1221 ± 0.0547	-
S97-V11E-RV-FX	-2.66 ± 2.00	1.324 ± 0.108	0.0096 ± 0.0052	0.317 ± 0.335
S97-V12A-RV-CX	-	3.656 ± 1.640	-	-
S97-V12A-RV-FX	-	3.278 ± 0.250	0.0194 ± 0.0106	-
S97-V12B-RV-CX	-	3.647 ± 2.055	0.4268 ± 0.1075	-
S97-V12B-RV-FX	11.15 ± 15.24	3.187 ± 0.263	0.0742 ± 0.0374	2.836 ± 2.709
S97-V12C-RV-CX	-	2.605 ± 1.991	0.2831 ± 0.1021	0.258 ± 1.694
S97-V12C-RV-FX	15.31 ± 11.41	2.264 ± 0.185	0.0624 ± 0.0157	-
S97-V12D-RV-CX	-	2.931 ± 1.959	0.3619 ± 0.1120	-
S97-V12D-RV-FX	-	3.073 ± 0.257	-	2.513 ± 1.413
S97-V12D-RV-MX5	-	0.162 ± 0.181	0.0409 ± 0.0119	3.895 ± 1.587
S97-V12D-RV-MX6	-	0.961 ± 0.199	0.0323 ± 0.0188	0.158 ± 0.516
S97-V12D-RV-MX7	-	1.817 ± 0.233	0.0049 ± 0.0129	0.129 ± 0.490
S97-V12D-RV-MX8	-	1.532 ± 0.224	0.0115 ± 0.0154	1.014 ± 0.972
S97-V12D-RV-MX9	-	0.505 ± 0.188	0.0089 ± 0.0143	-
S97-V12D-RV-MX10	-	0.305 ± 0.184	0.0238 ± 0.1459	-

Table D.10: Trace Metals Aerosol Concentration Data (Rb, Sb, Sc, Se) (continued)

Sample	Aerosol Concentration (ng m^{-3})			
	Rb	Sb	Sc	Se
S97-V12E-RV-CX	-	3.018 ± 1.109	0.2624 ± 0.0742	-
S97-V12E-RV-FX	-1.82 ± 2.00	2.736 ± 0.212	0.1440 ± 0.0116	1.364 ± 0.194
S97-V21A-LA-CX	-	5.690 ± 1.506	0.1418 ± 0.0742	0.322 ± 1.352
S97-V21A-LA-FX	-	8.608 ± 0.653	-	1.981 ± 1.456
S97-V21B-LA-CX	-	5.586 ± 1.866	0.1976 ± 0.0929	1.970 ± 2.119
S97-V21B-LA-FX	-	5.776 ± 0.436	0.0078 ± 0.0178	6.158 ± 0.592
S97-V21B-LA-MX5	-	0.813 ± 0.197	-	3.128 ± 1.634
S97-V21B-LA-MX6	-	0.431 ± 0.190	0.0001 ± 0.0124	0.309 ± 0.479
S97-V21B-LA-MX7	-	0.754 ± 0.196	-0.0037 ± 0.0113	0.074 ± 0.343
S97-V21B-LA-MX8	-1.86 ± 2.53	1.224 ± 0.211	-0.0037 ± 0.0113	-0.164 ± 0.277
S97-V21B-LA-MX9	-	0.519 ± 0.190	0.0004 ± 0.0115	-0.102 ± 0.349
S97-V21B-LA-MX10	0.90 ± 2.63	0.372 ± 0.190	0.0538 ± 0.0129	0.750 ± 0.479
S97-V21C-LA-CX	-	8.129 ± 1.880	0.3861 ± 0.1043	4.023 ± 3.258
S97-V21C-LA-FX	-	5.934 ± 0.456	0.0076 ± 0.0090	6.005 ± 0.750
S97-V21D-LA-CX	-9.25 ± 6.19	1.155 ± 1.791	0.1962 ± 0.0923	-
S97-V21D-LA-FX	-	1.605 ± 0.144	-	3.693 ± 2.303
S97-V21E-LA-CX	-	1.699 ± 1.011	0.1189 ± 0.0555	0.802 ± 1.133
S97-V21E-LA-FX	-	1.308 ± 0.116	-0.0020 ± 0.0060	0.813 ± 0.751
S97-V22A-LA-CX	-	0.594 ± 1.466	0.1326 ± 0.0779	2.027 ± 2.531
S97-V22A-LA-FX	-	1.706 ± 0.148	0.0192 ± 0.0167	3.810 ± 1.796
S97-V22B-LA-CX	-	3.820 ± 1.822	0.2476 ± 0.1177	4.879 ± 5.385
S97-V22B-LA-FX	-	3.283 ± 0.264	0.0262 ± 0.0150	-
S97-V22B-LA-MX5	-	0.574 ± 0.192	0.0138 ± 0.0185	-
S97-V22B-LA-MX6	2.65 ± 3.40	0.866 ± 0.201	0.0243 ± 0.0189	0.045 ± 0.298
S97-V22B-LA-MX7	-2.49 ± 2.47	0.399 ± 0.189	0.0007 ± 0.0123	-0.282 ± 0.253
S97-V22B-LA-MX8	-	0.428 ± 0.188	-	-
S97-V22B-LA-MX9	-1.44 ± 2.77	0.924 ± 0.202	0.0021 ± 0.0137	0.511 ± 0.633
S97-V22B-LA-MX10	-	0.253 ± 0.187	-	9.236 ± 3.219
S97-V22C-LA-CX	-	4.485 ± 1.826	0.1950 ± 0.0917	4.083 ± 3.871
S97-V22C-LA-FX	-	5.982 ± 0.459	0.0168 ± 0.0202	12.439 ± 4.869
S97-V22D-LA-CX	-	1.440 ± 1.829	0.1385 ± 0.1076	-
S97-V22D-LA-FX	-	1.128 ± 0.113	0.0095 ± 0.0144	-
S97-V22D-LA-MX5	-	0.513 ± 0.194	0.0271 ± 0.0159	-
S97-V22D-LA-MX6	-	4.224 ± 0.342	0.0041 ± 0.0128	0.392 ± 0.656
S97-V22D-LA-MX7	-	-0.003 ± 0.183	0.0015 ± 0.0131	-
S97-V22D-LA-MX8	-	-	-0.0034 ± 0.0113	-0.127 ± 0.319
S97-V22D-LA-MX9	-	-0.012 ± 0.183	-	0.334 ± 0.524
S97-V22D-LA-MX10	1.18 ± 2.67	2.194 ± 0.264	0.0329 ± 0.0186	-0.014 ± 0.304
S97-V22E-LA-CX	-	2.543 ± 1.015	0.1085 ± 0.0571	-
S97-V22E-LA-FX	-	2.512 ± 0.191	0.0004 ± 0.0078	1.696 ± 1.203
S97-V21A-AZ-CX	-	3.894 ± 1.582	0.3253 ± 0.0845	2.728 ± 2.802
S97-V21A-AZ-FX	-	3.941 ± 0.305	0.0119 ± 0.0082	0.531 ± 0.529
S97-V21B-AZ-CX	-	5.175 ± 2.029	0.7873 ± 0.1002	4.253 ± 5.030
S97-V21B-AZ-FX	-	3.823 ± 0.065	0.0475 ± 0.0202	2.721 ± 2.269
S97-V21C-AZ-CX	-	4.734 ± 2.001	0.5426 ± 0.1220	2.039 ± 1.796
S97-V21C-AZ-FX	-	3.110 ± 0.251	0.0274 ± 0.0091	1.643 ± 0.738

Table D.10: Trace Metals Aerosol Concentration Data (Rb, Sb, Sc, Se) (continued)

Sample	Aerosol Concentration (ng m^{-3})			
	Rb	Sb	Sc	Se
S97-V21D-AZ-CX	-3.26 ± 7.28	3.906 ± 2.039	0.4619 ± 0.1063	0.552 ± 1.627
S97-V21D-AZ-FX	-	4.866 ± 0.369	0.0315 ± 0.0152	4.281 ± 0.573
S97-V21D-AZ-MX5	-	0.127 ± 0.210	0.0799 ± 0.0636	3.825 ± 2.706
S97-V21D-AZ-MX6	-	0.285 ± 0.209	-	0.739 ± 0.536
S97-V21D-AZ-MX7	-	0.580 ± 0.213	0.0221 ± 0.0154	-
S97-V21D-AZ-MX8	-	0.009 ± 0.207	-0.0012 ± 0.0141	-
S97-V21D-AZ-MX9	-	0.311 ± 0.210	-0.0029 ± 0.0126	1.166 ± 0.991
S97-V21D-AZ-MX10	-	0.013 ± 0.207	-	-
S97-V21E-AZ-CX	5.72 ± 8.54	1.870 ± 1.110	0.2787 ± 0.0614	0.513 ± 1.164
S97-V21E-AZ-FX	-	1.412 ± 0.115	0.0136 ± 0.0070	1.055 ± 0.469
S97-V22A-AZ-CX	-	3.738 ± 1.639	0.0910 ± 0.0881	6.851 ± 6.958
S97-V22A-AZ-FX	-	2.202 ± 0.182	0.0198 ± 0.0273	2.606 ± 2.162
S97-V22B-AZ-CX	-	3.846 ± 2.059	0.5248 ± 0.1262	-
S97-V22B-AZ-FX	-	3.849 ± 0.296	0.0248 ± 0.0249	1.883 ± 1.336
S97-V22B-AZ-MX5	-	0.346 ± 0.208	0.0302 ± 0.0274	0.923 ± 1.008
S97-V22B-AZ-MX6	-	0.126 ± 0.205	0.0075 ± 0.0178	0.697 ± 1.102
S97-V22B-AZ-MX7	-2.50 ± 3.00	0.637 ± 0.211	-0.0028 ± 0.0131	1.085 ± 0.702
S97-V22B-AZ-MX8	-	1.090 ± 0.224	0.0140 ± 0.0178	1.021 ± 1.008
S97-V22B-AZ-MX9	-	0.378 ± 0.207	-0.0044 ± 0.0127	0.082 ± 0.448
S97-V22B-AZ-MX10	-3.28 ± 2.75	0.572 ± 0.211	-0.0044 ± 0.0126	0.244 ± 0.371
S97-V22C-AZ-CX	-	2.736 ± 2.017	0.3447 ± 0.1202	2.477 ± 3.103
S97-V22C-AZ-FX	-	3.535 ± 0.265	0.0216 ± 0.0118	1.063 ± 0.603
S97-V22D-AZ-CX	-	1.971 ± 2.015	0.3552 ± 0.1169	-
S97-V22D-AZ-FX	12.32 ± 11.61	1.294 ± 0.122	0.0928 ± 0.0370	3.226 ± 2.872
S97-V22D-AZ-MX5	-	0.376 ± 0.209	0.0088 ± 0.0149	-
S97-V22D-AZ-MX6	-	0.103 ± 0.204	-	-
S97-V22D-AZ-MX7	-	0.183 ± 0.204	-	0.371 ± 0.554
S97-V22D-AZ-MX8	-	5.338 ± 0.465	0.0220 ± 0.0140	8.910 ± 3.555
S97-V22D-AZ-MX9	-	0.570 ± 0.210	-	9.232 ± 3.555
S97-V22D-AZ-MX10	-	0.570 ± 0.210	0.0268 ± 0.0125	9.232 ± 3.555
S97-V22E-AZ-CX	-	2.363 ± 1.128	0.2436 ± 0.0735	1.953 ± 2.305
S97-V22E-AZ-FX	9.46 ± 10.74	1.911 ± 0.150	0.0260 ± 0.0238	6.249 ± 2.866
S97-V21A-RV-CX	-	1.263 ± 1.603	0.0984 ± 0.0860	-
S97-V21A-RV-FX	-	2.219 ± 0.180	0.0678 ± 0.0105	0.182 ± 0.306
S97-V21B-RV-CX	-	5.072 ± 2.373	0.5673 ± 0.1452	-
S97-V21C-RV-CX	-	2.870 ± 1.920	0.3636 ± 0.1039	-
S97-V21C-RV-FX	-	2.072 ± 0.176	0.1182 ± 0.0209	0.665 ± 0.967
S97-V21D-RV-CX	-	1.053 ± 1.922	0.4134 ± 0.1211	3.297 ± 4.263
S97-V21D-RV-FX	-	1.181 ± 0.112	0.1109 ± 0.0137	0.293 ± 0.646
S97-V21D-RV-MX5	-	0.017 ± 0.180	0.0095 ± 0.0185	-
S97-V21D-RV-MX6	-	0.191 ± 0.181	-	0.186 ± 0.442
S97-V21D-RV-MX7	-1.44 ± 2.55	0.191 ± 0.288	-0.0049 ± 0.0109	-0.099 ± 0.294
S97-V21D-RV-MX8	-1.52 ± 2.75	0.097 ± 0.180	0.0029 ± 0.0115	-
S97-V21D-RV-MX9	-	0.028 ± 0.180	0.0049 ± 0.0135	0.728 ± 0.699
S97-V21D-RV-MX10	-0.27 ± 2.39	-	-	-
S97-V21E-RV-CX	-	2.218 ± 1.082	0.2697 ± 0.0773	-

Table D.10: Trace Metals Aerosol Concentration Data (Rb, Sb, Sc, Se) (continued)

Sample	Aerosol Concentration (ng m^{-3})			
	Rb	Sb	Sc	Se
S97-V21E-RV-FX	-	1.032 ± 0.088	0.0527 ± 0.0078	0.641 ± 0.413
S97-V22A-RV-CX	-	2.199 ± 1.621	0.1222 ± 0.0826	1.604 ± 1.766
S97-V22A-RV-FX	-	0.928 ± 0.096	0.0014 ± 0.0082	0.525 ± 0.578
S97-V22B-RV-CX	-	4.234 ± 1.975	0.3243 ± 0.1052	4.355 ± 5.292
S97-V22B-RV-FX	-	1.696 ± 0.143	0.0181 ± 0.0113	0.626 ± 0.690
S97-V22B-RV-MX5	-	0.582 ± 0.189	-0.0002 ± 0.0359	-
S97-V22B-RV-MX6	-	0.142 ± 0.181	-0.0028 ± 0.0113	-0.110 ± 0.343
S97-V22B-RV-MX7	-	0.276 ± 0.182	-0.0036 ± 0.0109	-0.165 ± 0.314
S97-V22B-RV-MX8	-	1.651 ± 0.222	0.0029 ± 0.0212	-0.165 ± 0.282
S97-V22B-RV-MX9	-2.24 ± 2.54	0.091 ± 0.180	-0.0029 ± 0.0112	-
S97-V22B-RV-MX10	-	0.005 ± 0.179	-0.0005 ± 0.0112	-
S97-V22C-RV-CX	-	2.109 ± 1.965	0.2897 ± 0.1102	2.514 ± 2.780
S97-V22C-RV-FX	-	5.064 ± 0.407	0.0152 ± 0.0138	-
S97-V22D-RV-CX	-	1.174 ± 1.970	0.3670 ± 0.1079	6.218 ± 1.809
S97-V22D-RV-FX	-	3.818 ± 0.300	0.0246 ± 0.0135	-
S97-V22D-RV-MX5	-	0.048 ± 0.176	-0.0008 ± 0.0108	-
S97-V22D-RV-MX6	-1.59 ± 2.77	0.156 ± 0.178	-0.0038 ± 0.0109	0.087 ± 0.421
S97-V22D-RV-MX7	-	0.028 ± 0.176	-	0.238 ± 0.530
S97-V22D-RV-MX8	-	-0.014 ± 0.176	-0.0035 ± 0.0108	-0.097 ± 0.265
S97-V22D-RV-MX9	-	0.036 ± 0.176	-	-
S97-V22D-RV-MX10	-	-0.070 ± 0.176	-	-0.041 ± 0.361
S97-V22E-RV-CX	-	1.527 ± 1.088	0.1702 ± 0.0569	-
S97-V22E-RV-FX	-2.56 ± 2.03	0.719 ± 0.063	0.0027 ± 0.0054	0.165 ± 0.216
S97-N21D-ML-FX	-	1.751 ± 0.158	0.0075 ± 0.0123	2.060 ± 0.973
S97-N21E-ML-FX	34.18 ± 5.04	3.176 ± 0.243	-	4.421 ± 2.130
S97-N22A-ML-FX	-	2.811 ± 0.235	-	1.744 ± 0.836
S97-N22B-ML-FX	-2.30 ± 3.98	3.855 ± 0.295	0.0013 ± 0.0091	2.708 ± 0.863
S97-N22C-ML-FX	-	0.706 ± 0.087	0.0023 ± 0.0101	0.328 ± 0.472
S97-N22C-ML-MX5	-2.12 ± 2.57	-0.091 ± 0.184	0.0001 ± 0.0121	0.045 ± 0.429
S97-N22C-ML-MX6	-2.26 ± 2.62	-0.009 ± 0.184	-	0.425 ± 0.478
S97-N22C-ML-MX7	2.95 ± 2.77	0.073 ± 0.185	0.0106 ± 0.0117	2.035 ± 0.689
S97-N22C-ML-MX8	-1.53 ± 2.75	0.146 ± 0.185	-	-0.014 ± 0.369
S97-N22C-ML-MX9	6.46 ± 3.07	0.254 ± 0.187	0.0302 ± 0.0124	5.459 ± 1.225
S97-N22C-ML-MX10	-	-0.091 ± 0.184	-0.0023 ± 0.0119	-
S97-N22D-ML-FX	-	1.283 ± 0.110	0.0114 ± 0.0167	1.168 ± 0.936
S97-N22E-ML-FX	-	2.153 ± 0.165	0.0243 ± 0.0136	4.119 ± 3.058
S97-N23A-ML-FX	-	1.281 ± 0.113	0.0006 ± 0.0082	1.909 ± 0.591
S97-N23B-ML-FX	-	1.819 ± 0.170	0.0052 ± 0.0181	3.016 ± 1.426
S97-N23C-ML-FX	-	1.274 ± 0.112	0.0324 ± 0.0254	3.623 ± 2.348
S97-N23C-ML-MX5	-2.65 ± 2.47	0.223 ± 0.184	-0.0025 ± 0.0110	-
S97-N23C-ML-MX6	-	0.055 ± 0.183	-0.0048 ± 0.0111	0.393 ± 0.603
S97-N23C-ML-MX7	-	0.397 ± 0.187	0.0004 ± 0.0118	4.833 ± 0.285
S97-N23C-ML-MX8	-	0.223 ± 0.185	0.0030 ± 0.0138	1.380 ± 1.329
S97-N23C-ML-MX9	-	0.194 ± 0.184	-0.0043 ± 0.0111	-
S97-N23C-ML-MX10	-	-0.061 ± 0.182	-0.0025 ± 0.0120	-

Table D.10: Trace Metals Aerosol Concentration Data (Rb, Sb, Sc, Se) (continued)

Sample	Aerosol Concentration (ng m^{-3})			
	Rb	Sb	Sc	Se
S97-N23D-ML-FX	-	3.678 ± 0.292	-0.0015 ± 0.0095	0.290 ± 0.380
S97-N23E-ML-FX	-	0.520 ± 0.063	0.0185 ± 0.0155	2.590 ± 0.398
S97-N23E-ML-MX5	-	0.058 ± 0.111	-	-
S97-N23E-ML-MX6	2.84 ± 3.30	0.058 ± 0.107	0.0007 ± 0.0072	0.109 ± 0.286
S97-N23E-ML-MX7	-	0.727 ± 0.120	-	-0.008 ± 0.158
S97-N23E-ML-MX8	-	0.053 ± 0.110	-	0.392 ± 0.487
S97-N23E-ML-MX9	-	0.161 ± 0.106	-0.0023 ± 0.0065	-
S97-N23E-ML-MX10	-0.56 ± 1.87	-0.042 ± 0.106	0.0040 ± 0.0077	-
S97-N31A-DB-CX	-	6.754 ± 1.549	0.2017 ± 0.0749	0.751 ± 1.092
S97-N31A-DB-FX	-	5.006 ± 0.395	-0.0012 ± 0.0085	0.715 ± 0.754
S97-N31B-DB-CX	-	10.342 ± 2.023	0.4423 ± 0.0989	0.152 ± 1.359
S97-N31B-DB-FX	-	-	0.0112 ± 0.0095	2.200 ± 1.921
S97-N31C-DB-CX	-	5.179 ± 1.867	0.3033 ± 0.0959	1.457 ± 1.609
S97-N31C-DB-FX	-	4.360 ± 0.355	0.0176 ± 0.0110	1.247 ± 0.979
S97-N31C-DB-MX5	-	0.848 ± 0.200	0.0099 ± 0.0114	-0.112 ± 0.307
S97-N31C-DB-MX6	-	0.848 ± 0.202	-0.0032 ± 0.0117	-
S97-N31C-DB-MX7	-	0.405 ± 0.190	0.1785 ± 0.1100	0.548 ± 0.865
S97-N31C-DB-MX8	0.61 ± 3.03	0.819 ± 0.199	0.0007 ± 0.0117	0.282 ± 0.669
S97-N31C-DB-MX9	-2.64 ± 2.56	0.227 ± 0.188	-0.0043 ± 0.0115	0.075 ± 0.382
S97-N31C-DB-MX10	-	-0.045 ± 0.186	-0.0035 ± 0.0115	-0.159 ± 0.343
S97-N31D-DB-CX	-	6.774 ± 1.843	0.2678 ± 0.0968	-
S97-N31D-DB-FX	19.42 ± 4.48	5.557 ± 0.429	0.0162 ± 0.0213	2.588 ± 1.835
S97-N31D-DB-MX5	-1.09 ± 3.55	1.350 ± 0.247	0.0001 ± 0.0141	1.030 ± 0.757
S97-N31D-DB-MX6	-	0.757 ± 0.231	-	0.751 ± 1.222
S97-N31D-DB-MX7	1.42 ± 3.85	1.105 ± 0.238	-	0.681 ± 0.570
S97-N31D-DB-MX8	-	1.175 ± 0.241	-	1.274 ± 0.854
S97-N31D-DB-MX9	-0.67 ± 3.15	0.024 ± 0.220	-0.0030 ± 0.0136	-0.051 ± 0.364
S97-N31D-DB-MX10	-	0.146 ± 0.220	-	0.332 ± 0.345
S97-N31E-DB-CX	-	6.100 ± 1.109	0.2451 ± 0.0605	3.606 ± 2.460
S97-N31E-DB-FX	-	4.888 ± 0.364	0.0049 ± 0.0053	2.180 ± 0.667
S97-N32A-DB-CX	0.59 ± 6.59	5.331 ± 1.538	0.1964 ± 0.0756	1.182 ± 1.452
S97-N32A-DB-FX	-3.46 ± 2.83	0.024 ± 0.047	-0.0045 ± 0.0076	0.155 ± 0.325
S97-N32B-DB-CX	2.44 ± 7.12	2.887 ± 1.814	0.6203 ± 0.1012	-
S97-N32B-DB-FX	-	1.835 ± 0.166	0.0091 ± 0.0140	-
S97-N32C-DB-CX	-	6.402 ± 1.847	0.2359 ± 0.0962	4.985 ± 3.519
S97-N32C-DB-FX	-	3.921 ± 0.312	0.0178 ± 0.0094	0.648 ± 0.502
S97-N32C-DB-MX5	-	1.048 ± 0.204	0.0110 ± 0.0112	-0.117 ± 0.277
S97-N32C-DB-MX6	-	0.519 ± 0.191	-0.0005 ± 0.0111	-0.128 ± 0.310
S97-N32C-DB-MX7	-	0.549 ± 0.191	-	-
S97-N32C-DB-MX8	-	0.284 ± 0.187	-	-
S97-N32C-DB-MX9	-	0.196 ± 0.186	-	-
S97-N32C-DB-MX10	-	-0.006 ± 0.185	0.0033 ± 0.0120	-
S97-N32D-DB-CX	-	3.467 ± 1.810	0.2384 ± 0.0959	-
S97-N32D-DB-FX	-	3.008 ± 0.250	0.0110 ± 0.0137	4.024 ± 2.232
S97-N32E-DB-CX	-1.56 ± 4.06	3.027 ± 1.057	0.3292 ± 0.0564	0.085 ± 0.784
S97-N32E-DB-FX	-2.26 ± 1.99	2.149 ± 0.175	0.0045 ± 0.0052	1.500 ± 0.478

Table D.10: Trace Metals Aerosol Concentration Data (Rb, Sb, Sc, Se) (continued)

Sample	Aerosol Concentration (ng m^{-3})			
	Rb	Sb	Sc	Se
S97-N31A-ML-CX	-	7.353 ± 1.703	0.5704 ± 0.1005	-
S97-N31A-ML-FX	4.48 ± 3.74	4.428 ± 0.348	0.0173 ± 0.0092	1.570 ± 1.339
S97-N31B-ML-CX	-1.40 ± 10.36	7.440 ± 2.067	0.8614 ± 0.1173	-0.473 ± 1.357
S97-N31B-ML-FX	-	8.294 ± 0.629	0.0412 ± 0.0099	1.618 ± 1.335
S97-N31C-ML-CX	8.86 ± 16.22	2.047 ± 2.092	0.6399 ± 0.1199	-
S97-N31C-ML-FX	-	5.162 ± 0.392	0.0757 ± 0.0172	1.024 ± 0.740
S97-N31C-ML-MX5	-	0.171 ± 0.217	0.0032 ± 0.0135	-0.085 ± 0.447
S97-N31C-ML-MX6	-	0.298 ± 0.218	-0.0037 ± 0.0133	-
S97-N31C-ML-MX7	-	0.914 ± 0.230	-	0.087 ± 0.502
S97-N31C-ML-MX8	-	0.366 ± 0.219	-	-
S97-N31C-ML-MX9	-2.07 ± 3.24	0.082 ± 0.217	-	0.121 ± 0.502
S97-N31C-ML-MX10	-	-	0.0227 ± 0.0167	0.532 ± 0.839
S97-N31D-ML-CX	-	4.498 ± 2.011	0.8140 ± 0.1143	1.017 ± 1.634
S97-N31D-ML-FX	-	2.470 ± 0.210	0.0252 ± 0.0100	0.640 ± 0.705
S97-N31D-ML-MX5	-	0.495 ± 0.234	-	3.495 ± 2.014
S97-N31D-ML-MX6	-	0.532 ± 0.234	0.0041 ± 0.0144	-
S97-N31D-ML-MX7	-	0.894 ± 0.241	-0.0010 ± 0.0140	0.381 ± 0.501
S97-N31D-ML-MX8	-	0.423 ± 0.231	0.0048 ± 0.0154	-
S97-N31D-ML-MX9	-	0.112 ± 0.228	-	-
S97-N31D-ML-MX10	-	-0.037 ± 0.228	0.0016 ± 0.0148	0.779 ± 1.163
S97-N31E-ML-CX	8.85 ± 4.37	9.276 ± 1.314	1.1188 ± 0.0917	1.089 ± 0.906
S97-N31E-ML-FX	-	5.649 ± 0.425	0.0599 ± 0.0090	2.562 ± 1.845
S97-N32A-ML-CX	-4.23 ± 6.28	4.605 ± 1.686	0.5108 ± 0.0909	-
S97-N32A-ML-FX	-	3.957 ± 0.305	0.0506 ± 0.0284	1.397 ± 0.759
S97-N32B-ML-CX	-	0.435 ± 2.046	1.5065 ± 0.1565	-
S97-N32B-ML-FX	-	1.413 ± 0.139	0.0212 ± 0.0124	-
S97-N32C-ML-CX	-	-0.711 ± 1.964	0.8804 ± 0.1227	-
S97-N32C-ML-FX	-	0.516 ± 0.080	0.0417 ± 0.0119	0.714 ± 0.589
S97-N32C-ML-MX5	-	0.148 ± 0.204	-	-
S97-N32C-ML-MX6	-2.17 ± 2.91	-0.071 ± 0.202	-0.0012 ± 0.0129	-
S97-N32C-ML-MX7	-	-0.039 ± 0.203	-0.0015 ± 0.0126	-
S97-N32C-ML-MX8	-	-0.042 ± 0.203	0.0017 ± 0.0124	-
S97-N32C-ML-MX9	-2.85 ± 2.79	-0.039 ± 0.203	-0.0022 ± 0.0123	0.114 ± 0.526
S97-N32C-ML-MX10	-	-0.097 ± 0.202	-0.0051 ± 0.0123	-
S97-N32D-ML-CX	-	-0.660 ± 1.982	0.1990 ± 0.1021	-
S97-N32D-ML-FX	-0.11 ± 3.70	0.191 ± 0.069	0.0091 ± 0.0120	0.608 ± 0.736
S97-N32E-ML-CX	-2.99 ± 6.62	-0.321 ± 1.093	0.1994 ± 0.0598	0.935 ± 2.088
S97-N32E-ML-FX	-	0.229 ± 0.043	0.0041 ± 0.0059	0.225 ± 0.390
S97-N31A-RV-CX	-	-0.952 ± 1.536	-0.0487 ± 0.0772	-0.207 ± 1.141
S97-N31A-RV-FX	-	2.690 ± 0.161	0.0144 ± 0.0092	2.186 ± 0.940
S97-N31B-RV-CX	-1.57 ± 6.39	2.202 ± 1.964	0.3931 ± 0.1026	0.632 ± 1.487
S97-N31B-RV-FX	-	2.790 ± 0.238	0.0056 ± 0.0140	0.761 ± 0.662
S97-N31C-RV-CX	-	0.591 ± 1.914	0.2839 ± 0.1034	-
S97-N31C-RV-FX	-	1.288 ± 0.172	0.0094 ± 0.0118	1.235 ± 1.666
S97-N31C-RV-MX5	-	-0.107 ± 0.181	-0.0025 ± 0.0111	-0.014 ± 0.398
S97-N31C-RV-MX6	-	0.094 ± 0.182	-0.0051 ± 0.0109	-0.149 ± 0.280

Table D.10: Trace Metals Aerosol Concentration Data (Rb, Sb, Sc, Se) (continued)

Sample	Aerosol Concentration (ng m^{-3})			
	Rb	Sb	Sc	Se
S97-N31C-RV-MX7	-	0.509 ± 0.187	-0.0051 ± 0.0109	-0.137 ± 0.346
S97-N31C-RV-MX8	-	-0.118 ± 0.181	-0.0028 ± 0.0109	-
S97-N31C-RV-MX9	-	-0.012 ± 0.181	-	-0.111 ± 0.281
S97-N31C-RV-MX10	-	-0.081 ± 0.181	-0.0037 ± 0.0109	-
S97-N31D-RV-CX	-6.77 ± 5.88	3.085 ± 1.830	0.3728 ± 0.0956	12.958 ± 2.885
S97-N31D-RV-FX	-	2.621 ± 0.221	0.0196 ± 0.0096	2.754 ± 1.058
S97-N31D-RV-MX5	-	0.041 ± 0.216	-	-
S97-N31D-RV-MX6	-	0.366 ± 0.223	0.0032 ± 0.0140	-
S97-N31D-RV-MX7	-	0.571 ± 0.223	0.0015 ± 0.0140	2.141 ± 1.534
S97-N31D-RV-MX8	-2.00 ± 3.06	0.297 ± 0.218	-0.0057 ± 0.0132	0.189 ± 0.589
S97-N31D-RV-MX9	-	0.088 ± 0.216	0.0025 ± 0.0129	-0.300 ± 0.316
S97-N31D-RV-MX10	-	-0.021 ± 0.216	0.0018 ± 0.0142	-
S97-N31E-RV-CX	3.18 ± 5.73	9.614 ± 1.362	0.3531 ± 0.0631	0.965 ± 1.160
S97-N31E-RV-FX	-	3.973 ± 0.308	0.0297 ± 0.0082	0.213 ± 0.348
S97-N32A-RV-CX	-	3.076 ± 1.609	0.1887 ± 0.0848	1.120 ± 1.798
S97-N32A-RV-FX	-	2.235 ± 0.180	0.0115 ± 0.0130	1.698 ± 0.917
S97-N32B-RV-CX	-	0.132 ± 1.943	0.3258 ± 0.1110	2.221 ± 2.933
S97-N32B-RV-FX	-	4.836 ± 0.370	0.0163 ± 0.0108	-
S97-N32C-RV-CX	-	-0.505 ± 1.903	0.1726 ± 0.0972	-0.532 ± 1.330
S97-N32C-RV-FX	-	0.478 ± 0.066	0.0059 ± 0.0098	-
S97-N32C-RV-MX5	-	-0.097 ± 0.195	-	-
S97-N32C-RV-MX6	-	-0.075 ± 0.196	-0.0021 ± 0.0127	0.234 ± 0.562
S97-N32C-RV-MX7	0.95 ± 4.30	0.012 ± 0.196	0.0001 ± 0.0122	-
S97-N32C-RV-MX9	-	0.152 ± 0.197	0.0001 ± 0.0132	-
S97-N32C-RV-MX10	-	-0.010 ± 0.196	-	0.950 ± 1.090
S97-N32D-RV-CX	-	-0.655 ± 1.860	0.1508 ± 0.0946	-
S97-N32D-RV-FX	-	0.465 ± 0.064	0.0101 ± 0.0111	-
S97-N32E-RV-CX	-	-0.082 ± 1.066	0.0503 ± 0.0551	-
S97-N32E-RV-FX	5.19 ± 2.15	0.221 ± 0.039	0.0037 ± 0.0072	0.285 ± 0.445
S97-T11B-TI-CX	-	25.535 ± 3.034	0.1273 ± 0.1215	5.370 ± 4.988
S97-T11B-TI-FX	-	16.155 ± 1.205	0.1745 ± 0.0355	5.700 ± 4.860
S97-T11B-TI-MX5	10.21 ± 12.19	4.529 ± 0.436	0.0154 ± 0.0226	2.487 ± 1.946
S97-T11B-TI-MX6	-	1.084 ± 0.265	0.0044 ± 0.0188	0.725 ± 0.849
S97-T11B-TI-MX7	-	0.301 ± 0.248	-	0.295 ± 0.573
S97-T11B-TI-MX8	-	0.156 ± 0.247	-	1.117 ± 0.465
S97-T11B-TI-MX9	-3.58 ± 3.35	-0.036 ± 0.246	-0.0076 ± 0.0149	-
S97-T11B-TI-MX10	-	-0.095 ± 0.246	-	0.765 ± 1.182
S97-T11B-TO-CX	-	-0.187 ± 2.434	0.0444 ± 0.1330	-
S97-T11B-TO-FX	-	10.375 ± 0.777	0.0347 ± 0.0199	1.919 ± 0.421
S97-T11B-TO-MX5	-	0.008 ± 0.260	-0.0032 ± 0.0158	-
S97-T11B-TO-MX6	-	-0.046 ± 0.261	0.0014 ± 0.0169	-
S97-T11B-TO-MX7	-	0.041 ± 0.261	0.0005 ± 0.0182	-
S97-T11B-TO-MX8	-	-0.112 ± 0.260	-0.0069 ± 0.0157	-0.437 ± 0.360
S97-T11B-TO-MX9	-	-0.125 ± 0.259	0.0047 ± 0.0176	-
S97-T11B-TO-MX10	-	-0.151 ± 0.260	-0.0011 ± 0.0170	-

Table D.10: Trace Metals Aerosol Concentration Data (Rb, Sb, Sc, Se) (continued)

Sample	Aerosol Concentration (ng m^{-3})			
	Rb	Sb	Sc	Se
S97-T21B-TI-CX	-	13.726 ± 2.496	0.1388 ± 0.1149	-0.476 ± 1.555
S97-T21B-TI-FX	-	0.906 ± 0.106	0.0391 ± 0.0398	2.671 ± 3.036
S97-T21B-TI-MX5	-	3.500 ± 0.367	-0.0026 ± 0.0152	1.035 ± 1.519
S97-T21B-TI-MX6	-	9.197 ± 0.744	-0.0050 ± 0.0149	0.762 ± 0.992
S97-T21B-TI-MX7	-	0.109 ± 0.247	0.0025 ± 0.0192	0.801 ± 0.883
S97-T21B-TI-MX8	-	-0.051 ± 0.246	-0.0082 ± 0.0148	-
S97-T21B-TI-MX9	-	1.041 ± 0.261	-0.0050 ± 0.0148	-
S97-T21B-TI-MX10	-	4.904 ± 0.441	0.0068 ± 0.0195	-0.198 ± 0.368
S97-T21B-TO-FX	-	1.084 ± 0.136	0.0098 ± 0.0161	1.918 ± 1.199
S97-T31B-TI-CX	-	16.983 ± 2.654	0.0009 ± 0.1144	1.923 ± 2.742
S97-T31B-TI-FX	-	9.560 ± 0.743	-0.0069 ± 0.0128	-
S97-T31B-TI-MX5	-	2.914 ± 0.336	0.0212 ± 0.0283	-
S97-T31B-TI-MX6	-	0.885 ± 0.258	0.0099 ± 0.0220	3.767 ± 0.883
S97-T31B-TI-MX7	-	1.080 ± 0.262	-	-0.096 ± 0.405
S97-T31B-TI-MX9	-	0.729 ± 0.255	0.0224 ± 0.0190	0.879 ± 0.919
S97-T31B-TI-MX10	-	0.109 ± 0.246	-	-
S97-T31B-TO-CX	-2.36 ± 9.31	-0.580 ± 2.360	-0.0560 ± 0.1190	-
S97-T31B-TO-FX	-	0.302 ± 0.079	-0.0066 ± 0.0119	-
S97-T31B-TO-MX5	-	-0.117 ± 0.243	-	-
S97-T31B-TO-MX6	-	-0.024 ± 0.244	-	-
S97-T31B-TO-MX7	-	-0.124 ± 0.243	-0.0061 ± 0.0147	-
S97-T31B-TO-MX8	-2.53 ± 3.51	-0.142 ± 0.243	-0.0066 ± 0.0150	-
S97-T31B-TO-MX9	-	-0.032 ± 0.243	-0.0041 ± 0.0147	-
S97-T31B-TO-MX10	-	-	0.0268 ± 0.0198	-
S97-T41B-TI-CX	-	30.826 ± 3.288	0.0422 ± 0.1220	3.091 ± 3.896
S97-T41B-TI-FX	-	13.612 ± 1.025	-0.0057 ± 0.0118	0.332 ± 0.632
S97-T41B-TI-MX5	-	2.095 ± 0.316	-	-
S97-T41B-TI-MX6	-	-	-	-
S97-T41B-TI-MX7	-	0.042 ± 0.249	0.0017 ± 0.0170	-
S97-T41B-TI-MX8	-	-0.086 ± 0.247	-	-
S97-T41B-TI-MX9	-	0.378 ± 0.249	-0.0050 ± 0.0155	0.255 ± 0.540
S97-T41B-TI-MX10	-3.92 ± 3.33	-0.020 ± 0.245	-0.0050 ± 0.0153	-
S97-T41B-TO-CX	-	-1.145 ± 2.259	-0.0406 ± 0.1139	-
S97-T41B-TO-FX	-	9.030 ± 0.678	0.0096 ± 0.0175	11.105 ± 4.210
S97-B11A-AZ-MX5	-	0.600 ± 0.060	-	-
S97-B11A-AZ-MX6	6.80 ± 6.00	0.540 ± 0.076	0.0380 ± 0.0200	3.400 ± 2.800
S97-B11A-AZ-MX7	-	0.200 ± 0.100	0.0380 ± 0.0260	2.600 ± 2.100
S97-B11A-AZ-MX8	-	-	-	5.200 ± 3.200
S97-B11A-AZ-MX9	-	0.180 ± 0.040	0.0520 ± 0.0400	4.600 ± 3.600
S97-B11A-AZ-MX10	-	1.900 ± 0.166	0.0300 ± 0.0180	3.200 ± 2.400
S97-B11A-DB-CX	-	11.400 ± 0.860	0.6000 ± 0.0840	8.400 ± 7.000
S97-B11A-DB-FX	-	0.620 ± 0.060	0.0170 ± 0.0130	-
S97-B11A-DB-MX5	-	0.740 ± 0.064	0.0138 ± 0.0126	-
S97-B11A-DB-MX6	-	0.660 ± 0.070	-	-

Table D.10: Trace Metals Aerosol Concentration Data (Rb, Sb, Sc, Se) (continued)

Sample	Aerosol Concentration (ng m^{-3})			
	Rb	Sb	Sc	Se
S97-B11A-DB-MX7	-	0.540 ± 0.062	-	-
S97-B11A-DB-MX8	-	1.400 ± 0.124	0.0920 ± 0.0500	3.800 ± 2.800
S97-B11A-DB-MX9	7.80 ± 6.00	3.400 ± 0.260	0.0150 ± 0.0100	-
S97-B11A-DB-MX10	-	0.340 ± 0.068	0.0660 ± 0.0380	-
S97-B11A-ML-CX	-	0.400 ± 0.050	0.0380 ± 0.0122	-
S97-B11A-ML-FX	-	0.250 ± 0.300	0.0180 ± 0.0075	0.720 ± 0.470
S97-B11A-RV-CX	-	0.400 ± 0.120	0.1260 ± 0.0580	-
S97-B11A-RV-FX	-	0.300 ± 0.100	0.0300 ± 0.0200	-
S97-B11A-RV-MX5	-	0.320 ± 0.054	0.0560 ± 0.0300	4.600 ± 4.400
S97-B11A-RV-MX6	-	0.360 ± 0.062	0.0138 ± 0.0136	2.800 ± 1.780
S97-B11A-RV-MX7	-	0.300 ± 0.046	0.0400 ± 0.0120	1.020 ± 0.760
S97-B11A-RV-MX8	-	0.080 ± 0.040	-	0.500 ± 0.420
S97-B11A-RV-MX9	-	0.060 ± 0.016	0.0320 ± 0.0120	-
S97-B11A-RV-MX10	-	0.260 ± 0.060	0.0640 ± 0.0380	-
S97-B11A-TI-CX	-	4.400 ± 0.320	0.0260 ± 0.0150	-
S97-B11A-TI-FX	19.00 ± 5.00	0.200 ± 0.000	-	2.000 ± 1.000
S97-B11A-TI-MX5	12.60 ± 9.20	0.700 ± 0.106	0.0500 ± 0.0184	-
S97-B11A-TI-MX6	22.00 ± 13.20	0.240 ± 0.050	-	3.200 ± 3.000
S97-B11A-TI-MX7	-	0.380 ± 0.062	0.0260 ± 0.0106	1.520 ± 1.320
S97-B11A-TI-MX8	-	0.880 ± 0.070	0.0480 ± 0.0176	-
S97-B11A-TI-MX9	-	0.360 ± 0.088	0.0420 ± 0.0360	2.400 ± 2.200
S97-B11A-TI-MX10	-	5.800 ± 0.420	0.0340 ± 0.0200	-
S97-B21A-DB-CX	-	2.200 ± 0.178	-	-
S97-B21A-DB-FX	-	0.496 ± 0.077	-	-
S97-B21A-DB-MX5	-	1.800 ± 0.164	0.1080 ± 0.0280	-
S97-B21A-DB-MX6	-	0.200 ± 0.032	-	-
S97-B21A-DB-MX7	-	0.112 ± 0.038	0.0460 ± 0.0260	-
S97-B21A-DB-MX9	42.00 ± 9.20	-	0.3800 ± 0.0540	5.600 ± 1.940
S97-B21A-DB-MX10	40.00 ± 14.60	1.320 ± 0.136	0.3400 ± 0.1080	5.200 ± 1.800
S97-B21A-ML-CX	-	0.122 ± 0.046	0.0500 ± 0.0380	2.600 ± 1.660
S97-B21A-ML-FX	-	0.100 ± 0.000	-	-
S97-B21A-ML-MX5	-	0.280 ± 0.050	-	-
S97-B21A-ML-MX6	17.80 ± 14.40	1.020 ± 0.110	-	-
S97-B21A-ML-MX7	4.60 ± 2.80	1.400 ± 0.122	-	-
S97-B21A-ML-MX8	-	0.340 ± 0.054	0.0800 ± 0.0500	-
S97-B21A-ML-MX9	-	0.580 ± 0.120	-	-
S97-B21A-ML-MX10	-	-	-	-
S97-B21A-RV-CX	-	0.106 ± 0.020	-	-
S97-B21A-RV-FX	-	0.300 ± 0.000	0.0100 ± 0.0000	-
S97-B21A-RV-MX5	15.80 ± 6.00	0.300 ± 0.060	0.0220 ± 0.0120	-
S97-B21A-RV-MX6	-	5.200 ± 0.400	0.0380 ± 0.0280	2.680 ± 2.280
S97-B21A-RV-MX7	-	0.640 ± 0.164	0.0660 ± 0.0640	-
S97-B21A-RV-MX8	7.60 ± 5.00	0.160 ± 0.020	0.0240 ± 0.0140	-
S97-B21A-RV-MX9	-	0.122 ± 0.042	-	3.400 ± 2.600

Table D.10: Trace Metals Aerosol Concentration Data (Rb, Sb, Sc, Se) (continued)

Sample	Aerosol Concentration (ng m^{-3})			
	Rb	Sb	Sc	Se
S97-B21A-RV-MX10	-	0.440 ± 0.046	0.0260 ± 0.0240	3.380 ± 3.000

D.11 Trace Elements Aerosol Concentration Data (Sm, Sr, Th, Ti)

Table D.11: Trace Metals Aerosol Concentration Data (Sm, Sr, Th, Ti)

Sample	Aerosol Concentration (ng m^{-3})			
	Sm	Sr	Th	Ti
S97-V11A-LA-CX	0.02642 ± 0.03314	30.03 ± 10.04	-	218.65 ± 70.50
S97-V11A-LA-FX	0.00526 ± 0.00225	0.66 ± 1.95	0.024 ± 0.079	5.14 ± 8.27
S97-V11B-LA-CX	0.07480 ± 0.04589	-9.39 ± 7.56	-	194.52 ± 81.02
S97-V11B-LA-FX	0.00734 ± 0.00334	3.47 ± 3.93	-	16.70 ± 14.24
S97-V11C-LA-CX	0.05976 ± 0.04227	7.83 ± 10.54	-	460.79 ± 148.55
S97-V11C-LA-FX	0.00367 ± 0.00277	-	-	-
S97-V11D-LA-CX	0.04076 ± 0.04346	-	-	147.75 ± 102.84
S97-V11D-LA-FX	0.00052 ± 0.00274	-	-	12.56 ± 10.08
S97-V11E-LA-CX	0.01553 ± 0.02324	-	0.384 ± 0.305	2.50 ± 36.09
S97-V11E-LA-FX	0.00028 ± 0.00226	-	-	-
S97-V12A-LA-CX	0.03117 ± 0.03440	1.37 ± 7.87	-0.084 ± 0.055	11.75 ± 44.34
S97-V12A-LA-FX	0.00067 ± 0.00241	1.10 ± 2.18	-	5.25 ± 7.99
S97-V12B-LA-CX	0.09185 ± 0.04176	19.50 ± 15.97	0.038 ± 0.086	112.64 ± 68.49
S97-V12B-LA-FX	0.01253 ± 0.00382	-	0.177 ± 0.098	-
S97-V12B-LA-MX5	-	-	-	-4.12 ± 6.81
S97-V12B-LA-MX6	-	0.91 ± 3.63	-0.037 ± 0.095	-1.01 ± 7.19
S97-V12B-LA-MX7	-	-0.35 ± 3.29	-	-
S97-V12B-LA-MX8	-	-	-	-
S97-V12B-LA-MX9	-	-	-	-4.12 ± 7.13
S97-V12B-LA-MX10	-	-0.41 ± 3.32	-0.042 ± 0.092	-
S97-V12C-LA-CX	0.09985 ± 0.04181	-	0.920 ± 0.085	162.95 ± 70.08
S97-V12C-LA-FX	0.02770 ± 0.00383	6.11 ± 3.49	0.153 ± 0.127	39.96 ± 11.85
S97-V12D-LA-CX	0.04541 ± 0.04251	-	-	100.37 ± 76.08
S97-V12D-LA-FX	0.01981 ± 0.00407	-	-	-
S97-V12E-LA-CX	0.03758 ± 0.02340	-	0.205 ± 0.215	78.38 ± 39.95
S97-V12E-LA-FX	0.00553 ± 0.00222	0.91 ± 1.56	-0.052 ± 0.022	-
S97-V11A-AZ-CX	0.07586 ± 0.03757	-	0.228 ± 0.177	79.26 ± 46.77
S97-V11A-AZ-FX	0.00564 ± 0.00229	-	-	15.46 ± 5.88
S97-V11B-AZ-CX	0.28447 ± 0.05428	6.79 ± 14.17	0.291 ± 0.187	624.98 ± 90.38
S97-V11B-AZ-FX	0.01413 ± 0.00283	-	0.070 ± 0.126	184.20 ± 15.79
S97-V11C-AZ-CX	0.13159 ± 0.04679	-	-0.025 ± 0.094	193.11 ± 70.44
S97-V11C-AZ-FX	0.01259 ± 0.00341	0.69 ± 2.47	-	30.06 ± 8.69
S97-V11D-AZ-CX	0.11300 ± 0.04673	-0.41 ± 9.90	0.004 ± 0.075	222.81 ± 72.13
S97-V11D-AZ-FX	0.00378 ± 0.00272	-	0.002 ± 0.064	4.27 ± 8.70
S97-V11D-AZ-MX5	-0.00000 ± 0.00433	-	-	-
S97-V11D-AZ-MX6	0.00033 ± 0.00467	1.37 ± 3.66	-	0.82 ± 8.35
S97-V11D-AZ-MX7	-	-	-	-
S97-V11D-AZ-MX8	-0.00000 ± 0.00427	-	-	-
S97-V11D-AZ-MX9	0.00067 ± 0.00467	-	-	-4.50 ± 7.79
S97-V11D-AZ-MX10	-0.00167 ± 0.00423	-	-	-5.53 ± 7.85
S97-V11E-AZ-CX	0.06436 ± 0.02646	-1.55 ± 4.89	0.194 ± 0.038	-
S97-V11E-AZ-FX	0.00404 ± 0.00184	-	-	18.02 ± 7.68

Table D.11: Trace Metals Aerosol Concentration Data (Sm, Sr, Th, Ti) (continued)

Sample	Aerosol Concentration (ng m^{-3})			
	Sm	Sr	Th	Ti
S97-V12A-AZ-CX	0.07443 ± 0.03686	1.43 ± 10.29	-0.004 ± 0.089	54.92 ± 66.53
S97-V12A-AZ-FX	-	-	-0.049 ± 0.040	11.77 ± 4.96
S97-V12B-AZ-CX	0.20077 ± 0.05025	-	-	581.97 ± 144.44
S97-V12B-AZ-FX	0.05444 ± 0.00723	-	-0.031 ± 0.069	261.49 ± 28.26
S97-V12C-AZ-CX	0.23476 ± 0.05013	-	0.412 ± 0.093	456.90 ± 106.93
S97-V12C-AZ-FX	0.01045 ± 0.00419	-	-	174.10 ± 21.65
S97-V12D-AZ-CX	-	-	-	219.97 ± 115.41
S97-V12D-AZ-FX	0.03030 ± 0.00419	-	-0.054 ± 0.070	7.31 ± 10.39
S97-V12D-AZ-MX5	0.00882 ± 0.00443	-0.92 ± 3.75	-	3.45 ± 8.76
S97-V12D-AZ-MX6	-	-	-	-3.09 ± 7.91
S97-V12D-AZ-MX7	0.00196 ± 0.00432	-1.50 ± 3.61	-	-
S97-V12D-AZ-MX8	-	-	-	-
S97-V12D-AZ-MX9	-	-	-	-
S97-V12D-AZ-MX10	-0.00163 ± 0.00413	-	-	-
S97-V12E-AZ-CX	0.14433 ± 0.02826	10.33 ± 8.80	0.169 ± 0.065	546.79 ± 148.03
S97-V12E-AZ-FX	0.00756 ± 0.00230	-	-	21.66 ± 7.29
S97-V11A-RV-CX	0.01261 ± 0.03764	-	-	22.56 ± 50.04
S97-V11A-RV-FX	0.00327 ± 0.00235	1.75 ± 1.89	-	-
S97-V11B-RV-CX	0.12312 ± 0.04721	23.01 ± 16.32	0.178 ± 0.210	223.75 ± 89.71
S97-V11B-RV-FX	0.00378 ± 0.00286	-	-0.053 ± 0.057	-
S97-V11C-RV-CX	0.01670 ± 0.04431	-	-	27.43 ± 85.40
S97-V11C-RV-FX	0.00580 ± 0.00278	1.19 ± 2.81	-	2.57 ± 10.51
S97-V11D-RV-CX	0.07313 ± 0.14781	-	0.032 ± 0.097	105.48 ± 72.76
S97-V11D-RV-FX	0.07402 ± 0.00686	4.54 ± 4.30	0.063 ± 0.043	179.66 ± 19.07
S97-V11D-RV-MX5	-	-	-	-
S97-V11D-RV-MX6	-0.00114 ± 0.00361	-	-	-3.27 ± 6.62
S97-V11D-RV-MX7	0.00086 ± 0.00370	-	-	2.73 ± 7.37
S97-V11D-RV-MX8	-0.00086 ± 0.00364	-1.40 ± 3.12	-	-
S97-V11D-RV-MX9	-	-	-	-3.55 ± 7.12
S97-V11D-RV-MX10	-	-	-0.038 ± 0.089	-
S97-V11E-RV-CX	0.03991 ± 0.02460	-	0.002 ± 0.044	62.70 ± 46.10
S97-V11E-RV-FX	0.00901 ± 0.00221	-	-	12.60 ± 4.40
S97-V12A-RV-CX	0.01520 ± 0.03635	-	-	55.60 ± 50.28
S97-V12A-RV-FX	0.01075 ± 0.00327	-	0.100 ± 0.084	10.62 ± 8.33
S97-V12B-RV-CX	0.17323 ± 0.04907	-	0.111 ± 0.176	158.01 ± 74.66
S97-V12B-RV-FX	0.02028 ± 0.00417	-	-	-
S97-V12C-RV-CX	0.11190 ± 0.04655	0.83 ± 10.86	0.090 ± 0.076	78.04 ± 85.33
S97-V12C-RV-FX	0.02930 ± 0.00405	-	-	29.46 ± 9.52
S97-V12D-RV-CX	0.75377 ± 0.08162	2.68 ± 12.61	-	113.95 ± 65.58
S97-V12D-RV-FX	0.03544 ± 0.00481	42.31 ± 10.54	-	57.84 ± 16.54
S97-V12D-RV-MX5	0.01969 ± 0.00426	-	0.113 ± 0.099	-
S97-V12D-RV-MX6	0.00685 ± 0.00377	-	-0.030 ± 0.095	7.86 ± 8.31
S97-V12D-RV-MX7	0.00086 ± 0.00370	-	0.022 ± 0.096	-
S97-V12D-RV-MX8	0.00143 ± 0.00398	-	-	-
S97-V12D-RV-MX9	0.00200 ± 0.00377	-	-	-0.98 ± 6.71
S97-V12D-RV-MX10	0.00285 ± 0.00387	2.31 ± 3.74	-	0.44 ± 7.24

Table D.11: Trace Metals Aerosol Concentration Data (Sm, Sr, Th, Ti) (continued)

Sample	Aerosol Concentration (ng m^{-3})			
	Sm	Sr	Th	Ti
S97-V12E-RV-CX	0.20031 ± 0.03174	-	-	130.24 ± 41.89
S97-V12E-RV-FX	0.12770 ± 0.01229	9.98 ± 3.03	0.061 ± 0.029	73.68 ± 10.08
S97-V21A-LA-CX	0.06666 ± 0.03302	-	0.030 ± 0.085	165.17 ± 59.05
S97-V21A-LA-FX	0.01968 ± 0.00305	10.18 ± 3.95	-	27.04 ± 11.21
S97-V21B-LA-CX	0.08475 ± 0.04222	-	-	131.91 ± 65.79
S97-V21B-LA-FX	0.01286 ± 0.00392	9.96 ± 6.28	-	34.67 ± 14.08
S97-V21B-LA-MX5	0.01762 ± 0.00423	6.49 ± 3.70	-	6.04 ± 7.32
S97-V21B-LA-MX6	-0.00000 ± 0.00371	-	-	2.22 ± 6.75
S97-V21B-LA-MX7	-	3.85 ± 3.56	-0.049 ± 0.092	4.27 ± 7.18
S97-V21B-LA-MX8	-0.00117 ± 0.00381	-0.21 ± 3.45	-	-2.48 ± 6.98
S97-V21B-LA-MX9	-0.00147 ± 0.00371	-	-0.049 ± 0.092	-
S97-V21B-LA-MX10	0.01909 ± 0.00455	4.73 ± 3.55	-	-
S97-V21C-LA-CX	0.14142 ± 0.04311	-	-	43.93 ± 72.98
S97-V21C-LA-FX	0.01254 ± 0.00382	-	-	12.09 ± 9.22
S97-V21D-LA-CX	0.07553 ± 0.04145	-	0.004 ± 0.082	79.31 ± 74.53
S97-V21D-LA-FX	0.00669 ± 0.00393	-	-	-
S97-V21E-LA-CX	0.03729 ± 0.02298	-	0.036 ± 0.091	44.19 ± 38.90
S97-V21E-LA-FX	0.02962 ± 0.00535	-	0.101 ± 0.053	-
S97-V22A-LA-CX	0.06897 ± 0.03416	2.73 ± 10.12	0.038 ± 0.101	93.24 ± 51.54
S97-V22A-LA-FX	0.00909 ± 0.00267	-	-	13.56 ± 11.87
S97-V22B-LA-CX	0.10987 ± 0.04331	-	-	113.64 ± 70.41
S97-V22B-LA-FX	0.01586 ± 0.00302	5.90 ± 1.24	-	19.09 ± 12.87
S97-V22B-LA-MX5	0.01021 ± 0.00436	-	-	-
S97-V22B-LA-MX6	0.00584 ± 0.00386	-	0.004 ± 0.095	-
S97-V22B-LA-MX7	-0.00117 ± 0.00378	-	-	-0.42 ± 7.10
S97-V22B-LA-MX8	-	-	-	-
S97-V22B-LA-MX9	0.00117 ± 0.00407	-	-	-
S97-V22B-LA-MX10	0.00554 ± 0.00386	4.11 ± 4.20	-	42.76 ± 11.48
S97-V22C-LA-CX	0.13497 ± 0.04277	-	-0.104 ± 0.075	275.64 ± 235.35
S97-V22C-LA-FX	0.02085 ± 0.00409	-	-	20.70 ± 24.31
S97-V22D-LA-CX	0.07697 ± 0.04247	-	-	107.15 ± 59.38
S97-V22D-LA-FX	0.01501 ± 0.00352	-	0.024 ± 0.077	-
S97-V22D-LA-MX5	0.01972 ± 0.00614	5.25 ± 6.10	0.045 ± 0.113	-
S97-V22D-LA-MX6	0.00899 ± 0.00418	1.19 ± 3.67	-	7.41 ± 6.77
S97-V22D-LA-MX7	-0.00174 ± 0.00367	1.77 ± 3.18	-0.036 ± 0.094	-
S97-V22D-LA-MX8	-	0.81 ± 3.82	-	-
S97-V22D-LA-MX9	0.00029 ± 0.00384	-	-0.027 ± 0.099	-
S97-V22D-LA-MX10	0.01044 ± 0.00433	2.93 ± 4.29	-	-
S97-V22E-LA-CX	0.04652 ± 0.02317	4.70 ± 6.82	-	86.69 ± 30.76
S97-V22E-LA-FX	0.00609 ± 0.00168	-	-	7.37 ± 7.17
S97-V21A-AZ-CX	0.10233 ± 0.03639	-	0.040 ± 0.169	321.07 ± 77.33
S97-V21A-AZ-FX	0.00718 ± 0.00263	-	-0.039 ± 0.040	-
S97-V21B-AZ-CX	0.31168 ± 0.05378	22.70 ± 13.63	0.689 ± 0.282	1095.72 ± 133.25
S97-V21B-AZ-FX	0.01296 ± 0.00342	3.01 ± 3.16	-	279.00 ± 62.48
S97-V21C-AZ-CX	0.14810 ± 0.04660	8.33 ± 15.07	0.361 ± 0.269	283.69 ± 140.33
S97-V21C-AZ-FX	0.01208 ± 0.00297	-	-	39.24 ± 13.17

Table D.11: Trace Metals Aerosol Concentration Data (Sm, Sr, Th, Ti) (continued)

Sample	Aerosol Concentration (ng m^{-3})			
	Sm	Sr	Th	Ti
S97-V21D-AZ-CX	0.18144 ± 0.04866	-	0.004 ± 0.076	282.34 ± 71.25
S97-V21D-AZ-FX	0.01014 ± 0.00420	-	-	53.74 ± 31.71
S97-V21D-AZ-MX5	0.00033 ± 0.00445	9.55 ± 4.20	-	18.23 ± 10.65
S97-V21D-AZ-MX6	0.00098 ± 0.00425	-	-	-
S97-V21D-AZ-MX7	0.00033 ± 0.00425	-	-	-1.79 ± 8.33
S97-V21D-AZ-MX8	-	-	-0.021 ± 0.105	-2.77 ± 8.03
S97-V21D-AZ-MX9	-	0.13 ± 3.91	-	-
S97-V21D-AZ-MX10	-0.00164 ± 0.00419	-0.33 ± 3.68	-	-4.08 ± 7.77
S97-V21E-AZ-CX	0.10968 ± 0.02722	-	0.134 ± 0.090	96.16 ± 39.68
S97-V21E-AZ-FX	0.00646 ± 0.00190	-0.31 ± 0.92	-	23.98 ± 10.48
S97-V22A-AZ-CX	0.04534 ± 0.03666	-	0.057 ± 0.221	94.29 ± 59.71
S97-V22A-AZ-FX	0.00383 ± 0.00243	-	0.096 ± 0.088	-0.24 ± 6.43
S97-V22B-AZ-CX	0.17342 ± 0.04950	25.25 ± 13.99	0.277 ± 0.289	919.32 ± 101.55
S97-V22B-AZ-FX	0.01931 ± 0.00345	-	0.137 ± 0.089	270.97 ± 23.79
S97-V22B-AZ-MX5	0.00809 ± 0.00439	-	-	14.75 ± 8.68
S97-V22B-AZ-MX6	-0.00065 ± 0.00420	-	-	28.02 ± 8.68
S97-V22B-AZ-MX7	0.00032 ± 0.00420	-0.78 ± 3.61	-0.034 ± 0.104	102.46 ± 11.96
S97-V22B-AZ-MX8	-	-0.42 ± 3.64	0.057 ± 0.115	50.67 ± 9.23
S97-V22B-AZ-MX9	-	-	-	2.45 ± 7.69
S97-V22B-AZ-MX10	-0.00129 ± 0.00409	-0.75 ± 3.61	-	-5.71 ± 7.60
S97-V22C-AZ-CX	0.19044 ± 0.04925	-	0.187 ± 0.323	185.03 ± 180.53
S97-V22C-AZ-FX	0.01443 ± 0.00325	5.36 ± 6.40	-0.011 ± 0.070	50.36 ± 16.62
S97-V22D-AZ-CX	0.16195 ± 0.04898	41.40 ± 16.35	-	243.43 ± 68.51
S97-V22D-AZ-FX	0.01679 ± 0.00340	-	-	16.95 ± 9.17
S97-V22D-AZ-MX5	0.00870 ± 0.00465	2.29 ± 4.68	-	27.89 ± 11.40
S97-V22D-AZ-MX6	0.00226 ± 0.00426	-	-	16.61 ± 10.23
S97-V22D-AZ-MX7	0.01675 ± 0.00481	6.48 ± 4.99	-	-
S97-V22D-AZ-MX8	-	-	-	-
S97-V22D-AZ-MX9	0.00419 ± 0.00411	-	0.472 ± 0.136	-
S97-V22D-AZ-MX10	0.00419 ± 0.00411	0.06 ± 3.65	-	-
S97-V22E-AZ-CX	0.13179 ± 0.02840	3.66 ± 7.19	-	86.24 ± 35.34
S97-V22E-AZ-FX	0.01102 ± 0.00227	0.43 ± 1.35	-	14.69 ± 10.00
S97-V21A-RV-CX	0.03903 ± 0.03687	-	0.157 ± 0.161	70.89 ± 56.74
S97-V21A-RV-FX	0.02342 ± 0.00324	-	-	46.82 ± 10.48
S97-V21B-RV-CX	0.18735 ± 0.05666	-	0.574 ± 0.507	415.65 ± 136.03
S97-V21C-RV-CX	0.08016 ± 0.04377	-	0.242 ± 0.173	276.07 ± 91.96
S97-V21C-RV-FX	0.04145 ± 0.00399	-	-	60.51 ± 18.49
S97-V21D-RV-CX	-	-	-	177.31 ± 76.26
S97-V21D-RV-FX	0.04869 ± 0.00543	13.24 ± 4.32	0.124 ± 0.068	58.49 ± 12.01
S97-V21D-RV-MX5	0.00029 ± 0.00364	-1.51 ± 3.19	-	-1.84 ± 7.65
S97-V21D-RV-MX6	-0.00086 ± 0.00364	-1.37 ± 3.14	-	-
S97-V21D-RV-MX7	-	-0.43 ± 3.23	-	-
S97-V21D-RV-MX8	-0.00143 ± 0.00364	10.87 ± 4.63	-	64.64 ± 10.32
S97-V21D-RV-MX9	-	-	0.002 ± 0.097	-
S97-V21D-RV-MX10	-	-1.84 ± 3.11	-	0.44 ± 7.24
S97-V21E-RV-CX	0.07547 ± 0.02535	11.17 ± 8.20	0.375 ± 0.212	128.81 ± 41.04

Table D.11: Trace Metals Aerosol Concentration Data (Sm, Sr, Th, Ti) (continued)

Sample	Aerosol Concentration (ng m^{-3})			
	Sm	Sr	Th	Ti
S97-V21E-RV-FX	0.02098 ± 0.00247	-	-0.018 ± 0.032	26.25 ± 6.15
S97-V22A-RV-CX	0.05165 ± 0.03708	-	-	55.82 ± 61.59
S97-V22A-RV-FX	0.00593 ± 0.00348	-	-	-3.27 ± 6.01
S97-V22B-RV-CX	0.10975 ± 0.04595	-	-	356.25 ± 210.82
S97-V22B-RV-FX	0.01362 ± 0.00415	0.26 ± 2.00	-	3.96 ± 11.40
S97-V22B-RV-MX5	0.00656 ± 0.00497	-0.46 ± 3.23	-	-0.41 ± 7.12
S97-V22B-RV-MX6	0.00029 ± 0.00398	-	-0.038 ± 0.090	0.44 ± 7.24
S97-V22B-RV-MX7	-0.00114 ± 0.00364	-0.94 ± 3.20	-0.046 ± 0.089	-
S97-V22B-RV-MX8	-0.00143 ± 0.00364	-	-	-4.66 ± 6.70
S97-V22B-RV-MX9	-	-	-	-2.69 ± 6.65
S97-V22B-RV-MX10	-	-	-	-
S97-V22C-RV-CX	-	-2.38 ± 9.89	-	152.53 ± 93.89
S97-V22C-RV-FX	0.00725 ± 0.00425	-0.64 ± 1.50	0.100 ± 0.122	-
S97-V22D-RV-CX	0.13030 ± 0.04728	-7.03 ± 9.88	-	153.37 ± 78.91
S97-V22D-RV-FX	0.00705 ± 0.00414	4.58 ± 2.64	-	-5.53 ± 8.23
S97-V22D-RV-MX5	0.00028 ± 0.00379	-	-	-
S97-V22D-RV-MX6	-	1.42 ± 3.27	-	-4.07 ± 6.59
S97-V22D-RV-MX7	-0.00140 ± 0.00357	-	-	-
S97-V22D-RV-MX8	-	-1.68 ± 3.06	-	-
S97-V22D-RV-MX9	-	-0.81 ± 3.07	-	-0.40 ± 6.71
S97-V22D-RV-MX10	-	-	-0.040 ± 0.089	-
S97-V22E-RV-CX	0.06112 ± 0.02559	-	0.013 ± 0.089	68.59 ± 48.32
S97-V22E-RV-FX	0.00571 ± 0.00229	-	-	3.63 ± 6.61
S97-N21D-ML-FX	0.01120 ± 0.00377	-	0.035 ± 0.091	22.68 ± 14.12
S97-N21E-ML-FX	0.02451 ± 0.00329	-	-	3.16 ± 3.30
S97-N22A-ML-FX	0.01039 ± 0.00345	-	-	6.94 ± 9.80
S97-N22B-ML-FX	0.02014 ± 0.00460	2.00 ± 3.41	-	17.41 ± 10.10
S97-N22C-ML-FX	0.00603 ± 0.00318	-	-	-1.92 ± 6.41
S97-N22C-ML-MX5	-	-	-	54.60 ± 17.70
S97-N22C-ML-MX6	-0.00117 ± 0.00379	5.30 ± 5.43	-	-
S97-N22C-ML-MX7	-	-	-	-
S97-N22C-ML-MX8	-	-	-	-
S97-N22C-ML-MX9	0.02283 ± 0.00490	-	0.192 ± 0.111	-3.93 ± 7.31
S97-N22C-ML-MX10	-	-	-	-
S97-N22D-ML-FX	0.00553 ± 0.00262	0.06 ± 1.67	-0.029 ± 0.050	-
S97-N22E-ML-FX	-	0.25 ± 1.33	0.109 ± 0.065	17.09 ± 10.90
S97-N23A-ML-FX	0.01122 ± 0.00269	-	-	-
S97-N23B-ML-FX	0.01268 ± 0.00357	-0.26 ± 3.09	-	-
S97-N23C-ML-FX	0.00563 ± 0.00267	1.35 ± 2.51	0.012 ± 0.078	-
S97-N23C-ML-MX5	0.00464 ± 0.00384	-0.58 ± 3.25	-	-
S97-N23C-ML-MX6	-	-	-0.063 ± 0.090	-3.90 ± 7.16
S97-N23C-ML-MX7	-	-1.25 ± 3.24	-0.007 ± 0.093	-3.03 ± 7.25
S97-N23C-ML-MX8	-	-	-0.068 ± 0.089	-
S97-N23C-ML-MX9	-	-	-	-
S97-N23C-ML-MX10	-0.00174 ± 0.00367	-	-0.051 ± 0.089	-

Table D.11: Trace Metals Aerosol Concentration Data (Sm, Sr, Th, Ti) (continued)

Sample	Aerosol Concentration (ng m^{-3})			
	Sm	Sr	Th	Ti
S97-N23D-ML-FX	0.00050 ± 0.00402	4.23 ± 1.22	-	-
S97-N23E-ML-FX	0.00101 ± 0.00178	-	-	-
S97-N23E-ML-MX5	-	17.16 ± 8.52	-	31.05 ± 14.49
S97-N23E-ML-MX6	-	-	0.013 ± 0.059	-
S97-N23E-ML-MX7	-	-0.35 ± 1.90	-	-
S97-N23E-ML-MX8	-	0.85 ± 2.39	-	-
S97-N23E-ML-MX9	-	-	-	-
S97-N23E-ML-MX10	0.00632 ± 0.00394	-	-	11.74 ± 7.96
S97-N31A-DB-CX	0.12450 ± 0.03554	-	0.031 ± 0.060	-
S97-N31A-DB-FX	0.02987 ± 0.00527	-	-	-
S97-N31B-DB-CX	0.17565 ± 0.04542	23.87 ± 15.04	0.128 ± 0.100	348.34 ± 99.45
S97-N31B-DB-FX	0.02914 ± 0.00403	-	-	59.22 ± 16.57
S97-N31C-DB-CX	0.12006 ± 0.04326	-	0.082 ± 0.117	115.17 ± 78.98
S97-N31C-DB-FX	0.01644 ± 0.00404	-	-	35.73 ± 18.10
S97-N31C-DB-MX5	0.01331 ± 0.00401	-	-	7.56 ± 7.51
S97-N31C-DB-MX6	-	18.37 ± 12.84	-0.028 ± 0.099	-0.72 ± 7.51
S97-N31C-DB-MX7	0.01479 ± 0.00413	-1.24 ± 3.35	-	-3.39 ± 7.34
S97-N31C-DB-MX8	-	-0.06 ± 3.23	-	-
S97-N31C-DB-MX9	-	-0.80 ± 3.40	-0.050 ± 0.092	-
S97-N31C-DB-MX10	-0.00177 ± 0.00374	-	-0.031 ± 0.093	-
S97-N31D-DB-CX	0.13286 ± 0.04210	4.95 ± 9.74	-	111.29 ± 64.52
S97-N31D-DB-FX	0.03697 ± 0.00487	5.84 ± 1.22	-	28.91 ± 12.73
S97-N31D-DB-MX5	-0.00105 ± 0.00462	-1.47 ± 3.87	-0.023 ± 0.112	-0.16 ± 9.18
S97-N31D-DB-MX6	0.00244 ± 0.00462	3.52 ± 4.05	-	1.24 ± 11.32
S97-N31D-DB-MX7	-0.00140 ± 0.00441	-	-	-4.73 ± 8.67
S97-N31D-DB-MX8	-0.00174 ± 0.00445	-	-0.030 ± 0.115	-
S97-N31D-DB-MX9	-	-	-0.065 ± 0.109	-2.95 ± 8.14
S97-N31D-DB-MX10	-0.00209 ± 0.00441	-	-	-
S97-N31E-DB-CX	0.10507 ± 0.02509	-	0.296 ± 0.176	218.18 ± 45.71
S97-N31E-DB-FX	0.02447 ± 0.00277	3.66 ± 1.99	-	37.18 ± 10.97
S97-N32A-DB-CX	0.11150 ± 0.03533	0.62 ± 6.61	0.017 ± 0.068	135.81 ± 52.12
S97-N32A-DB-FX	-	-	-	-5.28 ± 4.71
S97-N32B-DB-CX	0.22269 ± 0.04744	-	0.237 ± 0.094	88.22 ± 78.28
S97-N32B-DB-FX	0.00174 ± 0.00327	9.12 ± 4.51	-	44.38 ± 20.73
S97-N32C-DB-CX	0.08296 ± 0.04087	3.29 ± 9.45	-	247.99 ± 59.10
S97-N32C-DB-FX	0.01368 ± 0.00301	1.60 ± 2.96	-0.068 ± 0.043	16.29 ± 9.38
S97-N32C-DB-MX5	0.00558 ± 0.00410	-	-	1.34 ± 7.88
S97-N32C-DB-MX6	0.00088 ± 0.00388	-	-0.061 ± 0.091	10.73 ± 9.95
S97-N32C-DB-MX7	-0.00088 ± 0.00371	-	-	2.81 ± 8.92
S97-N32C-DB-MX8	-	-	-	-0.72 ± 6.74
S97-N32C-DB-MX9	-0.00088 ± 0.00381	-	-	-2.48 ± 6.86
S97-N32C-DB-MX10	-	-0.29 ± 3.20	-	-4.27 ± 6.98
S97-N32D-DB-CX	0.08384 ± 0.04152	-	-	96.18 ± 88.55
S97-N32D-DB-FX	0.00596 ± 0.00281	2.19 ± 1.86	-	14.04 ± 9.06
S97-N32E-DB-CX	0.12212 ± 0.02563	2.89 ± 8.35	0.120 ± 0.042	30.61 ± 32.14
S97-N32E-DB-FX	0.00837 ± 0.00218	-	-	3.63 ± 4.10

Table D.11: Trace Metals Aerosol Concentration Data (Sm, Sr, Th, Ti) (continued)

Sample	Aerosol Concentration (ng m^{-3})			
	Sm	Sr	Th	Ti
S97-N31A-ML-CX	0.28045 ± 0.04446	-	1.056 ± 0.293	215.16 ± 92.88
S97-N31A-ML-FX	0.02166 ± 0.00336	-	-	-4.49 ± 12.83
S97-N31B-ML-CX	0.35839 ± 0.05589	34.99 ± 16.91	0.554 ± 0.171	438.46 ± 102.04
S97-N31B-ML-FX	0.03346 ± 0.00707	9.59 ± 4.40	-0.064 ± 0.046	33.96 ± 15.30
S97-N31C-ML-CX	0.21841 ± 0.05215	-	0.115 ± 0.209	293.03 ± 110.53
S97-N31C-ML-FX	0.02517 ± 0.00445	-	-	-
S97-N31C-ML-MX5	0.00617 ± 0.00453	-	0.040 ± 0.119	8.07 ± 9.19
S97-N31C-ML-MX6	0.00103 ± 0.00444	0.58 ± 3.83	-	-
S97-N31C-ML-MX7	-	-	-	9.44 ± 9.19
S97-N31C-ML-MX8	-	-	-	-2.89 ± 8.11
S97-N31C-ML-MX9	-	-	-	-
S97-N31C-ML-MX10	-	-	-	-
S97-N31D-ML-CX	0.32992 ± 0.05475	8.42 ± 11.91	0.251 ± 0.110	466.92 ± 93.06
S97-N31D-ML-FX	0.04740 ± 0.00424	-	-0.065 ± 0.045	24.80 ± 16.49
S97-N31D-ML-MX5	0.01810 ± 0.00506	-	-	20.84 ± 12.27
S97-N31D-ML-MX6	0.00434 ± 0.00506	-1.49 ± 4.03	-0.045 ± 0.118	9.25 ± 9.71
S97-N31D-ML-MX7	-0.00072 ± 0.00462	-	-	-
S97-N31D-ML-MX8	-0.00145 ± 0.00462	-	-	-6.06 ± 8.29
S97-N31D-ML-MX9	-0.00181 ± 0.00458	-	-	-3.42 ± 8.71
S97-N31D-ML-MX10	-0.00109 ± 0.00462	-	-	-6.32 ± 8.49
S97-N31E-ML-CX	0.48780 ± 0.05051	11.50 ± 10.32	0.833 ± 0.080	479.59 ± 98.55
S97-N31E-ML-FX	0.04632 ± 0.00395	-	-	34.27 ± 10.28
S97-N32A-ML-CX	0.22684 ± 0.04329	-	0.303 ± 0.157	214.53 ± 61.55
S97-N32A-ML-FX	0.02749 ± 0.00368	1.69 ± 2.31	-	37.75 ± 14.49
S97-N32B-ML-CX	0.50062 ± 0.06598	13.68 ± 14.14	1.168 ± 0.418	613.41 ± 90.13
S97-N32B-ML-FX	0.01819 ± 0.00554	-	-	26.66 ± 15.12
S97-N32C-ML-CX	0.32992 ± 0.05419	4.62 ± 10.70	0.649 ± 0.225	334.09 ± 71.98
S97-N32C-ML-FX	0.01286 ± 0.00396	-	-	-1.64 ± 6.13
S97-N32C-ML-MX5	0.00032 ± 0.00411	-1.39 ± 3.53	-	-
S97-N32C-ML-MX6	-0.00097 ± 0.00408	-	-	-5.62 ± 7.50
S97-N32C-ML-MX7	-0.00097 ± 0.00408	-1.58 ± 3.53	-	-
S97-N32C-ML-MX8	-0.00129 ± 0.00411	-1.32 ± 3.57	-0.050 ± 0.102	-
S97-N32C-ML-MX9	-0.00032 ± 0.00426	-1.10 ± 3.58	-	-
S97-N32C-ML-MX10	-	-	-0.068 ± 0.100	-
S97-N32D-ML-CX	0.06484 ± 0.04547	0.83 ± 9.40	0.004 ± 0.111	69.04 ± 58.67
S97-N32D-ML-FX	0.00356 ± 0.00330	-0.84 ± 1.48	-	-
S97-N32E-ML-CX	0.06211 ± 0.02584	-	0.039 ± 0.136	106.64 ± 48.67
S97-N32E-ML-FX	0.00289 ± 0.00171	-	-	4.10 ± 3.42
S97-N31A-RV-CX	-	-	-0.125 ± 0.049	-
S97-N31A-RV-FX	0.01530 ± 0.00268	-	0.048 ± 0.033	28.01 ± 11.93
S97-N31B-RV-CX	0.14836 ± 0.04668	21.52 ± 13.49	0.239 ± 0.077	199.52 ± 114.56
S97-N31B-RV-FX	0.01237 ± 0.00304	2.04 ± 2.28	-	19.12 ± 8.77
S97-N31C-RV-CX	0.09011 ± 0.04439	-	0.354 ± 0.273	177.16 ± 71.31
S97-N31C-RV-FX	0.00861 ± 0.00283	-	-	5.53 ± 8.15
S97-N31C-RV-MX5	-0.00173 ± 0.00364	-	-	0.45 ± 7.57
S97-N31C-RV-MX6	-0.00000 ± 0.00367	-0.92 ± 3.18	0.076 ± 0.091	-3.58 ± 6.80

Table D.11: Trace Metals Aerosol Concentration Data (Sm, Sr, Th, Ti) (continued)

Sample	Aerosol Concentration (ng m^{-3})			
	Sm	Sr	Th	Ti
S97-N31C-RV-MX7	-	0.86 ± 3.15	-	-4.93 ± 6.69
S97-N31C-RV-MX8	-	-1.58 ± 3.15	-0.061 ± 0.089	-3.87 ± 6.83
S97-N31C-RV-MX9	-	-1.70 ± 3.15	-	-
S97-N31C-RV-MX10	-	-	-	-0.99 ± 7.08
S97-N31D-RV-CX	0.13742 ± 0.04323	-	0.161 ± 0.091	298.07 ± 98.31
S97-N31D-RV-FX	0.01851 ± 0.00411	-	-0.047 ± 0.055	12.86 ± 8.14
S97-N31D-RV-MX5	-	-	-	33.06 ± 19.14
S97-N31D-RV-MX6	0.00753 ± 0.00697	-	-	57.02 ± 22.31
S97-N31D-RV-MX7	-0.00137 ± 0.00437	-0.31 ± 4.24	-	6.01 ± 7.88
S97-N31D-RV-MX8	-	-	-	6.70 ± 7.88
S97-N31D-RV-MX9	1.02437 ± 0.61628	-	-	-
S97-N31D-RV-MX10	0.00103 ± 0.10280	-0.10 ± 3.86	-0.032 ± 0.109	-
S97-N31E-RV-CX	0.13500 ± 0.02883	-	0.302 ± 0.093	170.09 ± 56.72
S97-N31E-RV-FX	0.02975 ± 0.00323	-	-	29.47 ± 7.32
S97-N32A-RV-CX	0.05916 ± 0.03629	-	0.003 ± 0.123	54.89 ± 55.05
S97-N32A-RV-FX	0.00602 ± 0.00262	4.85 ± 2.11	-	13.62 ± 9.97
S97-N32B-RV-CX	0.05031 ± 0.04447	-2.84 ± 8.82	-	76.90 ± 56.90
S97-N32B-RV-FX	0.00749 ± 0.00420	-	-	-
S97-N32C-RV-CX	0.05119 ± 0.04346	5.39 ± 8.70	-0.014 ± 0.085	47.87 ± 51.08
S97-N32C-RV-FX	0.00213 ± 0.00299	1.36 ± 2.82	-0.040 ± 0.061	47.25 ± 7.27
S97-N32C-RV-MX5	-	-1.77 ± 3.40	-	-2.32 ± 7.27
S97-N32C-RV-MX6	-	-	-	4.53 ± 7.77
S97-N32C-RV-MX7	-	-1.15 ± 3.44	-	-0.45 ± 7.13
S97-N32C-RV-MX9	-	-0.03 ± 3.52	-	-
S97-N32C-RV-MX10	-	-	-	-5.21 ± 7.15
S97-N32D-RV-CX	0.04107 ± 0.04235	-	-0.014 ± 0.065	100.71 ± 54.13
S97-N32D-RV-FX	0.00522 ± 0.00275	0.69 ± 1.67	-0.017 ± 0.062	9.48 ± 8.63
S97-N32E-RV-CX	-	-	-	-
S97-N32E-RV-FX	0.00228 ± 0.00151	-	-	-
S97-T11B-TI-CX	0.01805 ± 0.05109	16.06 ± 14.59	-	131.88 ± 131.53
S97-T11B-TI-FX	0.03272 ± 0.00540	0.88 ± 6.57	-0.021 ± 0.289	83.86 ± 29.73
S97-T11B-TI-MX5	-0.00039 ± 0.00518	-	-	0.61 ± 10.50
S97-T11B-TI-MX6	-0.00157 ± 0.00500	-	-0.049 ± 0.129	-1.74 ± 10.30
S97-T11B-TI-MX7	-	-	-	-
S97-T11B-TI-MX8	-	-	-	-5.66 ± 9.45
S97-T11B-TI-MX9	-0.00235 ± 0.00495	-	-	21.36 ± 14.46
S97-T11B-TI-MX10	-0.00196 ± 0.00495	-1.92 ± 4.30	-	-
S97-T11B-TO-CX	-	-	0.146 ± 0.325	190.38 ± 108.32
S97-T11B-TO-FX	0.01530 ± 0.00724	-	-	-
S97-T11B-TO-MX5	0.00041 ± 0.00535	-	-	68.82 ± 26.92
S97-T11B-TO-MX6	-	-	-	35.76 ± 15.26
S97-T11B-TO-MX7	-	-	-	-3.49 ± 9.94
S97-T11B-TO-MX8	-	-	-0.078 ± 0.128	-4.73 ± 9.46
S97-T11B-TO-MX9	-0.00248 ± 0.00523	-	-0.075 ± 0.128	-3.49 ± 9.57
S97-T11B-TO-MX10	-0.00041 ± 0.00535	-	-0.051 ± 0.129	-

Table D.11: Trace Metals Aerosol Concentration Data (Sm, Sr, Th, Ti) (continued)

Sample	Aerosol Concentration (ng m^{-3})			
	Sm	Sr	Th	Ti
S97-T21B-TI-CX	0.01489 ± 0.05155	8.55 ± 11.64	-	89.15 ± 67.10
S97-T21B-TI-FX	0.00102 ± 0.00368	7.24 ± 1.60	-	29.88 ± 20.35
S97-T21B-TI-MX5	-0.00156 ± 0.00498	0.31 ± 4.47	0.014 ± 0.120	2.95 ± 9.91
S97-T21B-TI-MX6	-	-	-	-4.47 ± 9.37
S97-T21B-TI-MX7	-	-2.22 ± 4.28	-0.067 ± 0.123	1.78 ± 10.08
S97-T21B-TI-MX8	-	-	-	-4.86 ± 9.51
S97-T21B-TI-MX9	-	-1.29 ± 4.37	-0.081 ± 0.121	-
S97-T21B-TI-MX10	-	-	-	-
S97-T21B-TO-FX	-	-	0.159 ± 0.051	-
S97-T31B-TI-CX	-0.00140 ± 0.05136	-	0.189 ± 0.078	-11.84 ± 65.97
S97-T31B-TI-FX	0.00106 ± 0.00359	15.69 ± 43.56	-	-
S97-T31B-TI-MX5	-	-1.48 ± 4.37	-	-
S97-T31B-TI-MX6	-	-	-	-
S97-T31B-TI-MX7	-	-	-	-5.68 ± 9.20
S97-T31B-TI-MX9	-0.00234 ± 0.00494	-	-	-5.36 ± 9.24
S97-T31B-TI-MX10	-	-	-	-2.12 ± 9.17
S97-T31B-TO-CX	-0.02882 ± 0.05325	-	-	41.15 ± 70.45
S97-T31B-TO-FX	-0.00133 ± 0.00340	-	-	4.70 ± 11.26
S97-T31B-TO-MX5	-	25.17 ± 5.01	-	-
S97-T31B-TO-MX6	-	-	-	37.33 ± 25.19
S97-T31B-TO-MX7	-	-	-	56.66 ± 36.27
S97-T31B-TO-MX8	-	-	-	-
S97-T31B-TO-MX9	-0.00193 ± 0.00494	2.74 ± 5.18	-	-
S97-T31B-TO-MX10	0.00966 ± 0.01187	-	-	4.47 ± 12.27
S97-T41B-TI-CX	-0.01593 ± 0.05229	-	-	-
S97-T41B-TI-FX	-0.00018 ± 0.00357	-	-	6.58 ± 8.95
S97-T41B-TI-MX5	-	9.01 ± 7.24	-	18.95 ± 26.15
S97-T41B-TI-MX6	-	-	-	-
S97-T41B-TI-MX7	-	-	-	-
S97-T41B-TI-MX8	-	-	0.267 ± 0.122	-
S97-T41B-TI-MX9	-0.00117 ± 0.00516	-	-	-
S97-T41B-TI-MX10	-	-	-	-1.34 ± 9.46
S97-T41B-TO-CX	-0.02542 ± 0.05093	-	-	-
S97-T41B-TO-FX	0.00538 ± 0.00346	3.25 ± 3.83	0.058 ± 0.136	17.48 ± 12.45
S97-B11A-AZ-MX5	-	-	-	-
S97-B11A-AZ-MX6	-	-	-	-
S97-B11A-AZ-MX7	-	1.50 ± 2.20	-	-
S97-B11A-AZ-MX8	-	5.40 ± 3.00	-	26.00 ± 11.80
S97-B11A-AZ-MX9	-	-	0.420 ± 0.260	14.60 ± 10.00
S97-B11A-AZ-MX10	-	-	0.220 ± 0.124	-
S97-B11A-DB-CX	0.26000 ± 0.02400	42.00 ± 38.00	-	320.00 ± 144.00
S97-B11A-DB-FX	-	5.80 ± 2.50	-	-
S97-B11A-DB-MX5	-	-	0.166 ± 0.104	-
S97-B11A-DB-MX6	-	-	-	-

Table D.11: Trace Metals Aerosol Concentration Data (Sm, Sr, Th, Ti) (continued)

Sample	Aerosol Concentration (ng m^{-3})			
	Sm	Sr	Th	Ti
S97-B11A-DB-MX7	-	5.40 ± 0.42	-	-
S97-B11A-DB-MX8	-	-	-	-
S97-B11A-DB-MX9	-	4.00 ± 2.00	-	32.00 ± 15.40
S97-B11A-DB-MX10	-	-	0.400 ± 0.300	-
S97-B11A-ML-CX	-	-	0.400 ± 0.132	72.00 ± 60.00
S97-B11A-ML-FX	-	0.75 ± 0.65	-	2.40 ± 1.20
S97-B11A-RV-CX	-	-	-	-
S97-B11A-RV-FX	-	-	0.290 ± 0.120	15.00 ± 7.00
S97-B11A-RV-MX5	-	-	-	-
S97-B11A-RV-MX6	-	-	-	-
S97-B11A-RV-MX7	0.00600 ± 0.00400	-	0.076 ± 0.056	34.00 ± 17.00
S97-B11A-RV-MX8	-	-	-	-
S97-B11A-RV-MX9	-	-	0.092 ± 0.054	9.40 ± 3.80
S97-B11A-RV-MX10	-	-	-	-
S97-B11A-TI-CX	-	8.40 ± 2.80	-	20.00 ± 7.60
S97-B11A-TI-FX	-	5.20 ± 2.30	-	-
S97-B11A-TI-MX5	0.00800 ± 0.00600	-	-	-
S97-B11A-TI-MX6	-	-	0.300 ± 0.220	-
S97-B11A-TI-MX7	0.00800 ± 0.00400	-	-	-
S97-B11A-TI-MX8	-	-	-	-
S97-B11A-TI-MX9	-	-	0.300 ± 0.260	-
S97-B11A-TI-MX10	-	-	-	-
S97-B21A-DB-CX	0.11000 ± 0.01200	-	-	60.00 ± 32.00
S97-B21A-DB-FX	-	-	-	33.00 ± 0.69
S97-B21A-DB-MX5	0.02400 ± 0.00600	-	-	-
S97-B21A-DB-MX6	-	-	-	128.00 ± 74.00
S97-B21A-DB-MX7	-	16.80 ± 7.00	0.220 ± 0.170	10.40 ± 5.40
S97-B21A-DB-MX9	0.16200 ± 0.02200	-	3.800 ± 0.400	-
S97-B21A-DB-MX10	-	-	0.920 ± 0.220	50.00 ± 13.60
S97-B21A-ML-CX	-	-	0.340 ± 0.220	12.60 ± 7.00
S97-B21A-ML-FX	0.00300 ± 0.00200	-	-	-
S97-B21A-ML-MX5	-	1.54 ± 1.50	-	-
S97-B21A-ML-MX6	-	-	-	-
S97-B21A-ML-MX7	-	-	-	-
S97-B21A-ML-MX8	-	-	0.380 ± 0.240	-
S97-B21A-ML-MX9	-	-	-	-
S97-B21A-ML-MX10	-	-	-	-
S97-B21A-RV-CX	-	40.00 ± 32.00	-	-
S97-B21A-RV-FX	-	-	0.170 ± 0.010	-
S97-B21A-RV-MX5	-	-	0.280 ± 0.140	-
S97-B21A-RV-MX6	-	-	0.400 ± 0.200	-
S97-B21A-RV-MX7	0.03000 ± 0.02000	-	-	-
S97-B21A-RV-MX8	0.01200 ± 0.00800	-	0.340 ± 0.160	26.00 ± 14.80
S97-B21A-RV-MX9	-	-	-	220.00 ± 14.20

Table D.11: Trace Metals Aerosol Concentration Data (Sm, Sr, Th, Ti) (continued)

Sample	Aerosol Concentration (ng m^{-3})			
	Sm	Sr	Th	Ti
S97-B21A-RV-MX10	-	-	-	-

D.12 Trace Elements Aerosol Concentration Data (U, V, Yb, Zn)

Table D.12: Trace Metals Aerosol Concentration Data (U, V, Yb, Zn)

Sample	Aerosol Concentration (ng m^{-3})			
	U	V	Yb	Zn
S97-V11A-LA-CX	-	4.98 ± 1.45	-	698.0 ± 277.9
S97-V11A-LA-FX	-	2.66 ± 0.17	-	32.6 ± 16.5
S97-V11B-LA-CX	-0.0685 ± 0.1347	4.92 ± 1.93	-	1440.1 ± 288.4
S97-V11B-LA-FX	-	4.74 ± 0.27	-	253.0 ± 35.1
S97-V11C-LA-CX	-	6.27 ± 1.91	-	6086.5 ± 1091.6
S97-V11C-LA-FX	-	1.98 ± 0.13	-	71.0 ± 21.1
S97-V11D-LA-CX	-	4.75 ± 1.89	-	2548.7 ± 515.7
S97-V11D-LA-FX	-	4.26 ± 0.23	-	26.6 ± 16.9
S97-V11E-LA-CX	-	4.21 ± 1.00	-	174.4 ± 153.6
S97-V11E-LA-FX	-	3.19 ± 0.16	-	13.1 ± 10.5
S97-V12A-LA-CX	-	5.19 ± 1.49	-	296.5 ± 238.4
S97-V12A-LA-FX	-	3.38 ± 0.16	-	100.2 ± 18.8
S97-V12B-LA-CX	-	5.29 ± 1.72	-	1617.0 ± 461.0
S97-V12B-LA-FX	-	3.90 ± 0.21	-	79.5 ± 18.8
S97-V12B-LA-MX5	-	-7.98 ± 51.07	-0.070 ± 0.241	-0.3 ± 5.6
S97-V12B-LA-MX6	0.0452 ± 0.0584	-7.67 ± 51.07	-	1.7 ± 5.7
S97-V12B-LA-MX7	-	-6.53 ± 51.07	-	13.8 ± 5.9
S97-V12B-LA-MX8	-	-7.35 ± 51.07	-	-0.9 ± 5.4
S97-V12B-LA-MX9	-	-8.02 ± 51.07	-	0.9 ± 5.6
S97-V12B-LA-MX10	-	-8.09 ± 51.07	-0.064 ± 0.241	-3.6 ± 5.4
S97-V12C-LA-CX	-	5.18 ± 1.70	-	1099.6 ± 325.7
S97-V12C-LA-FX	-	4.21 ± 0.21	-	85.8 ± 21.1
S97-V12D-LA-CX	-	4.30 ± 1.78	-	1160.7 ± 349.4
S97-V12D-LA-FX	-	3.84 ± 0.21	0.094 ± 0.084	23.7 ± 18.0
S97-V12E-LA-CX	-	5.37 ± 1.03	-	868.5 ± 219.1
S97-V12E-LA-FX	-	2.26 ± 0.12	-	21.6 ± 10.5
S97-V11A-AZ-CX	-	3.34 ± 1.55	-	-41.7 ± 235.1
S97-V11A-AZ-FX	-	1.73 ± 0.11	-	5.4 ± 13.7
S97-V11B-AZ-CX	-	19.88 ± 2.26	0.139 ± 0.214	629.1 ± 356.2
S97-V11B-AZ-FX	-	8.81 ± 0.41	-	42.0 ± 25.5
S97-V11C-AZ-CX	0.0467 ± 0.1748	9.66 ± 1.97	0.010 ± 0.094	292.7 ± 329.2
S97-V11C-AZ-FX	0.0007 ± 0.0575	3.18 ± 0.17	-	27.3 ± 17.4
S97-V11D-AZ-CX	-	7.30 ± 1.96	-0.019 ± 0.073	-100.5 ± 289.4
S97-V11D-AZ-FX	-	2.88 ± 0.17	-	-7.6 ± 16.4
S97-V11D-AZ-MX5	-	-9.08 ± 58.17	-	0.0 ± 6.2
S97-V11D-AZ-MX6	-	-8.90 ± 58.17	-	32.4 ± 7.8
S97-V11D-AZ-MX7	-	-8.27 ± 58.17	-	20.7 ± 7.6
S97-V11D-AZ-MX8	-	-8.10 ± 58.17	-	-2.0 ± 6.3
S97-V11D-AZ-MX9	-	-8.87 ± 58.17	-	-1.0 ± 6.4
S97-V11D-AZ-MX10	-	-	-	14.7 ± 6.7
S97-V11E-AZ-CX	-	-	0.126 ± 0.118	14.4 ± 169.4
S97-V11E-AZ-FX	0.0286 ± 0.0527	3.17 ± 0.17	-	62.6 ± 14.7

Table D.12: Trace Metals Aerosol Concentration Data (U, V, Yb, Zn) (continued)

Sample	Aerosol Concentration (ng m^{-3})			
	U	V	Yb	Zn
S97-V12A-AZ-CX	-	9.22 ± 2.07	-0.045 ± 0.060	134.3 ± 230.4
S97-V12A-AZ-FX	-	3.99 ± 0.27	-	24.2 ± 22.1
S97-V12B-AZ-CX	-	32.00 ± 3.87	-	5022.6 ± 622.4
S97-V12B-AZ-FX	-	22.21 ± 1.69	-	166.0 ± 40.6
S97-V12C-AZ-CX	-	27.59 ± 3.55	0.010 ± 0.072	176.5 ± 286.6
S97-V12C-AZ-FX	-	14.87 ± 0.99	-	34.3 ± 19.3
S97-V12D-AZ-CX	-	8.63 ± 2.22	0.143 ± 0.168	375.6 ± 291.2
S97-V12D-AZ-FX	-	4.28 ± 0.33	-0.022 ± 0.058	31.3 ± 19.3
S97-V12D-AZ-MX5	-	-8.85 ± 56.81	-	6.4 ± 10.1
S97-V12D-AZ-MX6	-	-	-	5.8 ± 6.3
S97-V12D-AZ-MX7	-	-6.97 ± 56.81	-0.061 ± 0.268	12.4 ± 6.7
S97-V12D-AZ-MX8	-	-7.78 ± 56.81	-	20.5 ± 6.9
S97-V12D-AZ-MX9	-	-8.92 ± 56.81	-	0.9 ± 6.2
S97-V12D-AZ-MX10	-	-8.88 ± 56.81	-	-2.7 ± 6.2
S97-V12E-AZ-CX	-	5.77 ± 1.57	-	351.5 ± 163.2
S97-V12E-AZ-FX	-	2.17 ± 0.18	-	37.2 ± 23.9
S97-V11A-RV-CX	0.0713 ± 0.1340	1.45 ± 1.58	0.049 ± 0.050	-85.7 ± 241.0
S97-V11A-RV-FX	-	0.91 ± 0.06	-0.030 ± 0.041	-7.1 ± 13.9
S97-V11B-RV-CX	-	5.02 ± 1.98	-	594.1 ± 302.2
S97-V11B-RV-FX	-	1.38 ± 0.14	-	236.6 ± 32.0
S97-V11C-RV-CX	-0.0388 ± 0.1648	1.80 ± 1.86	-	1033.5 ± 350.4
S97-V11C-RV-FX	0.0145 ± 0.0461	0.91 ± 0.10	-0.019 ± 0.052	5.2 ± 16.3
S97-V11D-RV-CX	-	5.75 ± 1.89	0.123 ± 0.158	2913.5 ± 597.6
S97-V11D-RV-FX	0.0231 ± 0.0442	5.09 ± 0.26	-	-2.0 ± 15.8
S97-V11D-RV-MX5	-	-7.67 ± 49.62	-	-4.8 ± 5.2
S97-V11D-RV-MX6	-	-6.60 ± 49.62	-	-2.0 ± 5.3
S97-V11D-RV-MX7	-	-6.88 ± 49.62	-	-0.0 ± 5.4
S97-V11D-RV-MX8	-	-7.31 ± 49.62	-	2.3 ± 6.5
S97-V11D-RV-MX9	-	-7.57 ± 49.62	-	14.2 ± 5.7
S97-V11D-RV-MX10	-	-7.72 ± 49.62	-	-3.7 ± 5.3
S97-V11E-RV-CX	0.0097 ± 0.0818	6.73 ± 1.09	-	1487.2 ± 308.2
S97-V11E-RV-FX	-	4.53 ± 0.21	-	-0.4 ± 8.8
S97-V12A-RV-CX	-	6.02 ± 1.56	0.178 ± 0.197	290.2 ± 273.6
S97-V12A-RV-FX	-	4.12 ± 0.21	-	8.5 ± 14.3
S97-V12B-RV-CX	-	7.61 ± 2.00	-	162.1 ± 307.9
S97-V12B-RV-FX	-	4.26 ± 0.25	-	251.5 ± 36.7
S97-V12C-RV-CX	-	5.62 ± 1.92	-	3133.4 ± 965.0
S97-V12C-RV-FX	-	2.28 ± 0.15	0.036 ± 0.071	10.8 ± 17.6
S97-V12D-RV-CX	-	6.54 ± 1.88	-	1209.7 ± 489.1
S97-V12D-RV-FX	-	6.97 ± 0.38	0.058 ± 0.055	7.2 ± 17.6
S97-V12D-RV-MX5	-	7.52 ± 49.62	0.229 ± 0.241	0.8 ± 5.3
S97-V12D-RV-MX6	-	-6.71 ± 49.62	-	5.4 ± 5.7
S97-V12D-RV-MX7	-	-4.17 ± 49.62	-	10.5 ± 6.5
S97-V12D-RV-MX8	-	-6.48 ± 49.62	-0.034 ± 0.236	0.8 ± 5.6
S97-V12D-RV-MX9	0.0239 ± 0.0825	-7.31 ± 49.62	0.006 ± 0.239	-0.9 ± 5.4
S97-V12D-RV-MX10	-	-7.40 ± 49.62	-	3.4 ± 9.5

Table D.12: Trace Metals Aerosol Concentration Data (U, V, Yb, Zn) (continued)

Sample	Aerosol Concentration (ng m^{-3})			
	U	V	Yb	Zn
S97-V12E-RV-CX	-	10.39 ± 1.15	-	669.7 ± 262.4
S97-V12E-RV-FX	-	7.67 ± 0.38	0.002 ± 0.030	12.9 ± 8.9
S97-V21A-LA-CX	-	6.90 ± 1.44	-	140.7 ± 211.8
S97-V21A-LA-FX	0.0174 ± 0.0477	3.84 ± 0.19	-	143.2 ± 22.6
S97-V21B-LA-CX	-	6.34 ± 1.76	-	-174.0 ± 259.9
S97-V21B-LA-FX	-	3.38 ± 0.22	-	66.1 ± 19.0
S97-V21B-LA-MX5	-	-7.44 ± 51.07	-	7.3 ± 6.9
S97-V21B-LA-MX6	-	-7.76 ± 51.07	-0.075 ± 0.241	11.1 ± 6.1
S97-V21B-LA-MX7	-	-6.79 ± 51.07	-	-3.4 ± 5.4
S97-V21B-LA-MX8	-0.0370 ± 0.0624	-7.23 ± 51.07	-	6.4 ± 5.8
S97-V21B-LA-MX9	-	-8.04 ± 51.07	-	-3.6 ± 5.4
S97-V21B-LA-MX10	-	-7.82 ± 51.07	0.500 ± 0.276	-0.9 ± 5.5
S97-V21C-LA-CX	-	4.81 ± 1.71	0.481 ± 0.110	1936.2 ± 649.8
S97-V21C-LA-FX	-	3.60 ± 0.21	-	46.3 ± 16.4
S97-V21D-LA-CX	-	3.97 ± 1.73	-	7144.1 ± 3969.6
S97-V21D-LA-FX	-	-	-	29.0 ± 18.1
S97-V21E-LA-CX	-	3.31 ± 0.99	-	123.0 ± 150.1
S97-V21E-LA-FX	-	2.06 ± 0.12	-	52.4 ± 11.1
S97-V22A-LA-CX	-	3.18 ± 1.43	-	188.0 ± 230.6
S97-V22A-LA-FX	0.0415 ± 0.0566	2.33 ± 0.26	-	110.8 ± 24.2
S97-V22B-LA-CX	-	4.74 ± 1.72	-	-168.4 ± 257.8
S97-V22B-LA-FX	-	2.99 ± 0.17	-	84.1 ± 23.6
S97-V22B-LA-MX5	-	-7.80 ± 50.74	-	-
S97-V22B-LA-MX6	-	-7.83 ± 50.74	-	6.7 ± 6.5
S97-V22B-LA-MX7	-	-7.16 ± 50.74	-	-2.1 ± 5.4
S97-V22B-LA-MX8	-	-7.07 ± 50.74	-	-0.9 ± 6.5
S97-V22B-LA-MX9	-	-7.62 ± 50.74	-	7.6 ± 5.9
S97-V22B-LA-MX10	-	-7.65 ± 50.74	0.292 ± 0.249	9.6 ± 5.8
S97-V22C-LA-CX	-	16.35 ± 3.35	0.060 ± 0.090	938.2 ± 400.8
S97-V22C-LA-FX	-	7.88 ± 0.46	0.058 ± 0.082	223.1 ± 36.6
S97-V22D-LA-CX	-	5.89 ± 1.76	-	698.8 ± 359.9
S97-V22D-LA-FX	-	4.39 ± 0.22	-	20.1 ± 17.6
S97-V22D-LA-MX5	0.1983 ± 0.0585	-7.43 ± 50.42	-	12.7 ± 8.3
S97-V22D-LA-MX6	-	-7.08 ± 50.42	-0.040 ± 0.239	1.7 ± 5.7
S97-V22D-LA-MX7	-	-	-	10.7 ± 9.2
S97-V22D-LA-MX8	-	-6.47 ± 50.42	-0.071 ± 0.238	-1.8 ± 5.3
S97-V22D-LA-MX9	-	-7.37 ± 50.42	-	-
S97-V22D-LA-MX10	-	-7.49 ± 50.42	0.320 ± 0.270	10.1 ± 7.0
S97-V22E-LA-CX	-	5.29 ± 0.99	-	-95.8 ± 142.6
S97-V22E-LA-FX	-	3.41 ± 0.17	-	110.2 ± 17.5
S97-V21A-AZ-CX	-	7.51 ± 1.56	-	584.2 ± 271.9
S97-V21A-AZ-FX	-	4.26 ± 1.11	-	18.5 ± 13.1
S97-V21B-AZ-CX	0.1130 ± 0.1818	35.29 ± 2.86	-	243.7 ± 300.4
S97-V21B-AZ-FX	-	24.53 ± 6.22	-	56.9 ± 20.5
S97-V21C-AZ-CX	0.1210 ± 0.1955	17.00 ± 3.60	-	-150.9 ± 281.5
S97-V21C-AZ-FX	-	5.44 ± 1.58	0.007 ± 0.062	-0.1 ± 16.5

Table D.12: Trace Metals Aerosol Concentration Data (U, V, Yb, Zn) (continued)

Sample	Aerosol Concentration (ng m^{-3})			
	U	V	Yb	Zn
S97-V21D-AZ-CX	0.1535 ± 0.1019	10.74 ± 2.02	-0.009 ± 0.060	1156.3 ± 798.6
S97-V21D-AZ-FX	-	33.13 ± 10.28	-	51.0 ± 18.3
S97-V21D-AZ-MX5	-	-8.81 ± 57.08	-	-
S97-V21D-AZ-MX6	-	-8.71 ± 57.08	-	6.2 ± 11.8
S97-V21D-AZ-MX7	-	-7.62 ± 57.08	-0.066 ± 0.270	1.0 ± 7.1
S97-V21D-AZ-MX8	-	-7.39 ± 57.08	-	-
S97-V21D-AZ-MX9	-	-8.41 ± 57.08	-	-3.6 ± 6.0
S97-V21D-AZ-MX10	-0.0526 ± 0.0708	-8.80 ± 57.08	-	-2.7 ± 6.5
S97-V21E-AZ-CX	0.1684 ± 0.0562	4.49 ± 1.07	-	1846.2 ± 1067.9
S97-V21E-AZ-FX	-	2.35 ± 0.67	-	9.7 ± 9.5
S97-V22A-AZ-CX	-	4.33 ± 1.56	-	352.4 ± 249.3
S97-V22A-AZ-FX	-	1.95 ± 0.16	-	29.9 ± 20.3
S97-V22B-AZ-CX	0.2526 ± 0.2377	48.90 ± 3.17	-	747.8 ± 357.1
S97-V22B-AZ-FX	-	27.66 ± 1.25	-0.019 ± 0.060	40.8 ± 19.8
S97-V22B-AZ-MX5	-0.0311 ± 0.0720	-8.00 ± 56.29	-	3.9 ± 8.0
S97-V22B-AZ-MX6	-	-6.00 ± 56.29	-	3.5 ± 7.0
S97-V22B-AZ-MX7	-	3.03 ± 56.29	-	10.3 ± 6.3
S97-V22B-AZ-MX8	-	-1.82 ± 56.29	-0.073 ± 0.266	4.8 ± 6.6
S97-V22B-AZ-MX9	-	-7.81 ± 56.29	-0.086 ± 0.265	-2.3 ± 6.0
S97-V22B-AZ-MX10	-	-8.78 ± 56.29	-	-2.3 ± 5.9
S97-V22C-AZ-CX	-	9.74 ± 2.90	0.155 ± 0.208	-194.9 ± 288.6
S97-V22C-AZ-FX	-	7.59 ± 0.43	-	236.3 ± 18.5
S97-V22D-AZ-CX	0.1631 ± 0.2528	14.59 ± 2.11	-	344.0 ± 311.7
S97-V22D-AZ-FX	-	4.86 ± 0.27	0.024 ± 0.070	30.5 ± 19.8
S97-V22D-AZ-MX5	-	-8.32 ± 56.03	-	2.2 ± 7.8
S97-V22D-AZ-MX6	-	-5.36 ± 56.03	-	1.9 ± 6.3
S97-V22D-AZ-MX7	-	-6.13 ± 56.03	-	-0.0 ± 6.0
S97-V22D-AZ-MX8	-	-6.58 ± 56.03	0.223 ± 0.278	-0.0 ± 6.0
S97-V22D-AZ-MX9	-	-8.16 ± 56.03	-	13.5 ± 6.8
S97-V22D-AZ-MX10	-	-8.48 ± 56.03	-	13.5 ± 6.8
S97-V22E-AZ-CX	-	5.38 ± 1.10	-	902.5 ± 555.4
S97-V22E-AZ-FX	-	3.21 ± 0.17	0.093 ± 0.073	31.1 ± 19.9
S97-V21A-RV-CX	-	3.78 ± 1.53	-	7309.1 ± 230.7
S97-V21A-RV-FX	-	-	-	39.6 ± 15.2
S97-V21B-RV-CX	0.5684 ± 0.5488	7.94 ± 2.30	0.436 ± 0.439	-223.4 ± 334.7
S97-V21C-RV-CX	-	7.04 ± 1.87	-	3012.3 ± 1130.3
S97-V21C-RV-FX	-	3.44 ± 0.27	0.029 ± 0.063	29.5 ± 21.8
S97-V21D-RV-CX	-	4.53 ± 1.85	0.222 ± 0.290	458.1 ± 305.3
S97-V21D-RV-FX	0.0264 ± 0.0544	4.48 ± 0.25	-0.032 ± 0.050	-2.0 ± 16.6
S97-V21D-RV-MX5	-	-7.78 ± 49.62	-	3.1 ± 8.8
S97-V21D-RV-MX6	-	-7.74 ± 49.62	-	-1.2 ± 5.6
S97-V21D-RV-MX7	-	-7.14 ± 49.62	-	-3.7 ± 5.2
S97-V21D-RV-MX8	-	-3.89 ± 49.62	-0.077 ± 0.234	-3.9 ± 5.2
S97-V21D-RV-MX9	-	-7.57 ± 49.62	-	0.3 ± 6.9
S97-V21D-RV-MX10	-	-7.68 ± 49.62	-	-2.9 ± 5.2
S97-V21E-RV-CX	-	7.72 ± 1.10	0.179 ± 0.156	396.6 ± 227.7

Table D.12: Trace Metals Aerosol Concentration Data (U, V, Yb, Zn) (continued)

Sample	Aerosol Concentration (ng m^{-3})			
	U	V	Yb	Zn
S97-V21E-RV-FX	0.0021 ± 0.0252	4.82 ± 0.23	-	5.8 ± 9.4
S97-V22A-RV-CX	0.0378 ± 0.1233	1.71 ± 1.58	-	1622.8 ± 312.2
S97-V22A-RV-FX	-	0.81 ± 0.03	-	9.0 ± 14.4
S97-V22B-RV-CX	-	22.48 ± 5.09	-	3166.5 ± 488.6
S97-V22B-RV-FX	-	2.27 ± 0.33	-	126.7 ± 31.3
S97-V22B-RV-MX5	-	-7.82 ± 49.62	-	5.0 ± 5.5
S97-V22B-RV-MX6	-	-7.45 ± 49.62	-0.057 ± 0.234	18.1 ± 5.9
S97-V22B-RV-MX7	-	-6.51 ± 49.62	-0.067 ± 0.234	4.8 ± 5.4
S97-V22B-RV-MX8	-	-7.35 ± 49.62	-	5.2 ± 5.4
S97-V22B-RV-MX9	-0.0554 ± 0.0577	-7.83 ± 49.62	-	-1.1 ± 5.3
S97-V22B-RV-MX10	-	-	-	2.3 ± 5.9
S97-V22C-RV-CX	-	3.21 ± 2.00	-	5830.6 ± 751.2
S97-V22C-RV-FX	-	1.99 ± 0.34	-	40.5 ± 37.1
S97-V22D-RV-CX	0.1408 ± 0.2740	3.41 ± 2.02	-	3686.6 ± 535.4
S97-V22D-RV-FX	-	1.61 ± 0.04	-	-8.0 ± 17.8
S97-V22D-RV-MX5	-	-7.60 ± 48.60	-0.075 ± 0.230	-0.9 ± 5.2
S97-V22D-RV-MX6	-	-7.51 ± 48.60	-	25.6 ± 6.7
S97-V22D-RV-MX7	-	-6.94 ± 48.60	-	0.5 ± 5.3
S97-V22D-RV-MX8	-	-7.53 ± 48.60	-0.066 ± 0.229	-3.8 ± 5.1
S97-V22D-RV-MX9	-	-7.55 ± 48.60	-	-3.4 ± 5.1
S97-V22D-RV-MX10	-	-7.60 ± 48.60	-	-1.1 ± 5.1
S97-V22E-RV-CX	-	2.96 ± 1.21	-	1815.4 ± 272.1
S97-V22E-RV-FX	-	3.06 ± 0.18	-	5.5 ± 9.5
S97-N21D-ML-FX	-	3.62 ± 0.95	-	57.7 ± 17.7
S97-N21E-ML-FX	-	8.31 ± 0.64	0.106 ± 0.072	11.2 ± 12.8
S97-N22A-ML-FX	-	6.02 ± 0.41	-	-6.0 ± 12.6
S97-N22B-ML-FX	-	4.90 ± 0.32	-	-16.2 ± 15.8
S97-N22C-ML-FX	0.0072 ± 0.0572	0.72 ± 0.07	-	-5.6 ± 16.1
S97-N22C-ML-MX5	-	-7.35 ± 50.90	-0.060 ± 0.241	-2.4 ± 5.6
S97-N22C-ML-MX6	0.0187 ± 0.0664	-7.47 ± 50.90	-0.040 ± 0.241	-2.4 ± 5.6
S97-N22C-ML-MX7	-	-7.76 ± 50.90	-0.037 ± 0.241	-
S97-N22C-ML-MX8	-	-8.03 ± 50.90	-0.020 ± 0.240	13.1 ± 6.5
S97-N22C-ML-MX9	-	-	0.033 ± 0.242	17.5 ± 6.5
S97-N22C-ML-MX10	-	-8.04 ± 50.90	-	26.6 ± 6.9
S97-N22D-ML-FX	-	3.04 ± 0.17	-	-10.5 ± 16.2
S97-N22E-ML-FX	-	6.82 ± 0.54	0.006 ± 0.031	15.2 ± 13.2
S97-N23A-ML-FX	-	5.08 ± 0.34	-	0.2 ± 12.8
S97-N23B-ML-FX	-	4.68 ± 0.32	-	22.3 ± 17.4
S97-N23C-ML-FX	-	3.27 ± 0.19	0.033 ± 0.048	14.3 ± 17.4
S97-N23C-ML-MX5	-	-7.79 ± 50.48	-0.066 ± 0.238	3.7 ± 5.4
S97-N23C-ML-MX6	-	-7.12 ± 50.48	-0.071 ± 0.238	-1.2 ± 5.5
S97-N23C-ML-MX7	-	-6.36 ± 50.48	-0.062 ± 0.239	4.3 ± 7.4
S97-N23C-ML-MX8	-	-7.83 ± 50.48	-	20.0 ± 6.3
S97-N23C-ML-MX9	-	-7.98 ± 50.48	-	-
S97-N23C-ML-MX10	-	-7.99 ± 50.48	-	1.4 ± 7.4

Table D.12: Trace Metals Aerosol Concentration Data (U, V, Yb, Zn) (continued)

Sample	Aerosol Concentration (ng m^{-3})			
	U	V	Yb	Zn
S97-N23D-ML-FX	-	3.16 ± 0.32	-	11.3 ± 20.9
S97-N23E-ML-FX	-	1.99 ± 0.12	-	21.7 ± 10.9
S97-N23E-ML-MX5	-	-3.63 ± 28.95	0.017 ± 0.145	2.8 ± 5.5
S97-N23E-ML-MX6	-	-1.93 ± 28.95	-	-
S97-N23E-ML-MX7	-	-3.47 ± 28.95	-	1.8 ± 3.3
S97-N23E-ML-MX8	-	-0.27 ± 28.95	-	3.6 ± 4.1
S97-N23E-ML-MX9	-	-4.55 ± 28.95	-	-1.9 ± 3.1
S97-N23E-ML-MX10	0.0722 ± 0.0849	-	-	1.3 ± 4.6
S97-N31A-DB-CX	0.0623 ± 0.1459	13.39 ± 1.95	-	698.0 ± 231.7
S97-N31A-DB-FX	-	12.76 ± 0.98	-	481.4 ± 211.4
S97-N31B-DB-CX	0.0612 ± 0.1553	12.53 ± 2.29	0.001 ± 0.084	885.1 ± 293.8
S97-N31B-DB-FX	-	9.21 ± 0.64	0.042 ± 0.056	137.1 ± 34.8
S97-N31C-DB-CX	-0.0184 ± 0.1238	12.30 ± 2.37	-	284.5 ± 266.4
S97-N31C-DB-FX	-	6.67 ± 0.64	-	341.6 ± 65.9
S97-N31C-DB-MX5	-0.0456 ± 0.0615	-7.43 ± 51.44	-	2.9 ± 5.5
S97-N31C-DB-MX6	-	-7.05 ± 51.44	-	0.3 ± 5.4
S97-N31C-DB-MX7	-	-7.17 ± 51.44	-0.029 ± 0.244	2.0 ± 8.7
S97-N31C-DB-MX8	-0.0136 ± 0.0635	-7.25 ± 51.44	-	1.2 ± 6.3
S97-N31C-DB-MX9	-	-7.91 ± 51.44	-	-4.5 ± 5.4
S97-N31C-DB-MX10	-	-8.11 ± 51.44	-	-4.4 ± 5.4
S97-N31D-DB-CX	-	25.36 ± 3.08	0.026 ± 0.134	47.4 ± 254.1
S97-N31D-DB-FX	-	19.65 ± 1.33	-	20.6 ± 16.8
S97-N31D-DB-MX5	-	-7.16 ± 60.67	-	5.5 ± 6.7
S97-N31D-DB-MX6	-	-7.61 ± 60.67	-	-1.8 ± 6.7
S97-N31D-DB-MX7	-	0.13 ± 60.68	-	3.8 ± 6.3
S97-N31D-DB-MX8	-	-4.40 ± 60.67	-	6.9 ± 8.7
S97-N31D-DB-MX9	-0.0583 ± 0.0741	-9.43 ± 60.67	-	-0.7 ± 6.6
S97-N31D-DB-MX10	-	-8.66 ± 60.67	-	-3.2 ± 6.5
S97-N31E-DB-CX	0.0139 ± 0.1005	41.55 ± 5.39	-	-50.1 ± 144.8
S97-N31E-DB-FX	0.0108 ± 0.0282	28.61 ± 1.61	-	55.8 ± 11.6
S97-N32A-DB-CX	-	12.09 ± 1.52	-0.063 ± 0.038	61.0 ± 214.4
S97-N32A-DB-FX	-	0.31 ± 0.04	-	-15.7 ± 12.4
S97-N32B-DB-CX	-	11.33 ± 1.87	0.182 ± 0.113	860.9 ± 302.0
S97-N32B-DB-FX	-	3.47 ± 0.27	-	85.5 ± 20.3
S97-N32C-DB-CX	-0.0519 ± 0.1155	-	-	-151.7 ± 254.6
S97-N32C-DB-FX	-	2.29 ± 0.15	-	342.4 ± 45.2
S97-N32C-DB-MX5	-	-7.64 ± 51.07	-	13.8 ± 5.7
S97-N32C-DB-MX6	-	-7.67 ± 51.07	-0.072 ± 0.241	5.8 ± 5.5
S97-N32C-DB-MX7	-	-7.17 ± 51.07	-	2.9 ± 5.6
S97-N32C-DB-MX8	-	-7.79 ± 51.07	-	-1.2 ± 5.7
S97-N32C-DB-MX9	-0.0564 ± 0.0599	-8.05 ± 51.07	-0.014 ± 0.242	5.5 ± 5.7
S97-N32C-DB-MX10	-	-8.08 ± 51.07	-0.052 ± 0.242	2.6 ± 5.7
S97-N32D-DB-CX	-	6.96 ± 1.73	-	-71.8 ± 257.8
S97-N32D-DB-FX	-	4.69 ± 0.29	-	102.2 ± 24.5
S97-N32E-DB-CX	-0.0252 ± 0.0649	3.80 ± 1.00	-0.042 ± 0.034	-26.5 ± 148.2
S97-N32E-DB-FX	0.0124 ± 0.0341	1.91 ± 0.10	-	7.2 ± 8.8

Table D.12: Trace Metals Aerosol Concentration Data (U, V, Yb, Zn) (continued)

Sample	Aerosol Concentration (ng m^{-3})			
	U	V	Yb	Zn
S97-N31A-ML-CX	-	22.96 ± 2.99	0.039 ± 0.121	-2.8 ± 229.7
S97-N31A-ML-FX	-	13.52 ± 1.06	-	117.3 ± 29.8
S97-N31B-ML-CX	-0.0979 ± 0.1169	20.98 ± 2.93	0.001 ± 0.090	451.9 ± 292.9
S97-N31B-ML-FX	0.0633 ± 0.0927	7.88 ± 0.66	-	130.3 ± 33.7
S97-N31C-ML-CX	-	12.15 ± 2.66	-	16.3 ± 302.0
S97-N31C-ML-FX	-	2.79 ± 0.35	-	53.3 ± 36.9
S97-N31C-ML-MX5	-0.0658 ± 0.0703	-9.12 ± 59.59	-	2.4 ± 6.6
S97-N31C-ML-MX6	-	-8.81 ± 59.59	-	8.9 ± 7.0
S97-N31C-ML-MX7	-	-8.30 ± 59.59	-	1.3 ± 6.5
S97-N31C-ML-MX8	-	-9.05 ± 59.59	-	5.8 ± 6.9
S97-N31C-ML-MX9	-	-9.34 ± 59.59	-	-3.4 ± 6.4
S97-N31C-ML-MX10	-	-9.41 ± 59.59	-	-0.7 ± 6.7
S97-N31D-ML-CX	-	16.23 ± 2.45	0.020 ± 0.082	195.7 ± 287.4
S97-N31D-ML-FX	-	6.67 ± 0.67	-	33.7 ± 19.2
S97-N31D-ML-MX5	-	-9.31 ± 62.96	-	1.8 ± 8.3
S97-N31D-ML-MX6	-	-8.37 ± 62.96	-	9.4 ± 7.0
S97-N31D-ML-MX7	-	-6.96 ± 62.96	-0.061 ± 0.297	6.8 ± 6.8
S97-N31D-ML-MX8	-	-9.83 ± 62.96	-	1.0 ± 7.7
S97-N31D-ML-MX9	-	-9.68 ± 62.96	-	-1.5 ± 6.7
S97-N31D-ML-MX10	-	-9.82 ± 62.96	-0.068 ± 0.298	-1.5 ± 6.9
S97-N31E-ML-CX	0.3622 ± 0.1377	23.72 ± 2.48	0.105 ± 0.059	76.9 ± 158.8
S97-N31E-ML-FX	-	11.96 ± 0.92	-	166.4 ± 36.3
S97-N32A-ML-CX	-	12.70 ± 1.72	-0.054 ± 0.067	446.5 ± 251.7
S97-N32A-ML-FX	-	7.36 ± 0.38	-	28.6 ± 15.7
S97-N32B-ML-CX	-	16.87 ± 2.20	-	-13.5 ± 297.4
S97-N32B-ML-FX	-	1.26 ± 0.13	0.023 ± 0.072	-4.6 ± 17.2
S97-N32C-ML-CX	-0.0865 ± 0.1113	12.44 ± 2.05	-	-103.2 ± 285.1
S97-N32C-ML-FX	-	0.05 ± 0.04	-	-13.5 ± 16.5
S97-N32C-ML-MX5	-	-8.86 ± 56.03	-	-5.0 ± 5.8
S97-N32C-ML-MX6	-	-8.86 ± 56.03	-0.083 ± 0.264	-4.7 ± 5.9
S97-N32C-ML-MX7	-	-8.84 ± 56.03	-	-2.6 ± 6.5
S97-N32C-ML-MX8	-	-8.84 ± 56.03	-	-5.3 ± 5.9
S97-N32C-ML-MX9	-	-8.83 ± 56.03	-	-2.6 ± 5.9
S97-N32C-ML-MX10	-	-8.89 ± 56.03	-	-4.8 ± 5.8
S97-N32D-ML-CX	-0.1036 ± 0.1087	2.78 ± 1.90	-	-61.0 ± 287.6
S97-N32D-ML-FX	-	-0.00 ± 0.04	-	-12.9 ± 16.7
S97-N32E-ML-CX	-	2.80 ± 1.09	-	404.3 ± 174.5
S97-N32E-ML-FX	-	0.14 ± 0.03	-0.024 ± 0.027	-2.5 ± 9.3
S97-N31A-RV-CX	-	-	-	-143.1 ± 222.4
S97-N31A-RV-FX	0.0186 ± 0.0377	6.41 ± 0.44	-	74.4 ± 17.2
S97-N31B-RV-CX	0.1024 ± 0.1570	9.51 ± 2.37	-0.028 ± 0.066	212.9 ± 285.5
S97-N31B-RV-FX	-	3.62 ± 0.23	-0.022 ± 0.051	34.1 ± 19.0
S97-N31C-RV-CX	-	6.19 ± 2.06	-	33.5 ± 277.5
S97-N31C-RV-FX	-0.0057 ± 0.0509	1.70 ± 0.13	-	46.5 ± 19.9
S97-N31C-RV-MX5	-	-7.80 ± 50.03	-0.074 ± 0.236	0.8 ± 5.4
S97-N31C-RV-MX6	-	-7.63 ± 50.03	-	3.7 ± 5.4

Table D.12: Trace Metals Aerosol Concentration Data (U, V, Yb, Zn) (continued)

Sample	Aerosol Concentration (ng m^{-3})			
	U	V	Yb	Zn
S97-N31C-RV-MX7	-	-7.40 ± 50.03	-0.066 ± 0.236	-2.0 ± 5.2
S97-N31C-RV-MX8	-	-7.63 ± 50.03	-0.079 ± 0.236	5.4 ± 5.4
S97-N31C-RV-MX9	-	-7.84 ± 50.03	-	-3.0 ± 5.3
S97-N31C-RV-MX10	-	-7.86 ± 50.03	-	-3.3 ± 5.3
S97-N31D-RV-CX	-0.0184 ± 0.1208	9.68 ± 2.25	0.027 ± 0.079	301.7 ± 266.6
S97-N31D-RV-FX	0.0526 ± 0.0702	3.80 ± 0.20	-	16.4 ± 15.7
S97-N31D-RV-MX5	-	-6.96 ± 59.54	-0.016 ± 0.281	-2.8 ± 6.4
S97-N31D-RV-MX6	-	0.81 ± 59.54	-	6.8 ± 7.2
S97-N31D-RV-MX7	-	-7.44 ± 59.54	-0.070 ± 0.282	18.5 ± 8.7
S97-N31D-RV-MX8	-0.0630 ± 0.0696	-8.67 ± 59.54	-	27.7 ± 7.8
S97-N31D-RV-MX9	-	-9.30 ± 59.54	-0.082 ± 0.281	3.0 ± 8.0
S97-N31D-RV-MX10	-	-9.39 ± 59.54	-	-5.8 ± 6.2
S97-N31E-RV-CX	0.0212 ± 0.0953	12.05 ± 1.95	0.028 ± 0.059	79.7 ± 164.7
S97-N31E-RV-FX	-	6.91 ± 0.42	-	19.8 ± 10.2
S97-N32A-RV-CX	0.1362 ± 0.1392	3.96 ± 1.53	-	-118.5 ± 228.2
S97-N32A-RV-FX	-	2.62 ± 0.16	-	61.8 ± 19.2
S97-N32B-RV-CX	-	2.07 ± 1.84	-	-130.9 ± 281.0
S97-N32B-RV-FX	-	0.38 ± 0.10	-0.022 ± 0.058	65.3 ± 19.7
S97-N32C-RV-CX	0.0173 ± 0.1330	0.83 ± 1.80	-0.090 ± 0.059	-176.2 ± 275.3
S97-N32C-RV-FX	-	0.48 ± 0.11	0.020 ± 0.048	-14.3 ± 15.9
S97-N32C-RV-MX5	-0.0567 ± 0.0647	-	-0.078 ± 0.255	-3.6 ± 5.7
S97-N32C-RV-MX6	-	-8.58 ± 54.13	-	-
S97-N32C-RV-MX7	-	-8.54 ± 54.13	-0.077 ± 0.255	-
S97-N32C-RV-MX9	-	-	-	-1.3 ± 6.6
S97-N32C-RV-MX10	-	-	-	-
S97-N32D-RV-CX	-	0.81 ± 1.76	0.001 ± 0.065	-161.5 ± 269.2
S97-N32D-RV-FX	-	-	-	-0.4 ± 16.4
S97-N32E-RV-CX	-	-0.04 ± 1.01	-	-1.9 ± 155.4
S97-N32E-RV-FX	-	0.00 ± 0.02	-	23.3 ± 11.2
S97-T11B-TI-CX	-	4.98 ± 2.31	0.292 ± 0.276	2048.2 ± 408.0
S97-T11B-TI-FX	-	3.68 ± 0.40	-	422.2 ± 56.8
S97-T11B-TI-MX5	-0.0376 ± 0.0908	-10.72 ± 68.09	-0.054 ± 0.326	98.2 ± 47.5
S97-T11B-TI-MX6	-	-10.67 ± 68.09	-	26.6 ± 11.1
S97-T11B-TI-MX7	-	-10.39 ± 68.09	-	17.2 ± 8.3
S97-T11B-TI-MX8	-0.0838 ± 0.0787	-10.11 ± 68.09	-	6.2 ± 7.5
S97-T11B-TI-MX9	-	-9.48 ± 68.09	-	7.8 ± 7.4
S97-T11B-TI-MX10	-	-10.77 ± 68.09	-	8.6 ± 8.0
S97-T11B-TO-CX	0.0809 ± 0.2345	3.41 ± 2.68	-	113.1 ± 354.3
S97-T11B-TO-FX	-	1.85 ± 0.20	-	264.2 ± 39.2
S97-T11B-TO-MX5	-	-9.97 ± 71.85	-	1.6 ± 7.9
S97-T11B-TO-MX6	-	-10.13 ± 71.85	-	-2.5 ± 7.9
S97-T11B-TO-MX7	-	-10.96 ± 71.85	-	29.7 ± 9.2
S97-T11B-TO-MX8	-	-10.79 ± 71.85	-0.100 ± 0.339	-
S97-T11B-TO-MX9	-	-11.28 ± 71.85	-	-0.5 ± 9.7
S97-T11B-TO-MX10	-	-	-	3.7 ± 11.1

Table D.12: Trace Metals Aerosol Concentration Data (U, V, Yb, Zn) (continued)

Sample	Aerosol Concentration (ng m^{-3})			
	U	V	Yb	Zn
S97-T21B-TI-CX	-	1.64 ± 2.14	-	-90.9 ± 325.7
S97-T21B-TI-FX	-	0.35 ± 0.18	0.069 ± 0.104	52.8 ± 23.5
S97-T21B-TI-MX5	-	-10.72 ± 67.86	-0.094 ± 0.321	22.6 ± 8.5
S97-T21B-TI-MX6	-	-10.73 ± 67.86	-	12.8 ± 7.7
S97-T21B-TI-MX7	-0.0024 ± 0.0995	-10.70 ± 67.86	-	16.7 ± 8.5
S97-T21B-TI-MX8	0.0132 ± 0.0948	-10.74 ± 67.86	-	3.9 ± 7.3
S97-T21B-TI-MX9	-	-	-	11.3 ± 7.4
S97-T21B-TI-MX10	-	-10.76 ± 67.86	-0.079 ± 0.321	-
S97-T21B-TO-FX	-	0.75 ± 0.04	-	44.8 ± 36.9
S97-T31B-TI-CX	0.7588 ± 0.5653	4.13 ± 2.19	-	126.3 ± 327.7
S97-T31B-TI-FX	-	1.95 ± 0.19	-0.020 ± 0.072	11.0 ± 20.7
S97-T31B-TI-MX5	-0.0598 ± 0.0819	-10.55 ± 67.86	-	5.0 ± 11.4
S97-T31B-TI-MX6	-	-10.64 ± 67.86	-0.046 ± 0.322	-0.4 ± 7.8
S97-T31B-TI-MX7	-	-10.48 ± 67.86	-	-3.2 ± 8.0
S97-T31B-TI-MX9	-	-10.63 ± 67.86	-0.073 ± 0.321	-0.0 ± 8.3
S97-T31B-TI-MX10	-	-10.68 ± 67.86	-0.084 ± 0.320	-2.0 ± 8.7
S97-T31B-TO-CX	-	2.52 ± 2.25	-	337.8 ± 347.1
S97-T31B-TO-FX	-	1.94 ± 0.17	-	-17.2 ± 19.1
S97-T31B-TO-MX5	-	-8.44 ± 67.23	-	1.1 ± 7.2
S97-T31B-TO-MX6	-	-9.40 ± 67.23	-	-1.2 ± 7.6
S97-T31B-TO-MX7	-0.0410 ± 0.0799	-6.43 ± 67.23	-	-0.8 ± 7.3
S97-T31B-TO-MX8	-	-4.88 ± 67.23	-	3.1 ± 7.4
S97-T31B-TO-MX9	-	-9.44 ± 67.23	-0.093 ± 0.318	-4.0 ± 7.3
S97-T31B-TO-MX10	-	-	-	13.9 ± 17.7
S97-T41B-TI-CX	-	1.35 ± 2.27	-	308.1 ± 339.8
S97-T41B-TI-FX	-	0.33 ± 0.06	-	35.5 ± 21.3
S97-T41B-TI-MX5	-	-10.16 ± 67.86	-	17.5 ± 15.7
S97-T41B-TI-MX6	-	-10.35 ± 67.86	-	6.6 ± 8.9
S97-T41B-TI-MX7	0.0405 ± 0.1371	-10.23 ± 67.86	-	3.9 ± 8.3
S97-T41B-TI-MX8	0.3332 ± 0.0813	-10.43 ± 67.86	-	3.1 ± 8.0
S97-T41B-TI-MX9	-0.0629 ± 0.0828	-	-	8.5 ± 7.5
S97-T41B-TI-MX10	-	-10.75 ± 67.86	-	7.8 ± 7.4
S97-T41B-TO-CX	-	-0.64 ± 2.14	-	-102.3 ± 327.3
S97-T41B-TO-FX	-	0.94 ± 0.15	-	118.8 ± 30.1
S97-B11A-AZ-MX5	-	-	-	154.0 ± 20.0
S97-B11A-AZ-MX6	-	-	0.130 ± 0.100	12.0 ± 6.8
S97-B11A-AZ-MX7	-	-	0.180 ± 0.160	28.0 ± 9.0
S97-B11A-AZ-MX8	-	-	-	132.0 ± 17.6
S97-B11A-AZ-MX9	-	-	-	40.0 ± 14.4
S97-B11A-AZ-MX10	-	-	-	20.0 ± 14.0
S97-B11A-DB-CX	0.5400 ± 0.3600	10.60 ± 1.86	0.420 ± 0.320	1680.0 ± 198.0
S97-B11A-DB-FX	-	0.08 ± 0.03	-	15.3 ± 6.4
S97-B11A-DB-MX5	-	0.46 ± 0.28	0.096 ± 0.060	15.8 ± 4.6
S97-B11A-DB-MX6	0.3200 ± 0.1780	-	0.130 ± 0.090	8.6 ± 3.4

Table D.12: Trace Metals Aerosol Concentration Data (U, V, Yb, Zn) (continued)

Sample	Aerosol Concentration (ng m^{-3})			
	U	V	Yb	Zn
S97-B11A-DB-MX7	-	-	0.162 ± 0.106	9.2 ± 8.8
S97-B11A-DB-MX8	-	-	-	22.0 ± 17.2
S97-B11A-DB-MX9	-	-	-	6.6 ± 3.6
S97-B11A-DB-MX10	0.0640 ± 0.0600	0.22 ± 0.07	-	22.0 ± 18.6
S97-B11A-ML-CX	-	-	-	66.0 ± 9.4
S97-B11A-ML-FX	-	-	0.044 ± 0.023	13.8 ± 3.1
S97-B11A-RV-CX	0.3800 ± 0.2800	-	0.220 ± 0.132	640.0 ± 74.0
S97-B11A-RV-FX	-	-	-	73.0 ± 39.0
S97-B11A-RV-MX5	-	-	-	24.0 ± 13.0
S97-B11A-RV-MX6	-	-	-	13.4 ± 5.8
S97-B11A-RV-MX7	-	-	-	32.0 ± 22.0
S97-B11A-RV-MX8	-	-	0.096 ± 0.074	15.6 ± 8.6
S97-B11A-RV-MX9	-	-	-	20.0 ± 12.8
S97-B11A-RV-MX10	-	0.13 ± 0.03	-	142.0 ± 18.0
S97-B11A-TI-CX	-	-	-	58.0 ± 9.0
S97-B11A-TI-FX	-	0.00 ± 0.00	0.100 ± 0.100	68.0 ± 14.0
S97-B11A-TI-MX5	-	-	0.176 ± 0.146	42.0 ± 10.6
S97-B11A-TI-MX6	-	-	-	42.0 ± 13.0
S97-B11A-TI-MX7	-	-	-	36.0 ± 5.8
S97-B11A-TI-MX8	-	-	-	40.0 ± 8.2
S97-B11A-TI-MX9	0.1560 ± 0.1200	-	-	28.0 ± 10.2
S97-B11A-TI-MX10	-	-	0.118 ± 0.088	34.0 ± 6.4
S97-B21A-DB-CX	-	0.48 ± 0.17	-	136.0 ± 16.8
S97-B21A-DB-FX	-	0.08 ± 0.03	-	121.1 ± 18.1
S97-B21A-DB-MX5	0.3600 ± 0.1440	0.86 ± 0.44	-	102.0 ± 15.8
S97-B21A-DB-MX6	-	-	-	44.0 ± 7.6
S97-B21A-DB-MX7	0.2000 ± 0.1240	-	-	32.0 ± 28.0
S97-B21A-DB-MX9	-	-	10.200 ± 2.600	98.0 ± 22.0
S97-B21A-DB-MX10	-	-	3.800 ± 0.860	30.0 ± 13.0
S97-B21A-ML-CX	0.2000 ± 0.1120	-	-	32.0 ± 15.0
S97-B21A-ML-FX	-	-	0.090 ± 0.060	36.0 ± 8.0
S97-B21A-ML-MX5	0.3000 ± 0.0060	-	-	26.0 ± 7.6
S97-B21A-ML-MX6	-	-	0.340 ± 0.162	-
S97-B21A-ML-MX7	-	-	-	7.8 ± 5.8
S97-B21A-ML-MX8	-	-	-	14.4 ± 13.0
S97-B21A-ML-MX9	-	-	-	13.2 ± 6.8
S97-B21A-ML-MX10	-	-	-	64.0 ± 14.8
S97-B21A-RV-CX	-	-	-	240.0 ± 36.0
S97-B21A-RV-FX	-	0.00 ± 0.00	-	137.0 ± 24.0
S97-B21A-RV-MX5	-	-	-	24.0 ± 5.4
S97-B21A-RV-MX6	-	-	0.114 ± 0.106	36.0 ± 24.0
S97-B21A-RV-MX7	-	-	0.540 ± 0.420	42.0 ± 18.0
S97-B21A-RV-MX8	0.2600 ± 0.2000	0.24 ± 0.04	-	34.0 ± 8.0
S97-B21A-RV-MX9	-	-	-	14.0 ± 9.8

Table D.12: Trace Metals Aerosol Concentration Data (U, V, Yb, Zn) (continued)

Sample	Aerosol Concentration (ng m^{-3})			
	U	V	Yb	Zn
S97-B21A-RV-MX10	-	-	-	40.0 ± 14.2